THE UNIVERSITY OF QUEENSLAND

AUSTRALIA

The Growth Hormone Receptor Mediated Oncogenesis

Yash Chhabra

B.Tech, MS

A thesis submitted for the degree of Doctor of Philosophy at

The University of Queensland in 2014

Institute for Molecular Bioscience

Abstract

Growth hormone (GH) is a major regulator of postnatal growth, cellular proliferation and differentiation, as well as of metabolism. All actions of GH are mediated via its cognate Growth Hormone Receptor (GHR). It is now clear that the role of GH extends well beyond the conventional notions of longitudinal growth and childhood development. A substantial body of evidence supports a role for the GH/IGF-1 axis in cancer incidence and progression in animals and humans and because of widespread clinical application of GH, there has been considerable interest in the mechanism of activation of its receptor. It was originally thought that GH initiated its actions by sequentially binding two GHR monomers, resulting in receptor dimerisation and initiation of intracellular signalling cascades, including Jak/STAT and MAPK pathways. However, recent evidence by our group and others has indicated that the GHR is constitutively dimerised, and that dimerisation alone is not sufficient for GHR activation.

To this end the main objective of this thesis was to evaluate the role of GH-mediated signalling via its GHR in mediating oncogenesis. We have taken a multi-disciplinary approach by first determining how the GHR is activated via its transmembrane domain (TMD) and the nature of its interaction with Src family of tyrosine kinase (Lyn). We have determined the basis of the contrasting actions of autocrine GH from independent publications and sought to evaluate the effect of various constitutively active GHR constructs in cancer promotion *in vitro* and *in vivo* by establishing a tissue-specific delivery system (TVA system) for introducing multiple genes in a spatial and temporally controlled manner. We have provided the molecular basis of increased cancer susceptibility of the first reported GHR variant from two independent epidemiological studies. Finally, we have evaluated cancer resistance and anti-aging pathways in various GHR knockin and knockout mice models.

In order to determine the role of GHR transmembrane domain (TMD) and upper juxtamembrane domain (JMD) in signalling, cysteine-scanning mutagenesis was employed with truncated and full length receptors in a thiol-free background. Using these GHR constructs and sequentially substituting residues along the GHR JMD and TMD with cysteine we observed a ligand-independent spontaneous dimerisation pattern of upper JMD and TMD residues with evidence for a ‘tilt and twist’ movement for this region of GHR during activation. By using Cu-o-phenanthroline we were able to show that GHR activation could occur following disulfide bond formation at the upper TMD boundary resulting in constitutive activation. Finally we were able to conclude that GHR activation requires the JMD residues to come in close proximity which results in separation of

the lower TMD residues and activation. Another outcome of this study was the generation of the first full-length constitutively active receptor.

GHR has been shown to activate numerous pathways and one such pathway involves Src Family Kinase (SFK), which have been shown to be activated independently of Jak2. As a part of determining the structure-function aspect of GHR, we have defined the region in the intracellular domain (ICD) of GHR that interacts with Lyn (a SFK member) to lie between Box1 and Box2 motif. SFK pathways have been implicated in GH-dependent migration, invasion and even radio-resistance in MCF-7 mammary cancer cells. Actions of GH occur through two systems: the classical endocrine system and through extra-pituitary mechanisms (autocrine and paracrine), the latter being associated with worst survival outcomes in cancers. Using promoter-driven systems for autocrine GH secretion (high levels via CMV and low levels via MT promoter) we have demonstrated contrasting effects of differential level of GH autocrine expression on proliferation. In doing so, we were able to bridge the gap between conflicting findings from three independent groups. We report here that the level of GH for the same level of GHR determines 'cancer-like' features.

In addition, we have also determined the molecular basis for oncogenesis by the P495TGHR variant that has been reported in two separate GWAS population studies linking it with increased lung cancer susceptibility (OR= 12.98 and 2.04). We found that P495TGHR increased STAT5 and AKT signalling in a cell-dependent manner. Although not constitutively active by itself this variant has prolonged downstream signalling and proliferation after GH stimulation due to a delay in GHR degradation at the cell surface. This appears to be the direct result of steric hindrance to SOCS2 ubiquitin ligase binding at Y487 that lies in close proximity to P495T in GHR. Additionally, the P495T variant was less prone to the ligand-independent constitutive endocytosis that was unaffected by proteasomal and/or γ-secretase inhibitors. This is the first time that a polymorphism in GHR has been associated with cancer and highlights the importance of GHR turnover in tumour promotion.

We have successfully established RCAS/TVA system for tissue-specific gene delivery in mice and zebrafish models to directly determine the oncogenic potential of GHR *in vivo*. Using this system we intend to analyse constitutively active or gain-of-function GHR constructs generated in this project.

Finally, the GHR models lacking the full repertoire of GHR signalling (GHR 391 truncated, GHR-Box1 mutated and *ghr* null) were used to analyse cancer-related cause of death and its effect on lifespan. We have also determined the potential cancer resistance mechanisms (and signalling pathways) already at play in these mouse models. Based on our results, protection against cancer is due to multiple interacting pathways that include but are not limited to reduction in activation of growth-promoting pathways, increased stress resistance, reduced inflammation markers and increased insulin sensitivity. Although, most of these effects have been attributed to calorie restriction-mediated lifespan extension but we did not find any correlation with longevity in the GHR mutants. Based on the survival curves were able to conclude that cancer and longevity in these models are sexually dimorphic with a possible correlation of IGF-1 with lymphoma incidence in males and lymphoma aggressiveness in females GHR mutant mice.

Declaration by author

This thesis is composed of my original work, and contains no material previously published or written by another person except where due reference has been made in the text. I have clearly stated the contribution by others to jointly-authored works that I have included in my thesis.

I have clearly stated the contribution of others to my thesis as a whole, including statistical assistance, survey design, data analysis, significant technical procedures, professional editorial advice, and any other original research work used or reported in my thesis. The content of my thesis is the result of work I have carried out since the commencement of my research higher degree candidature and does not include a substantial part of work that has been submitted to qualify for the award of any other degree or diploma in any university or other tertiary institution. I have clearly stated which parts of my thesis, if any, have been submitted to qualify for another award.

I acknowledge that an electronic copy of my thesis must be lodged with the University Library and, subject to the General Award Rules of The University of Queensland, immediately made available for research and study in accordance with the *Copyright Act 1968*.

I acknowledge that copyright of all material contained in my thesis resides with the copyright holder(s) of that material. Where appropriate I have obtained copyright permission from the copyright holder to reproduce material in this thesis.

Publications during candidature

Chhabra Y*., Waters M. J. & Brooks A. J. (2011). Role of the growth hormone–IGF-1 axis in cancer. *Expert Review of Endocrinology & Metabolism* **6**, 71-84.

Andrew J. Brooks*, Wei Dai, Megan L. O'Mara, Daniel Abankwa, **Yash Chhabra**, Rebecca A. Pelekanos, Olivier Gardon, Kathryn A. Tunny, Kristopher M. Blucher, Craig J. Morton, Michael W. Parker, Emma Sierecki, Yann Gambin, Kirill Alexandrov, Ian A Wilson, Manolis Doxastakis, Alan E. Mark, Michael J. Waters (2014). A new cytokine receptor activation paradigm: activation of JAK2 by the Growth Hormone Receptor. *Manuscript accepted in the journal "Science".*

Mayumi Ishikawa*, Andrew J. Brooks*, Manuel A. Fernández-Rojo*, **Yash Chhabra**, Shiro Minami, Robert G. Parton, Michael J. Waters (2014). Growth hormone (GH) induction of the immunotolerance protein H2-Bl/HLA-G is essential for survival after partial hepatectomy. *Manuscript reviewed by Gastroenterology, manuscript number: GASTRO-D-13-01801; revision requested by May 2014.*

Waters, M. J*., Brooks A. J., & **Chhabra, Y**. (2014). A new mechanism for GH receptor activation of JAK2, and implications for related cytokine receptors. *JAK-STAT. In press.*

Conference Presentations

Presenting author underlined

Chhabra Y., Nelson C., Plescher M., Brooks T. & Waters M.J. (2014) The choice of Growth Hormone Receptor signalling pathway determines longevity. *Abstract submitted at 7th International Congress of GRS and IGF society, 15-18 October 2014, Singapore.*

Chhabra Y., Wong, H., Brooks A. J. & Waters M. J. (2014) The First Cancer-Associated Variant of the Growth Hormone Receptor. *Oral presentation at ICE/ENDO 2014, June 21-24, Chicago, IL, USA.*

Chhabra Y., Wong, H., Brooks A. J. & Waters M. J. (2013) The First Cancer-Associated Variant of the Growth Hormone Receptor. *Poster presentation at 6th Barossa Meeting: Cell Signalling in the Omics Era, November 20-23, Barossa Valley, SA, Australia.*

Brooks, A. J., Ishikawa, M., Fernández-Rojo, M. A., **Chhabra, Y**., Minami, S., Parton, R. G. & Waters, M. J. (2013) Growth hormone (GH) induction of the immunotolerance protein H2-Bl/HLA-G is essential for survival and liver regeneration after partial hepatectomy. *Australasian Society for Stem Cell Research 2013 Conference, 27-29 October, Brisbane, Australia.*

Brooks, A. J., Abankwa D., **Chhabra Y**., Gardon, O., Tunny, K.A., Blucher, K., O'Mara, M. L., Mark, A. E., Doxastakis, M., Morton, C.J., Parker, M.W. & Waters, M.J. (2012) Activation of the Growth Hormone Receptor requires separation of the Intracellular Domain of the Receptor leading to activation of Jak2. *Oral Presentation at FASEB: The Growth Hormone/Prolactin Family in Biology and Disease, 8-13 July 2012, Snowmass Village, Colorado, USA*.

Brooks, A. J., Abankwa D., **Chhabra Y**., Gardon, O., Tunny, K.A., Blucher, K., Morton, C.J., Parker, M.W. & Waters, M.J. (2011) The Molecular Mechanism of Jak2 Activation by a Class I Cytokine Receptor. *Oral presentation at Combio2011, Cairns, QLD, Australia.*

Publications included in this thesis

Chhabra Y*., Waters M. J*. & Brooks A. J. (2011). Role of the growth hormone–IGF-1 axis in cancer. *Expert Review of Endocrinology & Metabolism* **6**, 71-84. – **(Included in Appendix X)**

Contributor	Statement of contribution
Chhabra Y (Candidate)	Wrote the review (60%) Made all the figures and tables
Waters M.J.	Co-wrote the review (30%) Edited the paper
Brooks A.J	Wrote a section of the review (10%)

Andrew J. Brooks*, Wei Dai, Megan L. O'Mara, Daniel Abankwa, **Yash Chhabra**, Rebecca A. Pelekanos, Olivier Gardon, Kathryn A. Tunny, Kristopher M. Blucher, Craig J. Morton, Michael W. Parker, Emma Sierecki, Yann Gambin, Guillermo A. Gomez, Kirill Alexandrov, Ian A. Wilson, Manolis Doxastakis, Alan E. Mark, Michael J. Waters†. A new cytokine receptor activation paradigm: activation of JAK2 by the Growth Hormone Receptor. *Science*. Accepted for publication. – **My 6% contribution in the paper (included in Appendix IX as currently not listed on pubmed) has been incorporated into Chapter 3 and makes up less than a third of the contents of that Chapter.**

Contributor	Statement of contribution
Yash Chhabra (Candidate)	All work pertaining the data regarding hGHR cysteine crosslinks and constitutive activation in fig.3B, 3C, 3D and supplementary fig.S3 (incorporated in Chapter 3). (6%) Also responsible for standardising the co-IP protocol used in figure S4 and S5 (not included in the thesis).
Andrew J. Brooks	Performed FRET and Jak2 kinase domain swap experiments. Designed experiments with collaborations and wrote major parts of the paper. (25%)

Wei Dai and Manolis Doxastakis	Performed molecular dynamics studies. (10%)
Megan L. O'Mara and Alan E. Mark	Performed Jak2 modelling studies. (6%)
Daniel Abankwa	FRET studies. (5%)
Rebecca A Pelekanos	Performed ToxR experiments. (4%)
Olivier Gardon	Responsible MTS-2-MTS crosslink in fig.3A and made few hGHR cys truncated residues. (3%)
Kristopher M. Blucher and Kathryn A. Tunny	Performed jun zipper and alanine insertion proliferation studies. (6%)
Craig J. Morton and Michael W. Parker	Performed GHR TMD modelling (5%)
Emma Sierecki, Yann Gambin and Kirill Alexandrov	Designed and performed alpha screen experiments. (5%).
Guillermo A. Gomez	Performed FRET-anisotropy experiments. (3%)
Ian A. Wilson	Critical review of manuscript. (2%)
Michael J. Waters	Co-wrote the manuscript and conceptualised the study. (20%)

Contributions by others to the thesis

Some of the truncated hGHR cysteine constructs described in Chapter 3 were made by Olivier Gardon while all full length and other truncated hGHR cysteine constructs were made by the candidate himself.

The FACS for live cell sorting for generating stables in Chapter 3 and 6 was performed in conjunction with Paula Hall at QIMR Beecroft while the candidate himself performed all the staining procedures.

The prostate cancer slides obtained from Australian Prostate Cancer BioResource were H&E stained and graded by a histopathologist at the source itself. The candidate performed the genomic DNA and RNA extractions and subsequent analysis (Chapter 4). The extracted DNA was sent to Dr. Sean Grimmond (QCMG, IMB, UQ) for sequencing.

The *tva*-zebrafish (Chapter 5) was made in collaboration with Dr. Kaska Koltowska from Dr. Ben Hogan's Group (IMB, UQ).

The mouse tissue and serum used in Chapter 8 were collected with Dr. Caroline Nelson. The GH ELISA on mouse serum listed in Chapter 8 was performed under the guidance of Dr. Frederik Steyn at SBMS, UQ. The Survival Curves were compiled by Tania Brooks and mouse histopathological analysis reported in Chapter 8 was carried out by Dr. Helle Bielefeldt-ohmann at School of Veterinary Science, University of Queensland Gatton campus.

Professor Michael Waters and Dr. Andrew Brooks provided ongoing guidance throughout the project and edited publications.

Statement of parts of the thesis submitted to qualify for the award of another degree

None.

Acknowledgements

The research work presented in this thesis has been carried out in the Waters' Group at the Institute for Molecular Bioscience at University of Queensland. The path towards this thesis spans decades of hard work within the group and elsewhere. I acknowledge my debt to all those who have helped me along the way and influenced the understanding and the approach to representation of data and ideas in this report directly or indirectly.

In particular, I wish to express my gratitude to my supervisor and the 'GHR Guru', Professor Mike Waters for allowing me to work under his aegis and for his ongoing support and invaluable suggestions during the PhD. I am thankful for inculcating in me the ability to think critically and allowing me to come up with my own ideas and letting me run with them. I would especially like to thank Mike for providing me with such a challenging project. It has most certainly had its moments, has been a roller coaster in its own right but has taught me valuable lessons at professional and personal level. I will cherish our candid discussions on history, politics and life on numerous occasions.

I am indebted to my co-supervisor Dr. Andrew Brooks for providing a conducive environment to work in the lab and teaching me the nuances of cloning and virology. Without his encouragement and support especially during the phase of self-doubt, I could not have finished this thesis. I am grateful for his advice and teaching me that persistence always pays off and also for enduring numerous proofreads of the report contents.

I would sincerely like to thank Dr. Caroline Nelson for her valuable experiences, support with mice collections and insights as a fellow PhD student. We had some wonderful conversations on GHR's role on obesity and longevity and most importantly 'Game of Thrones'. I think that between the two of us we can give George RR Martin a run for his money!

A big thank you is also extended to other lab members past and present especially Tania Brooks for the delicious cakes and pavs and dinner invitations, Kathryn Tunny for technical assistance in the lab. Not to forget Ho Yi Wong (Bonbon) and Monika Plescher for their help and wonderful company during late hours in the lab and weekends (which happened quite often). Also thankful to Makerita Ieremia, Mannon Vullings, Morganne Roussel for the fun times, coffee breaks and loud radio karaoke sessions in tissue culture.

I am thankful to my thesis committee, especially Dr. Aaron Smith and Dr Melissa Little, for their suggestions during the milestone committee and would also like to extend my gratitude to Dr. Amanda Carozzi for her support and encouragement. She is truly a miracle worker. Thanks also to the fellow inhabitants of Level 6 North and the microscope facility. IMB has been a great working environment and everyone from Animal House staff, CSF facility to IT staff and IMB store has been extremely helpful during this journey.

I also would like to acknowledge the financial support from Australian Government's International Post-graduate Research Scholarship, the University of Queensland International Living Allowance Scholarship and Mike's support for sustaining me through the course of my PhD that provided me with the utmost essential – caffeine!

To all those people who became close friends in Australia: Aditi, Sourabh, Vikram, Rashmi, Praveer, Adnan, Srikanth, and Amrita I thank you with all my heart! Finally, many thanks to all the adorable toddlers Aarna, Roma, and Fia and others who clearly had no idea how much of a stress-buster they have been for me.

In the end would like to acknowledge the entire Chhabra clan especially Mom, Dad, Shivi and also to Aai for their support and cousins Jazz and Anil for their encouragement throughout my time here in Australia. Thank you for not being judgemental every time I forgot to return your call.

In every sense, none of this work would have been possible without the love and support of my wife Kasturee. Immensely thankful for taking good care of me and being my pillar of strength. She always knew that I could finish it, but for whom it didn't matter if I did or not. Her patience truly amazes me since putting up with me so far would surely not have been easy, but she has taken it all in her stride. This PhD is as much yours as it is mine!

I would like to dedicate this thesis in loving memory of my Naani and Joy who passed away midway during the PhD. Although you were not around to see me finish this chapter of my life I hope I have done you proud.

Keywords

growth hormone receptor, cancer, stat5 activation, polymorphism, longevity, tva system, signal transduction, src family kinase, autocrine GH, GHR mutants

Australian and New Zealand Standard Research Classifications (ANZSRC)

ANZSRC code: 060111, Signal Transduction: 70%
ANZSRC code: 060110 Receptors and Membrane Biology: 20%
ANZSRC code: 060603 Animal Physiology – Systems: 10%

Fields of Research (FoR) Classification

FoR code: 0601, Biochemistry and Cell Biology, 70%
FoR code: 0604, Genetics, 10%
FoR code: 0606, Physiology, 20%

Table of Contents

List of Figures and Tables

List of Abbreviations

ACSL3	Acyl-CoA synthetase long-chain family member 3
AGRF	Australian Genome Research Facility
AMPK	Adenosine 5'-monophosphate-activated protein kinase
ANOVA	Analysis of variance
APCB	Australian Prostate Cancer BioResource
ApoE	Apolipoprotein E
APS	Ammonium persulphate
ASLV	Avian Sarcoma Leukosis Virus
ATP	Adenosine triphosphate
ATP5a	ATP synthase, H+ transporting, mitochondrial F1 complex, α subunit
B2M	Beta-2 microglobulin
Ba/F3	Murine pro-B (cell line)
BFA	Brefeldin A
bGH	Bovine growth hormone
BPH	Benign prostate hyperplasia
BrdU	Bromodeoxyuridine
BRET	Bioluminescence resonance energy transfer
BSA	Bovine serum albumin
CaMKKβ	Ca^{2+}/calmodulin-dependent protein kinase kinase beta
CAT	Catalase
CD36	Cluster of Differentiation 36/Fatty acid translocase
Cdc4	Cell division control protein 4
CDK	Cyclin-dependent kinase
CHO	Chinese hamster ovary (cell line)
CHYSEL	cis-acting hydrolase elements
CIS	Cytokine inducible SH2-containing protein
CMV	Cytomegalovirus promoter
co-IP	Co-Immunoprecipitation
CoAA	Coactivator activator
COS	African green monkey kidney (cell line)
COX IV	Cytochrome c oxidase IV
CR	Calorie restriction
CuP	Copper-o-phenanthroline (crosslinking agent)
DAPI	4', 6-Diamidino-2-Phenylindole
DTT	Dithiothreitol
DV	Destination vector

E2	Estrogen (estradiol)
E2R	Estrogen receptor
ECD	Extracellular domain
EDTA	Ethylenediaminetetraacetate
EGF	Epidermal growth factor
EGFR	Epidermal growth factor receptor
eNOS	Endothelial nitric oxide synthase
EnvA	Envelope A
EPO	Erythropoietin
EPOR	Erythropoietin Receptor
ER	Endoplasmic Reticulum
ERAD	ER-associated degradation
ERK	Extracellular signal-regulated kinase
ERR	Estrogen-related receptor
ETC	Electron transport chain
EV	Empty vector (devoid of gene of interest)
FACS	Fluorescence activated Cell Sorting
FAK	Focal adhesion kinase
FBS	Foetal bovine serum
FDC-P1	Factor dependent cell-Paterson1 (cell line)
FFPE	Formalin-fixed, paraffin-embedded
FGF	Fibroblast Growth Factor
FLAG	an epitope tag
FMO2	Flavin containing monoxygenase 2
FRET	Fluorescence resonance energy transfer
Fwd	Forward
GAS	Interferon-gamma activated sequence
G-CSF	Granulocyte-colony stimulating factor
G-PCR	G-protein coupled receptor
G120R	GHR antagonist, hGH mutated at G120 to R
GAPDH	Glyceraldehyde-3-phosphate dehydrogenase
GFP	Green fluorescent protein
GH	Growth hormone
GHBP	Growth hormone binding protein
GHD	Growth hormone deficiency
GHR	Growth hormone receptor
GHR K1	Ghr-569 mutant (Knockin transgenic mouse with truncation of growth hormone receptor at residue 569)

GHR K2	Ghr-391 mutant (Knockin transgenic mouse with truncation of the growth hormone receptor at residue 391)
GHR K4	Ghr-Box1 mutant (Knockin transgenic mouse with mutation of growth hormone receptor Box1 domain alanine residues to proline)
GHR KO	Ghr null mutant (Growth hormone receptor knockout mouse)
GHRD	Growth hormone receptor deficient
GHRE	Growth hormone response element
GHRH	Growth hormone-releasing hormone
GLE	Gamma-interferon activated sequence-like element
Glut2	Glucose transporter 2
GM-CSF	Granulocyte/macrophage colony-stimulating factor
GPx	Glutathione peroxidase
Grb	Growth factor receptor-bound
GSK	Glycogen synthase kinase
GST	Glutathione-S- transferase
GusB	beta glucuronidase
GWAS	Genome wide association studies
h	human (prefix)
HA	Haemagglutinin epitope tag
HDAC	Histone deacetylase
HEK293	Human embryonic kidney293 (cell line)
HIF-1α	Hypoxia-inducible factor-1α
HNF	Hepatocyte nuclear factor
HRP	Horse radish peroxidase
i.m.	Intra-muscular
i.p.	Intra-peritoneal
ICD	Intracellular domain
IDH	Isocitrate dehydrogenase
IF	Immunofluoresnce
IGF	Insulin-like growth factor
IGFBP	Insulin-like growth factor binding protein
IGFR	Insulin-like growth factor receptor
IgG	Immunoglobulin class G
IHC	Immuno-histochemistry
IL	Interleukin
IL-1RA	Interleukin1-receptor antagonist
IR	Insulin receptor
IRS	Insulin receptor substrate

ITT	Insulin tolerance test
Jak	Janus kinase
JH	Jak homology domain
JM	Juxtamembrane
JMD	Juxtamembrane domain
JNK	c-Jun N-terminal kinase
KAT2A	K(lysine) acetyltransferase 2A (GCN5)
kDa	Kilo dalton
Keap1	Kelch-like ECH-associated protein1
KO	knockout
LEPROT	Leptin receptor overlapping transcript
LKB1	Liver kinase B1
LTR	Long terminal repeat
m	mouse (prefix)
MAb	monoclonal antibody
MAPK	Mitogen-activated protein kinase
MAPPIT	Mammalian protein-protein interaction trap
MCF-7	Michigan cancer foundation-7 (cell line)
MD	molecular dynamics
MFN2	Mitofusin2
miR	Micro RNA
MT	Metallothionein promoter
mt	Mitochondrial
mt-CO1	Mitochondrially encoded cytochrome c oxidase 1
mTFAM	mitochondria transcription factor A
mTOR	Mammalian target of rapamycin
NCOR	Nuclear receptor co-repressor
Ndufa5	NADH dehydrogenase (ubiquinone) 1 alpha subcomplex 5
NLS	Nuclear localisation signal
NMR	Nuclear magnetic resonance
Nqo1	NAD(P)H dehydrogenase quinone 1
Nrf1	Nuclear respiratory factor
Nrf2	Nuclear Factor-erythroid 2-related factor 2
OR	Odd's ratio
OxPhos	Oxidative phosphorylation
p	pig (prefix)
PAGE	Polyacrylamide gel electrophoresis
PBS	phosphate buffered saline

PCR	Polymerase chain reaction
PFA	paraformaldehyde
PGC	Peroxisome proliferator-activated receptor gamma coactivator
PGK	Phosphoglycerate kinase
PI3-K	Phosphatidyl Inositol-3-kinase
PKA	Protein kinase A
PKC	Protein kinase C
PLC	Phospholipase C
Ppar	Peroxisome proliferator-activated receptor
PRL	Prolactin
PRLR	Prolactin receptor
PROP1	Paired like homeodomain factor 1
PTB	Phosphotyrosine binding
PTEN	Protein tyrosine phosphatase, non-receptor type
PTP	Protein tyrosine phosphatase
pY	Phosphotyrosine
qPCR	Quantitative real time polymerase chain reaction
QTL	Quantitative trait locus
r	rabbit (prefix)
RCAS	Replication-Competent ASLV long terminal repeat (LTR) with a Splice acceptor
RCASBP	RCAS- with Bryan Polymerase
Rev	Reverse (Rvs)
rhGH	Recombinant GH
RIPA	Radio immunoprecipitation buffer
RNS	Reactive nitrogen species
ROR	RAR-related orphan receptor
ROS	Reactive oxygen species
RSV	Rous sarcoma virus
RTK	Receptor tyrosine kinase
s.c.	Sub-cutaneous
SCAM	Substituted-cysteine accessibility method
SCF	Skp, Cullin, F-box containing complex
SCID	Severe combined immunodeficiency
SDHA	Succinate dehydrogenase complex, subunit A, flavoprotein
SDHB	Succinate dehydrogenase complex, subunit B, iron sulfur
SDS	Sodium dodecyl sulfate
SFK	Src family kinase
SH	Src homology

Shc	Src homology/α-collagen-related adaptor protein
SHP	Src Homology 2 domain-containing protein tyrosine phosphatase
SIE	c-sis inducible element
siRNA	Small interfering RNA
SIN	Self-inactivating lentiviral vector
Sirt	Sirtuin
SNP	Single nucleotide polymorphism
SOCS	Suppressors of cytokine signalling
SOD	Superoxide dismutase
SOS	Son-of-sevenless (drosophila homologue)
spi	serine protease inhibitor
SRE	Serum response element
SRF	Serum response factor
Srxn1	Sulfiredoxin
SS	Serum supreme
STAT	Signal transducers and activators of transcription
T2	Diiodothyronine
T2DM	Type 2 diabetes mellitus
T3	Triiodothyronine
T4	Tetraiodothyronine
TACE	Tumour necrosis factor-α-converting enzyme
TAE	Tris-acetate-ethylenediaminetetraacetate
TBST	Tris buffered saline containing 0.1% Tween-20
TCA	Tricarboxylic acid
TEMED	N,N,N,N'- tetra-methylethylenediamine
tg	Transgenic
TMD	Transmembrane domain
TNFα	Tumour necrosis factor α
ToxR	cholera toxin transcriptional regulator from *Vibrio cholerae*
TPO	Thrombopoietin
TPOR	Thrombopoietin receptor
tr	Truncated
TrCP	Transducing repeat-containing protein
TritC	Tetramethylrhodamine
Trx	Thioredoxin
UbE	ubiquitin-mediated endocytosis
UCP	Uncoupling protein
Uqcrc2	Ubiquinol cytochrome c reductase core protein 2

UTR	Untranslated region
VSVG	Vesicular stomatitis virus glycoprotein
WT	Wildtype (control)

Amino Acid	**3 letter code**	**1 letter code**
Alanine	Ala	A
Arginine	Arg	R
Asparagine	Asn	N
Aspartic acid	Asp	D
Cysteine	Cys	C
Glutamic acid	Glu	E
Glutamine	Gln	Q
Glycine	Gly	G
Histidine	His	H
Isoleucine	Ile	I
Leucine	Leu	L
Lysine	Lys	K
Methionine	Met	M
Phenylalanine	Phe	F
Proline	Pro	P
Serine	Ser	S
Threonine	Thr	T
Tryptophan	Trp	W
Tyrosine	Tyr	Y
Valine	Val	V
Any amino acid	X	X

काममय एवायं पुरुष इति।
स यथाकामो भवति तत्क्रतुर्भवति।
यत्क्रतुर्भवति तत्कर्म कुरुते।
यत्कर्म कुरुते तदभिसंपद्यते॥

kāmamaya evāyaṃ puruṣa iti |
sa yathākāmo bhavati tatkratur bhavati |
yatkratur bhavati tat karma kurute |
yat karma kurute tad abhisaṃpadyate ||

You are what your deep, driving desire is
As your desire is, so is your will
As your will is, so is your deed
As your deed is, so is your destiny

Brihadaranyakopanishat 4.4.5

Chapter 1
Introduction

Preface

The Growth Hormone Receptor (GHR) was first proposed by Tsushima and Friesen following detection in tissues of specific high affinity ^{125}I-hGH binding (Tsushima & Friesen, 1973). All initial studies were primarily focused on GH-GHR interactions, regulation of GHR expression and species specificity with regards to binding and GH-related disorders (Zhu et al, 2001). Cloning of this receptor by the Genentech team has led to the discovery of a new Class of transmembrane receptors, the Class I cytokine receptors (Bazan, 1990; Leung et al, 1987). The proof that the cloned gene was the bona fide GH receptor was provided by the demonstration of loss of function mutations in Laron dwarfism (Godowski et al, 1989). Since then considerable information has been generated in regards to the structure-function relationships, mechanisms of action, signal transduction pathways, single nucleotide polymorphisms and receptor antagonists of clinical significance. In the last decade a considerable paradigm shift has occurred in understanding its activation mechanism from GH-induced dimerisation to conformational change within a constitutive homodimer. This has been accompanied by recognition of Jak-independent signalling, receptor crosstalk signalling, and autocrine mode of GH activation, and finally function of nuclear-localised receptor function.

This chapter contains information on the pleiotropic actions of GHR and its ligand, GH that make them indispensable molecules in the field of endocrinology as of 2014.

Introduction

The Growth Hormone Receptor is expressed in almost all cell types (Waters & Shang, 2002) and its transcript and protein have been reported as early as a 2-cell embryo (Pantaleon et al, 1997) together with functional responses to exogenous GH in the blastocyst which also expresses GH. GHR-mediated effects occur upon binding to its only ligand Growth Hormone, also known as somatotropin.

Growth Hormone

GH is a member of a hormone family that evolved over the last 350 million years from a common ancestral gene (Miller & Eberhardt, 1983). Other members of this family include prolactin, placental lactogen, somatolactin, and proliferin. The human GH (*hGH*) gene is a part of gene cluster consisting of five closely related genes including GH-N (normal), GH-V (variant), CSH-1 (chorionic somatomammotropin-1), CSH-2 (chorionic somatomammotropin-2) and CSH-L (CS-like) (Okada & Kopchick, 2001) illustrated in figure 1.1. GH-N is expressed in the pituitary gland and at low level in some extra-pituitary tissues such as lymphocytes. GH-N translation results in 22kDa (191 amino acids) and 20kDa (176 amino acid splice minor variant) proteins (Longhi et al, 2003) (Harvey, 2010). GH-V encodes for 22kDa and 20kDa placental GH, which differ from classical GH-N by 13 amino acids (Alsat et al, 1998; Vickers et al, 2009). Functionally, the 22kDa GH-V has high somatogenic and low lactogenic activities whereas the 20kDa GH-V retains some of the growth promoting and all anti-lipogenic activities of 22kDa GH-N but has diminished diabetogenic and lactogenic properties compared with the native 22kDa GH-N (Vickers et al, 2009).

GH-N is secreted in circulation by the anterior pituitary and is primarily responsible for post-natal growth. It is also important for nutrient partitioning hence body composition and metabolism (Casanueva, 1992). It has significant roles in every physiological system, notably reproductive, immune, skeletal, cardiovascular, gastrointestinal tract, adipose and hepato-biliary systems (fig.1.2) (Lichanska & Waters, 2008). It mainly acts in an endocrine manner and its pulsatile sexually dimorphic secretion is regulated by a complex balance of factors (stress, exercise and sleep etc.) and neuro-endocrine processes (Hattori, 2009). The ability of GH to induce Insulin like Growth Factor-1 (IGF-1) expression, in an endocrine manner via its action on liver as well as locally in a paracrine and autocrine manner, results in a potent growth and anabolic stimulus (Okada & Kopchick, 2001). At the cellular level, GH has been implicated in proliferation, differentiation and survival (Zhu et al, 2001). Indeed, GH has been reported to have over 450 different actions in over 80 cell types

(Waters & Shang, 2002). All of these biological actions believed to be a result of interacting with its specific membrane bound receptor, GHR. Additionally, the prolactin receptor can, in many species including mouse and human, also be stimulated by human growth hormone (Goffin et al, 1996). Failure to adequately regulate GH signalling leads to metabolic disorders evident in acromegaly and cachexia while excessive GH signalling is linked to cancer and increasing cardiovascular risk (Pilecka et al, 2007).

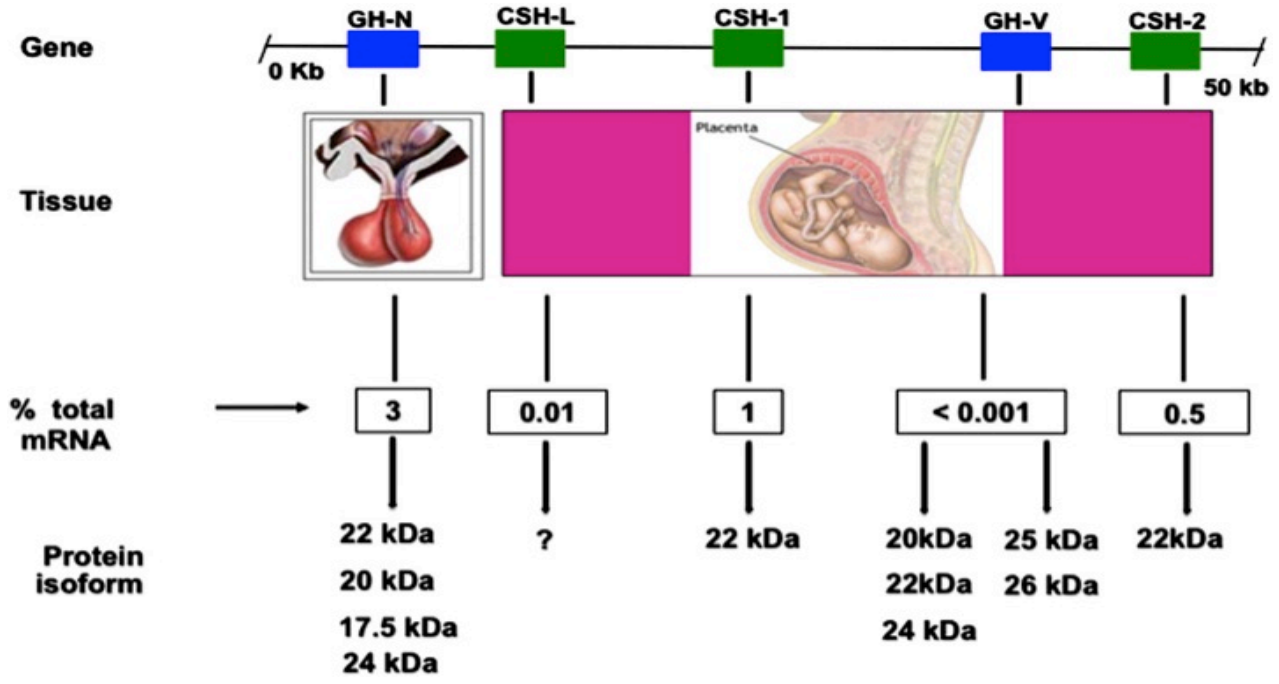

Figure 1.1: The human GH locus.

Locus structure, tissue site of expression, levels of mRNAs, and protein isoforms resulting from the gene members of the GH multigene family are shown (Perez-Ibave et al, 2014).

Extra-pituitary production of GH-N has been reported from sites such as neuronal cells (Scheepens et al, 2005), retinal cells (Harvey et al, 2004), lung cells (Beyea et al, 2006), bone (Kirpensteijn et al, 2002) and numerous immune cell types (Lantinga van Leeuwen et al, 2000). Certain embryonic cell types (notably in the brain) produce GH before ontogenic differentiation of pituitary somatotrophs (Lobie et al, 1993; Sanders & Harvey, 2004). In addition, many tumour cells have been reported to express GH and GHR (Perry et al, 2006; Chhabra et al, 2011). The GH-V is produced in a continuous manner by the placenta, gradually replacing the pituitary GH-N in pregnancy, so that GH-N becomes undetectable in the maternal circulation (Lacroix et al, 2002). This continuous secretion appears to have important implications for physiological adjustment to gestation especially in the control of maternal IGF-1 levels (Alsat et al, 1998). GH-N, GH-V and hPL are known to act through the GH receptor, although prolactin does not.

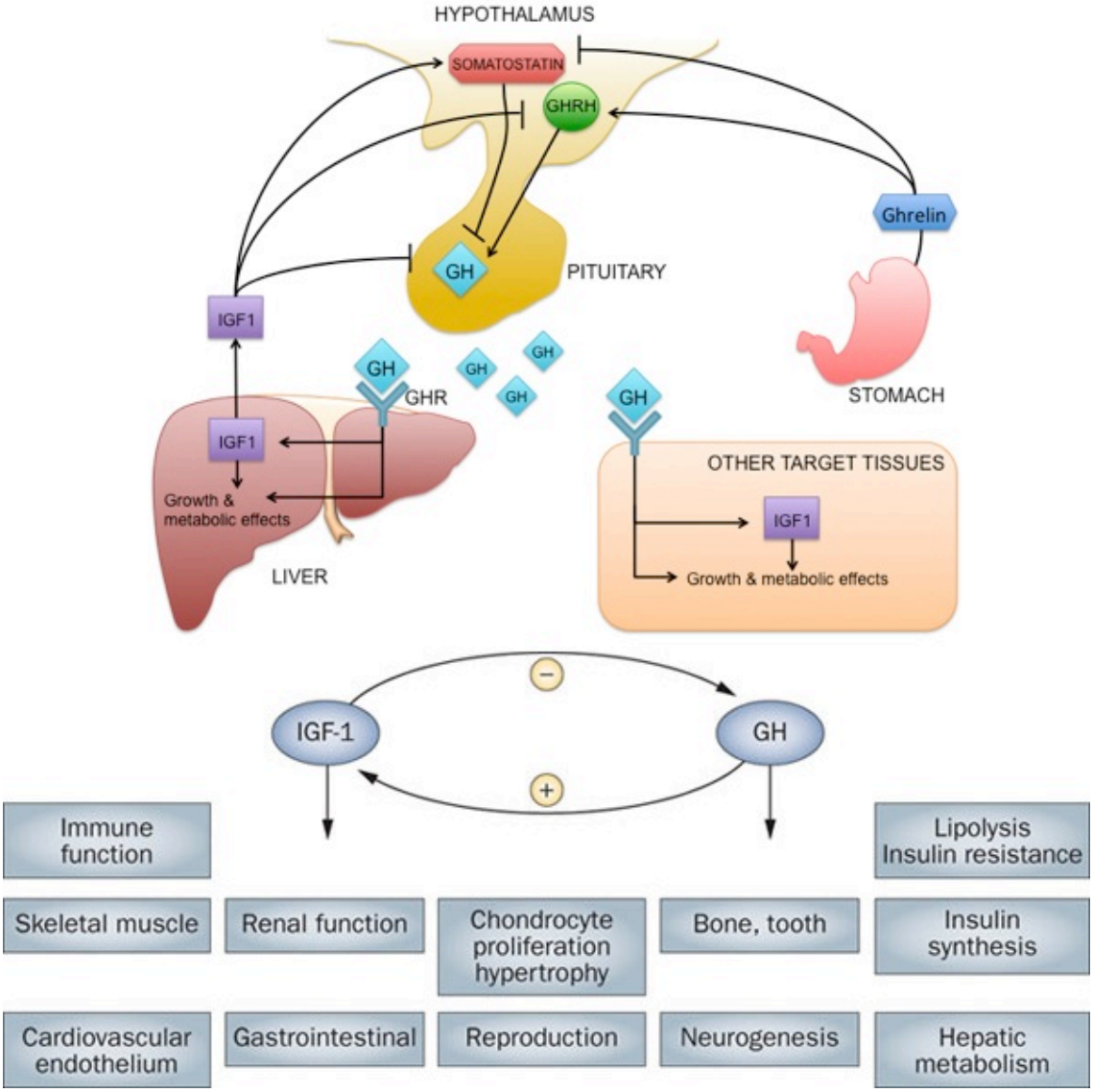

Figure 1.2: Regulation of Growth Hormone secretion and its actions on the physiological systems.
Hypothalamic growth hormone-releasing hormone (GHRH) and somatostatin positively and negatively regulate GH and secretion in the pituitary gland. Ghrelin, produced by the stomach, also stimulates GH secretion by stimulating hypothalamic release of GHRH and antagonising somatostatin. GH acts via the growth hormone receptor (GHR) stimulating production of insulin like growth factor (IGF)-1. IGF-1 is released into the circulation by the liver in response to GH and provides negative feedback on hypothalamic GHRH and pituitary GH release. IGF-1 has growth-promoting effects and acts independently or in conjunction with GH on numerous physiological systems and mediates cellular functions such as growth and metabolism in maintaining normal homeostasis.

Growth Hormone Receptor

Structure

GHR is a transmembrane glycoprotein with key structural features that characterise it as a member of Class I cytokine receptor family of 30 receptors, which includes erythropoietin, prolactin, leptin and thrombopoietin receptors (Kotenko & Langer, 2004). The mature GHR is composed of 620 amino acids comprising of 246-residue glycosylated GH-binding extracellular domain, a single

transmembrane domain predicted to be 24 amino acids in length, and an approximately 350-residue intracellular domain, which bears the C-terminus (Leung et al, 1987). The extracellular domain consists of two fibronectin type III (FNIII) subdomains, 3 conserved cysteine pairs and a conserved YGEFS motif (corresponding to WSxWS in other such receptors) (fig.1.3). The first FNIII domain spans residues 1-123 and the second residues 128-238, joined by a 4 residue long linker. Each of the domains contains 7 anti-parallel β-strands forming a β-sandwich similar in topology to immunoglobulins (Bazan, 1990). GH binds the receptor in both subdomains 1 through 2 assymetrically placed binding sites. Even though site 1 and 2 in GH molecule are different, they bind to essentially same residues on the GHR. In subdomain 1, the loops connecting the β–strands form a 'patch', with residues important for GH binding (Clackson et al, 1998; Wells, 1996; Gobius et al, 1992). Peptide mapping studies have revealed the extracellular domain of the GHR contains seven cysteines, six of them are located in subdomain 1 and form three disulfide bonds (C38-48, C83-94 and C108-122) (Fuh et al, 1990).

The lower subdomain 2 provides an interface where two GHR molecules interact connecting similar residues (Asn143, Ser145, Leu146, Thr147, His150, Asp152, Tyr200 and Ser201) in the opposite GHR via salt bridges and hydrogen bonds and called 'dimerisation domains' (Chen et al, 1997; Bernat et al, 2003). These residues are not necessary for constitutive dimerisation but are necessary for signal transduction (Gent et al, 2003). The subdomain 2 also possesses the cytokine receptor WSxWS equivalent motif ^{222}YGEFS^{226} (tyrosine-glycine-glutamate-phenylalanine-serine). Mutations in this motif have been shown to decrease signalling owing to lower ligand binding affinity and impaired receptor processing (Bazan, 1990) (Baumgartner et al, 1994). The extracellular domain also contains 5 well-conserved Asp-glycosylation sites at positions 28, 97, 138, 143 and 182 (Leung et al, 1987). Mutagenesis studies have revealed that these residues are not important for GH binding but are necessary for maintaining a high-affinity binding state and internalisation of GHR (Harding et al, 1994). An unpaired cysteine residue, C241 close to transmembrane domain has been shown to form an intermolecular disulfide bond on ligand binding (Zhang et al, 1999) but mutation of this cysteine to a serine did not affect dimerisation or phosphorylation status of the receptor (Gent et al, 2003).

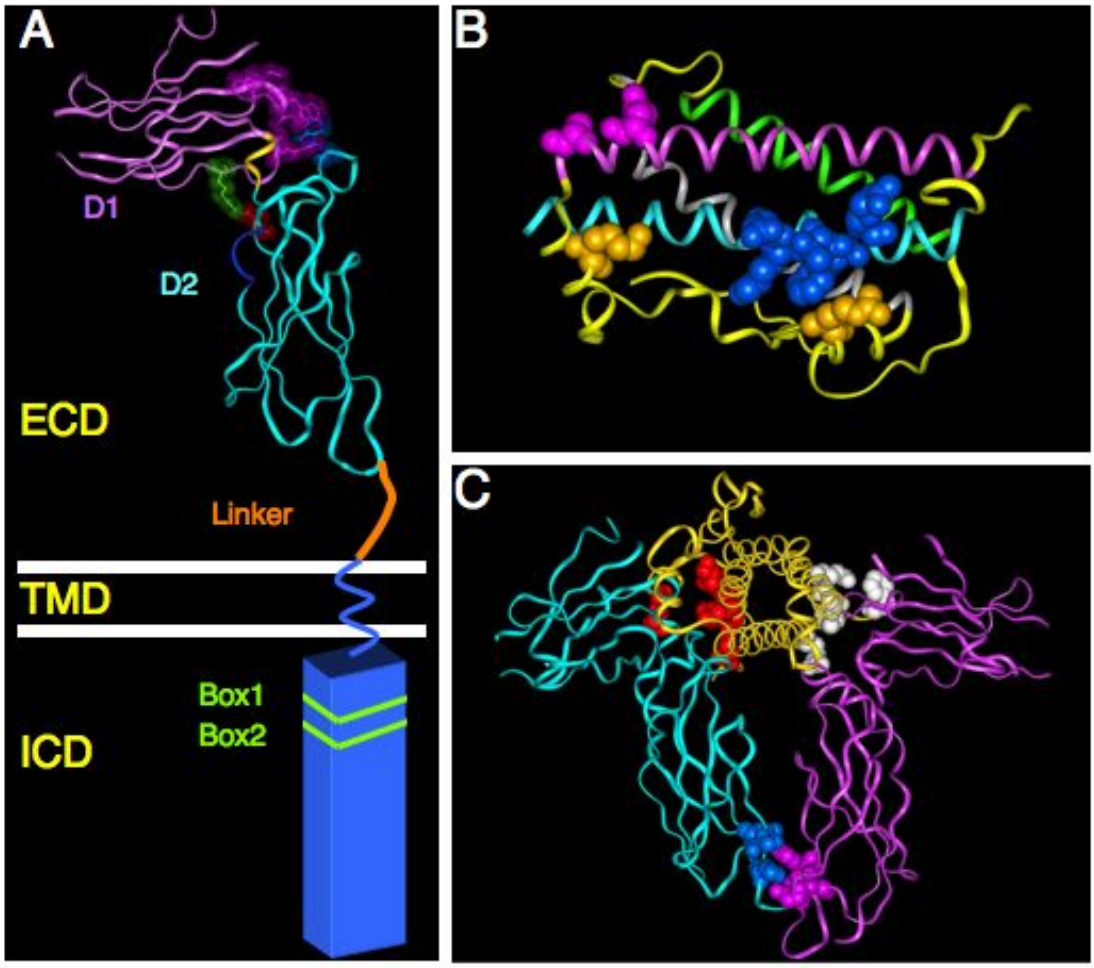

Figure 1.3: The structure of human Growth Hormone and its receptor.

(A) Illustration of a monomeric hGHR with the extracellular domain (ECD) shown as the crystal structure. Subdomain1 (D1) is shown in pink, the interdomain linker region is shown in yellow and subdomain 2 (D2) is shown in blue. Residues, including Trp104 (D1) and Trp169 (D2), involved in forming the hydrophobic patch that binds the hormone at site 1 are shown in semi-transparent space filling models (pink from subdomain 1, blue from subdomain 2). Arg39 and Asp132 form a salt bridge that stabilises the interdomain angle are shown as green and red semi-transparent space filling models respectively. The extracellular juxtamembrane linker region, transmembrane domain (TMD) and Intracellular domains (ICD) with no crystal structure are drawn in below the ECD. The approximate location of the Box1 and Box2 in the ICD are indicated by green lines. (B) The crystal structure of hGH with helices 1 through 4 are shown as ribbon and are coloured as follows: pink, green, grey and blue, with unstructured regions coloured yellow. Helix 4 residues that are important for binding to site1 are shown as blue space filling models, while those from the unstructured region are coloured yellow. (C) The GH:GHR2 complex structure with hGH (yellow ribbon), hGHR 1 (blue ribbon) and hGHR 2 (pink ribbon). Receptor interactive GH site1 residues are shown in red space filling model, receptor interactive GH site 2 residues are shown in white space filling model and residues in the dimerisation domain are shown in pink and blue space filling models (Behncken & Waters, 1999).

For the GHR a single transmembrane domain (TMD) comprised of hydrophobic residues spans the membrane as a potential helix as for other homomeric Class I cytokine receptors (Grotzinger, 2002). The crystal structure was able to reveal the organisation of the ECD only, so the structure of the transmembrane and intracellular domain are unknown. However, NMR studies have shown that the intracellular juxtamembrane region (residues 272-280) is α–helical up to the proline-rich motif

referred to as Box1 (^{281}PPVPVP^{286}) (Waters et al, 2006), common to the cytokine receptor family, and required for Jak2 binding (Dinerstein et al, 1995; Postel-Vinay & Finidori, 1995). Another well-conserved but less defined motif called Box2, spanning 15 amino acids is located ~23 amino acids downstream to Box1. This domain begins with a cluster of hydrophobic residues and ends with 2 positively charged amino acids (Postel-Vinay & Finidori, 1995; Argetsinger & Carter-Su, 1996). It has been shown that Box1 domain is sufficient for Jak2 binding with no requirement for the Box2 domain (Colosi et al, 1993; Brooks et al, 2014). The distal intracellular domain possesses of 9 tyrosine residues in the human sequence, and these are phosphorylated by Jak2 upon activation by GH, and serve as docking sites for signalling molecules such as STAT5.

In addition to domains important for signalling the ICD consists of motifs important for receptor internalisation and degradation. One such unstructured motif is the Ubiquitin-dependent Endocytosis (UbE) comprised of residues ^{322}DSWVEFIELD^{331} in the Box2 region (Govers et al, 1999; da Silva Almeida et al, 2013). Finally, the ICD contains di-leucine motifs and a DSGxxS degradon discussed in detail later.

Isoforms and species variation

The human GHR gene is located on the short arm of chromosome 5, spanning at least 87kb and comprising of 9 exons in addition to several non-coding exons in the 5' untranslated region (UTR) represented in figure 1.4 (Godowski et al, 1989). Exon 2 encodes the peptide signal sequence, exons 3-7 encode the extracellular domain and exon 8 encodes for three residues of ECD, the entire TMD and first four residues of ICD. The remaining exons encode the cytoplasmic domain and also the 2kb of 3` UTR (Edens & Talamantes, 1998). There are at least 13 alternatively spliced human GHR mRNAs generated in the 5` untranslated exons all of which splice into a common acceptor site upstream of the translation initiation site of exon 2. This results in generation of full-length receptor polypeptide but with expression levels varying in a spatial-temporal manner (Wei et al, 2006). Amino acid sequences of rabbit and human GHRs show 84% identity. For other species, homology in the sequence of the receptors is as high as 70% (Postel-Vinay & Finidori, 1995). Binding and activation of GHR of primate origin cannot be achieved with a non-primate GH whereas primate GH can bind and activate non-primate GHR (Knobil E, 1959). This species specificity is attributed to the Leu43Arg change in hGHR and His171Asp change in hGH (Behncken et al, 1997; Liu et al, 2001). Similarly, mutagenic analysis has also identified a second determinant Lys165, which in addition to His169 restricts the ability of non-primate hormones to activate primate GHR (Wan et al, 2004).

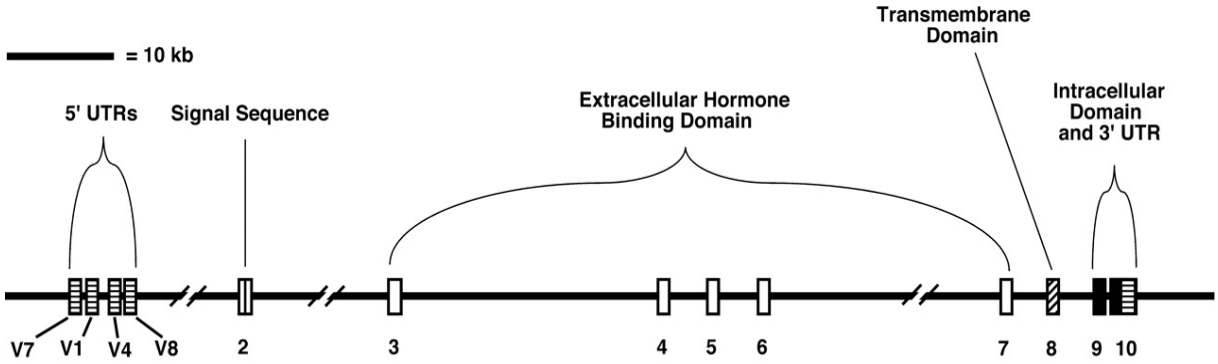

Figure 1.4: Human GHR gene structure.

The black horizontal line represents the intron sequence while the diagonal breaks in the lines indicate portions of introns. Boxes represent exons with numerical designation of the exon listed below each box. Exons with horizontal stripes encode untranslated regions (UTRs) of the transcripts (5'-UTRs and 3'-UTRs). Vertical striped exons encode signal sequence. White exons encode the hormone-binding domain. Diagonal striped exons encode the transmembrane domain. Black exons encode the intracellular domain. Human liver GHR transcripts have eight known alternative 5'-UTR sequences (V1-V8). The exons encoding four of the 5'-UTRs (V1, V4, V7, and V8) have been cloned and are shown on the gene map. The human UTR V5 sequence corresponds to the intron sequence immediately upstream of exon 2. (Edens & Talamantes, 1998).

A number of naturally occurring isoforms, alternatively spliced transcripts of GHR have been reported. Splice variants lacking 97% of the ICD occur in humans (corresponding to GHR 1-259 and GHR 1-261) although, present at a small proportion of the full-length receptor (Ross et al, 1997). These membrane-bound cytoplasmically truncated splice variants of GHR have also been reported in numerous tissues and cell lines with protein expression levels differing across tissues (Amit et al, 1997; Ayling et al, 1999; Ballesteros et al, 2000). One such receptor variant is generated due to 26bp deletion in the exon 9 that introduces a stop codon at amino acid position 280 of the receptor (Dastot et al, 1996). The variants (truncations) generated can form heterodimers with full-length GHR and are therefore inhibitory to the downstream signalling due to lack of Jak2 and STAT5 binding sites acting as dominant negative receptors. These truncated isoforms also generate large amounts of GH binding proteins (Dastot et al, 1996) and have been reported as a contributor to short stature (Ross et al, 1997; Minamitani, 2002).

One common isoform of GHR that is well characterised and widely expressed is exon-3 deleted GHR (d3-GHR) in humans. This isoform is the outcome of a genetic polymorphism resulting in deletion of the entire exon from mRNA without compromising the structure or function of the resultant protein (Stallings-Mann et al, 1996). It was initially thought that this isoform was tissue-dependent (Urbanek et al, 1992). However, it became apparent that the exon-3 deletion was not tissue-dependent but individual-dependent (Wickelgren et al, 1995). The d3-GHR lacks amino acids

7-28 in the extracellular domain, but this does not affect GHR binding or internalisation (Mercado et al, 1994; Urbanek et al, 1992). There are discrepant results on the role of the d3-GHR in the GH/IGF-1 axis and in some studies it has been reported to increase sensitivity to exogenous GH in children (Wassenaar et al, 2009) and GH pharmacogenetics (Dos Santos et al, 2004; Filopanti et al, 2011).

Growth Hormone Binding Protein

In humans, the GHBP is generated at the cell surface due to proteolytic cleavage of GHR ECD by ADAM-17 metalloprotease, also known as Tumour Necrosis Factor-α Converting Enzyme (TACE) (Zhang et al, 2000). The exact cleavage site is unknown but a site eight residues N-terminal to the TMD (around Glu242, Glu243, Asp244) was reported to be an important determinant for cleavage (Baumann & Frank, 2002; Wang et al, 2002). It was reported that spacing of the residues is more important than their identity. This proteolytic cleavage process (or shedding) results in a soluble, freely circulating GHBP in the blood that is measurable by a LIFA assay (Sotiropoulos et al, 1993) and provides an indication of GHR expression. It has been reported that GH protects the GHR from shedding, probably by creating a conformational change blocking access for TACE (Zhang et al, 2000; van Kerkhof et al, 2002). GHBP has the ability to bind to circulating GH and thereby increase the half-life (prolong bioavailability) of GH by decreasing its clearance from circulation, since the complex formed is too large for glomerular filtration. Therefore GHBP functions as a GH reservoir by damping free GH pulses (Baumann, 2001). In contrast, excessive GHBP produced by cells expressing truncated GHR can compete with GH for ligand binding and form an inactive GHR/GHBP complex (Lim et al, 1990). In addition to extracellular generation of GHBP it has been shown that it can be found intracellularly in the nucleus (Lobie et al, 1994a) where it interacts with coactivator activator (CoAA) to promote cell proliferation and this activity is dependent on S226 of the consensus WSXWS box equivalent YGEFS motif (Conway-Campbell et al, 2008). In addition to shedding, GHBP can also be synthesised by alternative splicing of mRNA especially in the case of rodents as evident from the presence of hydrophilic C-terminal extension in the GHBP (Edens et al, 1994).

GHR Turnover

GHR is present on almost every cell throughout the body at varying levels and the surface expression levels can vary temporally (Waters, 1999). Cell surface GHR availability is a key determinant of GH responsiveness. It is regulated by mechanisms that govern changes in GHR abundance (downregulation) in response to ligand stimulation. In addition, GH-independent

regulation occurs by factors that regulate receptor gene expression (Edens & Talamantes, 1998; Schwartzbauer & Menon, 1998) as well as factors that govern receptor protein stability, such as the ability of Jak2 to chaperone nascent receptor to the cell surface and to stabilise to the mature receptor against constitutive endocytosis and degradation (Deng et al, 2007; Schwartzbauer & Menon, 1998), as well as metalloproteolytic processing (Wang et al, 2002; Zhang et al, 2000) illustrated in figure 1.5. Metalloproteolytic GHR degradation involves cleavage of the extracellular domain by ADAM-17 followed by C-terminal transmembrane cleavage by presenilin-dependent γ–secretase (Wang et al, 2002; Cowan et al, 2005). Jak2 has been reported to be a key player in determining susceptibility of GHR to proteolysis, suggesting yet another role for this kinase in determining GH sensitivity (Loesch et al, 2006).

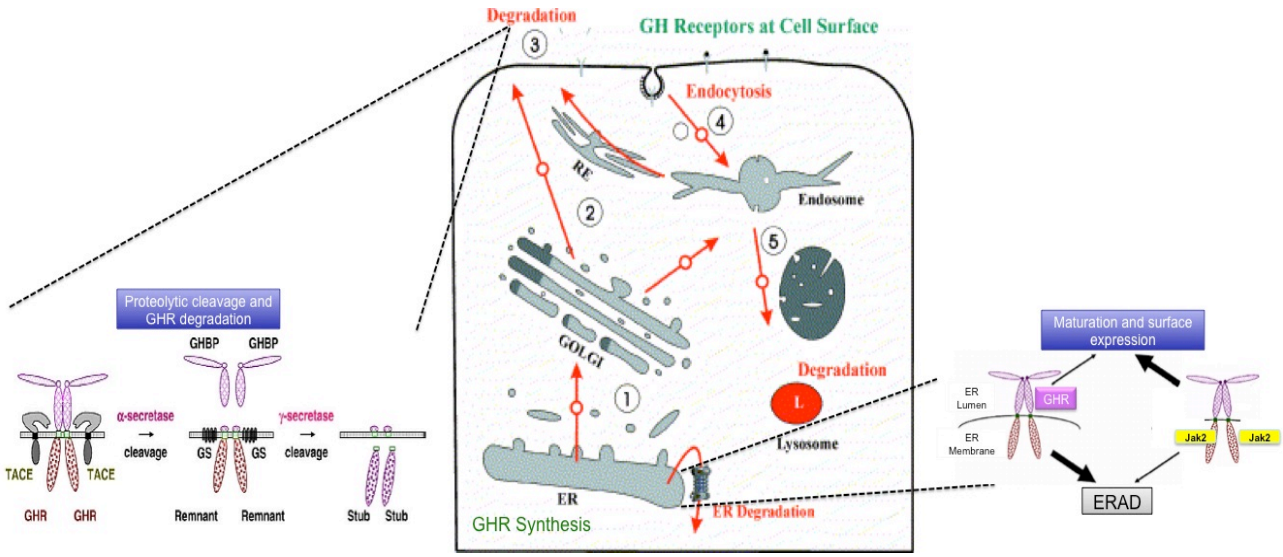

Figure 1.5: Growth Hormone Receptor turnover.

GHR is synthesised in the endoplasmic reticulum (ER) (1), sorted in the Golgi complex and transported to the cell surface (2). Degradation of the GHR occurs in several ways: the extracellular domain (ECD) is shed into the circulation (3), endocytosed into the cell (4) and transported to the lysosome for degradation (5). Availability of GHR at the cell surface is determined by the rate of endocytosis, the rate of shedding and other unknown mechanisms. Jak2 mediates increased maturation and reduced ER-associated degradation (ERAD) of GHR (right panel). The GHR at cell surface undergoes metalloproteolytic GHR degradation (left panel) involving cleavage of the extracellular domain by ADAM-17 generating Growth Hormone Binding Portein (GHBP) followed by C-terminal transmembrane cleavage by presenilin-dependent γ–secretase (Strous & van Kerkhof, 2002).

GHR synthesis

GHR synthesis and expression can be regulated at transcriptional, translational and post-translational levels and therefore regulate GH sensitivity. Factors such as nutritional status, endocrine context, developmental stage and various tissue-specific control mechanisms (Schwartzbauer and Menon 1998) are summarised in Table 1.1. GHR is synthesised and folded as a precursor protein in the endoplasmic reticulum, and complex-glycosylated at five potential sites

(Asn-X-Ser/Thr) (Harding et al, 1994) in the Golgi, resulting in a mature receptor that is transported to plasma membrane (Leung et al, 1987). In the ER, the three disulfide bonds (in subdomain 1) are formed and GHR dimerises. The immature GHR in the ER is detected on the western blot running at 110kDa while any misfolded GHR is subjected to ER-associated degradation mechanism with the aid of associated ubiquitin ligases (Loesch et al, 2007; Brodsky, 2012; Nelson et al, 2006). The mature 'glycosylated' GHR in the Golgi or at the plasma membrane is detected at 130kDa (due to the addition of high mannose oligosaccharides). At the cell surface the GHR is subjected to proteolytic cleavage, or remains unmodified until it ends up in clathrin-coated pits as a remnant (after proteolysis) or intact (with or without bound GH) for internalisation and degradation in the endosomal or lysosomal systems (van Kerkhof & Strous, 2001; Sachse et al, 2002a). Internalisation requires a ubiquitin/proteasome system (Strous et al, 1996). In addition, internalisation of GHR via caveolae has also been reported as a trafficking pathway to mitochondria (Yang et al, 2004; Perret-Vivancos et al, 2006) but this is not widely accepted (Sachse et al, 2002b).

Table 1.1: Regulation of GHR expression
Developed from (Flores-Morales et al, 2006).

Factor	Effect on GHR Expression	System
Nutrition		
Undernutrition and fasting	↓ GHR (mRNA)	Liver, rat
	↓ GHR (mRNA)	Hepatocytes, rat
Glucose starvation	↓ GHR (mRNA)	Hepatocytes, pig
Endocrine System		
Chronic GH treatment	↑ GHR (binding)	Liver, rat, pig, and sheep
GH deficiency	↓ GHR (number)	Liver, rabbit
Acute GH treatment	↑ GHR, 1 h (binding)	Liver, rat
	↓ GHR, 6 h (binding)	
GH overexpression	↑ GHR (binding)	Liver, transgenic mice
Pregnancy	↑ GHR (mRNA and binding)	Liver, mouse
Estrogen	↓ GHR (mRNA)	Liver, rat
Dexamethasone	↓ GHR (mRNA)	Liver, rat
Insulin	↑ GHR (mRNA and protein)	HuH7 cells
	↓ GHR surface	
	↓ GHR (binding)	H4 cells
T_3	↑ GHR (mRNA)	HuH7 cells
IGF-1	↑ GHR (mRNA)	Liver, rat
FGF-21	↓ GHR surface	Liver, transgenic mice
LEPROT & LEPROTL1	↓ GHR surface	Liver, transgenic mice
	↓ GHR surface	Hepatocytes, myoblasts

Ubiquitin system

Ubiquitin-dependent GHR internalisation

The GHR was initially found to be ubiquitinated upon amino acid sequencing of the receptor from rabbit liver (Leung et al, 1987). It was first suggested by Allevato *et al*. that amino acids 318-380 in the cytosolic tail of GHR were important for degradation (Allevato et al, 1995) nad this was later extended by Strous *et al*. who highlighted the role of a functional ubiquitin conjugating system in endocytosis within this region (Strous et al, 1996). In a Chinese hamster lung cell line, GHR availability was shown to be determined by UbE (ubiquitin-dependent endocytosis) motif (75%), ECD shedding (10%) and undetermined factors (15%) (van Kerkhof et al, 2003). The endocytosis of GHR has been reported to be relatively rapid, constitutive and GH-independent (van Kerkhof et al, 2002). However, binding of GH does enhance receptor ubiquitination, internalisation and degradation (van Kerkhof et al, 2002). Multiple ubiquitin moieties are covalently conjugated to the GHR protein on one or more of its 19 lysine residues in ICD as branched polymeric chains, resulting in the targeting of these substrates to 26S proteasomes (Strous et al, 1996).

Strous's Group have identified the target of the ubiquitin system in the GHR cytosolic tail as a 10 residue long sequence, ^{322}DSWVEFIELD^{331} (Strous et al, 1996; Govers et al, 1999). A key role for the ubiquitin system in GH-dependent GHR internalisation emerges from both genetic and molecular studies showing that GHR molecules accumulate at the plasma membrane if the ubiquitin system is inhibited (Strous & Govers, 1999). Moreover, GHR ubiquitination coincides with its recruitment into clathrin-coated pits (van Kerkhof et al, 2000). Strikingly, ubiquitination of the GHR itself is not required for internalisation because replacement of all lysine residues with arginine in the ICD did not alter the rate of internalisation (Govers et al, 1999). This indicates that for internalisation the ubiquitin conjugation system needs to be recruited to the UbE motif rather than the conjugation of ubiquitin to lysine residues of the GHR for this process, presumably dependent on an accessory protein. After internalisation, the GH-GHR complex is directed to early endosomes and then either to the proteasome or lysosome compartments (van Kerkhof & Strous, 2001; Sachse et al, 2002a).

By examining truncated receptors, the endocytosis-deficient receptor mutant F327A, and conditions under which clathrin-mediated endocytosis is inhibited it was found that GHR ubiquitination and internalisation are coupled events (Govers et al, 1997). GHR dimerisation has been shown to be necessary for UbE-mediated internalisation since a chimeric GHR that cannot form dimers was shown to undergo ubiquitin-independent internalisation (Gent et al, 2002). Importantly, GHR ubiquitination and internalisation besides being ligand-independent are also independent of downstream signalling by the GHR (Strous et al, 1996; van Kerkhof et al, 2000). However, GHR

internalisation is inhibited in the presence of proteasomal inhibitors and its C-terminal cytosolic tail is required for proteasome interaction (van Kerkhof et al, 2000). Thus, proteasomal inhibition was shown to prolong GHR/Jak2 phosphorylation (Alves dos Santos et al, 2001) although this may be because the GHR can signal even after internalisation (Frank, 2001). Recently Putters *et al*. have proposed a model with Jak2 as a negative regulator of ubiquitin-dependent endocytosis so that its detachment from GHR following activation is necessary for efficient endocytosis by ubiquitin ligases (Putters et al, 2011). This has been supported by marked reduction in surface receptor as determined by the fate of immunologically detectable receptor owing to GH-induced Jak2 activation (Deng et al, 2012). In contrast, a catalytically inactive Jak2 mutant incapable of associating with GHR, or a receptor mutant deficient in Jak2 binding rendered GH far less able to promote receptor downregulation compared with expression of wildtype receptor (Deng et al, 2012).

An important accessory protein in GHR internalisation is β-TrCP (β-transducing repeat-containing protein) (van Kerkhof et al, 2007) which forms the F-box substrate recognition subunit of a multi-subunit cullin-based E3 ligase, SCF (Skp, Cullin, F-box containing complex) (Winston et al, 1999). For most of its substrates, β-TrCP recognises the degron DSGxxS (where X is a hydrophobic residue) only when both the serine residues are phosphorylated (Latres et al, 1999; van Kerkhof et al, 2007). It has been implicated in the ubiquitination of β–catenin, IκBα and numerous homologous cytokine receptors (PRLR, EPOR, etc.) via its WD-40 domain which has been shown to bind to the DSGxxS motif of target proteins (Winston et al, 1999; Li et al, 2004; Meyer et al, 2007). In the case of GHR however β-TrCP has been shown to bind to the highly conserved but unstructured DSWVEFIELD (UbE) motif and the 30 residue downstream DSGRTS motif (da Silva Almeida et al, 2012). The β-TrCP binding to the UbE motif although specific is unconventional and with a lower affinity than the phosphorylated DSGxxS motif (da Silva Almeida et al, 2013). Using the F327A (UbE mutant), a DAGxxA mutant and double mutants it was shown that β-TrCP acts mainly via UbE motif in GH-induced conditions, whereas both the motifs supported ubiquitination in the basal conditions contributing to GHR homeostasis in the cells (da Silva Almeida et al, 2012).

Despite a specific interaction between β-TrCP and GHR, the receptor was reported not to be a necessary target for β-TrCP-directed Lys^{48} polyubiquitination. This meant that the GHR needs to interact with β-TrCP for internalisation but this does not require Lys^{48} ubiquitination. Slotman *et al*. have recently shown that Lys^{63}-linked ubiquitin chain conjugation is however required for GHR endocytosis as it is for the prolactin receptor. These workers identified both the ubiquitin-conjugating enzyme Ubc13 and the ubiquitin ligase COOH terminus of Hsp70 interacting protein

(CHIP) as required for Lys^{63} ubiquitination (Slotman et al, 2012). Ubc13 activity and its interaction with CHIP appear to precede endocytosis into clathrin-coated pits, but occur after β-TrCP directed Lys^{48} ubiquitination. These processes regulate cell surface availability of GHR.

Ubiquitin-independent GHR internalisation

GHR degradation has also been reported independently of ubiquitin through a di-leucine motif (Govers et al, 1997; Sachse et al, 2002b). This is however not the case of full-length GHR but for a truncated GHR (1-349), and possibly some GHR isoforms (Govers et al, 1998).

Mechanism of Action

GH Binding

The team at Genentech (James Wells' team) have conducted exhaustive mutagenic and phage display analyses and mapped the residues contributing energy to the binding interactions at site 1, site 2, and the receptor-receptor interaction domain of site 3 (Clackson et al, 1998; Walsh et al, 2003; Bernat et al, 2003). The major energy contribution for site 1 involves two tryptophans, one contributed by the upper cytokine receptor β-sandwich (W104) and one by the lower sandwich (W169). W104 is also key for the weaker site 2 interaction, and this interaction is blocked by substituting a bulky arginine or lysine at the glycine 120 position in helix 3 of the hormone, which binds tightly to W104 of the second receptor, as shown in the case of GH receptor antagonist pegvisomant. The electrostatic interactions allow GH to tightly interact with the tryptophan residues, while hydrogen bonds also contribute to the binding energy for both the hormone-receptor interaction and the receptor-receptor interaction (Walsh et al, 2003; Bernat et al, 2003).

Activation of constitutively dimerised receptor

The crystal structure of the GH bound to GHR extracellular domain showed that two GHR molecules were bound to a single GH molecule in 2:1 stoichiometry and physicochemical studies showed that this required a sequential 2-step binding process (Cunningham & Wells, 1991; de Vos et al, 1992). The GH molecule binds asymmetrically via its opposite face to a single binding site on each of the two GHR molecules with different affinities (de Vos et al, 1992; Wells, 1996). These observations led to the hormone-induced dimerisation model for GH action (Fuh et al, 1992). It was reported that binding of the three bivalent monoclonal antibodies to the ECD of the receptor was capable of activating a hybrid receptor expressed in a FDC-P1 cell line, while monovalent fragments of these could not dimerise and activate this receptor. The hybrid receptor consisted of the ECD of the human GHR fused to the N-terminal fibronectin domain of the granulocyte colony-

stimulating factor (G-CSF) receptor. Hence, this led to the measurement of G-CSF signalling rather than GHR. A second line of evidence for induced dimerisation was the bell shaped dose response curve for GH with this hybrid receptor, which led to a proposal that a second GH would occupy the second receptor at high concentration, preventing effective signalling (Ilondo et al, 1994).

However when the full-length GHR was subjected to similar study undertaken by Fuh *et al*. (Fuh et al, 1992), only 2 of the 15 antibodies were able to weakly activate GHR stably expressed in BaF/3 cells while no activation was observed in FDCP-1 (Rowlinson et al, 1998). As a positive control of dimerisation ability 8 of the 15 antibodies were able to activate the G-CSF/GH receptor chimera used by Genentech (Rowlinson et al, 1998). Based on this, it was proposed that receptor dimerisation alone could not activate the receptor, which required a specific conformation/orientation of receptor subunits. This was later supported by binding studies with the G120R antagonist that was shown to bind to a dimeric GHR at the cell surface (Ross et al, 2001) indicative that its mechanism must be induction of an antagonist conformation of the receptor dimer. Subsequently, co-immunoprecipitation data demonstrated that a proportion of the receptor exists as a constitutive dimer (Gent et al, 2002) and that the ligand-receptor complex had a differential susceptibility to proteasomal digestion than the G120R-receptor complex (van Kerkhof et al, 2002). The co-IP studies using truncated receptors also highlighted that the ECD was not needed for its formation since its removal with proteinase K treatment did not influence the extent of dimer formation in intact cells (Gent et al, 2002). In addition, it was also reported that receptor dimer formation occurred in the ER, which remained unaffected even after the addition of hormone to receptor-expressing cells. This also meant that there were separate confirmations of receptor dimer, one that could promote signalling (upon GH binding) and other that would inhibit it as in the case of G120R (Rowlinson et al, 1998).

These findings were supported by co-IP studies indicating constitutive dimer formation when the ICD was truncated just below the Box2 sequence at residue 360 and that these dimers were held together by either TMD or juxtamembrane domain (Brown et al, 2005). The same study also reported an increase in the proportion of GHR dimer that got immunoprecipitated after GH addition. This was confirmed by using both fluorescent resonance energy transfer (FRET) and bioluminescence resonance energy target (BRET) techniques to monitor receptor association in intact cell membranes by appropriate placing of specific fluorescent or bioluminescent tags/reporters.

From the FRET/BRET analysis it was evident that addition of 6 residues to the C-terminus was sufficient to drive dimer formation. Importantly, when the reporters were successively placed closer to the cytoplasmic membrane surface, both FRET and BRET ratios increased markedly, indicating proximity of the Jak2 binding Box1 sequences. Notably, deletion of the Box1 motif by alanine substitution did not change the FRET or BRET ratio, indicating that receptor dimer was not a consequence of Jak2 association. Placement of the FRET reporters at the receptor C-terminus resulted in a low FRET value, indicating a wider separation. Contrary to the ligand-induced dimerisation model, addition of GH to cell membrane preparations overexpressing GHR did not change the FRET or BRET ratios when the reporters were attached at the N- or C-terminus of the receptor (Brown et al, 2005). These have since been confirmed using cysteine crosslinking, Tox-R bacterial assay and homo-FRET anisotropy (Brooks et al, 2014). It was evident from these studies that GHR got dimerised within the cell and that addition of GH had no effect on the dimerisation state. The association between the GHR monomers to form a dimer was proposed to occur via its TMD (Brown et al, 2005).

The finding that the transmembrane helix was primarily responsible for formation of the constitutive GHR dimer was concordant with previous studies on EPOR and TPOR. By utilising the bacterial Tox-R/Tox-CAT assay of TM helix association and immunofluorescence co-patching to show that the homologous EPOR is constitutively dimerised through its TM helix domains by a leucine zipper-like motif (Kubatzky et al, 2001; Constantinescu et al, 2001). Similarly, Tox-R assay and cysteine substitution and crosslinking have shown that TPOR at the cell surface exists as a ligand-independent dimer (Matthews et al, 2011). Likewise, the homologous PRL receptor was shown to exist as a homodimer in ligand-independent manner and this association appears to be mediated by the TM helices (Qazi et al, 2006; Gadd & Clevenger, 2006). Based on these evidences it was clear that homo-dimerised type I cytokine receptors signalling involves a conformational change or a subunit arrangement.

In order to determine the mechanism of GH-induced receptor conformation, crystal structure of unbound receptor was analysed (Brown et al, 2005). Interestingly, there was little difference in comparison to the receptor bound complex, indicating a rotation of the lower domain by 7° to 9° as a result of hormone binding. No alterations in the position of residues involved in the extracellular receptor-receptor “dimerisation domain” were evident, despite being reported in the 1:1 complex formed with the G120R antagonist (Clackson et al, 1998). There were minor changes observed in residue position relating to the ligand binding sites (around Trp104 and Trp169), and an alteration of the F’G’ loop position in the lower receptor domain. The latter has been shown to regulate

receptor signalling by a novel Src/ERK pathway (Rowlinson et al, 2008), but did not influence the Jak2 activation. On closer inspection, it was revealed that receptor 1 gets rotated approximately 25° respective to receptor 2, and elevated by 8 angstroms to allow the two receptor domains to lock together (Brown et al, 2005), which had previously been shown to be essential for signalling (Chen et al, 1997; Gent et al, 2003). In addition, a subunit rotation could account for the lack of change observed in the FRET/BRET ratio after hormone binding since the relative distances would change only marginally. Support for a rigid body subunit rearrangement was also achieved by molecular dynamics that showed when the hormone was removed from the 2:1 complex *in silico*, the second receptor subunit rotated approximately 45° counterclockwise with respect to the first (Poger & Mark, 2010). This model was also consistent with the epitope location for the agonist monoclonal antibody, which could rotate receptor subunits in molecular simulations of docking (Wan et al, 2003).

The locking of dimerisation domains could be emulated by replacing just the GHR ECD with jun-jun zipper. This construct upon stable transduction in Ba/F3 cells was found to be constitutively active and could eliminate ECD movements by holding the receptor tightly at TMD and ICD in one configuration (Behncken et al, 2000). Initial placement of the zipper close to the cell membrane in 4-residue increments revealed that GHR activation increased as the distance between the zipper and cell surface decreased (Brooks et al, 2014). In order to determine the precise movement involved, alanine insertions were carried out in the zipper construct near the TMD, which revealed that a rotation of the receptor could induce constitutive activation of Jak2/STAT5 only when the receptor was in a particular configuration. In particular, it was shown alanine insertion above the TMD resulted in an optimal rotational position for activation (approximately a 40° turn). These experiments showed that there was a preferred orientation for activation, suggesting a rotation of the transmembrane helix was involved in activation.

A key element in understanding the receptor activation mechanism came from more FRET studies that involved the reporters to be placed just below Box1 motif (Brooks et al, 2014). These GHR constructs although 37 residues downstream to Box1 were able to bind and activate Jak2 normally upon GH binding. Contrary to the view that ligand binding induced proximity of the Box1 sequences, a decrease in FRET signal was reported indicating increased separation. Additionally, an inverse relationship between cell proliferation and FRET signal that was established by using the alanine insertions above the TMD in a jun zipper constructs was used to determine the gating mechanism at TMD. In particular, the acidic residues (^{242}EED^{245}) in the region juxtamembrane to the TM helix were replaced with non-repulsive alanine residues in the jun zipper chimera enhanced

cell proliferation, and resulted in an even lower FRET efficiency (Brooks et al, 2014). In addition, co-transfection of full-length GHR (containing EED) with a mutant receptor containing a charge reversal of EED to KKR was associated with decreased FRET efficiency and constitutive activation. It was evident that these conserved acidic residues act as a gating mechanism for receptor activation, where the electrostatic repulsion was overcome by GH binding. Similarly, alanine substitution of the first lysine in submembrane SKQQRIK sequence in a jun zipper construct resulted in increased receptor activation as in the case of TPOR (Staerk et al, 2006).

Finally by performing FRET analysis on cell membrane extract transfected with low levels of receptors, GH binding was shown to result in a substantial decrease in FRET efficiency. This was confirmed by blocking the separation movement by pre-incubation of cells with the G120R hGH antagonist. Importantly, in the case of D152H mutation (Duquesnoy et al, 1994) implicated in Laron dwarfism, no change in the FRET efficiency was observed after the addition of GH.

GHR-mediated Jak2 activation

Structurally Jak family members comprise of a modified FERM domain at its N-terminus (JH7-JH5) which is used for binding to the receptor via the receptor Box1 motif. This domain is followed by an apparently non-functional SH2 domain (JH4-JH3) that links to the pseudokinase domain (JH2) that is followed by the kinase domain (JH1) at the C-terminus. The crystal structures of the kinase and pseudokinase domains have been resolved (Lucet et al, 2006; Bandaranayake et al, 2012). It has recently been established that the pseudokinase domain functions as a serine/threonine kinase and in doing so the pseudokinase domain can regulate JH1 kinase activity (Ungureanu et al, 2011). There are many other regulatory tyrosine phosphorylation sites in Jak2 identified by mass spectrometry analysis but not much is known in regards to their interaction and function (Argetsinger et al, 2010).

In order to determine how the separation of the TMD helices at the C-termini Box1 sequences could result in Jak2 activation, few approaches were utilised by Waters' Group (Brooks et al, 2014). Firstly, by strategic placements of the FRET reporters the movement of kinase and pseudokinase domains were measured in conjunction with the receptors made constitutively active by co-transfecting receptor constructs with wildtype juxtamembrane EED sequence and with KKR replacing it, so that charge attraction at this point led to receptor activation. This showed that receptor activation resulted in an increased FRET for the C-terminal kinase domain placement of reporters, but a decrease in FRET for the pseudokinase reporter placement. This data was supported by Jak2 and STAT5 activation when the kinase and pseudokinase domains were swapped and co-

transfected at very low levels. These were suggestive that upon receptor activation the kinase domains would come together in close proximity in the receptor/Jak2 assembly, resulting in activation, in a receptor-dependent manner. The importance of receptor requirement for these domains to mediate activation has been confirmed by that have reported EPOR requirement for oncogenic *V617FJak2* to manifest its constitutive activity (Lu et al, 2008). Based on the current model it can be reasoned that the pseudokinase domain of one Jak2 molecule could be inhibiting the kinase domain of the other Jak2 and vice versa. Pulling them apart would allow the kinase domains to come into proximity, facilitating *trans* activation and Jak2 action (Brooks et al, 2014).

Another approach employed was the quantification of interactions between two pseudokinase-kinase domains, or these domains separately, using Alpha screen and single molecule FRET. These experiments demonstrated that the pseudokinase-kinase domain pair was able to associate *in trans* with another such pair, as proposed (Brooks et al, 2014). Finally, crystal structures of the kinase and pseudokinase domains were docked *in silico* in the predicted orientation using HADDOCK (high ambiguity driven biomolecular docking) to attain two optimum minimum energy states. The docked structures predicted a close complementary interaction between the opposing kinase and pseudokinase domains. Moreover, the structure showed proximity between the activation loop and V617 residue in the pseudokinase domain which, when mutated resulted in oncogenesis because of impaired kinase inhibition. In support of the experimental data of Jak2/STAT5 activation covalently linked pseudokinase and kinase (PK-K) domains of one Jak2 were then placed with another PK-K pair in alternative orientations, highlighting two arrangements that were also consistent with the recent study which has reported that the PK-K domains are linear in solution, and bound *in trans* (Varghese et al, 2014).

Signal Transduction

Like all Class I Cytokine Receptor Family, the GHR lacks the intrinsic kinase activity and is therefore dependent on other kinases to initiate intracellular signalling. Recent evidence has indicated that GHR exists as a homodimer in its non-liganded state and each GHR monomer is associated with one or more inactive kinases (Gent et al, 2002; Rowlinson et al, 2008). The most widely reported kinase that has been reported to associate with GHR and get activated by GH is Jak2 (Janus Kinase 2) (Carter-Su et al, 1994). Jak2 is also known for stabilising the GHR dimer (He et al, 2005), which initially forms in the endoplasmic reticulum and translocates to plasma membrane via Golgi (Frank & Fuchs, 2008). In addition to Jak2, members of the Src family kinases (SFK) have also been implicated in GHR interaction (Rowlinson et al, 2008). The signalling pathways are illustrated in figure 1.6.

Jak2-dependent Signalling

Jak2 is a major component of GHR signalling and is one of the four Janus tyrosine kinases (Jak1, Jak2, Jak3 and Tyk2) (Argetsinger & Carter-Su, 1996) used by Class I cytokine receptors (Tanner et al, 1995; Frank et al, 1995). Structurally, Jak2 contains seven highly conserved domains, including N-terminal FERM which binds constitutively with GHR box1 motif, an inactive-kinase like (pseudokinase) domain and a functional C-terminal kinase domain (Harpur et al, 1992).

As mentioned, the asymmetric ligand binding to the pre-dimerised receptors in the plasma membrane results in relative reorientation of the GHR molecules, each bound to a single Jak2. This conformational change was initially postulated to bring the two Jak2 molecules into sufficient proximity to allow each Jak2 molecule to transactivate (i.e. cross-phosphorylate) tyrosine residues in the kinase domain of the other Jak2 (Argetsinger et al, 2004; Argetsinger et al, 1993). However, Brooks *et al*. have recently provided a model for GHR bound Jak2 activation that shows that upon GH stimulation there is an increased separation of Box1 sequence between the two GHR molecules. This movement results in the removal of the inhibitory pseudokinase domain from the kinase domain of Jak2, which then aligns the kinase domains for transactivation and signal initiation (Brooks et al, 2014).

Using Jak2 overexpression systems, some of the auto-phosphorylation sites in Jak2 appear to be regulatory in function as is evident from mutation of residues that decrease (Y221) or increase (Y119, Y570, Y1007) in Jak2 activity (Argetsinger et al, 2004; Feng et al, 1997). It is proposed that phosphorylation of Tyr119 promotes its dissociation from its associated cytokine receptor (Funakoshi-Tago et al, 2008). After transactivation Jak2 phosphorylates multiple GHR cytosolic domain tyrosine residues (Argetsinger et al, 2010; Carter-Su et al, 1994). Hansen *et al*. have identified three redundant tyrosine residues at positions 534, 566, and 627 (in mature GHR) by mutagenesis, responsible for activation of GH-stimulated transcription of the serine protease inhibitor (Spi) 2.1 promoter (Hansen et al, 1996). In addition, Rowland *et al.* have identified Y487 on GHR to get tyrosine phosphorylated using GHR knockin mouse models following GH stimulation (Rowland et al, 2005b). The generation of the activated GH/GHR-Jak2 complex allows for the recruitment of multiple signalling molecules, triggering numerous pathways which are dependent on the cell type, compartmentalisation and differentiation status (Waters & Brooks, 2011; Yang et al, 2004). In addition to Jak2, GH is known to activate Jak1 and 3, although this represents only a minor event (Hansen et al, 1996).

Jak2 contains 48 tyrosine residues and hGHR has 7 in its ICD that can serve as docking sites for other signal transduction molecules containing Src homology 2 (SH2) or phosphotyrosine binding (PTP) motifs that can positively or negatively regulate GH signalling. Serine phosphorylation had initially been suggested not to occur (Carter-Su et al, 1989; Foster et al, 1988) however, Ishida-Takahashi *et al*. have shown the Ser523 of Jak2 is phosphorylated and inhibits Jak2 activity (Ishida-Takahashi et al, 2006). FRET studies suggest that activation of Jak2 after GH binding is a rapid and transient event with the signal lasting only for 2-3 minutes. This transient nature was not caused by receptor internalisation but suggested to be due to additional conformational changes in the cytosolic domains following phosphorylation and recruitment of other signalling molecules (Biener-Ramanujan et al, 2006).

Signal Transducer and Activator of Transcription molecules

An important and direct pathway from activated GHR to gene transcription involves a family of transcription factors called STATs (Signal Transducer and Activator of Trancription). At least seven mammalian STATs have been identified of which STAT1, 3, 5a and 5b have been shown to be activated by GHR upon GH action, with STAT5A and B being the key mediators (Herrington et al, 2000b). The regions on GHR required for activation of different STATs have been mapped. STAT1, 3 and 5 all require the membrane proximal part of the receptor, including Box1, and therefore Jak2, to become activated. Further, STAT5 binds to phosphorylated tyrosines within the C-terminal tail at position Y487 (Rowland et al, 2005b), Y534, Y566 and Y627 (Hansen et al, 1996).

STATs themselves harbor a highly conserved tyrosine residue near their C-terminus that following phosphorylation by Jak2 allows the two STATs to dimerise via their SH2 domains and the dimeric phosphorylated-STAT5 are then translocated to the nucleus (Herrington et al, 2000b; Waxman & O'Connor, 2006). Iyer *et al*. have reported that STAT5A is continually shuttling to and from nucleus and its phosphorylation allows it to bind to DNA resulting in its retention in the nucleus (Iyer & Reich, 2008). In the nucleus STAT1 and 3 bind the c-sis inducible element (SIE) and co-activate the *c-fos* gene whereas the STAT5 isoforms activate transcription of GH-regulated genes such as *igf-1* and serum protease inhibitor 2.1 (spi2.1) by binding to GH responsive element (GHRE) or interferon-gamma activated sequence (GAS)-like response element (GLE) with the sequence TTCNNNGAA (Wood et al, 1997). In addition to their ubiquitous tyrosine-phosphorylation sites STATs also contain serine phosphorylation site, which is utlised by a few

MAPK members for activation or inhibition of their transcriptional abilities (Frank, 2001; Wen et al, 1995; Chatterjee-Kishore et al, 2000).

Mitogen-Activated Protein Kinase

In addition to STAT activation, phosphorylated Jak2 has been reported to bind other adaptor proteins. Binding of Src-homology domain containing (Shc) (Thirone et al, 1999) leads to sequential activation of growth factor receptor-bound protein 2 (Grb2), binding and activation of sons of sevenless (SOS) and finally RAS, RAF and MEK-mediated ERK1/2 serine/threonine kinase activation (Vanderkuur et al, 1997). The RAS-MAPK pathway has been implicated in the regulation of *fos* protooncogene expression by ternary complex factors (TCFs), $p62^{TCF}$/ELK-1, which act in concert with serum response factor (SRF) and bind the serum response element (SRE) on the *c-fos* gene leading to its expression, then to transcription of specific gene sets (Vanderkuur et al, 1997; Piwien-Pilipuk et al, 2002).

The MAPK pathway regulates RAF-1, phospholipase A2, cytoskeletal proteins and the transcription factors *c-jun* and *c-myc* (Pilecka et al, 2007). MAP kinases are important regulators of cellular growth and differentiation (Cobb & Goldsmith, 1995). GH-induced MAPK activity may also be important in modulating signalling by other growth factors, like Erb2, a member of EGF receptor family (Kim et al, 1999). In addition to p44/42 MAP kinase, GH also stimulates other members of the MAPK superfamily, namely p38 MAPK and c-Jun N-terminal kinase (JNK) (Zhu & Lobie, 2000; Zhu et al, 1998a) that can be Jak2-dependent and/or independent.

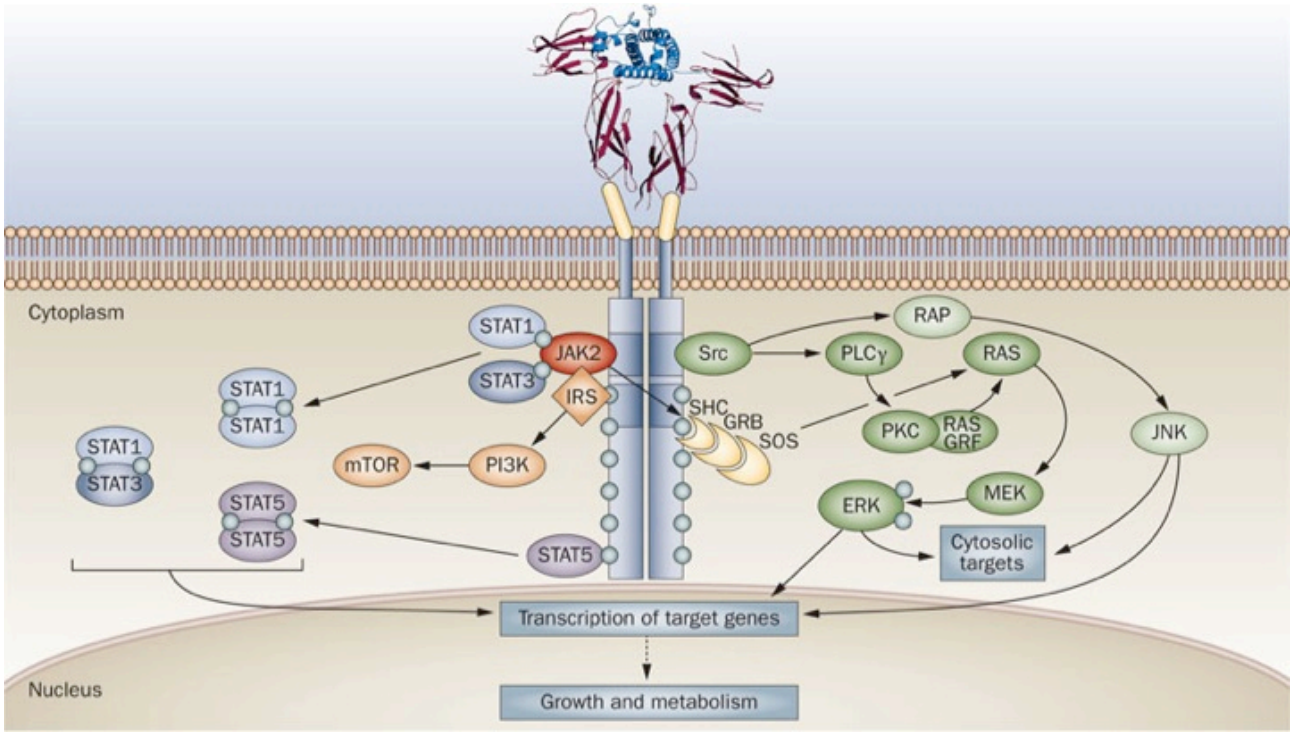

Figure 1.6: Growth Hormone Receptor-mediated signal transduction.

The extent of the individual pathways varies between cell types, depending on the relative expression of the component parts. Canonical protein-tyrosine kinase Jak2 signalling via STAT5 involves phosphorylation of key tyrosine residues in the cytoplasmic domain (below residue 350), which bind the Src homology 2 (SH2) domain of STAT5A and STAT5B, recruiting these STATs to the activated JAK2 and thus facilitating their tyrosine phosphorylation and subsequent dimerisation through their SH2 motifs. Dimerised STAT5 translocates to the nucleus to regulate gene transcription in complex ways. Conversely, STAT1 and STAT3 undergo direct tyrosine phosphorylation by Jak2 without the requirement for receptor binding. ERK can be activated either by SRC and/or phospholipase Cγ and Ras, or by Jak2 via the adaptors SHC, GRB and SOS. JNK is activated by SRC via RAP. The PI3-K and the serine–threonine-protein kinase mTOR pathway is activated by JAK2 via IRS phosphorylation. Signals are initially damped or terminated by the action of specific tyrosine phosphatases and receptor internalisation, then by the actions of induced SOCS proteins (Brooks & Waters, 2010).

Insulin Receptor Substrate and Phosphoinositide 3-Kinase

GHR activation of Jak2 can also result in phosphorylation of Insulin Receptor Substrate (IRS) family members, which results in PI3-Kinase/Akt pathway activation (Yamauchi et al, 1998a). IRS's are large cytosolic proteins that serve as mobile adapter proteins and upon tyrosine phosphorylation provide binding sites for other signalling molecules such as PI3-K, SHP-2 and SFK. The PI3-K pathway was initially reported in insulin activation. The phosphorylated IRS-1 provides binding sites for p85, the regulatory subunit of PI3-K resulting in the release of the catalytic subunit, p110 (Dey et al, 1998a; Hanada et al, 2004). Activated PI3-K phosphorylates the conversion of PIP-2 (Phosphatidylinositol 4,5-bisphosphate) to PIP-3 (Phosphatidylinositol 3,4,5-triphosphate). Subsequently PIP-3 recruits PDK1 (3-Phosphoinositide-dependent kinase 1 and Akt to the plasma membrane through the interaction with the pleckstrin homology (PH) domains. This

recruitment facilitates the phosphorylation of Thr308 in Akt, triggering downstream pathways (Currie et al, 1999; Stokoe et al, 1997). The PI3-K pathway is implicated in several physiological processes such as DNA synthesis, glucose uptake, cell cycle regulation, activation and inhibition of apoptosis (Cheatham et al, 1994; Songyang et al, 1997). Additionally, it is implicated in cell proliferation by inducing expression of c-myc and cyclins A and E (Jeay et al, 2001; Jeay et al, 2002).

Focal Adhesion Kinase-multiprotein signalling complex

GH-induced reorganisation of actin cytoskeleton and motility has been reported as a consequence of FAK (Focal Adhesion Kinase) activation that requires direct interaction between Jak2 and SH2-Bβ (Herrington et al, 2000a; Zhu et al, 1998b; Takahashi et al, 1999). These cytoskeletal changes are important in regulation of cell morphology and movement (Herrington & Carter-Su, 2001). GH is reported to stimulate the assembly of a multiprotein complex including Jak2, FAK and its substrates paxillin and tensin and several other proteins during cell adhesion and/or movement (Zhu et al, 1998b). c-Src and c-Fyn kinases, c-Cbl, Bck and JNK/p38 proteins have also been reported to be part of the large multimeric protein complex (Zhu et al, 1998a). PI3-K and SFK pathways have been reported to activate FAK and may provide an alternate pathway for GH-mediated cell modulation (Xing et al, 1994; Chen et al, 1996; Schlaepfer et al, 1998).

Activation of SIRPα and SHP-2 complex

The tyrosine phosphatase Src-homology domain 2 containing tyrosine phosphatase (SHP-2) can both positively and negatively regulate GH signalling. SHP-2 is recruited to the GH-induced complex of GHR, Jak2, Grb2 and SIRPα (signal-regulatory protein) (Kim et al, 1998). The SH2 domain of SHP-2 specifically associates with phosphorylated Y595 on GHR. Mutation of Y595 has been shown to prolong GH signalling (Stofega et al, 2000). On the contrary, expression of catalytically inactive SHP-2 reduces the transcriptional activity downstream of GHR (Kim et al, 1998).

Protein Kinase C Activation

An increase in intracellular Ca^{2+} concentration induced by GH is dependent on calcium channel activation by mechanism including protein kinase C (PKC) activation. The PKC pathway is induced by an increase in diacylglycerol (DAG) caused by phospholipase C (PLC) activation (Sjoholm et al, 2000). The activated PLC then hydrolyses inositol phospholipids to generate inositol phosphates and DAG, activator of PKC (Wakai et al, 1998). The PKC pathway is implicated in cellular growth and differentiation as well as lipogenesis and metabolism (Bergan et al, 2013). It has been

suggested that calcium transport pathway activation does not require Box1 or Jak2 activation but only the C-terminal part of the GHR (Billestrup et al, 1995) and therefore can be SFK-mediated.

Nuclear factor-κB Activation

A relatively recent report has shown that GH signalling pathway can mediate the activation of Nuclear Factor (NF)- κB via the PI3-K/Akt pathway (Jeay et al, 2001). NF- κB activation is responsible for cell survival by regulating anti-apoptotic proteins Bcl-2 and Bcl-X_L and induction of cyclins D1 and D3 (Jeay et al, 2002). It is unclear if the NF- κB induction by GH occurs only under stress conditions or during normal endocrine/autocrine GH signalling (Jeay et al, 2000).

Jak2-independent Signalling

Src Family Kinase Activation

Emerging evidence suggests that GHR can signal through additional pathways as has been reported in patients with GH resistance, that exhibit normal Jak2-mediated STAT5 activation but impaired ERK activation (Clayton et al, 1999). This has been supported by *in vitro* demonstration of Jak2-independent Src activation (Manabe et al, 2006; Zhu et al, 2002). Zhu *et al*. provide evidence using both pharmacological inhibitors and kinase inactive proteins in NIH-3T3 cells that tyrosine kinase Src is activated by GH-independent of Jak2 (Zhu et al, 2002). Further, constitutive binding of Lyn kinase (member of SFK) with GHR has been shown in FDCP-1 myeloid cell line (Rowlinson et al, 2008). Additionally, GH has been shown to activate Src and the ERK pathway in Jak2-deficient fibrosarcoma γ2A cells (Rowlinson et al, 2008). It was proposed by Rowlinson *et al*. that a movement in the F`G` loop of the lower cytokine module of GHR extracellular domain alters the signalling choice between Jak2 and Lyn kinase by regulating transmembrane domain realignment (Rowlinson et al, 2008). The existence of SFK-mediated signalling by GHR *in vivo* has been demonstrated in targeted Box-1 mutated mouse model (complete abrogation of GHR-mediated Jak2/STAT signalling) and transcripts resulting from Jak-independent Src activation were reported (Barclay et al, 2010).

Manabe *et al*. have shown that Src can bind and phosphorylate GHR in F-36P human leukemia cells (Manabe et al, 2006). They reported treatment of cells with Src inhibitors and anti-sense oligonucleotides decreased STAT5 activity, which was independent of Jak2. In contrast, Guren *et al*. reported no such STAT5 inhibition in primary rat hepatocytes after treatment with Src inhibitor (Guren et al, 2003). This discrepancy can be attributed to different cell types used in the two studies. Finally, GH-induced increase in the free cytosolic Ca^{2+} is not blocked by Jak2 inhibitor and therefore can be SFK-mediated, although it has been shown to be mediated by PRLR rather than

GHR (Zhang et al, 2006). Indeed, both PRLR and EPOR, close homologs of the GHR, have been shown to signal via SFK as well as Jak2 (Fresno Vara et al, 2000; Chin et al, 1998).

Transcription Factors regulated by GHR

GH regulated gene expression contributes to many of its action on cellular growth, differentiation and metabolism. GH first stimulates the expression of early response proto-oncogenes including *c-fos* (de Vos et al, 1992), *c-jun* (Foster et al, 1988), *c-myc* (Winston & Bertics, 1992), early growth response (*egr-1* and *2*) (Campbell et al, 1993; Clarkson et al, 1999).

MAPK pathway associated regulation

Transcriptional regulation of *c-fos* and *egr-1* through SRE in response to GH requires transcription factors *Elk-1* and serum response factor (SRF) (Clarkson et al, 1999; Davey et al, 2001). GH-induced serine phosphorylation of Elk1 and Elk1-dependent transcriptional activation is mediated by MAPK signalling components RAS, MEK, ERK1/2 (Sotiropoulos et al, 1995; Wen et al, 1995). GH also increases formation of complexes bound to *c-fos* at a consensus AP-1 site (Pircher et al, 1999; Teglund et al, 1998).

STAT association with SIE

Upon activation, the activated STAT molecules shuttle to nucleus and bind to specific DNA sequences referred to as interferon gamma activated sequences (GAS) or sis-inducible element (SIE) of the c-fos promoter to activate transcription (Rui & Carter-Su, 1999). STAT proteins also contain a conserved consensus sequence for phosphorylation by MAPKs (Bergad et al, 1995; Ram et al, 1996). Additionally, a serine kinase downstream of PI3-K and Akt, PKC-γ or methylation (Meton et al, 1999) can also modulate transcriptional activity of STAT1 and 3 indicative of supporting interactions between GH-regulated STATs, MAPK and PI3-K signalling members.

PI3-K and MAPK regulation of C/EBP

Another GH-responsive site in c-fos is a CCAAT/enhancer-binding protein (C/EBP) site that overlaps the SRE (Chen et al, 1997) as evident from the binding of *C/EBPβ* and *C/EBPδ* containing complexes (Piwien Pilipuk et al, 2003). GH has been shown to regulate the activity of C/EBPβ via two signalling cascades namely PI3-K, Akt/PKB and by phosphorylation of C/EBPβ at MAPK consensus sequence by activation of ERK1/2. This clearly indicates that numerous signalling pathways can be integrated via multiple phosphorylation sites, in order to regulate a single transcription factor.

Physiological role of GHR

In humans, the GHR is highly expressed in the liver, adipose tissue, heart, kidneys, intestine, lung, brain, pancreas, kidney, cartilage and skeletal muscle (Ballesteros et al, 2000; Castro et al, 2000; Chin et al, 1992). GHR protein has been demonstrated in all of these tissues by IHC together with many others (Waters, 1999). The signalling cascades downstream of GHR lead to a variety of cellular responses, including altered gene transcription, proliferation, differentiation, and motility. The resulting signalling pathways are cell-type specific and show differences with age, gender and signal dynamics (pulsatile *vs* continuous) (Pilecka et al, 2007).

Longitudinal Growth

The primary role of GH prior to adulthood has long been considered to be increased height through long bone growth. This is a complex process requiring the precise regulation of many endocrine and nutritional factors, including GH. This process involves the proliferation and mineralisation of the cartilaginous growth plate at the ends of long bones. Longitudinal bone growth is a limited process that in humans is completed by sexual maturity (van der Eerden et al, 2003). Long bone growth eventually ceases due to cessation of chondrocyte proliferation and epiphyseal fusion. The growth plate present at the ends of long bones is made up of resting zone chondrocytes (stem-like cells) which are acted on by GH to cause their rapid proliferation, resulting in columns of chondrocytes extending into the proliferative zone cartilage and elongation of the growth plate (Nilsson et al, 2005). Chondrocytes differentiate and cease dividing in the adjacent hypertrophic zone, then undergo cellular hypertrophy and become calcified. GH is responsible for "recruiting" resting chondrocytes, inducing proliferative zone chondrocytes to proliferate in an IGF-1-dependent process involving local generation of IGF-1 (Nilsson et al, 2005).

The "dual effector hypothesis" states that GH acts locally at the growth plate to recruit resting chondrocytes into a proliferative state (Ohlsson et al, 2009), and to stimulate local IGF-1 production, which then stimulates proliferation of proliferative zone chondrocytes (Nilsson et al, 2005). However, there are IGF-1-independent actions of GH in growth and these were elegantly demonstrated by Lupu *et al.* who reported that dual GHR and IGF-1 knockout mice showed a more dramatic loss in size than either mutation alone (Lupu et al, 2001).

Rowland *et al*. have used transgenic mouse models to determine the signalling pathways of GHR that are responsible for GH-induced growth. Knockin mouse models with truncations and mutations of the GHR intracellular domain (ICD) at residue 569 or a more severe 391 truncation were compared to GHR knockout mice. The gross phenotype and *in vivo* GH-induced signalling pathway

activation, demonstrated that STAT5 signalling below residue 391 was responsible for growth effects of GH (Rowland et al, 2005b). The GHR 391 truncation retained full Jak2 and MAPK pathway activity but had no ability for STAT5 activation. This transgenic GHR 391 mouse showed a dramatic decrease in postnatal growth of almost 50%, comparable to that of the GHR knockout (KO) mouse.

Metabolism

GH has an important role in carbohydrate, fat and protein metabolism by acting on liver, skeletal muscle, kidney, heart and adipose tissue in particular. These tissues maintain normal energy balance and homeostasis (Barclay et al, 2011) and when disturbed can result in metabolic disorders such as diabetes, obesity, muscle wasting and cancer. GH actions *in vivo* are complex.

The ability of GH to regulate glucose levels in plasma has been known for many years (McCann et al, 1987) and is the direct outcome both of increased gluconeogenesis in the liver and insulin antagonism in muscle. GH-mediated insulin-resistance is a consequence of downstream signalling mechanisms that inhibit the insulin pathway rather than the downregulation of insulin receptors (Davidson, 1987). The GH-mediated decrease in insulin sensitivity in mice (Dominici et al, 2005) is associated with decreased adiposity and hepatic lipid accumulation. Conversely, lack of GH signalling with its consequent obesity (and Non-Alcohol Fatty Liver Disease) is associated with insulin sensitivity (Dominici et al, 2002; Liu et al, 2004) as evident in GHR knockout and knockin mice models (Rowland et al, 2005b; Berryman et al, 2004). The state of GH excess results in insulin resistance as seen in bovine GH overexpressing mice and acromegalic patients (Coculescu et al, 2007; Olsson et al, 2005) with a correlation between increased severity of insulin resistance and higher circulating GH levels (Coculescu et al, 2007). These observations represent the anti-insulin actions of GH.

In addition, GH is also responsible for regulation of synthesis of enzymes involved in steroid and drug metabolism. These effects are mediated in part by cytochrome P450 (Legraverend et al, 1992) enzymes and sulfotransferases (Klaassen et al, 1998) induced as a result of the direct actions of GH on liver (Waxman & Holloway, 2009).

Proliferation and Differentiation

In the liver, IGF-1 production owing to GH action is well documented. However GH and not IGF-1 promotes hepatocyte proliferation since there are no IGF-1 receptors expressed in the liver (Caro et al, 1988). Therefore IGF-1 secretion is an endocrine function allowing it to act systemically on

other target tissues and for regulating GH secretion via a negative feedback loop at the hypothalamus and pituitary gland (Ceda et al, 1987). Liver has been shown to have a high proliferative index following chemical and physical injury and this regeneration rate can be enhanced by exogenous GH administration (Asakawa et al, 1989) and is absent or naturally low in GHR knockout or GH antagonist animal models, particularly in C57Bl/6 mice (Pennisi et al, 2004) (Zerrad-Saadi et al, 2011). GH results in increase of hepatocyte growth factor and EGFR in the liver, both of which are potent mitogens (Ekberg et al, 1992; Jansson et al, 1988), but the lethal aspect relates to the production of a powerful immunotolerance protein (H2-Bl) by GH (Barclay et al, 2010).

GH has been shown *in vitro* to directly stimulate proliferation of less differentiated cells in the osteoblast lineage derived from both trabecular and stromal sources (Kassem, 1997). This mechanism may in part mediate the *in vivo* effects of GH on bone formation. In the immune system, GH induces cell proliferation in the thymus (Savino et al, 2003) and spleen (Takada et al, 1991). *In vitro*, GH has been shown to stimulate cell numbers in lymphocytes particularly CD4 T-cells (Lempereur et al, 2003), plasma cells (Kimata & Yoshida, 1994), erythroid precursors (Claustres et al, 1987), myeloid precursors (Kotzmann et al, 1996), and adult neural stem cells (Blackmore et al, 2012). Likewise in β-cell of pancreas, besides proliferation GH has a well established ability to directly increase insulin synthesis and secretion (Billestrup & Nielsen, 1991; Cousin et al, 1999).

In response to GH stimulation, fibroblasts exhibit increased proliferation, collagen synthesis and angiogenesis and chemotaxis, which accelerates the wound healing process (Sobiczewska & Szmigielski, 1997). GHR expression is widespread in epidermis and dermal fibroblasts throughout the body (Lobie et al, 1990a) and GH is known to increase the thickness and strength of the skin, partly by inducing collagen synthesis (Wilson et al, 1995). This is supported by the observation that acromegalics have epidermal hyperplasia while GH deficient individuals have thin, elastic skin (Lange et al, 2001).

As mentioned above, besides proliferation GH can increase chondrocyte differentiation, resulting in extracellular mineralisation and proteoglycan synthesis (Olney, 2003). This differentiation process is marked by an increase in type II collagen, cathepsin D and acid phosphatase. GH also promotes upregulation of enzymes, matrix proteins, and differentiation markers involved in mineralisation of tooth and bone matrices directly and augments the role of IGF-1 in promoting bone and tooth formation (Li et al, 2001). Further, GH is proposed to have necessary role in differentiation of pre-adipocytes to functional mature adipocytes (Shang & Waters, 2003). More recently, Lu *et al*. have

provided a novel mechanism by which GH can control adipogenesis. This involves GH-mediated decrease in secretion of interleukin-1β by the macrophage and increase adipocyte differentiation (Lu et al, 2010).

In light of its importance in neural development, GH can function as an autocrine mitogen, augmenting the proliferation of adult neurosphere cultures (McLenachan et al, 2009). Recently, a new population of neural stem cells has been reported which is activated by GH infusion, and can differentiate into neurons in mice (Blackmore et al, 2012). These stem cells are activated by voluntary exercise in a GH-dependent manner (Blackmore et al, 2009). GH has been shown to influence male sexual differentiation and alter the androgen-binding activity of the foetal reproductive tract (Nguyen et al, 1996).

Development

GH primarily regulates post-natal growth whereas embryonic and foetal growth is considered to be independent of GH. However, newborn Laron dwarf babies are 2 standard deviations shorter than normal (Laron, 1972) and congenitally GH deficient newborn babies are shorter as well (Waters & Kaye, 2002). In animal models, the growth of rat foetus transplanted under the renal capsule of hypophysectomised host was impaired as compared to normal foetus and this could be corrected with GH administration (Liu et al, 1987). In GHR KO mice GH was found to have an important role in early development evident from reduced litter size, smaller foetus and prolonged pregnancy (Danilovich et al, 1999).

A number of foetal tissues and embryonic stem cells have been shown to express GHR and to respond to GH *in vitro* (Ohlsson et al, 1993) with both GHR protein and mRNA detectable from two-cell embryo stage to blastocyst stage in both mouse and bovine (Pantaleon et al, 1997; Kolle et al, 2001). Locally produced GH also plays a role in the development of the central and peripheral nervous system pre-natally, prior to its expression by the pituitary gland (Harvey & Hull, 2003). Turnley *et al*. have reported that neural GH promotes glial cell formation in preference to neurons by downregulation of neurogenin-1 (Turnley et al, 2002). However, GH also promotes proliferation of neural precursors and neurogenesis during brain development (Ajo et al, 2003), and brain structure and cell population are altered in *ghr* null mice (Ransome et al, 2004).

Subcellular localisation of GHR

The general paradigm for cytokine signalling involves binding of the ligand to the cell surface localised GHR and control of receptor expression occurs at various points in the receptor life cycle (Strous & van Kerkhof, 2002) which determine its localisation in a spatial and temporal manner. The plasma membrane is made of numerous lipids and proteins forming different structural entities such as coated pits, glycolipid rafts and caveolae (Nabi & Le, 2003). In the plasma membrane of epithelial cells GHR has been found to reside within microdomains, specifically glycolipid rafts and caveolae (Lobie et al, 1999; Yang et al, 2004).

However, it was early established that the majority of binding sites for GH in hepatocytes are not on the cell surface (Bergeron et al, 1978). The GHR (or GH specific binding sites) was initially reported in rough endoplasmic reticulum (ER), cytoplasmic matrix, golgi appartus and microsomal fraction (Postel-Vinay et al, 1982; Gorin et al, 1984; Mertani et al, 1999). Since then it has been reported in mitochondria (Mertani et al, 1996) where it is transported via the caveolar pathway and hypothesised to be required for GH stimulation of cellular oxygen consumption, dependent on the receptor Box1 motif for trafficking (Perret-Vivancos et al, 2006).

Nuclear localisation

Although a large population of GHR resides in ER and at the cell surface, an unexpected location for GHR and GHBP is in the nucleus. There is clear evidence of pronounced nuclear localisation in various cell types including cells of the blastocyst, hepatocytes and cancer cells (Lincoln et al, 1998; Lobie et al, 1994b). The nuclear localised GHR/GHBP has been reported to have normal affinity for GH and a panel of anti-GHR antibodies, indicating it is antigenically identical to the surface GHR (Lobie et al, 1991). Inside the nucleus the GHR was localised in nuclear membrane, heterochromatin and nucleolus by immunogold electron microscopy (Lobie et al, 1992).

The exact functional role of nuclear GHR is yet unknown but it is a common feature of tissues demonstrating high proliferative status; placenta (Garcia-Aragon et al, 1992), gastrointestinal tract (Lobie et al, 1990b), pre-implantation embryo (Pantaleon et al, 1997), epithelia of prostate gland, and ovaries. Analysis of a number of clinical cancer samples has shown GHR localised to the nucleus, including B-cell lymphomas, mammary carcinoma, melanoma and prostate tumours (Lincoln et al, 1998; Mertani et al, 1996). The GHBP, and by implication the nuclear GHR, has been shown to act as a transcription factor capable of direct transactivation in a mammalian β-galactosidase reporter assay (Graichen et al, 2003; Conway-Campbell et al, 2008).

GHR translocates rapidly into the nucleus after GH stimulation of serum-starved cells and this receptor is full-length and glycosylated like the cell surface receptor. The kinetics of nuclear translocation is rapid and transient, occurring within 10 minutes of GH stimulation and ceasing within 60 minutes (Lobie et al, 1994a). *In vitro* and *in vivo* studies have also shown that exogenous GH is also translocated into the nucleus (Lobie et al, 1994a). This *in vitro* uptake of GH was not blocked by microtubule or microfilament blockers but could be increased by blocking lysosomal degradation (Lobie et al, 1994a) indicating that cells utilise a different nuclear localisation mechanism that is independent of cytoskeletal network. Importantly, the internalisation and nuclear uptake of GH was not observed in the absence of an intact GHR. Graichen *et al*. have reported that GH and GHR co-translocate to the nucleus and receptor phosphorylation may be the stimulus for nuclear translocation (Graichen et al, 2003).

The phenomenon of nuclear translocation is not unique to GHR and is an attribute of several growth factors, cytokines and their receptors (Jans & Hassan, 1998), including the homologous PRLR (Rycyzyn et al, 2000). It has been shown that tyrosine kinase receptors EGFR, FGFR1, IGF-1R and endothelial growth factor receptors as well some G-PCRs, translocate as full-length receptors to the nucleus (Lin et al, 2001; Stachowiak et al, 1997; Sarfstein et al, 2012; Gobeil et al, 2006). The members of the EGFR (Epidermal Growth Factor Receptor) family (ErbB-1, ErbB2) have been reported to translocate in the nucleus by binding of their nuclear localisation signal (NLS) to the importin α/β complex (Lo et al, 2006). FGFR1 (Fibroblast Growth Factor Receptor) lacks a NLS sequence and so cannot directly bind to importin α, and as a result is translocated into the nucleus by binding to its ligand that contains the NLS sequence, a phenomenon referred to as 'piggy-backing' (Reilly & Maher, 2001). This is thought to occur with the GHR which associates with importin β *in vitro* (Conway-Campbell et al, 2008). GHR has been reported to interact directly with CoAA by GST-pull down and co-immunoprecipitation assays. This association was shown to occur only in the presence of GH and overexpression of CoAA in GH responsive cells led to a specific increased proliferative response to GH (Conway-Campbell et al, 2008). CoAA is a known coactivator of a number of nuclear steroid receptors and has a role in mRNA splicing regulation (Auboeuf et al, 2004) and contains several nuclear localisation signals that could bind directly to importin β and be used to transport the full-length GHR protein in the nucleus (Conway-Campbell et al, 2007). Nuclear expression of GHR in cancer cells shows an association with the frequent overexpression of CoAA (Sui et al, 2007).

Although considerable evidence indicates the recruitment of importin α/β complex for nuclear translocation of cytokine receptor, the phenomenon of cytosol access by the receptor and its ligand

remained unclear until the recent study by Wang *et al*. (Wang et al, 2010b). They showed by co-IP studies that activated EGFR utilises the Sec61 translocon complex for its transport from the cell surface through endosomes via the Golgi/ER to the nuclear pore complex associated with importin β. This entire process of nuclear translocation takes 30-60 min and is referred to as the INTERNET (Integral trafficking from the ER to NE transport) pathway. The Sec61 translocon normally detects misfolded proteins in the ER and sends it back into the cytoplasm for degradation by 'retrograde transport' via the ERAD (ER-associated degradation) pathway.

Waters' lab have shown that nuclear localised GHR correlates with high proliferation status, and that constitutively targeting the GHR to the nucleus results in cell cycle progression, dysregulation of proliferative arrest, and oncogenesis (Conway-Campbell et al, 2007). This has prompted in-depth analysis of the effect of nuclear localisation in cellular transformation.

Autocrine mode of GH signalling

As mentioned earlier, several tissues express GH locally and it has been suggested that autocrine GH can serve as a cytokine, promoting cell cycle progression and preventing apoptosis (Chhabra et al, 2011). Autocrine GH has been implicated in oncogenic transformation and metastasis in several different types of malignancies (Perry et al, 2006; Waters & Barclay, 2007). Autocrine GH is thought to enhance the *in vitro* oncogenic potential of endometrial carcinoma and colorectal cells while its forced expression in immortalised endometrial carcinoma and breast cancer cell lines increased their cell number through enhanced cell cycle progression and decreased apoptotic cell death while promoting anchorage-independent growth and increased cell migration and invasion (Jenkins & Bustin, 2004; Pandey et al, 2008; Zhu et al, 2005). Both GH and GHR are expressed in immune cells and are implicated in the development of leukemia and lymphoma (Hooghe et al, 1998) along with IGF-1 and its receptor (Weigent & Arnold, 2005). The overexpression of GH and GHR in lymphoma cells have been shown to have anti-apoptotic effects (besides increasing IGF-1) by decreasing the production of superoxide and associated expression of *bax*, *Bad* and *caspases 3,8 and 9* (Arnold & Weigent, 2003).

Autocrine production of GH in immortalised human epithelial cells enhances proliferation and protects against apoptosis and promotes abnormal mammary morphogenesis with oncogenic transformation and tumour formation *in vivo* (Liu et al, 1997). Exogenous GH cannot, however, mimic these actions (Kaulsay et al, 2000). This is supported by microarray analysis of 19,000 human genes that identified a subset of 305 genes that were differentially responsive to exogenous

or endogenous GH, as well as 167 genes that were regulated in common in mammary carcinoma (Xu et al, 2005).

A more recent study by Nakonechnaya *et al*. in the LNCaP prostate cancer line revealed differential effects of exogenous and autocrine growth hormone cell proliferation and survival. In contrast to the proliferative effects observed in mammary and colorectal carcinoma lines, autocrine GH overexpression reduced LNCaP cell proliferation and increased apoptosis (Nakonechnaya et al, 2013). The differential actions of endogenous and exogenous GH could be attributable to differences in GH concentration and secretion, since endocrine GH is secreted episodically whereas endogenous GH is released continuously at low concentrations (Vouyovitch et al, 2008). Moreover, endogenous GH is released in closer proximity to GHR and potentially at higher microenvironment concentrations than exogenous GH, allowing it to bind with available intracellular receptors in compartments not readily accessible to exogenous GH e.g. following synthesis in the ER (van den Eijnden & Strous, 2007). Additionally, Nakonechnaya *et al*. have also shown that the distinct actions of exogenous and autocrine GH were accompanied by differences in the involvement of GHR signal transduction pathways, and were paralleled by an alteration in the subcellular localisation of GHR, in which autocrine GH appeared to sequester GHR in the Golgi and ER (Nakonechnaya et al, 2013). This GH-GHR complex is then transported to the plasma membrane where exogenous GH is unable to bind these receptors, but signal transduction by endogenous GH only occurs after exiting the endoplasmic reticulum (Perry et al, 2006). This mechanism explains why GHR antagonists have been reported as ineffective in blocking the actions of autocrine GH (Tallet et al, 2008). This alteration of GHR trafficking may underlie a distinct mode of GH-mediated signalling associated with the effect of autocrine GH. The autocrine GH can also act through nuclear localised GHR, which is upregulated in cancerous tissues. (Brooks et al, 2008; Conway-Campbell et al, 2007; Perry et al, 2008).

In addition to above findings, the study of Mol *et al.* (Mol et al, 1995a) reported the presence of GH transcripts in human mammary tissue but with no evident relation to presence of carcinogenesis, and apparently decreased transcript in most carcinomas. A search of the Oncomine database reveals underexpression of GH1 and no listing for GH2 transcripts in invasive ductal breast carcinoma against normal tissue, in contrast to the prolactin transcript, which is highly expressed. Many human prostate cancers overexpress GH1 or GH2 and GHR transcripts as evidenced in the Oncomine database (Chhabra et al, 2011). Furthermore, an immunohistochemical study of 20 prostate cancers and 17 controls reported a four-fold increase in human GH expression in prostatic carcinoma where it is believed to act locally as almost all of them express GHR (Chopin et al, 2002; van Garderen &

Schalken, 2002). More recently, expression of both hGH and hPRL has been reported in mammary and endometrial carcinoma which associated with poor survival outcome for patients with these tumours (Wu et al, 2011). A similar result was also evident in dogs with high intratumoural levels of GH and IGF-1 reported in dogs with malignant mammary cancer (Queiroga et al, 2010).

Mechanisms that control GHR signalling

Depending on the cell type, as well as the time and extent of exposure to GH, the intracellular response to GH will vary. The steady state receptor turnover of receptor is rapid (half-life ~ 30-60 minutes), and two mechanisms contribute to receptor clearance from the plasma membrane: proteolytic cleavage by metalloproteases, resulting in the release of soluble GH-binding protein, and continuous ubiquitin-dependent internalisation. The deactivation of GHR signalling occurs at various levels in the signalling cascade and is tightly controlled.

Termination of GHR Signalling

In vivo, GH signalling is tightly regulated by numerous mechanisms that attenuate or terminate GH-induced signalling and operate following a GH secretory pulse. One such mechanism is endocytosis but since GHR/Jak2 complex is active in the endosomes additional mechanisms are required that can terminate the signalling cascades (Flores-Morales et al, 2006). The most important mechanisms involve phosphatases, members of Suppressors of Cytokine Signalling (SOCS) family and PIAS.

Phosphatases

Phosphatase activity is an important terminator of GH signalling, both at the receptor level and its downstream cascade. GHR is dephosphorylated by several protein tyrosine phosphatase (PTP) family members (Pasquali et al, 2003). Among the 44 PTPs tested, TC-PTP, PTP1B, SAP-1, PTP-H1, PTP-β, Meg1/2 and SHP-1/2 showed binary interaction with phosphorylated GHR (Pasquali et al, 2003). However, further *in vivo* functional studies narrowed this list to PTP-H1 (Pilecka et al, 2007) and PTP1B (Klaman et al, 2000).

Earlier studies had focused on tyrosine phosphatases (SHP-1 and 2). The binding of these molecules is increased upon Jak2 activation by tyrosine phosphorylation, which recruits and phosphorylates SHP phosphatases. The enzymatic activity of SHP-1 limits the extent and duration of Jak2 activation upon GH stimulation in *in vitro* expression systems (Hackett et al, 1997). By contrast, SHP-2 has been shown to be a both positive and negative regulator of GH signalling, depending on its cellular concentration and cell context. SHP-2 is recruited to the GH-induced complex, which

includes GHR, Jak2 and a transmembrane glycoprotein signal-regulatory protein (SIRPα) that upon GH stimulation induces SHP-2 binding to Grb2 (Kim et al, 1998). The SH2 domain of SHP-2 specifically associates with phosphorylated tyr595 of human GHR and mutation of this tyrosine prolongs signalling *in vitro* (Stofega et al, 2000). The tyrosine phosphatases also bind and dephosphorylate other downstream signalling molecules, such as IRS-1 and FAK (Myers et al, 1998; Yu et al, 1998).

Phosphorylated Jak2 is also a physiological substrate of PTP1B, which in addition dephosphorylates STAT5B and B (Gu et al, 2003; Aoki & Matsuda, 2000). This has been supported by the studies showing that deletion of *ptp1b* gene results in GH-induced hyper-phosphorylation of Jak2 and therefore of STATs whereas its overexpression reduces GH-mediated gene expression (Gu et al, 2003). In addition to tyrosine phosphorylation, Jak2 can be serine phosphorylated at position 523, potentially by ERK1/2 and this has been shown to inhibit its kinase activity (Mazurkiewicz-Munoz et al, 2006). Eventually Pilecka *et al*. have tested all the potential GH-induced tyrosine phosphorylated players as substrates for a large panel of PTPs in biochemical and cellular studies and from this identified PTP-H1 and PTP1B as major players. In support of this they reported enhanced growth in mice (significant for males) lacking the PTP-H1 catalytic domain over their wild type littermates (Pilecka et al, 2007). These mice have increased body size with a high level of IGF-1 owing to enhanced GHR sensitivity. In contrast PTP1B deleted male mice were smaller than wild type littermates and possessed of lower fat content due to increased energy expenditure in those mice (Klaman et al, 2000), suggesting that PTP-H1, but not PTP1B opposes the actions of GH *in vivo*.

Suppressors of Cytokine Signalling

SOCS proteins are negative regulators of Jak/STAT signalling (Wormald & Hilton, 2004) that have been shown to modify cytokine action through a classic negative feedback loop. Normally, SOCS protein levels are constitutively low, but their expression increases rapidly following cytokine stimulation (Aoki & Matsuda, 2000). There are 8 members of the SOCS family, of which SOCS1, 2, 3 and CIS (Cytokine Inducible SH2 protein) are the key SOCSs involved with GH action (Flores-Morales et al, 2006). GH has been reported to induce the expression of these SOCS proteins to varying degrees and with different kinetics *in vitro* (Gu et al, 2003; Hackett et al, 1997) and *in vivo* (Pasquali et al, 2003). Generally, SOCS1, SOCS3 and CIS expression is rapidly induced following GH stimulation but is transient, whereas SOCS2 expression increases steadily with time (Flores-Morales et al, 2006). Each SOCS member has a different mechanism of action on GH signalling (Flores-Morales et al, 2006; Ram & Waxman, 1999). Structurally, all SOCS family members

comprise of a variable N-terminus, a central SH2 domain and a conserved C-terminal motif called the SOCS box (Flores-Morales et al, 2006). In addition SOCS1 and 3 contain at their N-terminus a kinase inhibitory region (KIR) for terminating the Jak kinase activity (Ungureanu et al, 2002). The common and key function of SOCS proteins is their ability to form an E3 ligase complex with their SOCS box and Elongin BC, cullin 2 or 5 and ring finger proteins Rbx1 or 2 (Kamura et al, 2004) leading to proteasome degradation of the GHR.

SOCS1 and 3 can directly bind within the Jak2 activation loop on Tyr1007, blocking its kinase activity through their KIR (kinase inhibitory region) motif and promoting its proteasomal degradation (Stofega et al, 2000; Kershaw et al, 2013; Kim et al, 1998; Ungureanu et al, 2002). SOCS2, SOCS3 and CIS have been shown to interact with tyrosine phosphorylated GHR. Good evidence indicates that binding to Y487 and Y595 is required for SOCS2 and Y333 (Ram & Waxman, 1999) and Y338 for SOCS3-mediated inhibitory actions (Udy et al, 1997). Since Y487 and Y595 are known STAT5 binding sites (Fuh et al, 1992), SOCS2 can competitively inhibit STAT5 binding to the receptor. Vesterlund *et al*. have recently reported the mechanistic importance of phosphorylated Y487 rather than Y595 on GHR for its regulation by SOCS2 (Vesterlund et al, 2011). Little is known about CIS interaction with the GHR but phosphorylated Y487 and Y595 have been predicted as binding sites using the mammalian two-hybrid method (Uyttendaele et al, 2007). The effects of SOCS proteins are also reflected in knockout mouse models. SOCS1 knockout mice are contradictorily growth retarded and die before weaning due to fatty degeneration of the liver and infiltration by monocytes (Starr et al, 1998) in contrast with the inhibitory effects due to overexpression *in vitro*. The thymus size is also markedly reduced in these animals and is associated with progressive loss of maturing B-cells in the bone marrow, spleen, and peripheral blood reported as well. These defects have been traced to increased interferon sensitivity since SOCS1 is a critical inhibitor of IFN-gamma signalling and prevents the potentially fatal neonatal actions of this cytokine (Alexander et al, 1999).

SOCS3 knockout mice do not exhibit any growth phenotype (Croker et al, 2003) raising the issue of functional redundancy across the family. Functionally only SOCS2 knockout mice are 40% larger compared to wild type mice (Metcalf et al, 2000). This SOCS2 deficiency mediated gigantism is STAT5-dependent and can be reversed by GH deficiency indicating a direct relationship of GH and SOCS2 (Greenhalgh et al, 2002; Greenhalgh et al, 2005). In addition, SOCS2 knockout mice only partially mimic state of GH excess, but also result in changes that cannot be related to known GH effects (Rico-Bautista et al, 2005). SOCS2 has also been shown to interact with IGF-1R and therefore may have the major role in growth regulation (Dey et al, 1998b).

The importance of tyrosine residues in GHR is evident from studies carried out on the receptor mutant with all intracellular tyrosine residues changed to phenylalanine, which allowed acute GH-induced Jak2 activation but, this tyrosine phosphorylation-defective receptor underwent markedly reduced GH-induced ubiquitination and was only modestly downregulated (Deng et al, 2012).

PIAS-mediated signalling termination

Protein inhibitors of activated STATs (PIAS) share a common structure; the N-terminal nuclear receptor interaction motif and central RING-like zinc-binding domain (Schmidt & Muller, 2003). All members of PIAS family display E3 small ubiquitin-related modifier (SUMO) ligase activity (Pilecka et al, 2007). The mechanism by sumolyation leads to STAT inactivation is not clear. PIAS1 and 3 bind STAT1 and 3 respectively following cytokine stimulation and thus inhibit the association of STAT with DNA. By contrast, PIASx and PIASy inhibit their respective targets STAT4 and STAT1 through other mechanisms, without interfering with DNA binding of these STATs (Pilecka et al, 2007). Studies on PIAS1 deficient mice show a selective effect of PIAS1 on blocking the transcriptional activity of STAT1 (Liu et al, 2004). It should be noted that STAT5B can also be negatively regulated by phosphorylation on Tyr740 and Tyr743 (Kloth et al, 2002; Weaver & Silva, 2007).

GHR signalling crosstalk

Recent evidence highlights the significant crosstalk between GHR and other Class I cytokine receptors and receptor tyrosine kinase (RTK) members. GH-mediated phosphorylation of the ErbB receptor family such as EGFR has been reported to regulate EGF responsiveness (Frank, 2008). Indeed, GH action via Jak2 directly phosphorylates EGFR *in vivo* and *in vitro* resulting in enhanced binding and activation of Grb2-mediated ERK1/2 pathway (Yamauchi et al, 1998b). In addition GH and EGF were shown to specifically synergise for activation of ERK in murine pre-adipocytes leading to serine-threonine phosphorylation of EGFR (Li et al, 2011). This crosstalk results in EGF-induced ERK1/2 activation and reduced EGF-mediated EGFR downregulation.

GH and Insulin are known mediators of growth and metabolic regulation, utilizing common signalling pathways and can directly interact and influence each other. Essentially insulin has been shown to regulate the GH signalling in a time-dependent manner; with short exposures leading to induction of MAPK pathway downstream of GHR and longer exposures (of insulin) having reverse effects due to negative-feedback regulation (Xu & Messina, 2009). In contrast long-term GH

administration has inhibitory effects on insulin signalling, producing the well-known insulin resistance (Dominici et al, 2005).

Both GH and IGF-1 are responsible for promotion of cellular proliferation and growth. Recently it has been shown that both mitogens have a much closer interaction than previously thought. Huang *et al*. have reported that GH can induce a functional complex between GHR, Jak2 and IGF-1R (Huang et al, 2004) which is at least partially independent of the kinase activity of IGF-1R (and therefore IGF-1) (Gan et al, 2010). In addition by using a Cre-loxP system these authors have shown that deletion of IGF-1R markedly inhibits acute GH-induced STAT5 activity, while sparing GH-induced ERK activity in primary osteoblasts (Gan et al, 2010). Similar results on functional collaboration of GHR and IGF-1R but not insulin receptors were obtained in another study on mouse calvarial cells (Gan et al, 2013). Ma *et al*. have reported that signalling crosstalk between GH and IGF-1 in pancreatic islet β-cells promotes synergistic activation of STAT5 and Akt pathways (Ma et al, 2011).

An important facet of human GH and human PRL biology is that although hPRL interacts only with hPRLR, hGH binds and activates both hGHR and hPRLR (Goffin et al, 1996). Although homo- or heterodimerisation are common mechanisms for activation of cytokine receptors, crosstalk between two distinct receptors in this superfamily has not been shown until recently. A heterodimerisation interaction between PRLR and GHR has been postulated to be a novel mechanism contributing to the diversity of cytokine signalling (Herman et al, 2000; Xu et al, 2011). This GHR and PRLR interaction as well as GHR binding preferences have been shown to depend on the relative amounts of GHR and PRLR (Xu et al, 2011). Using both surface plasmon resonance and gel filtration techniques it was established early that ovine placental lactogen hetero-dimerises the extracellular domains of both the receptors (Herman et al, 2000) but no such effect was observed with ovine GH or ovine PRL (Biener et al, 2003). Functionally, homodimerisation or heterodimerisation of PRLR and GHR had no differential effect on activation of STAT5 and MAPK. On the contrary their heterodimerisation resulted in a prolonged phosphorylation of STAT1 and STAT3, suggesting that the heterodimerisation of α-oGHR and β-oPRLR is able to transduce a signal, which is distinct from that occurring on homodimeric associations (Biener et al, 2003). Furthermore, Xu *et al*. have shown by immunoprecipitation that GHR and PRLR associate in a fashion augmented acutely by GH, even though GH primarily activates PRLR, rather than GHR, in T47D breast cancer cells (Xu et al, 2013). It is likely that transmembrane helix interactions are responsible for full-length GHR/PRLR association (Pelekanos RA PhD thesis, 2006).

Pathophysiological role of GH/GHR

Clinical manifestations of GH secretory disorders

GH/GHR-mediated signalling is involved in numerous basic physiological processes, therefore incorrect GH function results in several pathologies.

GH deficiency

When GH levels are low, or the GHR is rendered non-functional, post-natal growth retardation occurs. Hence defects in GHR signalling or in GH/IGF-1 axis account for a proportion of human short stature (Okada & Kopchick, 2001; Pilecka et al, 2007). Adults with congenital GH deficiency (GHD) or following surgical hypophysectomy (treatment for pituitary tumour) show decreased muscle strength and bone density, increased body fat and cardiovascular dysfunction (Rosen et al, 1995). All these complications can be reversed by exogenous GH administration. Other evidence implicates GH in reproduction, regulation of immune function, mental health and aging (Savine & Sonksen, 2000; Brooks & Waters, 2010). The anabolic actions of GH can be beneficial in patients with chronic illness such as those suffering from post-surgical stress, AIDS and Prader-Willi syndrome (Napolitano et al, 2008; Stafler & Wallis, 2008). GH has been reported to accelerate wound healing in surgical and burn patients (Saito, 1998) and also prevent autoimmune diabetes in non-obese diabetic mice models (Villares et al, 2013). However, in adults GH treatment has resulted in significant side effects such as peripheral edema, carpal tunnel syndrome and insulin resistance (Cummings & Merriam, 1999). The use of GH agonists in GHD in regards to cancer is considered safe (Pekic & Popovic, 2013). However, in children with thyroid neoplasia, the risk of second neoplasms were increased, suggesting that GH could aggravate neoplastic tendencies resulting from underlying genetic abnormalities or radiotherapy (Bell et al, 2010). More recently, sustained-release recombinant human GH formulation (LB03002) has been shown to be effective and well tolerated in individuals with GH deficiency (Biller et al, 2011).

GH excess

Gigantism and acromegaly are clinical conditions that result from chronic secretion at supraphysiological levels of GH in childhood and adults respectively. These are primarily a result of pituitary adenomas and activating mutations in the subunit of Gsα protein, which activates Growth Hormone Releasing Hormone (GHRH) receptor (Faglia et al, 1996). GH excess is associated with increased morbidity and mortality; around 2-3 fold higher than age and sex matched normal population (Wass et al, 1999) resulting in death before the age of 50. Since GH signalling antagonises the insulin pathway, acromegalics have been reported to be insulin resistant causing diabetes-associated pathologies (Andersen, 2014). GH transgenic mice develop progressive

glomerulosclerosis, not reported for IGF-1 transgenic mice (Doi et al, 1988). Patients with GH excess are predisposed to cardiovascular and respiratory diseases and cancers (Palmeiro et al, 2012; Hernandez-Gordillo et al, 2012).

Growth disorders owing to GHR

Mutations in GHR

In a small cohort of the human population, growth defects arise as a result of mutations of GHR resulting in partial or complete loss of its function (Brooks & Waters, 2010). These mutations have been reported to alter features of the GHR that are required for activation of the receptor or other components of its signalling cascades such as STAT5B. Laron syndrome or GH insensitivity is one such disorder that is an autosomal, fully penetrant recessive disease. It is characterised by severe growth retardation, small gonads and genitalia, truncal adiposity, thin skin and hair and high levels of GH with low levels of IGF-1, IGFBP3 (IGF-1 binding protein), and ALS (acid labile subunit) in circulation (Laron et al, 1966; Brooks & Waters, 2010). The molecular defects affecting *GHR*, include exon deletion or nonsense, missense and frameshift mutations (Laron, 2002). Most of the mutations affect the ECD and these are diagnosed by the absence of circulating GHBP. In contrast, normal or high GHBP indicates that the mutation resides in the ICD of the GHR or in downstream components (Feigerlova et al, 2013). No mutations have been reported in the 24 amino acid residue TMD, although 4 splicing mutations that have resulted in excision of exon 8 and subsequent supraphysiological concentrations of GHBP (Aalbers et al, 2009). More recently, a second intronic GHR mutation has ben identified that activates a cryptic 5' donor splice site resulting in an abnormal splicing event leading to early protein termination and undetectable serum GHBP (Feigerlova et al, 2013).

Expression and Activation failure

A novel type of mutation leading to GH insensitivity has been described which results from a point mutation that activates an intronic pseudoexon leading to insertion of 36 residues in the extracellular dimerisation domain (after residue 207) (Maamra et al, 2006). This elongated receptor (~ 656 residues) retains the ability to bind to GH but is poorly expressed on the cell surface (trapped in the ER) and as a result has reduced downstream signalling, highlighting a trafficking defect.

GHR mutations leading to a decrease in surface-localised GHR can manifest as a clinical phenotype as reported in patients expressing GHR with I153T, Q154P or V155G. These mutations result in a decreased level of GHR at the surface due to impaired cellular trafficking from ER as shown by co-

localisation studies (Wojcik et al, 1998). Additionally, the substitution of aspartate at histidine152 (D152H mutation) has been described in detail in the context of familial GH resistance (Esposito et al, 1998). The histidine residue is part of the dimerisation domain and was initially believed to be important for receptor homodimerisation (Bernat et al, 2003). This is necessarily not the case since the GHR was reported to be a constitutive dimer (Gent et al, 2003; Brown et al, 2005). It has now been proposed that D152H allows GH binding but allow locking of the dimerisation domains, hence abrogates signalling (Brooks et al, 2014).

Signalling failure

GH insensitivity arising from the failure to signal is largely attributed to GHR truncated mutants arising from mutation of splice acceptor site of exon 9. This truncated receptor lacks the entire cytosolic domain and besides being signalling-incompetent, exhibits impaired degradation (lack of UbE-motif) and therefore acts as dominant-negative towards the full-length GHR in heterozygotes (Ross et al, 1997). In addition, truncations have been reported in individuals arising due to frameshift mutations and as a result of a premature stop codon. These include mutants truncated after residues 449 and 581 respectively (Milward et al, 2004; Tiulpakov et al, 2005). In these truncations, the receptor expression, cellular distribution, GH binding and Jak2, STAT3, MAPK activation ability was similar to full-length receptor. In contrast, the ability to phosphorylate STAT5 and STAT5-mediated gene transactivation was impaired, in agreement with observations reported in analogous mouse models (Rowland et al, 2005a; Rowland et al, 2005b).

'Downstream to GHR' defects

Realisation of the key role of STAT5 in GHR signalling has led to the discovery of STAT5B mutations linked to GH insensitivity (Kofoed et al, 2003). The first mutation involved substitution of proline at alanine 630 leading to incorrectly folded protein and formation of proteasome-stable aggregates in the cells (Chia et al, 2006b). Since this mutation lies in the SH2 domain it prevented interaction with cytokine receptor interaction (including GHR) and also was unable to bind to DNA, hence initiate transcription (Fang et al, 2006). This mutation manifested not only as severe growth retardation but also immunodeficiency indicative of genetic defects shared with cytokines. Additional mutations in STAT5B resulting in an inactive truncated protein or others with total absence of mature protein have also been reported (Vidarsdottir et al, 2006; Rosenfeld et al, 2005; Hwa et al, 2005).

Modulation of GHR Activity

GHR agonists

GH deficiency (GHD) in paediatric and adult patients currently necessitates many years or lifelong treatment and persistence with a daily injection regimen. This regimen of GH replacement with daily injections of the hormone is inconvenient and can be distressing in young patients (de Schepper et al, 2011). Consequently, several approaches have been developed to produce long-acting GH. Covalent attachment of polyethylene glycol to GH molecules has been shown to increase its half-life by reducing the rate of GH clearance in the kidney, and also imparts less susceptibility to intravascular proteolysis (Clark et al, 1996). Pegylated GH is well tolerated within the body and is now used as a weekly therapy in GHD patients (Sondergaard et al, 2011).

As an alternative strategy sustained release of GH formulation in form of encapsulated recombinant GH in biodegradable polymers or microspheres are being increasingly employed (Nutropin Depot® and Biosphere®) (Silverman et al, 2002; Kemp et al, 2004; Jostel et al, 2005) in GHD patients. Another approach for long-acting GHR agonists has been developed by Wilkinson *et al*. based on ligand-receptor fusion proteins. This approach requires linking the recombinant GH C-terminus to a GHBP molecule via a flexible linker allowing reduced clearance rate due to size constraints. *In vivo* studies have shown that this fusion molecule has a half-life 100-fold longer than GH and clearance rate 300-fold slower than GH (Wilkinson et al, 2007).

GHR antagonists

Increased understanding of GH-GHR interactions and downstream GH signalling pathways have fostered the development of analogs. The rationale of design to generate the most potent antagonist was based on ability of molecules to bind preformed GHR dimers but prevent subsequent conformational changes within the receptor-GH complex necessary for intracellular signalling to occur (Zhang et al, 1999). These are all based on introduction of mutations into native GH polypeptide that increases its binding affinity to receptor 1 but simultaneously reduces the receptor 2 binding, resulting in a molecule that can bind to GHR but cannot elicit the conformational change for activity. Such an approach was used by Chen *et al*. who discovered that substitution of residues E117 to L, G119 to R and A122 to D, in site 2 of bovine GH resulted in dwarfism in transgenic mice (Chen et al, 1991). This was followed by other studies highlighting the importance of glycine at position 120 in helix 3 of the GH site 2 for its biological activity. As shown by Fuh *et al.* Gly120Arg resulted in a GH analogue that was unable to bind the second receptor and therefore block signalling (Fuh et al, 1992). Incorporation of 8 site 1 amino acid residues determined from phage display to increase GHR affinity and decrease PRLR affinity, making it GHR-specific

(Goffin et al, 1999) has led to the development of a potent antagonist, known as B2036-PEG. This is commercially known as Pegvisomant (brand names Somavert® or Trovert®) and pegylation increased its half-life from 30 minutes to 70 hours (Ross et al, 2001; van Neck et al, 2000), reduced its immunogenicity. Pegvisomant is used as an effective alternative to somatostatin analogues to treat acromegaly (Feelders et al, 2009; Neggers & van der Lely, 2011).

Considerable success in reducing hepatic GHR expression and body weight gain has been shown in normal mice by sub-cutaneous injection of GHR antisense oligonucleotide (ATL227446). This was shown to be effective in reducing normal postnatal growth and plasma IGF-1 in mice (Tachas et al, 2006). More recently, a second-generation antisense DNA drug (ATL1103, Antisense Therapeutics, Victoria, Australia) is currently in Phase II clinical trails for acromegaly and diabetic retinopathy. In recent Phase I studies, ATL1103 was shown to reduce IGF-1 levels and was well tolerated. This molecule has also demonstrated efficacy in an animal model of retinopathy, significantly reducing retinal neovascularisation (Wilkinson-Berka et al, 2007). Guesdon *et al*. have reported development of a glycophosphatidylinositol (GPI)-anchored (membrane tethered) GH or GHR ECD molecules that has antagonist properties (Guesdon et al, 2012). Surprisingly GH-GPI when expressed on the cell surface formed inactive receptor complexes that failed to internalise and blocked receptor activation. In addition, inhibitory mAbs that target the GHR at the dimerisation interface have also been reported to inhibit GH action (Jiang et al, 2011). Other strategies that reduce circulating GH levels include somatostatin analogues that inhibit GH release from the anterior pituitary gland, used widely for treatment of acromegaly (Hasskarl et al, 2011). Further benefit may be obtained in combination with pegvisomant. However, whether somatostatin analogues can inhibit extrapituitary GH action to inhibit autocrine/local GH production has not been tested.

Sexual dimorphism

The Jak2-STAT5 pathway has been shown to be central to GH-induced metabolic function, body growth and IGF-1 transcription (Waxman & O'Connor, 2006; Chia et al, 2006a). As reviewed earlier, GH acts to regulate a diverse set of target genes in hepatic tissue, including genes coding for receptors, secretory products, enzymes and transcription factors. Many of these genes respond to GH in a sex-dependent manner, giving rise to a sexually dimorphic pattern of liver metabolic function that is most dramatic in rodents but significant male-female differences in GH secretory pattern also occur in humans (Veldhuis et al, 2001).

GH production in the somatotrophs of anterior pituitary is tightly controlled by the hypothalamus, which releases factors that stimulate (GHRH) or inhibit pituitary GH secretion (somatostatin). The GH is released in to the circulation in an intermittent or pulsatile manner which is ultimately regulated by the action of gonadal hormones on the hypothalamus giving rise to sex differences in the temporal pattern of GH secretion (Jansson et al, 1985). Sex-dependent differential plasma GH profile emerges at puberty and is regulated not only by the post-pubertal sex steroids but also by gonadal steroid imprinting during the neonatal period (Jansson & Frohman, 1987; Fernandez-Perez et al, 2013). Gender-specific GH secretion is an important determinant of the metabolic and somatic actions of GH in rodents. In the plasma of adult male rats, GH is secreted in a highly regular, pulsatile manner with hormone peaking (200-300ng/ml) every ~3.5hrs, separated by periods during which GH is virtually undetectable in circulation. In contrast, adult female rat have continuous presence of GH in plasma concentrations typically ranging from 15-40ng/ml (Jansson et al, 1985). Interestingly, depletion of liver-derived IGF-1 in male mice (LID mice) causes a feminisation of some of the GH-regulated sexually dimorphic markers of liver functions (Ohlsson et al, 2009). This is a consequence of losing the feedback effect exerted by IGF-1 on the hypothalamic-pituitary system, which results in increased GH secretion, including elevated baseline GH levels between pulses, resembling a female pattern of pituitary GH release.

In humans, the metabolic effects of pulsatile versus continuous exposure to GH are different, as exemplified by sex-dependent effects in body growth and metabolism, differences in IGF-1 production, transcriptional regulation of sex-dependent *CYP* genes and other hepatic phase I and II genes relating to drug metabolism (Shapiro et al, 1995; Jaffe et al, 2002). This suggests that GH pulse pattern is an independent parameter of GH action in humans.

Knockout of STAT5B (Udy et al, 1997) and of STAT5A and B (Teglund et al, 1998) but not STAT5A alone abrogated sexual dimorphism in mice because body size and IGF-1 levels of STAT5B knockout males were equivalent to female mice in which these parameters were not affected. Male-characteristic body growth rates and male-specific liver gene expression were decreased to wild-type female levels in STAT5B knockout males, while female-predominant liver gene products were increased to a level intermediate between wildtype male and female levels. Although these responses are similar to those observed in GH-deficient Little mice (non-functional GHRH receptor), STAT5B knockout mice are not GH-deficient, suggesting that they may be GH pulse-resistant (Udy et al, 1997).

GHR and Cancer

Traditionally, GHR is expressed on cell surface (and ER) while GH is secreted by the pituitary gland (Okada & Kopchick, 2001). Evidence from Waters' Group has shown that GHR (and GHBP) is expressed in the nucleus (Lincoln et al, 1998; Lobie et al, 1994b) and is antigenically identical to the surface GHR (Lobie et al, 1991). Additionally, the nuclear-localised GHR was associated with increased proliferation and shown to act as a transcriptional activator (Conway-Campbell et al, 2007; Zatelli et al, 2009). Similarly, the concept that GH-N synthesis occurs only in the pituitary gland has been changing since the last quarter century as evident from the presence of *GH* gene in numerous extra-pituitary tissues (Perez-Ibave et al, 2014). These discoveries clearly indicate towards a more complex role of somatotropic axis than previously thought (Waters & Barclay, 2007).

One of the main regulators of height is the GH/IGF-1 axis and a positive correlation exists between height and risk of various cancers (Gunnell et al, 2003; Tripaldi et al, 2013). Acromegaly, a condition attributable to GH excess is associated with considerable morbidity and reduced life expectancy mostly due to cardiovascular diseases and can be reduced when serum GH and IGF-1 are effectively lowered by treatment (Andersen, 2014). In addition to numerous animal studies (reviewed in (Chhabra et al, 2011), human studies have associated the GH/IGF-1 axis with the development of some of the most common cancers in the western world (Khandwala et al, 2000). Several population studies indicate that individuals with higher GH/IGF-1 levels have an increased risk for colorectal cancer, breast cancer, thyroid cancer (Wolinski et al, 2014) and prostate cancer even though causality has not yet been established. Conversely, studies evaluating cancer incidence in patients with GH/IGF-1 deficiency and GH-resistance or Laron syndrome showed no reports of any malignancy whereas first- and second-degree relatives had normal cancer incidence rate (Shevah & Laron, 2007; Guevara-Aguirre et al, 2011).

GHR-mediated signalling and mammary neoplasia

There is increasing evidence that the GH/IGF-1 axis might provide a major link between genetic and environmental factors and development of cancer through its influence on the regulation of normal breast cell proliferation, differentiation, and apoptosis (Kleinberg et al, 2009). Pathological conditions that affect GH signalling in humans, both defective and excessive, may influence breast cancer risk (Perry et al, 2008). Epidemiological studies showed that breast cancer patients have significantly higher serum GH levels compared with healthy individuals (Emerman et al, 1985) and high IGF-1 predicts a higher breast cancer risk in premenopausal women (Renehan et al, 2004).

Moreover, an earlier study reported a four fold higher risk for breast cancer in female patients with acromegaly (Nabarro, 1987), but this finding has not been confirmed by subsequent study (Orme et al, 1998) or indicates only a marginal correlation that requires more number of patients (Jenkins, 2004). The increased mortality in acromegalic patients may be attributed to GH-induced radioresistance (Bougen et al, 2011) and chemoresistance as reported in MCF-7 cell line with the latter shown to be independent of autocrine GH (Zatelli et al, 2009). Felice *et al*. have reported that GH promotes β-estradiol-dependent proliferation of T47D breast cancer cells independent of IGF-1 and the combination of GH and β-estradiol could overcome IGF-1R activity inhibition (Felice et al, 2013). A more recent study has shown that GHR blockade *in vitro* can inhibit GH-induced chemoresistance by restoring doxorubicin-induced apoptosis in breast cancer cells (independently of estrogen receptor expression) by increasing JNK phosphorylation (Minoia et al, 2012). More importantly, it has been reported that after exposure to cytotoxic drugs in mammary neoplasia there is a progression from a hormone-dependent, non-metastatic, anti-estrogen-sensitive phenotype to a hormone-independent, invasive, metastatic, anti-estrogen-resistant phenotype (Campbell et al, 2001). Animal studies have demonstrated that deregulation of somatotropic axis has resulted in reduced tumour severity. A high frequency of mammary adenocarcinoma was reported in metallothionein promoter-driven hGH female mice (Tornell et al, 1992). The Lit/Lit mice due to inactive GHRH receptor resulting in secondary suppression of GH and IGF-1 secretion has been shown to significantly reduce tumour growth of mammary xenografts as compared to control mice (Yang et al, 1996). Moreover, five different human sarcoma cell lines have demonstrated similar reduced effects in xenograft assays in Lit/Lit mice (Deitel et al, 2002). Another animal model, liver IGF-1 delete (LID) mice with low IGF-1 levels (25% of controls) were reported to have reduced growth of colon cancer (Wu et al, 2002) and chemically-induced mammary cancer (Wu et al, 2003). In the same study, LID mice crossed with C3(1)/SV40 large T-antigen transgenic mice, the mean age of onset of mammary tumours was delayed as compared with controls (Wu et al, 2003).

In addition to GHR, PRLR expression is present in ~70% of breast biopsies and is reportedly increased in breast cancer (Mertani et al, 1998; Touraine et al, 1998), whereas expression of the shorter, dominant-negative, form of this receptor is decreased (Meng et al, 2004). Other studies have shown increased stability of PRLR in breast tumours (Li et al, 2006). PRL in humans was shown to be produced by 70% of breast cancer lines (Clevenger et al, 1995) and by a similar proportion of biopsies, and antibody neutralisation of secreted autocrine PRL decreased the proliferation of breast cancer lines (Vonderhaar, 1998). However, a more recent study has reported low or undetectable PRL mRNA expression in 144 breast cancer patients and in 13 of 14 breast cancer cell lines when analysed by qPCR (Nitze et al, 2013). In animal model of local PRL

overexpression in differentiating mouse mammary gland functional defects and benign lesions were evident, but no carcinoma was reported (Manhes et al, 2006) while autocrine PRL (under the control hormonally nonresponsive promoter) overexpressing mice develop mammary adenocarcinoma at 15months of age (Rose-Hellekant et al, 2003). These data were strongly indicative that PRL signalling in the context of local *vs* systemic levels might be involved in promoting tumour growth in breast cancer patients. These two paralogous cytokine hormones seem to have parallel and interconnected roles in breast cancer as they do in breast development.

GHR-mediated signalling and prostate cancer

Several lines of evidence suggest the potential for endocrine GH to affect prostate tumourigenesis in addition to normal prostate development and function. GH has a growth stimulatory role in the prostate, and plasma GH-mediated IGF-1 levels may be an indicator of prostate cancer risk (Ozkan, 2011). The first evidence came from increased expression of GHR protein in the epithelial cells of the tumour acini while no GHR was detectable in normal prostatic epithelium (Kolle et al, 1999). An increase in the incidence of benign prostate hyperplasia (BPH) is associated with increased GH concentrations in individuals with acromegaly (Jenkins & Besser, 2001; Clemmons, 2002), and increased endogenous GH expression was observed in prostate tissue biopsies taken from individuals with BPH that ultimately progressed to prostate cancer (Slater & Murphy, 2006). An inverse correlation between serum GH concentration and prostate cancer incidence has also been reported (Fuhrman et al, 2005). *GHR* transcripts have been reported in benign prostate hyperplasia (BPH) and prostate adenocarcinoma patient tissues, as well as in LNCaP, PC3 and DU145 human prostate cancer cell lines (Weiss-Messer et al, 2004). In addition, GHR mRNA levels were reported to be 80% higher in the carcinoma tissues than in BPH in the same study.

In direct tests of the role of GH in prostate cancer, the absence of GH signalling due to GHR deficiency abrogated prostate tumourigenesis in rat and mouse models of prostate cancer susceptibility, consistent with a contribution of the GH/IGF-1 axis to prostate tumourigenesis (Kurmasheva & Houghton, 2006; Guan et al, 2002). Takahara *et al*. have shown that circulating GH and IGF-1 can promote androgen-responsive growth, castration-resistant progression, and androgen-independent expansion of PTEN-deficient human prostate cancer (PCa) cell xenografts in SCID Lit/Lit mice and that IGF-1 can promote cancer growth even in a suppressed GH environment (Takahara et al, 2011). IGF-1 has been shown to induce clusterin, a cytoprotective molecular chaperone through STAT3-Twist1 pathway, that can promote PCa growth (Takeuchi et al, 2014). In addition, GH levels have been shown to increase in prostate cancer patients undergoing androgen-deprivation (Galvao et al, 2008). Taken together, these findings indicate that endocrine GH may

have the potential to influence prostate cancer, but the direct effects of GH on prostate cancer cell function are not well understood.

GHR-mediated signalling and colon and endometrial cancer

GH was reported to be produced by the glandular cells of the human endometrium during mid to late luteal phase of the female menstrual cycle (Sbracia et al, 2004). A Polish study has reported higher incidences of endometrium and colon cancers (Baldys-Waligorska et al, 2010). The levels of hGH were significantly increased in both endometriosis and endometrial adenocarcinoma (Slater et al, 2006) and both PRL and GH serum levels are part of five-biomarker panel that allows accurate discrimination between cancer and control groups and early detection of endometrial cancer in high-risk populations (Yurkovetsky et al, 2007). An epidemiological study in Italian population has reported increased colon cancer incidences in acromegalic patients (Terzolo et al, 2005). While colonoscopy-based studies of adenoma prevalence rates in acromegalic patients are misleading, the population-based studies on colorectal cancer risk are more consistent as estimated by meta-analysis study indicating a pooled risk ratio of 2.04 (95 % CI: 1.32, 3.14) (Renehan et al, 2003). At the functional level the increased colonic neoplasia in acromegalics has been attributed due to increased proliferation rather than reduced apoptosis (Ishizaka-Ikeda et al, 1993). This has been confirmed at cellular level where siRNA-mediated knockdown of GHR in SW480 colon cancer cell line was reported to be anti-tumourigenic (Zhou et al, 2013).

GHR-mediated signalling in other cancers

The role of the GH/IGF-1 axis has been studied on glioma cell lines. In one study both the GHR and IGF-1R were found to be expressed in few immortalised glioma cell lines. Treatment of two of these lines (U251 and U373) with IGF-1 resulted in increased mitogenesis as assessed by thymidine uptake (Friend et al, 2001). However these results could not be shown in xenograft models in SCID mice. GHR has been identified as one of the marker genes for lung adenocarcinoma (Wu et al, 2012) with the first reported variant P495TGHR associated with increased lung cancer susceptibility in two separate GWAS studies (Cao et al, 2008; Rudd et al, 2006). Additionally, elevated levels of GHR have been reported in NCI60 panel of non-small cell lung carcinoma, CNS cancer and melanoma cell lines (Sustarsic et al, 2013).

Aims and objectives of the thesis

GH acting through its receptor is a direct regulator of many physiological and pathological processes, and it is therefore important to understand the mechanism by which the GHR is activated following GH binding. Recent emerging findings on GHR polymorphism in relation to GH responsiveness and disease susceptibilities have given significant attention to the receptor signalling outcomes. Although over 60 loss of function mutations in GHR have been associated with deficient post-natal growth, to date no constitutively active GHR mutations has been reported. This study is aimed at identifying gain of function mutations in the receptor and analysing their consequence *in vivo* using the RCAS/TVA system. This study will focus on oncogenesis, since GHR loss of function results in abrogation of cancer susceptibility in men and autocrine expression of GH correlates with stage of cancer progression. I will also examine forced nuclear localisation of GHR since this has been shown to promote proliferation *in vivo*. This thesis will undertake a multi-faceted approach to determine the role of GHR in mediating oncogenesis.

1. **Determine the structure-function basis of GHR-mediated oncogenesis**

Using cysteine scanning mutagenesis, the transmembrane domain helix interface of GHR will be revealed to determine the mechanism of Jak2 activation upon ligand binding. This will form the basis of creating mutants with constitutive Jak2/STAT5 activity. Because our group has shown that Src Family Kinases (SFKs) are activated by GHR independent of Jak2, mapping studies of the SFK binding to GHR will be undertaken to determine the basis of Jak2-independent mechanism of SFK activation because this may be important for oncogenesis. Finally, we intend to determine the molecular basis for the first cancer-associated variant of GHR identified from GWAS studies. This will be supported by genomic DNA analysis of polymorphisms associated with GHR and other signalling molecules in clinical prostate cancer at different Gleason stages.

2. ***In vitro* role of GHR-mediated oncogenesis**

Based on Waters' Group earlier result that constitutive nuclear localised GHR is oncogenic we intend to determine its role in cancer cell lines *in vitro*. This will be carried out simultaneously with other constitutively active GHR constructs or those arising from the cysteine mutagenesis studies in Aim 1. Finally, we seek to evaluate the role of GH/GHR signalling in the autocrine MCF-7 model amidst reports citing contradictory effects of autocrine GH on cell transformation and proliferation.

3. ***In vivo* role of GHR-mediated oncogenesis**

Based on preliminary results from Aim 2, the potentially oncogenic GHR constructs will be tested for oncogenic effects *in vivo* to determine if GHR is a tumour initiator or a tumour promoter. The *in*

vivo delivery will be carried out using the RCAS/TVA delivery system to achieve tissue-specific expression. These studies will be complemented with naturally occurring end of life tumour incidences in GHR knockin and knockout models available in our group and their potential effect on longevity. These mice models will be used to analyse the potential cancer resistance pathways based on earlier report of reduced cancer incidences in long lived *ghr* null mice and lack of cancer-related deaths in Laron dwarves.

Chapter 2
Materials and General Methods

Chemicals

Analytical grade chemicals were purchased from Sigma-Aldrich (MO, USA), Ajax Finechem (Australia). Other reagents were purchased from Invitrogen Australia Pty Ltd (Mt Waverly, VIC, Australia), Amersham Pharmacia (Uppsala, Sweden), Roche Boehringer (Castle Hill, NSW, Australia) and BioRad laboratories (Hercules, CA, USA).

Tissue culture consumables

All plastic consumables were supplied by Nunc industries (Thermo Scientific, IL, USA). Growth media (DMEM, RPMI 1640, LHC-9) were supplied by Invitrogen™ Life Technologies (NY, USA). Foetal Bovine Serum (FBS) and Serum Supreme (SS, a foetal bovine serum substitute) were purchased from Lonza Group Ltd (Basel, Switzerland). Geneticin418 (G418) was supplied by Invitrogen™ Life Technologies (NY, USA). Puromycin and Hygromycin B were purchased from Sigma-Aldrich (MO, USA).

Antibodies and Enzymes

Primary antibodies were supplied by Cell Signaling Technology® (MA, USA), Santa Cruz Biotechnology® Inc (Santa Cruz CA, USA) and Abcam® Inc (MA, USA) and Covance (NJ, USA) (details are listed in the Appendix VI). Secondary antibodies HRP conjugated were purchased from Santa Cruz Biotechnology®, Inc (Santa Cruz, CA, USA) and GE Healthcare Life Sciences (Dusseldorf, Germany). Enzymes used for molecular cloning were supplied by New England Biolabs (Genesearch Ltd, Australia).

Hormones

Recombinant human GH was expressed and purified in the laboratory of Professor Mike Waters (Behncken et al, 1997; Rowlinson et al, 1994). Recombinant Interleukin-3 (IL-3) was expressed and purified using Baculovirus expression by SRC Protein Expression Facility of Institute for Molecular Bioscience at University of Queensland.

Buffers and Solutions

Luria Bertani (LB) medium and LB agar plates

Growth medium for bacteria containing 10g of tryptone, 5g of yeast extract and 5g of NaCl, was made up to 1L with water, the pH adjusted to 7.5 with NaOH, then autoclaved at 121°C and 20 PSI for 20min. For making LB agar plates, 15g of agar was dissolved in LB broth to a final volume of 1L, then autoclaved at 121°C and 20 PSI for 20min and cooled to 50°C before the addition of the appropriate antibiotics. 20ml of the liquid agar was poured into 100mm petri dishes and left at room

temperature to solidify and plates were stored in darkness at 4°C.

Phosphate Buffered Saline (PBS)

A 10x concentrated stock was made by mixing 438.5g of NaCl (1.5M), 61.66g of Na_2HPO_4 (87mM) and 11.5g of NaH_2PO_4 (15mM) in 5L of distilled water. After 10-fold dilution, the pH was adjusted to 7.4 prior to use.

20% Sodium Dodecyl Sulfate (SDS) solution

A 20% (w/v) SDS stock solution was prepared by dissolving 200g SDS in 1L of water.

Tris EDTA (TE) Buffer

TE buffer consisted of 10mM Tris base and 1mM EDTA (final concentration) in 1L of distilled water, adjusted to pH 8.0 with NaOH.

Tris-acetate EDTA (TAE) buffer

A 10x concentrated stock was made by mixing 48.4g Tris base (400mM), 3.72g EDTA (10mM) and 11.42ml of acetic acid in a final volume of 1L of water. The stock was adjusted to pH 8.3 with acetic acid after dilution. This was diluted to 1x TAE buffer with distilled water prior to use.

Laemmli resolving gel buffer

Resolving gel buffer consisted of 2.5ml 20% SDS, 22.7g Tris Base and 30ml 1M HCl made up to a final of 100ml with distilled water (final 0.5% SDS, 625mM Tris-HCl, pH 8.8).

Laemmli stacking gel buffer

Laemmli stacking gel buffer was made with 62.5ml 1M Tris-HCl, 2.5ml 20% SDS and distilled water added to 100ml (final 0.5% SDS, 625mM Tris HCl, pH 6.8).

Laemmli running buffer

A 10x Laemmli running buffer concentrate consisted of 30.25g Tris Base, and 144.2g Glycine added to 950mL distilled water. When these had dissolved, 50ml of 20% SDS solution was added, then the solution was diluted 10-fold with distilled water to make 1x Laemmli Running buffer prior to use.

6x DNA Loading Buffer

The DNA loading buffer consisted of 30ml glycerol (final 30%) and 500ml loading dye concentrate

(5% glycerol, 0.5% Bromophenol blue, 0.5% Xylene cyanol in distilled water), made up to 100ml with distilled water (stored at room temperature).

Tris Buffered Saline

A 10x Tris buffered saline (TBS) was made by combining 24.4g Tris base, 80g NaCl, and 38ml of 1M HCl, made up to 1L with distilled water, pH 8.6. This was diluted 10-fold prior to use as a washing or blocking buffer, to give a final concentration of 30mM Tris, 140mM NaCl.

Plasmid manipulation

Preparation of chemically competent E. coli cells

A starter culture of *E. coli* (DH5a or stbl3 or ccdB resistant) was prepared by inoculating 15ml LB broth without antibiotics with a scraping of glycerol stock and incubated for 16hrs at 37°C with continuous shaking. The starter culture was then diluted in 500ml of LB broth without antibiotics and grown to an OD_{540} of 0.4-0.6 over a period of 3-4hrs. The cells were transferred to centrifuge tubes and cooled on ice. Cells were centrifuged at 6000rpm for 5min at 4°C and the pellet was resuspended in 250ml of ice cold 50mM $CaCl_2$, then incubated for 60min on ice. The cells were centrifuged again as before and resuspended in 50ml of a solution containing 50mM $CaCl_2$ and 15% (v/v) sterile glycerol. 0.5ml of the cell suspension was dispensed into microfuge tubes, rapidly frozen on dry ice and stored at -80°C. These cells were verified for competence with low concentrations of DNA.

Plasmid or ligation mixture transformation

Calcium chloride competent *E.coli* cells (200µl) were added to an ice-cold microfuge tube containing 10µl of the transforming plasmid DNA at an approximate concentration of 10µg/ml. The mixture was incubated on ice for 30min after which it was subjected to heat-shock at 42°C for 1min. 1ml of LB broth was added and the tube was incubated for 1hr at 37°C with shaking. Subsequently the bacterial cells were centrifuged for 1min at 8000rpm at room temperature and 900µl of the supernatant was removed. The pellet was resuspended with the remaining supernatant and spread over an agar plate containing the specific antibiotic. The plates were inverted and placed in a 37°C incubator overnight.

Plasmid DNA Isolation

For routine screening of bacterial colonies, individual colonies were picked with a 200µl tip and cultured in 2-3ml of LB broth with antibiotics overnight in a shaking incubator at 37°C. The bacterial cell suspension was used for plasmid DNA extraction using Invitrogen™ Mini-Prep kit (CA, USA). For larger DNA preparations, Nucleobond™ Midi Plasmid Extraction kit (Macherey-

Nagel GmbH & Co. Duren, Germany) was used as per manufacturer's guidelines. Plasmid concentration was determined on NanoDrop™ spectrometer (Thermo Scientific). Integrity of the plasmid was determined by agarose gel electrophoresis.

DNA Sequencing

The DNA to be sequenced (800-1000ng) and each primer (0.64µM) in a total volume of 12µl were sent to Australian Genome Research Facility (AGRF, University of Queensland, QLD, Australia) for the 'purified DNA' sequencing service. The primer sequences used for sequencing analysis are listed in Appendix II.

Animals

Animals were housed in the Institute for Molecular Biosciences animal facility under a 12hr light/dark cycle at 20±2°C. Water and food (Meat-free rat and mouse diet, Specialty Feeds, Australia) was available *ad libitum*. All experiments were approved by and performed in accordance with the guidelines set by the University of Queensland Animal Ethics Committee.

GHR Mutant Mice

GHR knockin mutant mice (GHR K1 (ghr 569tr), GHR K2 (ghr 391tr) and GHR K4 (Box1 prolines mutated to alanines) were generated previously (Barclay et al, 2010; Rowland et al, 2005b). GHR knockout mice (GHR KO or ghr null) were generated previously (Zhou et al, 1997a) and kindly provided by Prof. John Kopchick (Department of Biomedical Sciences, Ohio University, Athens, OH, USA).

Genotyping

Genotyping was performed by PCR on mouse genomic DNA extracted from 8 –12 day old mouse toe tissue (toe selection was also used as a means of identification). DNA was extracted using hot NaOH as described earlier (Truett et al, 2000). PCR reactions for genotyping were carried out in 20µL reactions consisting of: 10-200ng genomic DNA, 1x Phire® Reaction Buffer (Thermo Scientific, Finland), 200µM dNTPs, 0.5µM primers (Table 2.1), 0.4µL Phire® Hot Start DNA Polymerase (Thermo Scientific, Finland). PCR reactions were performed in a Biorad i-Cycler® or my-Cycler® thermal cycler (BioRad) with the reaction conditions specified below.

Table 2.1: List of pimers and their sequences used for genotyping

Primer	Sequence
9F	5'CCTACTTCCTGCTTAGAACTCTC
10R	5' GCTCAATGAACTCGACCCAGG
In3+1	5' CCTCCCAGAGAGACTGGCTT
In4-1	5' CCCTGAGACCTCCTCAGTTC
Neo3	5' GCTCGACATTGGGTGGAAACAT
Cre Fwd	5' CGAGTGATGAGGTTCGCAAG
Cre Rev2	5' CACCAGCTTGCATGATCTCC
Cre Ctrl Fwd	5' CTAGGCCACAGAATTGAAAGATCT
Cre Ctrl Rev	5' GTAGGTGGAAATTCTAGCATCATCC

GHR Knockin genotyping

In order to genotype the GHR knockin mutants, the 9F and 10R primers (Table 2.1) were used to amplify the intronic region between *ghr* exon 9 and 10. This produced a 593bp product in the WT allelles and a 746bp product in mutant alleles that included the remaining loxP site from the Cre deletion of the neomycin-resistant (neo) selection cassette used in the original transgene construct to generate the mice (Barclay et al, 2010; Rowland et al, 2005b) (fig.2.1). The PCR cycle conditions used were:

Initial denaturation: 98°C for 2 min

35 cycles of:

Denaturation: 98°C for 5 sec

Annealing: 58°C for 5 sec

Extension: 72°C for 20 sec

Final extension: 72°C for 1 min

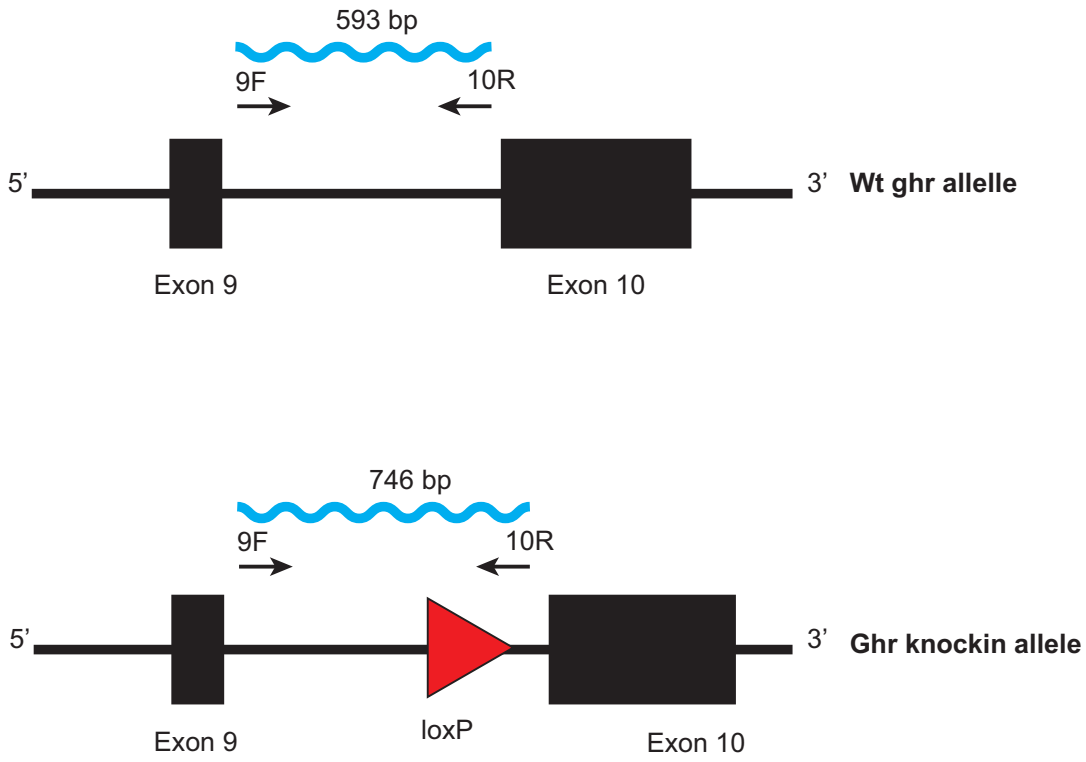

Figure 2.1: Schematic Diagram of Genotyping PCR for GHR knockin mutants.

Primers 9F and 10R amplify a 593 bp product within *ghr* intron 9/10 in the WT allele. Ghr mutants (GHR K1, GHR K2 and GHR k4) were created as described (Rowland et al, 2005b; Barclay et al, 2010). The original construct used to create the mice contained a loxP neomycin resistance selection cassette within ghr intron 9/10 which was excised by Cre recombinase. The remaining loxP site results in a 746bp product amplified by the genotyping PCR from the *ghr* mutant allele.

GHR KO Genotyping

The In3+1, In4-1 and Neo3 primers (Table 2.1) were used to genotype the GHR KO mutants. Primers In3+1 and In4-1 amplify the region containing exon 4 (plus some flanking intronic regions) in the WT allele, yielding a 390bp product. The GHR KO mutant allele contains the neo-selection cassette that has replaced the majority of exon 4 and ~500bp of the intron 4/5 (Zhou et al, 1997a). Neo3 primer binds to a repeat sequences in the neo cassette. The primers In3+1 and Neo3 amplify 290bp and 220bp products in the GHR KO allele (fig.2.2).

The PCR cycling conditions used were:

Initial denaturation: 98°C for 2 min

35 cycles of:

Denaturation: 98°C for 5 sec

Annealing: 62°C for 5 sec

Extension: 72°C for 10 sec

Final extension: 72°C for 1 min

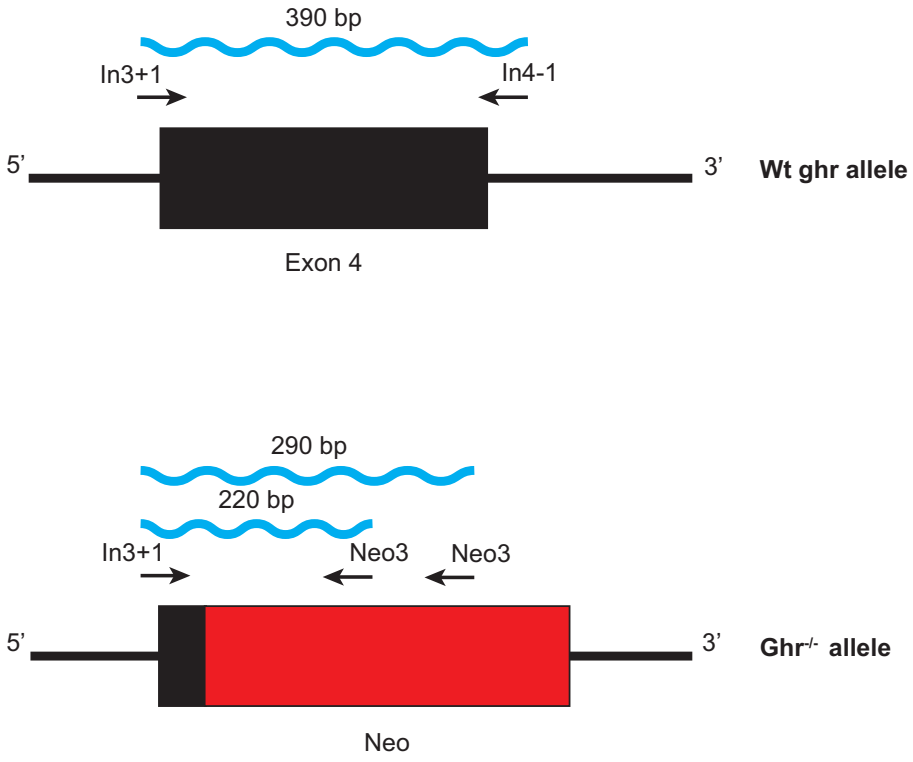

Figure 2.2: Schematic Diagram of Genotyping PCR for GHR KO Mutants.

Primers In3+1 and In4-1 amplify a 390bp product spanning *ghr* exon 4 in the WT allele. GHR KO mutants were created as described (Zhou et al, 1997a). A neomycin resistance gene replaces most of ghr exon 4 and ~500 bp of intron 4/5. The Neo3 primer binds to a repeat sequence in the neomycin resistance gene. The In3+1 and Neo3 primers amplify 2 products (220bp and 290bp).

DNA Agarose Gel Electrophoresis

PCR products were identified by size by electrophoresis on agarose gels. Agarose gels were made at 2% (w/v) with analytical grade agarose (Amresco, Ohio, USA) in Trisacetate-ethylenediaminetetraacetate (TAE) buffer (40mM Tris, 20mM acetic acid, 1mM EDTA). Gels were pre-stained with Sybr Safe (Invitrogen, Australia). PCR reactions were mixed with 10x loading buffer (50% red food colouring, 50% glycerol) and electrophoresed at 80–100V in TAE buffer. A 100bp DNA ladder (New England Biolabs, MA, USA) was used as a size reference. Gels were visualized using the Universal Hood UV Transilluminator (BioRad, Sydney, Australia) and Quantity One (v 4.4.0) software.

Tissue Collection

Unless, specified, all mice were 12–14 weeks (young) and 78-80 weeks (old) of age at collection. Mice used in this thesis were in the fed state prior to tissue collection. Mice were anaesthetised by placing them into a chamber flushed with CO_2 until unconscious.

Serum samples were obtained by blood collection via cardiac puncture using 27 gauge needles.

Blood was kept at room temperature for 1hr until centrifugation at 3000rpm, at 4°C for 20min for serum separation. After cardiac puncture, mice were euthanized by cervical dislocation. Tissue samples were dissected and snap frozen in liquid-nitrogen or fixed for histology. Snap frozen tissue and serum (aliquoted into tubes) was stored at -80°C until used for analysis.

Tissue Processing for Histology

Small pieces of liver or muscle were fixed in 4% paraformaldehyde (PFA) in phosphate buffered saline (PBS) at 4°C with gentle rocking overnight. Fixed tissue was then washed in PBS and either stored in 70% ethanol at 4°C for paraffin embedding or cryopreserved in Tissue-Tek®O.C.T™ compound (Sakura Fine technical, Tokyo, Japan). Tissue was paraffin embedded using a TP1020 Tissue Processor (Leicia Microsystems, Australia). Cryopreserved samples were incubated in 30% sucrose in PBS at 4°C overnight, followed by embedding in Tissue-Tek® O.C.T™ compound. The cryopreserved samples in O.C.T compound were stored in -80°C.

Quantitative Reverse Transcription Polymerase Chain Reaction (qPCR)

RNA extraction and reverse transcription

Cell pellets, mouse tissues and whole zebrafish were homogenised in Trizol Reagent (Invitrogen, USA) and RNA was extracted according to the manufacturer's instructions. RNA was then further purified and DNase treated using RNeasy® Mini Kit clean up protocol (Qiagen, Maryland, USA). RNA was reverse transcribed using Superscript III (Invitrogen, USA) using the random hexamers protocol and used for qPCR with Sybr® Green Technology (ABI, CA, USA) in the 7500HT Real Time Cycler (ABI, CA, USA), 7900 Real Time Cycler (ABI, CA, USA) or ViiA7 Real Time Cycler (ABI, CA, USA). For all qPCR experiments, triplicate reactions were performed for each gene including controls using a two-step amplification program (Initial denaturation at 95°C for 10 minutes, followed by 40cycles of 95°C for 20seconds and 60°C for 30seconds). A melting curve analysis step was added at the end of amplification, consisting of denaturation at 95°C and re-annealing at 55°C for 1minute each. A comparative Ct method was used to determine relative expression in samples.

Primer design for SYBR® Green Technology

Primers for qPCR were designed using Primer Express 2.0 software (ABI, CA, USA). Standard curves were generated from each experimental plate using 5-fold serial dilutions of cDNA. The geometric mean of Ct-value for each reaction was calculated along with amplication efficiency for each primer pair using the equation $E=10^{(-1/slope)}$. Primer pairs that showed efficiency between 90%-105% were chosen. No non-specific amplication or primer dimer was observed as confirmed by melting curve analysis. Final analysis was performed by calculating the change in Ct between the

gene of interest normalised against the housekeeping gene (such as glyceraldehyde-3-phosphate dehydrogenase (Gapdh) or glucoronidase beta (GusB) or beta-2 microglobulin (B2M) where specified) and expressed as a mRNA levels relative to control or fold change above control as indicated.

Western Blot Analysis

Protein Extraction

Pieces of liver, heart, skeletal muscle and kidney tissues were homogenised or cells were scraped in radioimmunoprecipitation (RIPA) buffer (150mM NaCl, 1% NP-40, 0.5% sodium deoxycholate, 0.1% SDS, 50mM Tris (pH8.0), 1mM Na_3VO_4, 30mM NaF, 10mM $Na_4P_2O_7$, 10mM EDTA plus Complete EDTA-free protease inhibitor cocktail (Roche, Mannhein, Germany). Tissue homogenates were cleared by centrifugation at full speed for 10min at 4°C. Protein concentration was determined by BCA assay (Pierce, IL, USA).

SDS Polyacrylamide Gel Electrophoresis (SDS-PAGE)

Equal amounts of protein were incubated at 100°C for 5min in sample buffer (15mM Tris-HCl (pH 6.8), 2% SDS, 10% glycerol, 10mM DTT), loaded into SDS-PAGE gels and separated by electrophoresis. Precision Plus Protein™ Dual Color Standards (BioRad, CA, USA) was used as a size reference. Gels were prepared according to the Laemmli system (Laemmli, 1970). Gradient gels (4–20%) were purchased from BioRad (CA, USA). For single percentage gels, the appropriate amount of 40% acrylamide/bis (29:1 acrylamide:bis) solution (BioRad), 1mL of resolving gel buffer (0.5% SDS, 62.5mM Tris-HCl, pH8.8), 5µL N,N,N'-tetra-methylethylenediamine (TEMED [ICN Biomedicals Inc, Costa Mesa, USA]) and 30µL 10% ammonium persulphate (APS) made up to 5mL with distilled water (dH_2O) was set in a Mini-PROTEAN® casting apparatus (BioRad). Water-saturated isobutanol was overlaid onto the gel to ensure a straight interface. After polymerisation, the isobutanol was removed and a stacking gel (250µL 40% acrylamide/bis solution, 500µL stacking gel buffer (62.5mM Tris-HCl, 0.5% SDS, pH 6.8), 5µL TEMED and 30µL 10% APS made up to 2 mL with dH_2O) was set on top of the resolving gel with a spacer comb inserted. Electrophoresis was performed in Mini-PROTEAN® Tetra cell tanks (BioRad) in Laemlli running buffer (0.1% SDS, 200 mM Tris-HCl, pH 8.0).

Electroblotting and Probing of Membranes

After electrophoresis, gels were transferred onto 0.2µm PVDF membranes either using the semi-dry Hoefer® TE-70 semi-dry electroblotter or the Trans-Blot® Turbo™ Transfer System (BioRad). Membranes were blocked with 5% Bovine Serum Albumin (BSA) or 5% skim milk in Tris-

Buffered Saline containing 0.1% Tween-20 (TBST) for 1hr at room temperature. Blots were probed by incubating with specific primary antibody (listed in Appendix VI) diluted in blocking buffer overnight at 4°C or 1hr at room temperature. Blots were washed and incubated with 1:10000 dilution of secondary anti-IgG conjugated to horseradish peroxidase (HRP) (GE Healthcare, Dusseldorf, Germany) in blocking buffer for 1hr at room temperature. Membranes were washed and proteins visualised with a chemi-luminescent reagent (GE Healthcare, Dusseldorf, Germany) via exposure to X-ray film (Fuji Film, Japan). The X-ray film was imaged using Epson Perfection™ scanner. All densitometry quantitation was performed on immunoblots using ImageJ® software. All test values were normalised to respective loading control and represented relative to experimental control and graphed with Prism 5.

Stripping of PVDF Membranes

PVDF blots were routinely stripped and re-probed for loading controls after detection of the protein of interest. Blots were stripped using Re-Blot Plus Mild Stripping Solution (Millipore, CA, USA) according to the manufacturer's instructions. Blots were washed with TBST for 10min before re-blocking and re-probing.

Immunohistochemical analysis

Formalin-fixed/paraffin-embedded sections were deparaffinised and rehydrated by passage through a graded xylene/ethanol series before antigen retrieval by boiling in 10mM Sodium Citrate Buffer for 5min. The sections were then washed and subjected to various blocking steps at room temperature with intermittent washes: (i) 3% H_2O_2/PBS for 30 min (blocking endogenous peroxidise activity), (ii) 10% animal serum in 2% BSA (IgG free Fraction V) in 0.025% Triton containing PBS for 1hr (blocking non-specific sites), (iii) Avidin and Biotin block for 15min each (blocking endogenous biotin). Rabbit anti-GFP polyclonal primary antibody (Invitrogen; 1:200 dilution in serum containing blocking buffer) incubation was carried out in a humidified chamber at 4°C overnight, slides were washed and subjected to goat anti-rabbit biotinylated secondary antibody (Sigma; 1:250 dilution in serum containing blocking buffer). The signal was amplified using VectaStain® ABC kit as per manufacturer's conditions (Vector labs) and subjected to diaminobenzidine (DAB) staining. The reaction was stopped by incubating the slides in tap water and counter stained with hematoxylin for nuclear staining. The slides were dehydrated by ethanol gradation series, xylene treated and mounted in Entellan (Merck). The slides were then analysed on an Olympus IX70 Microscope.

Immunofluorescence analysis

Frozen sections were allowed to equilibrate to room temperature and rehydrated in PBS. Antigen retrieval was performed by boiling the slides for 5min in 10mM Sodium Citrate buffer and the sections were blocked in 10% animal serum, 2% BSA in 0.025% triton containing PBS for 1hr at room temperature. Primary antibodies used were rabbit anti-GFP (Invitrogen; 1:5000) and incubated overnight at 4°C and mouse anti-HA (Covance; 1:200) incubated for 1h at room temperature in a humidified chamber. Following incubation, the slides were washed 5 times in 0.1% Tris Buffered Saline with Tween-20 (TBST) and incubated in the dark with goat anti-rabbit Alexa Fluor 488/594/647 conjugated secondary antibody (Invitrogen; 1:200) for visualising GFP and goat anti-mouse TritC conjugated secondary antibody (Sigma; 1:100) for HA tag, for 1h at room temperature. The slides were then washed five times in 0.1% TBST and mounted with VectaShield® containing DAPI, sealed and stored at 4°C for visualization.

For direct visualisation of cells and tissues expressing GFP, the cells and tissues slides fixed in 4% PFA were mounted with VectaShield® containing DAPI, sealed and stored at 4°C. The slides were then analysed under an Olympus IX70 Fluoro microscope and analysed by the Fluoroview v. 1.6A software.

Data analysis and statistics

Statistical analysis was performed in GraphPad Prism® version 5.0 with multiple comparisons by ANOVA, using Tukey's post hoc test. Comparisons of two groups utilized an unpaired student t-test.

Chapter 3
Structure-Function Aspects of Growth Hormone Receptor Transmembrane Domain

Introduction

Given that a conformational change in ECD induced by ligand binding activates Jak2 (Brown et al, 2005), these structural changes must be transmitted through the transmembrane domain and intervening sequences from the extracellular domain to the Box1 motif. The constitutive dimerisation of GHR (Brown et al, 2005) and EPOR (Constantinescu et al, 2001) is mediated predominantly through interactions in the TMD; however, other regions such as the ECD may also play a role in the dimerisation process or provide specificity to homodimer formation (Yang et al, 2007). Unlike the ECD (Clackson et al, 1998; de Vos et al, 1992), there has not been any direct structural data about the TMD or ICD of the GHR. Comparison of the unliganded and GH-bound GHR ECD structures revealed that the orientations of the main chain, including residues in the dimerisation interface, are almost identical in both (Brown et al, 2005). The lack of major difference between the structures of the unliganded and GH-bound ECDs led to the hypothesis that GH initiates signalling by inducing rotation within the inactive preformed dimer so as to change the relative orientations of the cytoplasmic domains and bring Jak2 molecules bound to each GHR dimer partner within proximity for activation. This model suggested that both the ECD and ICD juxtamembrane domains of the GHR adopted a rigid conformation to allow the transmission of the torque force resulting from the asymmetrical binding of GH to both receptors. Furthermore, Brown *et al.* have reported that GHR can be activated in the absence of ligand by inserting a defined number of alanine residues within the TMD, presumably by causing a specific rotation of the dimerised receptor monomers relative to each other (Brown et al, 2005).

Random mutagenesis experiments have revealed constitutively active mutations in the TMD of homologous EPOR (Lu et al, 2006) and TPOR (Onishi et al, 1996). Mutation Ser505Asn in the TMD of the related thrombopoietin receptor is linked to familial thrombocythemia, and this mutation (experimentally mutated to glutamic acid, aspartic acid or glutamine) results in constitutive activation of the receptor, which was proposed to be due to receptor dimerisation and alteration of the TMD conformation or rotation to an active form (Ding et al, 2009). Additionally, several non-peptide thrombopoietin mimetics interact only with residues within the transmembrane domain and extracellular juxtamembrane linker (Kuter, 2009), which underscores the role of the TMD as an important target for novel drug development to modulate cytokine receptor activation.

The human GHR TMD is composed of a single 24 amino acids from F265 to S288 in a mature receptor (Leung et al, 1987; Waters, 1999) and is encoded entirely by exon 8 of the *ghr*. Numerous mutations in human GHR leading to loss of function attributes such as in Laron dwarfism and GHIS (Bronson & Lipman, 1991; Waters, 1999) have been reported. Interestingly all these mutations lie

in the ECD and ICD regions of the GHR and so far only a single case report with a mutation in the splice donor site of exon 8 that disrupts normal splicing has been reported (Woods et al, 1996). This resulted in the complete skipping of exon 8, producing a mutant GHR protein lacking TMD and ICD domains. Thus, the precise role of TMD in the initiation of receptor signalling is currently unknown and will be evaluated in this chapter. This chapter will discuss in detail the structural information generated from cysteine scanning mutagenesis studies and correlate it with downstream signalling in order to determine the exact role of TMD in mediating a signalling response upon GH binding.

Materials and Methods

Construction of full-length human GHR cysteine mutant constructs

Truncated HA (haemagglutinin) tagged hGHR (human growth hormone receptor) with cysteine substitutions in pCDNA3.1 plasmid were created by site-directed mutagenesis (primers listed in Appendix I). Each GHR mutant created was truncated at C389 (stop codon inserted after C389) while cys259 was also converted to serine. Full-length HA-tagged Cys mutant hGHR constructs were created by carrying out *AvaI* partial digestion of wild-type full-length hGHR pCDNA3.1 vector and a 2002bp fragment was isolated, purified and ligated to the dephosphorylated 5669bp fragment produced by *AvaI* digestion of truncated Cys mutant hGHR constructs. The ligation reaction was carried out using T4 DNA ligase at 16°C overnight and subsequently used to transform competent *E. coli* DH5α. Ampicillin resistant colonies were screened, sequenced and a correct clone for each construct was used for large-scale DNA preparations. Double cysteine hGHR mutant constructs were made by three-fragment ligations in which the wild-type vector was digested with *Eco*RI and *Kpn*I and dephosphorylated. The vector carrying the first cysteine mutation was digested with *Eco*RI and *Nco*I and a 1075bp product was obtained. The vector carrying the second cysteine mutation was digested with *Nco*I and *Kpn*I digestion and a 427bp product was obtained. The two products were then ligated into the dephosphorylated vector backbone and transformed into DH5α strain.

The full-length cysteine hGHR constructs were cloned from pCDNA3.1 into viral expression vector pMX-IRES-GFP. This was carried out by PCR reaction along the entire length of the insert (HA-hGHR), digestion with *Nco*I and finally ligation into partially digested pMX-IRES-GFP vector (6595bp) which expresses GFP via an Internal Ribosomal Entry Site (IRES). The correct clones were selected following transformation into *E.coli* DH5α and confirmed by restriction digestion and

sequencing. The pCDNA3.1-STAT5B(WT) plasmid was a kind gift from Dr. J. Barclay (Waters' Group, IMB).

Cell lines

The African green monkey kidney cell line, COS-1 (purchased from ATCC) and human embryonic kidney cell line, HEK293 (a kind gift from Dr. F. Fontaine, Cooper Group, IMB) and retroviral packaging cell line, PLAT-E (Morita et al, 2000) a gift from Dr. T. Kitamura from University of Tokyo, Japan) were maintained in DMEM media supplemented with 10% FBS. The murine pro-B Ba/F3 cell line were chosen for the convenience of analysing GHR constructs (based on GH selection) as they are devoid of any endogenous GHR. Ba/F3 cells were maintained in RPMI 1640 media supplemented with 10% SS, 2mM L-glutamine and 100units/ml IL-3 or 100ng/ml hGH (where indicated). All cell lines were maintained at 37°C in a humidified incubator containing 5% CO_2.

Signalling analysis with hGH treatment

COS-1, HEK293 and Ba/F3 cell lines were starved overnight and then treated with hGH (expressed and purified by Waters' Group) at 50ng/ml in reduced-serum media. The starve media (or reduced-serum media) for COS-1 and HEK293 was DMEM supplemented with 0.5% FBS and for Ba/F3 cell lines was RPMI 1640 supplemented with 5% FBS without IL-3 or GH. All GH stimulations (where indicated) were carried out for 10 minutes at 25°C. Following stimulation of COS-1 and HEK293, the media was aspirated and the cells were washed twice with chilled PBS. Treated Ba/F3 cells were collected by centrifugation at 4°C and washed twice with ice-cold PBS before final pellet collection. The cells were then harvested in RIPA lysis buffer, the lysates quantified for total protein and these were subjected to reducing SDS-PAGE and immunoblotting.

Cysteine Crosslinking Studies

Crosslinking in membrane extracts

COS-1 cells were plated at a seeding density of $4x10^5$ cells per well (6 well plate format) and transfected with a series of N-terminal HA-tagged hGHR truncated cysteine mutants (L251C to S288C) in pcDNA3.1 backbone using lipofectamine 2000 as per manufacturer's guidelines. Cells expressing receptor constructs were homogenised and diluted to give a minimal level of expression for clear detection with 100ng/well hGHR cys construct transfected per well. Crosslinking was

performed 24hrs after transfection. Briefly, to obtain membrane extracts wells were washed with ice-cold phosphate-buffered saline (pH 7.4) and scraped in 1ml of cold Buffer A (25mM sodium phosphate, 5mM $MgCl_2$, 2mM Na_3VO_4, pH 7.4 with 1×Complete Protease Inhibitor Cocktail (Roche) and homogenised using handheld Kinematica Polytron homogenizer (Fisher Scientific) at full speed for 10sec. Membrane extracts were then centrifuged at 17000g for 20min, and resuspended in 100µl of buffer A. The extracts were subjected to crosslinking by disulfide bond formation by treatment with Cu-o-phenanthroline comprised of 0.40mM $CuSO_4$ and 1.60mM o-phenanthroline (Sigma Aldrich), for 10min at 37°C after addition of 500ng/ml hGH. The reaction was terminated with 10mM EDTA prior to SDS-PAGE on a non-reducing gel, blotted on PVDF membrane and probed with anti-HA antibody (Covance) to reveal monomers and dimers. Due to interference from crosslinking reagents protein quantification of membrane extracts by Bradford or BCA were not compatible and as a result equal volumes of lysates were loaded onto the gel.

Crosslinking in intact cells

For signalling analysis on intact cells, HEK293 cells were plated at seeding density of 2×10^5 cells per well and transfected next day with full-length hGHR expression constructs with cysteine mutations or WT GHR construct (C259). GH at 50ng/ml was then added for 10min at 37°C and Cu-o-phenanthroline where indicated (at the concentrations indicated above). Crosslinking was stopped with 2mM EDTA and GH treatment was stopped with two washes in cold PBS.

For signalling analysis of spontaneous cysteine dimers in the absence of hGH, 30ng of STAT5B pCDNA3.1 expression construct was also transfected along with 300ng of full-length hGHR constructs to increase sensitivity. The cells were incubated for 24-36hrs then starved overnight in reduced serum media (DMEM supplemented with 0.5% FBS) and harvested. STAT5 phosphorylation and GHR levels were analysed by resolving quantified protein lysates on a reducing SDS-PAGE. In addition, dimerisation of full-length GHR was analysed simultaneously on a non-reducing SDS-PAGE gel.

Production of replication defective ecotropic retrovirus

In order to generate retrovirus for stable transduction of Ba/F3 cell line, the potent retroviral packaging cell line, Plat-E was used. The cells were plated at a cell density of 8.5×10^4 cells per well in a 6-well format and transiently transfected with 4µg of pMX-HA-hGHR-IRES-GFP constructs for each of the full-length cys mutant constructs using lipofectamine 2000 as per manufacturer's guidelines. The media was replenished 24hrs post-transfection and the plates were further incubated

at 37°C for 24hrs. The plates were then incubated for 24hrs at 32°C and supernatant collected and filtered through 0.45µm (low protein binding) polyethersulfone membrane filter and used for transducing the Ba/F3 cell line.

Stable transduction of Ba/F3 cell line

A total of 2×10^5 starved Ba/F3 cells were harvested and seeded in each well of a 6-well cell culture plate for viral transduction with different cysteine hGHR mutants (full-length). The starved cells were resuspended in the harvested viral supernatant. Polybrene was added at a final concentration of 8µg/ml and the plates were incubated at 37°C for 1-2 hours. After incubation, an equal volume of RPMI growth media with twice the standard concentration of IL-3 was added and the plates were incubated at 37°C further for 48h. Ba/F3 cells were analysed for stable transduction by FACS sorted for GFP expression (via the IRES cassette) from untransduced cells (at FACS Facility, QIMR). These GFP expressing cells were then grown in IL-3 containing media and selected on GH.

Ba/F3 proliferation assay

For measuring proliferation of Ba/F3 cells transduced with full-length hGHR cys mutants, the cells were starved overnight and seeded at a cell density $2x10^4$ cells/ml in duplicate in growth media supplemented with 2mM glutamine and 10% charcoal-stripped serum (Hyclone) (Day 0) and cells were counted daily by trypan blue (Sigma Aldrich) exclusion using a hemocytometer.

Surface expression of GHR

For analysis of the surface expression of GHR in stably transduced Ba/F3 cell lines, 10^7 cells were starved overnight in medium devoid of IL-3/GH. The cells were washed in cold PBS and treated with mouse anti-HA antibody (1:200) for 2hrs on ice. Note that all reactions were carried on ice and without any permeabilisation agent to prevent receptor downregulation and antibody internalisation. Following subsequent washes, cells were incubated in dark and on ice with TritC conjugated goat anti-mouse secondary antibody (1:50, Sigma Aldrich MO, USA) for 40 min. The cells were washed in cold PBS, fixed in 2% PFA and analysed at QBI FACS Facility.

Results

Cysteine-scanning analysis is a valuable and established method for predicting the topology of membrane proteins, determining structural parameters such as distance, torsion angle and investigating different functional states of proteins (Friedbichler et al, 2011). This approach has been expanded into Substituted-Cysteine Accessibility Method (SCAM), in which cysteine residues are introduced sequentially along the TMD that allows characterisation of the interacting interfaces, either by detection of spontaneously formed disulphide bonds or by chemical crosslinking (Friedbichler et al, 2011; Kubatzky et al, 2001).

Construction of GHR cysteine mutants

Using the WT hGHR as template, C259S and C389stop truncation were introduced sequentially, illustrated in figure 3.1A. The resulting PCR product was used as template to sequentially introduce cysteine mutants from L251 to S288 in the C259S background, truncated at residue 389. Modification of cys to ser is important as it provides a thiol-free background for sulfydryl crosslinking solely between the introduced cysteine residues in the juxtamembrane linker (L251 to Y264C) and the TMD (F265 to S288). Each mutant was confirmed by sequencing and transient expression in COS-1 cells. Using HA tag antibody revealed that all GHR truncations were expressed at a similar level (fig.3.1B). The same truncated constructs were later made full-length to assess the effect of targeted cys crosslinking on Jak2/STAT5 signalling.

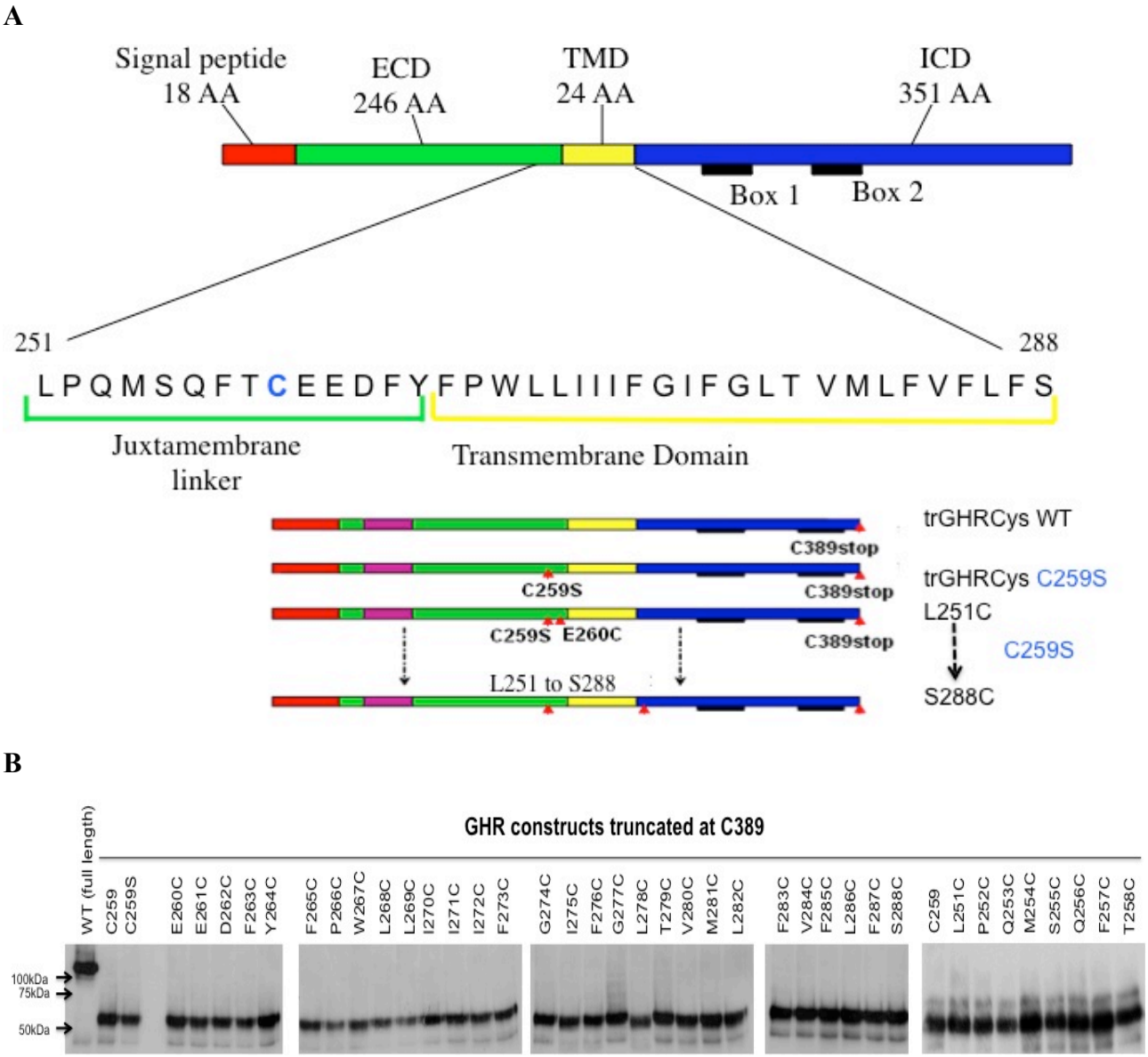

Figure 3.1: Schematic illustration of hGHR cysteine mutant constructs and their expression.

(A) Schematic illustration of the wildtype (WT) GHR construct and design of truncated and full-length versions of the hGHR Cys mutant constructs. Each juxtamembrane linker or TMD residue was sequentially mutated to cysteine in a C259S background, truncated at C389. (AA-amino acid; tr- truncated; ECD: extracellular domain, TMD: transmembrane domain, ICD: intracellular domain). (B) Similar expression levels of hGHR cys mutants by transient transfection in COS-1 cells with lysates resolved on an reducing gel before immunoblotting with an anti-HA antibody.

Spontaneous dimerisation pattern of GHR cysteine mutants

Disulfide bond formation is possible only under oxidising conditions. This means that spontaneous disulfide bond formation between two cysteine residues in close spatial proximity is possible in the ECD but not in the ICD due to the reducing environment in the cytosol. COS-1 cells transiently expressing the different GHR constructs were lysed and proteins resolved under non-reducing conditions as shown in figure 3.2. As is evident from the blot, 6 GHRcys mutants (E260C, E261C, D262C, F263C, Y264C and F265C) were strongly dimerised (based on dimer to monomer ratio)

while 4 mutants (P266C, W267C, L268C and L269C) were dimerised to a lesser extent. In addition, the upper linker region (L251C to T258C) above C259 did not form any detectable spontaneous dimers (not shown). Thus, every cysteine substitution located between E260C to L269C was able to form an intermolecular disulfide bond between the two GHR molecules.

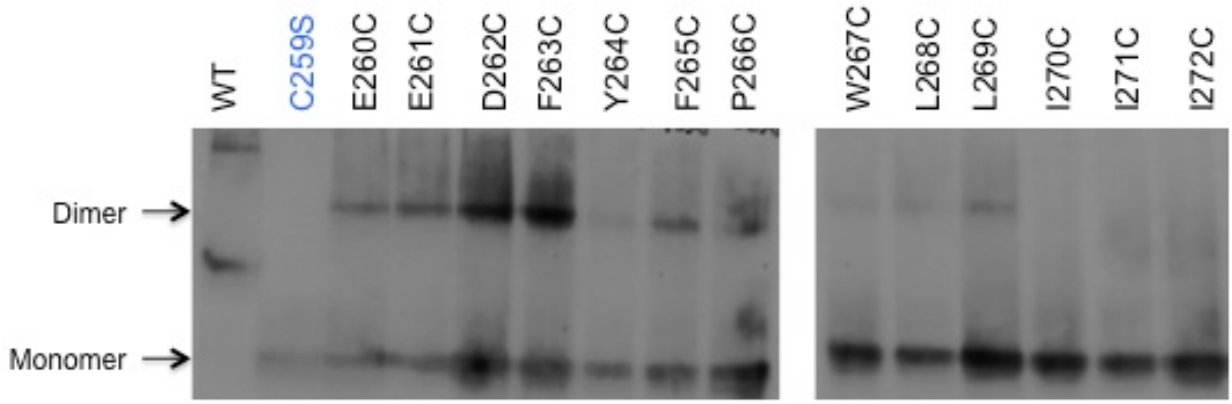

Figure 3.2: Spontaneous dimerisation pattern of the hGHR cysteine mutant.

Transiently expressing hGHR cys truncations in COS-1 cells were lysed and protein lysates resolved on a non-reducing SDS-PAGE gel before immunoblotting with an anti-HA antibody (for GHR). The GHR dimers and monomers are indicated in comparison to full-length WT and truncated C259S. Based on the dimer to monomer ratio few residues (E260C to F265C) dimerised strongly in comparison to those modestly dimerised (P266C-L269C) for equal amount of lysate loaded, while no dimerisation was evident from I270C residue onwards. Blots representative of n=3 independent experiments.

Cysteine crosslinking analysis of membrane extracts

In order to overcome the limitations of crosslinker penetration into the membrane observed previously with MTS-2-MTS (Gardon O Masters Thesis, 2006), Cu-o-phenanthroline [Cu(II)-(1,10-*phenanthroline*)$_3$] was used. It is a zero-length crosslinker as it does not introduce any linker to bridge the targeted cysteines, instead copper withdraws electrons from the sulfhydryl on cysteine side chains creating an oxidising environment that favours disulfide bond formation between the sulfhydryl groups in immediate proximity. The use of Cu-o-phenanthroline (CuP) to form disulfide bonds is more likely to reveal minor structural changes compared to other crosslinkers such as MTS-2-MTS owing to the short distance of crosslink.

The use of CuP on membrane extracts provided deeper access into the membrane as compared to the previously used crosslinkers and intact cell treatment. It was consistently observed that CuP was unable to crosslink the residues in the middle of the TMD (G274C-T279C) but could crosslink those positioned at its ends. Such an effect could be due to inability of CuP to provide an oxidising environment for disulfide bond formation in the middle of the TMD but since these studies were conducted on crude membrane extracts, the crosslinks could be formed at the ends of the TMD with

two-way accessibility for CuP (fig.3.3A). However, the upper linker region E260C to L269C was strongly crosslinked, similar to spontaneous dimerisation (fig.3.2). In addition, there was CuP facilitated crosslinks evident for other TMD residues (I270C to F273C) before disappearing at G274C and this became evident again at V280C. Note that no crosslinking was evident for C259S indicating that the dimers observed are solely due to the introduced cysteine residues.

There were few consistent observations in the CuP-mediated crosslinking analysis with added GH based on the dimer to monomer ratio. Nevertheless, increased crosslinking at D262C (fig.3.3B) and a reduced crosslinking of V284C and F287C positions (fig.3.3C) was consistently observed following GH addition. Based on the helix wheel projection the V284 and F287 are on the same interface.

A

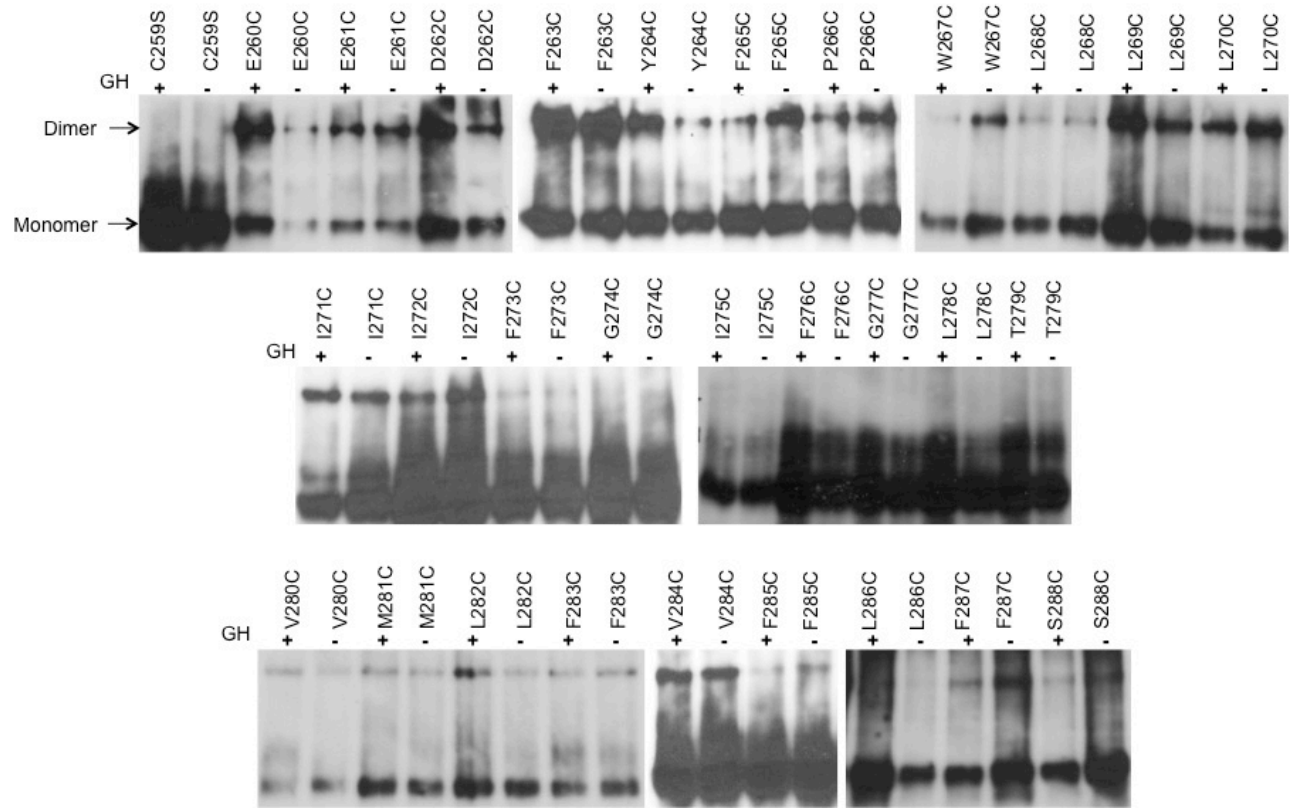
GH
C259S C259S E260C E260C E261C E261C D262C D262C
F263C F263C Y264C Y264C F265C F265C P266C P266C
W267C W267C L268C L268C L269C L269C L270C L270C
Dimer
Monomer
GH
I271C I271C I272C I272C F273C F273C G274C G274C
I275C I275C F276C F276C G277C G277C L278C L278C T279C T279C
GH
V280C V280C M281C M281C L282C L282C F283C F283C
V284C V284C F285C F285C L286C L286C F287C F287C S288C S288C

B

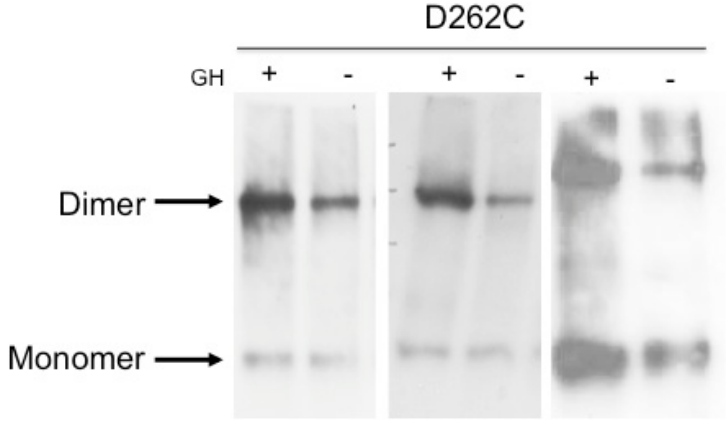
D262C
GH
Dimer
Monomer

C

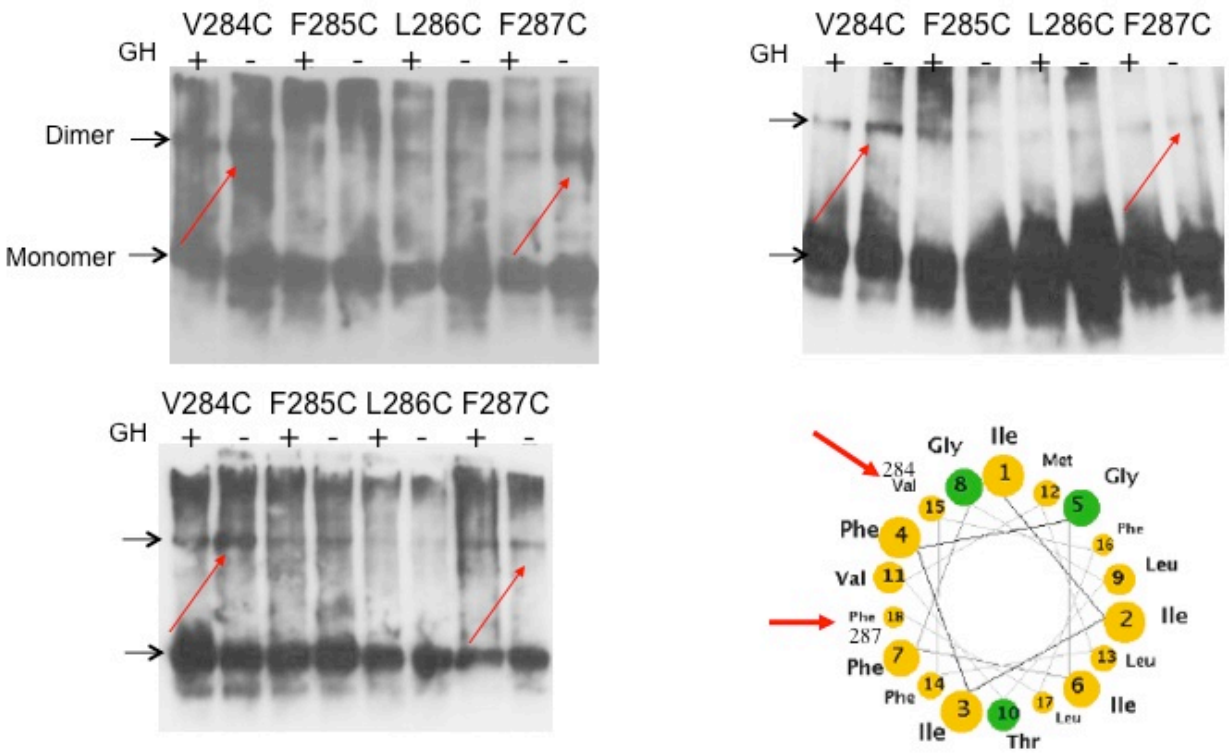

Figure 3.3: Effect of GH on Copper-o-phenanthroline-induced GHR dimerisation.

Transiently transfected COS-1 with GHR cys truncated mutants were subjected to GH treatment, membrane extract preparation and copper phenanthroline treatment (refer methods section) and analysed on non-reducing SDS-PAGE gels. (A) The entire TMD and upper linker region show crosslinking from E260C to F273C and V280C to S288C. No crosslinking is evident for C259S and for the stretch of residues from G274C to T279C. Blots representative of n=4 independent experiments (B) Increased CuP-mediated crosslinking in D262C subsequent to GH addition evident from 3 independent blots. (C) Decreased CuP-mediated crosslinking in V284C and F287C (indicated with red arrows) subsequent to GH addition evident from 3 independent blots. The helical wheel projection indicates that both residues reside on same side of the interface.

GHR cysteine mutant signalling analysis

Based on the spontaneous dimerisation pattern, we also sought to determine if targeted dimerisation alone could induce STAT5 activation. Initially, a comparative analysis of HEK293 and COS-1 cell lines was carried out and HEK293 was chosen based on the fact that they have low levels of endogenous GHR and active STAT5 (fig.3.4). The full-length versions of each of the truncated cys mutant constructs were created in the current studies by removing the stop codon but retaining all the other mutations. All the full-length constructs were also able to activate STAT5 at similar levels after GH addition (not shown).

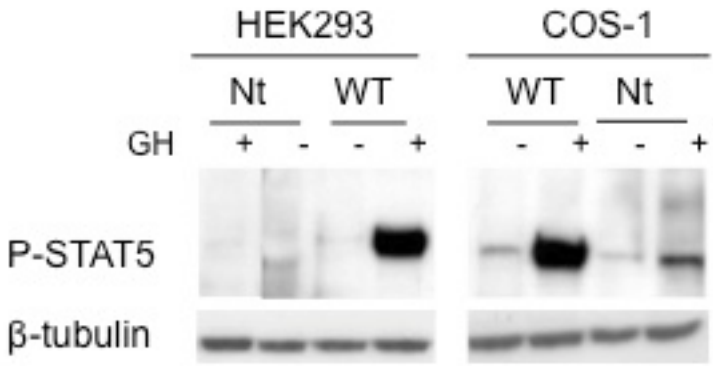

Figure 3.4: Choice of cell line for STAT5 activation in full-length hGHR cys mutants.

HEK293 and COS-1 cell lines were transiently transfected with low levels of full-length GHR (WT) or empty vector (Nt) and subjected to GH treatment (50ng/ml) for 10 minutes and STAT5 phosphorylation was determined. For the equal amount of protein loaded based on β-tubulin no STAT5 phosphorylation was detectable for empty vector transfected HEK293 following GH treatment but this was evident in COS-1 cells. Blots representative of n=2 independent experiments.

Based on differences in spontaneous dimer formation ability the full-length GHR cys mutants from L251C to I271C were analysed for STAT5 activation. Since HEK293 also have low levels of endogenous STAT5, small amounts of a STAT5B encoding plasmid were transfected with the GHR vector in order to sensitise the cells to changes induced by crosslinking of residues in JMD and upper TMD. By starving the transfected cells overnight in reduced serum media, any endogenous levels of STAT5 was reduced to basal levels and only the GHR-mediated effects on STAT5 activation could be observed. Phosphorylation of STAT5 in the absence of GH showed considerable differences between the different constructs on comparison with wildtype hGHR (fig.3.5A). From the blot it is evident that mutants from E260C to P266C have STAT5 activity comparable to WT whereas the upper linker mutants L251C to T258C except S255C had significantly reduced STAT5 activity. Interestingly, the STAT5 activity reduced to greater extent as the N-terminal distance from C259 increased and became comparable to that observed for C259S mutant. The only mutant with a high level of STAT5 activity was the double cysteine mutant (E260C, I270C). The rationale for using double cysteine mutant was to determine if increased helix interaction (disulfide bond formation) between residues on opposing face of the helix wheel could promote constitutive receptor activation. The corresponding dimer formation of full-length GHR cys mutants is shown in figure 3.5B by running the same lysate on a non-reducing gel and probing for HA-tag. In addition, importance of cysteine in upper linker region in GHR-mediated signalling is evident from significantly increased STAT5 activation relative to C259S. As shown in graph by normalising phospho-STAT5 to GHR expression (fig.3.5C), the entire region from C259 to P266 when crosslinked with a cysteine can induce STAT5 activation and that dimerisation at the N-terminal

juxtamembrane sequence, or the upper TMD can activate the receptor. Use of two disulfide crosslinks here strongly activates the receptor.

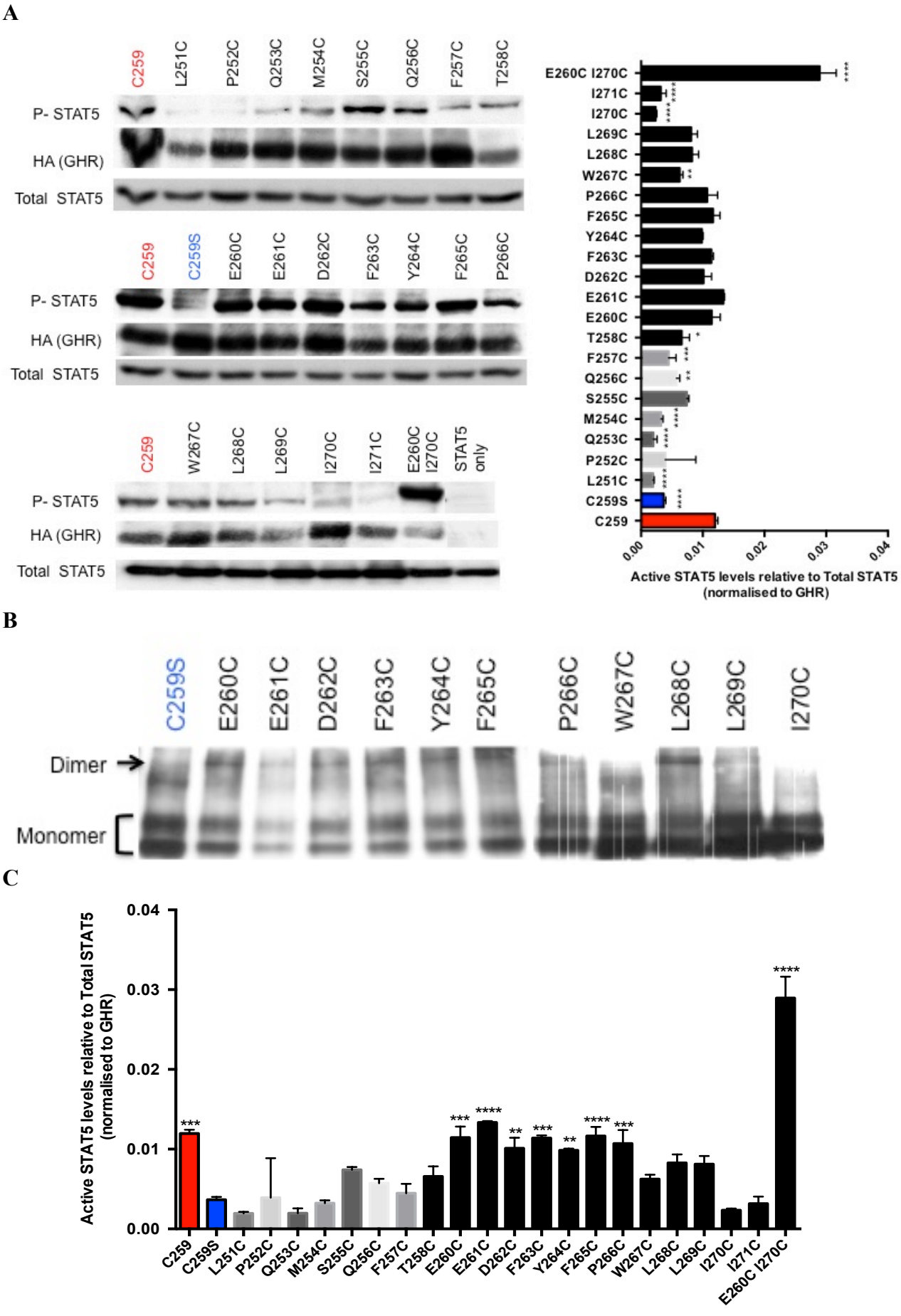

Figure 3.5: Signalling analysis of juxtamembrane linker and transmembrane domain residues of hGHR in the

absence of GH and crosslinker.

Western Blot analysis of hGHR cys mutants transfected with STAT5B in HEK293 cells in the absence of GH stimulation following an overnight starve. Equal quantity of each lysate was resolved on a reducing SDS-PAGE gel and analysed for STAT5 activity and receptor expression. (A) Constitutive activation of spontaneously crosslinked cysteine substituted receptors is evident in the immunoblot (left panel) and histogram depicts ratio of active STAT5 to total STAT5 level normalised to receptor expression and statistical significance relative to WT (C259) (right panel). (B) GHR dimerisation for full-length GHR cys mutants (from the same lysates represented in panel above) shown in a non-reducing SDS-PAGE gel. (C) Histogram depicting ratio of active STAT5 to total STAT5 level normalised to receptor expression with statistical significance relative to C259S mutant (thiol-free background) shown. Data representative of n=3 independent experiments (mean ±SEM; ****:P <0.0001, ***:P <0.001, **:P <0.01, *:P <0.05) by ANOVA.

Crosslinker treatment on live cells

Because crosslinking studies on membrane extracts have been quite informative, we sought to analyse if there was a difference in the GH-induced signalling on crosslinked receptor at various positions in the TMD. In this experiment, five set of treatments were carried out on HEK293 cells transiently transfected with cys hGHR constructs. These treatments included; addition of GH alone, addition of CuP alone, no treatment and addition of CuP and then GH and vice versa. The crosslinking reaction in all the treatment regimes was stopped using EDTA while washing the cells in PBS twice stopped the GH stimulation. All the TMD mutants were subjected to these methods but due to difficulty of crosslinker to penetrate the TMD only the upper region at the N-terminal TMD was tractable.

There were significant differences in GHR activation when the receptor had been previously crosslinked previously indicative of a positional preference of activation due to positional difference in crosslinking. There was a ‘ON’ position evident at residue L268 as shown in figure 3.6. When this residue was crosslinked and subjected to GH treatment, the STAT5 activation was of similar intensity as observed with the addition of GH alone or with GH first and then CuP. Such an observation indicates that crosslinking at L268 position is conducive to GHR activation or occurs naturally during GHR activation. This observation was in complete contrast from I270 where there was no GHR activation observed if GHR is previously crosslinked at this position before GH addition. This represented a ‘OFF’ position at I270 that if crosslinked could inhibit GH-induced activation.

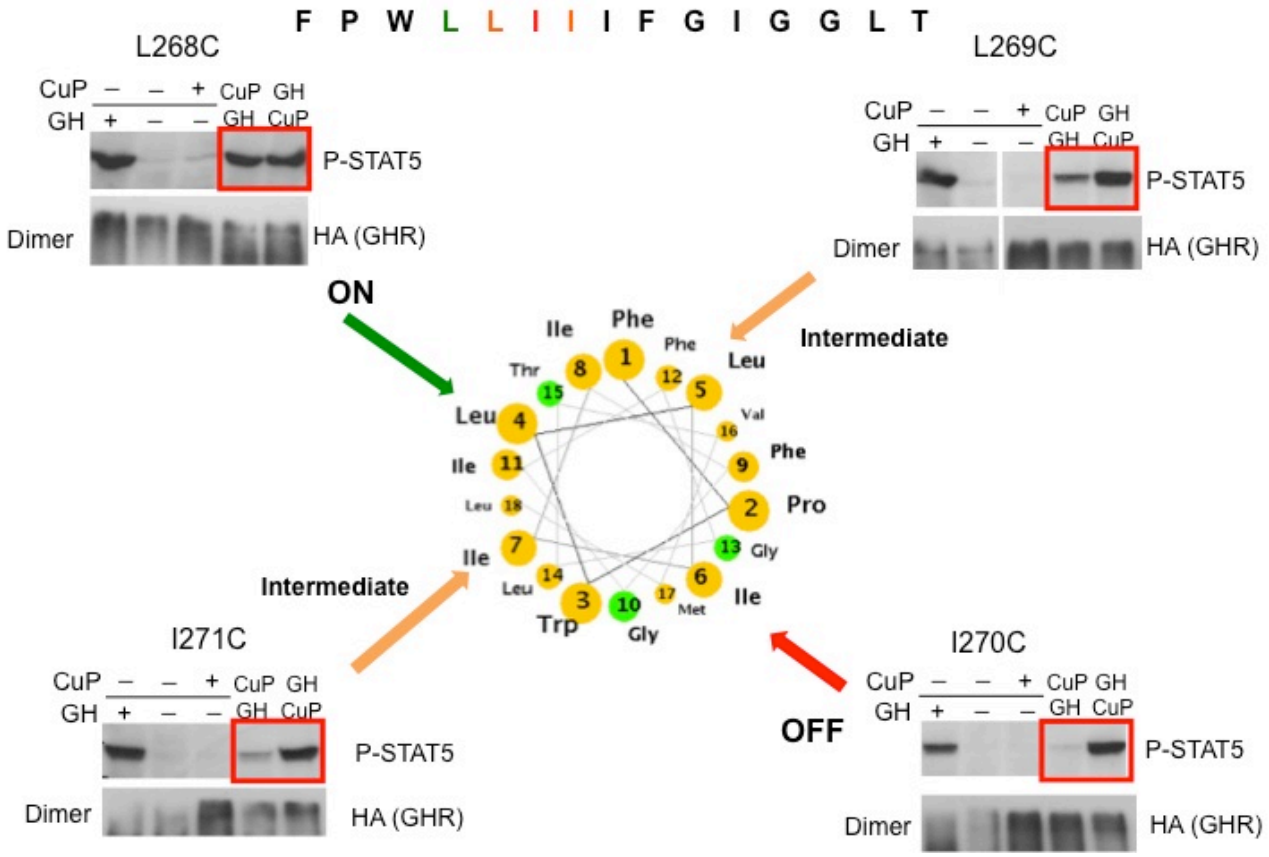

Figure 3.6: Helical wheel representation of the residues indicating 'ON', 'OFF' and intermediate positions in the upper Transmembrane domain region of GHR.

Transiently transfected HEK293 cells indicating phosphorylated-STAT5 on reducing gel (indicating GHR activation) and HA blot on non-reducing gel (indicating crosslinking and dimer formation) from L268C to I271C residues are shown. Following CuP and GH treatments (refer text), a helical interface is evident for these residues that matches the helical wheel projections. Blots representative of n=3 independent experiments.

Signalling analysis in Ba/F3 cells stably transduced with GHR cysteine mutants

In order to support the above findings from transient transfection, the stably expressing Ba/F3 cell lines were created by retroviral transduction with the hGHR cys constructs. Since all these constructs have been shown to be GH responsive, stable cell lines were selected in GH. For signalling analysis, cell lines were starved overnight in low serum media to reduce level of phospho-STAT5 and the cell lysates were analysed for pSTAT5, total STAT5 and GHR expression. From figure 3.7A it is evident that there is significant activation observed in the constructs E260C, E261C, D262C, F265C, L268C and the double cysteine mutants PM1 (E260C, I270C) and PM2 (F263C, I270C).

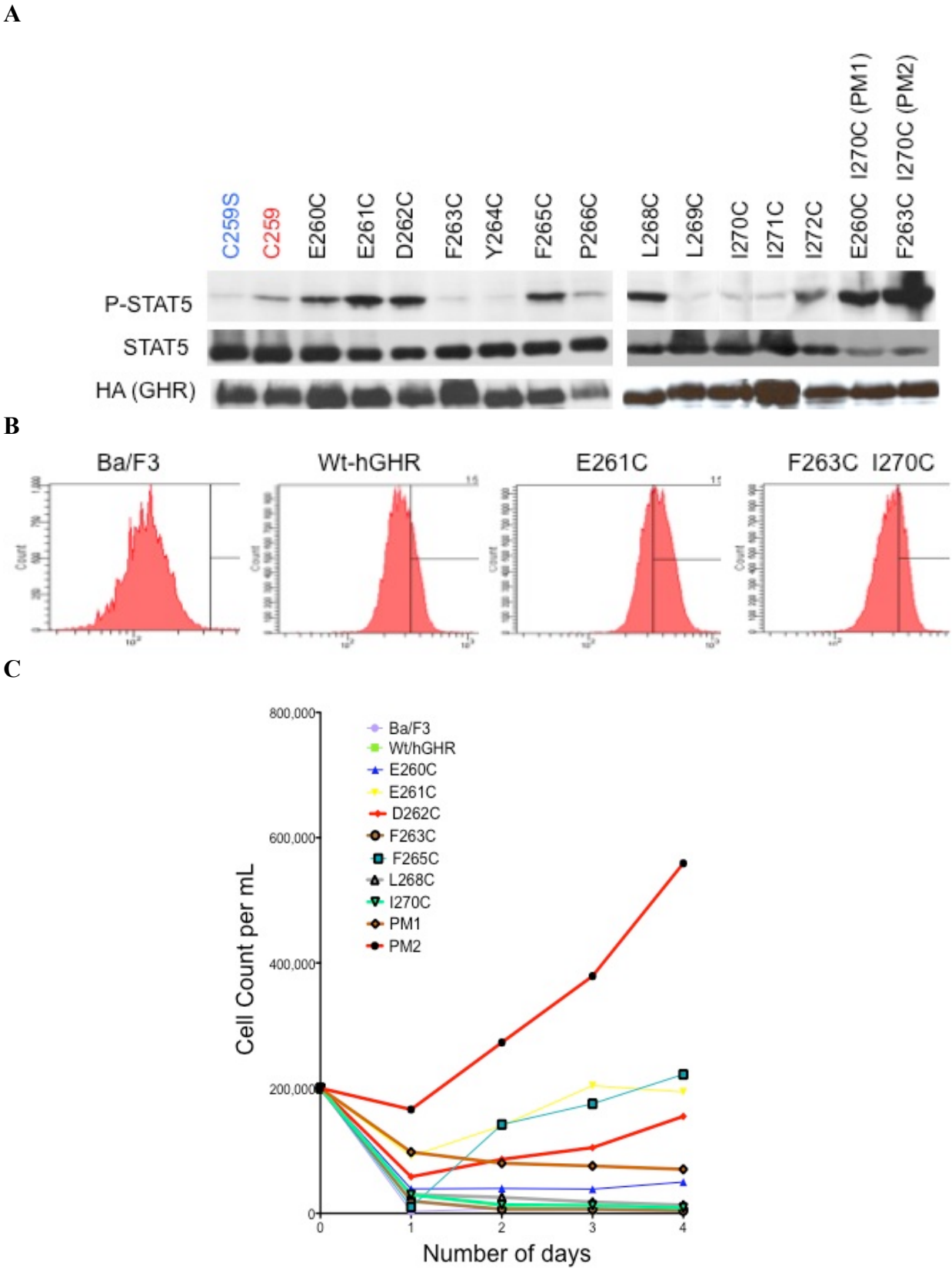

Figure 3.7: Analysis of the effects of full-length hGHR cys mutants in stably transduced Ba/F3 cell line in the absence of GH.

(A) Western Blot analysis of different cys hGHR mutants in retroviral transduced Ba/F3 cell lines without GH stimulation following an overnight starve (in IL-3/GH lacking media). Equal quantity of each lysate was run on a reducing SDS-PAGE gel and analysed for STAT5 activity evident in few juxtamembrane linker sequences. (B) Representative graph indicating surface expression of GHR of some hGHR cys mutants in Ba/F3 cell lines stained using anti-HA antibody

and TritC-labelled secondary antibody, then analysed by FACS. Note the shift in gating set using Ba/F3 as negative control and WT hGHR (B2B2 clone) as positive control. Two cell lines E261C and PM2 (F263C, I270C) are shown to express receptor at the surface. (C) Proliferation analysis of stably transduced Ba/F3 cells in charcoal-stripped serum containing media in the absence of IL-3 and GH indicates that PM2 mutant (F263C, I270C) is the most constitutively active. Data representative of n=2 independent experiments in two separate population studies and clonal lines from two independent transductions.

All the Ba/F3 cell lines stably expressing the different hGHR cys constructs were analysed for surface expression of GHR by FACS using mouse anti-HA primary antibody and a TritC-labelled secondary anti-mouse antibody. Parental Ba/F3 cells were used as negative control while WT-hGHR expressing Ba/F3 (B2B2 clone) (Rowland et al, 2002) served as a positive control for setting the gating channel. In addition, care was taken in choosing the gating so that it did not interfere with the GFP channel since the stable Ba/F3 mutants were selected for IRES driven GFP expression. For the entire set of hGHR cys mutant cell lines significant surface expression of GHR was observed and data for two such cell lines is shown (fig.3.7B). All the stable cell lines were subjected to proliferation analysis in growth media with routine FBS replaced with charcoal stripped serum to avoid effects from other cytokines. From these analysis the double cysteine PM2 (F263C, L268C) appears to be the most active hGHR construct although low level constitutive proliferation was also seen in other juxtamembrane residues (fig.3.7C) that showed STAT5 activation in the absence of GH.

Conservation of GHR TMD and upper linker region sequences

The GHR sequences from species across varied genus were analysed for evolutionary conservation since conservation can be correlated with functional importance of a particular amino acid specific to that position. The cysteine and acidic residues in the juxtamembrane linker region and potential TMD initiating residues FPW were highly conserved along with the GxxG motif in the TMD. Towards the end of the TMD, the terminal FS residues were also preserved across the species analysed here (fig.3.8).

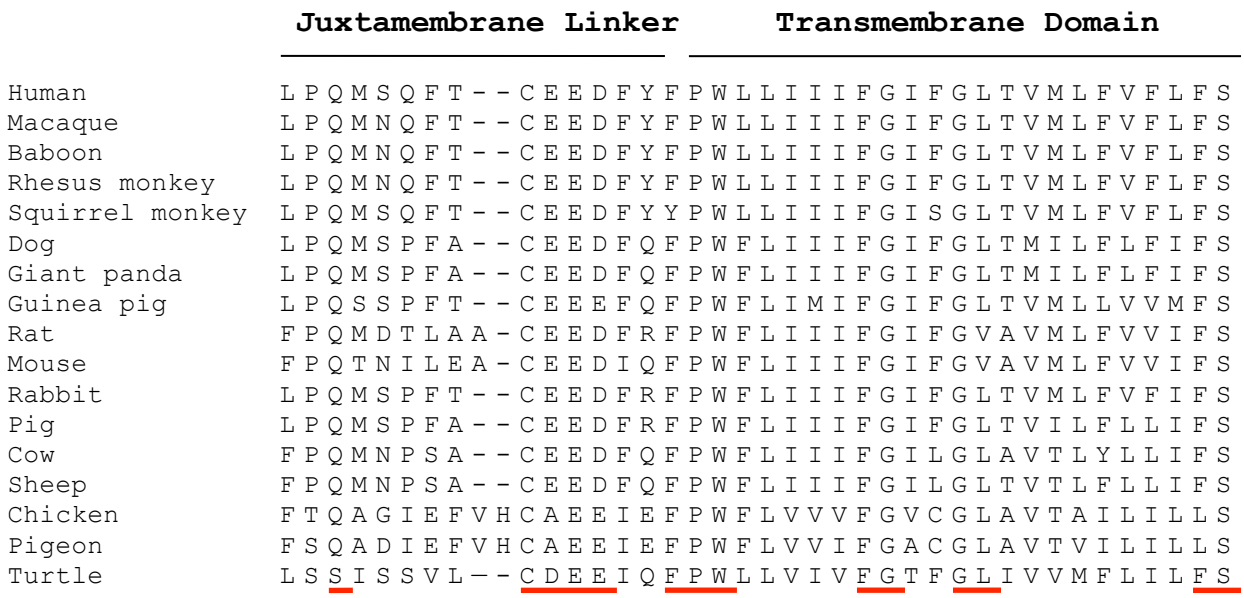

Figure 3.8: Multiple Alignments of GHR juxtamembrane linker and transmembrane domain amino acid sequences from various species.

Sequence alignments of GHR TMDs and upper linker region shows key conserved residues (underlined in red) including the GxxG motif and CEED (or CDEE) gating across species.

Discussion

The main aim of using SCAM here was to demonstrate that GHR, which exists as a pre-formed dimer is activated by a 'movement' of its subunits rather than by dimerisation alone. In order to test this hypothesis, cysteine-scanning mutagenesis and crosslinking analysis of the TMD was undertaken in truncated and full-length GHR and the latter was compared with the downstream GHR-mediated STAT5 activation.

Initial studies were undertaken in truncated GHR to determine if cysteine mutants in and around the TMD revealed a dimerisation pattern and if GH addition had any affect on that pattern. Indeed these GHR mutants were able to form dimers in the absence of GH consistent with the previous reports that GHR is a pre-formed dimer (Brown et al, 2005; Gent et al, 2003). However after GH addition few obvious differences in dimerisation pattern were evident. This lack of periodicity in the dimerisation pattern of the juxtamembrane linker region indicates that this sequence is not helical but unstructured. However, there was an increase in the ratio of dimers to monomers after GH addition at D262. It can be assumed that the 4 substitutions from P266 that undergo dimerisation to a lesser extent may be located at the interface between the JMD and the TMD and this is indicative that the TMD would actually start with the P266. Other SCAM studies have indicated that cysteine substitutions which are either completely buried in the membrane or at the cytosolic surface cannot form disulfide bonds because these residues are not exposed to enzymes such as protein disulfide

isomerase that catalyse disulfide bond formation in the ER lumen (Lu et al, 2006). This would explain why the spontaneous crosslinking is only evident for the first 3 or 4 residues in the TMD.

The unpaired cysteine at position 259 in the extracellular domain has been reported to be critical for GH-induced disulfide linkage of GHR molecules (Zhang et al, 1999). In our system, the C259S mutation had no effect on GH-induced signalling but in the absence of GH no spontaneous dimers were observed, which is consistent with the findings reported by Gent *et al.* (Gent et al, 2003). This is suggestive that cysteine may just serve to stabilise the GH-induced GHR binding. The relevance of disulfide bridge formation at this position is now clear from the recent studies in Waters' Group. In particular, removal of the conserved acidic sequence (EED) which caps the TMD and replacing it with non-repulsive alanine residues in jun zipper chimera resulted in lowering of FRET ratio indicative of receptor monomers coming close together (Brooks et al, 2014). In addition, when WT GHR (containing EED) was co-transfected with a mutant receptor containing KKR sequence (charge reversal) this resulted in constitutive activation and a decreased FRET ratio (Brooks et al, 2014). It appears that these acidic residues act as a gating mechanism for receptor activation, where the electrostatic repulsion must be overcome by ligand-induced proximity of the surrounding upper TM residues and the cysteine disulfide bond.

The MTS-2-MTS crosslinker analysis of TMD residues plotted onto a helix wheel projection indicated that one side of each helix is in contact. This was used to define the relative orientation of the two helices in the basal state and provided not only further evidence for constitutive dimerisation. This information provided the orientation of the basal state in molecular dynamics simulations of the two helices as they approached in lipid membranes. In addition, the spontaneous crosslinking of the introduced cysteines in the upper helix and juxtamembrane sequence down to I271 showed that this was associated with STAT5 activation in full-length GHR, which supported the view that increased receptor proximity in the upper TM/juxtamembrane sequence results in receptor activation. Activation was even stronger when two cysteine residues (at least 2 helix turns apart) were crosslinked (intermolecular) as in the case of double cysteine mutant (PM2), evident in constitutive activation both transiently in HEK293 and stably in Ba/F3 cells.

The STAT5 activation associated with GHR full-length TM mutants determined in this study supports the findings from the related EpoR where two such mutations in the first two residues in the TMD (L226C and I227C) were shown to confer-ligand independent activation (Lu et al, 2006). Our data therefore indicates that activation of pre-dimerised GHR by ligand binding is achieved by reorientation of the TMDs and their juxtamembrane ICDs and that certain disulfide bonded dimers

recapitulate the activated dimeric conformation, constitutively activating downstream signalling. Based on our data and the previously determined structure of GHR ECD bound to GH, this provides useful information on structure-function aspects of receptor.

The CuP treatment of intact cells indicated that L268 residue is present on the interaction interface between the two TM helices. This evidence was further supported by the fact that neighbouring residues to both 'on' and 'off' positions, L269C and I271C, give intermediate intensity of STAT5 activation if crosslinked before GH addition. The experiment indicates that there could be a potential 'rotation movement' in the α–helix that provides residue positions with on and off effect, separated by residues with intermediate effects on GHR activation. Considering the TMD to be α–helical, it is expected there will be a similar outcome every 3.6 residues from L272 onwards. However, no 'on' and 'off' positions were found lower into the membrane which was indicative either of the inability of CuP to crosslink further into the TMD due to the hydrophobic conditions within the membrane or a 'fork' like positioning of the helix. The inability of CuP to reach within the membrane seems more plausible since the CuP treatment of membrane extracts was able to form dimers for the TMD residues adjoining the ICD. In support, a previous study by Guo *et al.* on G-PCRs has reported decreased CuP-induced crosslinking in the middle of membrane (Guo et al, 2005). The lack of consistent disulfide bond pattern on membrane extracts in the presence or absence of GH suggests that there is some flexibility in the TMDs making it difficult to determine the precise movement. However, in the case of V284C and F287C there was decreased CuP-mediated dimer formation while in D262C there was an increased dimer formation following GH treatment suggestive of separation of lower TM helices and proximity of upper linker region for activation of GHR.

In order to further validate these findings, *in silico* molecular dynamics modeling of the TM helices in lipid membranes were performed in collaboration with M. Doxastakis (University of Houston). To obtain the free energy profile as a function of distance (PMF) between two transmembrane domains (TMDs), exhaustive Monte Carlo simulations using 128 replica pairs were performed for a range of separations between the centers of mass of the helices as they approach. The fact that this profile has a deep minimum at a separation of 0.7-0.8nm supports the finding that the two TMDs interact strongly. The simulations showed that as the two helices approached, they first interact at their C-termini as a result of repulsive interactions at the N-termini (especially the EED sequence). Subsequently, the TMDs follow a path that maximises interactions between the Phe residues and Thr-Thr hydrogen bonding. This initially led to an essentially parallel dimer (State 1) corresponding to the crosslink pattern seen in the absence of hormone. Closer approach of the helices (as could

result from hormone binding) leads to a close-packed structure (State 2) with increased tilting and TMD rotation, resulting in a left handed cross over dimer with increased separation at the C-terminus. Both State 1 and 2 were within the identified energy minimum, indicating a relatively facile State1-State2 transition. The GHR TMDs form the active left hand crossover dimer by rotating F276 and F283 out of the interface. Importantly, when the inactive State 1 is compared with the left-handed crossover form, separation between the C-termini had increased substantially. This parallels the finding that activity correlates with higher separation of the C-termini as monitored by FRET (Brooks et al, 2014). In the proposed active State2 form the N-terminal W267 sits favourably at the upper membrane interface, facing outward to favour association, while the C-terminal K289 is in an unfavourable configuration for helix interaction. This model can therefore also explain how alanine substitution of K289 promotes the left-handed dimer form, correlating with the increased activation as seen in the mutation K289A GHR (Brooks et al, 2014) and can be extended to TPOR. It is important to note that these helix movements are essentially sequence independent, so can be applicable to other Class I receptors.

Evidently the receptor activation mechanism does not have a specific sequence requirement for the TMD helix, but rather the 'tilt and twist' movement observed is a function of helix dynamics in a lipid membrane contingent on close apposition of the N-terminal end of the paired helices.

Interestingly, the only known variant in the TMD sequence was identified by quantitative trait locus (QTL) mapping of the bovine TMD (Blott et al, 2003) as Phe279Tyr (corresponding to F283Y in humans), and this was associated with a major change in the milk yield and composition. The molecular basis of this alteration was shown not to be STAT5-dependent (Zhou & Jiang, 2006). Therefore it seems that another signalling pathway is affected for the strong effect on milk yield and composition. There may be a possibility that similar to the conformational change in F'G' loop in ECD, resulting in induced biased signalling to SFK/ERK (Rowlinson et al, 2008), certain TMD residues may be involved in the same. A similar observation has been reported in the same study where perturbing the relative orientations of the two TM helices with glycine and proline substitutions resulted in changed ratio of Jak2/STAT5 to ERK signalling (Rowlinson et al, 2008). Based on these results it would be worthwhile to determine if any of the hGHR cysteine mutants upon crosslinking can signal via other pathways.

Determining the oncogenic potential of GHR

The constitutively active jun zipper GHR constructs (Brown et al, 2005; Brooks et al, 2014) as well the double cysteine arising from this chapter will be used to determine the oncogenic role of GHR

and define cellular location of any transformation ability. The leucine zipper domain from the transcription factor jun has been employed for functional replacement of GHR ECD and used to confer ligand-independent growth when transfected into Ba/F3 cell line by clamping the receptor together from the top and resulting in continuous downstream signalling (Behncken et al, 2000). This construct has been used to make transgenic zebrafish *in vivo* and was reported to double the size (and IGF-1 levels) in comparison to overexpression with GH, GHR or both together (Ishtiaq Ahmed et al, 2010). Eventually by utilising the TVA system, these constructs will be used to investigate the *in vivo* effects of constitutively active GHR and nuclear-targeted GHR, in a tissue-specific manner.

Chapter 4
The First Cancer-Associated Variant of the Growth Hormone Receptor

Introduction

The Growth Hormone Receptor (GHR) is a member of Class I cytokine receptors superfamily that exists as a dimer on the cell surface of virtually all cells of the body (Brooks & Waters, 2010). Upon binding of growth hormone (GH) to GHR, Janus kinase 2 (Jak2) which is associated within the intracellular domain at a conserved box1 motif is activated and downstream signalling cascades are triggered (Argetsinger et al, 1993). GHR can also activate Src family kinases (SFK: c-src, lyn, fyn, yes, hck) independently of Jak2 but the exact receptor binding region is yet unknown (Rowlinson et al, 2008). Numerous signalling pathways activated by GH have been identified, including those for STATs (signal transducer and activator of transcription), MAPK (mitogen activated protein kinase), and the PI3-K (phosphatidylinositol-3-kinase). Interestingly these pathways can be activated independently in a cell dependent manner (Rowlinson et al, 2008). Apart from promoting longitudinal body growth, GHR signalling regulates post-natal metabolism and cellular functions of proliferation and differentiation (Chhabra et al, 2011). A substantial body of evidence supports a role for the growth hormone (GH)–IGF-1 (Insulin like growth factor-1) axis in organomegaly and cancer incidence and progression (Miquet et al, 2008). This includes epidemiological evidence relating elevated plasma IGF-1 to cancer incidence as well as a lack of cancer in human GHR mutations resulting in IGF-1 deficiency (Gunnell et al, 2001), (Guevara-Aguirre et al, 2011). Moreover, rodent models lacking GH or its receptor are strikingly resistant to the induction of a wide range of cancers (Ikeno et al, 2009; Miquet et al, 2008), and treatment with the GH antagonist pegvisomant slows tumour progression (Divisova et al, 2006). While GH receptor expression is elevated in many cancers, autocrine GH is present in several types, and overexpression of autocrine GH can induce cell transformation (Chhabra et al, 2011).

GHR signalling is tightly regulated at numerous levels via different mechanisms. These involve the regulation of cell surface receptor level by internalisation and degradation and attenuation of receptor signalling by negative feedback mechanisms, following a GH secretory pulse. In addition, GHR displays a rapid turnover in the absence of GH (van Kerkhof et al, 2007). This constitutive turnover of GHR is probably cell type-dependent and is fast in most cell types: in rat adipocytes (T1/2= 45minutes) (Gorin & Goodman, 1985), in rat liver (T1/2= 40 minutes) (Donaghy et al, 2002) and in mouse fibroblasts (T1/2=75minutes) (Murphy & Lazarus, 1984). GH-induced GHR endocytosis/degradation requires an intact ubiquitination system and depends on the ubiquitin-dependent motif (UbE: DDSWVEFIELD) present in the juxtamembrane cytoplasmic sequence (Strous et al, 2004). Mutations in the UbE motif lead to a dramatic decrease in endocytosis and lysosomal degradation, rendering the cells more GH-sensitive. Protein ubiquitination involves the

sequential action of three classes of enzymes; E1 activating enzymes, E2 conjugase and the E3 ligases that introduce the substrate specificity (da Silva Almeida et al, 2013).

Recently, Beta-transducin repeat-containing protein (β-TrCP) has been reported to be (van Kerkhof et al, 2007) necessary for GHR endocytosis where it serves as the substrate recognition subunit for the SCF(β-TrCP) ubiquitin ligase (van Kerkhof et al, 2007). After GH binding, the serine residues of the DSGxxS motif get phosphorylated and SCF(β-TrCP) is recruited, mediating its ubiquitin-dependent endocytosis. However, it has been recently demonstrated that the DSGxxS motif of GHR is not involved in ligand-mediated, but rather in GH-independent, basal GHR endocytosis and degradation (da Silva Almeida et al, 2012). In addition the GHR UbE motif regulates endocytosis and degradation, in both the presence and the absence of GH stimulation. β-TrCP interacts with its substrates through its WD40 domain and nuclear magnetic resonance studies have characterized the interaction of β-TrCP with classical phosphorylated degrons $DSG(x)_{2+n}S$ in several other substrates (Evrard-Todeschi et al, 2008). For the binding of the GHR DSGxxS motif to β-TrCP, the same residues in the WD40 domain are involved. However, in the case of UbE motif sequence, which differs substantially from the classical DSGxxS motif this interaction is unconventional and has a lower affinity (da Silva Almeida et al, 2013). Although β-TrCP ubiquitinate specifically phosphorylated substrates, in the case of GHR, ubiquitination was shown to be dispensable, since β-TrCP silencing was shown to decrease the degradation of GHR mutant with all lysine residues mutated (in cytosolic tail) as efficiently as wildtype GHR (van Kerkhof et al, 2007). Functionally the SCF-ubiquitin ligases have been shown to play a pivotal role in the regulation of cell division and various signal transduction pathways (Fuchs et al, 2004).

The GHR is synthesized as a precursor protein in the endoplasmic reticulum where it dimerises (Gent et al, 2002) and becomes glycosylated at five potential sites (Asn-X-Ser/Thr) in the Golgi before being transported to plasma membrane (Leung et al, 1987). Cell surface GHR availability is a key determinant of GH responsiveness. Regulation of GHR abundance include factors that regulate receptor gene expression (Edens & Talamantes, 1998; Schwartzbauer & Menon, 1998) as well as those that govern receptor protein stability, such as the propensity of Jak2 to chaperone nascent receptor to the cell surface and therefore provide stability to the mature receptor from constitutive endocytosis and degradation (Deng et al, 2007) (Schwartzbauer & Menon, 1998). Susceptibility of the surface receptor to inducible metalloproteolytic processing by TACE/ADAM17 is another factor that determines surface availability (Zhang et al, 2000; He et al, 2003). GH-induced Jak2 activation markedly reduces surface receptor; such that a catalytically-inactive Jak2, a Jak2 mutant incapable of associating with GHR, or a receptor mutant deficient in

Jak2 binding are far less able to promote receptor downregulation compared with expression of wild-type receptor and Jak2 (Deng et al, 2007). In addition, a receptor mutant with all intracellular tyrosine residues changed to phenylalanine allowed acute GH-induced Jak2 activation, this tyrosine phosphorylation-defective receptor underwent markedly less GH-induced ubiquitination and was only modestly downregulated (Deng et al, 2012). This indicates the importance of downstream phosphorylation of tyrosine residues in receptor turnover, suggesting that they serve as docking sites for not only transcription factors but also negative regulators of GHR signalling.

Activation of GH-dependent signalling pathways is based on protein phosphorylation on tyrosine, serine or threonine residues. The mechanism for deactivation of these phosphorylations is the action of protein phosphatases (PP) and suppressors of cytokine signalling (SOCS). Pasquali *et al*. (Pasquali et al, 2003) have identified four protein tyrosine phosphatases (PTPs): PTP-H1, PTP1B, Sap1, and TC-PTP with binding affinity towards GH-induced phosphorylated GHR. Of the 4, PTP-H1 has strong affinity for Y534, Sap1 only but strongly for Y487, TC-PTP for Y332, Y87, Y534, and Y595, and PTP1B for Y487 and Y332 as determined by substrate recognition by trapping mutants. In addition, SHP2 has been shown to negatively regulate GHR-mediated Jak2/STAT5 signalling by binding to Y595 (Stofega et al, 2000). PTP-H1 knockout mice are larger with the difference being particularly significant for males (Pilecka et al, 2007). Although PTP1B has been strongly linked to some aspects of GHR signalling, PTP1B knockout mice are in fact smaller than wild type animals because of their lower fat content, which is linked to increased energy expenditure (Klaman et al, 2000).

SOCS proteins are negative regulators of Jak/STAT signalling (Wormald & Hilton, 2004) that have been shown to modify cytokine action through a classic negative feedback loop. Normally, SOCS protein levels are constitutively low, but their expression increases rapidly following cytokine stimulation (Fujimoto & Naka, 2003). GH has been shown to induce the expression of several SOCS proteins *in vitro* (Adams et al, 1998; Paul et al, 2000) and *in vivo* (Tollet-Egnell et al, 1999). Generally, SOCS1, SOCS3 and CIS expression is rapidly induced following GH stimulation but is transient, whereas SOCS2 expression increases steadily with time (Flores-Morales et al, 2006). Each SOCS member has a different mechanism of action on GH signalling. SOCS1 and 3 can directly bind within the Jak2 activation loop blocking kinase activity and promoting its proteasomal degradation (Nicholson et al, 1999; Endo et al, 1997). SOCS2, SOCS3 and CIS have been shown to bind to tyrosine phosphorylated GHR. Strong evidence indicates that binding to Y487 and Y595 is required for SOCS2-mediated inhibitory actions (Greenhalgh et al, 2002). Since both tyrosines are known STAT5 binding sites (Wang et al, 1996), SOCS2 can competitively inhibit STAT5 binding

to the receptor. Vesterlund *et al*. (Vesterlund et al, 2011) have recently reported the mechanistic importance of phosphorylated Y487 rather than Y595 on GHR for its regulation by SOCS2. Not much is known about CIS interaction on GHR but phosphorylated Y487 and Y595 have been predicted as binding sites using mammalian two-hybrid method (Uyttendaele et al, 2007). Functionally only SOCS2 knockout mice are 40% larger compared to wild type mice (Metcalf et al, 2000). Evidence also indicates that growth factors (e.g., insulin), xenobiotics (e.g., dioxin, statins), and estrogens, can induce SOCS2 expression (Leong et al, 2004; Rico-Bautista et al, 2006). Consequently, regulation of SOCS2 protein expression provides a mechanism for crosstalk where multiple factors can regulate the activity of GH.

The loss of GH signalling evident in Laron dwarfism is due to lack of a functional receptor. These mutations reported for GHR include 153T, Q154P, and V155G that mainly affect intracellular trafficking and binding affinity of the receptor, whereas the D152H mutation affects receptor expression, dimerisation, and signalling (Wojcik et al, 1998). In addition membrane bound cytoplasmically truncated splice variants of GHR have also been reported. These variants can form heterodimers with full-length GHR and inhibit the downstream signalling due to lack of Jak2 and STAT5 binding sites, and generate large amounts of GH binding proteins (Ross et al, 1997). The most important manifestation of loss of GHR activity, as evident in the Ecuadorian cohort was a lack of cancer incidence in individuals with GHR deficiency as compared to their normal relatives (Guevara-Aguirre et al, 2011) highlighting the fact that altered GH signalling can alter cancer risk. Besides loss of function mutations a number of naturally occurring variants, alternatively spliced transcripts of GHR have been reported with no functional implications as yet. There are at least 13 alternatively spliced human GHR mRNAs generated in the 5` untranslated exons all of which splice into a common acceptor site upstream of the translation initiation site of exon 2. This results in generation of full-length receptor polypeptide but with expression levels varying in a spatial-temporal manner (Wei et al, 2006).

A widely expressed GHR variant is the exon-3 deleted GHR isoform in humans. It lacks amino acids 7-28 in the extracellular domain which does not affect GHR binding or internalisation (Urbanek et al, 1992; Mercado et al, 1994). However it does influence the sensitivity to GH activation and is associated with enhanced responsiveness to GH in children (Wassenaar et al, 2009) and reportedly altered GH pharmacogenetics (Dos Santos et al, 2004; Filopanti et al, 2011). Recently the first mutation for GHR *that was* associated with lung cancer risk in a Chinese population was identified (Cao et al, 2008). A base substitution from C to A on 1526nt of cDNA of *ghr* resulted in an amino acid change at position 495 from proline to threonine. The subjects

heterozygous and homozygous for the A allele at Pro495Thr polymorphism had a higher risk for lung cancer (OR= 2.02, *P*= 0.007, 95% CI: 1.20–3.41) with significant risk of small cell and squamous cell lung cancer (OR= 2.59, *P*= 0.006, 95% CI: 1.35–4.95) but not adenocarcinoma, which suggests a potential interaction between this polymorphism and pathological pathways related to smoking. Further analyses revealed P495T variant was more significantly associated with lung cancer in the male subpopulation, still-smokers subpopulation and the subpopulation with familial history of cancer. A similar correlation of this GHR variant was reported in a large-scale genome-wide association studies in UK Caucasians with an odds ratio of over 12 (Rudd et al, 2006). This chapter characterises the P495T GHR variant in regards to its effect on the downstream signalling from GHR in different cell lines and determine the molecular basis for it.

Materials and Methods

Materials

Fetal Bovine Serum (FBS) and Serum Supreme (SS) were purchased from Lonza Group Ltd (Basel, Switzerland). Lipofectamine, Bovine serum albumin (BSA) fraction V, IgG free, L-glutamine, Hygromycin B in PBS, RPMI 1640 media, and LHC-9 media were purchased from Invitrogen Life Technology (NY, USA). Human fibronectin was purchased from Becton Dickinson (NJ, USA). Collagen solution and puromycin was purchased from Sigma Aldrich (NSW, Australia). Complete Protease Inhibitor Cocktail Tablets were purchased from Roche (NSW, Australia). Immobilon Western Chemiluminescent HRP substrate and mild Re-blot stripping buffer were purchased from Millipore (MA, USA). Chemicals: DAPT, MG132 (Z-Leu-Leu-Leu-al), clasto-Lactacystin beta-lactone were obtained from Sigma Aldrich (NSW, Australia). Brefeldin A (BFA) was kindly provided by Prof. Jenny Stow (IMB). Human growth hormone was expressed and purified within the Waters lab (IMB).

Construction of plasmids

The P495TGHR coding sequence was derived from wild type GHR by site directed mutagenesis and PCR amplified with KOD Hot Start polymerase (Roche) with primers containing *attB* sequences. The PCR products were cloned into two different destination vector backbones pMX and pQCXP using a modified Gateway cloning based on the previously described protocol by (Loftus et al, 2001). Haemagglutinin A (HA) tag was introduced N-terminal to GHR coding sequence for ease of detection during immunoblotting. The integrity of the cloned GHR vectors were confirmed by DNA sequencing using a set of 8 different primers to provide clear overlapping sequencing results spanning the entire GHR coding sequence. DNA sequencing was performed by

AGRF and sequence data was analysed. The pCMV-SOCS2 plasmid was purchased from Origene (Maryland, USA).

Cell culture

Murine pro-B cell lines (Ba/F3) were cultured in RPMI 1640 medium supplemented with 2mM L-glutamine, 10% SS, 100units/ml interleukin-3 (IL-3) and 900μg/ml hygromycin B. For serum starvation, Ba/F3 cells were washed and maintained in RPMI 1640 media containing10% FBS and 2mM glutamine but devoid of IL-3 or GH for 16hrs.

Transformed normal bronchial epithelium cells (BEAS-2B) were maintained in LHC-9 medium (Life Technologies) with 50μg/ml hygromycin B. Flasks were pre-coated with a mixture of 0.01mg/ml fibronectin, 0.03mg/ml collagen and 1μg/ml bovine serum albumin dissolved in LHC-9 medium overnight at 37^{o}C. Excess coating mixture was removed and flasks/plates were dried overnight at 37^{o}C. Pre-coated flasks were subjected to three PBS washes prior to addition of cells. For serum starvation, BEAS-2B cells were kept in RPMI 1640 supplemented with 2mM L-glutamine and 0.5% BSA medium for 16hrs.

The androgen independent DU145 cell line was cultured in RPMI 1640 medium supplemented with 10% FBS, 2mM L-glutamine and 250μg/ml hygromycin B. Cells were starved in 2mM L-glutamine and 0.5% BSA-RPMI 1640 medium for 24 hours. HEK293 and HEK293T cell lines were cultured in DMEM supplemented with 10% FBS. Cells were starved in DMEM with 0.5% FBS for 16hrs. All cells were maintained in 37^{o}C and 5% CO_2.

Production of replication incompetent ecotropic retroviruses

For generation of cell lines stably expressing wild type or the variant P495TGHR, Platinum-E (PLAT-E) cells were transfected by Lipofectamine as per manufacturer's instructions. Supernatant was collected 3 days post-transfection, centrifuged at 400g for 5min and filtered with 0.4 μM PDVF filter. Murine (Ba/F3) cells were incubated in growth media containing 50% filtered PLAT-E supernatant in the presence of 4μg/ml polybrene. Cells were then selected for hygromycin B resistance three days post infection.

Production of replication incompetent pantropic viruses

Pantropic retrovirus production was performed in a similar manner to ecotropic retroviruses. Lenti-X cells (derived from 293T cells; Clontech) were transfected with pVPack-GP, pVPack-VSVG, and the expression vector; pQCXP-HA-GHR-IRES-hygromycin. The virus containing supernatant was harvested, filtered and used to transduce BEAS-2B, HEK293 and DU145 cells lines as above. The transduced cells were selected for GHR on puromycin.

Proliferation assay

For measuring proliferation of Ba/F3 cells transduced with WT and P495TGHR, the cells were starved overnight and seeded at a cell density of 1×10^4 cells/mL in duplicates in growth media supplemented with GH at 100ng/mL instead of IL-3 (Day 0). The cells were counted everyday by trypan blue exclusion using a hemocytometer.

Time course assay for GH signalling

Cells were serum starved as described above on attaining 80% confluency and stimulated with 50ng/ml GH in reduced-serum medium for 15minutes. GH was removed by two PBS washes. Washed cells were maintained in reduced-serum medium at 37^{o}C until harvested by scraping (for adherent cell lines) or centrifugation (for suspension cell lines) at different time points as described in the results section. For Brefeldin A experiment starved cells were pretreated with 1µg/ml BFA for 1hr prior to GH treatment and BFA was added again when the media was replaced. Protein was extracted in cold RIPA buffer (radio immunoprecipitation assay): 150mM NaCl, 50mM Tris pH7.5; 0.5% SDS, 1% NP-40, Sodium Deoxycholate supplemented with Protease inhibitors (Roche, EDTA-free), 10mM Sodium Fluoride, 1mM Sodium Pyrophosphate, 2mM Sodium Orthovanadate. For co-immunoprecipitation, HEK293 stable cells were transfected with 2µg of SOCS2 plasmid (Origene) for 24hrs. The cells were starved for 16hrs prior to GH stimulation for 15 minutes (50ng/ml). Cells were harvested in buffer containing 150mM NaCl, 50mM Tris pH7.5, 5mM EDTA, 0.5% Triton and supplemented with 100mM Sodium Fluoride, 2mM Sodium orthovanadate, Protease inhibitor (EDTA-free) and 1mM PMSF. For animal studies, pieces of liver tissue were homogenised in RIPA lysis buffer, cleared by centrifugation. Equal amounts of quantified protein lysates were boiled in sample buffer (15mM Tris-HCl (pH 6.8), 2% SDS, 10% glycerol, 10mM DTT) at 100°C for 5 minutes and resolved on SDS-PAGE gels. The gels were transferred on to PVDF membranes and subjected to specific antibodies (listed in Appendix VI).

Co-Immunoprecipitation and Western blot analysis

HEK293 stably expressing WT and P495TGHR were plated in T-75 flask format at equal seeding density and transfected next day at 50% confluency with 2μg SOCS2 expression plasmid or 2μg CIS expression plasmid using lipofectamine 2000 (Invitrogen) as per manufacturer's conditions. For CIS and SOCS2 comparison, equal amount of CIS and SOCS2 plasmid were added (1μg each). For co-immunoprecipitation (co-IP), transfected cells were starved 16hrs before harvest in serum reduced media (DMEM with 0.5% FBS). On the subsequent day, cells were stimulated with 200ng/ml human GH for 12minutes at 37ºC. The cells were washed in cold PBS and harvested by scraping into cold lysis buffer comprising 150mM NaCl, 50mM Tris pH7.5, 5mM EDTA, 0.5% Trition-X-100 supplemented with 1x complete EDTA-free protease inhibitor tablets, 10mM Na_3VO_4, 30mM NaF, 10mM $Na_4P_20_7$. Protein lysates were spun at 12000g for 10minutes at 4ºC and quantified using a BCA Assay kit (Pierce). Equal amount of protein lysates were pre-cleared using Protein G sepharose beads (GE Healthcare) for 30minutes at 4ºC. The pre-cleared lysate was used for immunoprecipitation.

For SOCS2 co-IP, anti-SOCS2 antibody at (1:100 dilution) and for CIS co-IP, CIS antibody (1:100 dilution) (Cell signalling) were added to protein lysates and mixed gently on a rotating wheel at 4ºC. After 2hours, Protein G sepharose beads were added in the antibody-lysate tube which was then mixed gently on a rotating wheel at 4ºC for another 2hours. The beads were washed in lysis buffer (lacking Triton) twice and spun at 6000rpm for 1minute each time between washes and the supernatant was removed. Finally, the washed beads were boiled in SDS sample buffer with 0.1M DTT for 5minutes and spun at 12000g for 5minutes. The supernatant was removed and subjected to SDS PAGE gel electrophoresis.

Quantitative real time PCR (qPCR)

Liver tissue was homogenised in Trizol Reagent (Invitrogen, USA) and RNA extracted as per manufacturer's instructions. RNA was then further purified and DNase treated using the RNeasy Mini Kit clean up protocol (QIAGEN, Maryland, USA). RNA was reverse transcribed using Superscript III (Invitrogen, USA) and used for qPCR with Sybr Green Technology (ABI, CA, USA) in the 7500 Real Time Cycler (ABI, CA, USA). Analysis was performed by calculating the change in Ct between the gene of interest normalised against the housekeeping gene, β-2 microglobulin (B2M) using primers listed in Appendix V.

For HEK293 cells in the time course experiment, cells were washed in PBS and RNA extracted as per manufacturer's instructions. RNA was then further purified and DNase treated using RNeasy Mini Kit clean up protocol (QIAGEN, Maryland, USA). RNA was reverse transcribed using Superscript III (Invitrogen, USA) and used for qPCR with Sybr Green Technology (ABI, CA, USA) in the 7500 Real Time Cycler (ABI, CA, USA). Analysis was performed by calculating the change in Ct between the gene of interest normalised against the housekeeping gene, glyceraldehyde-3-phosphate (Gapdh) (listed in Appendix IV) and expressed as a fold change relative to wild type control.

Sequencing of Prostate Cancer slides

Prostate cancer formalin-fixed, paraffin-embedded tissue sections were obtained from Australian Prostate Cancer BioResource (APCB) after Human ethics approval from the UQ Ethics Committee. These slides were subjected to hematoxylin and eosin staining and subsequently graded and marked by a histopathologist. These marked slides were scanned on a NanoZoomer (Hamamatsu Photonics, Japan) and using as reference, the paraffin-embedded tissue (in unstained slides) was carefully scraped using a scalpel blade and collected in an eppendorf tube. Each tissue section (from a total of 40 sections) was scraped for corresponding 'cancerous' and normal region as marked by the histopathologist. The DNA and RNA were extracted simultaneously using AllPrep® DNA/RNA FFPE kit (Qiagen) as per manufacturer's guidelines. The DNA was sent to Dr. Sean Grimmond at Queensland Centre for Medical Genomics (at IMB, UQ) for sequencing while the RNA was reverse transcribed using Quantitect® Reverse Transcriptase kit (Qiagen) as per manufacturer's guidelines and subjected to qPCR using specific sybr and/or Taqman primers.

Results

P495TGHR enhances GHR signalling in Ba/F3 cells

To characterize the effect of the P495T variant on downstream signalling, the well-characterised murine pro-B cell line (Ba/F3) was used. This cell line is IL-3 dependent and does not express endogenous GHR. After retroviral transduction of the variant (P495T or 495) and wild type (WT) GHR into these cells they can proliferate in response to GH. The GHR expression was selected by hygromycin B and verified by western blot.

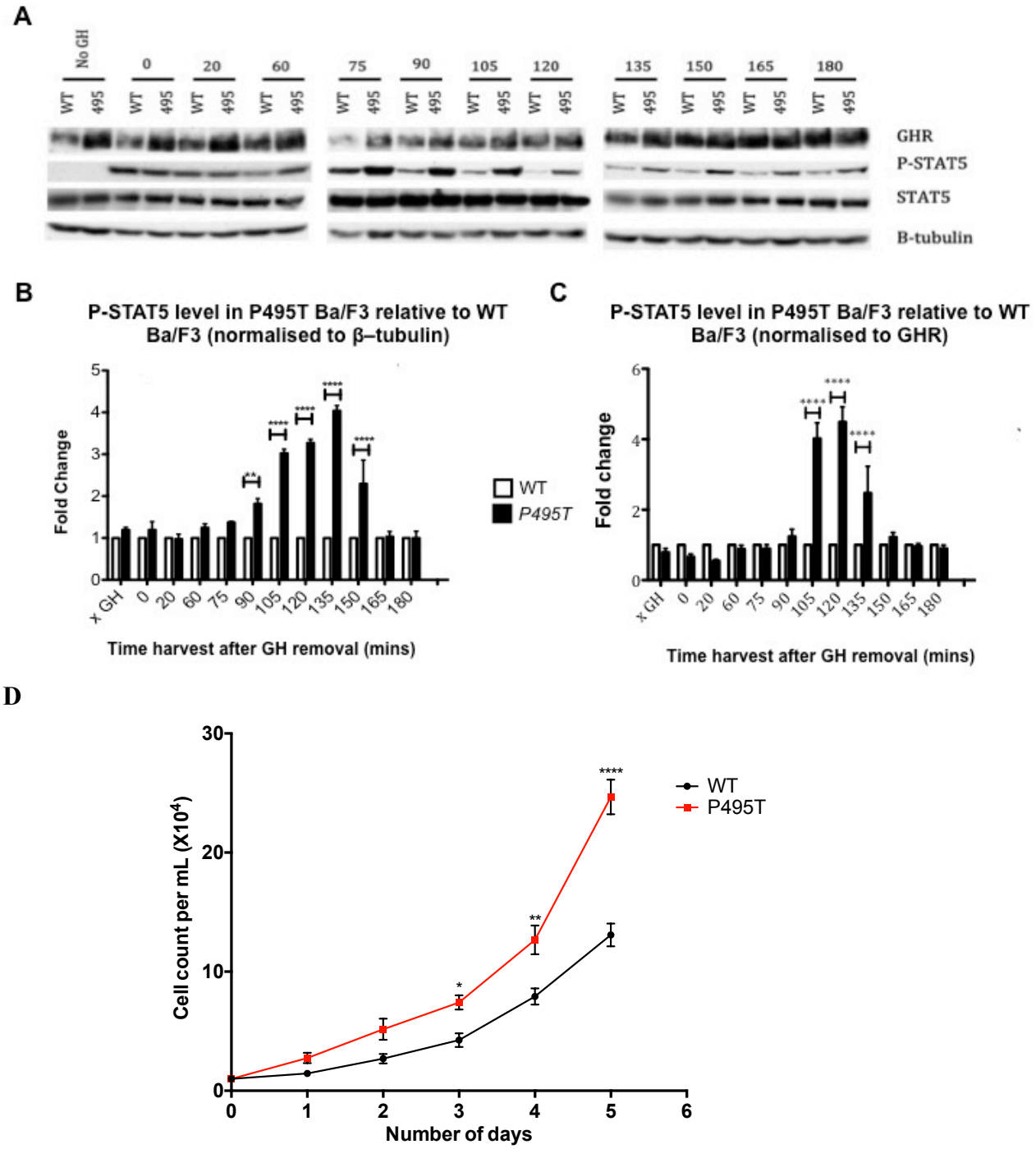

Figure 4.1: Time course analysis of GHR downstream signalling in WT and P495T Ba/F3 cells.

Cells were serum starved overnight and stimulated with 50ng/ml of GH for 15 minutes followed by PBS washes. Cells were returned back into serum starvation medium and harvested at the indicated time points. Enhanced P-STAT5 signalling was observed in P495T Ba/F3 compared to WT (post 90 minutes). (A) The immunoblot of the time course experiment, comparing P-STAT5 level in WT and P495T Ba/F3 cells. (B) P-STAT5 level was quantified and normalized to β-tubulin. The fold change of P-STAT5 levels in P495T Ba/F3 relative to WT is represented graphically. (C) P-STAT5 levels were quantified and normalised to respective GHR level. The fold change of P-STAT5 levels in P495T Ba/F3 relative to WT is represented graphically. (D) Proliferation assay of WT and P495T in growth medium containing GH (100ng/mL) over a period of 5 days starting at a seeding density of 10^4cells/mL. Data representative of n=3 independent experiments confirmed in three separate population studies and clonal lines from three independent transductions (mean ± SEM; ****: P <0.0001, **: P < 0.01, *:P<0.05) analysed by student t-test.

As shown in figure 4.1A, the initial response to GH was similar for both GHR expressing cell lines. The P-STAT5 levels normalised to beta-tubulin was enhanced in P495T Ba/F3 cells from 60 minutes and peaked at 135 minutes, when there was 4 fold more P-STAT5 in the P495T Ba/F3 relative to WT.

After serum starvation, P495T was found to have a higher basal GHR expression level than WT GHR. In order to determine if this was a clonal artifact, stably transduced cells were created by retroviral transduction in three independent experiments, and in each of the three rounds the P495T mutant exhibited higher GHR expression than WT after serum starvation. This suggested that the mutant receptor (P495T) had an inherent ability to enhance receptor expression in this cell line. However, the level of P495T and WT GHR became similar after 105 minutes following a GH pulse, which indicates that P495T GHR Ba/F3 retains the ability to downregulate in response to GH stimulation. Notably, activated STAT5 levels in P495T cells were still significantly higher than that in WT even when both the receptor levels became similar (fig.4.1A). The higher P-STAT5 level at the later time points despite the same level of GHR in both Ba/F3 lines is indicative that this GHR polymorphism hindered the termination of the Jak/STAT5 pathway.

As GHR levels determines the sensitivity to GH stimulation as well as the strength of P-STAT5 signalling, we sought to determine if the enhanced P-STAT5 level was solely due to the higher GHR expression in P495T Ba/F3 or an effect of polymorphism in enhancing the P-STAT5 level. This was achieved by normalising the levels of P-STAT5 to the respective GHR level as represented in figure 4.1C. Significantly, the P-STAT5 level was 4 fold higher in P495T Ba/F3 at 105 to 120 minutes. This suggested that the difference in the active STAT5 level is only partially a result of the enhanced GHR expression of P495T in Ba/F3 cells, and that this variant was intrinsically able to signal for a longer time following a GH pulse, as occurs *in vivo*. In addition, the proliferation assay on Ba/F3 cells indicated a significant increase in cell number of P495T Ba/F3 cells analysed over a period of days starting at the same cell density (fig.4.1D).

P495TGHR is a potential driver for lung tumourigenesis

According to the two GWAS studies, P495TGHR is strongly associated with lung tumourigenesis. To study the action of this mutant in lung cells, stably transduced human bronchial epithelial cells (BEAS-2B) with P495T and WT GHR were used. Similar to the Ba/F3 model, P495T BEAS-2B showed prolonged GHR downstream signalling and therefore a similar prolonged P-STAT5

signalling as observed in Ba/F3 cells was expected, but we found the STAT5 signal was weak and dropped to an undetectable level within 45 minutes (data not shown).

However, GHR activation of the PI3-K pathway was altered in BEAS-2B P495T line. The P-Akt response to GH was significantly stronger in P495T BEAS-2B at 45-60 minutes before falling to a similar level by 90 minutes suggesting that P495T BEAS-2B signalling via Akt was enhanced (fig.4.2B). This was more evident for P-Akt Thr308 than for P-Akt Ser473 and correlated with mature GHR levels (the upper band) representing the receptor on cell surface (fig.4.2A).

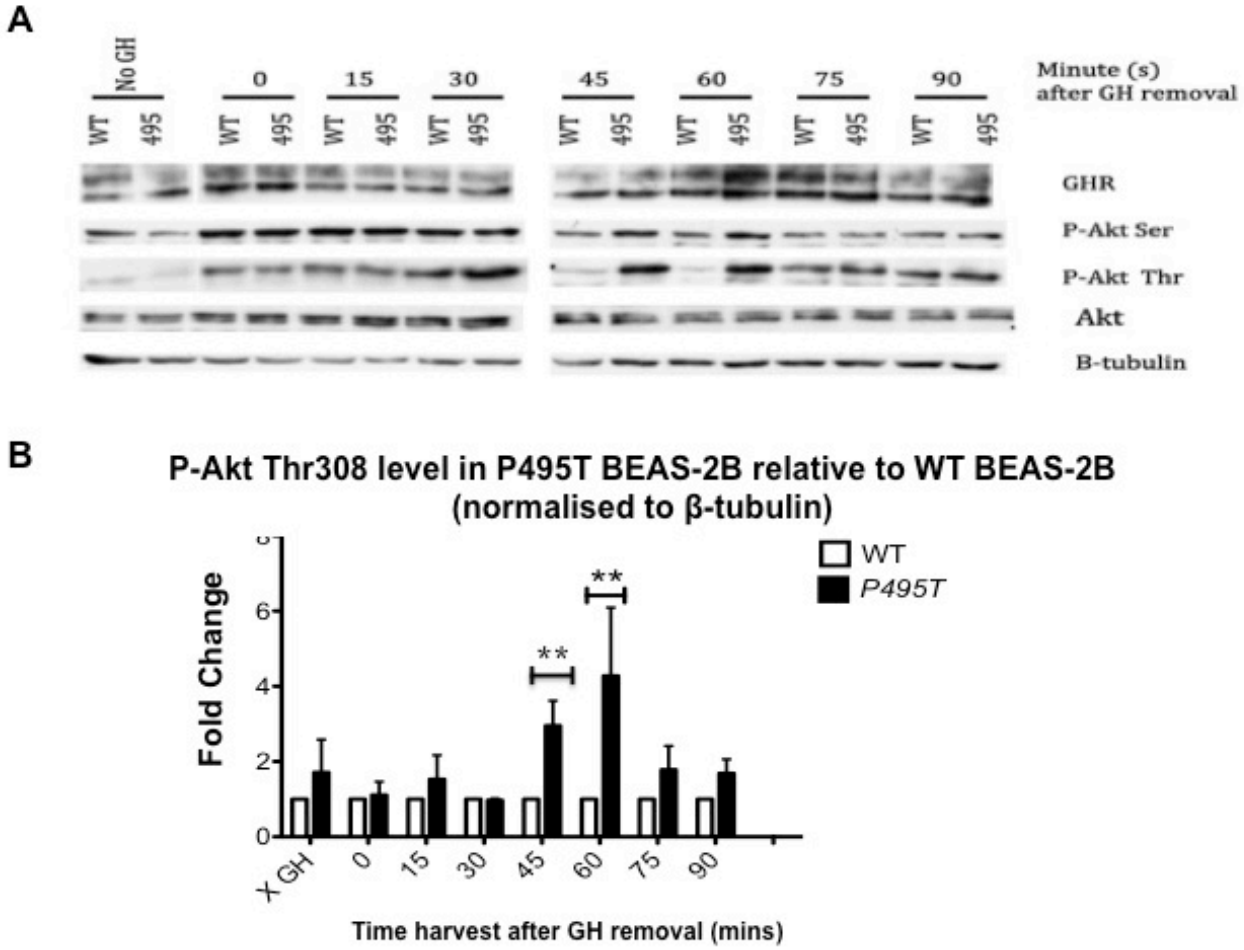

Figure 4.2: Time course of GHR downstream signalling in WT and P495T BEAS-2B.

Cells were serum starved overnight followed by acute GH (50ng/ml) stimulation for 15 minutes. The cells were washed and harvested at the indicated time points. (A) P495T BEAS-2B showed an enhanced P-Akt signalling particularly between 30-75 minutes. (B) P-Akt Thr308 levels were quantified and normalised to β-tubulin and represented as fold change of P-Akt levels in P495T BEAS-2B relative to WT. (n=3 independent experiments, mean ± SEM) **:P<0.01 analysed by student t-test.

Furthermore, P-Akt Ser473 followed the same trend as that of P-Akt Thr308 but with lower amplitude and did not reach statistical significance.

The difference in GHR level at early time points was not as significant in the BEAS-2B cells compared to that observed in Ba/F3 cells. Nonetheless, the GHR level of 495 BEAS-2B at 60 minutes was clearly higher. Again receptor levels came back to similar levels by 75 minutes, which implies the degradation mechanism of GHR in P495T BEAS-2B might be impaired leading to a delay in GHR downregulation. It is important to note that this result was consistent with the observation that we obtained in Ba/F3 cells where the GHR level in P495T mutants was higher than the WT.

To further demonstrate that the variant P495T has an altered GHR degradation system, the time course assay was repeated with a second dose of GH at 60 or 120 minutes where the GHR level differed to the greatest extent in the previous time course assays. Figure 4.3 shows the receptor level of WT and P495T BEAS-2B after this second acute GH stimulation. Similar to the above result, P495T was more resistant to GHR degradation as these cells had a higher GHR level after the second GH stimulation (indicated as 60+ and 120+) particularly of the mature, cell surface level. This indicates that the GHR P495T has a negative effect on the GHR degradation mechanism.

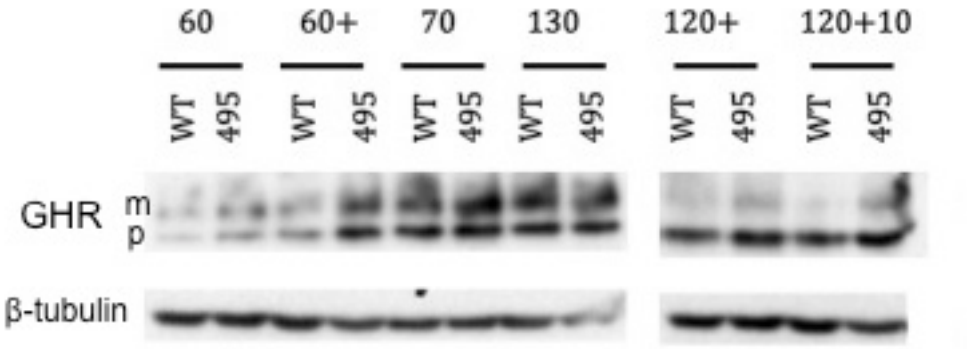

Figure 4.3: Time course of second acute GH stimulation at 60 and 120minutes following the first GH removal in WT and P495T BEAS-2B cells.

The GHR receptor level in P495T BEAS-2B cells was higher at 60 minutes and after 120minutes following the initial acute GH stimulation. After a second GH treatment at 50ng/ml for 15minutes (indicated as +), cells were harvested after 10 minutes indicated as (60+10 and 120+10 time point), WT BEAS-2B showed degradation of GHR level as compared to P495T BEAS-2B, which seems to be impaired as evident from the level of mature receptor (m) and precursor (p).

P495TGHR enhances GHR surface cells in DU145 cells

Although the outcome of P495TGHR polymorphism has only been analysed in context with lung cancer, there is a possibility that this polymorphism can have an impact on prostate tumourigenesis. Therefore, GHR were retrovirally transduced into DU145 (human prostate cancer cell line) and time course analysis was carried out as for the two other cell lines described above.

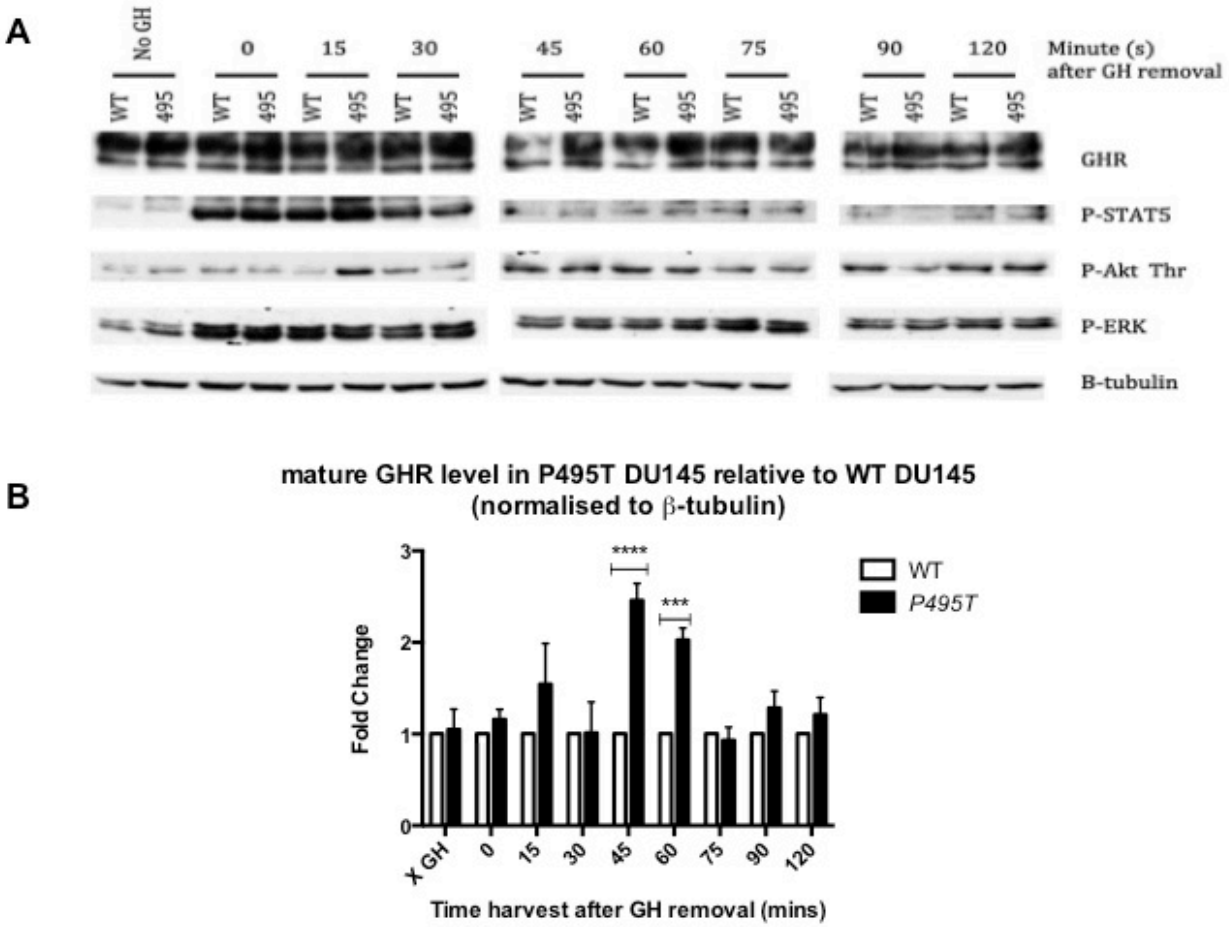

Figure 4.4: Time course analysis of GHR downstream signalling in WT and P495T DU145 cells.

WT and P495T DU145 cells were serum starved for 24hrs and subjected to acute (50ng/ml) stimulation followed by subsequent washes and harvested at indicated time points following GH removal. (A) The representative immunoblot for shows the level of signalling molecules. (B) Fold change of P495T GHR relative to WT normalised to β-tubulin. (n=3 independent experiments, mean ± SEM) ****:P<0.0001, ***:P<0.001 analysed by student t-test.

Similar to Ba/F3 and BEAS-2B, P495T DU145 showed a higher level of mature GHR upon stimulation, suggesting that P495T has an impaired GHR regulation system. Consistently, the GHR levels of P495T DU145 were higher at 45-60 minutes (fig.4.4B) but no distinct effect on the P-STAT5 and P-Akt signalling was observed at these time points. This may be due to the low endogenous levels of total STAT5 and Akt. Since DU145 is primarily an ERK-driven cancer cell line, we analysed the levels of active ERK. However, no statistical significance was achieved.

Impaired SOCS2 binding on P495T GHR

The Tyrosine at 487 has been shown to be the binding site for SOCS2 (Vesterlund et al, 2011). Due to the close proximity of the P495T polymorphism to this tyrosine we hypothesised that SOCS2 binding to this variant might be impaired due to steric hindrance. This was analysed by co-immunoprecipitation (co-IP) studies on HEK293 stables expressing WT and P495T GHR. As evident in figure 4.5A, SOCS2 binds to the mature glycosylated GHR (m) present on the cell

surface after GH stimulation in both cell lines but this is significantly less in the case of P495T GHR (fig.4.5B). Since CIS has been shown to bind to Y487 there is a possibility that CIS binding to the GHR might also be impaired in P495T but has yet to be analysed. In addition, the level of SOCS2 transcript in HEK293 stables was determined following a time course assay to evaluate if P495T had any effect on SOCS2 at transcriptional level. No difference in SOCS2 mRNA was observed at matching time intervals between WT and P495T (fig.4.5C) but there was a clear induction of *Socs2* transcription following GH treatment at all the time points analysed.

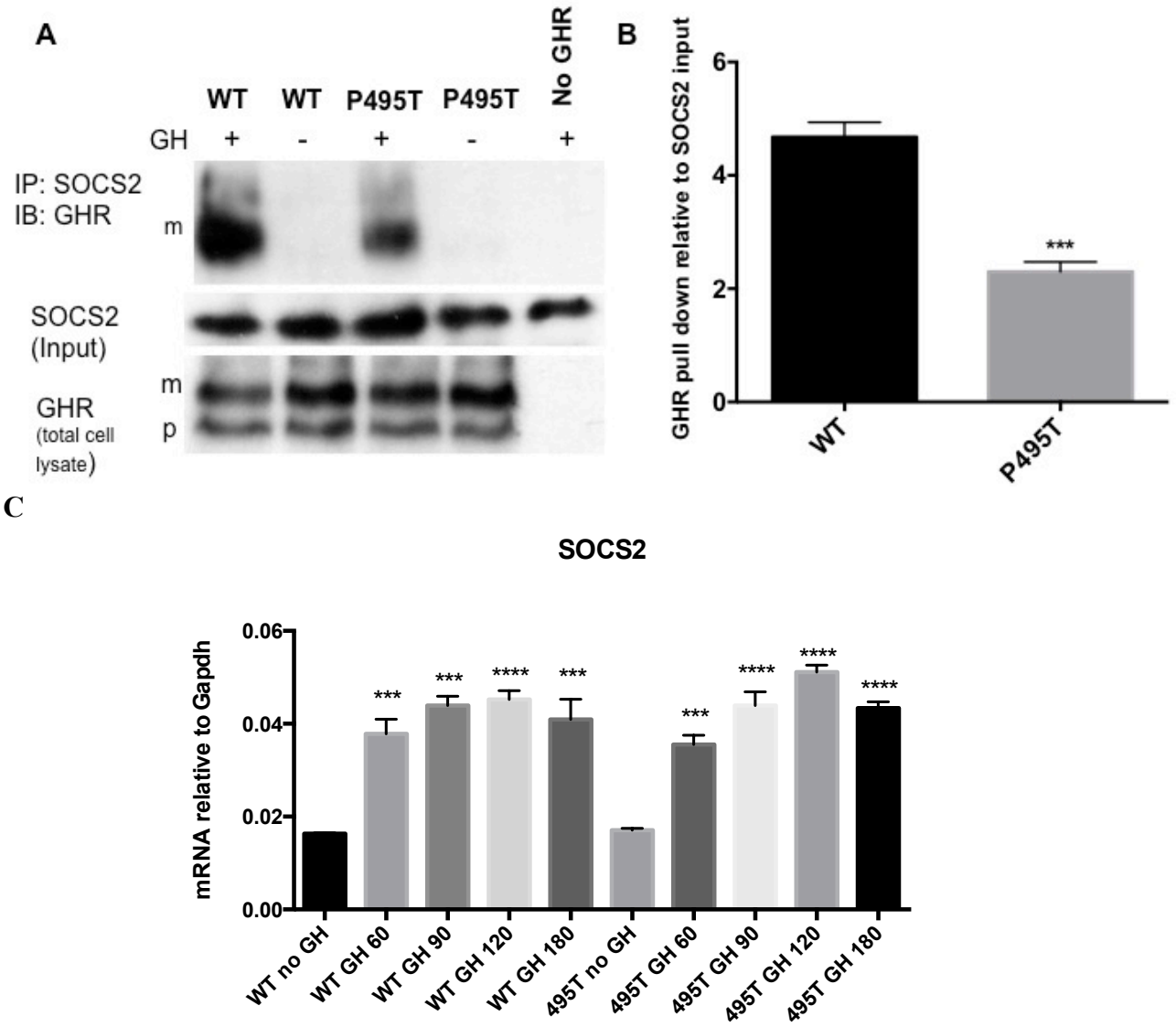

Figure 4.5: SOCS2 induction and impaired binding of SOCS2 to P495TGHR in HEK293 cells.

Parental cells (no GHR) and cells stably expressing WT and P495T GHR were transfected with 2μg SOCS2 for 24hrs and starved for overnight before GH stimulation (100ng/ml) for 15 were minutes. Cells were harvested in co-immunoprecipitation buffer (refer materials and method) and lysates subjected to SOCS2 antibody pull down and with antibody coated on sepharose beads. The protein complex was boiled and resolved on a gradient gel. (A) The immunoblot for SOCS2 pull down was probed for GHR using HA antibody. m refers to the mature glycosylated form, p is the precursor or unglycosylated form and SOCS2 was used as input along with GHR expression in total cell lysates. (B) The GHR pull down was quantified for WT and 495 relative to the SOCS2 input (corrected for GHR expression) and

represented as densitometry units. (C) SOCS2 mRNA levels in HEK293 WT and P495T stables following a time course experiment are similar (mean ± SD) ****:P<0.0001, ***:P<0.001,**:P<0.01, n=4 independent experiments analysed by student t-test (in B) and ANOVA (in C).

CIS is not a direct binding partner of GHR

Based on MAPPIT analysis, phosphorylated Y487 and Y595 on GHR have been predicted to be binding sites for CIS ubiquitin ligase as well (Uyttendaele et al, 2007). To date, no direct interaction of CIS with GHR has been shown. In order to determine if P495T hinders the CIS interaction as for SOCS2, a co-IP analysis was performed. HEK293 cells stably expressing WT GHR was transfected with equal amounts of SOCS2 and CIS expression plasmids. The same lysate was divided in to two parts and subjected to CIS and SOCS2 co-IP. However, no CIS interaction was detectable in comparison to SOCS2 as shown in figure 4.6. Other experiments of CIS co-IP in the absence of SOCS2 in HEK293 stable or transiently transfected WT GHR levels did not reveal any detectable interaction with GHR (data not shown). It is evident from the blot (fig.4.6) that the CIS interaction with GHR is not direct like that of SOCS2.

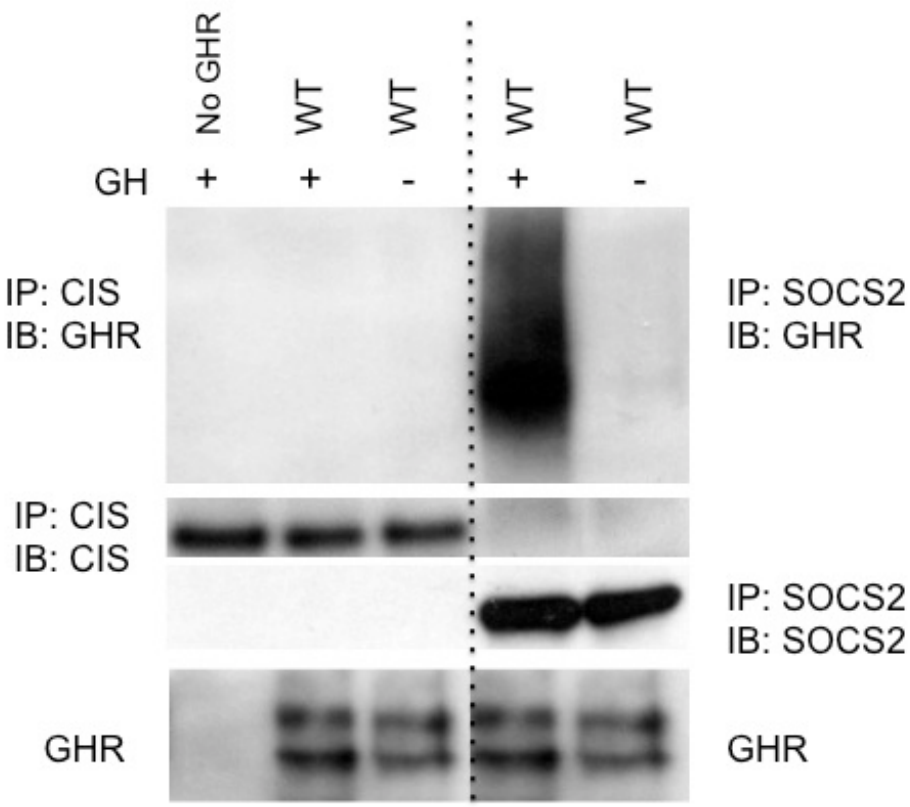

Figure 4.6: CIS protein does not interact strongly with GHR as compared to SOCS2.

HEK293 cells stable for WT GHR were transfected with CIS and SOCS2 plasmid (1μg each) simultaneously for 24hrs and starved overnight before GH stimulation (100ng/ml) for 15minutes. Cells were harvested in co-immunoprecipitation buffer and lysates were divided into two equal parts and subjected to SOCS2 or CIS antibody pull down separately and simultaneously and complexed on sepharose beads. The protein complexes was boiled and resolved on a SDS-PAGE gel. The blot shows clear pull down of GHR by SOCS2 indicating direct binary interaction whereas no such interaction

was seen in CIS. The blots are representative of n=2 independent experiments.

Continuous turnover of SOCS *in vivo*

In order to determine the physiological levels of SOCS2 and CIS with regards to GHR status in liver, both qPCR and western blot was carried out in tissues from WT and GHR KO (GHBP/GHR null) mice. As expected there was a decline in SOCS2 and CIS mRNA in GHR KO owing to lack of GHR activated STAT5. Interestingly, the protein levels for both of these were in contrast to their mRNA levels, with more SOCS2 protein in GHR KO and no significant change in CIS as compared to WT mice (fig.4.7). The latter result is consistent with impaired turnover of SOCS2 protein as a result of lack of GHR-mediated proteolysis, unlike CIS. Even though CIS transcript was higher in WT mice no change was observed at the protein level when compared to GHR KO confirming that CIS does not directly interact with GHR.

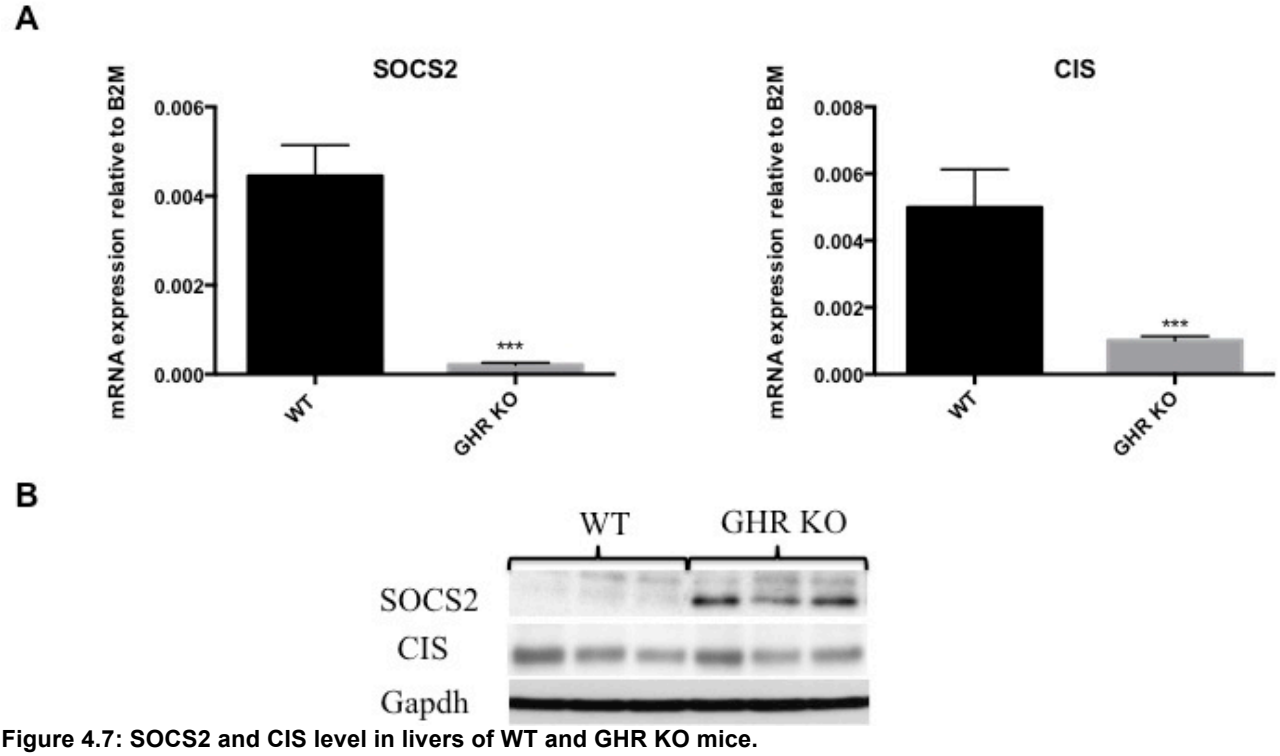

Figure 4.7: SOCS2 and CIS level in livers of WT and GHR KO mice.

(A) SOCS2 and CIS mRNA hepatic levels from age-matched male mice (age 12weeks) represented as relative to B2M. (B) Immunoblot of SOCS2 and CIS in the liver of the same mice shows contrasting levels of protein as compared to the transcript. (n=4/genotype, mean ± SEM) ***:P<0.001,**:P<0.01 analysed by student t-test.

Effect of Brefeldin A on P495TGHR

In order to ensure that the difference observed in mature GHR isoform between WT and P495T is due to delay in GHR degradation rather than increased synthesis, Brefeldin A (BFA) was used. BFA is an inhibitor of protein transport from Endoplasmic Reticulum (ER) to Golgi therefore

decreasing surface GHR incorporation. A similar time course experiment was carried out on HEK293 stable cells that were continuously treated with BFA (1µg/ml) starting 1hr before GH stimulation until harvesting at indicated time points.

A

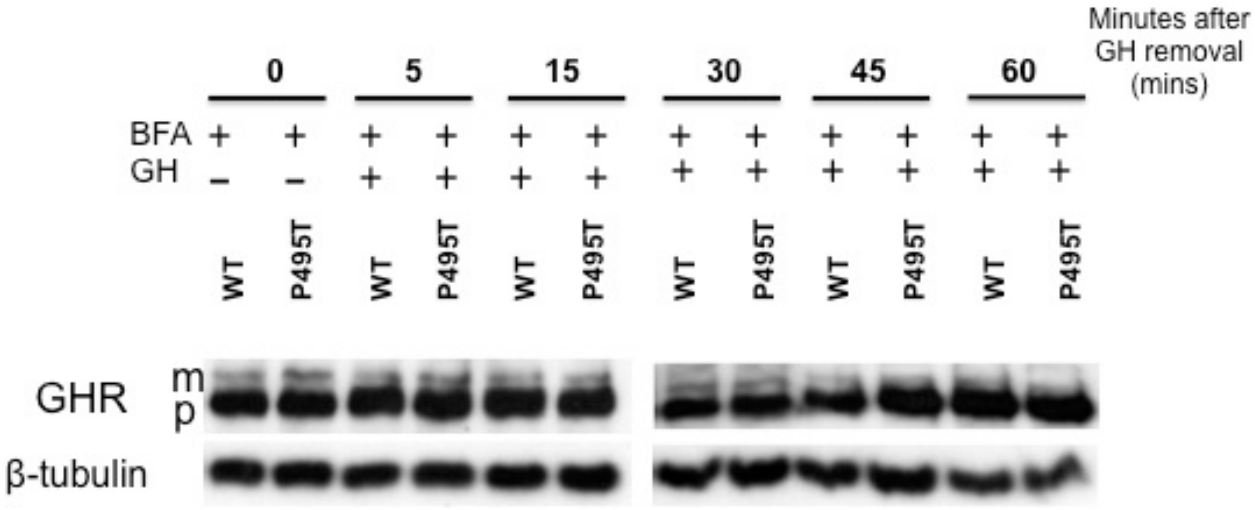

B

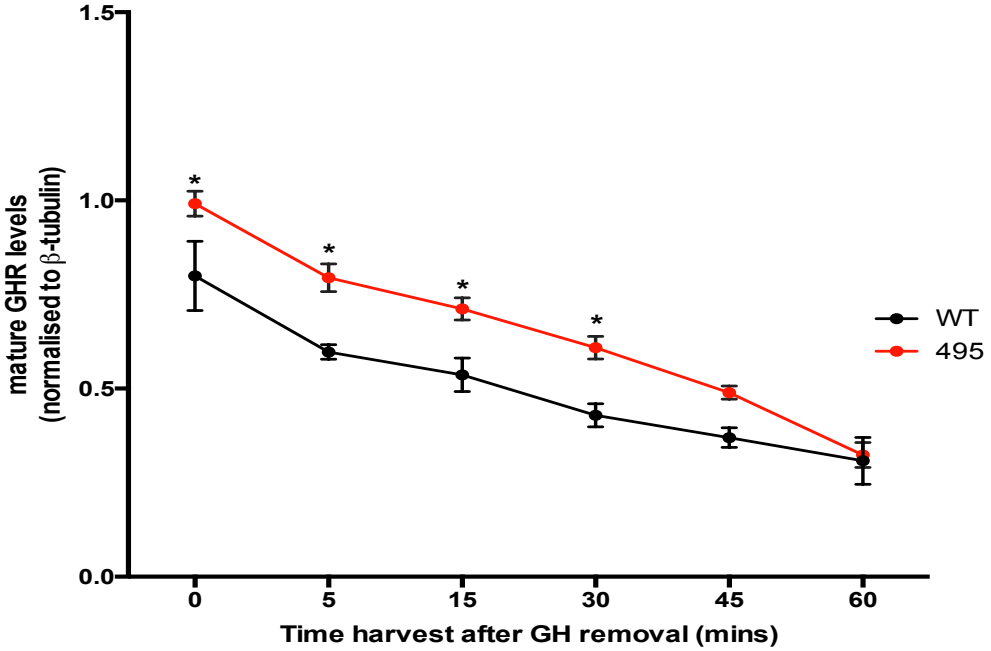

Figure 4.8: Effect of Brefeldin A treatment on HEK293 WT and P495T GHR.

Cells stably expressing WT and P495T were starved overnight and treated with BFA starting 1hr before the GH stimulation (50ng/ml) of 15 minutes and subjected to time course analysis described earlier with continuous BFA treatment till harvest. (A) Immunoblot depicting the effects of BFA treatment. Before the addition of GH there is a clear difference between the levels of mature (m) GHR in WT and P495T that is maintained through the different time points analysed. With subsequent BFA treatment the ratio of mature GHR to precursor GHR decreases. (B) Graph representing the downregulation of mature GHR levels (m) in WT and P495T HEK293, following BFA and acute GH treatment, normalised to β-tubulin. (n=4 independent experiments, mean ± SEM) *:P<0.05 analysed by student t-test.

The addition of BFA resulted in a decrease in the level of glycosylated mature GHR (m) and an increase in precursor (p) levels in both WT and P495T. There is however a clear difference between the levels of mature GHR isoform (m) suggesting less receptor on the surface of WT as compared

to P495T before and after a GH pulse as shown in figure 4.8. This is consistent with increased cell surface GHR (m) observed in three different P495T cell lines.

Altered receptor turnover in P495T GHR

Further analysis of P495T HEK293 stable revealed undetectable bands that were otherwise evident at 60kDa and 43kDa for GHR remnants (indicated by arrows) in WT cell lysates. These bands were only observed in HEK293 stables for the WT receptor (as opposed to transiently transfected) indicating that it was part of routine receptor endocytosis (or turnover) that occurs *in vitro*. Another observation (fig.4.9A) was that the generation of these bands was independent of GH treatment. In order to determine if these bands were an outcome of reduced endocytosis owing to decreased proteolytic or γ–secretase activity, specific inhibitors were used. A potent 26S proteasomal inhibitor, MG132 pre-treatment at 10μM for 2hrs on HEK293 stables did increase the mature GHR form but had no effect on the two remnants in WT or P495T as compared to treatment of the cell lines with DMSO alone (control). A similar effect was seen following treatment with another irreversible proteasomal inhibitor clasto-lactacystin β-lactone at 10μM for 4hrs. Finally, a γ–secretase inhibitor, DAPT was used and no difference was observed evident with higher dose up to 10μM for 4hrs. These analyses with inhibitors were indicative that the remnants seen in WT appear not to be due to proteasomal degradation.

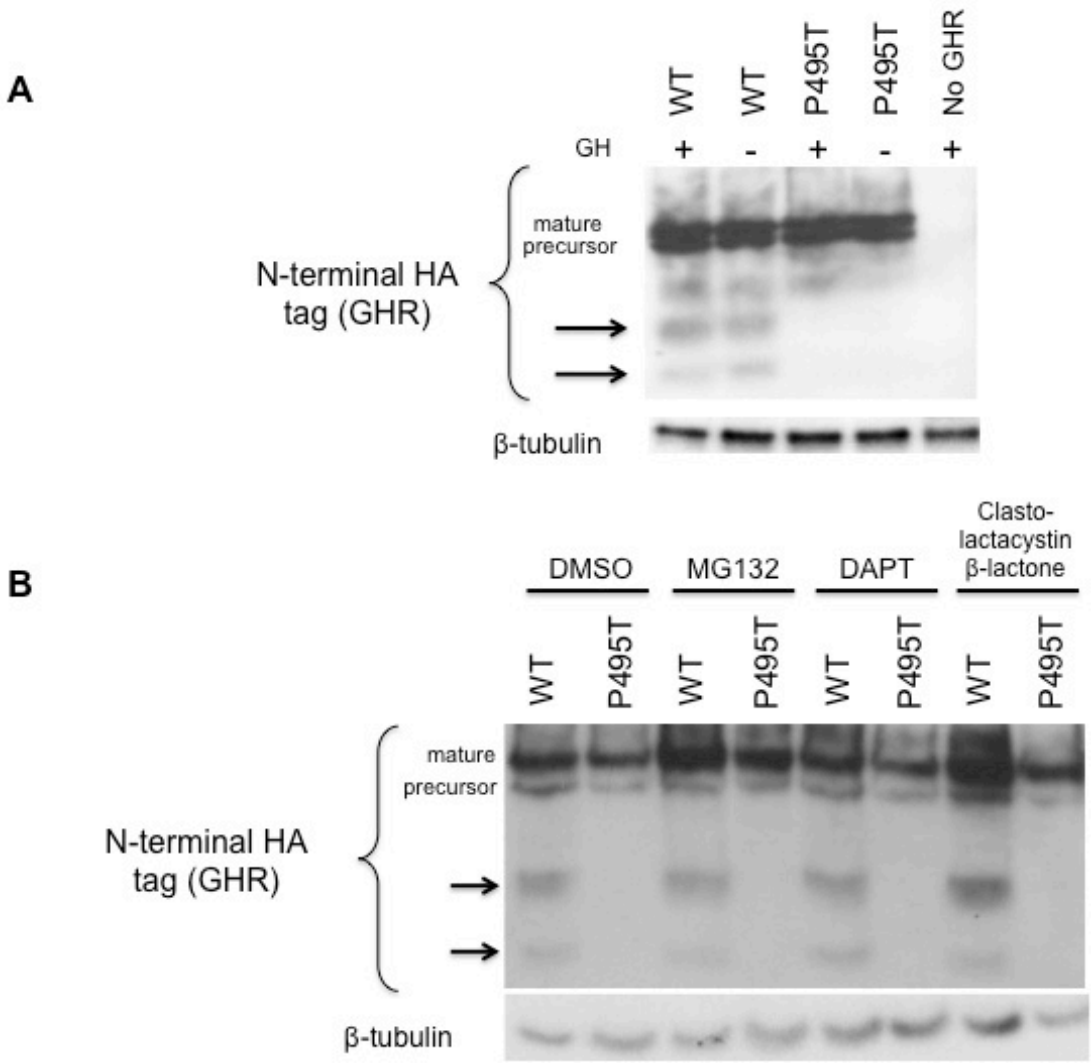

Figure 4.9: Appearance of remnants in WT GHR and the effect of proteasomal and γ–secretase inhibitors on WT and P495TGHR in HEK293.

(A) HEK293 WT and P495T stables were starved overnight and stimulated with GH (50ng/ml) for 15 minutes and harvested. The lysate were subjected to SDS-PAGE. There were 2 remnant bands observed at 60kDa and 43kDa (indicated with arrows) only in WT and undetectable in P495T. Blots representative of n=10 independent experiments. (B) HEK293 WT and P495T were subjected to MG132 (2hrs), DAPT (4hrs) and clasto-lactacystin β-lactone (4hrs) at 10μM each, harvested and analysed on SDS-PAGE. No effect of these inhibitors was evident on the WT remnants while none were detectable in P495T. Blots representative of n=4 independent experiments.

Conserved P495 and surrounding residues of GHR

To determine if P495 (highlighted in red fig.4.10) and the residues surrounding it were conserved in other species, a multiple alignment analysis was performed using ClustalW2 program (EMBL-EBI) as shown in figure 4.10. Intriguingly, besides proline at 495 a stretch of amino acids upstream and downstream of it was also conserved. The distinctive cyclic structure of proline's side chain gives it an exceptional conformational rigidity compared to other amino acids and since there is no known structure of the GHR intracellular domain, it can only be postulated that the proline to threonine

conversion might cause significant structural changes since patients heterozygous for the variant GHR allele were also susceptible to lung cancer (Cao et al, 2008).

Figure 4.10: Multiple sequence alignment of the GHR polypeptide around P495.

The residue Proline at 495 is highlighted in red and is conserved all through the species along with ~8 residues both upstream and downstream to it.

Sequencing of Prostate Cancer slides

To determine if other GHR polymorphism similar to P495T as well as variants in GH1, GH2, STAT5A and B, and Jak2 occurs in prostate cancer, the extracted genomic DNA was sent for sequencing. The analysis was not completed at the time of writing the thesis. However, the RNA extracted from the same specimens, although clean was not amenable to amplification by PCR for house keeping gene-specific primers (Ct values over 32) and therefore not pursued further.

Discussion

Lung cancer is frequently cited as a malignancy solely attributable to environmental exposure. However, it has long been postulated that individuals may differ in their susceptibility with increasing evidence from epidemiological studies for a familial risk (Matakidou et al, 2005). Direct evidence for a genetic predisposition is evident from the increased risk of lung cancer associated with a number of rare Mendelian cancer syndromes, such as carriers of tumour protein p53 (TP53) (Hwang et al, 2003) and retinoblastoma (Sanders et al, 1989) gene mutations. The impact of alterations of GH-induced signalling on the development and progression of lung neoplasia is not fully understood although elevated levels of IGF-1 have been associated with lung cancer (Wang et al, 2013). The P495TGHR polymorphism has been associated with a 2-12-fold increase susceptibility to lung cancer (Rudd et al, 2006; Cao et al, 2008) and is the first GHR mutation that is directly linked to cancer development. We sought to identify the pathway that might be involved and examine its role in cancer development. Three different cell lines were transduced with the WT or P495T GHR expression constructs and subjected to GH-stimulated time course experiments. We identified that the affected signalling pathway was cell line-dependent and hypothesised that

negative regulators of GHR signalling like SOCS and Phosphatases as well as GHR turnover might be impaired and can thus prolong the signalling rather than the P495T receptor being constitutively active.

We found that Ba/F3 cells transduced with P495T GHR have a prolonged active STAT5 signal following a GH pulse as well as a higher basal receptor expression than WT. Although the receptor levels were higher the increase in active STAT5 was statistically significant when normalised to GHR levels. STAT5 activation has been reported in cancers of the breast, prostate, lung, and leukaemia while there is evidence for increased oncogenicity when its constitutively activated (Xiong et al, 2009; Chhabra et al, 2011). Direct evidence comes from constitutively active STAT5 transgenic mice that show a 22% increase incidence of developing mammary tumours (Iavnilovitch et al, 2004). STAT5 can also induce production of reactive oxygen species (ROS) and DNA damage, requirements for cancer initiation (Mallette & Ferbeyre, 2007), however the underlying mechanisms are not clear. In addition, enhanced proliferation of P495T following GH stimulation in Ba/F3 cells suggests that the expression of this mutant in a hematopoietic cell lineage may promote oncogenesis in a similar manner to the Jak2*V617F* or thrombopoietin receptor MPL*W515L/K* (mutation in the cytoplasmic domain), which can result in constitutively active Jak/STAT myeloproliferative disorders (Constantinescu et al, 2008).

In BEAS-2B cells there was a significant increase in active Akt(Thr308) and GHR levels evident in P495T compared to WT. Importantly the increase in GHR levels was further exacerbated following a second GH pulse indicating that GH-induced degradation is impaired in P495T GHR. The role of PI3-K/Akt pathway in cancer progression is still emerging as many of the underlying mechanisms are not well understood but a recent finding has indicated that active Akt at Thr308 is a better prognostic indicator for non-small cell lung cancer (Vincent et al, 2011). Interestingly, the same cancer modality was found to be significant in the GWAS studies associated with P495TGHR polymorphism (Cao et al, 2008). In ERK-driven DU145 prostate cancer cell line the signalling molecules analysed failed to reach significance but GHR levels were clearly elevated in P495T compared to WT cells.

STAT-mediated negative feedback via SOCS and phosphatases have been studied to a considerable extent with evidence that GH induces expression of SOCS1-3 and CIS. It has been shown that SOCS1-3 terminate GHR signalling largely by ubiquitination through binding at specific tyrosine residues on the GHR (Adams et al, 1998; Tollet-Egnell et al, 1999; Vesterlund et al, 2011). Since the binding of SOCS1 and 3 is either on Jak2 or the tyrosine residues upstream of P495 we analysed

the effect of P495T on SOCS2 and CIS binding as it has been shown to bind to Y487 on GHR by co-IP and MAPPIT studies respectively (Vesterlund et al, 2011; Uyttendaele et al, 2007). Definitive experiments have proven difficult at this stage, at least in part, because endogenous ubiquitinated complexes are expressed at low levels and are short lived and secondly SOCS abundance from ligand induction to protein level takes time. As a consequence, the majority of experiments have been performed by overexpression of SOCS molecules. On similar lines, in HEK293 cells stably expressing WT and P495T and overexpressing SOCS2 we found significantly decreased SOCS2 binding to P495TGHR after GH stimulation. This observation may be attributable to steric hindrance and can explain the increase in STAT5 and Akt signals observed in P495T Ba/F3 and P495T BEAS-2B as a result of delayed degradation of GHR at a given time point by SOCS2. Interestingly, no direct interaction of GHR with CIS has been shown to date and with Y487 and Y595 on GHR predicted as binding site for CIS, it was important to confirm the effect of this variant on CIS binding. Essentially, both CIS and SOCS2 protein are expressed in wide range of tissues with highest expression in lung, liver, heart and skeletal muscle. But we were not able to detect any physical interaction between CIS and GHR as compared to SOCS2 even when the 2 co-IPs were performed on the same lysate (containing both SOCS2 and CIS) simultaneously.

Another important attribute of SOCS2 and CIS is their turnover rate *in vivo*. Both SOCS2 and CIS are maintained at low levels but increase steadily after a GH pulse (Flores-Morales et al, 2006). As a result in the GHR KO mice one would expect less SOCS2 and CIS protein as compared to WT due to complete absence of GH-mediated STAT5-induction of SOCS expression evident from the mRNA transcript analysis. On the contrary we observe more protein levels of SOCS2 and equal level of CIS in mice livers. This highlights two important observations; firstly SOCS2 and CIS transcript expression are dependent on GHR function. Secondly, SOCS2 actions may be exclusive to GHR unlike CIS, as the level of CIS protein does not change between WT and GHR KO unlike the transcript. However, absence of GHR allows SOCS2 protein to accumulate to high levels in liver implying that extent of SOCS2 binding to GHR is important in regulating its action. In relation to the P495T polymorphism *in vivo*, the steady state levels of SOCS2 should be enough to show a prolonged signalling after a GH pulse and secondly due to the pulsatile nature of GH secretion there is a stronger correlation between P495TGHR and lung cancer susceptibility with males over females (Cao et al, 2008). The role of SOCS2 in growth is evident from the fact that SOCS2 KO mice are giant (Greenhalgh et al, 2002) and idiopathic short stature (ISS) patients express high levels of SOCS2 transcripts under basal condition as compared to controls (Ocaranza et al, 2012).

In order to confirm that increased signalling in P495T cells is a surface phenomenon BFA experiments were carried out. Pre-treatment with BFA prior to GH stimulation results in a significant decrease in WT receptor on cell surface (as indicated by mature glycosylated form) compared to P495T in HEK293. This increase in GHR level in P495T is maintained throughout the time course analysis although the rate of decrease appears similar with WT. An important analysis would be to carry out a similar experiment but in the presence of SOCS2 to determine the difference in kinetics due to decreased SOCS2 interaction with P495T GHR. This would give a better idea of the scenario *in vivo*.

The 43kDa and 60kDa bands WT GHR cell lysates differ from the one reported earlier as a consequence of ERAD (endoplasmic reticulum-associated degradation) mechanism (Loesch et al, 2007). The ERAD mechanism occurs in precursor form due to inefficient protein folding and is pronounced in cells where GHR and Jak2 interaction is hindered or absent. Since HEK293 cells express Jak2 and activate STAT5 downstream following GH stimulation in both WT and P495T stable cell lines indicates the remnants we observed are not due to Jak2 and GHR interaction. Additionally, these bands differ from the metalloproteolytic cleavage-induced remnant since that occurs in region (^{242}EED^{244}) proximal to the extracellular domain of the GHR while the residue at 495 position is close to the C-terminal of the intracellular domain. The treatment of HEK293 stables with 26S proteasomal inhibitors; MG132 and clasto-lactacystin β-lactone at high concentrations was unable to reduce these remnants in WT or make them appear in P495T cells. Similar effects were observed with γ–secretase inhibitor, DAPT suggesting that these remnants are not generated as a part of metalloproteolytic or secretase activity since the bands were observed using an anti-HA antibody against the HA-tag present on the N-terminus of the GHR. The effect of lysosomal inhibitors on WT and P495T cells has not yet been analysed.

The existing literature on GHR structure and function have featured mainly on tyrosine phosphorylation which only forms 2.8% of total GHR polypeptide as compared to serine and threonine phosphorylation which form 9% and 6% respectively. It is unknown which of the serine and threonine residues are phosphorylated and the kinases that may be involved especially those in the absence of GH (van Kerkhof et al, 2007). In the case of PRLR, GSK-3β (glycogen synthase kinase-3β) was shown to be the bona fide kinase that phosphorylates the receptor on Ser349 and is required for the recognition of PRLR by β-TrCP, as well as for its ubiquitination and degradation (Plotnikov et al, 2008). The same residue was reported to enhance the stabilisation of PRLR in breast cancer cells (Li et al, 2006) due to reduced phosphorylation by GSK-3β (which itself is inactivated due to inhibitory phosphorylation by ErbB2 and Ras) (Plotnikov et al, 2008).

As observed earlier there was an increase in the level of GHR in P495T stable cells following serum starvation suggesting differential GHR turnover that is GH independent. Based on the unconventional interaction reported for GHR with β-TrCP in the absence of the GH there is no ruling out the possibility of involvement of other E3 ubiquitin ligases that can bind to this well conserved serine/threonine rich sequence. Indeed the potential binding site of cdc4 (cell division control protein 4) contains phosphorylated serine or threonine followed by a proline and a basic amino acid (Orlicky et al, 2003). Although no functional interaction of cdc4 with GHR has been analysed yet it is possible that such an interaction would be impaired in P495T variant (lack of consensus motif due to proline to threonine mutation). Intriguingly another such consensus motif for cdc4 lies 7 residues downstream to 495 and therefore suggests that the variant P495T does not completely inhibit the GHR ubiquitination and degradation but only delays it, enough to prolong the downstream signalling as seen earlier. Cdc4 has been shown to be an important molecule with cdc4 KO mice being embryonically lethal (Tsunematsu et al, 2004) and has been shown to control levels of c-myc, Notch, cyclin E (Teng et al, 2012).

This chapter highlights the attributes associated with the first gain of function variant in GHR and shows that it prolongs signalling in a cell line context owing to delayed degradation of the GHR. This delay can occur in a GH dependent manner due to decreased SOCS2 binding or in the absence of GH by alteration of the GHR turnover due to alteration in degradation, synthesis and/or transport to the surface. The interaction of the variant with other ubiquitin ligases that control the level of receptor at the surface cannot be ruled out. Finally, the increase in susceptibility to cancer by activation of specific signal transduction molecules to GHR can be tissue-specific and ultimately depends on protein abundance of signal activators and suppressors in those tissues. Therefore it remains to be determined if P495TGHR polymorphism is associated with other cancers.

Chapter 5
Establishing the RCAS/TVA System

Introduction

Need for an appropriate animal model

Current research on tumourigenesis seeks to understand the molecular events driving tumour initiation and progression. Gene knockout and transgenic mice have yielded important insights into the contribution of specific mutations to tumourigenesis. However these models carry germline mutations with an inherent potential to affect tissue development and predispose all the cells or tissue to neoplasia. In contrast, the majority of cancers occur somatically due to multiple, heterogeneous mutations in a single cell (Hanahan & Weinberg, 2011). In addition, most transgenic models can be used to study only one or two genetic lesions, but practically several mutations are likely required to produce most tumours. Furthermore, studying interactions of germline mutations requires extensive, expensive, and time-consuming breeding protocols. Previous attempts of generating one such transgenic murine model, over-expressing the NLS-GHR have proven unsuccessful probably because of embryonic lethality as the only transgenic mice produced from this strategy carried a severely truncated GHR gene (Wooh JW PhD thesis, 2008). The recent studies (reviewed in (Chhabra et al, 2011) have provided significant data on the proliferative and tumourigenic effects GH/GHR in addition to its forced localisation into the nucleus. However this data was generated in GHR knockout or GH transgenic mice and athymic nude mice with xenografts, which is not an adequate representation of long-term tumourigenesis. Therefore, in order to define the *in vivo* effects resulting from nuclear localisation of GHR or a constitutively active GHR or cancer associated variant P495TGHR, a tissue-specific gene delivery system is required which allows restriction of expression to a particular cell or tissue. We have therefore sought to establish a strategy to circumvent some of the limitations of a typical transgenic model. This strategy is based on use of the receptor for subgroup-A Avian Sarcoma Leukosis Virus, TVA that allows multiple genes to be introduced somatically into a single transgenic mouse strain.

The RCAS/TVA technology

The RCAS/TVA system (Replication-Competent ASLV long terminal repeat (LTR) with a Splice acceptor) is based on the use of the receptor for subgroup-A of avian sarcoma leukosis virus, TVA that allows genes to be delivered in a tissue specific manner into small animal models (Federspiel et al, 1994). TVA-based systems rely on tissue-specific or generalized expression of a transgene encoding TVA; the expression of TVA on the surface of mammalian cells is sufficient to mediate retroviral infection by subgroup-A Avian Sarcoma Leukosis Viruses (ALSV-A) (Hughes, 2004).

This serves as an important tool for a cell and developmental stage specific delivery of the gene(s) of interest (Orsulic, 2002).

Different retroviral envelopes have been shown to recognise different receptors on the host cell surface (Fisher et al, 1999). The ALSV family, which includes ALSVs, RSV and RCAS vectors have a variety of envelope subtypes, designated from A-J, where A to E have been used in laboratories (Gilbert et al, 1994). The *tva* gene was first cloned from chicken and quail DNA based on its ability to allow infection of mammalian cells by ALSV-A (Bates et al, 1993). The mRNA transcribed from the avian *tva* gene is alternatively spliced to produce at least two proteins- a transmembrane and a GPI-anchored isoform that have identical 83 amino acid ECD, and both are sufficient to permit infection of mammalian cells. While there is no recognised mammalian homolog, a 40 amino acid region ECD is related to a cysteine-rich element found in low density lipoprotein receptor (LDLR) (Rong & Bates, 1995). The role of TVA in avian biology, other than acting as a receptor for subgroup ASLV-A retroviruses, is unknown. The TV-B, D and E receptors recognise aspects of a single receptor, TVB, which is a membrane protein of *fas* ligand receptor family (Adkins et al, 2000; Brojatsch et al, 1996). The receptor for envelope C has not yet been identified. There is evidence that ALSV envelopes mediate viral entry into cell and fusion to host cell membrane only after receptor binding at low pH (Melikyan et al, 2004; Mothes et al, 2000).

Development of the RCAS system

A molecular clone of the DNA genome of the SR-A strain of Rous Sarcoma Virus was modified to delete the *src* oncogene and a unique restriction site (*Cla*I) was inserted in place of the deleted *src* gene (Hughes & Kosik, 1984; Hughes et al, 1987). In RSV, the *src* gene is expressed from a spliced mRNA; the splice acceptor that is needed to generate the *src* message is derived from the cellular *src* gene. The *src* gene is flanked by 100 bp long repeats known as direct repeats (DR). ALVs have one copy of the DR sequence, as only one copy of DR is both necessary and sufficient for viral replication (Sorge & Hughes, 1982). The RCAS vectors contain the downstream copy of DR while the upstream copy of DR was deleted to reduce the loss of inserted genes by a recombination event (Hughes, 2004).

Although one copy of DR substantially reduces the rate at which inserted genes can be removed, inserted sequences still can be lost. This is probably the result of reverse transcriptase jumping between fragments that have no homology. In general, viruses with smaller genomes (RCAS vectors that have lost the inserted gene) replicate more rapidly than those that retain an inserted sequence (Hughes, 2004). However, it is understandable that with every viral passage (reverse

transcription) there occurs a loss of inserted sequences. Unlike the RSV, the ALSV-derived viruses can take up to 2.5kb insert, which is a little larger than the *src* gene (Greenhouse et al, 1988). However, in some cases inserts larger than 2.5kb have been successfully cloned in RCAS vectors and some inserts smaller than 2.5kb have not worked well. A simple, plausible explanation is that the key issue is not the length of the RNA genome but the volume it occupies when it is optimally folded. As a result, sequences that interfere with the expression of the full-length viral genome (sequences containing polyadenylation signals) or those containing direct repeats should be avoided.

Upon viral infection, reverse transcriptase produces a linear viral DNA that is subsequently integrated into the host genome. However, in the nucleus of infected cells, a portion of the linear viral DNA is circularized by host enzymes to produce either one-LTR circles (by homologous recombination within the LTRs) or two LTR circles (by end to end joining of the linear viral DNA) (Butler et al, 2002). These circular forms have no direct role in the viral life cycle, but are extremely useful because they are easy to clone and provide information about mutations and the process of reverse transcription *in vivo*.

In the RCAS vectors, the inserted genes are expressed from the LTR promoter and therefore the LTR completely controls the expression of the insert. There are two key elements that govern the LTR promoter efficiency; the enhancer and the sequence of *pol* gene. The ALV LTR contains a strong enhancer while the mechanism governing the *pol* gene expression is not very clear. But, it has been demonstrated that the substitution of the *pol* gene by Bryan high-titre strain of RSV results in an increase of the infectious titre with enhanced LTR promoter activity by 5-10 fold (Petropoulos & Hughes, 1991). The Bryan strain of RSV was selected for its rapid growth and the resultant RCAS derivatives containing Bryan *pol* gene are called RCASBP (RCAS-Bryan Polymerase). The main advantage of using RCASBP vector is that it does not alter the tissue specificity of the internal promoter (Petropoulos et al, 1992). The original RCAS vectors have two *ClaI* sites, of which one is used to insert foreign gees and the other site is non-functional due to Dam methylation when propagated in the majority of common *E. coli* strains used for cloning (fig.5.1). Hence, the insertion of a DNA segment into the RCAS vector requires their conversion into a *Cla*I fragment using adaptors (Hughes et al, 1987).

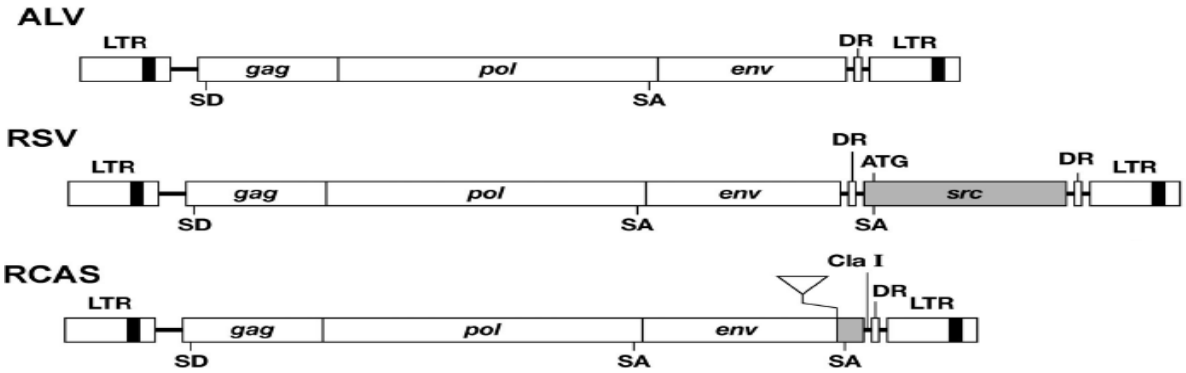

Figure 5.1: Comparison of RSV, ALV and RCAS genomes.

The diagram shows the organisation of viral DNA genomes, the location of the genes (*gag*, *pol*, and *env*), the direct repeats (DR), the splice donor (SD) and splice acceptor (SA) sites. The *src* gene of RSV carries a splice acceptor (SA) that leads to the production of a separate spliced *src* message. The *src* gene also contains its own initiator ATG. The upstream DR has been deleted from RCAS; *src* has also been deleted and replaced by a *Cla*I site. There is a small segment of the *src* gene in RCAS; this segment carries the *src* splice acceptor (Adapted from (Hughes, 2004)).

RCAS Vector Propagation

The RCAS vectors are propagated in cells of avian origin. Originally, chicken embryo fibroblasts (CEFs) were prepared from chicken embryos. Like other primary cells, CEFs have a limited lifespan in culture, usually 20-30 passages. However, due to the presence of inherent endogenous proviruses (closely related to ALSV virus and RCAS vectors) leading to recombination between the vectors and endogenous viruses, a line of chickens, called EV-0, were developed that lacked any endogenous proviruses closely related to the ALSVs. This further led to development of a permanent, non-transformed chicken fibroblastic cell line DF-1 from an EV-0 embryo now routinely used to propagate the RCAS vectors (Himly et al, 1998; Schaefer-Klein et al, 1998).

ALSV viruses do not infect mammalian cells because mammalian cells lack the cognate receptors that recognise one of the standard envelope subgroups (A-J) expressed on the virus envelope. Secondly, even if the entry barrier is overcome, the virus is incapable of producing infectious progenies, thereby making these ALSV viruses doubly-defective in mammalian cells (Young et al, 1993). These problems can be overcome by firstly, using envelope genes from the viruses that are capable of infecting mammalian cells. An example of this strategy is the replication-competent RCAS vectors that use either the ecotropic or the amphotropic envelopes from the murine leukaemia virus (MLV) (Barsov et al, 1996; Barsov et al, 2001). Alternatively, VSVG protein can also be used to prepare viral stocks; however these viruses are replication-defective and other attempts to make replication-competent VSVG/RCAS derivatives have failed as VSVG is too toxic for the host cells to support the spread of a replication-competent retrovirus (Hughes, 2004).

Another solution to overcome the barrier is to express an ALSV receptor (*tva* for subgroup A) in a mammalian cell (or a transgenic animal); this allows efficient infection with RCAS derivatives that have the cognate envelope TVA (fig.5.2) (Federspiel et al, 1994; Fisher et al, 1999; Orsulic, 2002). This concept has been used to generate strains of mice that can be infected in specific cells or tissues.

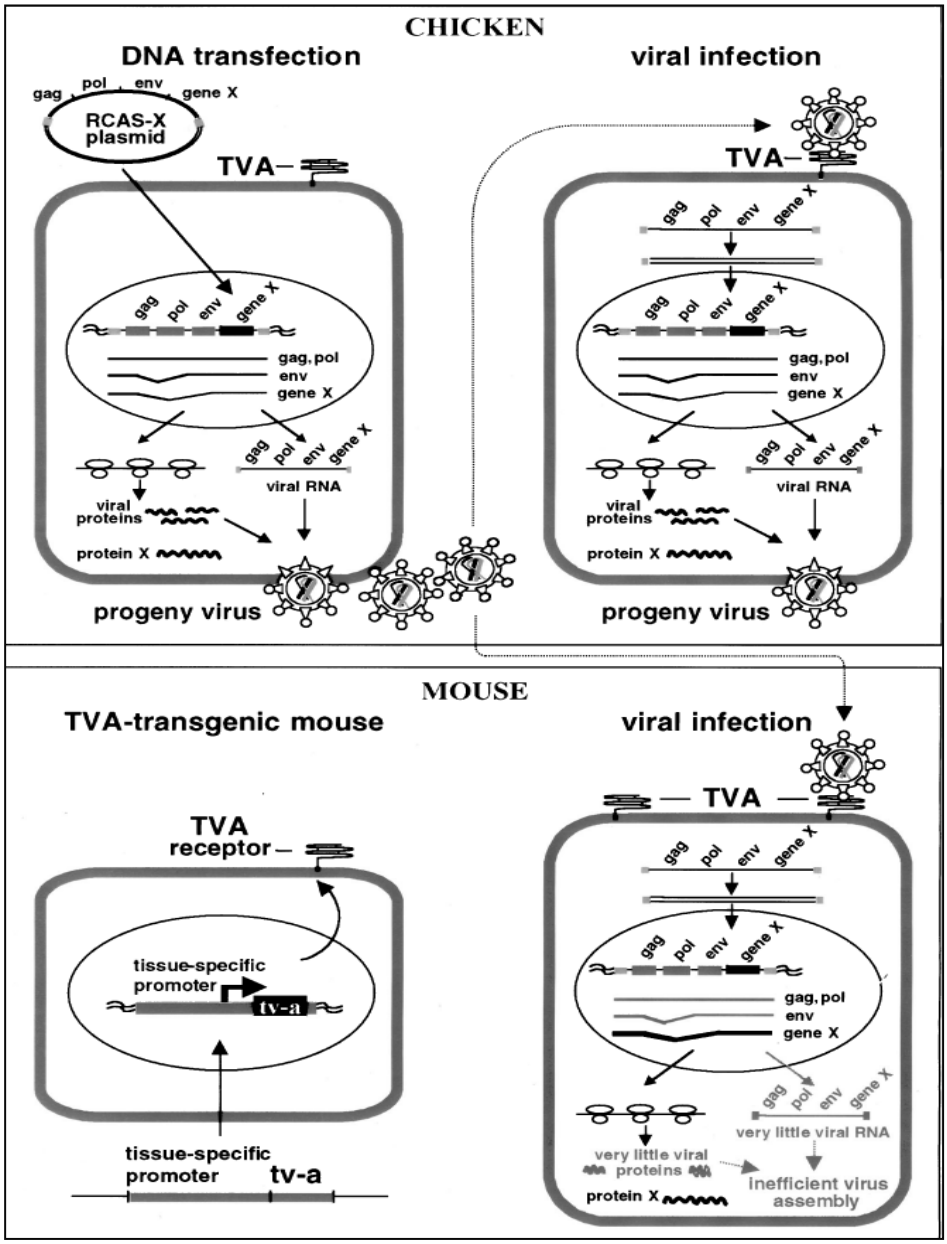

Figure 5.2: Generation of Replication competent retroviral particles

Chicken DF-1 cells are transfected with a plasmid encoding the replication-competent, subgroup-A avian viral vector RCAS which contains the viral genes *gag*, *pol* and *env* and a gene of interest (gene X). The virus is produced in high titre and can infect avian cells through the attachment of its surface glycoproteins to the extracellular domain of the TVA receptor on the cell surface. Mammalian cells do not encode the TVA receptor and therefore are not susceptible to virus infection. However, mammalian cells engineered to express *tva* cDNA under a tissue-specific promoter are susceptible to the viral infection. Unlike avian cells, mammalian cells do not produce infectious RCAS. Only the protein encoded by gene X is efficiently produced in mammalian cells. The lack of viral envelope protein production leaves the TVA receptor unoccupied, permitting repeated infection of mammalian cells with different RCAS viruses from chicken producer cells (Fisher et al, 1999).

Replication Defective Lentiviral Vector

During the past decade, gene delivery vehicles based on HIV-1, the best characterised of the lentiviruses, have been developed. Lentiviral vectors, a subclass of retroviruses, offer unique versatility and robustness as DNA delivery vehicles as they can transduce a wide range of cell types and integrate into the host genome in both dividing and post-mitotic cells, resulting in long-term expression of transgene both *in vitro* and *in vivo* (Tiscornia et al, 2006). Since they are replication-deficient they reduce the risk of insertional mutagenesis and oncogene activation as they lack overlapping sequences of the retroviral genome (Delenda, 2004).

The HIV-1 genome contains 9 open reading frames encoding at least 15 distinct structural and regulatory proteins that are involved in the infectious cycle. In addition, there are a number of *cis*-acting elements required at various stages of the viral life cycle. These include long terminal repeats (LTRs), the TAT activation region (TAR), splice donor and acceptor sites, packaging and dimerisation signal (ψ), Rev-responsive element (RRE) and the central and terminal polypurine tracts (PPT) (Trono, 2002). The general strategy for the production of the viral particles involves elimination of all the dispensable genes from HIV-1 genome and separating the *cis*-acting sequences from *trans*-acting factors that are absolutely important for viral production, infection and integration (Delenda, 2004).

In vitro, these vectors are produced by transient transfection or stable integration of the replication defective vector genomes in a packaging cell line containing stably integrated retroviral genome *trans*- sequences (*gag*, *pol*, *env*) but lacking the packaging signal sequence necessary to encapsidate them. One of the latest improvements in the lentiviral vector design has been the development of self-inactivating lentiviral vectors (SINs) (Zufferey et al, 1998). This is carried out by deletion in the 3`-LTR which reduces homologous recombination between the transfer vector and packaging constructs and also reduces the competition between the 5`-LTR promoter and internal promoter (Sclimenti et al, 2001; Zufferey et al, 1998). A second modification in the lentiviral utility is the envelope substitution which is achievable by transfecting an envelope negative packaging cell line with a heterologous *env* expression construct (Sakalian & Hunter, 1998) (fig.5.3). After efficient incorporation, these pseudotyped lentiviral particles reflect the host range of the virus from which the envelope protein has been derived.

The second generation systems were the most commonly utilized viral generation plasmids which separate packaging and gene transfer functions into three distinct plasmids and lacking certain viral accessory genes (Stewart et al, 2003). In general, lentiviral vectors with a wild type 5' LTR need the

second-generation packaging system because these vectors require TAT for activation. In contrast, the third generation systems go even further by using three helper plasmids: a packaging construct, an envelope construct and a Rev construct, along with a Tat-independent gene transfer vector, providing 4 separate plasmids in all. This lentiviral transfer vector is made TAT-independent by constructing a chimeric 5' LTR in which HIV-1 promoter is replaced with a CMV or RSV. This generation packaging system offers maximal biosafety (Dull et al, 1998; Klages et al, 2000). Although both 2nd and 3rd generation vectors are generally self-inactivating by virtue of promoter disabling mutations engineered into the U3 region of the 3' LTR, the elimination of the accessory gene *Tat* provides an additional level of safety.

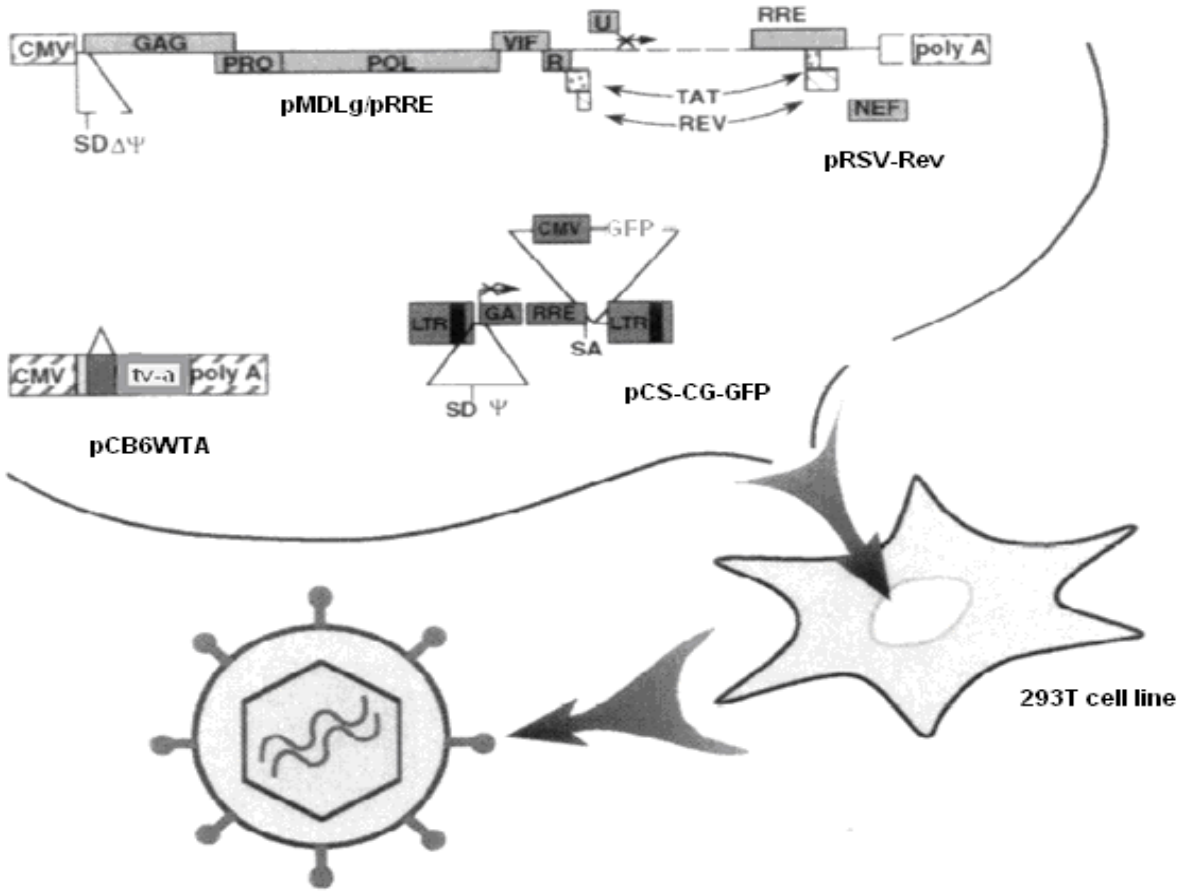

Figure 5.3: Schematic representation of generation of lentiviral vector.

The main elements of the four plasmids co-transfected into 293T cells are depicted. pMDLg/pRRE, the packaging construct, provides most of the viral structural proteins but the envelope. The viral genes are expressed from the CMV promoter and the polyadenylylation site. Proviral 5' leader and P sequences have been deleted together with a large portion of the *env* gene. A translation stop codon was inserted upstream of the remaining *env* segment. The major 5' splice donor site (SD) has been conserved. pRSV-Rev provides the Rev protein for nuclear export of RNA. pCS-CG-GFP, the transducing vector encoding for GFP, provides the vector genome. The viral long terminal repeats (LTRs) and the P sequence are indicated. The *gag* gene is truncated after 350bp and is out of frame (x), and it follows the Rev responsive element (RRE) and a splice acceptor site (SA). The position of a CMV-driven expression cassette for the GFP cDNA is shown. pCB6WTA encodes the ALSV-A envelope that pseudotypes the virus for binding specifically to the TVA receptor. (Adapted from (Naldini et al, 1996).

TVA in Animal Models

As indicated above, mammalian cells are not susceptible because of a lack of suitable cell surface receptors for viral entry and infection. This has however changed with the cloning of the *tva* gene, which encodes for the TVA receptor. It was shown that ectopic expression of *tva* gene in mammalian cells allows for viral entry and chromosomal integration by ALSV-A (Bates et al, 1993; Young et al, 1993). This discovery has enabled the generation of mammalian cell lines and transgenic mouse lines that express the TVA cell surface receptor, thus rendering the cells susceptible to infection with RCAS viruses or ALSV-A pseudotyped lentiviruses.

The TVA transgenic mice have an added advantage that TVA receptor can be expressed under the control of a specific promoter in order to develop a system for cell- or tissue specific gene targeting (Dunn et al, 2000; Federspiel et al, 1994). Therefore, only mice cells that are engineered to express the TVA receptor can be infected, while mouse cells that do not express the *tva* gene homolog are resistant to ALSV-A infections. After the viral entry into TVA-positive mammalian cells, a newly synthesised DNA copy of the viral genome integrates into the host DNA, and the viral LTR promotes a high level of transcription of the integrated provirus (Orsulic, 2002).

In contrast to replication-defective vectors, RCAS vectors do not need a packaging cell line and high titre viral stocks can be generated by transfecting the vector into a chicken fibroblast cell line (Himly et al, 1998; Schaefer-Klein et al, 1998). RCAS infection does not, however result in infectious progeny in mammalian cells (Federspiel et al, 1994) thereby preventing the spread of cell-to-cell infection and also limiting any cellular immune response by the host (Pinto et al, 2000). Another important consideration for using TVA mice is the fact that the expression of RCAS *env* gene is quite low in mammalian cells, therefore, the TVA receptor is not occupied by the viral envelope protein and is susceptible to multiple rounds of infection with RCAS vectors carrying the same or different inserts. This gives the added advantage of introducing multiple genes sequentially into specific cells of a single transgenic mouse strain (Federspiel et al, 1994; Holland & Varmus, 1998; Orsulic, 2002). A few strategies employed for retroviral vector-mediated gene delivery are highlighted below.

Utility of RCAS/TVA based gene delivery system

The first demonstration of expression of a *tva* transgene in specific mouse tissues in combination with recombinant ALSV-A for introducing the gene of interest (alkaline phosphatase) was

implemented with a *tva* transgene under the control of chicken α_{sk}-actin promoter (Federspiel et al, 1994). These mice expressed TVA in skeletal and cardiac muscle and proved that the *tva* based retroviral system was a viable means of introducing foreign genes in mice in a tissue-specific manner.

Cooperative oncogenesis

Cancer is thought to arise from an accumulation of multiple genetic alterations. Each genetic alteration contributes additional capability for progression from normal to a metastatic state (Hanahan & Weinberg, 2011) as evident in the case of colorectal carcinoma, where about seven sequential genetic alterations occur during the tumour development (Kinzler & Vogelstein, 1996). The most common approach for studying cooperative tumourigenesis has been the use of tumour-prone transgenic and or knockout mice to evaluate the acceleration of tumour development. This is particularly complex while analysing more than two genetic perturbations and therefore requires analysis of synergistic combination of mutations.

In the TVA system, a number of genetic lesions can be introduced simultaneously or sequentially into individual cells in a TVA transgenic mouse, thus allowing for the study of numerous combinations of genetic alterations (gain of function or loss of function) in specified cell types. This strategy has been employed to study cancer models of glioma by mimicking the genetic alterations that occur in human gliomas by rendering glial cells specifically susceptible to infection by viral vectors (Holland, 2000; Holland & Varmus, 1998). Using this approach in TVA mice, it was demonstrated that simultaneous activation of RAS and Akt pathways (Holland, 2000) or BRAF and Akt (Robinson et al, 2011) in progenitor cells was sufficient to induce formation of glioblastomas. Individually, neither RAS or BRAF or Akt pathways were able to induce glioblastoma suggesting the requirement for combined effects of two pathways. Additionally, Holland *et al*. have investigated the role of EGFR mutation in glioma pathogenesis using transgenic mice that expressed the TVA receptor under the control of the astrocyte specific glial fibrillary acidic protein (GFAP) promoter (Holland et al, 1998). Infection of GFAP–TVA transgenic mice with the virus encoding a constitutively active mutant EGFR did not result in glioma development. However, coinfection of GFAP–TVA transgenic mice with viruses carrying CDK4 and mutant EGFR or infection of GFAP–TVA transgenic mice deficient in INK4a–ARF with the mutant EGFR virus triggered gliomagenesis, suggesting that genetic alterations of EGFR and INK4a–ARF are two crucial genetic events in gliomagenesis (Holland et al, 1998).

Trace cell lineages and developmental processes

TVA-based systems have also proved useful in developmental studies as the infection by RCAS viruses are restricted to cell lineages due to replication defects in mammalian cells, the descendants of infected progenitors can be traced during development. In case of GFAP-TVA transgenic mice it was demonstrated that the GFAP-positive astrocytes of the sub-ventricular zone (SVZ) act as neural stem cells (Doetsch et al, 2002). Other studies have been conducted to investigate the megakaryocyte lineage (Murphy & Leavitt, 1999) and neural crest development (Dunn et al, 2000).

Generate transgenic animals

Retroviruses stably integrate into the genome of cells and therefore can be used as gene delivery vehicles to introduce experimental genes into blastocysts. So far there has only been one study in this regard, in which transgenic mouse line expressing *tva* under the control of β–actin promoter were used. This line therefore expresses the TVA receptor in the majority of adult tissues and in early embryonic tissues (Federspiel et al, 1996). New transgenic lines expressing chloramphenicol acetyl transferase (CAT) in all, or specific tissues were generated by infection of susceptible blastocysts (expressing *tva*) with retroviral vectors carrying the *CAT* gene under the control of constitutive viral promoter or an internal tissue-specific promoter (Federspiel et al, 1996).

Besides the examples listed in the Table 5.1 below, the TVA system is being utilized for extensive studies on development, receptor signalling and gene knockdown using RNA interference (Foppiano et al, 2007). Recently, the Cre-loxP-based system has been incorporated in conjunction with TVA system for conditional somatic gene expression and knockdown. In this method, a lox-P flanked stop cassette was used for conditional activation of TVA in a Cre-recombinase-dependent manner both *in vivo* and *in vitro* (Seidler et al, 2008). Combined with the growing number of *Cre* expression models, the *tva* gene expression and knockdown systems provide promising perspectives for analysing gene functions in a spatial-temporal manner. Finally, there have been recent modifications to the RCAS vectors to expand the repertoire of their applications. These include modifications to allow gene knockdown experiments by RNAi via expression of short hairpin RNAs (shRNAs), and drug regulated gene expression by utilisation of the tetracycline (tet)-dependent transcriptional regulation (Politi & Pao, 2011).

Table 5.1: RCAS/TVA system utility.

Some published studies conducted using RCAS/TVA system utilising replication competent retroviral vectors (RCAS/RCASBP) and EnvA-pseudotyped lentiviral vectors.

Mice or Model	Viral Construct	Delivery/ Technique	Fate	Reference
Chicken α_{sk}actin-TVA (Skeletal muscle)	RCASBP-*AP*	30-50µl retrovirus 2×10^5 DF-1 cells/leg injected intra-muscular in neonates	Culled after 7 days and muscle stained for AP	(Federspiel et al, 1994)
β-actin TVA (Ubiquitous expression)	RCASBP-*AP*	4×100mm DF-1 confluent plates in 1ml, 50µl injected intra-muscular in neonates	Analysed 14, 28 and 42 days post-injection	(Pinto et al, 2000)
β-actin TVA embryo derived fibroblasts (EF)	RCAS-$Kras^{G12D}$	10^6 EFs (retroviral transduced) injected sub-cutaneous into nude mice	Tumours formed in 8 weeks	(Pao et al, 2003)
$MiaPaCa2^{TVA}$ (Orthotopic Pancreatic Cancer Model)	RCASBP-EGFR RNAi RCASBP-p53 RNAi	$MiaPaCa2^{TVA}$ cells transplanted in pancreas of nude mice and injected intra-peritoneal with 10^7 DF-1 producer cells after 5 days	Analysed after 1 month	(Mayr et al, 2008)
Nestin-TVA (Neural progenitor cells in cerebella)	RCASBP-*IGF2* RCASBP-*Shh* RCASBP-*Akt* (active form of *Akt*)	10^5 DF-1 producer cells injected intra-cranially	Not Defined	(Rao et al, 2004)
Scl-TVA (Vascular Endothelial Progenitors)	RCASBP-*PyMT*	8-12weeks old mice injected intra-venous with retrovirus (10^7IU/ml, 300µl/mouse)	Analysed after 3-6 months	(Sausville et al, 2008)
MMTV-TVA (Mammary epithelium)	RCASBP-*PyMT* RCASBP-*Neu*	6weeks old pubertal mice injected with 10µl (or 10^8IU) intraductal via teat	7 days post-injection	(Du & Li, 2007)
Nestin-TVA (Neural progenitor cells in cerebella)	RCASBP-*Akt* RCASBP-*Braf* RCASBP-*Kras* (Active form of *Akt*, *Braf*, *Kras*) RCASBP-*Mek1* (Active form of *Erk1*)	10cm confluent dish with DF-1 producer cells trypsinised, into total 50µl and 5µl injected intra-cranial in neonates with genotype Nestin-TVA/Ink4a/$Arf^{lox/lox}$	Tumours analysed after 3-5 months	(Robinson et al, 2010) (Robinson et al, 2011)
RIP-TVA (B cells of pancreatic islets)	RCASBP-*cad* (dominant negative)	RIP-Tag and RIP-TVA crossed mice given intra-cardiac injections of 100µl (>10^8IU/ml) virus at 7weeks	Tumours analysed after 9 weeks	(Du et al, 2007)
DCT-TVA (Melanocytes)	RCASBP-$NRas^{Q61R}$	10cm confluent dish with DF-1 producer cells trypsinised, into total 50µl and 5µl injected sub-cutaneous near the ear of neonates with genotype DCT-TVA/Ink4a/$Arf^{lox/lox}$	Tumours visible after 4-6 weeks	(VanBrocklin et al, 2010)
Alb-TVA (Liver)	RCAS-*PyMT* RCAS-*c-myc*	3 day old neonates injected with 10^6 DF-1 producer cells in liver parenchyma	Tumours analysed after 4-6 months	(Lewis et al, 2005)
Keratin19-TVA (Epithelial cells) MMTV-TVA (Mammary epithelium)	HIV-1 (ALSV-A)-*PyMT* RCAS-*PyMT*	10µl of concentrated lentivirus (10^4 IU/ml) injected via the teat into the ductal lumen of mammary glands of 7weeks old mice.	Mice sacrificed 30 days post-injection and tumours analysed	(Siwko et al, 2008)

This chapter details the establishing of the TVA based avian retroviral and pseudotyped lentiviral gene delivery system both *in vitro* and *in vivo* with a methodological approach. Emphasis will be given on development, testing and significance of the system to generate more information on GHR-mediated oncogenesis *in vivo*.

Materials and Methods

Chemicals

Sudan Black B, copper sulphate and sodium butyrate were purchased from Sigma Aldrich (Australia). Ultraculture™ Serum-free media was purchased from Lonza (USA).

Plasmids

The plasmids pCS-CG-DV, pCS-CG-GFP, pCB6WTA (VCT) and (Δ513) were gifts from Prof. Brian Lewis (University of Massachusetts Medical School, MA, USA) and RCASBP-Y-DV were purchased from Addgene (plasmid# 11478). Lentiviral packaging plasmids pMDLg/pRRE and pRSV-Rev were a kind gift from Prof. Alpha Yap, University of Queensland. Lentiviral destination vectors with PGK-driven expression (pLenti-PGK-Puro DEST) were obtained from Addgene (plasmid# 19068) (Campeau et al, 2009). The pMSCV-TVA-puro vector (unpublished construct) was a gift from Dr. Jonas Nilsson, University Umea, Sweden. pVPack-GP® and pVPPack-VSVG® was purchased from Stratagene. pDONR221 vector was obtained from Invitrogen. All gateway destination vectors were maintained in OneShot® ccdB Survival™ *E. coli* strain (Invitrogen, Australia).

Construction of RCAS and ALSV-A pseudotyped replication defective lentiviral expression plasmids

RCAS constructs were constructed either by standard cloning or gateway cloning strategy. For standard cloning, each gene of interest was PCR amplified using specific primers (listed in Appendix III) designed to include *Acl*I recognition sequences. PCR reactions were carried out using *Pfu* Turbo DNA polymerase (2.5U/µl) as per manufacturer's recommendations (Stratagene). The PCR conditions used were 94°C for 20sec, 60°C for 20sec and 68°C for 150sec for 35 cycles in a thermal cycler (MyCycler, BioRad). The RCASBP-Y vector was digested with *Cla*I and dephosphorylated with Shrimp Alkaline Phosphatase (New England Biolabs, Genesearch Ltd, Australia) while all the *Acl*I site containing inserts were digested with *Acl*I to provide overhangs that were compatible for ligation with *Cla*I digested products. The gel-extracted purified, dephosphorylated RCASBP-Y vector and inserts were used in an equal molar ratio for ligation reactions using T4 DNA Ligase (Promega) at 16°C overnight.

For Gateway recombination cloning, each gene of interest was PCR amplified using *attB* cassette containing primers (listed in Appendix III). PCR reactions were carried out using *Pfu* Turbo DNA

polymerase (2.5U/µl) as per manufacturer's recommendations (Stratagene). The PCR conditions used above. Two series of reactions were carried out for each Gateway Cloning procedure. The first reaction was between the *attB* flanked PCR amplified fragment and pDONR221 donor vector (Invitrogen) using BP Clonase® enzyme mix (Invitrogen) in a total volume of 5µl in Tris EDTA (TE) buffer (10mM Tris pH8.0, 1mM EDTA) at room temperature for at least 3hrs. The second reaction between 4µl BP reaction end product and pCS-CG-DV, RCASBP-Y-DV or pLenti-PGK-DV plasmids (destination vectors) were catalysed by LR Clonase® enzyme mix (Invitrogen) in a total volume of 8µl TE buffer supplemented with 14mM NaCl, at room temperature overnight. The ligation end products and 1µl LR Clonase reaction were transformed into competent *E. coli* DH5α or Stbl3™ strains (Invitrogen) and plated on LB agar plates containing ampicillin (100µg/ml).

Cell Culture

Chicken embryonic fibroblast derived cell line; DF-1 (a kind gift from Prof Douglas Foster University of Minnesota USA via Dr. Matthias Ernst, Ludwig Institute, Melbourne) was maintained in DMEM supplemented with 10% FBS (Schaefer-Klein et al, 1998). The retroviral packaging cell line Plat-E (a gift from Dr. T. Kitamura from University of Tokyo, Japan) was also maintained in DMEM with 10% FBS. HEK293 derived 293T (Clontech) and 293FT (Life Technologies) cell lines were maintained in DMEM with 10% FBS. Human melanoma cell line MM96 and 293T derived Lenti-X cell line from Dr. Aaron Smith, UQ were maintained in DMEM with 10% FBS. MM96-TVA-puro cell line was maintained in normal growth medium supplemented with 0.4µg/ml puromycin (concentration determined by kill curve experiments).

The murine pro-B cell line, Ba/F3 was grown in RPMI 1640 media supplemented with 10% serum supreme, 2mM L-glutamine and 100U/ml IL-3. Ba/F3 cells expressing wildtype and nuclear localised GHR were maintained in 0.1ng/ml hGH instead of IL-3 to maintain the receptor expression. Ba/F3-TVA-puro cell line was maintained in normal growth medium supplemented with 1µg/ml puromycin (concentration determined by kill curve experiments). All cell lines were maintained in a humidified chamber 37°C incubator with 5% CO_2.

Production of replication competent ALSV-A virus

DF-1 cells were plated at a seeding density of 10^6 cells in a 6-well format a day prior to transfection. At 50% confluency, DF-1 cells were transiently transfected with 3µg of RCASBP vector with gene of interest per well using lipofectamine 2000 (Invitrogen) as per manufacturer's guidelines. The

media was removed 3-4 hours after transfection and replenished with 2 ml of fresh complete growth media. The viral supernatant was collected at several time points (i.e. 2, 3, 4, 5, 6, 7, 8, 9 days post-transfection) and centrifuged at 3000g for 5minutes. The supernatant was then filtered through a 0.45µm (low protein binding) polyethersulfone membrane filter (Merck) and stored at 4°C, concentrated or used fresh to test for functional virus production.

Production of replication defective ecotropic retrovirus

The potent retroviral packaging cell line, Plat-E was plated at a cell density of 8.5×10^4 cells per well in a 6-well format and transiently transfected with 4µg of pMSCV-TVA-puro plasmid using lipofectamine 2000 (Invitrogen) as per manufacturer's guidelines. The media was replenished 24hrs. post-transfection and the plates were further incubated at 37°C for 24hrs. The plates were then incubated for a further 24hrs at 32°C and supernatant collected. The supernatant was filtered through 0.45µm (low-protein binding) polyethersulfone membrane filter and used for transducing Ba/F3 cell line.

Generation of Ba/F3-TVA-puro cell line

A total of 2×10^5 Ba/F3 cells were harvested and seeded in each well of a 6-well cell culture plate for each viral transduction. The starved cells were resuspended in the harvested supernatant or concentrated virus. Polybrene (Sigma, USA) was added at a final concentration of 8µg/ml and the plates were incubated at 37°C for 1-2hrs. After incubation, an equal volume of complete growth media with twice the standard concentration of IL-3 was added and the plates were incubated at 37°C. 48hrs after infection Ba/F3 cells were selected on puromycin and analysed for infection.

Production of replication defective pantropic retrovirus

Lenti-X cells were plated in a 6-well format and upon attaining 50% confluency transiently transfected with 4µg each of pMSCV-TVA-puro plasmid, pVPPack-VSVG plasmid and pVPack-GP using lipofectamine 2000 (Invitrogen) as per manufacturer's guidelines. The media was replenished 24hrs post-transfection and the plates were further incubated at 37°C for 48hrs and supernatant collected. The supernatant was filtered through 0.45µm (low-protein binding) polyethersulfone membrane filter and used for infecting MM96 cell line in the presence of 4µg/ml polybrene. The cells were selected in puromycin 48hrs after transduction.

Harvesting and Concentration of Viruses

The centrifuged supernatant from transiently transfected DF-1 (containing replication competent virus) and 293T/Lenti-X cells (containing replication defective virus) were concentrated by ultrafiltration of the supernatant using Amicon Centricon® centrifugal filters (Millipore) with a 100,000 MWCO (molecular weight cut-off), at 4000rpm at 4°C. The centrifugation time can be increased in order to increase the concentration of the virus. Virus concentration by ultracentrifugation carried out in a fixed angle Beckman Coulter Optima 70Ti series rotor at 90,000g for 2h at 4°C. The viral pellet was resuspended in PBS and concentrated virus was used fresh or stored at 4°C for not more than two weeks.

Estimation of Viral Titre

MM96-TVA-puro cells were plated in a 24 well format a day prior to infections. On the day of infection, cells close to 75% confluency were mixed with limiting dilution of viral supernatant or concentrated virus in the range of 1 to 10^{12} in duplicates and incubated for 24hrs at 37°C. No polybrene was added during the process. Following 24hrs, the cells are replenished with fresh medium and plates incubated at 37°C. The infectious titre is determined by analysing the expression of reporter gene (GFP or mKate2) within 48-72hrs from the time of infection and GFP expressing cells were counted for each dilution under a fluorescence microscope. The viral titre is estimated by determining the dilution range that gives at least 10 positive cells. The formula used was:

Viral titre (TU/ml) = (number of GFP positive cells) x (dilution factor)

Animal Experiments

Mouse strains: α-actin TVA (expressing TVA receptor in skeletal muscles; TVM) and β–actin TVA (expressing TVA receptor ubiquitously; TVU) were sourced from Dr. Stephen Hughes (National Cancer Institute, USA) (Federspiel et al, 1994; Pinto et al, 2000). Albumin TVA (expressing TVA receptor in liver; TVL) was sourced from Brian Lewis, UMASS (Lewis et al, 2005). Genotyping was performed for TVA mice by PCR with DNA extracted from toes. The PCRs were carried out using *Taq* DNA Polymerase (5U/µl, NEB) in a thermal cycler with the following program: 95°C for 20sec, 59°C for 30sec, 72°C for 30sec for 30 cycles with *tva* specific primers.

Viral Delivery and Tissue collection

Retroviral Delivery:

Based on published studies with replication competent retrovirus, neonates were injected with DF-1 producer cells and the route of delivery was based on the tissue expressing *tva*. Due to volume constraints 10^6 producer cells were resuspended in minimal PBS volume of 30μL, of which 5μL was injected 2-day-old neonates; intra-muscularly (i.m.) into α–actin *tva* litters, intra-peritoneally (i.p.) close to liver for albumin *tva* litters (Lewis et al, 2005) and/or both for ubiquitous β–actin *tva* litters.

Lentiviral delivery:

Concentrated viruses (100-fold) with titre around 10^9 to 10^{11}IU/ml (Naldini, 1999) were injected intra-muscularly and intra-peritoneally in 2-4 week old α–actin *tva* mice and albumin *tva* mice respectively. Equal amount of empty expression vector concentrated virus was used as control when injecting virus. Intra-venous viral delivery via inferior vena cava following surgery was performed for albumin-*tva* mice. The mice and neonates were monitored regularly for any signs of toxicity, wound, and disease.

Subsequently mice were culled 2-4 weeks post-injection by cervical dislocation and liver and/or muscle tissues were collected and partly fixed in 4% PFA for histopathology and rest was snap-frozen in liquid-nitrogen and stored in -80°C freezer until use.

Generation of TVA expressing Zebrafish

The TVA expressing zebrafish was made by Dr Kaska Koltowska in the laboratory of Dr. Ben Hogan (IMB). All experiments were approved by and performed in accordance with the guidelines set by the University of Queensland Animal Ethics Committee. Briefly, tol2 transposase mRNA was prepared *in vitro* by transcription from XbaI-linearised pDB600 (Balciunas et al, 2006) using the mMESSAGE mMACHINE® T3 transcription kit (Ambion). RNA was purified using the RNeasy purification kit (Qiagen) and diluted to a final concentration of 100ng/μl and stored as 2μl aliquots at –80°C. The TVA construct was made using the Gateway cloning system (Kwan et al, 2007). For microinjections approximately 5μl mix was prepared with 2μl transposase, 2μl construct (100ng/μl) and lμl phenol red. Finally 2nl were injected in single embryo. Fish were raised to adulthood and screened for founders based on GFP expression in the heart (Bussmann & Schulte-Merker, 2011). The founders were crossed to Tg*(hsp70l:Gal4)*$^{1.5kca4}$ and larvae generated were given a heat shock treatment at 39°C for 1.5hrs and analysed for *tva* expression by qPCR using *hprt*

as an internal control. The zebrafish larvae and adults were held in E3 medium (5mM NaCl, 0.17mM KCl, 0.33mM $CaCl_2$, and 0.33mM $MgSO_4$, pH 6.8–6.9) at 29°C.

Results & Discussion

Construction of RCASBP(A) vectors

The most commonly used or the 'classical' cloning method is a restriction endonuclease dependent strategy for insertion of transgene into the vector of interest. Using this method, RCASBP vectors were digested with the *Cla*I enzyme and dephosphorylated. Since only one *Cla*I site is functional in the RCASBP vector, the other one being methylated, the insertion of DNA segment requires their conversion into a ClaI fragment using adaptors (Hughes et al, 1987). Therefore, the linearised plasmid was ligated to transgenes (amplified using *Acl*I specific primers and digested with *Acl*I to obtain compatible overhang with ClaI) to get the desired construct.

However, due to the large size of the retroviral vector (~12kb) and inherent repetitive viral sequences, the constructs were prone to recombination resulting in small sized plasmids (following the loss of gene of interest). In order to circumvent this problem the gateway® cloning method was employed. This cloning exploits the bacterial or viral site-specific recombinases like the bacteriophage P1 Cre, the *Saccharomyces cerevisiae* FLP or the bacteriophage lambda integrase (Magnani et al, 2006). These enzymes catalyse a reciprocal double-stranded DNA exchange between two specific DNA sites (Loftus et al, 2001) and summarised in the figure 5.4.

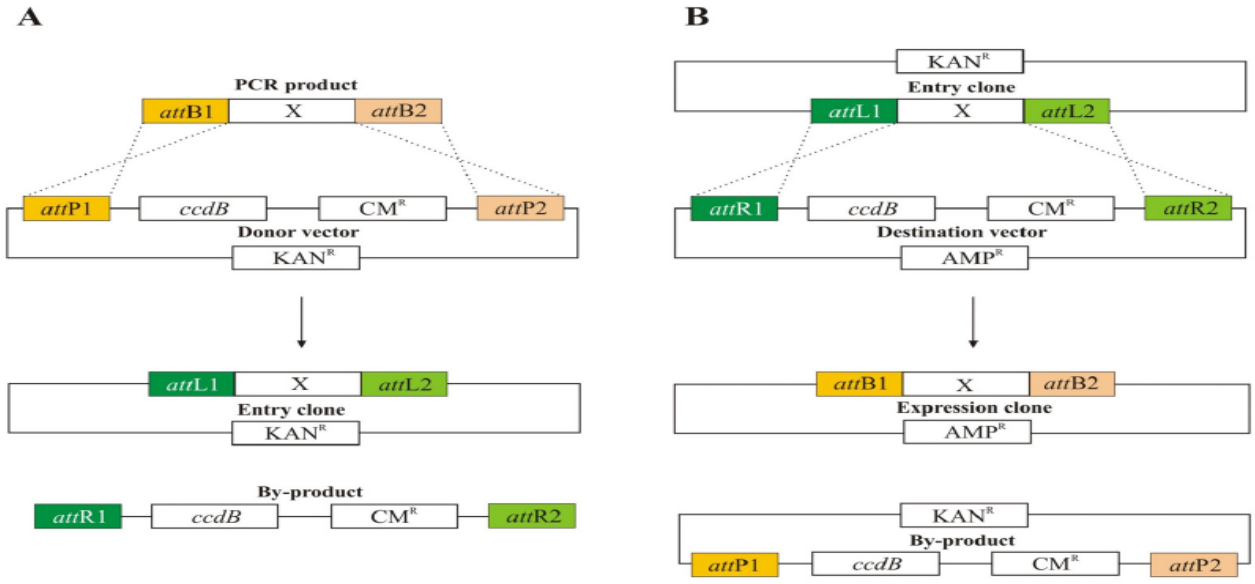

Figure 5.4: Gateway BP and LR reactions.

(A) BP recombination of a PCR product "X" flanked by *attB* sites with a Gateway donor vector resulting in generation of a entry clone with *attL* sites (B) LR recombination of the entry clone bearing a DNA fragment "X" with a Gateway

destination vector with *attR* sites. This results in the final expression clone with gene of interest 'X' (Magnani et al, 2006).

Consistent with published work expression clones generated using recombination based cloning had a higher success rate as compared to standard cloning (Loftus (Loftus et al, 2001). During the routine process of lentiviral and retroviral plasmid isolation from *E.coli* DH5α it was observed that the isolated plasmid DNA would often lose the insert. This issue was resolved by transforming the retroviral and lentiviral constructs into competent Stbl3™ *E. coli* strain. This strain lacks *recA* gene and is designed specifically to circumvent the problem of cloning direct repeats found in retroviral and lentiviral expression vectors as it reduces the unwanted recombination within the LTRs. Using gateway cloning strategy we have made numerous GHR constructs including wildtype, nuclear-localised and constitutively active receptor.

Establishing the RCAS/TVA system *in vitro*

Mammalian cells are resistant to infection by ALSV-A vectors, therefore a cell line expressing the ALSV-A receptor TVA was required to determine any functional viruses produced. For generation of such a cell line, two important questions need to be answered; the choice of cell line and the method to engineer that cell line of interest. Ba/F3 cells were chosen for the convenience of analysing GHR constructs (based on GH selection) as they are devoid of any endogenous GHR while an adherent human melanoma cell line MM96 was chosen for estimating the viral titre. A reasonable approach for generating such cell lines was the use of replication deficient retroviral particles that would carry the *tva* gene and stably integrate into the genome of transduced cells without any risk of viral replication.

Generation of ALSV-A based replication competent retroviruses

For the production of high titre recombinant retroviral stock, we took the advantage of a RSV-derived replication competent vector, RCASBP and an established chicken fibroblast cell line, DF-1 (free from any endogenous viruses). This cell line was transfected with the RCASBP vector carrying the desired insert. For their anticipated ease of detection, vectors containing GFP or far-red fluorescent protein, mKate2 were used and cloned into RCASBP vectors.

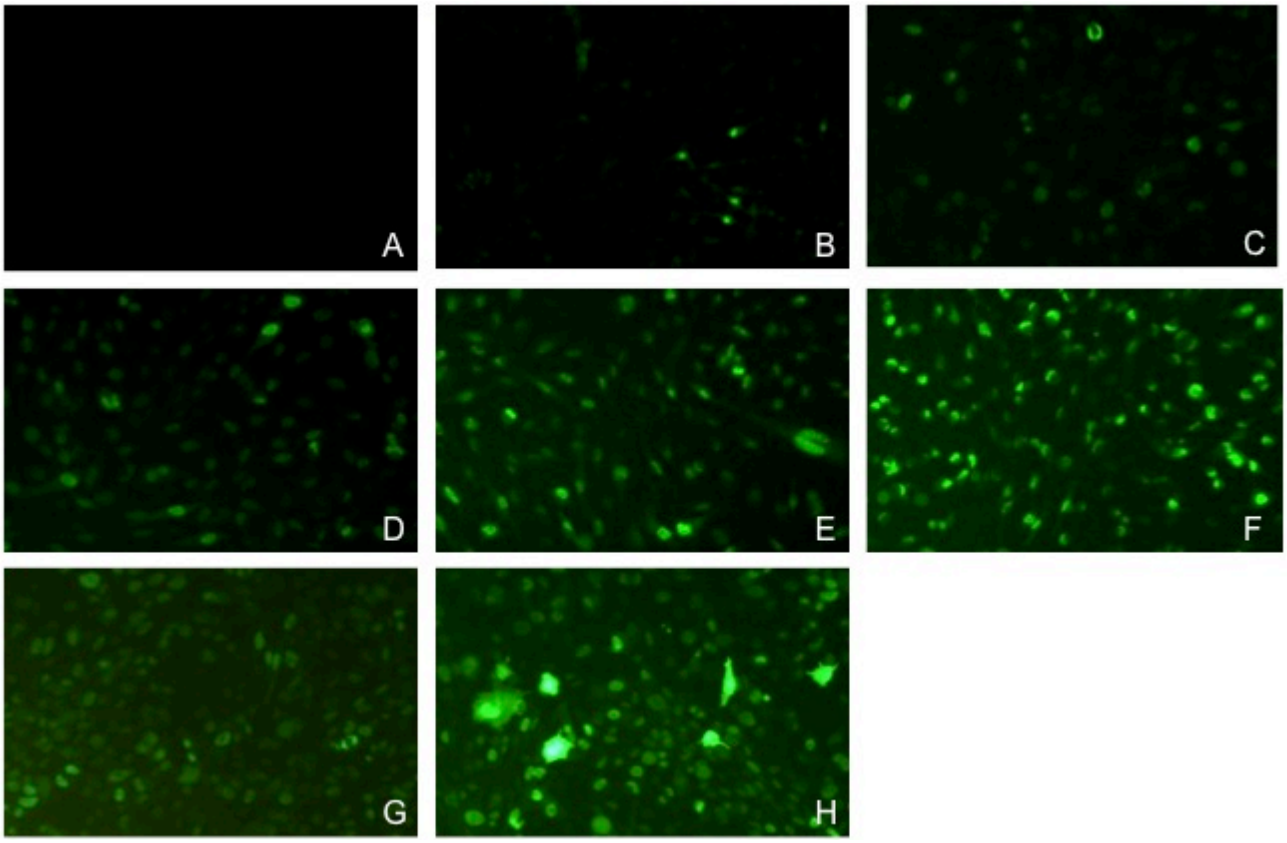

Figure 5.5: Generation of Replication Competent Retroviruses.

Chicken embryonic fibroblast cell line, DF-1 was transiently transfected with replication competent vector RCASBP(A)-HA-NLS-GFP. The DF-1 cells were analysed for nuclear GFP expression every day (24hrs interval) to determine transfection efficiency and viral production by DF-1 cells, which corresponds to percentage of cells expressing nuclear GFP and the intensity of brightness. (A) Represents day 0 of transfection, B – H represents subsequent analysis of cells every 24hrs till day 7. Untransfected DF-1 cells were used as a control and analysed everyday (image not shown). Images taken on Olympus Fluoro microscope.

A number of standardisation experiments were carried out in order to determine the most optimal time point of supernatant harvest for maximum viral yield. Cells were replenished, 24 hours post-transfection, with a minimal amount of media (to obtain concentrated virus). Initially the supernatant was collected every 24hrs and used promptly to infect MM96-TVA-puro cells to determine viral load. From the tests, it was also observed that Day 6-7 harvested media had the maximum viral load attributed to 100% DF-1 cells being transduced with the virus. As show in the fig.5.5, there was a gradual increase in the intensity of the GFP signal. Initially, only a few chicken cells express GFP, which increases subsequently as a result of multiple rounds of infections of the cells with the replication competent retrovirus (RCAS) being produced by the cells themselves. This observation corresponds to a previous study in which successful transfections of only a few DF-1 cells was sufficient since the replication competent virus spreads throughout the DF-1 culture (Schaefer-Klein et al, 1998). Even though the RCASBP vectors contain one copy of DR sequence, there is a possibility of the reverse transcriptase jumping fragments with little or no homology every time the viral RNA genome gets reverse transcribed following infection of dividing cells, resulting

in the loss of the gene of interest (Hughes, 2004). In general, viruses with smaller genomes (devoid of the gene of interest) replicate more rapidly than those that retain the inserted sequences. It is therefore recommended to generate fresh stock of RCAS vector by transfecting cells with cloned viral DNA than to passage continuously.

The majority of *in vivo* experiments with RCAS system have shown a 24 fold higher expression of the gene of interest by using transduced DF-1 cells instead of the virus itself (Federspiel et al, 1994). However, because of the requirement of dividing cells for infection by replication competent retroviruses, the age of mice at the time of injection is important as the infectivity has been shown to decreases significantly upon injections in pups over 5-days old (Federspiel et al, 1994). Following injections, the producer cells produce high titre retrovirus (~10^7IU/ml unconcentrated) as reported by studies (listed in Table 5.1) and infect the surrounding cells expressing the TVA receptor. In the case of muscles, this infectivity increases until 5 weeks and becomes constant. The producer cells are believed to be eliminated within 3 days from the time of injection (Holland & Varmus, 1998) although this would be dependent on the injection site (VanBrocklin et al, 2010). For all the injections untransfected or untransduced parental DF-1 cells were used as controls wherever required.

Even though the RCAS system has major advantages, the *in vivo* utility of this method has considerable limitations: firstly, there is a short bracket of 2-3 days available for injecting mice in order to get efficient gene delivery and at this age the mice are very vulnerable and often get cannibalised by parents. Secondly, the genotype of the mice is unknown at this age (unless at least one of the parents is homozygous, not the case for all mice models) and there is only a small volume of cells/virus that can be used due to size constraints. Most importantly, the replication competent system is not compatible in some cases where the gene of interest itself is detrimental to DF-1 cells such as in the case of potential oncogene (Himly et al, 1998). The RCAS system is also limited by the maximum size of the insert that can be incorporated which is 2.5kb (Orsulic, 2002) and the infection of mammalian cells with RCAS vectors can introduce genes encoding foreign viral proteins that can potentially elicit an immune response in the host (Orsulic, 2002). Additionally, the efficiency of infection depends on tissue/organ accessibility and most importantly, the rate of proliferation of the cells (Naldini et al, 1996).

Generation of Replication Defective ALSV-A pseudotyped lentiviral vector

The Avian leucosis sarcoma virus (ALSV) derived retroviral vectors offer potential advantages over their mammalian counterparts. First, they are self-sufficient as they can encode for all the proteins

required for assembly of infectious particles in addition to the gene of interest. Secondly, they can be produced in high titres in avian cells. Since the ALSV structural proteins are not efficiently produced (and devoid of packaging signal) in mammalian cells any chance of infectious particle production is rare and hence the vector cannot spread in the target cells, tissue or animal.

Like other classical retroviruses, ALSV and its derived vectors require cell division to efficiently establish a provirus after host infection. In contrast, lentiviral vectors are capable of integrating viral DNA into genomes of non-dividing cells. Therefore with the intention of initiating infection (tumourigenesis) in resting TVA positive cells, a system for preparation of HIV-1 based lentiviral vectors pseudotyped with the ALSV-A subgroup envelope protein (EnvA) was developed. This means that HIV-1 based lentiviral vectors retain the requirement for TVA receptor on the surface of target cell for entry and infection. Previously VSVG (vesicular stomatitis virus glycoprotein) pseudotyping of lentiviral vector has been shown and it is the most common envelope protein utilised for studies in different cell types across species (Naldini, 1999). Subsequently, other HIV-based pseudotypes have been utilised.

The HIV-1 based lentiviral vector pseudotyped with ALSV-A have previously been shown to be produced at titres greater than 5×10^4IU/ml and found to be stable during ultracentrifugation and can be concentrated to titres of 10^7IU/ml. It has been shown to infect both dividing and non-dividing cells including primary cultures from multiple mouse tissues, terminally differentiated cells, that are resistant to ALSV infection (Lewis et al, 2001). The HIV-1 (ALSV-A) pseudotyped vector contains a central polypurine tract, a short purine rich sequence within the *pol* gene that acts to generate a "plus-strand" flap in the double strand viral DNA prior to integration. This flap has been shown to be important for efficient nuclear import of viral DNA as well increase the viral titre by five fold (Zennou et al, 2000). The expression vectors used for viral production is a self-inactivating (SIN) vector made by deleting 133bp in the U3 region of the 3`LTR including the TATA box and binding sites for transcription factor SpI and NF- κB (Miyoshi et al, 1998). This deletion is transferred to the 5`LTR after reverse transcription and integration in infected cells, resulting in the transcriptional inactivation of the LTR in the provirus without significant decreases in titre. The expression of the desired gene from a SIN vector is under the control of its internal promoter (CMV or PGK) and is similar to the wild-type vector (with or without an internal promoter) indicating that the LTR is still transcriptionally active. However in some cases the LTR has been found to negatively influence the internal promoter. The third generation of lentiviral vectors have increased biosafety as the transfer vector used has a chimeric 5'LTR which means that a part of the upstream LTR is replaced by

constitutively active promoter sequences such as with CMV, PGK or RSV thus making it TAT-independent (Dull et al, 1998).

The steps outlined here were optimised in the context of the third–generation lentiviral vector packaging system and the production and handling of lentiviral vectors was carried out using appropriate biosafety containment. The third generation packaging system offers maximal biosafety but is more cumbersome, as it involves the transfection of four different plasmids in the producer cells. The protocol described here outlines detailed procedures to prepare, concentrate and titrate ALSV-A pseudotyped HIV-1 lentiviral vectors. In these third generation lentiviral packaging constructs the wildtype HIV-1 genome has been modified and divided into functional components on separate expression plasmids consisting of pMDLg/pRRE, pRSV/Rev, pCB6WTA and pCS-CG or pLenti. The plasmid pMDLg/pRRE contains the *gag* gene, coding for the virion main structural proteins; *pol* gene, responsible for the retrovirus-specific enzymes; and RRE, a binding site for the Rev protein. The plasmid pRSV-Rev lacks all accessory proteins and expresses the *rev* gene required for nuclear export of the viral RNA. Since the envelope protein of the virus determines its tropism, the commonly used VSVG envelope (that confers broad host range) was replaced with another plasmid that encodes for ALSV-A envelope-A glycoprotein. This ALSV-A envelope protein (EnvA) was expressed from the plasmids pCB6WTA/ (VCT or Δ513) and finally a self-inactivating lentiviral vector plasmid pCS-CG or pLenti expressing the gene of interest from an internal cytomegalovirus (CMV) promoter or phosphoglycerate kinase (PGK) promoter respectively were used as a transfer vector (Miyoshi et al, 1998; Naldini, 1999).

Use of altered ALSV-A envelope constructs

The ability of EnvA to pseudotype the HIV vector is poor relative to VSVG envelope glycoprotein, as demonstrated by its relatively low physical and infectious titres. While VSVG pseudotyped vector can be generated at titres of 10^6 to 10^7IU/ml, those from ALSV-A pseudotyped were consistently less than 10^4IU/ml (Lewis et al, 2001). A possible reason may lie in the different entry mechanisms of VSVG which fuses directly with the membrane phospholipids whereas ALSV utilises glycoprotein receptors on the membrane surface. Noteworthy was that the only difference between the two viruses was the envelope glycoprotein and since the cytoplasm tail of the transmembrane segment of the envelope is the only region that contacts the HIV core, it was hypothesised that cytoplasmic tail of the ALSV-A envelope might be inhibiting particle formation. As a result Lewis *et al*. (Lewis et al, 2001) have generated EnvA construct with truncation at residue 513, just beyond the membrane spanning region (pCB6WTA-Δ513), and a plasmid encoding a chimera in which the cytoplasmic tail of EnvA was replaced with that of VSVG

(pCB6WTA-VCT). These modified envelope proteins along with cPPT sequence were able to increase the viral titre by five fold as determined by serial dilution. Comparison between the two envelope constructs has shown that the use of pCB6WTA-VCT produced a significantly greater number of transduced cells as compared to the use of the Δ513 envelope construct. This result was in agreement to that of Lewis *et al*. who reported a decrease in the viral yield from 6.5×10^4 to 5×10^4IU/ml when Δ513 envelope was used (Lewis et al, 2001).

Optimal time point for harvesting supernatant

Optimisation was carried out by harvesting the media at 4 different time points; 24hrs, 48hrs, 72hrs and 96hrs post-transfection. The 293T cells were transiently co-transfected with the 3 helper plasmids along with pCS-CG-GFP or pLenti-PGK-GFP for ease of detection and titration. Typically 293T cells once transfected have been shown to produce virus for two to three days (Naldini et al, 1996). A similar finding was observed in our experiments where the viral production started within the first 24hrs and increased gradually over the next 24hrs, attaining a maximum yield by 72hrs. Around this time the 293T cells were close to confluency (fig.5.6). Media harvested after 72hrs had dead, floating producer cells with reduced viral titre. As a result all the supernatant harvesting was carried out at 72hrs post-transfection. The harvested media was used for transducing DF-1 or MM96-TVA-puro cell line using an appropriate control (media from untransfected 293T cells) and cells were analysed after 48hrs.

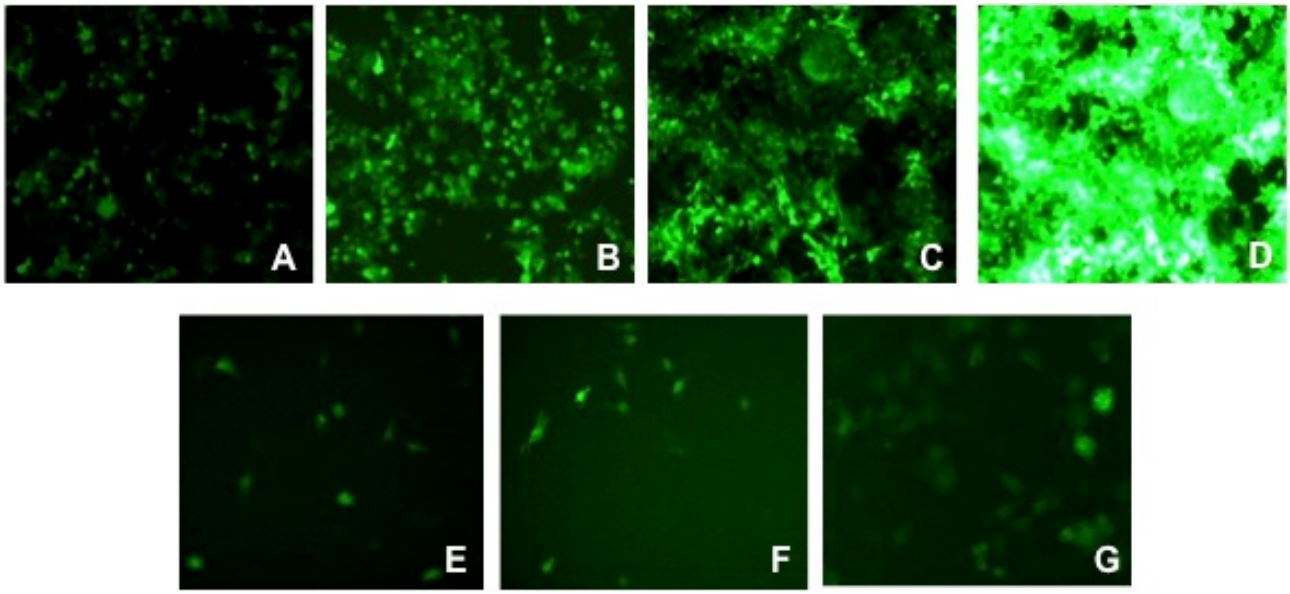

Figure 5.6: Generation of ALSV-A pseudotyped replication defective lentiviral vector.

An envelope-negative viral packaging cell line, 293T cell line was transiently transfected with third generation split vector plasmids and the transfer vector pCS-CG- GFP. The 293T cells were analysed for GFP expression every day starting at (A) 24hrs post-transfection up to 96hrs (D) to determine transfection efficiency, which directly corresponds to intensity and percentage of cells expressing GFP. The lower panel indicates the transduction of DF-1 cells with the 293T harvested supernatant for 48hrs from top panel. (E) DF-1 cells transduced with media 24hrs post-transfection from (A),

(F) DF-1 transduced with media from (B), (G) DF-1 transduced with media from (C). Media from untransfected 293T cells was used as control and used for transducing DF-1 cells (image not shown). Images taken on Olympus Fluoro microscope.

Optimisation of amount of DNA transfected for maximum lentivirus yield

For efficient viral yields, the relative amount of expression, packaging and envelope constructs were optimised on a case-by-case basis. The amount of DNA to cell ratio is critical to ensure a high level of transfection. A high ratio can lead to excessive cell death and barely detectable functional virus. Consequently, a number of experiments with different concentrations of the 4 plasmids were performed and the optimal plasmid concentration was determined to be a ratio of 1:2:3:4 which tallied to 8µg of pCB6WTA: 16µg of pRSV-Rev: 24µg of pMDLg/pRRE: 32µg of pCS-CG or pLenti for a 75cm^2 culture flask. This ratio resulted in the maximum viral titre that was higher than the one reported by Lewis *et al*. for unconcentrated virus (Lewis et al, 2001)**.** Any scale up done using the same plasmid ratio has produced consistently high titres. Emerging studies have indicated that CMV promoter, even though constitutive, can be subjected to epigenetic regulation and become silenced *in vivo* (Brooks et al, 2004; Loser et al, 1998; Mehta et al, 2009). As a result expression vectors with murine PGK promoter (pLenti plasmid) to drive the gene expression were therefore used.

Optimisation of transfection method for maximum lentivirus yield

Another set of experiments were carried out to determine the best method and mode for transfecting DNA into the producer cells. Transient transfections provide flexibility in the method that can be used for introducing DNA into the cells. For optimising this process two methods of transfection; lipofectamine 2000 and calcium phosphate-BES (*N,N*-bis(2-hydroxylethyl)-2-aminoethanesulphonic acid) were compared along with the forward and reverse modes of transfection for both reagents. Calcium phosphate-DNA precipitate in BES has been widely used to produce herpes simplex virus (Tognon et al, 1996) and lentiviral vectors (Sakoda et al, 1999) with reports indicating it to be more efficient than Hepes Buffered Saline (HBS) (Tognon et al, 1996). Therefore, in this optimisation a comparison was carried out between lipofectamine and calcium phosphate-BES.

Using forward co-transfection calcium phosphate-BES we achieved a more uniform expression in the cells (70% cells transfected) as compared to lipofectamine 2000 (60%). This was in contrast to the reverse co-transfection method, where 90% cells were transfected with lipofectamine 2000 as compared to calcium phosphate-BES (60%). In these transfections the cells transfected with

lipofectamine showed higher intensity of GFP expression. The supernatant from all four cases were titred by serial dilution and a significantly higher titre was obtained for reverse transfection method using lipofectamine, than for transfection using calcium phosphate-BES.

Optimisation of packaging cell line and effect of sodium butyrate on lentivirus yield

The choice of packaging cell line was based on experiments done on 3 different cell lines, selecting the one that gave maximum viral production based on a functional titre estimation. The cell lines tested were 293T, 293FT and Lenti-X. These cell lines are derived from the parental HEK293 cell line and contain SV40 large T antigen. 293FT (Invitrogen) and Lenti-X (Clontech) cell lines are two fast growing variants of 293T and are commonly used for lentiviral production for their ease of transfection and high temporal expression. In our study we found that lentiviral production from the Lenti-X cell line gave a five fold higher titre as compared to using 293FT or 293T cell lines.

Sodium butyrate is an inhibitor of histone deacetylase (Lea & Randolph, 1998). In the presence of sodium butyrate, histones are hyper-acetylated which promotes a chromatin structure permissive for transcription and has been previously shown to increase expression of transfected DNA (fig.5.7) (Workman & Kingston, 1998). A one time treatment with 10mM sodium butyrate for 8hrs before harvesting has been shown to increase the viral titre by three fold in experiments conducted by Karolewski *et al*. (Karolewski et al, 2003). The experimental data suggests an increase in titre by up to six fold upon treatment with sodium butyrate in Lenti-X cells.

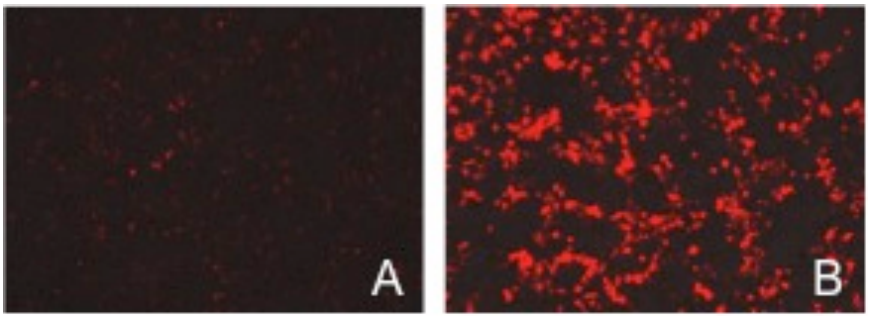

Figure 5.7: Effect of Sodium Butyrate treatment on Lenti-X expression.

Lenti-X cells transfected with pCS-CG-mKate2 and lentiviral packaging plasmids. (A) Untreated (B) Treated for 8hrs at 10mM Sodium Butyrate. Images taken using Olympus Fluoro microscope.

Lentivirus concentration

In the above studies, the estimated viral titre was considerably lower as compared to replication competent retrovirus. For *in vitro* cell transduction, crude (unconcentrated filtered) vector stocks are often sufficient whereas concentrated vector stocks are much needed for *in vivo* applications (Naldini et al, 1996). Concentrations of the lentiviral stocks were typically performed using two approaches. The harvested supernatant was subjected either to ultracentrifugation at high speed or

to ultrafiltration by passing it through a low protein binding cellulose filters with a 100,000 MW cut-off, then centrifugation at a low speed, to concentrate the virus by 100 fold. This concentrated suspension was then used for titre estimation in the absence of polybrene. Lewis *et al*. have demonstrated that the EnvA-pseudotyped lentiviral vectors are stable upon ultracentrifugation to yield a titre of 10^7IU/ml after a 100-fold reduction in volume (Lewis et al, 2001). Based on limiting dilution titre estimation from the 100 fold concentrated supernatant, a higher functional titre of 10^8IU/ml was obtained by ultracentrifugation in our experiments which was 10 fold higher as compared to the one reported by Lewis *et al*. (2001).

However, upon comparison it was evident that the viral concentration achieved using filters was much greater as it improved the transduction efficiency from ~20% to >90% in all the cell lines tested with viral titre estimated at 10^{10}IU/ml. It has been postulated that ultrafiltration can bypass resuspension problems that are encountered with virus stocks concentrated by ultracentrifugation and hence gives a higher titre (Reiser, 2000). An issue in this approach was that at the end of concentration, the retentate on the filter was a viscous soup containing viral particles and aggregated protein and serum components. For ease of injections, it was important to reduce the viscosity of virus-enriched suspension, and this was affected by replacing the normal growth media with Ultraculture™ Serum-free media. In addition, the lack of aggregating proteins allowed a much faster and manifold concentration of the supernatant resulting an estimated titre of 10^{11}IU/ml, which is considerably higher than the one reported for EnvA-pseudotyped lentivirus.

Lentiviral storage

A final experiment was performed to determine the stability of EnvA-pseudotyped lentivirus concentrated by ultrafiltration or ultracentrifugation during long-term storage at -80°C. There was a drastic decline in the viral titre after cold storage by nearly 5000 fold as compared to fresh virus. This meant that pseudotyping plays an important role in determining the stability of virus particles and unlike VSVG-pseudotyped virus that are stable for a long time at -80°C these EnvA ones need to made just prior to use.

Establishing the RCAS/TVA system for gene delivery *in vivo*

Currently there is no commercially available antibody for TVA receptor therefore we sought to detect *tva* transcript levels in different tissues (mainly liver, skeletal muscle and skin) of the three mouse models. The cDNA reverse transcribed from RNA was used as template to determine the *tva* expression using specific primers (listed in Table 5.2). It is evident in figure 5.8 that there was a

clear tissue-specific expression of *tva* gene depending on the promoter driving the *tva* gene with no leaky expression at least in the tissues analysed.

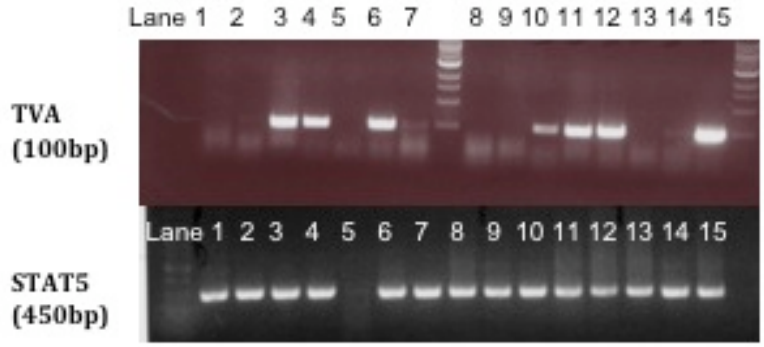

Lane	Sample
1	Muscle wt
2	Muscle TVL
3	Muscle TVM
4	Muscle TVU
5	BLANK
6	Skin TVU
7	Skin TVM
8	Skin TVL
9	Liver TVM
10	Liver TVU
11	Liver TVL
12	Skin TVM
13	Liver wt
14	Genomic DNA wt
15	Genomic DNA TVU

Figure 5.8: Detection of *tva* transcript in tissues of TVA mouse models.
Reverse-transcriptase PCR for *tva* gene and *STAT5* (control) from RNA extracted from tissues of different TVA mice (TVU: β-actin *tva*, TVM: α-actin *tva*, TVL: alb-*tva*). Genomic DNA from TVU mice was used positive control and from a wildtype mice (non-transgenic for *tva*) as a negative control with water used as template in the blank. The reaction was run on a 1.7% agarose gel, stained with sybr safe and visualised under a UV transilluminator.

Detection of viral-mediated gene delivery in mice

For the ease of detection all the virus standardisation experiments *in vitro* were carried out using fluorescent markers such as GFP and mKate2. It was thought that the *in vivo* analysis for viral-mediated gene delivery to muscle and liver could be analysed in a similar way by putting a thin tissue section directly under the microscope. However it was proven otherwise when the tissue sections (paraffin or OCT embedded) were observed under the microscope. What seemed like GFP fluorescence was actually a false positive due to autofluorescence visible even in the control tissues sections.

Natural fluorescence in tissues is mainly due to the presence of endogenous flavins, reduced NAD(P)H, lipofuscins, reticulin fibres, collagen and elastin. Flavins and NAD(P)H are co-enzymatic redox carriers that play important role in most metabolic pathways (Andersson et al, 1998). These molecules increase and accumulate with age, therefore while embryo and neonates do not have significant background, the older mice have high natural fluorescence. Collagen/elastins, which are typical constituents of blood vessels, are also a source of autofluorescence (Billinton & Knight, 2001). Reticular fibres similarly are prone to autofluorescence, the degree of which depends on the tissue type (Viegas et al, 2007). In our case the two tissues that we were most interested in were liver and muscle. Liver has a high metabolic rate with constant NADP-NADPH turnover with high accumulation of flavins and lipofuscins. Being highly vascularised it contains large amounts of

collagen and elastin, and its parenchyma is rich in reticular fibres. Skeletal muscle on the other hand is rich in NAD(P)H and flavins (Jackson et al, 2004).

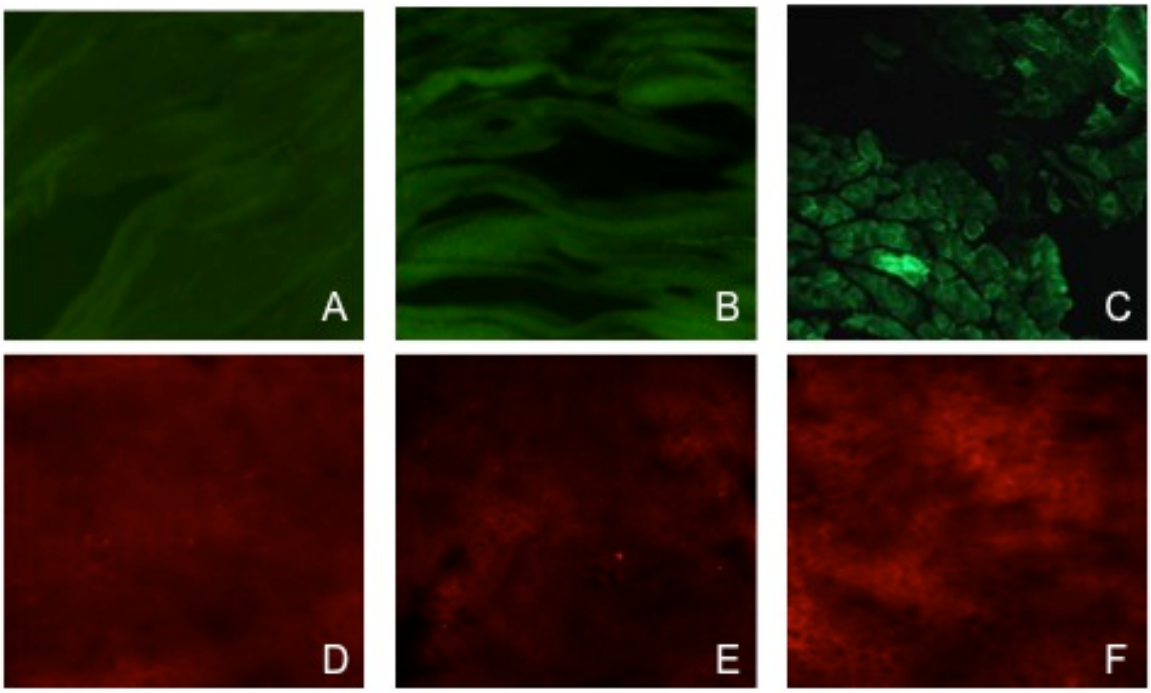

Figure 5.9: Autofluorescence detection in virus injected liver and muscle tissue of TVA mice.

PFA fixed muscle (A, B, C) and liver (D, E, F) tissue sections (7µm thickness) from mice injected with concentrated EnvA-pseudotyped lentivirus carrying GFP (of 10^7IU/ml titre, A, B, D, E) and empty vector (C, F) observed under two different filters on a Olympus Fluoro microscope. All the sections were subjected to similar parameters of fixation and treatment.

Tissue fixatives, which are used for preservation of morphological details, may further augment background fluorescence. Fixative-induced fluorescence occurs when aldehyde fixatives react with amines and proteins in the tissue to generate fluorescent products. This auto-fluorescence is fairly uniform, non-punctately distributed across the tissue, but may be brighter in some cells depending on the presence of the biogenic amines. One solution to this problem is performing aldehyde blocking by incubating the tissue with bland amino groups such as those provided by glycine post-fixation (Viegas et al, 2007). However, this treatment of tissue sections did not show any significant decrease in background autofluorescence. Such treatment also reduces the intensity of immunofluorescent labelling, which demands a compromise between autofluorescence reduction and antigen visualisation. Other chemical strategies using Sudan Black B and Copper Sulphate treatment of tissue sections have been tried with limited success.

The emission spectra of natural fluorescence or fixative-induced fluorescence is very broad compared to the spectra of any particular dyes, probes and proteins, making it difficult to separate wanted from unwanted fluorescence by traditional filtering methods of image acquisition. We

therefore tried separating the spectra of GFP/mKate2 from autofluorescence using confocal laser scanning microscopy but since the desired signal intensity from the tissue was fairly weak it was difficult to separate the two spectra.

Analysis of in vivo gene delivery by immunofluorescence detection

In order to circumvent the problem caused by autofluorescence in muscle and liver sections an antibody against GFP was used. This strategy can amplify weak signals and hence can be easier to analyse. A few different primary antibodies against GFP and HA-tag were used with combinations to different secondary antibodies. For these experiments corresponding tissues obtained from non-transgenic (WT) and GFP expressing mice (autosomal GFP expressing mice provided by Dr. Jo Bowles, Koopman Group, IMB) have been used as positive controls (Hadjantonakis et al, 2001; Hadjantonakis et al, 1998). The antibody was first tested out in cells for its ability to detect GFP (data not shown). This was however not the case in tissue sections from adult mice (as opposed to cells and embryo sections) indicating that it was not feasible to analyse the tissue sections by immunofluorescence (IF) due to inherent backgrounds for reasons mentioned earlier.

Since the main aim of this experiment was establishing the TVA system using viral delivery *in vivo*, we did not expect a widespread expression from viral-mediated delivery and because of the high autofluorescence it was not possible to conclusively determine viral-mediated gene delivery. For direct or indirect GFP expression analysis in tissue sections, observation of sections under any filter (on the fluorescent microscope) resulted in significant autofluorescence, which made it difficult to distinguish between control and lentiviral/retroviral injected tissue. In order to alleviate this issue immunohistochemistry (IHC) was performed on the tissue sections.

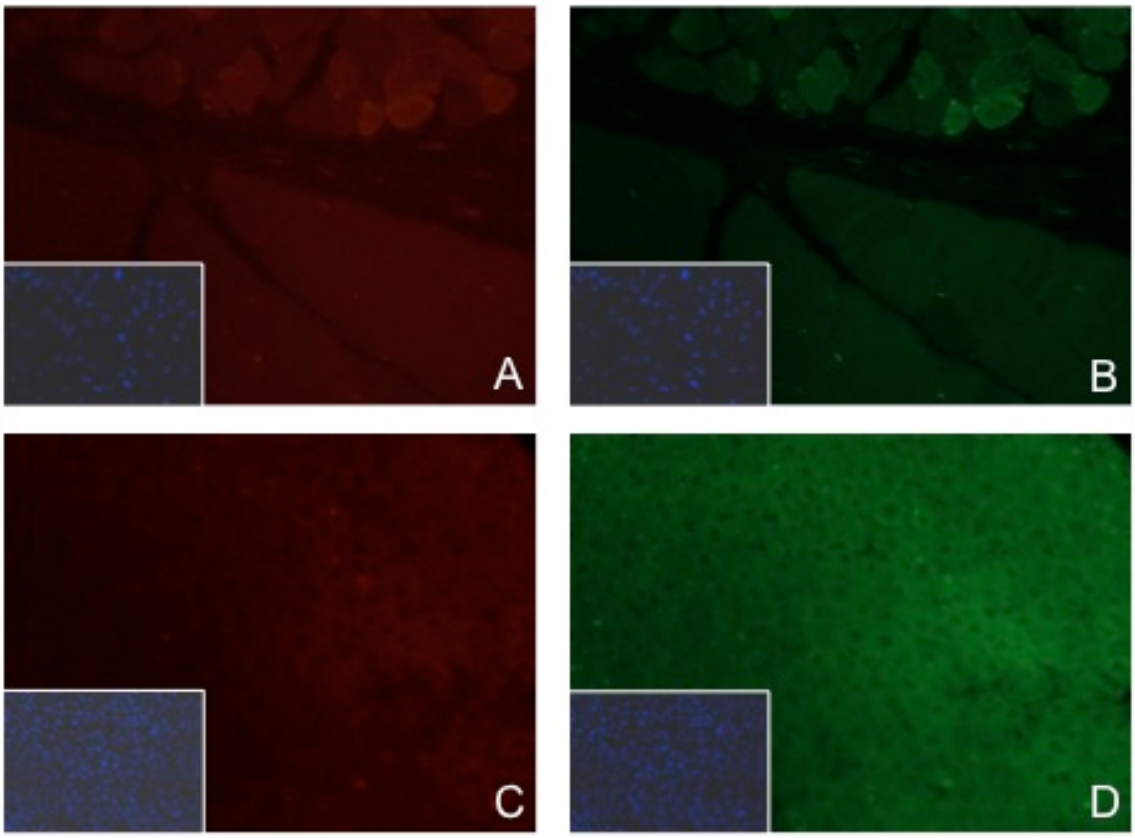

Figure 5.10: Indirect Immunofluorescence analysis of tissue sections from autosomal-GFP and WT mice.
7µm sections of muscle (A, B) and liver (C, D) tissue were subjected to anti-GFP primary antibody overnight in a humidified chamber and probed with Alexa Fluor conjugated secondary antibody 647 (A, C) and 488 (B, D). The slides were mounted in DAPI and visualised under Olympus Fluoro microscope. There was no evident difference between GFP expressing (A, C) and WT (B, D) tissues in terms of GFP detection following immunofluorescence.

Analysis of in vivo gene delivery by immunohistochemical detection

Immunohistochemical analysis was performed against GFP in tissue sections (muscle and liver) injected with EnvA GFP pseudotyped lentivirus (10^8-10^{10}IU/ml) for transduction with GFP (driven by PGK promoter) and positive (autosomal GFP mice tissue) and negative controls (empty vector injections). For IHC, the same anti-GFP antibody that was used for IF analysis was used on muscle sections that were subjected to prior blocking for endogenous peroxidase and biotin as both muscle and liver are rich in biotin (Wang & Pevsner, 1999).

The comparison of brown pigmentation (because of DAB staining) between the control and injected sample clearly shows there is significant detectable infection in muscle tissue with not much success in liver tissue (data not shown). Besides constraints imposed by the different routes of delivery, a possible reason for easier, prolonged detection of infection in muscle than liver can be attributed to lower $CD8^+$ T cells that can recognise transgenic protein and clear it from the system (Pinto et al, 2000).

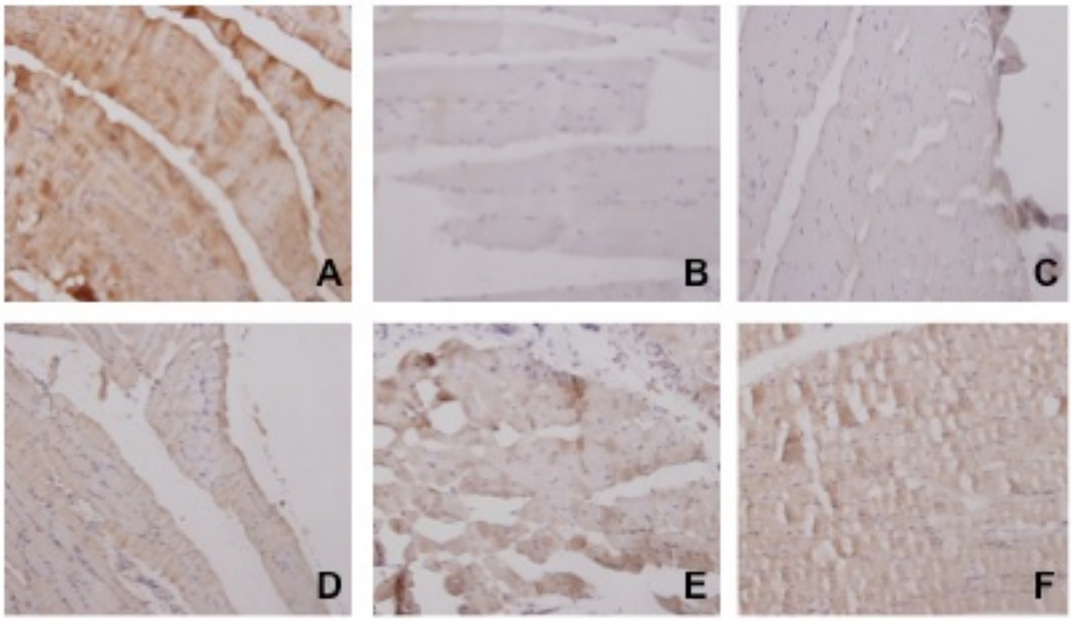

Figure 5.11: Immunohistochemical analysis of muscle sections injected with EnvA-pseudotyped lentivirus.
7µm muscle sections injected with EnvA-pseudotyped lentivirus for GFP using anti-GFP primary antibody and biotinylated secondary antibody incubated with diaminobenzidine (DAB) substrate (brown pigmentation) and counter-nuclear stained with hematoxylin (blue). Muscle sections from autosomal GFP mice (A and B) were used as controls and empty virus injected muscle section was used as negative control (C). Muscle section with no primary antibody is indicated in (B). Muscle sections injected with GFP virus (10^8-10^{10}IU/ml) at different concentrations show GFP reactivity as evident from brown pigmentation (D, E, F). All images visualised under Olympus Fluoro microscope.

Analysis of in vivo gene delivery by qPCR

In order to validate the gene delivery, quantitative PCR reaction was carried out on injected tissue samples, negative and positive controls (GFP-adenovirus injected mice liver, available in the Waters Group) using GFP and Gapdh (as internal control) primers. It is evident from the figure 5.12 that there is detectable infection occurring in most of TVA positive virus delivered tissues. Although detected at variable levels nevertheless expression was higher than the negative control especially in muscle. Liver samples on the other hand do not show a high level of expression (shown as fold change) compared to the positive control (liver tissues analysed 4 days after GFP adenovirus injected via tail vein). A high level of infection was achieved in mice injected with pLenti-PGK-GFP via inferior vena cava vein directly in the liver. No success was achieved with the GFP transduced DF-1 delivery in the liver (via i.p) but further experiments to improve delivery of concentrated viral supernatant by other routes are warranted.

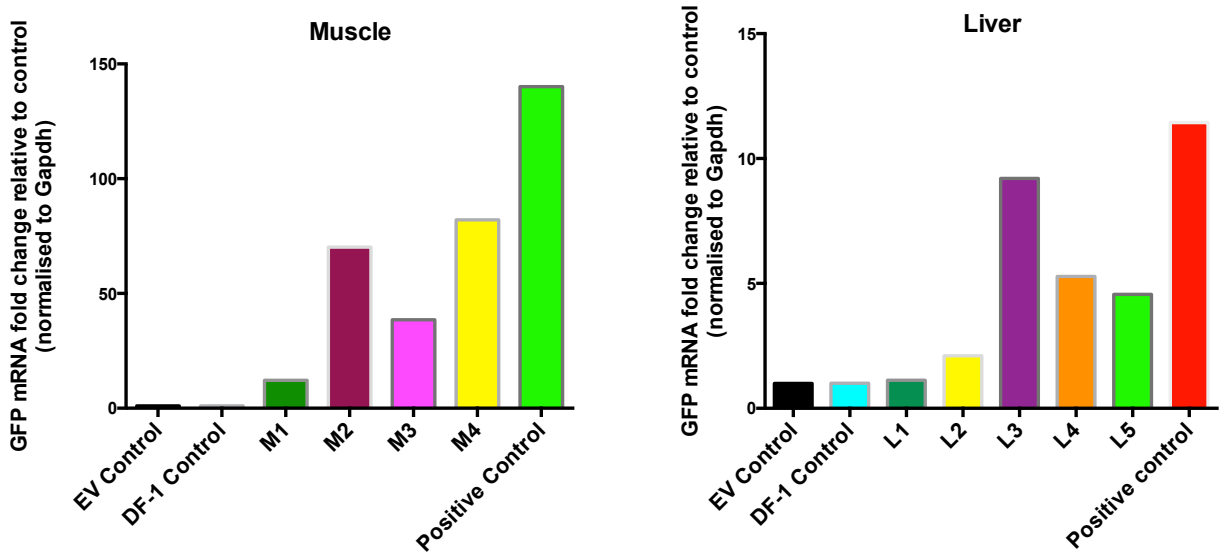

Figure 5.12: Detection of viral delivery in muscle and liver tissue *in vivo* by qPCR.

Fold activation of *GFP* gene expression in retroviral/lentiviral injected tissues. Gene expression was normalised to *Gapdh* and fold activation is reported relative to empty vector (EV) injected control. DF-1 control: Parental DF-1 injected, M1-2: Retroviral DF-1 GFP injected TVA muscles; M3-4: PGK-GFP lentivirus injected TVA muscle; Positive control: Autosomal GFP tissues; L1: Retroviral DF-1 GFP injected in liver intra-peritoneally L2-5: PGK-GFP lentivirus injected TVA liver via inferior vena cava injections; Positive control: adenovirus encoding GFP injected by tail vein.

Lentiviral Delivery in Zebrafish

Zebrafish larvae expressing the *tva* gene driven by a heat shock promoter (evident from GFP expression in the heart) were incubated at 39°C for 1.5hrs and transferred into E3 media containing PGK-GFP concentrated EnvA-pseudotyped lentivirus (1:5000 dilution). The larvae were analysed for GFP expression 2 days post-infection and are shown in fig5.13. As a control, non-transgenic zebrafish larvae (data not shown) and *tva*-transgenic zebrafish larvae without heat shock treatment were used and no virus-mediated GFP expression was detectable as compared to TVA expressing larvae following heat shock. Interestingly, we observed that the lentivirus was stable at the low pH of 6.8 (in E3 medium) and since the larvae generated were ubiquitously expressing TVA (after heat shock) GFP was detected all along the length of the larvae.

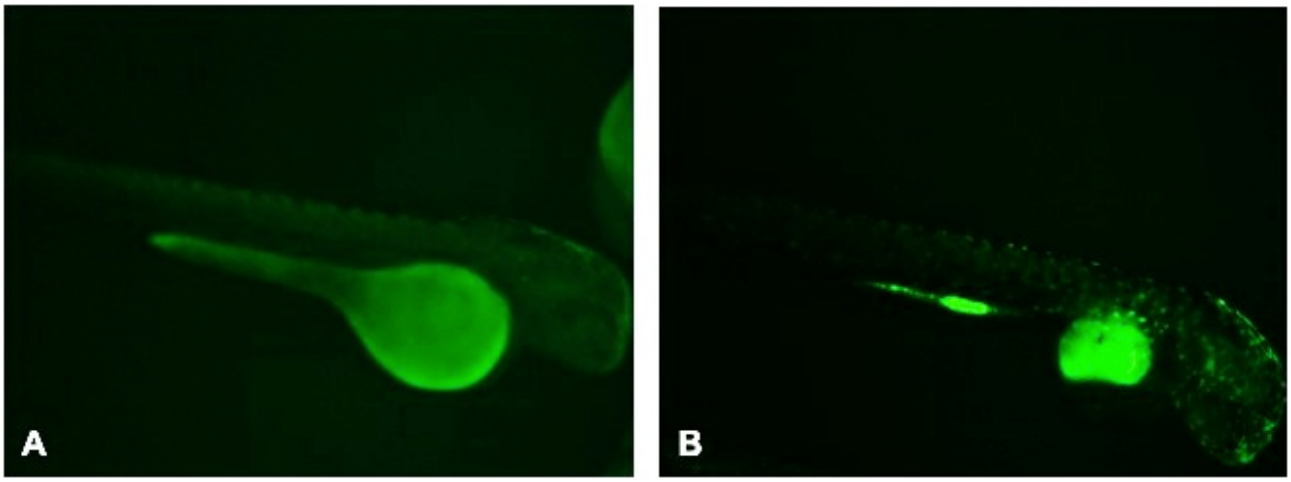

Figure 5.13: EnvA-pseudotyped lentivirus transduction of TVA transgenic zebrafish.

Zebrafish larvae transgenic for TVA receptor (evident from GFP expression in heart) were infected with PGK-GFP lentivirus (10^9IU/ml) at 1:5000 ratio in E3 medium. (A) TVA transgenic larvae infected with virus without heat shock treatment. (B) TVA transgenic larvae infected with virus following 1.5hrs of heat-shock treatment at 39°C. The live larvae were visualised 2 days post-infection under the Olympus Fluoro microscope.

Conclusion

Although the RCAS system has been established *in vivo*, we had limited success in our lab. One possible reason could be the amount of producer cells we injected into the mice was lower than what has been shown recently to achieve sufficient infection (von Werder et al, 2012).

We therefore decided to move focus from the use of retrovirus to a safer lentiviral delivery with the ability to transduce non-dividing cells. This has allowed efficient delivery in both liver and muscle tissues with a higher success rate as compared to retrovirus and most importantly can be utilised to transduce non-dividing cells in older animals. We have been the first to optimise the protocol for lentivirus pseudotyped for EnvA with the ability to produce titres in the range of VSVG envelope.

In addition, in conjunction with Dr Ben Hogan's laboratory, we have generated ubiquitously expressing TVA transgenic fish founders and shown that these can be transduced with EnvA-pseudotyped lentivirus. This approach can be used to generate fish with tissue-specific TVA expression and will be used to study the effect of various constitutively active GHR constructs (outlined in Chapter 6) associated with increased downstream signalling. This should allow a much faster and easier method to determine the direct oncogenic potential of GHR in cancer initiation, progression and maintenance.

EnvA-pseudotyped Lentivirus production protocol

The conditions that produced the highest titre for each of the standardisation experiments (mentioned earlier) were combined into one protocol detailed below. This protocol is now used by other labs in IMB for pseudotyping with VSVG envelope.

- **Day 1**: Make up cocktail of plasmids in OPTI-MEM (6ml)

  24µg of pMDLg/pRRE,

  16µg of pRSV-Rev,

  8µg of pCB6WTA (VCT or Δ513) and

  32µg pCS-CG/pLenti-PGK-GFP

  Scale up depends on culture dish and also the size of the insert

  Simultaneously incubate lipofectamine 2000 in 6ml of OPTI-MEM as per manufacturer's guidelines. Mix both the DNA and lipofectamine and incubate for at least 30 min at room temperature.

  Trypsinise Lenti-X cells from a confluent (not over-grown) T-75 cell culture flask and resuspend in 36ml of DMEM media with 10% FBS. Mix the resuspended cells with 12 ml of DNA-lipofectamine mix (reverse co-transfected with 4 plasmids) and plate into 4xT-75 flasks with total volume of 12ml per flask.

  Incubate at 37°C in humidified incubator with 5% CO_2 overnight (16hrs).
- **Day 2**: Change media in the morning for all the flasks replacing with 12ml of Ultraculture™ Serum-free media supplemented with L-glutamine (2mM), D-glucose (5.5mM) and sodium pyruvate (1mM).
- **Day 3**: Collect virus supernatant and store at 4°C and replace with 12ml of fresh media (as above) with 10mM sodium butyrate.
- **Day 4**: Harvest the virus supernatant and pool with the one collected on Day2. Centrifuge at 2000rpm for 5min at 4°C. Filter the supernatant containing the virus using 0.45um low protein binding PVDF filter before proceeding with virus concentration. Concentrate the supernatant using Amicon Ultra column (100,000 MWCO) by centrifugation at 4000rpm at 4°C by 100 fold.
- **Day 5**: Estimate the functional titre of the concentrated virus on a TVA positive cell line in triplicates by making a serial dilution of the virus by microscopy (based on a marker) or PCR analysis from DNA of transduced cells.

Chapter 6
Autocrine Growth Hormone and Growth Hormone Receptor-mediated Oncogenesis *in vitro*

Introduction

GHR-mediated cancer

The GHR is expressed in almost all cells, and its expression is subject to control by nine alternate first exons in humans. The GHR transcript has been found to be overexpressed in a range of cancers, notably prostate carcinoma, glioblastoma, neuroectodermal tumours, adult T-cell lymphoma, kidney clear cell carcinoma and parathyroid adenoma (reviewed in (Chhabra et al, 2011)) In addition, immunohistochemical and quantitative PCR studies have reported GHR overexpression in a high proportion of invasive breast ductal carcinoma, adrenal cortical neoplasms and in colorectal cancer. Moreover, elevated serum GH-binding protein is associated with a threefold increase in breast cancer incidence (Pazaitou-Panayiotou et al, 2007). Immunohistochemical assessment has also revealed GHR overexpression in melanoma (Lincoln et al, 1999) and prostate carcinoma (Weiss-Messer et al, 2004). This has been supported by a high level of *GHR* transcript expression reported in the NCI60 (National Cancer Institute) cancer cell lines (Sustarsic et al, 2013), Oncomine database (Chhabra et al, 2011) and more recently the development of the Cancer Cell Line Expression (CCLE) database (Barretina et al, 2012) (fig.S.1 in Appendix VII). To date, there are no reports of constitutively active GHR mutations but a coding mutation (Pro495 to Thr) has been reported to confer increase lung cancer susceptibility in GWAS studies (Cao et al, 2008; Rudd et al, 2006).

Humans deficient in GHR or harbouring a dysfunctional GHR have no reported deaths due to malignancy as compared to their relatives with functional receptor that die from malignancies (Shevah & Laron, 2007; Guevara-Aguirre et al, 2011). The animal models with lack of a functional GHR (GHR KO) have lower tumour burden and delayed incidences of fatal neoplastic lesions, particularly lymphomas and pulmonary adenoma/carcinomas as compared to WT mice (Ikeno et al, 2009). This was supported by other GH/IGF-1 axis deficient animal models that fail to signal efficiently via GHR (reviewed in (Chhabra et al, 2011). It is therefore no surprise that the level of endogenous GHR expression may be a critical target, which influences the tumourigenic effect of recombinant hGH (rhGH). This has recently been shown in gastric cancer xenograft model where rhGH was shown to activate tumour angiogenic factors mainly through the Jak2/STAT3 pathway (Lin et al, 2011). GHR may therefore be the key factor in determining if rhGH can be used in patients with a history of cancer.

The current view of GHR signalling requires activation of GHR at the cell surface by GH available exogenously (endocrine manner) or following synthesis/secretion by cells themselves (autocrine) or

from extracellular fluid following secretion by neighbouring cells (paracrine). This activates numerous signal transduction cascades in a cell-dependent manner resulting in transcription of specific genes in the nucleus that regulate cellular proliferation, differentiation, motility and other cellular functions. It is now apparent that several growth factors, cytokines, and their receptors become nuclear-localised, with nuclear localisation in many cases being necessary for full function, including cell proliferation (Lin et al, 2001; Johnson et al, 2004; Giri et al, 2005). The presence of GHR in the nucleus is a common feature of tissues and cells demonstrating a high proliferative status; examples include the chondrocytes of the epiphysial growth plate (Gevers et al, 2002), the gastrointestinal tract (Lobie et al, 1990b), placenta (Garcia-Aragon et al, 1992), and preimplantation embryos (Pantaleon et al, 1997). Nuclear-localised GHR and high GHR expression have also been reported in a number of cancers, including breast cancer (Mertani et al, 1998), colorectal carcinoma (Lincoln et al, 2000), hepatocellular carcinoma (Garcia-Caballero et al, 2000), cervical cancer (Dehari et al, 2008), and melanoma (Lincoln et al, 1999). Despite this, rigorous correlation with nuclear GHR, no correlated proliferative status had been reported before the study from Waters' Group indicating nuclear targeting of GHR to result in dysregulation of cellular proliferation and tumourigenesis (Conway-Campbell et al, 2007).

It was proposed that the normally limited period of nuclear localisation of GHR after GH addition (1h), which coincides with cell cycle initiation, might prevent cell transformation. However, during excessive nuclear uptake or extended residence time of GHR in the nucleus could result in oncogeneic transformation as shown in Ba/F3 cells with forced nuclear localisation using a nuclear localisation coding sequence (NLS) preceding the GHR cDNA sequence. Once transformed, these Ba/F3-NLS-GHR had more GH-responsive STAT5, GH-autonomous proliferation and rapid tumour formation *in vivo* in SCID mice, whereas Ba/F3-WT GHR were reported not to form a single tumour (Conway-Campbell et al, 2007). Microarray analysis revealed genes differentially expressed between Ba/F3-WT-GHR and Ba/F3-NLS-GHR cell lines. The constitutive transcripts upregulated in BaF-NLS-GHR were increased 2.5–4 fold in GHR-WT cells 1h after GH addition. These transcripts included those associated with highly proliferating normal tissues (regenerating liver) *Phgdh*, *F2r*, and *Ctsc*, and in cancers, *Phgdh*, *F2r*, *Ctsc*, *Mybbp1a*, *Eif5a*, and *dysadherin*. In addition, a majority of these (*Phgdh*, *Ctsc*, *Mybbp1a*, and *Survivin*) were shown to remain elevated during the entirety of the experiment in nuclear localised GHR Ba/F3 cell lines (Conway-Campbell et al, 2007). However, a majority of GH-regulated genes, including metabolic enzymes, did not show differential regulation in the forced nuclear GHR *vs* surface GHR expression cell lines, suggesting that nuclear targeting of the GHR did not influence the basic metabolic functions of GH.

A striking observation of this study was that nuclear localised rabbit GHR Ba/F3 cells exhibited increased STAT5 activation and proliferation as compared to the nuclear localised human GHR, independent of any exogenous GH addition. This was attributed to endogenous GH (autocrine) synthesised by the murine pre-B cell line that can selectively bind to rabbit receptor but not human GHR (Conway-Campbell et al, 2007). This result indicates clear clinical implications for nuclear GHR in cell lines and tumours expressing high levels of GHR. A large number of studies on tumours and cancer cell lines have indicated the higher expression and/or polymorphism of GHR and associated elevated signalling molecules but failed to study the origin of this signalling (GHR localisation) inside the cell.

Autocrine GH and Cancers

Mammary and endometrial cancer

The *GH* is expressed in normal and neoplastic mammary glands of cats and dogs (Mol et al, 1995b) as well as humans (Mol et al, 1995a). The GH mRNA in humans was demonstrated to be identical to pituitary GH and expressed by normal, benign (tumour) and malignant mammary tissue, although the immunoreactive hGH was restricted to epithelial cells (Mol et al, 1995a). Intriguingly, the pituitary and mammary gland GH transcripts originate from the same transcription start site but undergo differential regulation since mammary gland *GH* transcription occurs independently of *Pit-1* (Lantinga-van Leeuwen et al, 1999; Harvey et al, 2000). In addition, GHR mRNA and protein have also been detected in the mammary gland epithelia of rodents (Lincoln et al, 1990; Ilkbahar et al, 1995), bovine (Glimm et al, 1990), and humans (Mertani et al, 1998) as well as human mammary stromal and endothelial cells (Raccurt et al, 2002). In dogs, locally produced GH has been suggested to play a paracrine role in progesterone-induced proliferation and differentiation of mammary epithelium where the maximum expression occurs during the proliferation of epithelial cells, linking progestin-induced mammary GH synthesis to this proliferation (van Garderen et al, 1997). Intra-tumoural GH and IGF-1 concentrations are associated with malignant tumours in dogs and these canine mammary tumours closely resemble those observed in humans owing to clinical and molecular similarities (Queiroga et al, 2011). Together with the reported GHR expression, this is indicative of an autocrine or paracrine action of GH in canine mammary tumours (Rijnberk et al, 2003), independent of plasma GH and/or IGF-1 (Waters & Conway-Campbell, 2004). There is increasing evidence that the local mammary progestin/GH-axis is also operational in human breast cancer (Rijnberk et al, 2003). GH and PRL expression has been demonstrated in neoplastic human breast tissues (Wu et al, 2011) and progesterone is capable of promoting GH expression in human breast cancer cell lines (Gregoraszczuk et al, 2001). GHR expression in human breast cancer

correlates positively with progesterone receptor expression (Gebre-Medhin et al, 2001). In human breast tissue, increased GH expression is associated with increased epithelial proliferation and metastatic mammary carcinoma cells have the highest level of GH expression (Raccurt et al, 2002; Wu et al, 2011). In addition it has been shown that tissue overexpression of IGF-1 stimulates mammary tumourigenesis *in vivo* in transgenic mice (de Ostrovich et al, 2008). Both endocrine GH and autocrine (and paracrine) generated GH therefore possess the capacity to exert a direct effect on the development and differentiation of mammary epithelia *in vitro* and *in vivo* (Feldman et al, 1993). The *Pit-1* gene was reported to be expressed at both transcript and protein levels in normal and cancerous human breast tissue, where it regulates GH secretion and cell proliferation (Gil-Puig et al, 2005). Intriguingly, it may also be significant that vitamin D, a known inhibitor of mammary carcinogenesis, inhibits hGH expression at transcription level in human mammary carcinoma cells (Seoane et al, 2002) by repressing the transcription of *Pit-1* by recruitment of HDAC1 (Seoane & Perez-Fernandez, 2006).

Autocrine GH has also been shown to enhance the *in vitro* oncogenic potential of endometrial carcinoma and colorectal cells while its forced expression in immortalised endometrial carcinoma and breast cancer cell lines increased their cell number through enhanced cell cycle progression and decreased apoptotic cell death while promoting anchorage-independent growth and increased cell migration and invasion (Jenkins & Bustin, 2004; Pandey et al, 2008; Zhu et al, 2005). Both GH and GHR are expressed in immune cells and are implicated in the development of leukemia and lymphoma (Hooghe et al, 1998) along with IGF-1 and its receptor (Weigent & Arnold, 2005). The overexpression of GH and GHR in lymphoma cells have been shown to have anti-apoptotic effects (besides increasing IGF-1) by decreasing the production of superoxide and associated expression of *bax*, *Bad* and *caspases 3,8 and 9* (Arnold & Weigent, 2003). A high mRNA level of *GHR* and *GH1* transcripts have been reported in not only mammary cancer but numerous other cancer cell lines (including NCI60 panel (Sustarsic et al, 2013). An intriguing observation comes from the transcript data of *GH2* gene that is selectively expressed in higher levels in most cancerous cell lines but is barely detectable in their normal tissues of origin (fig.S.1 and S.2 in Appendix VII).

A model system to study the role of autocrine human GH-N (hGH) in mammary carcinoma by stable transfection of either the *GH* gene or a translation-deficient gene into cell lines has been developed by Lobie's Group (Kaulsay et al, 1999). The autocrine hGH producing cells display a marked IGF-1-independent increase in cell number in both serum-free and serum-containing conditions as well as a specific increase in STAT5-mediated transcription (Kaulsay et al, 1999). The same model system has been extended to endometrial cancer (Pandey et al, 2008). The increase in

mammary carcinoma cell number as a consequence of autocrine production of hGH is a result of both increased mitogenesis and decreased apoptosis and is dependent on the activities of both ERK1/2 and p38 MAPK that are mediated solely by its action on GHR (Kaulsay et al, 2001). Also, autocrine hGH production was shown to promote enhancement of the rate of MCF-7 cells spreading on a collagen substrate (Kaulsay et al, 2000).

The study by Mukhina *et al.* provides a clear demonstration that forced autocrine production of hGH confers an invasive phenotype on mammary carcinoma cells due to epithelial–mesenchymal transition (Mukhina et al, 2004). As shown in figure 6.1, this phenotypic conversion is associated with a loss of expression of plakoglobin, (γ-catenin), together with a relocalisation of E-cadherin to the cytoplasm. Notably, an increased secretion of matrix metalloproteases (MMPs) 2 and 9 along with increased cell migration and invasion was also evident. Migration and invasion were both blocked by specific Src-kinase inhibitors. The *in vitro* evidence for invasive phenotype is supported by studies in immune-compromised mice showing diffuse infiltration of autocrine GH-secreting MCF-7 breast cancer cells into mammary gland stroma, together with islands of tumour cells removed from the main tumour mass. The proliferative effects of GH (autocrine and endocrine) are also maintained in primary culture of mammary carcinoma cells (Chiesa et al, 2011).

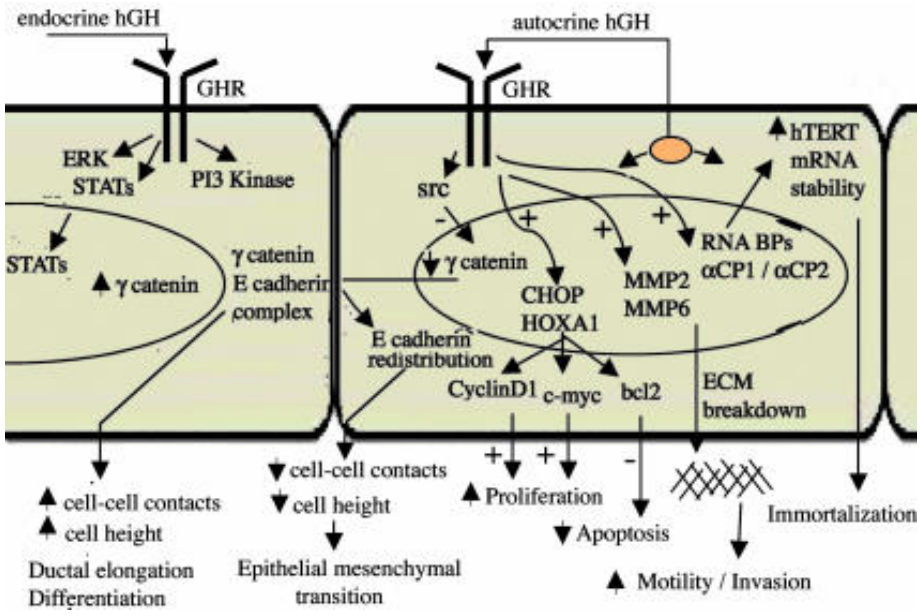

Figure 6.1: Endocrine hGH versus forced autocrine hGH actions on mammary epithelial cells.

The figure illustrates the differential effect of GH when administered exogenously or in an endocrine manner as opposed to synthesised by itself (Waters and Conway-Campbell, 2004).

BPs, binding proteins; ECM, extracellular matrix.

Autocrine production of GH in immortalised human epithelial cells enhances proliferation and protects against apoptosis and promotes abnormal mammary morphogenesis with oncogenic

transformation and tumour formation *in vivo* (Liu et al, 1997). Exogenous GH cannot, however, mimic these actions and this is supported by microarray analysis of 19,000 human genes that identified a subset of 305 genes that were differentially responsive to exogenous and endogenous GH, as well as 167 genes that were regulated in common (Xu et al, 2005). The differential actions of endogenous and exogenous GH could be attributable to differences in GH concentration and secretion, since endocrine GH is secreted episodically whereas endogenous GH is released continuously at low concentrations (Perry et al, 2008; Vouyovitch et al, 2008). Moreover, endogenous GH is released in closer proximity to GHR and potentially at higher microenvironment concentrations than exogenous GH, allowing it to bind with the available intracellular receptors (in compartments not readily accessible to exogenous GH) directly following synthesis in the ER (van den Eijnden & Strous, 2007). This GH-GHR complex is then transported to the plasma membrane where exogenous GH is unable to bind these receptors. This mechanism explains why GHR antagonists have been reported as ineffective in blocking the actions of autocrine GH (Tallet et al, 2008) at least in an overexpression autocrine system. The autocrine GH can also act through nuclear localised GHR, which is upregulated in cancerous tissues (Waters & Conway-Campbell, 2004; Brooks et al, 2008).

The mechanistic basis for these observations is not yet fully defined, but there are other studies from Lobie's Group that shed light on the subject. First, autocrine hGH upregulates the expression of HOXA1, a potent mammary oncogene that is required for increased c-myc, cyclin D1, and Bcl-2 expression (Zhang et al, 2003). Second, autocrine GH upregulated *gadd153* (CHOP), which has been reported to provide enhanced protection from apoptosis (Mertani et al, 2001), and downregulated the expression of transcripts for p53-regulated placental transforming growth factor β (PTGF-β). The latter is known to inhibit GH-stimulated cyclin D1 expression and promote apoptosis (Graichen et al, 2002). More recently, it has been reported that autocrine hGH increases telomerase catalytic subunit (*TERT*) transcript levels by stabilising the mRNA (Emerald et al, 2007), and increased TERT is known to immortalise human mammary epithelial cells. The means used by the activated GHR to elicit these changes in gene expression has been shown to be via Jak2-mediated STAT3 (Tang et al, 2010a) and STAT5A/B activation (Tang et al, 2010b), activation of src kinases (Bougen et al, 2012), and transactivation of the ErbB-2 receptor (Yamauchi et al, 1997). These pathways have been shown to associate with ERK1/2 and p38 MAPK activation, which are known to promote carcinogenesis (Aguirre-Ghiso et al, 2003). Indeed, inhibition of this pathway with MEK inhibitor abrogates the increased proliferation seen in autocrine hGH expressing cells (Kaulsay et al, 1999). These studies are indicative that autocrine hGH by carcinoma cells can promote cancer progression and this can have an impact on the clinical prognosis.

Prostate cancer

The binding of exogenous GH to GHR in the human prostate cancer cell line LNCaP and the concomitant activation of GHR-associated signal transduction pathways has been reported, but no effect of exogenous GH on LNCaP cell proliferation was observed (Weiss-Messer et al, 2004). This report contrasted with an earlier study that demonstrated an increase in LNCaP cell proliferation upon treatment with exogenous GH (Untergasser et al, 1999), illustrating the need for clarification of the role of GH in prostate cancer cell function. The ectopic expression of GH has also been observed in prostate cancer cell lines and tissue, indicating the possibility of autocrine signalling in prostate tumours that could affect tumour progression (Chopin et al, 2002; Slater & Murphy, 2006). It has also been reported that hGH can stimulate/modulate IGF-1 and β-estradiol receptor (ERβ) gene expression in PCa cancer cell lines and interact with IGF-1 and β-estradiol (E2) to stimulate androgen-dependent LNCaP cell proliferation (Bidosee et al, 2011). In addition, cell type-dependent, GH-mediated differential regulation of IGF axis gene expression was observed and increased cell proliferation was evident only when GH and IGF-1 were administered for 96hrs (Bidosee et al, 2011). GH also appeared to exert a synergistic effect on E2-stimulated LNCaP cell proliferation. However, the functional significance of autocrine GH in prostate cancer cells and the possible mechanistic distinction from the effects of endocrine GH has only recently been reported. The study by Nakonechnaya *et al.* have reported distinct actions of exogenous and autocrine GH in LNCaP cells, accompanied by differences in the involvement of GHR-associated signal transduction pathways, which paralleled an alteration in the subcellular localisation of GHR, in which autocrine GH appeared to sequester GHR in the Golgi and ER (Nakonechnaya et al, 2013). While the exogenous GH was proliferative, autocrine GH was shown to be more apoptotic and decreased cell proliferation. These findings indicate that the activity of autocrine GH may be distinct from that of endocrine GH in prostate cancer cells.

This chapter analyses the different GHR constructs (constitutively active *vs* wildtype) in prostate cancer cell lines to determine the molecular pathway downstream of GHR that may be involved in oncogenesis. In addition, based on the established model of autocrine GH as an oncogene in MCF7 breast cancer cell line we seek to evaluate the recent conflicting study by Nakonechnaya *et al*. indicating autocrine GH to be non-tumourigenic in LNCaP prostate cancer cell line and determine if the level of endogenous GH expression (and/or a particular signalling pathway) can explain this discrepancy.

Materials and Methods

Construction of plasmids

The pMT and pCDNA3.1 vectors containing hGH-N (GH1) gene as well as empty vectors were provided by Dr. Jo Perry (Liggins Institute, University of Auckland). The pMT-hGH vector drives the expression of hGH by a Metallothionein promoter while in pCDNA-hGH expression is under the control of Cytomegalovirus (CMV) promoter. CMV-driven expression has been shown to be much higher as compared to MT promoter *in vitro* and *in vivo* (Cheng et al, 1993). The empty pCDNA3.1 vector was digested with *Spe*I to remove the 700bp CMV promoter and ligated with an *Eco*R1 digested 4.1kb fragment from pMT-hGH containing the MT promoter and hGH fusion cassette to generate a vector containing MT-hGH in a pCDNA3.1 vector backbone with G418 selection. This was carried out since the original pMT-hGH vector was devoid of any selection marker. For a control plasmid in similar backbone, hGH was selectively removed by *Bam*H1 digestion and the resultant plasmid was re-ligated. All the plasmids were checked by restriction digestion and confirmed by sequencing at AGRF.

For construction of WT, nuclear localised (NLS), and the active GHR constructs (Jun3A-rGHR, PM2-hGHR) with co-expression of GFP in a single ORF, a self-cleaving 2A peptide bridge was encoded between the GHR and GFP sequences. Cloning was carried out using PCR-mediated overlap extension as detailed in Results section. Following the construction of ORFs, the joined fragments were gel extracted and used as template for Gateway Cloning (outlined in Chapter 5) into pLenti-PGK-Puro DEST (plasmid# 19068, Addgene). This lentiviral destination vector drives the expression of the gene of interest via the PGK promoter. All PCR reactions were carried out using Phusion DNA polymerase (Thermo Scientific). GFP was used as a reporter in all the GHR constructs with all of them expressing a HA tag at the N-terminus of the GHR for the ease of detection by immunoblotting or immunofluorescence.

Cell line and transfections

Murine Ba/F3 cells expressing the human GHR (Ba/F3-B2B2 clone) (Rowland et al, 2002) were passaged in RPMI 1640 medium supplemented with 10% (v/v) Serum Supreme (Biowhittaker, Walkersville, MD, USA), 10^5 units/l of IL-3 (or 100µg/l hGH). Prostate cancer cell lines; LNCaP-androgen dependent and DU145-androgen independent cell lines were maintained in RPMI 1640 containing 10% FBS supplemented with 2mM L-glutamine and were obtained from ATCC (USA).

The human mammary carcinoma cell line, MCF-7 cell lines was a kind gift from Dr. Jo Crawford (laboratory of Dr. Ryan Taft, IMB, UQ). These cells were maintained in DMEM supplemented with 10% FBS. The cell lines were stably transfected with the two expression vectors containing the entire *hGH-N* gene-driven via the CMV promoter (CMV-GH) or MT promoters (MT-GH) and their respective empty vectors as controls designated as CMV-EV and MT-EV using lipofectamine 2000 as per manufacturer's guidelines. The pooled stable transfectants were selected in 500µg/ml G418 (Life technologies, Australia) and analysed for expression. All cell lines were maintained in a 5% CO_2 humidified incubator at 37°C.

Generation of TVA transgenic cell lines

For making the mammalian cell lines susceptible to ALSV-A-pseudotyped lentivirus, the cell lines were made to express the avian *tva* gene (avian receptor that allows susceptibility to ALSV-A viruses) by using by using MSCV-TVA-IRES-PURO (a kind gift from Dr Jonas Nilsson, University of Gothenburg and Sahlgrenska University Hospital, Sweden) to produce replication defective pantropic retroviruses and selection with puromycin. A dose-dependent kill curve was established for all the cell lines that were made TVA positive (referred as LNCaP/tva and DU145/tva). The presence of functional TVA receptor was checked by infecting with ALSV-A pseudotyped virus with GFP and/or by RCASBP-GFP.

Infection of normal and cancer prostate cell lines

The two TVA+ prostate cell lines: LNCaP and DU145 were infected with concentrated ALSV-A-pseudotyped replication defective lentivirus carrying constructs 1 to 9 (fig.6.2). Three days post-infection, cells were expanded and cells were sorted for GFP expression at QIMR FACS Facility. The sorted cells were confirmed for receptor expression by immunoblot and used for experiments.

Anchorage-independent growth assay

For the soft-agar colony formation assay, 2×10^3 cells of DU145 stables and control cells in 2ml of RPMI 1640 media containing 10% FBS and 0.36% agar (Noble Agar Difco) were plated on a layer of 2ml of the same medium containing 0.7% agar. The plates were fed weekly with 0.5ml of RPMI/10% FBS. Three weeks after plating, the colonies were stained with 0.005% crystal violet, and photographed using an Olympus inverted microscope.

Cell morphogenesis on Matrigel.

Tissue culture dishes were coated with Matrigel (BD Bioscience, NJ) as per manufacturer's guidelines at 37°C for 30 minutes before adding 1×10^5 vector- or *hGH1*-transfected MCF-7 cells, which were then overlaid with a dilute solution of Matrigel (in growth media) in triplicates and incubated at 37°C. Images were recorded after 48hrs using Nikon inverted microscope.

GH assay

An equal number of MCF-7 stably expressing cells and parental line were seeded in a 6-well format and grown till confluence. The following day these cells were subjected to serum-free media for 24hrs and media was collected for GH secretion measurements. Simultaneously, the cells were washed in PBS and harvested in 25mM Tris–HCl, pH 7.4. The supernatant and cell lysates were diluted and assayed on murine Ba/F3 cells stably expressing the human GHR (Ba/F3-B2B2 clone) as previously described (Rowland et al, 2002) with an MTT formazan dye endpoint.

Preparation of total RNA and quantitative PCR (qPCR)

Total RNA was isolated from MCF-7 parental and stable cell lines using RNeasy Kit (Qiagen) as per manufacturer's guidelines. 1µg of total RNA was reverse transcribed to cDNA using Superscript III (Invitrogen, USA) and used for qPCR with Syber Green Technology (ABI, USA) using specific primers (listed in Appendix IV) in the 7500 Real Time Cycler (ABI, USA). Analysis was performed using Ct comparison for the gene of interest normalised against beta glucuronidase (GusB).

GH treatment and Western Blot Analysis

Before GH treatment the cells were subjected to 24hrs of serum starvation in their respective growth media devoid of 10% FBS then stimulated with 100ng/ml hGH for 12minutes. The cells were washed in cold PBS and harvested in RIPA lysis buffer. For normal growth medium analysis, the cells were left in growth medium and harvested after a cold PBS wash in RIPA lyis buffer. Protein quantification of lysates was performed using bicinchoninic acid (BCA) protein assay (Thermo Scientific) as per manufacturer's instructions. Equal amounts of protein were boiled in sample buffer (15mM Tris-HCl (pH 6.8), 2% SDS, 10% glycerol, 10mM DTT) at 100°C for 5 minutes and proteins were resolved on a 7% SDS PAGE gels followed by transfer on to polyvinylidene difluoride (PVDF) membranes using a semi-dry transfer apparatus (BioRad)

according to manufacturer's guidelines. Blocked membranes were then incubated overnight at 4^{o}C in primary antibodies (listed in Appendix VI) and washed in Tris Buffered Saline with 0.1% Tween (TBST) before the addition of appropriate secondary antibodies diluted 1:10000 in blocking buffer for 1hour. After TBST washes, immunoblots were visualised using Immobilon Western Chemiluminescent HRP substrate (Merck Millipore) and X-Ray films were developed by X-OMAT. Blots were reprobed with different antibodies after stripping with Re-blot mild stripping buffer (Merck Millipore) according to manufacturer's guidelines.

Sphere-forming Assay

To determine colony-forming efficiency, 120 single MCF-7 cells were seeded per well of a 6-well plate in triplicates in 2ml growth medium (DMEM with 10% FBS) and incubated for two weeks until macroscopic colonies were visible. Before counting, the colonies were washed with PBS and fixed and permeabilised using cold methanol for 10min. The colonies were stained for 1h with crystal violet solution (0.1% crystal violet, 20% methanol). Images were captured using a camera.

Bromodeoxyuridine (BrdU) Incorporation Assay

Cells were plated in duplicate in 6-well plates containing 3 cover slips at 2×10^4 cells/well complete growth media. The next day, complete media was removed, cells were washed with PBS, and serum-free media was added for 24hrs. After 24hrs, either normal growth medium or fresh reduced-serum medium (DMEM supplemented with 0.5% BSA) was added and cells were given 20μM BrdU treatment for 2hrs. The cells were then washed and fixed in PFA and subjected to immunofluorescence with BrdU specific antibody (Chemicon) and counterstained with DAPI (Vector Labs) for nuclei. The coverslips were mounted and analysed under the Olympus Fluoro microscope. A total population of over 400 cells was analysed in several arbitrarily chosen microscopic fields to determine the BrdU labelling index.

Results

Creation of GHR constructs using 2A peptide

In order to determine the effect of GHR in prostate cancer cell lines, various constructs (fig.6.2) were designed to be expressed under the control of murine phosphoglycerate kinase (PGK) promoter, based on ALSV-A-pseudotyped lentiviral system. The PGK promoter is less prone to silencing in stem cells and *in vivo* as compared to the cytomegalovirus (CMV) promoter (Qin et al, 2010).

For creating GHR constructs using 2A peptide (fig.6.3A), two individual PCRs were carried out. The first fragment was generated by attB1 sequence linked to a pig signal peptide (Fwd primer1) and with the reverse complement of half of a 2A peptide sequence linked to reverse complement of GHR C-terminus without the stop codon (Rvs primer1). The second fragment was generated by using half of 2A peptide linked with GFP start codon (Fwd primer2) and attB2 sequence linked with reverse complement of GFP C-terminus sequence with a stop codon between attB2 and GFP (Rvs primer2). Most importantly, a portion of DNA sequence of 2A peptide was kept overlapping between the two PCRs while designing the Rvs primer1 and Fwd primer2. This common region between the 2 PCR products was on the same principle as overlap extension PCR cloning (Bryksin & Matsumura, 2013) (fig.6.3B).

No.	Insert	Gene 1	Gene 2	Gene 3
1	c-myc-2A-GFP	c-myc	GFP	X
2	CDK4*-2A-GFP	CDK4*(R24C)	GFP	X
3	hGHR-2A-GFP	hGHR	GFP	X
4	rGHR-2A-GFP	rGHR	GFP	X
5	NLS-hGHR-2A-GFP	NLS- hGHR	GFP	X
6	NLS-rGHR-2A-GFP	NLS-rGHR	GFP	X
7	hGHR(C259S, F263C, I270C)-2A-GFP	hGHR(PM2)	GFP	X
8	JunAAA-rGHR-2A-GFP	JunAAA-rGHR	GFP	X
9	GFP	X	GFP	X
10	hGHR-2A-c-myc-2A-GFP	hGHR	c-myc	GFP
11	rGHR-2A-c-myc-2A-GFP	rGHR	c-myc	GFP
12	NLS-hGHR-2A-c-myc-2A-GFP	NLS- hGHR	c-myc	GFP
13	NLS-rGHR-2A-c-myc-2A-GFP	NLS-rGHR	c-myc	GFP
14	hGHR(C259S,F263C,I270C)-2A-c-myc-2A-GFP	hGHR(PM2)	c-myc	GFP
15	JunAAA-rGHR-2A-c-myc-2A-GFP	JunAAA-rGHR	c-myc	GFP
16	hGHR-2A-CDK4*-2A-GFP	hGHR	CDK4*	GFP
17	rGHR-2A-CDK4*-2A-GFP	rGHR	CDK4*	GFP
18	NLS-hGHR-2A-CDK4*-2A-GFP	NLS-hGHR	CDK4*	GFP
19	NLS-rGHR-2A-CDK4*-2A-GFP	NLS-rGHR	CDK4*	GFP
20	hGHR(C259S,F263C,I270C)-2A-CDK4*-2A-GFP	hGHR(PM2)	CDK4*	GFP
21	JunAAA-rGHR-2A-CDK4*-GFP	JunAAA-rGHR	CDK4*	GFP

Figure 6.2: List of GHR constructs made containing the 2A peptide using overlap extension PCR cloning.
The different combinations of cDNA for the insert as well the resulting proteins are indicated
CDK4*- CDK4(R24C), hGHR- human Growth Hormone Receptor, rGHR- rabbit GHR, WT- wildtype, GFP- Green Fluorescent Protein.

As mentioned, the 2A peptide sequence is a self-processing viral peptide bridge that can separate different protein coding sequences in a single ORF transcription unit (Ryan et al, 1991). Using these 2A peptide constructs it has been shown that quantitative co-expression of heterologous proteins,

driven by one promoter is possible for both *in vitro* and *in vivo* analysis (Tang et al, 2009). The *in vitro* expression using 2A peptide sequences are shown in figure 6.3C by immunoblotting of whole cell extracts of transiently transfected HEK293T cells with a set of GHR constructs containing the 2A peptide. The first 8 constructs (fig.6.2) were used in the first round of transduction. The vector with GFP alone was used as a lentiviral transduction control.

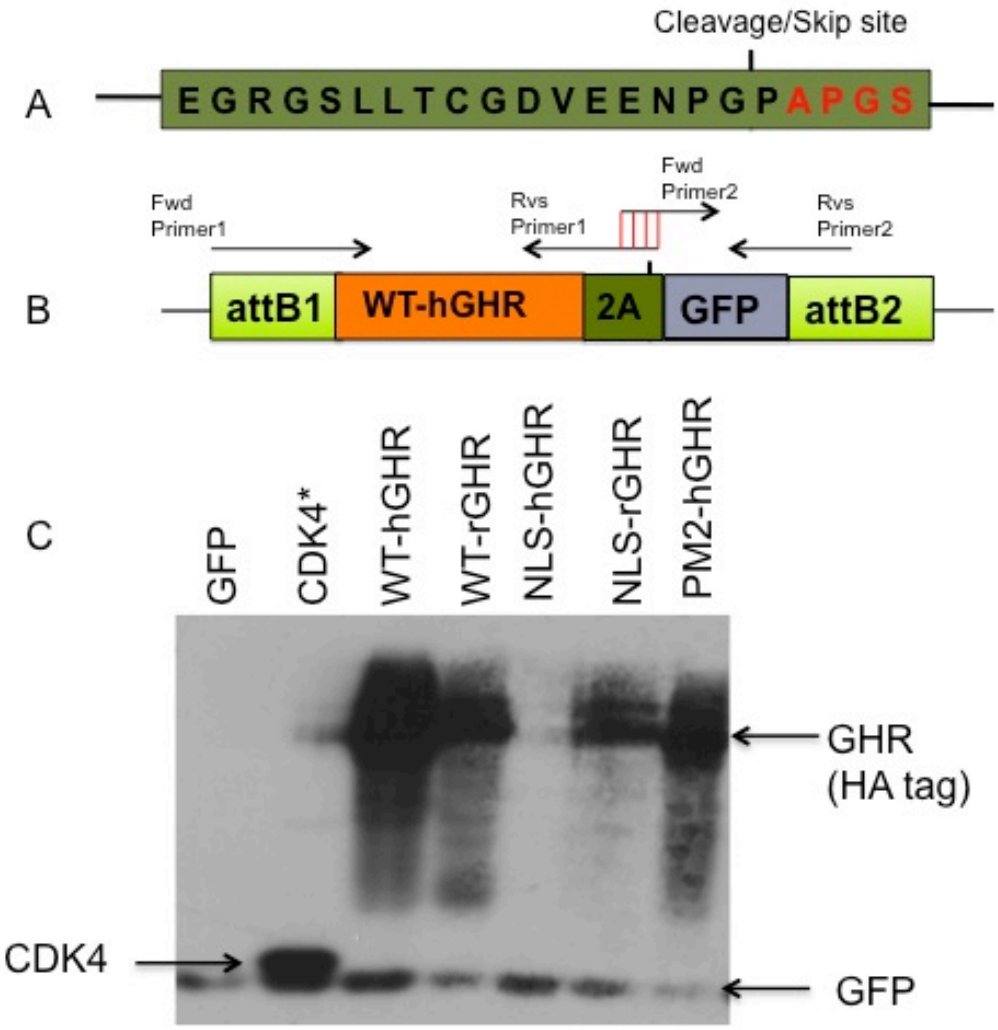

Figure 6.3: GHR constructs made using 2A peptide.

(A) Peptide sequence of 2A region with cleavage or ribosomal skip site (B) Representation of the 2A peptide containing ORF driven via a PGK promoter in a self-inactivating lentiviral construct. (C) Immunoblot showing expression of 2 heterologous proteins (GFP and GHR; GFP and CDK4) made using 2A peptide by transient transfection of HEK293 cells (20ug protein loaded). The GHR was probed against the N-terminal HA-tag. The expression of both proteins is evident as two separate molecules based on their respective molecular weights rather than a fusion protein.

PM2-hGHR- (C259S, F263C, I270C)-hGHR

The 2A elements used for the study were codon optimised for human expression and owing to the small size of only 66bp, they can be easily introduced between 2 or more genes, thus making them an ideal choice for lentivirus production since there are no size constraints with 2A peptide as opposed to IRES (internal ribosome entry sites) (~ 600bp). This approach therefore allows a single

virus particle to carry a set of genes into single cell. The precise mechanism of how 2A peptides bring about the expression of two separated proteins is not well understood but ultimately, a ribosomal-skip mechanism has been proposed, and 2A and 2A-like sequences are now referred to as CHYSELs (*cis*-acting hydrolase elements) rather than self-cleaving peptides (Donnelly et al, 2001). The rationale for the use of 2A peptide is the fact that oncogenesis is a multi-step process and requires accumulation of a number of genomic 'hits' leading to complete transformation and/or survival of partially transformed cells with one or a few hits (Hanahan & Weinberg, 2011). Using the RCAS/TVA system we can introduce desired genes with gain or loss of function that are hypothesised to cause neoplasia from our *in vitro* studies.

Immunoblot analysis for function GHR in prostate cancer cell lines

The two prostate cell lines stably transduced with lentiviral GHR constructs were FACS sorted for uniform GFP expression since 2A peptide results in proteins in equimolar ratio. Due to time constraints, only DU145 cell lines were analysed to determine the effect of the constitutively active and nuclear localised GHR constructs with respect to WT-GHR. The cells were subjected to three conditions before protein harvest: Cell supplemented in normal growth media (Normal Media), cells starved for 24hours in serum-free media (Serum-free media) and cells starved for 24hours in serum-free media then given an acute GH stimulation (GH+) for 12minutes. The resulting immunoblots on DU145/tva stably expressing GHR constructs are shown in figure 6.4. The lysates were initially probed with HA antibody to check for GHR expression and the two bands corresponding to mature (glycosylated) and immature forms of the receptor are evident.

Following exogenous GH stimulation (GH+), a clear STAT5 activation signal was observed in all GHR stables. No changes in ERK1/2 activation and a decrease in STAT3 activation were also evident following GH stimulation in all GHR constructs compared to GFP control. The Jun3A-rGHR construct lacks the receptor extracellular domain and is therefore not amenable to GH-mediated activation or degradation. In addition, the NLS-hGHR construct has been known to be poorly expressed as compared to WT-hGHR (Wooh JW PhD thesis, 2008). Under normal growth conditions, an activated STAT5 signal was observed for the constitutively active Jun3A-rGHR and PM2-hGHR as well as all the rGHR constructs. The rGHR constructs can bind to the bovine GH present in the serum and became activated. The P-STAT3 signal was selectively reduced in NLS cell lines. In the absence of GH stimulation and under starved condition, activated STAT5 was only detectable for Jun3A-rGHR cell line and P-ERK signals were elevated in WT-GHR and PM2-

hGHR specifically while P-STAT3 signal was quite weak. For subsequent experiments normal growth media conditions were chosen based on these signalling attributes.

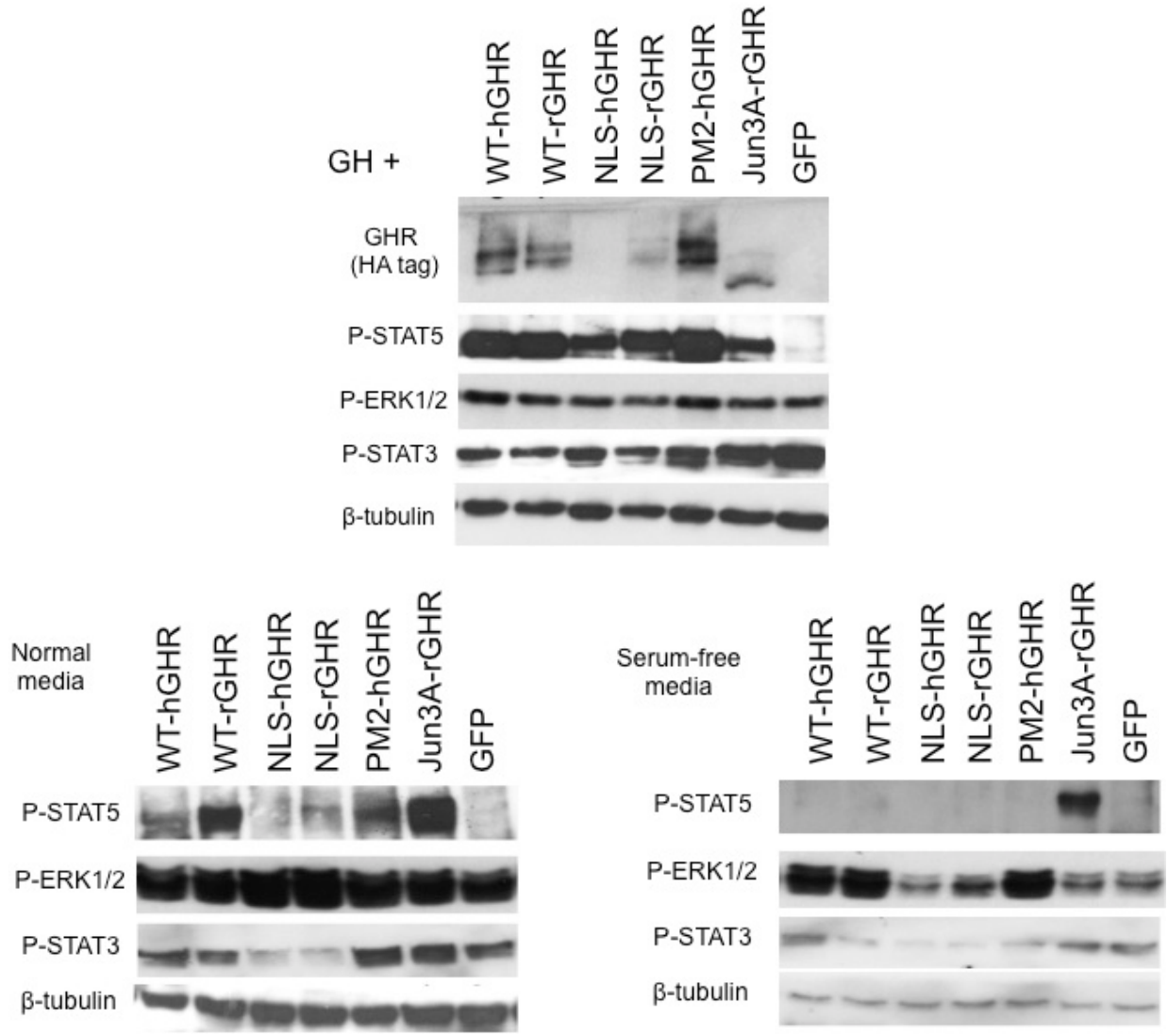

Figure 6.4: Immunoblot of DU145/tva cell lines stable for GHR constructs under different media conditions.
The DU145 stably expressing various GHR constructs and GFP control were subjected to three media conditions. GH+: 24hrs serum starvation and GH stimulation at 100ng/ml for 12minutes. Normal media: Complete growth media without serum starvation. Serum-free media: 24hrs serum starvation and no GH stimulation. The protein lysates were probed for downstream signalling molecules P-STAT5, P-STAT3 and P-ERK1/2 while β–tubulin was used as a loading control. Blots representative of n=2 independent experiments in three separate clonal lines made from three independent transductions.

Anchorage-independent growth assay

In order to determine a direct functional outcome of differential signalling in DU145 stables, soft-agar assay was performed. No change was evident in any of the GHR constructs in comparison to GFP control (fig.6.5). As a positive control c-myc DU145 stables were used.

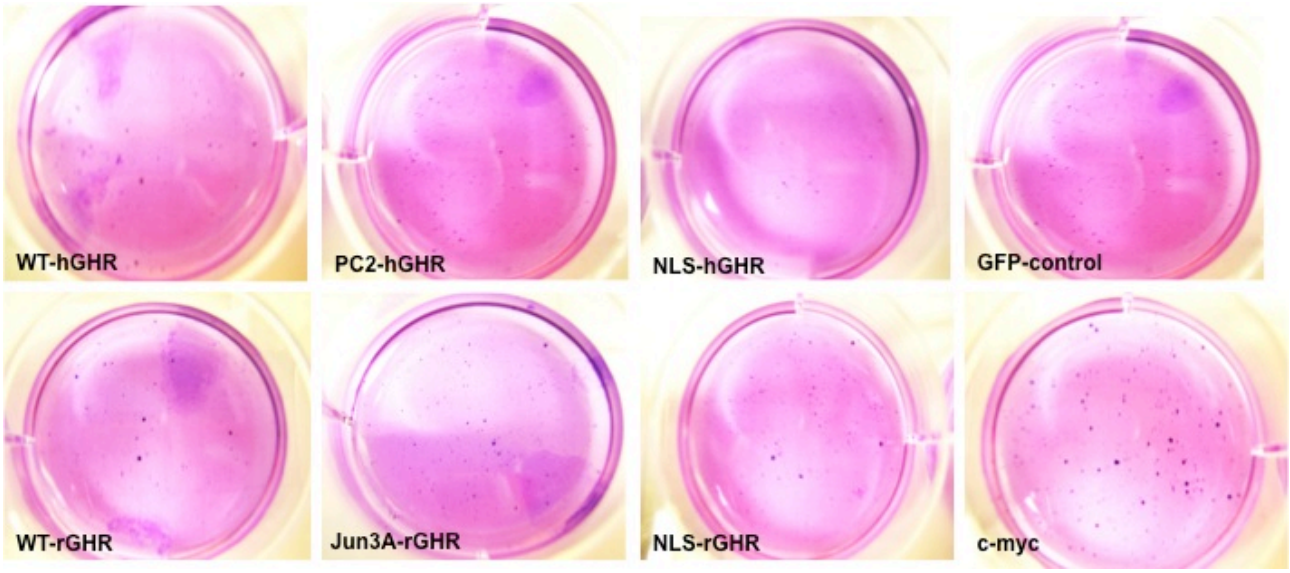

Figure 6.5: Anchorage-independent growth in DU145/tva cell lines stably expressing GHR constructs in normal growth media

There was no evident difference in soft agar colonies in any of the GHR constructs as compared to GFP control. DU145/c-myc stables were used as positive controls. Equal number of DU145 cells were layered in agarose and incubated for 3 weeks. The colonies were stained using crystal violet (0.005%) and images were taken on an inverted microscope. Images representative of n=3 independent experiments on two separate transduction derived clones.

Cell proliferation assay

The DU145/tva stables for GHR were analysed for proliferation under normal growth conditions based on BrdU incorporation in the nuclei, a marker for DNA synthesis. No significant change in proliferation was observed in any GHR stable cell lines (fig.6.6).

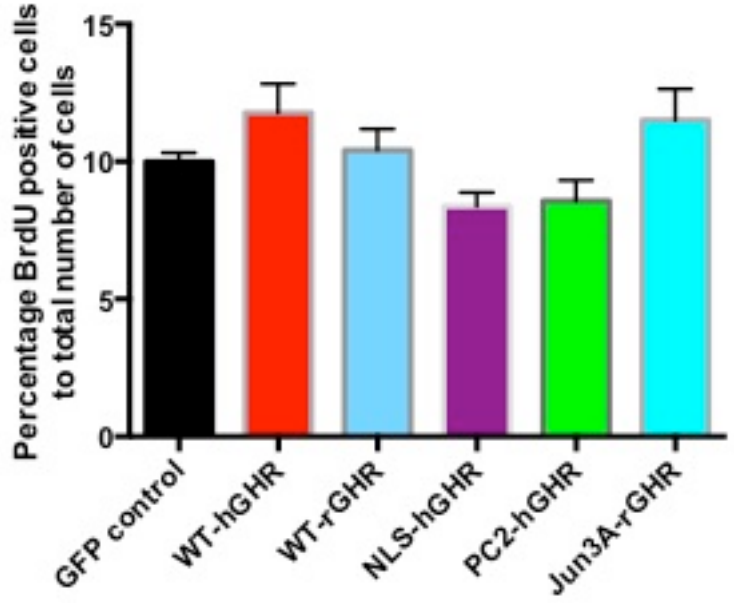

Figure 6.6: BrdU incorporation in DU145/tva cells cell lines stably expressing GHR constructs in normal growth media

Percentage of BrdU positive cells to total number of cells for GFP and GHR constructs in 10% Serum containing normal growth media counted in 8 random fields is represented graphically. No difference in proliferation is evident in any of the GHR constructs as compared to GFP control. Data pooled from three independent experiments was quantified and represented as mean ±SEM of n=2 independent experiments.

Since no differences were observed in DU145 cells we sought to test the GHR constructs in MCF7 cells since it is a well-characterised system of forced GH expression (Kaulsay *et al*, 1999). Our strategy initially was to evaluate and compare the downstream signalling in autocrine GH *vs* constitutively active GHR constructs in MCF7 cells. However, while generating the MCF7 stables for autocrine GH we observed opposing results to what has been published by Lobie's group and that was pursued instead. The GHR constructs were therefore not tested in MCF7 due to time constraints.

Generation of MCF-7 stables for GH expression: Two models of differential level of GH secretion

MCF-7 cell lines stably expressing the *GH1* gene under CMV and MT promoters were analysed for GH expression by qPCR relative to parental (untransfected) as shown in figure 6.7A. This was supported by western blot analysis using GH-specific antibody in stable clones. As expected CMV promoter-driven GH expression was significantly higher than MT promoter (fig.6.7B). In addition, to determine the functional concentration of GH secretion and production in the lysate, MTT assay was carried out with Ba/F3 cells expressing hGHR (Ba/F3-B2B2) following incubation of these

cells with MCF-7 supernatants and lysates at different concentrations. No detectable functional GH was evident in the any of the empty vector controls and parental cells even at the lowest dilution. The estimated value of GH secreted when driven via MT promoter was 95ng/ml ± 10 and in the lysate (inside the cell) was 45ng/ml ± 20 in preliminary studies. Consistent with qPCR and western blot these were lower than the CMV-driven autocrine GH expression, which resulted in secreted levels of GH in the range of 165ng/ml ± 22.

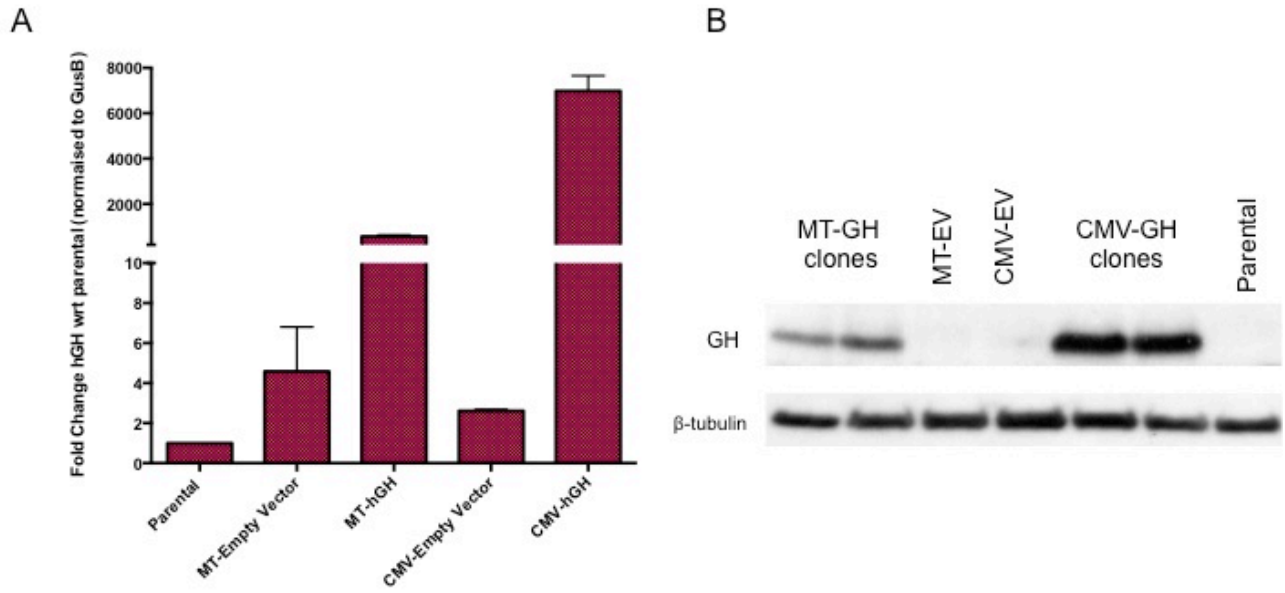

Figure 6.7: Growth Hormone expression in MCF-7 cell lines.

MCF-7 cell line stable clones for *GH1* gene expression using two different promoters CMV (CMV-GH) and MT (MT-GH) and the respective empty vectors (CMV-EV and MT-EV) were analysed for GH expression. (A) qPCR analysis representing fold change in *GH* expression normalised to *GusB* relative to parental cell line and (B) western blotting using GH-specific antibody indicates high levels of GH protein expression by CMV-driven *GH* gene as compared to MT. No GH protein was detectable in parental or empty vector stable cell lines. β–tubulin was used as loading control. Data representative of n=3 independent experiments confirmed in three separate clonal lines made from three independent transfections. (Mean±SEM). MT: metallothionein, CMV: cytomegalovirus, EV-empty vector.

GHR signal transduction in autocrine GH MCF-7 cell line

In order to determine the impact of different signalling molecules downstream of GHR, immunoblot analysis was undertaken for MCF-7 cells made stable for GH expression as well empty vector controls. These were starved for 24hrs and treated with and without exogenous GH at 100ng/mL for 12 minutes at 37°C. The cells were then harvested and probed with specific antibodies and represented in fig.6.8.

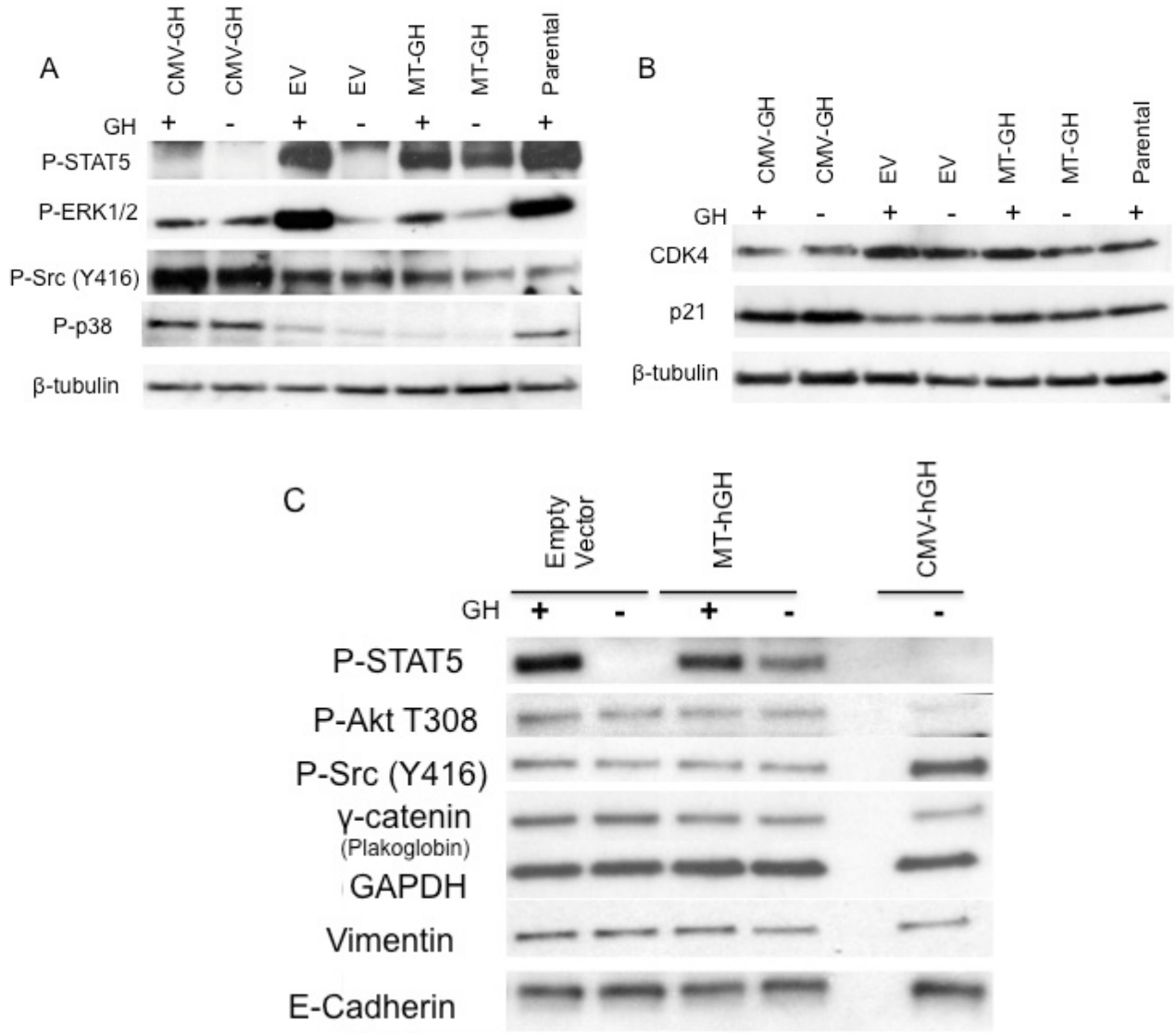

Figure 6.8: Immunoblot analysis of MCF-7 autocrine GH cell lines and controls.

Representative blot of signalling molecules in MCF-7 stables autocrine for GH under the control of MT and CMV promoters as well as empty vector (EV) and untransfected parental. All cell lines were starved for 24hrs and stimulated with GH at 100ng/ml for 12minutes where indicated (+). *Refer to text for explanation of results*. Blots representative of n=3 independent experiments.

A strong activated STAT5 signal was evident in parental and empty vector stables upon GH stimulation, reduced in MT-driven GH and completely undetectable in CMV-driven GH. In contrast, basal level of STAT5 activation was evident in MT-driven GH, which was absent in all other stables and parental in the absence of GH (fig.6.8A and 6.8C). A similar signalling pattern was observed for ERK1/2 with the highest level evident in controls (EV and parental) on GH stimulation. No ERK activation was seen in CMV-GH following exogenous GH stimulation and this level was independent of exogenous GH. The levels of active Src (Y416) was higher in CMV-GH as compared to MT-GH and parental cell line and was independent of GH. In contrast, the levels of active Akt (T308) were higher in MT-GH and EV as compared to CMV-GH and

independent of GH. Active p38 MAPK were highest in CMV-GH and parental cell lines and lowest in MT-GH. In addition, cell division protein kinase, CDK4 was downregulated and cyclin-dependent kinase 1-inhibitor (p21) was elevated selectively in CMV-GH stables (fig.6.8B). No change in CDK4 was observed between MT-GH and controls. However, p21 levels were lowest in EV as compared to MT-GH and parental. No changes in E-cadherin and vimentin protein levels were evident in any of the cell lines.

Increased proliferation in MCF-7 with lower levels of autocrine GH

Nuclear BrdU incorporation was carried out for MCF-7 cell lines and there was significantly increased proliferation under normal growth medium (10% Serum) and serum free media conditions selectively for MCF-7 cells with lower autocrine GH production via the MT promoter. In contrast, CMV-driven GH expression decreased cell proliferation as compared to parental cell lines or empty vector (fig.6.9).

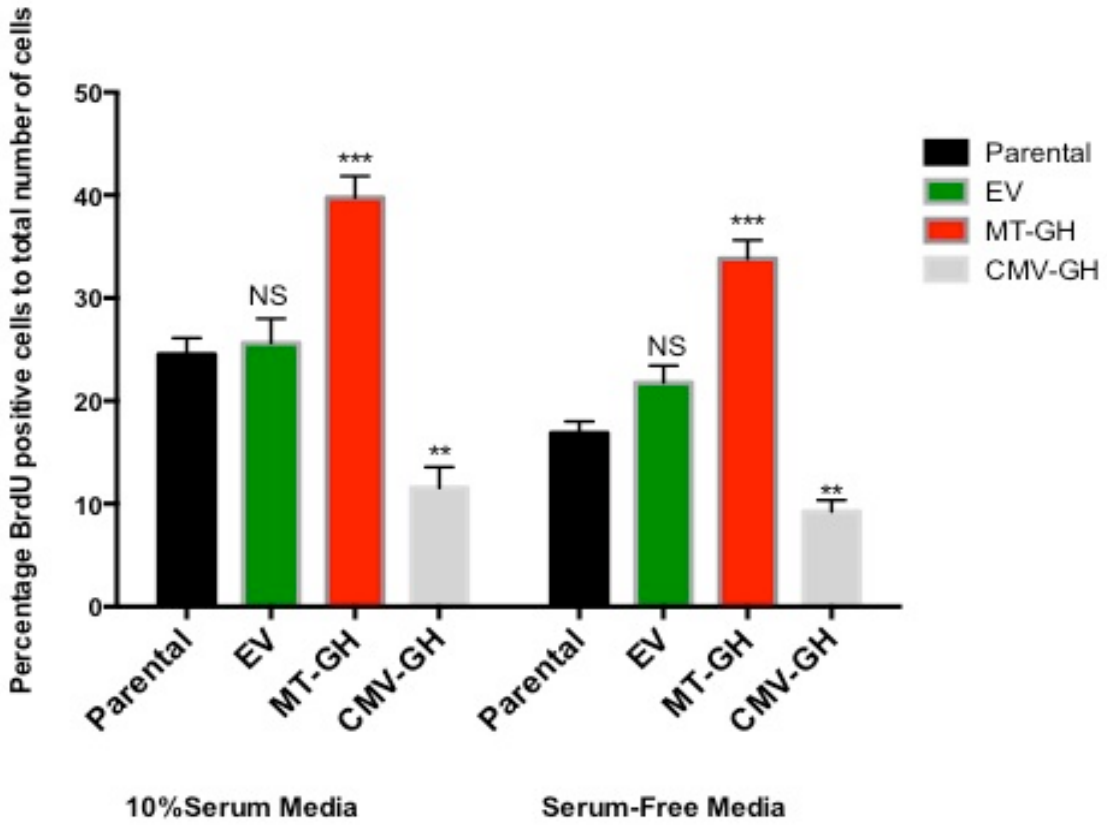

Figure 6.9: BrdU incorporation in MCF7 cell lines

Graphical representation of percentage of BrdU positive cells to total number of cells for parental, empty vector (EV) and MT and CM-driven GH MCF-7 cell lines in 10% Serum containing normal growth media and serum-free media (starved conditions) counted in 6 random fields (~400cells). Increased proliferation was evident in MT-driven GH while proliferation was reduced in CMV-driven GH as compared to parental cell line in both conditions of media supplementation. There was no evident difference in proliferation in EV under both conditions in comparison to the parental cell line. Data pooled from three independent experiments was quantified and represented as mean ±SEM of n=3 independent experiments. Statistical analysis performed using ANOVA (***, p< 0.001; **, p<0.01, NS = not

significant).

Increased colony formation in MCF-7 with lower levels of autocrine GH

The colony formation assay is an *in vitro* cell survival assay based on the ability of a single cell to grow into a colony. The colony is defined to consist of at least 30 cells and it essentially tests every cell in the population for its ability to undergo "unlimited" division bearing in mind that only a fraction of seeded cells retain the capacity to produce colonies. The colonies with greater than 30cells/colony were counted and broadly classified as holoclones, meroclones and paraclones depending on the morphology (fig.6.10). Holoclones are large with smooth edges and consist of small tightly packed cells at high density. Meroclones are smaller, have an irregular outline and consist of a mixture of small tightly packed cells and much larger loosely packed cells, particularly around the edge, with an average. Paraclones are small and diffuse and consist mainly of loosely packed enlarged cells. The highest number of clones for the same seeding density was observed in MT-driven GH MCF-7 cells as compared to the EV while no change was evident in any stable cell line driven via CMV promoter (fig.6.10).

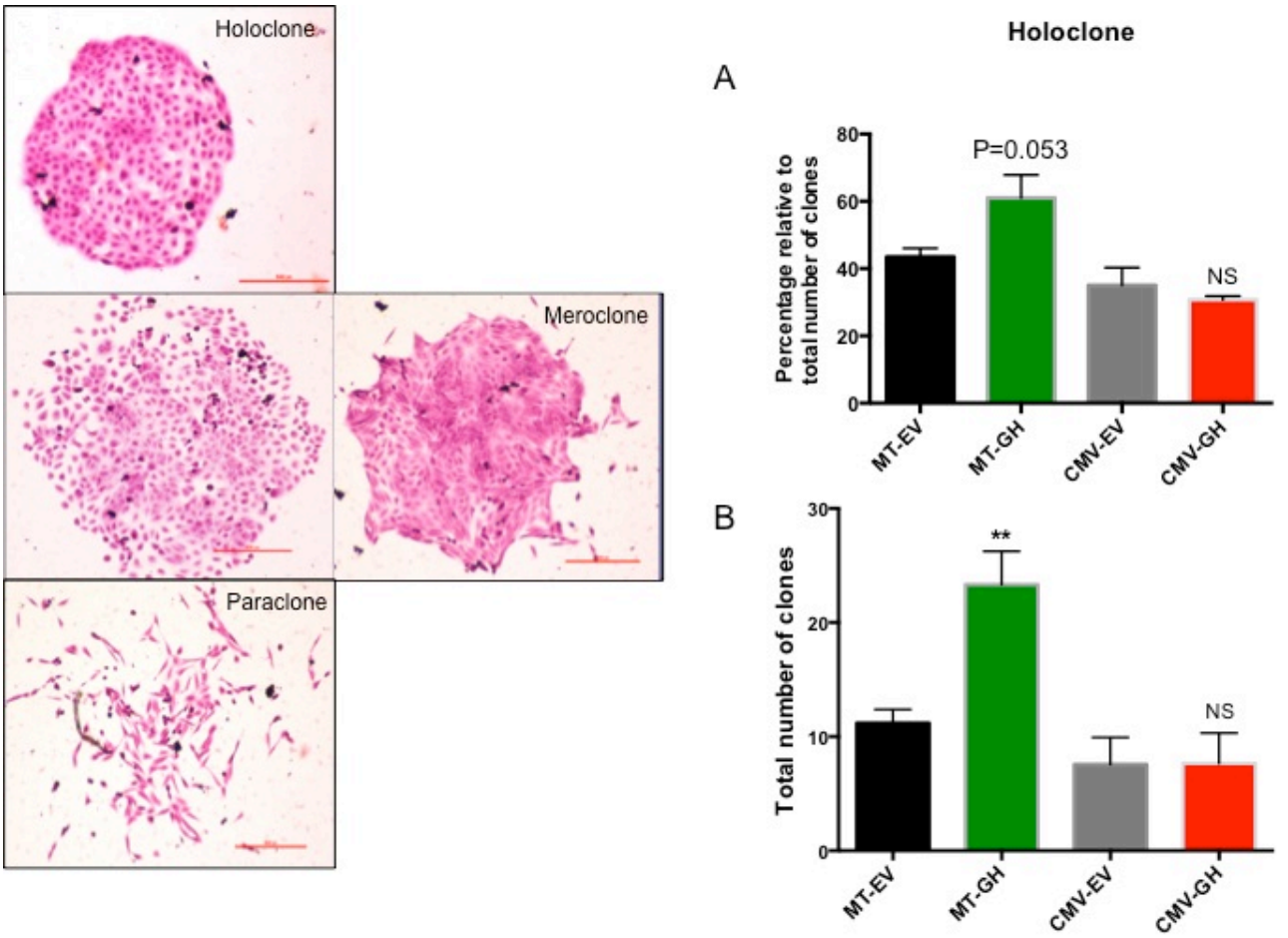

Figure 6.10: Increased Clonogenic ability of MCF-7 cell line autocrine for low levels of GH.

MCF-7 cells were plated at low seeding density and incubated for 2weeks, the generated colonies were stained with crystal violet (pink/purple) and only colonies greater than 30 were counted. Representative images of clones observed in MCF-7 cell lines for holoclone, meroclone and paraclone are shown. (A) Percentage of holoclones to the total number of clones is plotted for each cell line. An increase trend is evident in MT promoter driven GH cell line but did not reach significance. (B) Increased total numbers of clone were observed in MCF-7 stables with MT-driven GH as compared to EV control and no change was evident in CMV-driven GH as compared to parental cell line. Data representative of n=5 independent experiments (Mean±SEM). NS: not significant analysed by ANOVA.

Oncogenic transformation of MCF-7 cells with lower levels of autocrine GH

MCF-7 empty vector and CMV-GH cells organised into small colonies when cultured on Matrigel (fig.6.11). In contrast, MCF-7 MT-hGH cells adopted a very rapid stellate organisation within 48hrs.

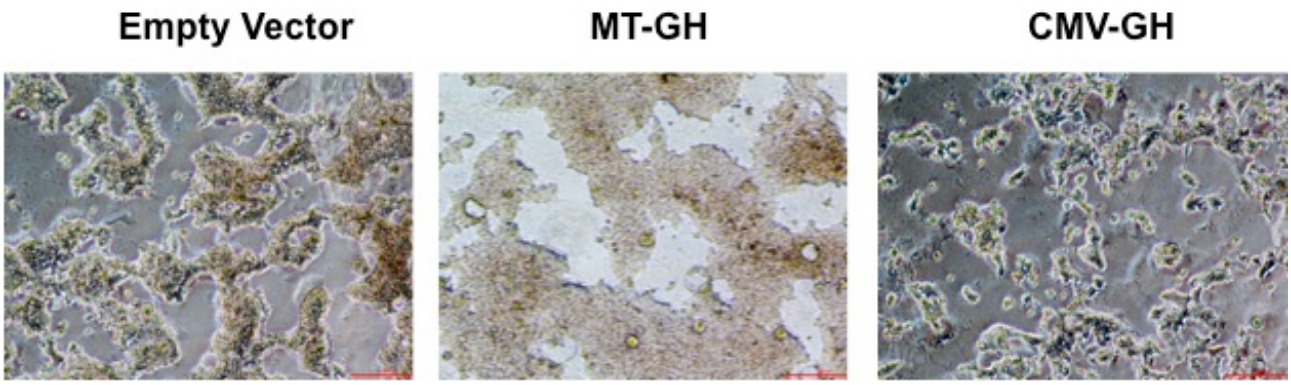

Figure 6.11: Phase contrast microscopy of MCF-7 stables on 2D-Matrigel

MCF-7 stables were seeded in equal numbers on a layer of Matrigel and overlayed with a dilute solution of matrigel ('On-Top' Assay). CMV-driven GH expression and Empty vector (EV) morphology formed small aggregates of cells while MT-driven GH had a more stellate organisation. Images representative of n=2 independent experiments.

Discussion

For this project prostate cancer was chosen as a suitable model for analysing GHR-mediated oncogenesis. While it is known that androgens play a central role in prostate cancer development and progression, other hormones and growth factors are also involved in prostate growth in both stages of androgen-dependent and independent neoplasia (Feldman & Feldman, 2001; Marques et al, 2010). IGF-1 plasma levels have been associated with prostate cancer risk, and GH/GHR axis, a major factor regulating IGF levels, also is able to prostate cancer cell proliferation and viability, with high expression of GHR reported in prostate cancer tissue (Chhabra et al, 2011). In addition active phosphorylated STAT3 and 5, key downstream molecule of GHR and PRLR signalling pathway are associated with high-grade (Gleason score) prostate tumours (Gu et al, 2010; Dagvadorj et al, 2007).

The action of GH/GHR has been associated with an increased incidence of several types of cancer, including those of epithelial origin. Several lines of evidence have suggested a specific correlation between endocrine or autocrine hGH-mediated signalling and prostate cancer. However, only a few published studies have directly tested the effect of hGH on prostate cancer cell function, and conflicting findings have been reported. An initial report indicated increased LNCaP cell proliferation in response to hGH (Untergasser et al, 1999). However, a second study failed to recapitulate this effect, although GHR binding and the activation of the STAT5, MAPK, and PI3-K signal transduction pathways by exogenous hGH was observed (Weiss-Messer et al, 2004). The role of these pathways in exogenous hGH-stimulated LNCaP cell proliferation has only recently been addressed and reported to be stimulatory (Nakonechnaya et al, 2013).

Due to time constraints we were only able to carry out analysis on DU145, an androgen-independent PCa cell line to investigate the effect of GHR activation in promoting prostate tumourigenesis. The preliminary studies with different GHR constructs driven via a PGK constitutive promoter have revealed no effect on cell proliferation by BrdU incorporation or anchorage-independence. There was no change in cell morphology even though a persistently activated STAT5 signal was evident in all rGHR constructs (WT, NLS and Jun3A) in the presence of complete growth media. Although no tests have been performed as yet in our study to determine the effect of exogenous GH, there seems to be no evident effect of autocrine GH on DU145 cells. This is supported by the fact that DU145 have no detectable *GH* transcript (Sustarsic et al, 2013). These reports do not discount for the fact that instead of proliferation, GHR-mediated signalling may increase cell survival by decreasing apoptosis as has been reported by exogenous GH administration in LNCaP cells (Nakonechnaya et al, 2013). In addition, the effect of these GHR constructs in the LNCaP cell line may provide more significant results as STAT5 has been reported to be a transcription-activator of androgen receptor (Tan et al, 2008) while SOCS2 (induced by STAT5) has recently been reported to mediate the cross-talk between the androgen and GH-mediated signalling (Iglesias-Gato et al, 2014).

Earlier studies have shown that activated Stat3 stimulates metastasis in human PCa cells *in vitro* and *in vivo*, while Stat5B preferentially promotes cell viability and tumour growth (Gu et al, 2010). This is supported by reports where STAT5 knockdown was shown to delay the progression of castration-resistant PCa (Ahonen et al, 2003; Thomas et al, 2011). The STAT5 overexpression studies have been carried out using an adenovirus system that results in very high expression of the downstream signalling molecules and therefore may not be similar to GHR or active GHR overexpression and most importantly would be cell line-dependent. It is important to highlight that Gu *et al.* have concluded that Stat5A/B activity related to metastatic behavior of human prostate cancer cells (DU145) is mediated by Src kinases rather than by Jak2 (Gu et al, 2010). In another study from the same laboratory it was reported that autocrine prolactin promoted PCa cell growth via Jak2/STAT5 signalling pathway (Dagvadorj et al, 2007).

Other reports have highlighted that both STAT5 and its promoter undergo increased methylation in PCa cell lines as compared to normal epithelial cell lines and this aberrant methylation has been correlated with a loss of gene expression and function (Mishra et al, 2010). On the contrary, the STAT5 locus has been shown to undergo amplification in clinical PCa specimen (Haddad et al, 2013), while other studies have emerged highlighting an opposite role of STAT5 isoforms during tumour progression (Shchelkunova et al, 2013).

Level of autocrine GH determines oncogenic ability

There is no doubt that GHR-mediated signalling by GH via an autocrine/paracrine manner promotes cell proliferation in numerous cancer models (Chhabra et al, 2011; Perry et al, 2013; Sustarsic et al, 2013) and results in a phenotypic conversion of others, especially human mammary carcinoma cells, into a more invasive phenotype as shown by elegant studies from Lobie's Group (Mukhina et al, 2004). However, these have been disputed with two independent studies indicating autocrine GH to be growth-inhibitory (Nakonechnaya et al, 2013) and the other implying that autocrine GH producing cells may be insensitive to GH antagonist (van den Eijnden & Strous, 2007).

We have utilised 2 model systems of autocrine GH in order to bridge the gap between the conflicting findings from Strous's Group, Lobie's Group, and Nakonechnaya *et al.* (2013). Using the MCF-7 cell line, the most widely published cell line exhibiting cancer-promoting autocrine GH effects we have made stably expressing lines in a similar manner to the previously reported studies using lipofectamine 2000 for transfection and pCDNA backbone to drive *GH1* expression via MT or CMV promoters and their respective empty vector controls, all with a selection marker. Consistent with the observation by Liu *et al.* (Liu et al, 1997) we also found that cytoplasmically localised GH (devoid of signal peptide) was not able to activate GHR (data not shown). We observed very contrasting effects in regards to 'cancer-like' features between the two promoters. There was a significant increase in cell proliferation under normal growth media (10% serum) and serum-free conditions for low level autocrine GH (MT-GH) whereas proliferation was dramatically reduced when a high level GH was expressed (CMV-GH) (Table 6.1). The former has been reported in vast majority of publications from Lobie's Group and the latter was used in the LNCaP cell line. Additionally, the level of GH reported by ELISA in these studies does not necessarily correspond to functional GH as opposed to our methods of bioactive GH measurement using the GH-responsive Ba/F3-B2B2 cell line. It is important here to note that some of the publications from Lobie's Group have used CMV to drive GH expression but the level of GH expression reported in their endometrial carcinoma cell line (Pandey et al, 2008) was significantly lower relative to the promoter-matched cell line in our study over a 24hour period. In comparison, the study of autocrine GH in the LNCaP cell line has only calculated GH levels over an 8hour period (Nakonechnaya et al, 2013) but based on the published graph it can be expected to strongly increase with time.

The model proposed by the Strous Group (van den Eijnden & Strous, 2007) is based on relatively high expression levels of GH and GHR in CHO cells and is valid for situations wherein the molar ratio of expression levels (GH/GHR) exceeds 0.5 in any given cell. In physiological systems however, the cellular levels of autocrine GH and GHR can vary widely between individuals (Hattori

et al, 2001). Strous's model proposes that the relative protein levels of GH and GHR synthesised will determine the fraction of receptor occupied by GH before arriving at the cell surface where high levels of autocrine GH would imply low levels or complete lack of unoccupied GHR as observed in some studies (van den Eijnden & Strous, 2007; Nakonechnaya et al, 2013). In line with the GH/GHR ratio as a factor, Segard *et al.* have reported enhanced proliferation and inhibition of differentiation in C2C12 myoblasts due to autocrine GH being observed only when the cells were forced to express GHR (six fold) even though they express low levels of endogenous GHR (Segard et al, 2003). A similar scenario exists in our study where the level of GH expression is much higher in cells expressing GH under a CMV promoter as compared to MT. This model can also explain the growth promoting effects of exogenous GH and growth-inhibitory effect by GH agonists reported in studies by Lobie's Group (Kaulsay et al, 1999) as opposed to lack of growth-promoting effects of exogenous GH reported by others (van den Eijnden & Strous, 2007; Nakonechnaya et al, 2013). This model also explains the disparity in growth inhibitory effects of pegvisomant treatment in GH-producing xenograft tumours (Divisova et al, 2006; Dagnaes-Hansen et al, 2004) and is illustrated in figure 6.12. Interestingly, the level of GH produced by non-invasive ductal carcinoma (DCIS) is higher than invasive ductal carcinoma (Table 6.1) (Raccurt et al, 2002), which suggests that high GH levels may prevent metastasis and that the GH secreted by them is actually used by surrounding cells (paracrine manner) that lack or secrete very low amounts of autocrine GH.

A similar phenomenon was observed in the case of PRL, where forced autocrine PRL-producing T47D cells displayed lower proliferation rate with reduced PRLR levels as compared to control cells but their conditioned medium (containing secreted PRL) promoted proliferation of lactogen-dependent Nb2 cells and control T47D cells (Nitze et al, 2013). Autocrine hGH has been shown to increase the sensitivity of the MCF-7 cell line (under CMV promoter but secreted GH levels not reported) to arsenic trioxide (ATO)-induced apoptosis (Zekri et al, 2013). In the light of the current data, this effect would likely be an additive effect of ATO on CMV-hGH driven apoptosis.

Interestingly, immunoreactivity for hGH was reported to be of variable intensity in different cells within the same primary culture of human mammary carcinoma cells established from malignant biopsies (Chiesa et al, 2011). Based on this observation, the pMT-GH model of autocrine GH (Kaulsay et al, 1999) would closely resemble the scenario found *in vivo* since MCF-7 made using the plasmid that does not contain a selection marker of its own. This is suggestive that one needs to examine the amount of unliganded receptors at the cell surface before an antagonist is administered. The same explanation holds for autocrine GH-producing cells that upon exogenous GH administration are insensitive (Segard et al, 2003; Nakonechnaya et al, 2013). This was also

supported by the fact that MCF-7 and MCF-10A cell lines stably transfected with human GH, showed reduction in anchorage-independent growth with exogenous GH (Zhu et al, 2005) while other studies from the same group have reported inhibition of 'cancer-like effects' when antagonists were used (Kaulsay et al, 1999; Kaulsay et al, 2001). Such a discrepancy can be attributed to the two different model systems used in these studies with MT promoter (Kaulsay et al, 1999) used in one and CMV in the other (Zhu et al, 2005) to drive the GH expression. We have shown here for the first time that the level of autocrine GH expression is the key to determining the oncogenic ability.

The significant inhibition of autocrine hGH–stimulated oncogenic transformation by exogenous hGH may simply be due to shift of the bell-shaped hGH dose-response curve. It has been shown that GH and GHR interact in the ER and that this association results in higher quantities of mature GHR (van den Eijnden & Strous, 2007). A remaining question is whether GH directly serves as a ligand chaperone or is dependent on Jak2 for assisting in folding of the GHR in the ER. In the experiments described by Strous's Group it was shown that since GHR gets folded relatively quickly, the role of GH in this process might be marginal. Additionally, the exogenously added GH or antagonist had no effect but the transiently transfected, CMV-driven autocrine GH-producing cells have minimal levels of activated STAT5, possibly a result of balance between activating factors, such as the Jak and STAT molecules and downregulating factors, like phosphatases and the SOCS proteins (van den Eijnden & Strous, 2007). Raccurt *et al*. have reported that SOCS gene expression is elevated in breast carcinoma, which may be a response to autocrine/paracrine GH (Raccurt et al, 2003). An alternative scenario as seen in the case of CIS, a member of the SOCS family and inhibitor of STAT5 signalling is its role in tumour promotion. CIS has been reported to correlate well with cell proliferation and colony formation with high expression level of CIS observed in proliferative areas corresponding to high level of GH synthesis in human breast cancers. CIS has been hypothesised to work via a negative feed back loop in MCF-7 cells stably transfected with the hGH gene (MCF-hGH) resulting in strong activation of MAPK pathway and inhibition of the cellular differentiation mediated through the Jak/STAT pathway (Borges et al, 2008; Raccurt et al, 2003).

Table 6.1: Autocrine GH secretion in cancer cell lines and breast cancer tissue based on published literature

Tissue/cell sample	Plasmid	Transfection reagent	GH levels in media secreted by cells	GH levels in protein extracted from cells	Reference
Normal breast tissue	n.a	n.a	n.a	69±21.5pg/mg lysate	(Raccurt et al, 2002)
Fibroadenoma tissue	n.a	n.a	n.a	99.5±12.5pg/mg lysate	(Raccurt et al, 2002)
DCIS (Intraductal carcinoma tissue)	n.a	n.a	n.a	195.5±12.5pg /mg lysate	(Raccurt et al, 2002)
Invasive ductal carcinoma tissue	n.a	n.a	n.a	102±13pg/mg lysate	(Raccurt et al, 2002)
Human mammary carcinoma cells (HMCC) derived from malignant biopsies	n.a	n.a	n.a	30 to 150 pg/ml Normalised to cell count: 1.5 to 6.5 pg/ml/million cells *In some cells hGH was undetectable*	(Chiesa et al, 2011)
Breast cancer explants	n.a	n.a	0.061±0.1 ng/mg tissue Secreted into media	n.a	(Milewicz et al, 2011)
MCF-7	pMT-GH (No selection marker)	DOTAP	2pg/ml	1100pg/mg cell lysate	(Kaulsay et al, 1999)
MCF-7	pCDNA-GH (Selection marker present)	SAINT-MIX	Not shown	Not shown	(Brunet-Dunand et al, 2009)
MCF-10A	pCDNA-GH (Selection marker present)	Effectene	100nM (2200ng/ml) (24hr end point)	n.a	(Zhu et al, 2005)
RL95-2	pCDNA-GH (Selection marker present)	SAINT-MIX	37.5ng/ml (1.7nM) (24hr end point)	n.a	(Pandey et al, 2008)
LNCaP Prostate cancer cell line	pCMV1-hGH (Selection marker present)	Lipofectamine 2000	15ng/ml (8hr end time point) *24hr levels undetermined*	n.a	(Nakonechnaya et al, 2013)

The ability of MCF-7–MT-GH to form an increased number of clones in the clonogenic assay supports increased proliferation and cell viability. In addition a significant increase in the number of holoclones generated from single cells was evident in our studies. This finding is consistent with the report that holoclones harbour cancer stem cell and are highly proliferative with self-renewal capacity as well as being serially tumourigenic (Beaver et al, 2014). In contrast, CMV-GH had no significant change in total number of clones or holoclones. Another point of difference between high and low levels of GH was morphology of cells on 2D-matrigel with close resemblance to *in vivo* assembly in low GH-driven cells as opposed to a more differentiated one seen in CMV-GH.

In regards to signalling, the autocrine GH has been shown to signal via Jak2/STAT3/5 (Kaulsay et al, 2001; Tang et al, 2010a; Tang et al, 2010b). The increase in mammary carcinoma cell number as a consequence of autocrine production of hGH is a result of both increased mitogenesis and decreased apoptosis and is dependent on the activities of both ERK1/2 and p38 MAPK that are mediated solely by its action on GHR (Kaulsay et al, 2001). Autocrine GH-mediated radioresistance in mammary and endometrial carcinoma cells has been attributed to Jak2 and Src kinases (Bougen et al, 2012). Remarkably, a converse correlation has been reported in signalling between the autocrine hGH and exogenous hGH administration in LNCaP cells. It was shown that inhibition of PI3-K or STAT5 was able to overcome the negative effect of autocrine hGH on LNCaP cell proliferation by returning it to a wildtype level (DMSO treated) (Nakonechnaya et al, 2013), which implies that these pathways also have a role in mediating growth inhibitory effects of overexpressed autocrine hGH. Finally, while MAPK pathway signalling appears to be required for basal LNCaP proliferation, ERK1/2 inhibition did not alter the effects of exogenous or autocrine hGH, indicating that MAPK pathway signalling is not likely involved in mediating the observed stimulatory effects of hGH.

Our results are in support with the role of STAT5 in autocrine GH-mediated proliferation as activated STAT5 was evident only in MCF-MT-GH both in the presence and absence of GH. The fact that there was more STAT5 and ERK signal following GH stimulation is indicative that low levels of GH in MT-GH as opposed to high levels in CMV-GH do not occupy all endogenous GHR. In addition, Src and p38 were higher in cells with more GH production suggesting a tumour suppressor role in our model. The decrease in BrdU incorporation and reduced clone numbers in CMV-GH are supported by reduction in CDK4 and increase in p21 protein levels. Similar to the earlier study by Mukhina *et al.* we also observed reduced plakoglobin levels in all cell lines with

GH indicative of a decrease in cell-cell contacts, essential for epithelial to mesenchymal transition (Mukhina et al, 2004).

These differences in signalling can be attributed to differential modes of GHR activation. It has been reported that GHR can be activated only when the receptor has exited the Golgi apparatus after glycosylation, a prerequisite for signalling. It is possible that very high levels of GH bound GHR complex are amenable to rapid degradation depending on the GH and GHR ratio, before they can even signal. This altered localisation has been shown in LNCaP cells overexpressing GH, with GHR location changing from peripheral patches on plasma membrane (in empty vector control) to cytoplasmic perinuclear intracellular compartments. These were later identified using specific marker enzymes assays to be Golgi and the endoplasmic reticulum with very little localisation on plasma membrane. The GHR was also shown to co-localise in Golgi with GH by confocal microscopy (Nakonechnaya et al, 2013).

The pulsatility of endocrine GH secretion does not seem to influence this difference in signalling, as the most extensively studied model of autocrine GH is mammary carcinoma in females that retain a more continuous level of GH secretion as opposed to males. This difference in signalling mediated through autocrine or endocrine GH may be caused by the fact that the receptors are already activated within the cell. Alternative signal transduction pathways might become activated through signalling from the Golgi system. The factors that can determine if the autocrine or endocrine will be promoting or inhibitory for proliferation are the signalling pathways that are differentially regulated as well as the concentration and location of activated receptor at that given time.

MCF-7 cells express *GHR* and *PRLR* transcripts at high levels while low levels of *GH* transcript and undetectable *PRL* transcript have been reported (Sustarsic et al, 2013). Wennbo *et al*. have suggested that the oncogenic effects of hGH are conducted only through interaction with the prolactin receptor (Wennbo et al, 1997). In the context of autocrine GH studies, the effects of the prolactin or IGF systems were not measured but the results reported by us and others are most likely only due to autocrine GH activating GHR because of their high expression levels. Further studies by using a TET-regulated system of autocrine GH synthesis are warranted and could aid in determining a ‘threshold’ level of autocrine GH that is tumourigenic above which it becomes growth inhibitory. Use of signalling and GHR inhibitors as well as cell transformation assays are required to further support our hypothesis. In addition, the direct effects of GH2 in cancer progression need to be evaluated by autocrine and endocrine mechanisms since GH2 transcript is elevated in numerous cancer cells (fig.S.1 in Appendix VII) as opposed to undetectable in corresponding normal tissues.

It is possible that different cell types and functional end points do not share the same requirement for intracellular *vs* extracellular hormone. More comprehensive analysis is needed to determine how the cellular site of GH action relates to the contrasting effects seen in our study and recapitulate these results with differential effects of GH expression levels in the LNCaP cell line.

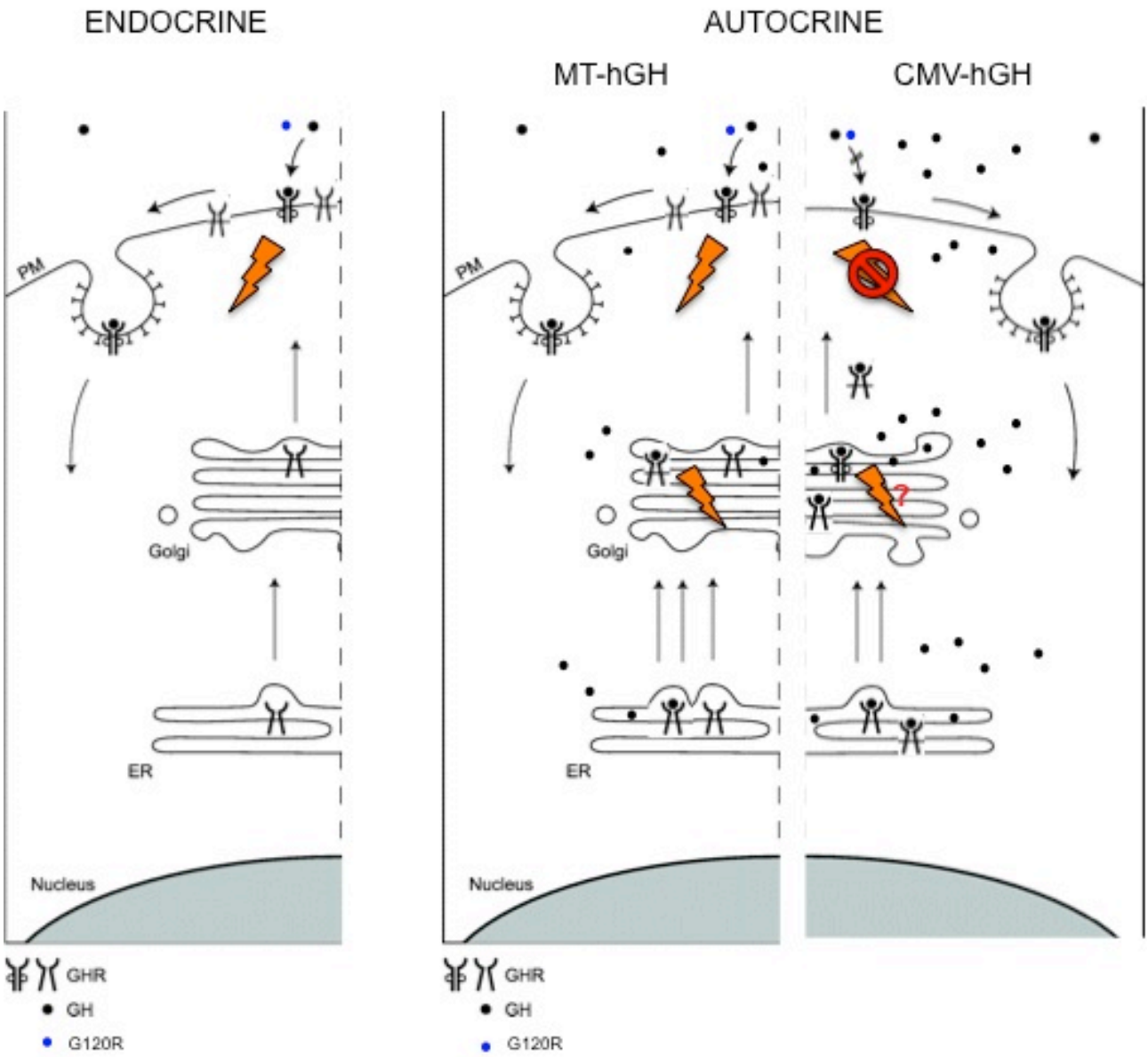

Figure 6.12: Model for endocrine *vs* differential autocrine GH actions on GHR in MCF-7 cells.

Schematic representation of endocrine (left panel) and autocrine (right panel) mode of signalling. Endocrine or exogenous GH administration results in GH binding to the receptor on cell surface and subsequent activation of downstream GHR signalling pathways. The complex is then internalised and degraded in the endosomal/lysosomal system. In the autocrine mode, GH can bind GHR following synthesis in the ER and signal transduction can start from Golgi itself and may continue until it is degraded. The level of endogenous GH can decide the GHR fate. During low level of autocrine GH (in MT-hGH stably transduced cells), reduced levels of GH do not occupy all the GHR and therefore some unbound receptor is still available on cell surface to bind exogenous GH (or G120R antagonist). However, during increased autocrine GH production (in CMV-hGH stably transduced cells) no exogenous GH (or G120R) binding can take place as all the receptors are pre-occupied by GH internally. In addition, the differential signal transduction pathways between low and high levels of autocrine GH need to be determined such that choice of pathway in former is transforming while latter is inhibitory to proliferation respectively. The precise location of cellular transformation signal is also currently unknown. (Developed from (van den Eijnden and Strous, 2007).

Chapter 7
Lyn interaction with Growth Hormone Receptor

Introduction

Src Family Kinase Structure

Src family non-receptor tyrosine kinases are present in essentially all metazoan cells, where their regulated activation by diverse growth factor, cytokine, adhesion, and antigen receptors is critical for generating an appropriate cellular response to external stimuli (Brown & Cooper, 1996). The nine members of the Src family include Src, Lck, Hck, Fyn, Blk, Lyn, Fgr, Yes, and Yrk. Src kinases share a conserved domain structure consisting of consecutive SH3, SH2, and tyrosine kinase (SH1) domains (fig.7.1). All family members also contain an SH4 membrane-targeting region at their N-terminus, which is always myristoylated and sometimes palmitoylated (Resh, 1999). The SH4 region is followed by a 'unique' domain of 50–70 residues, which is divergent among family members.

During myristoylation at the glycine residue on position 2, the terminal methionine is cleaved and a 14 carbon-myristoyl group is attached. This serves to provide membrane localisation but does not guarantee it. The function of the second ‘unique’ domain is currently unknown but has been suggested to play a role in individualized protein contacts (Brown & Cooper, 1996). This is followed by a SH3 domain that is 50-60 residues in length and has a β-barrel architecture consisting of five antiparallel β-strands and two prominent loops, termed the RT and n-Src loops (Noble et al, 1993). These loops lie at either end of a surface composed of aromatic and hydrophobic residues. An optimal Class I Src SH3 ligand has a consensus sequence RPLPPLP and a Class II ligand has ϕPPLPxR (where ϕ represents a hydrophobic residue and X denotes any amino acid). Therefore the recognition site for SH3 domain is the proline-rich sequences bearing the 'PxxP' motif (Lim et al, 1994). However, the SH3 domain of Fyn kinase, within the SFK family, has been shown to be promiscuous as it can even bind the proline-independent motif RKxxYxxY found in the immune cell adaptor SKAP55 (Kang et al, 2000). Even quite subtle changes in the sequence of SH3 domains and their binding peptides can alter the specificity of the peptide binding.

The SH2 domain is comprised of 100 residues and contains specific phosphotyrosine binding site. This phosphotyrosyl recognition site is highly conserved among SH2 domains, and contains a universally conserved arginine residue (Arg175 in Src) that forms requisite electrostatic interactions with the phosphorylated tyrosine (Waksman et al, 1993). Src-family SH2 domains bind preferentially to the pYEEI motif, coordinating the phosphotyrosine and isoleucine residues in the canonical recognition pocket. Polar and electrostatic interactions favour glutamic acid residues at

the pY +1 and +2 positions, but many other residues can be accommodated in these positions in Src SH2 domains (Songyang et al, 1993).

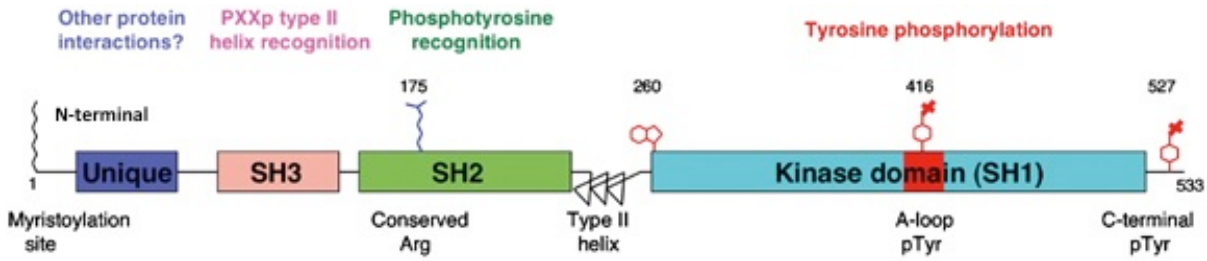

Figure 7.1: Schematic illustration of SFK structure.

At the N-terminal, SFK is myristoylated at the glycine residue on position 2 which lies in the SH4 domain (not shown here) and is followed by a unique domain of unknown function. The SH3 domain has a preferential binding for proline-rich sequences while the SH2 domain binds to phosphorylated tyrosine. The SH2 domain is connected to the Kinase/SH1 domain via a linker that allows SH3 domain to attach with the N-lobe. The activating phosphorylation site, Tyr 416 lies in the catalytic region of the SH1 domain while the inactivating phosphorylation site (Tyr527) lies outside the kinase domain on the C-terminal tail (Boggon & Eck, 2004).

The SH1 or Kinase domain is composed of 253 residues and follows the SH2 domain. The SH1 domain consists of a small N-terminal lobe and a large C-terminal lobe. The SFKs share the bilobal protein kinase fold that is a characteristic feature of all tyrosine kinases and ser/thr kinases. The N-terminal (or small) lobe is composed of five β-strands and a single α-helix, termed the C helix, which is an important component of the regulatory mechanism employed in Src kinases. The C-terminal (or large) lobe is predominantly α-helical, and contains the regulatory activation loop, which is the site of activating tyrosine phosphorylation in Src and other kinases (Boggon & Eck, 2004). Nucleotide binding and phosphor-transfer (via ATP) have been shown to occur in the cleft between the two lobes. The adenine moiety of the bound nucleotide is coordinated largely by interactions with the N-lobe and a short hinge segment that connects the two lobes. Bound nucleotide phosphates are in part coordinated by the glycine-rich G-loop (also termed the P-loop, for phosphate binding) (Taylor et al, 1992; Hubbard & Till, 2000). The activating tyrosine phosphorylation site at 416 is present in the catalytic site. There is a linker between SH2 and N-lobe that has prolines at positions 246, 250 and 263 whereby the SH3 domain attaches to the N-lobe. Towards the end of the kinase domain is an inhibitory phosphorylation site at Tyr527, which when phosphorylated allows it to attach to the SH2 domain and close the catalytic cleft. The proposed mechanism of its activation is described in figure 7.2.

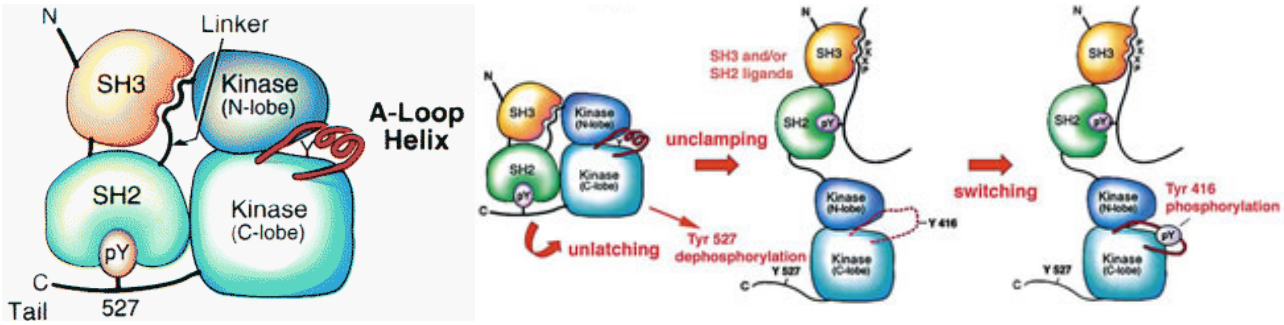

Figure 7.2: Illustration of proposed regulation of Src Family kinase

Generally SFK have an auto-inhibitory closed confirmation (left panel). This occurs as a result of stabilisation of SH3 domain by binding to the linker, which provides packaging of the N-lobe, while the SH2 domain attaches to the phosphorylated Tyr527 at the C-terminus. The ordered Activation "A" Loop forms a helix, stabilising the inactive conformation of the kinase domain while simultaneously blocking the peptide-substrate binding site and preventing phosphorylation of Tyr416. Following an activation stimuli (right panel), the SFK undergoes 3 steps: (i) unlatching where Tyr527 is dephosphorylated (by SHP1, PTPs) and detached from the SH2 domain. In addition to growth factor binding and Tyr527 dephosphorylation, a variety of SH2 and SH3 competitors may serve to alter SFK structure, leading to its activation (ii) unclamping where an opening and closing of the cleft between N-lobe and C-lobe is created (iii) switching where Tyr416 undergoes autophosphorylation (Bjorge et al, 2000; Boggon & Eck, 2004).

GHR and Src Family Kinases

Jak2 has been regarded as the classical GHR signalling kinase but there is strong evidence that indicates activation of the GHR also results in direct activation of SFKs (Zhang et al, 2006) (Rowlinson et al, 2008; Barclay et al, 2010), although the strength of the relative Jak2 and SFK signals is dependent on cell type (Jin et al, 2008). Activation of SFKs by ligand binding has already been shown for the related TPOR, EPOR, and PRLR (Lannutti & Drachman, 2004; Tilbrook et al, 1997; Chin et al, 1998; Fresno Vara et al, 2000). The activation of SFK by GH does not require Jak2 activation (Rowlinson et al, 2008) as is also the case for prolactin-mediated activation of PRLR (Fresno Vara et al, 2000). In addition, GH-driven SFK was shown to activate ERK1/2 through a phospholipase Cγ–Ras pathway (Rowlinson et al, 2008) similar to EPOR (Boudot et al, 2003).

Barclay *et al*. have described targeted knockin mutations to the Box1 sequence of GHR in mice, which completely abrogated Jak2 activation by GH *in vivo*, but did not decrease activation of hepatic ERK via SFK. These mice displayed an mRNA expression profile different from that of mice harboring a complete deletion of *ghr* gene, especially the transcripts regulated by ERK (Barclay et al, 2010). Relevant to the receptor activation mechanism, perturbing the relative orientations of the two transmembrane helices of the growth hormone receptor with glycine and proline substitutions changed the ratio of Jak2/STAT5 to ERK signalling (Rowlinson et al, 2008).

This has raised the possibility that some hGH analogues are able to activate ERK, but only weakly compared to STAT5, as reported for the I179M hGH mutant associated with deficient growth (Lewis et al, 2004). This residue sits next to W169 in receptor site 1. Moreover, a specific conformational change in the loop between the β-strands F' and G' of the lower fibronectin module of the GHR ECD was identified in the crystal structures, which differs between agonist-bound and antagonist-bound forms of the receptor, and mutating this loop markedly decreased ERK signalling but not Jak2/STAT5 signalling i.e. induced-biased signalling.

Of interest is the conserved YGEFS motif adjacent to the F'G' loop in the lower fibronectin module, which is equivalent to the WSXWS motif in the ECD of all Class 1 cytokine receptor family members. Mutations within this sequence have been shown to cause GH insensitivity and Laron syndrome (Brooks & Waters, 2010). Supporting the duality of GHR signalling, studies on the EPOR using numerous ECD conformations in conjunction with alanine insertions, at the boundary between transmembrane domain and cytoplasmic domain, which introduces helical rotations, showed differential STAT5 to ERK activation (Liu et al, 2009). These data clearly support that conformational changes in the ECD and rotation of the TMD are critical activation mechanisms for these receptors. Waters' Group has shown both *in vitro* in the Jak2-deficient cell line γ2A and *in vivo* in mice with mutated Box1 motif (alanine substitutions of the four prolines) that ERK can be activated by GHR independent of Jak2. These Box1 mutated mice (GHR K4) were similar to GHR-null mice in that they display severe growth retardation and lack Jak2/STAT5 phosphorylation in response to GH administration; however, they were able to activate ERK and a set of transcripts associated with SFK/ERK signalling (Barclay et al, 2010) (Thompson et al, 2000).

Further evidence that GH signalling utilises a Src family tyrosine kinase independently of Jak2, has come from Lobie's Group (Ling et al, 2003; Zhu et al, 2002). In NIH-3T3 cells it has been shown that GH activates c-Src, which in turn can activate ERK1/2 via a pathway involving the activation of the Ras-like small GTPases RalA and RalB, leading to Elk1-mediated transcription (Zhu et al, 2002). Further studies showed that both Jak2 and c-Src activate the additional Ras-like small GTPases Rap1 and Rap2 that acts to inhibit RalA-mediated activation of ERK1/2 (Ling et al, 2003). This chapter aims to determine the precise region of GHR to which Lyn kinase (and other SFK member) binds and vice versa as well if this binding is constitutive in nature. In addition, we seek to determine if there exists a competition between SFK (using Lyn kinase) and Jak2 binding on GHR and its functional consequence in terms of downstream signalling.

Materials and Methods

Construction of GHR mutants and truncations

Full-length human *ghr* encoded within a pQCXP plasmid was used as a template for the construction of GHR truncations and Box1 mutants with N-terminal HA tag. GHR truncations were made using specific primers with stop codon for early termination of receptor cDNA. The primers were designed to contain flanking attB sequence and are listed in Table 7.1. PCRs were carried out using Phusion® DNA polymerase (Thermo Scientific). For creation of the Box1 mutant in which all four prolines (PPVPVP) were mutated to alanine (AAVAVA), PCR-mediated overlap cloning (Bryksin & Matsumura, 2013) was used where two separate PCR products were ligated together (outlined in Chapter 6). All the mutants (represented in fig.7.3) were cloned into pQCXP-CMV-Puro DEST (plasmid# 17386, Addgene) by Gateway Cloning. The resulting clones were analysed by restriction digestion and sequencing. The pCMV-Lyn(WT)-myc tag vector was a kind gift from Prof. E. Ingley at Western Australian Institute of Medical Research, Perth Australia. The pCMV-Jak2 construct was made by Dr. A.J. Brooks (Brooks et al, 2014).

Table 7.1: Primer sequences used for construction of GHR truncation and Box1 mutants.

Primer	Sequence
hGHR 270tr stop attB2 Rvs	5'GGGGACCACTTTGTACAAGAAAGCTGGGTCTAAGAAAATAAGAATACAAATAGCATCACTGTTAGCCCAAATATTC
hGHR 280tr stop attB2 Rvs	5'GGGACCACTTTGTACAAGAAAGCTGGGTCTACAGAATCAGCATTTTAATCCTTTGCTGTTTAGAAAATAAG
hGHR 289tr stop attB2 Rvs	5'GGGGACCACTTTGTACAAGAAAGCTGGGTCTATTTAATCTTTGGAACTGGAACTGGGGGCAG
hGHR 312tr Rvs	5'GGGGACCACTTTGTACAAGAAAGCTGGGTC
hGHR 339tr stop attB2 Rvs	5'GGGGACCACTTTGTACAAGAAAGCTGGGTCTAAGTCTTTTCATCTGGCTCATCAATATCTAGCTCAATAAATTC
hGHR 364tr Rvs	5'GGGGACCACTTTGTACAAGAAAGCTGGGTC
hGHR Y314A/389tr Fwd	5'CCATTCATGATAGCGCTAAACCCGAGTTCCACA
hGHR Y314A/389tr Rvs	5'TGTGGAACTCGGGTTTAGCGCTATCATGAATGG
hGHR 389tr stop attB2 Rvs	5'GGGGACCACTTTGTACAAGAAAGCTGGGTCTAACCCTCATGTATGTCATTGGCATTGAAATCAG
hGHR 439tr stop attB2 Rvs	5'GGGGACCACTTTGTACAAGAAAGCTGGGTCTATTGTGGTTTGTTTTTCTCTGCTTGGATAACACTG
hGHR Box 1 mut Fwd:	5'TGGCCGCAGTTGCAGTTGCAAAGATTAAAGGAATCGATCCAGATCTCCTC
hGHR Box 1 mut Rvs	5'CTTTGCAACTGCAACTGCGGCCAGAATCAGCATTTTAATCCTTTGCTGTTTAGAA

attB1 pGHR sig Fwd	5’GGGGACAAGTTTGTACAAAAAAGCAGGCTATGGATCTCTGGCAGC TTCTGTTGACC
hGHR attB2 Rvs	5’GGGGACCACTTTGTACAAGAAAGCTGGGTCTAAGGCATGATTTTG TTCAGTTGGTCTGTG

Construction of Lyn mutants and truncations

The Lyn constructs were designed based on the earlier study by Chin *et al.* evaluating Lyn binding to EPOR (Chin et al, 1998). More constructs have been designed to analyse the effect of Lyn kinase domain on GHR binding. These constructs were created by overlap PCR extension method (Bryksin & Matsumura, 2013). The primers used are listed in Table 7.2.

Table 7.2: Primer sequences used for generating Lyn constructs

Primer	Sequence
pCMV-Tag Rev	5’GCTCCAGCTTTTGTTCCCTTTAGTGAGGG
pCMV-myc Fwd	5’GAGCAGAAACTCATCTCTGAAGAGGATCTGTAGGT
pCMV-Lyn1 Fwd	5’CCCTCACTAAAGGGAACAAAAGCTGGAGCATGGGATGTATTAAATC AAAAAGGAAAGACAATCTCA
Lyn119-myc Rvs	5’ACCTACAGATCCTCTTCAGAGATGAGTTTCTGCTCGGCCACGTAGTT GCTGGGGATGAAG
pCMV-Lyn67 Fwd	5’CCCTCACTAAAGGGAACAAAAGCTGGAGCATGATTGTGGTGGCCTTA TACCCTTATGATGGC
pCMV-Lyn120 Fwd	5’CCCTCACTAAAGGGAACAAAAGCTGGAGCATGAAGGTCAACACCTT AGAAACTGAAGAGTGGTTCTTC
Lyn230-myc Rvs	5’ACCTACAGATCCTCTTCAGAGATGAGTTTCTGCTCTTTGGGACTGATG CATGCCTTCTCCA
myc tag1 Rvs	5’ACCTACAGATCCTCTTCAGAGATGAGTTTCTGCTC
pCMV-Lyn234 Fwd	5’CCCTCACTAAAGGGAACAAAAGCTGGAGCATGCCATGGGATAAAGA TGCCTGGGAGATCC
Lyn-E260G Fwd	5’GGGCAGTTTGGGGGAGTCTGGATGGGTTAC
Lyn-E260G Rvs	5’GTAACCCATCCAGACTCCCCCAAACTGCCC
Lyn323-myc Rvs	5’ACCTACAGATCCTCTTCAGAGATGAGTTTCTGCTCAGCCATGAACTC GGTGATGATGTAGATGG
pCMV-Lyn322 Fwd	5’CCCTCACTAAAGGGAACAAAAGCTGGAGCATGGCTAAGGGTAGTTT GCTGGATTTCCTCA

Cell lines

Human embryonic kidney HEK293 cell line (a kind gift from Dr. F. Fontaine, Cooper Lab, IMB) and 293 derived HEK293T cell line together with African green monkey kidney COS-7 cell line (a

kind gift from Dr. M. Sweet, IMB) were maintained in DMEM supplemented with 10% FBS and maintained at 37ºC in a 5% CO_2 humidified incubator.

Signalling analysis

For signalling analysis, HEK293 and COS-7 cells were seeded at 1×10^5 cells per well and transfected using lipofectamine 2000 (Invitrogen) as per manufacturer's conditions with GHR expression constructs (300ng/well) or Lyn construct (100ng/well) where indicated. A total of 400ng of DNA was transfected per well with the residual quantity made up with pCMV-empty vector. Transfected cells 36hrs after transfection were starved in serum-reduced media (DMEM containing 0.5% FBS) and exposed to GH treatment at 200ng/ml hGH for 12minutes at 37ºC.

Co-Immunoprecipitation and Western Blotting

HEK293T cells were plated in T-75 flask format at equal seeding density and transfected next day at 50% confluency with 12µg GHR plasmid, 8µg Lyn plasmid or 8µg Jak2 plasmid using lipofectamine 2000 (Invitrogen) as per manufacturer's conditions. For Jak2 and Lyn competition assays, equal amount of Lyn and Jak2 plasmid were added (4µg each) with 12µg of GHR constructs. For co-immunoprecipitation (co-IP), transfected cells were starved 16hrs before harvest in serum reduced media (DMEM with 0.5% FBS). On the subsequent day, cells were stimulated with 200ng/ml human GH for 12minutes at 37ºC. The cells were washed in cold PBS and harvested by scraping into cold lysis buffer comprising 150mM NaCl, 50mM Tris pH7.5, 5mM EDTA, 0.5% Trition-X-100 supplemented with 1x complete EDTA-free protease inhibitor tablets, 10mM Na_3VO_4, 30mM NaF, 10mM $Na_4P_20_7$. Protein lysates were spun at 12000g for 10minutes at 4ºC and quantified using a BCA Assay kit (Pierce). Equal amount of protein lysates were pre-cleared using Protein G sepharose beads (GE Healthcare) for 30minutes at 4ºC. The pre-cleared lysate was used for immunoprecipitation.

For Jak2 co-IP, anti-Jak2 antibody at (1:100 dilution) and for Lyn co-IP, Lyn antibody (1:50 dilution) or myc-tag (at 1:100 dilution) (Cell signalling) were added to protein lysates and mixed gently on a rotating wheel at 4ºC. After 2hours, Protein G sepharose beads were added in the antibody-lysate tube which was then mixed gently on a rotating wheel at 4ºC for another 2hours. The beads were washed in lysis buffer (lacking Triton) twice and spun at 6000rpm for 1minute each time between washes and the supernatant was removed. Finally, the washed beads were boiled in

SDS sample buffer with 0.1M DTT for 5minutes and spun at 12000g for 5minutes. The supernatant was removed and subjected to SDS PAGE gel electrophoresis.

Results

Construction of GHR truncations and signalling analysis

A series of GHR truncations illustrated in figure 7.3A were constructed and verified for expression ability by transient transfection in HEK293 cells by immunoblotting for the HA tag (fig.7.3B). All GHR constructs excluding 364tr and 339tr expressed well (as compared to WT), and show two bands, a higher molecular weight representing mature glycosylated monomer and lower band representing the precursor form. The 339tr and 364tr failed to express even in the presence of proteasomal inhibitor, MG132 (data not shown) indicating that the decreased expression was independent of proteasomal degradation and may be the outcome of an unstable mRNA that undergoes rapid degradation. Most GHR truncations were expressed at higher levels as compared to full-length receptor owing to smaller size and reduced degradation especially 289tr and 270tr lacking both UbE motif and DSGxxS motif important for proteasomal degradation (da Silva Almeida et al, 2012). In addition, owing to lack of Box1 motif, no Jak2 binding could be expected with these constructs which would also reduce Jak2-mediated degradation.

As shown in figure 7.3B, STAT5 activation was only evident for WT GHR following GH stimulation. There are some endogenous GHR in the HEK293T cell line accounting for low level of STAT5 activation seen in all other mutants. However no difference in ERK activation was evident even in the presence of GH (data not shown). To establish a cell line to analyse Lyn-mediated ERK signalling HEK293 and COS-7 cells were tested by transient transfection of mutants. The STAT5 activation in HEK293 cells was similar to HEK293T but with increased ERK activation evident after GH stimulation (fig.7.4A). However, ERK activation was also evident in Lyn only transfected wells indicating that GH-mediated ERK pathway is already predominant in these cells due to endogenous GHR. It is also important to note that GHR truncations express at a higher level as compared to full-length constructs (fig.7.3B). The poorly expressed constructs (364tr and 339tr) have since been excluded from signalling analysis.

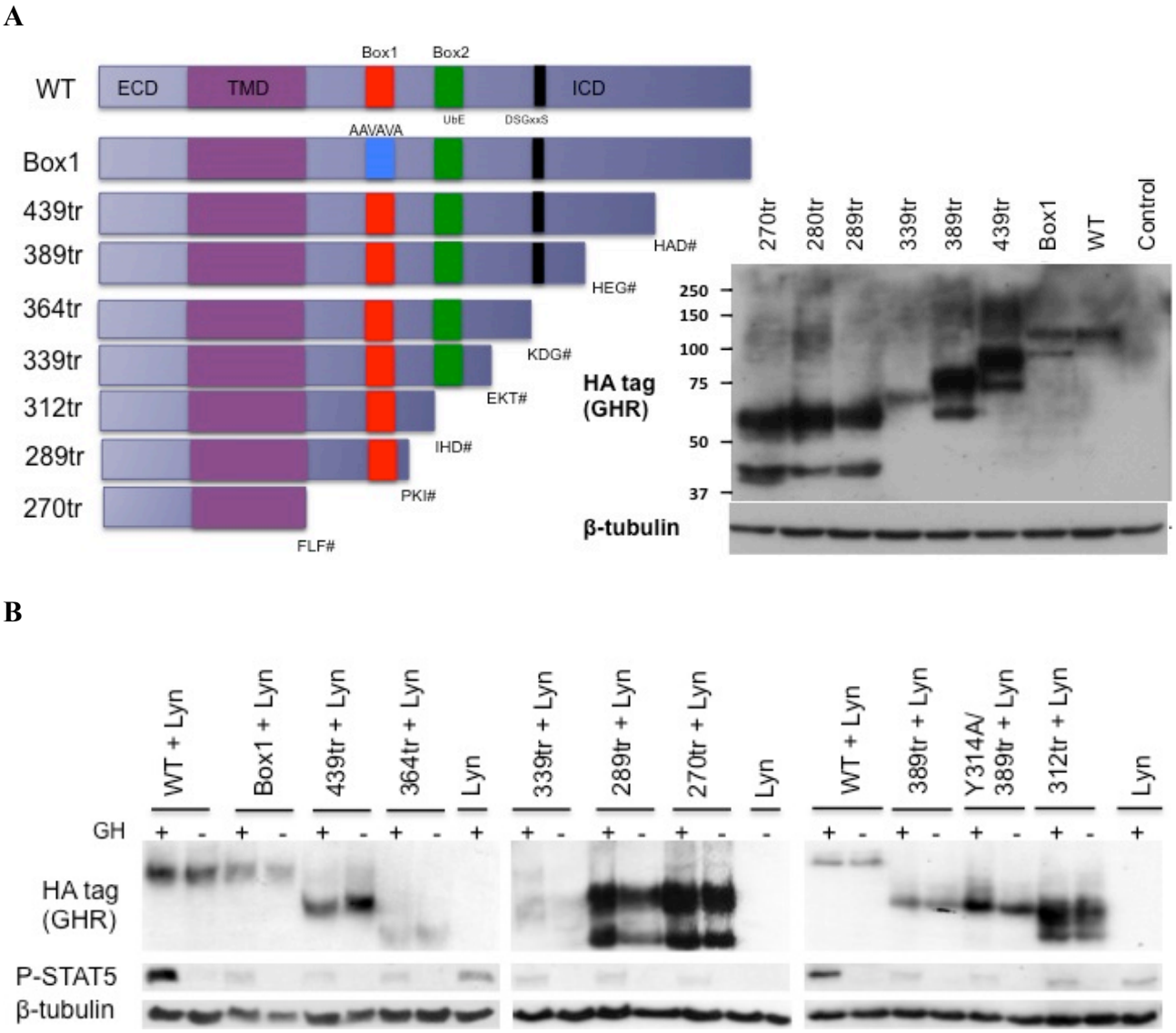

Figure 7.3: Construction of GHR mutants and signalling analysis in HEK293T.

(A) Schematic representation of GHR Box1 mutant and GHR truncations used for Lyn co-IP analysis. The WT hGHR is represented with extracellular domain (ECD), transmembrane domain (TMD) and intracellular domains and with Box1 (red box), Box2 (green box), UbE: ubiquitin motif, DSGxxS motif (black box) indicated. Each truncation is represented with the last three amino acids in the sequence followed by a stop codon (#). The box1 sequence with the prolines mutated to alanines is indicated in blue. HEK293T cells transiently transfected with GHR truncations, Box1 mutant (refered to as Box1) and WT receptor were immunoblotted for GHR (for HA tag) and represented on a molecular weight scale. (B) Western blot analysis of transiently transfected GHR mutants in HEK293T cell lysates using HA-tag for receptor expression and STAT5 activation after GH stimulation (+) at 200ng/ml for 12minutes. All GHR constructs except 339tr are expressed more efficiently than full-length WT and Box1 for an equal amount of protein loaded based on β–tubulin. Activated STAT5 after GH stimulation is strongest for WT GHR as compared to Lyn alone transfected control. Blots representative of n=3 independent experiments.

In the case of COS-7 cell line, GH-mediated STAT5 activation although weak was evident only when GHR was transfected. In addition, following GH stimulation there was increased ERK activation when GHR was transfected and it increased further upon Lyn transfection and was not evident in Lyn only control (fig.7.4B).

A

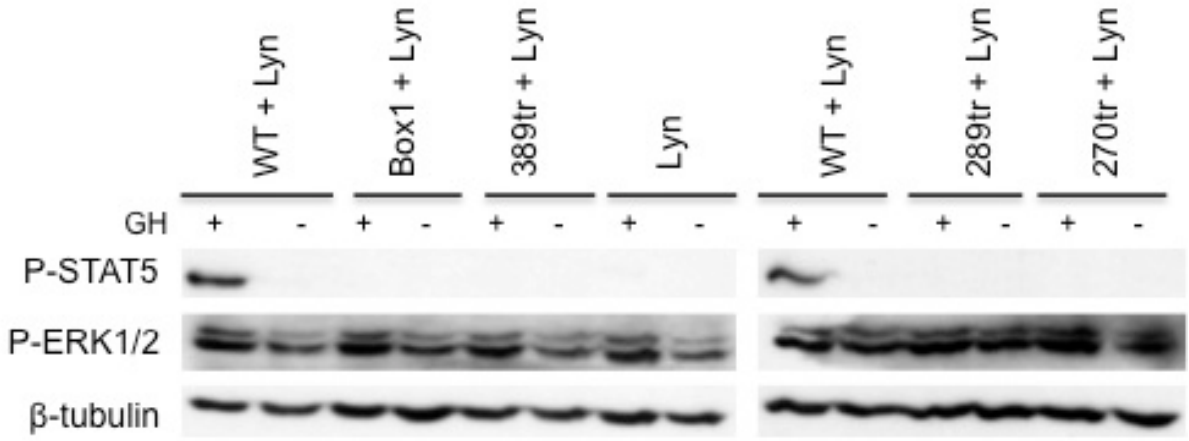

B

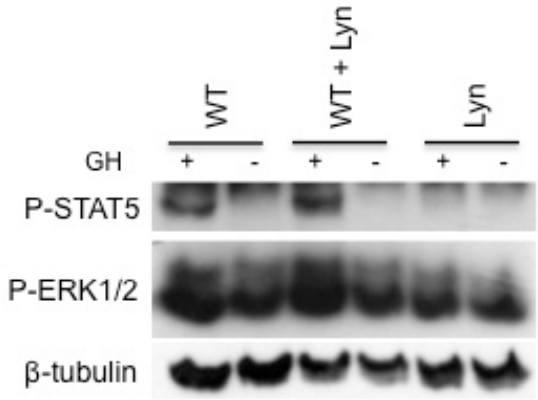

Figure 7.4: Downstream signalling from GHR mutants following GH stimulation.
Transiently transfected GHRtr and Box1 mutants with Lyn were analysed in HEK293 and COS-7 cell lines for downstream signalling after GH stimulation (+) at 200ng/ml for 12minutes. (A) HEK293 cells transfected with WT gave a strong activation of STAT5 that was not evident for other GHR constructs while ERK activity was detectable in all mutants and control cells following GH stimulation. Blots representative of n=2 independent experiments (B) COS-7 cells show STAT5 activation after GH stimulation that was only evident in WT transfected cells. Increased ERK activation was observed when both WT and Lyn were transfected as compared to WT alone and no GH-mediated ERK activation was observed in Lyn only control. Blots representative of n=2 independent experiments.

Co-immunoprecipitation of GHR truncations

The GHR truncations were subjected to co-IP following transient transfection in HEK293T. Since these cell lines have low endogenous SFKs, therefore based on the Waters' Group results of Lyn (a SFK member) interaction with GHR (Rowlinson et al, 2008), Lyn was transfected along with GHR. For co-IP, different buffers were standardised (to amount of Triton-X-100) to get maximum pull down of GHR and Lyn, without disrupting their interaction. The harvested protein lysate was pulled down with Lyn antibody and the blots were probed for HA tag. The immunoblot is shown in figure 7.5A and an interaction between full-length WT and Box1 mutant with Lyn is evident. In addition,

Lyn interaction was also observed for the truncations 439tr and 389tr. No interaction was evident in 289tr and 270tr even at higher level of expression of GHR in total cell lysate (fig.7.3) and also in the case of 339tr, which was shown to have reduced receptor expression (fig.7.4A). Following the first round of co-IP analysis further truncations were made between residues 364 and 289. In addition to truncation at 312, the tyrosine at 314 was mutated to alanine in the 389tr background and both were found to interact with Lyn (fig.7.4B). These co-IP results were confirmed using an anti-myc tag antibody (to detect C-terminal myc tag in Lyn) and gave similar results (data not shown).

A

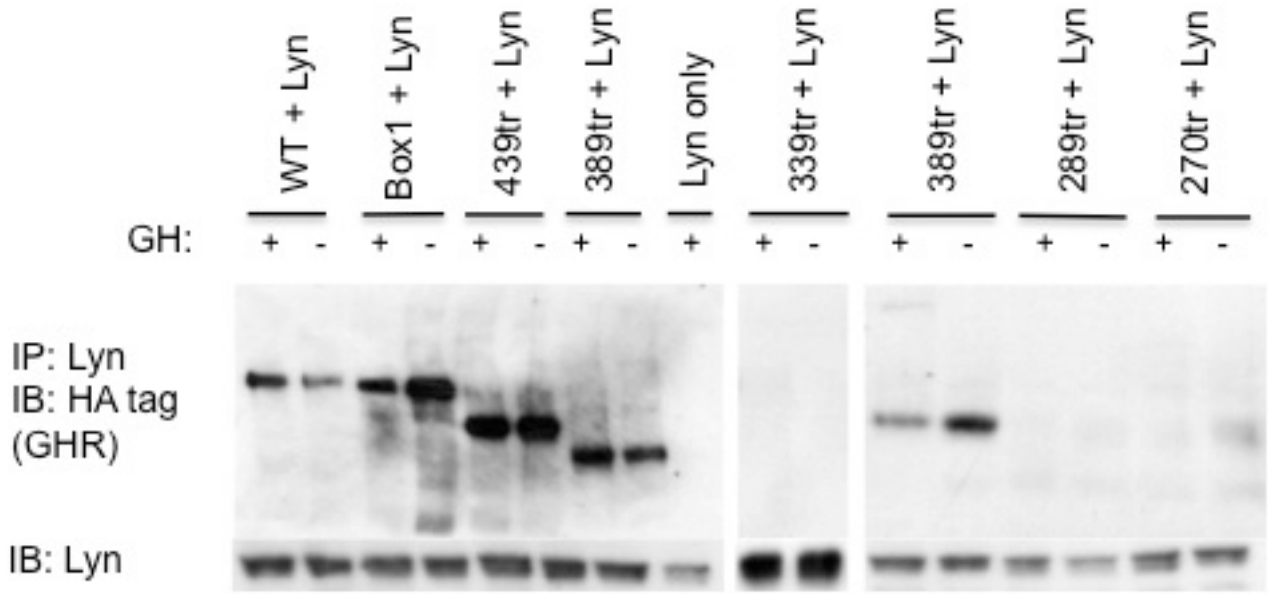

B

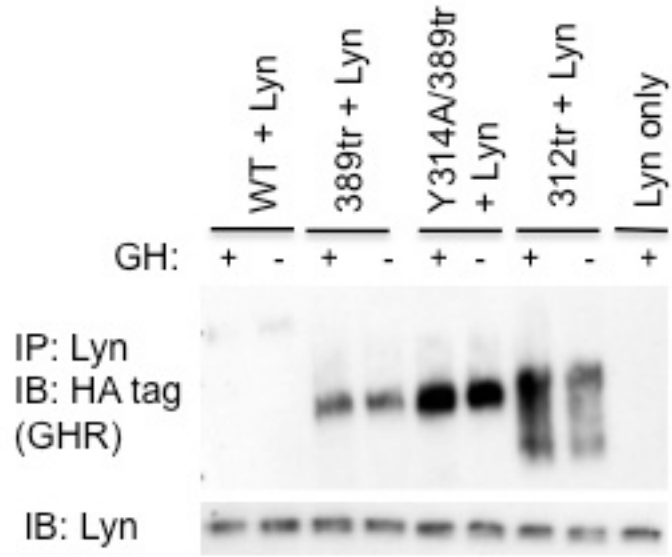

Figure 7.5: GHR interaction with Lyn in HEK293T cells

GHR mutants were subjected to co-IP analysis (refer materials and methods) to determine the region on GHR where Lyn binds. (A) Lyn binding is evident in full-length WT and Box1 mutant as well 439tr and 389tr. No binding was evident in the case of 339tr (issues with expression), 289tr and 270tr. Blots representative of n=3 independent experiments. (B) Lyn

binding to 312tr and Y314A/389tr is also evident. Blots representative of n=2 independent experiments.

Effect of Jak2 on Lyn GHR interaction

In order to determine if there was an effect of Jak2 on Lyn binding to GHR, HEK293T cells were transfected with WT GHR and both Jak2 and Lyn subjected to co-IP pull down simultaneously with Jak2 and Lyn antibody. Jak2 co-IP was first performed as a proof of principle to confirm if this binding was specific to Box1 motif. As evident from immunoblot in figure 7.6A Jak2 interaction with WT GHR was constitutive but required an intact Box1 motif as no interaction was evident in Box1 mutant. In addition, there was increased activation of Jak2 following GH addition in WT receptor as evident from the P-Jak2 immunoblot (fig.7.6A). The Lyn co-IP immunoblot (fig.7.6B) revealed two observations. Firstly, there was a decrease in Lyn interaction with WT receptor following GH stimulation when Jak2 was transfected. This was in contrast to the observation in Box1 mutant where the binding of Lyn to Box1 mutant was facilitated upon GH stimulation and was constitutive when no Jak2 was added (fig.7.6B, 7.5A). Interestingly, addition of Jak2 and its concomitant binding at Box1 motif in WT receptor resulted in an increase in mature GHR isoform in comparison to the precursor (fig.7.6B) as shown previously (He et al, 2005).

A

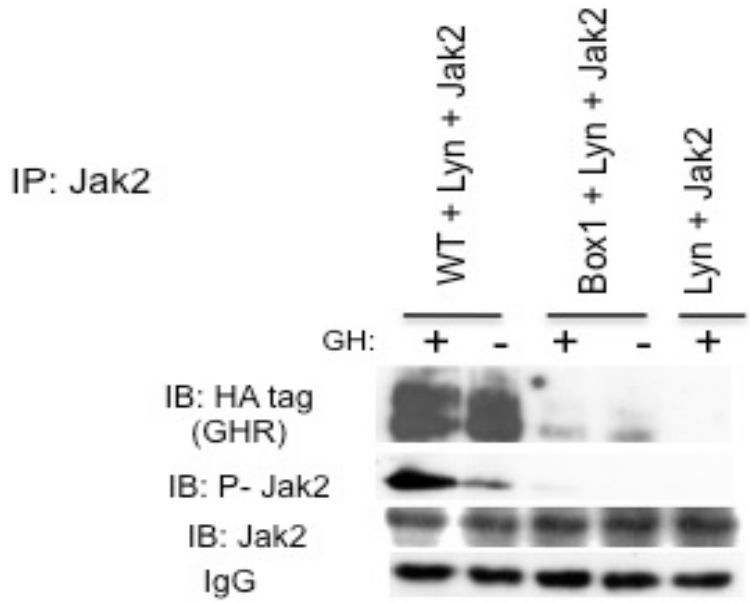

B

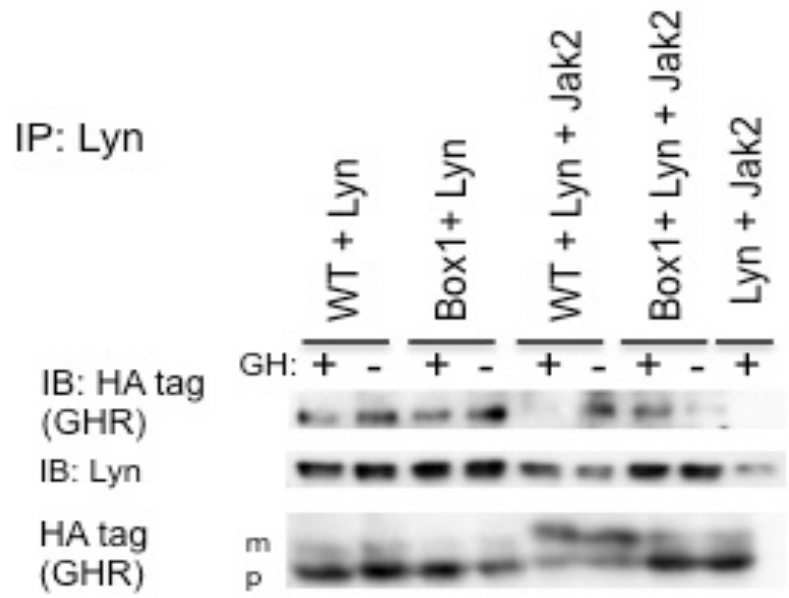

Figure 7.6: Effect of Jak2 on Lyn interaction with GHR.

Jak2 and Lyn constructs were transfected with WT and Box1 mutant GHR in combination or with Lyn alone in HEK293T cells and subjected to co-IP analysis (refer materials and method section). (A) Jak2 interaction with WT and Box1 mutant indicates that Jak2 binds only to the Box1 motif in the GHR and gets activated after GH stimulation evident from P-Jak2 blot. (B) Lyn co-IP was carried out to determine the effect of Jak2 on Lyn binding to GHR for WT and Box1 constructs. The remaining lysate left after using the half for the Jak2 co-IP above was used for Lyn co-IP and matched with lysate lacking exogenous Jak2. There was decrease in Lyn binding following GH treatment in the presence of Jak2 while no binding difference was evident in the absence of GH stimulation for WT GHR. In contrast Lyn binding to Box1 mutant increased after GH stimulation when Jak2 was transfected. Note the increase in mature receptor isoform following Jak2 transfection with WT GHR. Blot representative of n=2 independent experiments.

Lyn Constructs

Similar to the strategy used to determine Lyn interaction with EPOR (Chin et al, 1998), several Lyn constructs were made to determine the region on Lyn (fig.7.7) that interacts with GHR. Numerous constructs with different domains deleted and others mutated such as kinase dead (E260G) were made. These are currently being analysed for expression, signalling and co-IP analysis using antibody against its C-terminal myc tag.

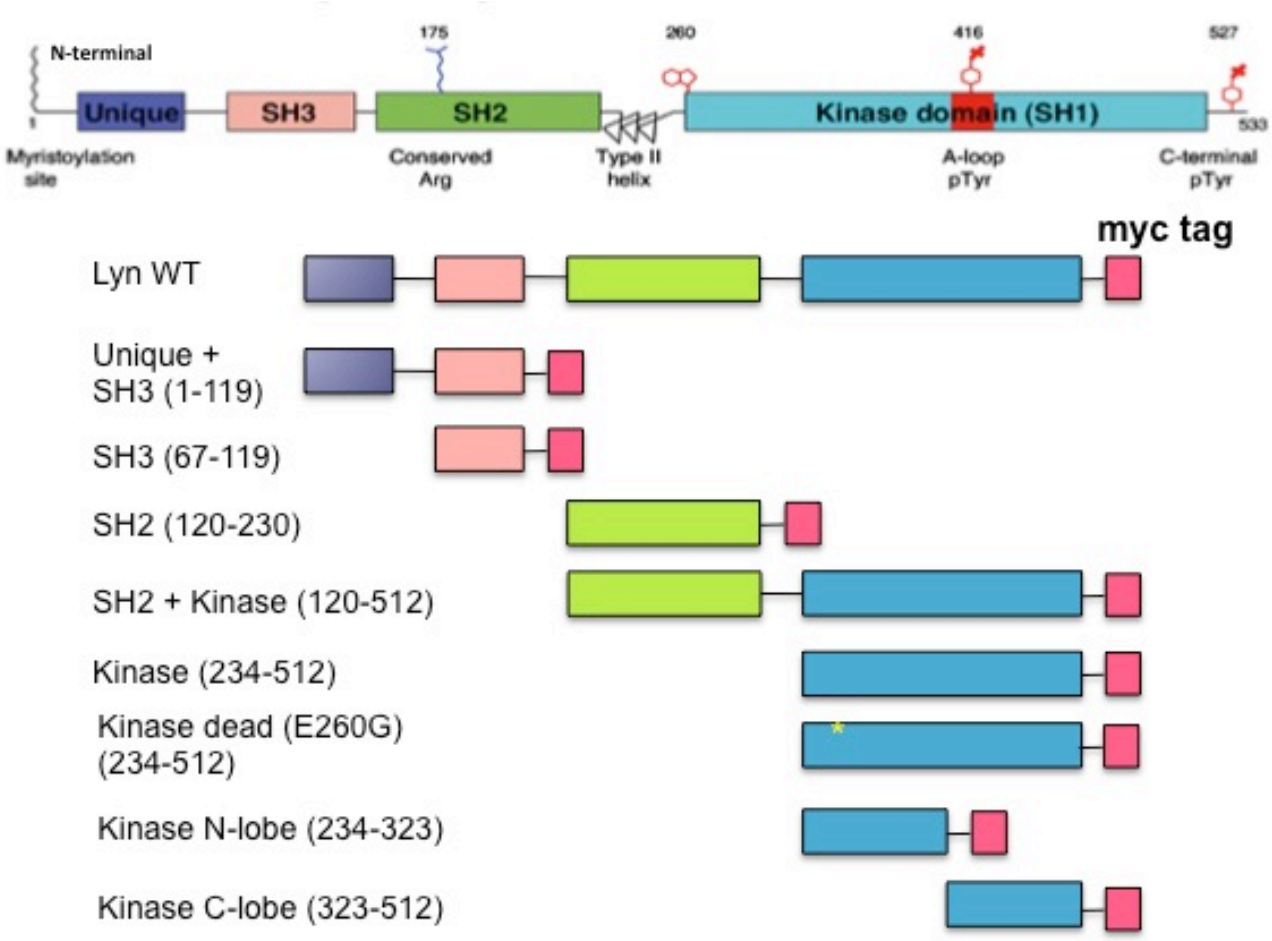

Figure 7.7: Schematic illustration of Lyn constructs.

Lyn constructs were designed to determine the region on Lyn that binds to GHR. Each illustrated construct indicates the domain and amino acid residues based on wildtype full-length Lyn (56kDa isoform). All constructs were designed to contain by a C-terminal myc tag for the ease of detection.

Discussion

There is strong evidence that GHR can activate SFK independently of Jak2 both *in vitro* and *in vivo* (Brooks & Waters, 2010). This study has used truncated GHR constructs to determine the precise region on GHR where Lyn, a predominantly hematopoietic SFK member binds by co-immunoprecipitation analysis. We report here for the first time that Lyn binds to GHR between the residues 312 and 289. This region lies between the Box1 motif and the Box2 motif (not inclusive) with no requirement for Box1 motif to bind Lyn as shown previously by Waters' Group (Barclay et

al, 2010). Based on the current study, Lyn binding occurs in the region in the sequence indicated in figure 7.8 and alignment of this region with GHR sequences of other species highlights that this region is very conserved.

	Box1	Lyn Binding Region
Human	PPVPVPKI	KGIDPDLLKEGKLEEVNTILAIHDSYKP
Macaque	PPVPVPKI	KGIDPDLLKEGKLEEVNTILAIHDSYKP
Baboon	PPVPVPKI	KGIDPDLLKEGKLEEVNTILAIHDSYKP
Rhesus monkey	PPVPVPKI	KGINPDLLKEGKLEEVNAILAIHDSYKP
Squirrel monkey	PPVPVPKI	KGIDPDLLKEGKLEEVNTILAIHDSYKP
Dog	PPVPVPKI	KGIDPDLLKEGKLEEVNTILAIHDNYKP
Giant Panda	PPVPVPKI	KGIDSDLLKEGKLEEVSTILAIHDNYKP
Guinea Pig	PPVPVPKI	KGIDPDLLKEGKLEEVNTILAIHDNSKP
Rat	PPVPVPKI	KGIDPDLLKEGKLEEVNTILGIHDNYKP
Mouse	PPVPVPKI	KGIDPDLLKEGKLEEVNTILGIHDNYKP
Rabbit	PPVPVPKI	KGIDPDLLKEGKLEEVNTILAIQDSYKP
Pig	PPVPVPKI	KGIDPDLLKEGKLEEVNTILAIHDNYKH
Cow	PPVPVPKI	KGIDPDLLKEGKLEEVNTILAIHDNYKH
Sheep	PPVPVPKI	KGIDPDLLKEGKLEEVNTILAIHDNYKH
Chicken	PPVPVPKI	KGIDPDLLKKGKLDEVNSILASHDNYKT
Pigeon	PPVPVPKI	KGIDPDLLKKGKLDEVNSILASHDNYKT
Turtle	PPVPAPKI	KGIDPDLLKKGKLDEVNSILASHDSCKP

Figure 7.8: Multiple alignment of potential Lyn binding amino acid sequence on GHR from various species.
Based on the co-IP results the Lyn binding region on human GHR was aligned to the corresponding GHR sequence of various species and appears conserved all along the Lyn binding region as well as proximal sequences.

The consensus sequence stated by earlier studies for SFK binding via its SH2 domain (Songyang et al, 1993) or SH3 domain (Lim et al, 1994) are not evident in GHR although numerous non-consensus binding regions have been reported for both domains. SFK binding to GHR does not appear to require a tyrosine residue for binding, since the mutation Y314A (in 389tr) did not affect GHR and Lyn binding but in fact increased the GHR expression compared to 389tr. An earlier study by Manabe *et al.* have reported that treatment of F-36P human leukemia cells with a Src inhibitor resulted in reduced GHR phosphorylation to the same extent as that of Jak2 inhibition (Manabe et al, 2006). However, with barely detectable levels of endogenous receptor phosphorylation evident from GHR immunoprecipitation, this study failed to determine subtle differences between Src and Jak2-mediated GHR phosphorylation. In addition, the level of tyrosine phosphorylation of GHR in COS-7 cells co-transfected with WT-Src was shown to be of a similar extent when Jak2 was transfected (Manabe et al, 2006). This study however failed to consider that the level of endogenous Jak2 in COS-7 cells would be enough to phosphorylate GHR independent of exogenous Src. Thus, it remains to be determined if SFK bound to GHR can phosphorylate the GHR. Previous studies on the closely related PRLR using immunoprecipitate kinase reactions have not been able to show any involvement of c-Src activity in PRLR tyrosine phosphorylation.

Moreover, in cells co-expressing PRLR (Box1 mutant) and c-Src, addition of PRL, although induced activation of c-Src, did not result in receptor phosphorylation (Fresno Vara et al, 2000).

GHR-mediated SFK activation has been implicated in mediating the autocrine actions of GHR (Tang et al, 2010a) with increased cancer cell attributes associated with SFK signalling (Bougen et al, 2012). Numerous reports of GH/GHR expression in immune system also suggest that GH acts on various types of immune cells, especially B-lymphocytes, monocytes and macrophages (Hattori et al, 2001) with Lyn kinase being predominantly expressed in hematopoietic lineage and SFK implicated in an array of signalling networks regulating metabolism, viability, proliferation, differentiation and migration within different immune cells (Parsons & Parsons, 2004). In contrast, it has been demonstrated that thrombopoietin-stimulated SFK inhibits cellular proliferation and megakaryocyte differentiation (Lannutti & Drachman, 2004). Engagement of the B-cell antigen receptor (BCR) initiated by the Lyn has been shown to trigger signalling cascades, leading to proliferation, differentiation or growth arrest of B cells (Wang et al, 2007) indicating that SFK can perform distinct roles in different cell types and cytokine receptor systems.

An interesting observation made by Chin *et al.* has been the binding of the Lyn SH2 domain to tyrosine-phosphorylated Jak2 *in vitro* although no *in vivo* binding could be demonstrated by co-immunoprecipitation in the same study (Chin et al, 1998). Similarly, Uddin *et al.* have reported that Fyn, another member of the Src family, associates via its SH2 domain with Tyk2 or Jak2 in cells stimulated with interferon IFNα or IFNγ, respectively (Uddin et al, 1997). More recently, it has been shown that SFK can control Jak2 activation in response to PRL through a tyrosine kinase-independent mechanism (Garcia-Martinez et al, 2010). PRLR was shown to utilise Src SH2 and SH3 domains for Jak2 signalling in W53 lymphoid cells and by using non-catalytic Src mutant, SrcK295M/Y527F, whose SH3 and SH2 domains are exposed, these workers could control Jak2/Stat5 activation. In contrast, the kinase inactive SrcK295M mutant, with inaccessible SH3 and SH2 domains, could not control Jak2 activation. These mutants were also shown to attenuate PRLR-induced Akt and p70S6K activation (Garcia-Martinez et al, 2010). Finally, Jak2/Stat5 pathway has been shown to be downregulated in $Src^{-/-}$ mice mammary glands in the same study.

Earlier study in F-36P leukemia cells has shown Src depletion using siRNA did not affect Jak2 expression or its tyrosine phosphorylation after GH stimulation although GH-mediated STAT5 activation was shown to be reduced in the absence of Src (Manabe et al, 2006). The same study also reported that when WT GHR, Jak2 and Src were co-transfected together, Jak2 and Src co-immunoprecipitated with GHR and this association was seen when non-catalytic Src mutants were

used, indicating that Src association with GHR does not require its tyrosine kinase activity (Manabe et al, 2006). Other studies have emerged that reporting that Jak2 inhibition can deactivate Lyn kinase (Samanta et al, 2009), further strengthening Jak2 and SFK association. However, studies from Waters' Group have indicated that both binding and activation of Lyn are independent of Jak2. These studies were carried out in both Jak2-deficient cell line and in Box1 mutant mice (GHR K4) where no activation of Jak2 was evident (Rowlinson et al, 2008). It is to be noted that there was increased ERK activity *in vivo* between in Box1 mutant's hepatic tissue with (no GH-mediated STAT5 activity) but this may have been a consequence of elevated plasma GH (Barclay et al, 2010). This result indicates that SFK-mediated STAT5 activation via GHR is either cell line-dependent or an artefact of overexpression system.

In the current study we have presented preliminary results indicating a reduction in Lyn binding to WT receptor after GH stimulation. It remains to be evaluated if this is a direct effect of Jak2 on Lyn or mediated due to rapid GHR degradation owing to the higher level of Jak2 (transfected) and GHR on cell surface. In contrast, a Box1 mutant that cannot interact with Jak2 showed increased Lyn binding following GH stimulation. It may be speculated that Lyn and GHR compete with each other for Jak2 binding and when Jak2 is unable to bind GHR (as in the case of Box1 mutant) this will facilitate Lyn binding to GHR either directly or via another signalling molecule such as PLCγ or FAK. As a result, these co-IP studies need to be performed in Jak2-deficient γ2A cell line to evaluate the effect that lack of endogenous Jak2 might have on SFK association with GHR.

SFK members have been shown to associate through their SH2 domains with several receptor-type tyrosine kinases (e.g. EGFR), resulting in the mutual stimulation of catalytic activity and enhanced phosphorylation of downstream targets of these tyrosine kinases (Parsons & Parsons, 2004) (Arbet-Engels et al, 1999). It may thus be speculated that the Lyn-Jak2 interaction may activate or stabilise the catalytic activity of both tyrosine kinases and mediate GHR crosstalk with other receptors. *In vitro* and *in vivo* binding studies have previously shown that Lyn also binds to Cbl, Shc, PI3-K, PLCγ, MAPK, and GAP47 most of which have also been implicated in signalling mediated through GHR (Brooks & Waters, 2010). Therefore, Lyn may also directly phosphorylate these signalling molecules involved in GHR-mediated signalling or indirectly potentiate their tyrosine phosphorylation.

Further studies are currently in progress to determine the precise binding region of Lyn binding to GHR and to investigate Lyn-mediated tyrosine phosphorylation of GHR (in the absence of Jak2). These findings will be re-evaluated in FDC-P1 cell lines (used in (Rowlinson et al, 2008) made

stable for GHRtr to evaluate the extent of Lyn activation in this SFK-dependent line. It should be noted that some GH-dependent ERK activation also occurs from Jak2 via Ras (Choi et al, 2006) in FDCP-1 cells evident from the residual activity in the presence of SFK inhibitors. This situation may be reversed in other cell types, so the relative extent of these alternate pathways (Jak2 or SFK) would depend on the relative expression levels of these two kinases. Since binding alone is necessarily not a measure of activation, the GHR truncations will be analysed for ERK1/2 activation in the COS-7 cell line, which has now been established as a suitable system for GH-stimulated Lyn-mediated ERK activation.

Chapter 8
Molecular Basis for Cancer resistance and Lifespan Extension in Growth Hormone Receptor Mouse Models

Introduction

Numerous cancers, including breast, prostate and colorectal, increase with advancing age, with the vast majority of cancer cases reported in people over 60 years of age (Ahmad et al, 2009). The risk of cancer mortality increases in an age-dependent manner, although both incidence and mortality rate apparently plateau and subsequently decline after 90 years of age (Smith, 1996). The increased incidence of cancer as a function of ageing has long been interpreted to suggest that multiple genetic changes are required for carcinogenesis to occur. Cancer is the primary cause of death in most mouse strains, although tumour type appears highly strain-specific (Anisimov, 2001). Hypophysectomy or surgical removal of the pituitary gland was the most common form of endocrine therapy used to reduce hormone action before the development of specific chemical agents and monoclonal antibodies for the treatment of cancer, diabetes and hypertension (Saglam et al, 1970). Reduced levels of endocrine hormone/growth factors have also been associated with anti-ageing effects that contribute to extend lifespan in nematodes, fruit flies, and rodent models (Tatar et al, 2003), supporting the link between cancer and longevity. This chapter will highlight some of the common attributes that may lead to reduced cancer incidences and in turn promote longevity based on the genetic murine models of altered GH/GHR signalling.

Mutant and genetically modified animal models, characterised by shortening or extension of the lifespan, provide an opportunity to evaluate the role of ageing genes in the mechanisms of carcinogenesis and *vice versa*. The most well characterised murine models in regards to longevity are the Ames and Snell dwarf mice. On an average, Ames mice live 69% and 49% longer (in Ames genetic stock background females and males, respectively), whereas Snell dwarfs live nearly 42-26% longer (DW/J Pit1^{dw} X C3H/HeJ Pit1^{dw-J} genetic background females and males, respectively) than wildtype littermates (Flurkey et al, 2002), these differences being largely a result of genetic background rather than differences in pituitary function (Brown-Borg et al, 2012). Both of these mice models have embryonic developmental arrest in the anterior pituitary arising from autosomal recessive mutations in *Prop-1* and *Pit-1* genes respectively, resulting in undetectable circulating GH, PRL and thyrotropin levels (Sornson et al, 1996; Magkou et al, 2007). Despite having a similar endocrine profile as Snell dwarf mice, old Ames dwarf mice exhibited a high incidence and burden of cancer at the time of death (Ikeno et al, 2003). Necropsy at the time of death revealed malignant lesions in 72% of Ames dwarf mice, in comparison to 95% of control mice where as in the case of Snell dwarf mice the cancer deaths accounted for only 18% as compared to 82% in control mice (Alderman et al, 2009).

Since these mice lack at least three hormones it was difficult to establish the exact role of GH and/or IGF-1 levels to lifespan extension until the generation of GHR/GHBP knockout (GHR KO) mice by targeted disruption of murine *ghr* (Zhou et al, 1997b; Coschigano et al, 2000). The GHR KO have been made in two different genetic backgrounds: 129Ola X BalbC with lifespan extension of 55% and 38% (females and males, respectively) (Coschigano et al, 2000) and C57Bl/6 with lifespan extension of 26 and 16% (females and males, respectively) (Coschigano et al, 2003). Although the GHR KO mice can synthesise GH normally they are GH insensitive and show deficiency in endocrine IGF-1 levels as well as retarded post-natal growth, similar to Laron patients (Coschigano et al, 2000). Owing to low IGF-1 levels (and therefore lack of negative feedback on GH synthesis) as well as reduced GH clearance these mice have high levels of circulating GH as compared to wildtype. Additionally plasma PRL levels that normally increase with age in wildtype mice were shown to decline in GHR KO males, and did not differ between aged GHR KO and controls (Chandrashekar et al, 2007). GHR KO have decreased levels of thyroid hormones (T_3 and T_4) (Hauck et al, 2001) and testosterone in males (Chandrashekar et al, 2007).

Ikeno *et al*. have reported reduced incidence (and burden) from 83% in C57Bl6 littermate controls to only 42% and delayed occurrence of neoplastic diseases as well as a decrease in the severity of non-neoplastic diseases in both male and female GHR KO mice of 129Ola X BalbC genetic background (Ikeno et al, 2009). These mice exhibit a pathological profile similar to mice subjected to calorie restriction (Bronson & Lipman, 1991) and consequently live longer than age and gender matched wildtype littermates (Coschigano et al, 2003). Similarly Lit/Lit mice harbouring a mutation in *Ghrhr* have reduced GH levels owing to lack of GH synthesis by pituitary somatotrophs and therefore a secondary reduction in IGF-1 levels (Lin et al, 1993), exhibit significantly reduced growth of breast cancer xenografts relative to controls (Yang et al, 1996). Since the common endocrine denominator between Lit/Lit, GHR KO, Ames, Snell dwarf mice and CR mouse models is the suppressed levels of GH/IGF-1, it is clear that low levels of GH and IGF-1 are unfavourable to tumourigenesis.

Human studies are in complete accordance with the results in mice models as indicated by non-existent tumour incidences (and diabetes) in patients with Laron syndrome (Steuerman et al, 2011; Guevara-Aguirre et al, 2011). In contrast to the dwarf animal models GH transgenic (GHtg) mice exhibit gigantism characterised by increased longitudinal body growth owing to increased IGF-1 levels in circulation as compared to wildtype littermates (Wolf et al, 1993). Increased inflammation, hepatocellular carcinoma and premature death have been reported in two different models of GHtg mice (Wanke et al, 1991; Friedbichler et al, 2011). Dysregulation of several oncogenic pathways

and signalling mediators were reported in the liver of GHtg mice of both genders as compared with normal controls, including Akt2, NF- κB, GSK3β, β-catenin, cyclin D1, cyclin E, c-myc, c-jun and c-fos (Miquet et al, 2013). Also, acromegalics have been reported to have a higher incidence of colon and thyroid cancers (Chhabra et al, 2011) while other increased tumour incidences have not been confirmed due to small sample size.

Potential cancer resistance mechanisms in dwarf mice

The observations highlighted above should be considered in the context of several aspects of GH/IGF-1 signalling such as inhibition of insulin signalling, promotion of inflammation, mitochondrial and oxidative pathways that correlate directly with longevity and are particularly relevant to tumour development.

Mitochondrial function

The mitochondria plays a central role in energy metabolism through oxidative phosphorylation (OxPhos), apoptosis, modulation of redox status, control of cytosolic Ca^{2+} levels and generation of free radicals as byproducts of the electron transport chain (Wallace, 2012). Changes in these elements can interrupt biosynthetic pathways, cellular signal transduction pathways, transcription factor action and even chromatin structures in order to shift the cell from a quiescent, differentiated state to an actively proliferating one (Wallace, 2012). A progressive decline in physiological function occurs with ageing that is associated with accumulated damage in DNA, RNA and protein resulting in loss of cellular function (Salvioli et al, 2001). Mitochondrial DNA (mtDNA) is characterized by high variability, maternal inheritance, and absence of recombination and can affect rate and quality of ageing. Differences in mitochondrial function arising from mtDNA germline inherited variants have been associated with extended ageing profile in an Italian population (de Benedictis et al, 2000) while other mitochondrial gene variants have been reported at higher frequencies in Japanese centenarians than in controls (Tanaka et al, 1998). In addition, mutations in genes encoding key mitochondrial enzymes such as succinate dehydrogenase (SDH), fumarate hydratase (FH), and isocitrate dehydrogenase (IDH1 and 2) arising in cancer cells are well established (Wallace, 2012).

The five-multimeric enzyme complexes that drive OxPhos and cellular respiration are contained within the inner mitochondrial membrane. Complex I (NADH dehydrogenase) forms the largest of the multimeric electron transport chain (ETC) proteins and contributes significantly to the generation of free radicals, respiration rate and overall control of ETC (Brown-Borg et al, 2012).

Inhibition of complex I alone by as little as 25% has been shown to negatively impact energy metabolism and production (Brown-Borg & Bartke, 2012) and is also reported to be a naturally occurring process during ageing (Ventura et al, 2002). Complex II or succinate dehydrogenase is a second entry point to the electron transport chain and is the only enzyme that is part of both the citric acid cycle and the electron transport chain (Cecchini, 2003). It is believed to be important in decreasing production of reactive oxygen species while it oxidises succinate to fumarate and reduces ubiquinone (Yankovskaya et al, 2003). The maintenance of succinate levels within the cells is important as it can serve as a metabolic signal in inflammation and has been shown to stabilise the transcription factor hypoxia-inducible factor-1α (HIF-1α) in specific tumours (Mills & O'Neill, 2013).

Q-cytochrome c-oxidoreductase or complex III is involved in the oxidation of one molecule of ubiquinol and the reduction of two molecules of cytochrome c, a heme protein loosely associated with the mitochondrion. This protein has been associated with oncogene-induced senescence and found to be upregulated in breast cancer cells and primary breast tumours (Owens et al, 2011). While complex I and II exert great control over the respiratory chain flux, complex IV (Cytochrome c oxidase) is the final and rate-limiting step of the ETC and along with complex I and III is responsible for ROS generation (Huttemann et al, 2012; Hoehn et al, 2009). Use of GHRH antagonists in the prostate cancer cell line LNCaP has been shown to prevent ROS generation by inhibition of Complex IV activity (Barabutis & Schally, 2008).

Age matched Ames mice liver has increased complex I and IV activity and protein levels as compared to wildtype with greater decline observed in wildtype tissues with age (Brown-Borg et al, 2012). This is also complemented by data obtained from fruit flies, rats and human livers (Salvioli et al, 2001). ATP synthase (Complex V) couples proton flow from the inter-membrane space back to the matrix with conversion of ADP and inorganic phosphate to ATP (Yoshida et al, 2001). This complex is key to energy availability and is not co-regulated with OxPhos proteins (Brown-Borg & Bartke, 2012). This is important because energy deficits are common in diseases with low ATP synthase protein or due to mutations in the genes encoding the ATP synthase complex, which results in increased membrane potential, delay in ETC and higher ROS production (Jonckheere et al, 2011).

PGC1α (peroxisome proliferator-activated receptor γ co-activator1α) has been identified as a key regulator of mitochondrial biogenesis and plays an important role in utilisation of fatty acids as a metabolic fuel, thereby controlling lipid homeostasis (Wu et al, 1999). Enhanced PGC1α expression

at transcript level in liver has been reported in GHR KO and Ames mice although this did not result in greater mitochondrial numbers per se (Al-Regaiey et al, 2005; Brown-Borg et al, 2012). Other factors involved in the regulation of mitochondrial biogenesis include AMP-activated protein kinase (AMPK), Sirtuins, endothelial nitric oxide synthase (eNOS), nuclear respiratory factor1 (Nrf1), mitofusin2 (MFN2) and calorie restriction (CR) (Pfeifer et al, 2001). Disturbances in mitochondrial biogenesis affect oxidative stress resistance, energy production and metabolism and may result in the development of age-associated degenerative diseases as evident in the case of GHtg mice that have markedly decreased level of complexes I, II and IV and shortened lifespan (Brown-Borg & Bartke, 2012).

During carcinogenesis cells shift their metabolism from aerobic energy production to glycolysis. This shift can take place even in the presence of oxygen and is therefore referred to as aerobic glycolysis, and it is known as the Warburg effect (Hanahan & Weinberg, 2000). Since 2000, considerable work has been done on the role of mitochondria in neoplastic transformation. Generally, two primary mitochondrial cancer promoting factors have been linked to cancer, i.e. metabolic switching to provide building blocks for the growing cells (Weinberg & Chandel, 2009), and/or increased mitochondrial ROS production resulting in the emergence of cells with oncogenic mutations (known as 'mitochondrial malignancy') (Ralph et al, 2010). This indicates that examination of changes in individual OxPhos components and mitochondrial enzymes due to differences in circulating levels of hormones in mice models has the potential to uncover areas of altered function relating to cancer.

Free Radicals and Reactive Oxygen Species

Reactive oxygen species (ROS) and reactive nitrogen species (RNS) can induce oxidative stress/damage but at lower levels are physiologically important for regulating cellular and stress signalling, integrating energy state, and survival (Hamanaka & Chandel, 2010). It has been proposed that oxidative damage due to excessive free radical generation by mitochondria as a by-product of OxPhos contributes to cancer, neurodegenerative disorders, diabetes, and inflammation (Ralph et al, 2010). Mitochondrial redox regulation is crucial for mitochondrial function and NADPH is used for reduction of mitochondrially generated H_2O_2 and other peroxides by glutathione and GPx. When ROS production is too high it will induce cellular apoptosis that if prevented can contribute to neoplastic transformation (Burdon, 1995). Recent investigations have suggested that during uncontrolled proliferation in cancer cells oxygen depletion in the tumour core stimulates mitochondria to elaborate increased ROS, with subsequent activation of signalling pathways, such as hypoxia inducible factor 1α (HIF-1α), that promote cancer cell survival and

tumour growth by increased inflammation and metabolic reprogramming (Semenza, 2010). Mitochondrial ROS from complex III has been shown to be essential for stabilising HIF-1α during hypoxia (Chandel et al, 2000). Additionally AMPK, a pro-survival kinase was reported to be highly sensitive to ROS/RNS and shown to function as a physiological repressor of NADPH oxidase (Nox) to maintain NADPH levels (Wang et al, 2010a).

Despite intensive investigations in this field, current antioxidant therapeutics (vitamin A, E and β-carotene) have not been clinically effective in combating the pathological conditions arising from oxidative stress, but rather promote mortality (Bjelakovic et al, 2014). There is clear evidence that demonstrates the GH/IGF-1 axis plays a role in antioxidative defense as in the case of GHtg mice that succumb to cancer early in life. These have increased superoxide radical and reduced antioxidant enzymes levels such as superoxide dismutase (SOD), catalase and GPx (Brown-Borg et al, 1999). In contrast, GH deficiency in dwarf mice results in enhanced antioxidative defense capacity in Ames mice but not GHR KO. Ames mice have been reported to harbour elevated transcripts of catalase, SOD and GPx in multiple tissues (Brown-Borg et al, 1999) (Brown-Borg & Rakoczy, 2000) which can be suppressed by exogenous GH administration (Brown-Borg & Rakoczy, 2003). In the case of GHR KO however, a lack of free radical scavenging in the liver and kidney has been reported (Hauck et al, 2002). Recently Marty *et al*. have reported a role for ROS in *Jak2*^{V617E} mediated progression of myeloproliferative neoplasm (Marty et al, 2013) while STAT3 and 5 transcription factors downstream of GH signal cascade have been implicated in cross-regulation of oxidative metabolism/ROS generation in cancer cells (Bourgeais et al, 2013).

Stress resistance: Ability to deal with ROS

Increased stress resistance against cytotoxic and metabolic stresses can contribute to differential neoplastic disease occurrence. Indeed, human mammary epithelial cells cultured in the serum of the GHR-deficient (GHRD) Ecuadorian cohort were protected from oxidative DNA damage, compared with cells cultured in the serum of their relatives (Guevara-Aguirre et al, 2011). In the setting of oxidative stress, increased cytotoxicity was also observed in the cells cultured in the serum from the GHR mutant patients, while the addition of IGF-1 to this serum or culturing cells in the serum from controls reduced the rate of cell death (Guevara-Aguirre et al, 2011). GHD/GHR mutation therefore appears to protect cells from oxidative damage while simultaneously increasing cytotoxic pathways for removing mutated/damaged cells.

Snell dwarf mice are resistant to chemically induced cancers and exhibit reduced growth of transplanted tumours compared to control mice that are either homozygous or heterozygous for the

wildtype *Pit1* allele (Flurkey et al, 2001). This resistance is also evident in cells derived from these dwarf mice. The skin-derived fibroblasts from Snell mice were resistant to multiple forms of oxidative and non-oxidative cellular stress (Murakami et al, 2003). Significant increases in LD_{50} values were observed in dwarf mice over those of wild-type mice following exposure to UV irradiation (45%), hydrogen peroxide (H_2O_2; 147%), paraquat (53%), cadmium (180%), and heat (102%). Similar studies were performed on other long-lived dwarf mice (Ames, GHR KO) and revealed increased resistance against UV, H_2O_2 and paraquat (Salmon et al, 2005). More recently it has been shown skin-derived fibroblasts from both Snell and GHR KO have diminished phosphorylation of mTOR, S6K and 4EBP1 after amino acid deprivation (in GHR KO and Snell fibroblasts), H_2O_2 (Snell fibroblasts), and paraquat (Snell fibroblasts), consistent with the higher levels of autophagy in these cells following a stress stimulus (Wang & Miller, 2012) Additionally it has been suggested that stress resistance might be dependent on developmental changes (hormone-dependent) that occur during the first few months after birth since no differences were observed in fibroblasts derived from neonates of dwarf mice and littermate controls (Salmon et al, 2005).

A different approach to studying oxidative stress in Snell dwarf mice challenged with 3-nitropropionic acid (OxPhos Complex II inhibitor) showed decreased activation in the MEK-Erk cascade and a lack of c-Jun (Ser63) phosphorylation as compared to wildtype, suggesting altered management of oxidative stress in the Snell dwarf (Madsen et al, 2004). Although antioxidative defence enzymes have not yet been systematically examined in the GHR KO mice (C57Bl/6 background), an overall enhancement of this system is likely responsible for increased resistance to oxidative insult as found in Ames and Snell dwarf mice.

The results above can be attributed to increase in Nrf2 (Nuclear Factor-erythroid 2-related factor 2) expression. Nrf2 is the master controller of oxidative and xenobiotic stress response that has been shown to influence oxidative stress-related physiological and pathological processes such as cancer, diabetes, and inflammation (Kensler et al, 2007). Snell dwarf mice derived skin-fibroblasts have been shown to maintain a steady-state level of Nrf2 as compared to control, which further increases transcription of antioxidant response element (ARE)-responsive genes in dwarf mice (Leiser & Miller, 2010). Gene expression array data from GH deficient mice models have revealed elevation in phase I enzymes which can also be attributed to Nrf2 activation *in vivo*, a hallmark of long-lived (Steinbaugh et al, 2012) and CR mice (Martin-Montalvo et al, 2011).

Glucose deprivation

Cancer cells are dependent on glycolysis for ATP production rather than OxPhos and so have a requirement of high levels for glucose for energy production (Matoba et al, 2006). Glucose deprivation (and starvation) has been shown to cause rapid cancer cell death as compared to healthy cells *in vitro* and *in vivo* (El Mjiyad et al, 2011; Shim et al, 1998). Accordingly, elevated circulating glucose increases the risk of cancer and reduces the effectiveness of medical treatment in cancer patients (Stattin et al, 2007; Malin et al, 2005). Importantly, Ames and Snell dwarfs, GHR KO, and non-transgenic calorie-restricted mice have reduced levels of glucose in peripheral circulation (Brooks et al, 2007; Alderman et al, 2009; Dominici et al, 2002; Liu et al, 2004; McCarter et al, 2007). The decrease in plasma glucose was proposed to not be an important factor in the action of calorie restriction on longevity (McCarter et al, 2007) although lower glucose by calorie restriction is inversely correlated to cancer incidence (Rondini et al, 2011). It is relevant that p53, one of the most frequently mutated genes in cancers, modulates the balance between the utilisation of respiratory and glycolytic pathways (Matoba et al, 2006).

IGF-1/IGF-1R in Cancer Promotion

IGF-1 has been shown to act *in vitro* as a tumour promoter by increasing proliferation and decreasing apoptosis, and by promoting angiogenesis and metastasis (Samani et al, 2007). Indeed, local expression of IGF-1 in mouse mammary tissue resulted in spontaneous mammary tumours in 30% of mice (de Ostrovich et al, 2008). Some conclusions have been drawn from mouse models with lower levels of circulating IGF-1 but with normal/elevated tissue expression as a result of selective knockout of hepatic IGF-1 expression (liver IGF-1-deleted or LID mice). These mice had approximately 50% of normal circulating IGF-1, which resulted in a 40% significant decline in azoxymethane-induced colon adenocarcinoma number, largely due to increased apoptosis (Olivo-Marston et al, 2009). An earlier study with orthotopically transplanted colon-38 adenocarcinomas has reported that the circulating IGF-1 in LID mice to be approximately 25% of normal, and this was associated with a substantial decrease in the number of mice with palpable colon tumours from 57% to 31% with a significant increase in tumour latency from 23 to 27 days (Wu et al, 2002). Hepatic metastases were also significantly decreased from 44% to 31%, and these improvements were reversed with IGF-1 administration. Generation of mammary tumours by chemical or genetic means is also decreased in LID mice (Wu et al, 2003). Besides IGF-1, GH has been shown to directly regulate the transcription of *igf2* in human liver (von Horn et al, 2002) and increased expression of IGF-2 has been reported in a variety of cancers, including geriatric malignancies such as brain tumours, mammary carcinoma, gastrointestinal cancer including pancreatic carcinoma and ovarian carcinoma (Pollak, 2008).

Similarly increased IGF-1R expression has been reported in numerous cancers and cancer cell lines and though not all data is consistent, it is generally associated with worse prognosis (Railo et al, 1994; Law et al, 2008; Ludovini et al, 2009). This elevated expression and/or increased activation of IGF-1R is mainly associated with pro-survival signalling pathways (Kurmasheva & Houghton, 2006) and can therefore tip the balance between apoptotic cell death versus survival of damaged cells towards survival and consequently favour the emergence of a malignant clone. Additionally, the IGF axis has been implicated in the maintenance of cancer stem cells and induction of EMT (Bodzin et al, 2012; Graham et al, 2008). This has been demonstrated in stem cell niches generated in hypoxic microenvironments that trigger the stabilisation and activation of hypoxia inducible factors (HIF) (Keith & Simon, 2007). Constitutive IGF-1R levels have been reported to be elevated in chemoresistant cell lines relative to parental cell lines (Dallas et al, 2009).

Disruption of an intracellular substrate of the IGF-1 receptor, p66Shc, provides a 30% increase in lifespan and increased resistance to hydrogen peroxide, UV-irradiation, and paraquat toxicity (Migliaccio et al, 1999). Low circulating levels of IGF-1 obtained by liver-specific IGF-1 inactivation (lv-IGF-$1^{-/-}$) (Svensson et al, 2011) or brain-specific IGF-1R knockout (Croce et al, 2014) also extend lifespan in mice. Holzenberger *et al*. have demonstrated that the longevity effect of IGF-1R on 129/SvPas genetic background was sexually dimorphic with female heterozygotes (IGF-$1R^{+/-}$) exhibiting 33% increase in longevity and resistance to oxidative stress (paraquat), while the effect was not significant in males (IGF-$1R^{+/-}$) (Holzenberger et al, 2003). However, Bokov *et al*. have reported only 5% extension of lifespan in female IGF-$1R^{+/-}$ mice on C57BL/6 genetic background and unchanged lifespan in mutant males (Bokov et al, 2011). Similarly, the modest longevity effect of low IGF-1 in lv-IGF-$1^{-/-}$ mice (on C57BL/6 genetic background) was seen in females, but not in males (Svensson et al, 2011). Indeed, it is now established that the longevity effect of IGF-1R hetrozygosity is dependent on the genetic background of the mice (Xu et al, 2014).

Insulin /Insulin Receptor in Cancer Promotion

Epidemiological studies have demonstrated a clear association between T2DM and cancer (Ko & Chaudhry, 2002; Calle & Kaaks, 2004; Noto et al, 2011). This association between diabetes and cancer is mediated in part by chronic hyperinsulinemia acting via IR as well as the effects that elevated insulin levels have on the IGF system (Calle & Kaaks, 2004). Elevated IR expression has been reported in cancers of the breast, lung, ovary, thyroid, and colon and associated with larger, higher-grade tumours as well as higher estrogen receptor concentrations (Cannata et al, 2010). Elevated insulin levels have been shown to promote activation of STAT5 inducing IGF-1 (Le et al,

2002) and elevated insulin levels have been shown to hinder IGFBP-1 and 2 expression therefore increasing IGF-1 availability locally (Lukanova et al, 2004). In addition, elevated insulin levels (as in the post-prandial surge in insulin-resistant subjects or after insulin injection) are likely to bind to IGF-1R, which has increased mitogenic potential as compared to IR (Vigneri et al, 2009). Experiments with insulin-deficient (diabetic) animals have shown that insulin promotes tumour growth and development in xenograft models and in chemical models of carcinogenesis (Cocca et al, 1998) and finally adipocyte-specific deletion of the *IR* gene (FIRKO mice) was shown to lower plasma insulin levels by more than 30% and increases lifespan by 15% to 18% in male and female mice, respectively (Bluher et al, 2003) while mutants with inactivation of its downstream signalling molecules like IRS-1 (Selman et al, 2008; Selman et al, 2011) and S6K1 (S6 Kinase1) have been (Selman et al, 2009) shown to have extended lifespan.

Hyperinsulinemia is directly associated with GH deficiency as evident in obesity, but with normal circulating IGF-1. Conversely, GH excess in the liver of GHtg mice was associated with a decrease in insulin receptor (IR) with simultaneous increase in the basal activity of IR/IRS-1 and PI3-K pathway, although these are unresponsive to exogenous insulin stimulation (Dominici et al, 1999). In skeletal muscle of GHtg mice, decreased levels of IR protein and decline in insulin-mediated signalling with increase in p85 (negative regulator of insulin signalling) are thought to be key element in promoting insulin resistance (Barbour et al, 2005). Additionally, prolonged exposure to GH is associated with hyperinsulinemia, insulin resistance and cardiomegaly due to persistent stimulation of PI3-K/Akt and p38 pathways in GHtg mice (Miquet et al, 2011; Izzard et al, 2009). Enhanced oxidative stress in the serum and tissues of GHtg rats (particularly heart) and serum of acromegalics has been reported by Nishizawa *et al*. but attributed to increased IGF-1 levels rather than GH in C2C12 myocytes (Nishizawa et al, 2012). Acquired metabolic alterations, such as hyperglycemia and hyperinsulinemia, can also promote the production of ROS, which damage mitochondria in insulin-responsive tissues (Szendroedi et al, 2012). Conversely, insulin resistance has been proposed to be a cellular antioxidant defense mechanism, one that is preceded by mitochondrial oxidative stress (Hoehn et al, 2009).

Conversely, GH deficient long-lived dwarf mice have reduced insulin levels and enhanced insulin sensitivity (Dominici et al, 2002) that can be reversed by exogenous GH administration (Masternak et al, 2009). Essentially, reduction in GH levels has been demonstrated to affect not only IGF-1 secretion but also that of insulin as evident in the case of GHR KO mice that have reduced pancreatic islet size (Liu et al, 2004) and in Ames dwarf mice that contain decreased islet number along with impaired secretory response to glucose (Parsons et al, 1995). The decrease in islet

growth in GHR KO was restored by pancreatic islet-specific expression of IGF-1 at least partially through cell hypertrophy (Guo et al, 2005). GH replacement can exacerbate insulin resistance in GHD patients associated with induction of p85 subunit of PI3-K and a switch from glucose metabolism to lipolysis (Bramnert et al, 2003). Additional GH-mediated indirect mechanisms for negatively regulating insulin sensitivity, such as reduction in adiponectin, enhanced mTOR signalling and alterations in serum lipid profile as well as fat accumulation, have also been reported (Bartke & Westbrook, 2012). Additionally, disruption in the expression of *klotho* gene, which encodes a circulating hormone that inhibits intracellular insulin and IGF-1 signalling, was demonstrated to extend lifespan and reduce age-related pathologies (Kurosu et al, 2005).

Inflammation

Cancer incidence increases with age and there is a decline in immune system function leading to chronic low-grade inflammatory activity that can lead to long term tissue damage and even mortality (Vasto et al, 2007). On the other hand calorie restriction has been shown to enhance immune function and ameliorate inflammation (Fernandes et al, 1997).

A body of evidence suggests the presence of low-grade inflammation in obesity, with altered levels of several circulating factors such as an increase in the plasma levels of C-reactive protein (CRP), tumour necrosis factor α (TNFα), interleukin-6 (IL-6), and other biological markers of inflammation (Olefsky & Glass, 2010). In addition, there is a correlation in healthy individuals between body mass index (BMI) and CRP levels (Choi et al, 2013). IL-6 has been reported to increase liver CRP production and is positively associated with oxidative resistance (Park et al, 2013). TNFα has been shown to exert its effects on metabolism through serine-phosphorylation of IRS-1, which inhibits its interaction with the β-subunit of the insulin receptor and blocks insulin signalling resulting in obesity-linked insulin resistance (Hotamisligil et al, 1993; Kern et al, 1995). In addition to *in vitro* studies daily GH injections for three weeks in healthy individuals was shown to increase pro-inflammatory cytokines TNFα and IL-6 in circulation that was not observed in pegvisomant-injected individuals (Andreassen et al, 2012).

Obesity and Adipokines

Obesity is linked to increased cancer risk and impacts the secretion of hormonal factors regulating tissue homeostasis and metabolism (Calle & Kaaks, 2004). Adult GHtg mice have increase in lean mass and reduction in fat mass consistent with the lipolytic action of GH while GHR KO are obese and accumulate excess subcutaneous fat independent of gender and age implying subcutaneous fat

is GH sensitive (Berryman et al, 2004). The lipid profile between the two mouse models is also altered with high levels of cholesterol, high-density lipoproteins (HDL) and low-density lipoproteins (LDL) in GHtg and opposite levels in GHR KO (Frick et al, 2001; Egecioglu et al, 2006). Additionally, Ding *et al*. using proteomics approach have identified biomarkers differentially secreted in plasma between GHR KO and GHtg mice (Ding et al, 2011; Ding et al, 2012).

Adiponectin is an adipocyte-secreted, circulating hormone with pleiotropic functions in lipid and glucose metabolism, and beneficial roles in cardiovascular functions and inflammation (Brooks et al, 2007). Adiponectin was shown to be negatively associated with GH activity in GHtg and GHR KO mice, regardless of age. Interestingly exogenous GH excess, but not IGF-1 could decrease circulating adiponectin levels (Lubbers et al, 2013). Acromegaly has also been shown to inhibit the expression of endothelial adhesion molecules and vascular smooth muscle cells proliferation, suppressing the transformation of macrophages and inducing production of anti-inflammatory factors like IL-10 (Vielma et al, 2013). Adiponectin is also known to suppress the secretion of TNFα (Park et al, 2008). Adipose tissue in obese subjects has been shown to be infiltrated by a large number of macrophages that secrete several chemokines that result in the recruitment of even more macrophages leading to a continuous low-grade inflammatory state (Makki et al, 2013).
Resistance to cancer and increased insulin sensitivity in dwarf mice has been attributed to the elevation of circulating adiponectin (Brooks et al, 2007; Berryman et al, 2004). Although its role in cancer remains controversial adiponectin has been shown to inhibit endogenous glucose production (Brooks et al, 2007) in the liver through the suppression G6Pase and PEPCK, the rate-limiting enzymes in hepatic glucose production and associated with improved insulin sensitivity (Berg et al, 2001). Numerous epidemiologic studies have suggested that cancer risk is decreased by elevated circulating adiponectin (Vansaun, 2013). Additionally, it stimulates fatty acid utilization through its intracellular target, AMP activated protein kinase (AMPK) (Brooks et al, 2007; Yamauchi et al, 2002). Elevation in adiponectin levels and increase in AMPK activation are important features of GH-deficient patients and dwarf mice and has been shown to reduce inflammatory NF- κB signalling (Salminen et al, 2011; Meazza et al, 2013).

Metabolic regulation by Sirtuins

Cancer cells meet their needs for energy by consuming high levels of glucose and rewiring metabolism to support continuous growth and metastasis. Since many metabolic intermediates that support cell growth are provided by mitochondria it is instructive to determine the factors that regulate these mitochondrial pathways. Sirtuins, a well conserved family of NAD-dependent enzymes have been implicated in the regulation of mitochondrial pathways as well as stress

responses and longevity in model organisms (Haigis & Sinclair, 2010). Sirtuins are known to possess diverse enzymatic activities that include ADP-ribosylation, desuccinylation, demalonylation, depropionylation and debutyrylation, in addition to deacetylation (Haigis & Sinclair, 2010; Du et al, 2011; Peng et al, 2011).

Acetylated proteins are found in the nucleus, cytoplasm and mitochondria, and the seven mammalian Sirtuins (Sirt1-7) are similarly distributed throughout the cell (Haigis & Sinclair, 2010). In particular, mitochondrial proteins appear to be acetylated dynamically and at the highest frequency at multiple lysine residues (Kim et al, 2006). This serves as an important mechanism of regulation in mitochondria by altering protein-protein interaction, protein stability, mitochondrial localisation or modulating enzymatic activity. Sirt1 targets a number of substrates that regulate DNA damage, stress response, mitochondrial biogenesis, and glucose and lipid metabolism (Houtkooper et al, 2012). Sirt2 controls cell cycle and glucose and lipid metabolism (Chalkiadaki & Guarente, 2012; Houtkooper et al, 2012). Sirt3, 4, and 5 regulate ATP production, metabolism, apoptosis, and cell signalling (Haigis et al, 2006; Michishita et al, 2005; Onyango et al, 2002). Sirt6 is involved in genomic DNA stability and repair, and crucial in metabolism and ageing (Zhong et al, 2010). Sirt7 is nucleolar and regulates transcription, oxidative stress resistance and inflammation (Vakhrusheva et al, 2008).

Dynamic mitochondrial acetylation is regulated by changes in nutrient status and calorie restriction, high fat diet, and ethanol feeding, as well as fasting and re-feeding that can all cause dramatic shifts in global mitochondrial protein acetylation *in vivo* (Schwer et al, 2009; Hirschey et al, 2011). These alterations in protein acetylation are kept in check by deacetylating sirtuins that respond to the changes in energy expenditure as well as exercise, and adiponectin (Ruderman et al, 2010; Shaw et al, 2005). Importantly, Sirt1 and Sirt3 can activate AMPK by deacetylating its upstream liver kinase B1 (LKB1), which promotes LKB1 translocation from the nucleus to the cytosol, where it is activated and in turn phosphorylates and activates AMPK (Palacios et al, 2009; Hou et al, 2008; Price et al, 2012). Conversely, AMPK has been shown to activate Sirt1 by increasing the NAD/NADH ratio or the expression/activity of NAMPT (Canto et al, 2009). Collectively, these findings suggest the existence of an AMPK-Sirt1/3 cycle that links the cell's energy and redox states (Ruderman et al, 2010). In addition, AMPK and SIRT1 (and other sirtuins) act on common transcriptional activators and coactivators, including the mitochondrial master regulator PGC1α and members of the FoxO family, most of which are negatively regulated by GH/IGF-1 signalling directly or indirectly (Pfeifer et al, 2001) except Sirt1 which was reported to be elevated in GHtg mice at protein level (Al-Regaiey et al, 2005).

There seems to be little doubt that sirtuins are involved in carcinogenesis but owing to complexity and diversity of effects, the mechanisms involved have remained elusive and there is as yet no consensus on role of each sirtuin in cancer (Bosch-Presegue & Vaquero, 2013). Overall, it appears that Sirt2 and Sirt6 may be tumour suppressors, whereas Sirt1 and 3 depending on the context, can either be a tumour suppressor or an oncogenic factor. Knockout mice models for five Sirtuins (Sirt1–4 and 6) have clearly shown increased levels of genome instability, as indicated by high levels of DNA damage, defective DNA repair and chromosomal aberrations (Bosch-Presegue & Vaquero, 2013). Furthermore, four of these five KO's undergo spontaneous tumourigenesis (the exception being Sirt1 KO mice, as Sirt1 functions appear to be more complex).

Sirt1 overexpression has been reported in several types of human tumours including breast, prostate, hepatocellular, and pancreatic cancer (Morris, 2013) where it could serve to silence tumour suppressors rather than being an oncogene itself. It is not known if Sirt1 overexpression causes or is a consequence of tumourigenesis (Morris, 2013). A possible mechanism of Sirt1 elevation in cancer could be loss of transcriptional repressors evident in the case of one such repressor, HIC1. Mice knocked out for *H1C1* are prone to cancer and exhibit Sirt1-dependent resistance to apoptosis during DNA damage (Chen et al, 2005). Tumour suppressor p53 has been shown to bind to Sirt1 proximal promoter and inhibit its expression (Nemoto et al, 2004). Since p53 is the first to be lost in most cancer, it can increase Sirt1 expression in tumours. Additionally, Sirt1 has been shown to inhibit p53 activity by deacetylation and block p53-dependent apoptosis (Luo et al, 2001).

On the other hand there is also a large body of evidence highlighting a tumour suppressor role for Sirt1. It has been shown to suppress growth of intestinal, colon, liver, ovarian, and bladder cancers (Morris, 2013) as well as breast cancers in various animal models (Wang et al, 2008a). Mice transgenic for Sirt1 exhibit a global decrease in carcinomas and sarcomas, but not lymphomas (Herranz & Serrano, 2010). Additionally, these mice are less prone to DNA damage and inflammation by deacetylating and inhibiting NF- κB (Yeung et al, 2004). Sirt1 has been shown to suppress tumours by deacetylation and inactivation of HIF-1α and the genes targeted by HIFs (Lim et al, 2010).

Numerous studies have supported a role for Sirt2 as a tumour suppressor (Bosch-Presegue & Vaquero, 2013) mainly because of its function as mitotic checkpoint during mitotic stress (Dryden et al, 2003). In gliomas, Sirt2 expression was found to decrease while in some cases the locus itself was lost (Hiratsuka et al, 2003). Sirt2 expression was also reduced in oesophageal, breast,

hepatocellular carcinoma and gastric adenocarcinomas (Peters et al, 2010; Kim et al, 2011) while in melanoma, an inactivating mutation has been identified in the catalytic domain of Sirt2 (Lennerz et al, 2005). Further evidence for its role as tumour suppressor comes from Sirt2 KO mice, which develop hepatocellular carcinoma in males and mammary tumours in females (Kim et al, 2011). Additionally cancer cells have been shown to display hyperacetylation of the lysine 53 of histone H3, a known target of Sirt2 (Das et al, 2009). In one reported study of acute myeloid leukemia cells, however, Sirt2 was upregulated and involved in the aberrant proliferation and survival of leukemic cells (Dan et al, 2012).

The mitochondrial Sirt3 has been shown to regulate metabolism and oxidative stress (Bell et al, 2011) and there is some evidence that Sirt3 acts as a mitochondrial tumour suppressor (Kim et al, 2010). Loss of Sirt3 expression can result in elevation of ROS that increases stabilisation of HIF-1α and thereby increase expression of HIF-dependent genes and metabolic reprogramming towards a cancer phenotype (Finley et al, 2011a; Bell et al, 2011). Adenovirus-mediated overexpression of Sirt3 inhibited hepatocellular carcinoma cell growth and induced apoptosis (Zhang & Zhou, 2012). This was reported to be associated with NAD^+ suppression, reduction in Erk1/2 and activation of Akt signalling, and downregulation of Mdm2, resulting in increased p53 levels due to reduction in p53 degradation (Zhang & Zhou, 2012). Sirt3 also has the ability to protect cells from oxidative stress that is dependent on inhibition of the mitochondrial matrix protein IDH2, which is mutated in majority of cancers (Yu et al, 2012). Sirt4 has been found to be elevated along with Sirt1 in photo-damaged skin cells (Benavente et al, 2012).

Sirt6 is the only member of the sirtuin family that has been shown to regulate mammalian lifespan conclusively especially in males by lowering the IGF-1 levels (Kanfi et al, 2012). It has been shown to have a tumour suppressor role and it deacetylates histones H3K9 and H3K56 (Michishita et al, 2008; Michishita et al, 2009) and is involved in DNA repair at double-stranded breaks (Kaidi et al, 2010). H3K56 is hyperacetylated in skin, thyroid, breast, liver, and colon cancers (Das et al, 2009). Induction of SIRT6 overexpression in cancer cell lines selectively resulted in massive apoptosis (Van Meter et al, 2011) that was dependent on its mono-ADP-ribosyltransferase activity rather than its deacetylase activity, leading to activation of p53 apoptotic signalling cascades (Van Meter et al, 2011).

Sirt7 levels were reported to be elevated in breast cancer, including node-positive breast cancer (Ashraf et al, 2006) and thyroid cancer (Bosch-Presegue & Vaquero, 2013). It seems to be important for maintaining the cancer phenotype (Martinez-Redondo et al, 2012) by deacetylating

acetylated histone H3K18 (Barber et al, 2012). The action of Sirt7 was shown to promote anchorage-independent growth, consistent with progression of tumours to aggressive phenotypes while its depletion was shown to markedly impede tumour development (Barber et al, 2012).

GHR knockin and knockout mouse models

GHR KO mice are devoid of any/all GH-mediated signalling and therefore inconclusive in determining the exact downstream molecule/pathway that can be attributed to cancer resistance. In order to overcome this issue, Waters' Group have generated mice with truncated or mutated GHR cytoplasmic domain. These GHR mutant mice have previously enabled the identification of STAT5B as essential for *igf-1* expression and post-natal growth (Rowland et al, 2005b), since loss of the terminal 260 residues of GHR (GHR K2) resulted in concomitant loss of STAT5 activation ability and IGF-1 expression in addition to dwarfism. This phenotype was however absent in 569 truncation mutant (GHR K1) mice that retained 30% of residual STAT5 activity (Rowland et al, 2005b). In addition, these mutants allowed identification of key Phase I and Phase II xenobiotic metabolising enzymes that were STAT5-dependent (Rowland et al, 2005b; Barclay et al, 2011). Another mutant with the inability to activate Jak2 (Box1 or K4 mutant) has allowed identification of Jak2-independent but SFK/Erk activated factors involved in GH action (Barclay et al, 2010). An important point to note here is that all the GHR knockin mice have an intact UbE motif, not allowing the GHR to accumulate at the cell surface and therefore the heterozygous mice do not harbor a dominant negative receptor and have only a partial impairment of post-natal growth (Rowland et al, 2005a) and closely resemble wildtype.

The other features common to GHR K2, K4 mutant and KO mice include small body size due to decreased IGF-1 concentration and increased adiposity with age (Barclay et al, 2010; Rowland et al, 2005b). Additionally, these mutant mice have increased GH concentration in serum (due to lack of IGF-1-mediated feedback inhibition) and lack STAT5 pulsatility resulting in feminising effects on males. This chapter seeks to determine the effect of lack of GHR-mediated signalling (absence of GH-mediated STAT5 activation and circulating IGF-1) on longevity and cancer incidences in male and female animal models of GHR and provides a more descriptive mechanism based on the measurement of transcript and protein levels of key genes.

Materials and Methods

Longevity Study

Animals in the longevity study were housed in pairs of same sex and kept under a 12hr light/dark cycle at 20±2°C with environment enrichment. Water and food (Meat-free rat and mouse diet, Specialty Feeds, Australia) was available *ad libitum*. Solid pellets were replaced with wet mash of the same composition when mice were old. All experiments were approved by and performed in accordance with the guidelines set by the University of Queensland Animal Ethics Committee. The animals were checked daily for health and survival and were handled for cage changes only. Animals that appeared to be near death (listless, unable to walk, and cold to the touch) or had large tumours or neoplastic growth approaching 10% of body weight were euthanised, and the date of euthanasia was considered as the date of death. Initial evaluation for the cause of death was based on any evident gross morphology changes (palpable tumours, lesions etc.) and classified into one of three categories: tumour, sick, and found dead as the cause of death. After death or euthanasia, all mice were fixed in 10% formalin as near as possible to the time of death and sent to Dr. Helle Bielefeldt-ohmann at School of Veterinary Science, University of Queensland Gatton campus for histopathological analysis to determine the exact cause of death.

Circulating GH estimation

The serum from old GHR mutant female mice was used for estimation of circulating GH levels based on the method described by Steyn *et al.* (Steyn et al, 2011). Briefly, a sensitive sandwich ELISA was carried out in a 96-well plate format (Corning Inc., NY, USA) that was coated with 50µl capture antibody (anti-ratGH-IC-1; a kind gift from Dr. F. Steyn) at a final dilution of 1:40,000 and incubated overnight at 4°C. To reduce non-specific binding, each well was subsequently incubated with 200µl blocking buffer (5% skim milk powder in 0.05% PBS with Tween-20 (PBST)). A standard curve was generated using a 2-fold serial dilution of mouse GH (mGH) in PBST supplemented with 0.2% BSA (PBST). Bound standards and samples were incubated with 50µl detection antibody (rabbit antiserum to ratGH) at a final dilution of 1:40,000). The bound complex was incubated with 50µl horseradish peroxidase-conjugated antibody (anti-rabbit, IgG; GE Healthcare Ltd., Bucks, UK) at a final dilution of 1:2000. Addition of 100µl O-phenylenediamine (Invitrogen, CA, USA) substrate to each well resulted in an enzymatic colorimetric reaction. This reaction was stopped by addition of 50µl 3M HCl, and the absorbance was read at a wavelength of 490nm with a Rainbow 96 monochromatic microplate reader. The concentration of GH in each well was calculated by regression of the standard curve.

Western blot analysis

All tissues (~100mg) were homogenised in 500µl of RIPA lysis buffer using handheld Kinematica Polytron homogenizer (Fisher Scientific) at full speed until no chunks were visible. Tissue homogenates were cleared by centrifugation at full speed for 10min at 4°C. Total protein was quantified by BCA Assay (Pierce) and resolved on Mini-PROTEAN® Precast gradient gels (BioRad). The gel was immunoblotted using the semi-dry Trans-Blot® Turbo™ Transfer System (BioRad). Membranes were blocked with 5% Bovine Serum Albumin (BSA) or 5% skim milk in Tris-Buffered Saline containing 0.1% Tween-20 (TBST) for 1hr at room temperature. Blots were probed by incubating with specific primary antibody (listed in Appendix VI).

DNA extraction and mitochondrial/nuclear ratio estimation

DNA was extracted from liver tissue (~20mg) using the DNeasy® Blood and Tissue kit (Qiagen, Maryland, USA) as per manufacturer's guidelines. The extracted DNA was subjected to qPCR using Sybr Green® primers specific for mitochondrial genome (*mt-rnr2*) and nuclear genome (*polg2*) listed in Appendix V.

Lipid peroxidation measurement

Quantification of lipid peroxidation, an indicator of oxidative injury was carried out using Lipid Hydroperoxide Assay kit (Cayman, Michigan, USA) as per manufacturer's guidelines.

Total antioxidant determination

The total antioxidant capacity in mouse serum was determined using the TAC Peroxyl kit (Applied Bioanalytical Labs, Florida, USA) as per manufacturer's guidelines.

Results

Waters' Group currently has GHR mutant knockin mouse models that were created to determine the molecular basis for GH control of postnatal growth (Barclay et al, 2010; Lichanska & Waters, 2008; Rowland et al, 2005b). These comprise mice with 30% STAT5 activation ability (GHR K1), no STAT5 activation ability (GHR K2) and mice with an inability to activate Jak2 as well as STAT5 (GHR K4) (fig.8.1A). In contrast, these mutants (K1, K2, K4) still retain the ability to activate SFK

members (Barclay et al, 2010; Rowlinson et al, 2008). Growth retardation was observed as shown in figure 8.1B (to a lesser extent in the K1 mutants) as was striking late onset obesity in male mutants with a marked increase in sub-cutaneous fat stores (Barclay et al, 2010; Rowland et al, 2005b). These targeted knockin mice are compared with GHR KO mice (gifted by Prof. J.J. Kopchick), transferred to a C57Bl/6 background.

To investigate the roles of pathways downstream of GHR, we sought to evaluate if the lack of GH-induced STAT5 activation and differential signalling in these mutants can affect cancer incidence and longevity. Since GH secretion is sexually dimorphic it is pertinent to analyse both females and males to determine the sex-dependent effects associated with GH-dependent secretory pattern.

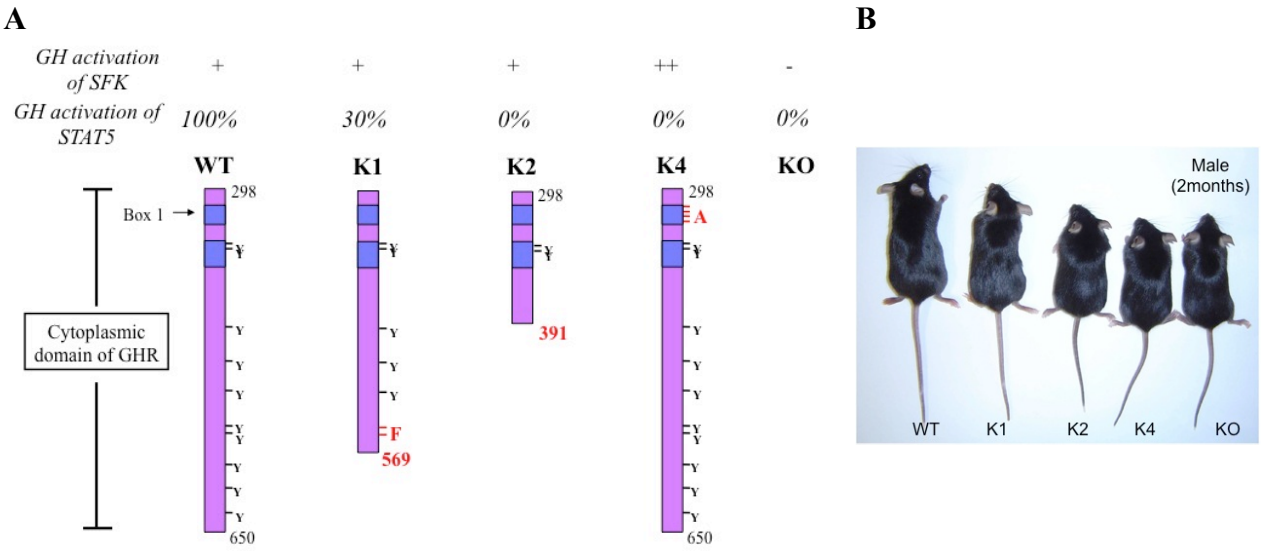

Figure 8.1: Cytoplasmic Domain of Targeted Growth Hormone Receptor Mutations and their attributes with regards to longevity and cancer.

(A) The cytoplasmic domains of murine WT, K1, K2 and K4 targeted GHR mutations (in red) are shown above. The K1 mutation is truncated at proline 569 in addition to conversion of tyrosines 539 and 545 to phenylalanine. The K2 mutant is truncated at lysine 391 while K4 mutant has four proline residues of the box1 domain converted to alanine in a full-length receptor. Compared to WT, GH activated STAT5 and SFK in mutant GHR receptors are indicated as percentage and signal intensity (+/-) respectively. (B) Male GHR mutant and WT mice at 2 months of age with evident difference in body size.

Robustly increased longevity in all GHR mutant females, but not all males

There was no significant difference in *median* lifespan in most male mutants except K4, with a median survival of 1044days *vs* 904days in control amounting to 15% median life extension. As shown in fig.8.1C, *median* survival of female GHR K2 (955days), K4 mutants (1104days) and GHR KO (909days) was increased approximately by 26%, 45% and 20% respectively relative to WT controls (759days). The GHR K1 female mutants with only 30% residual GH-mediated STAT5 activity had median survival of 807days, hence a marginal 6% increase in median lifespan extension and were not further analysed. In addition, there is an increase in *maximal* lifespan evident in both male and female GHR K4 and female K2 mutants.

C

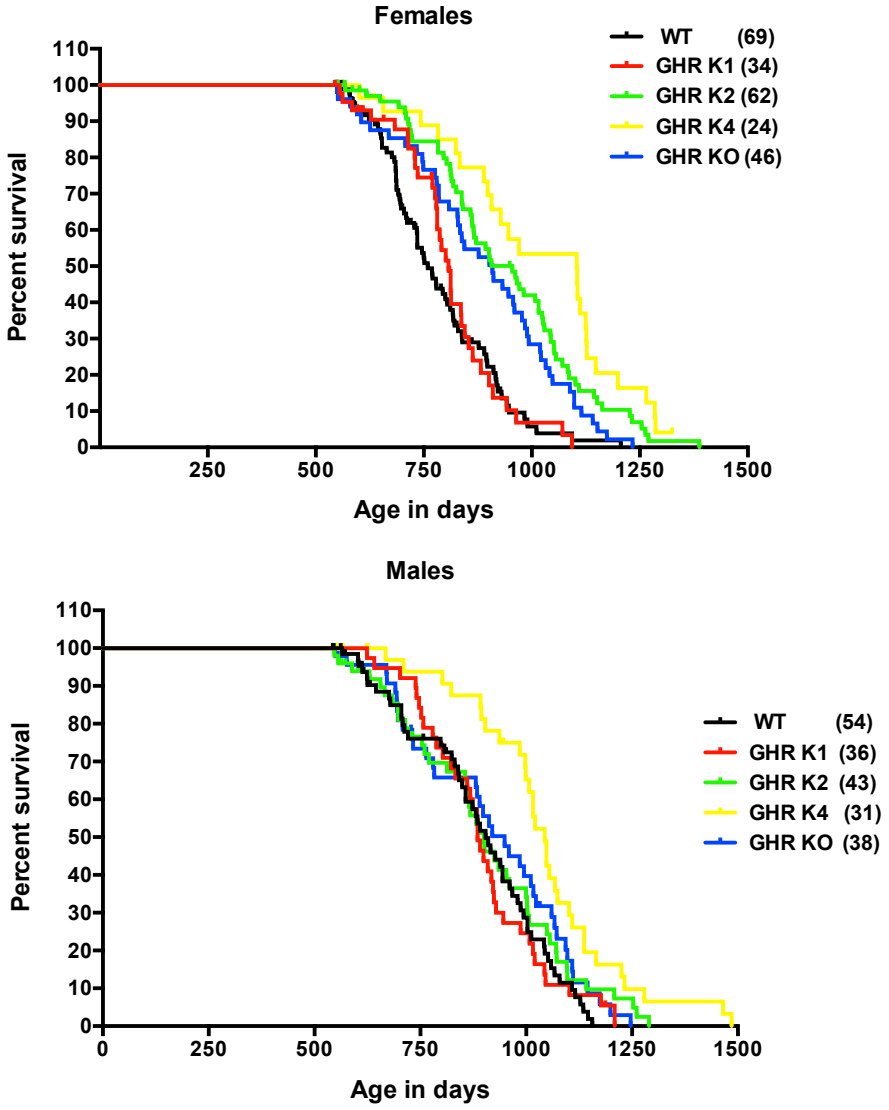

Figure 8.1C: Kaplan-Meier Plots for GHR knockin and knockout mice.

Survival curves of GHR knockin and knockout models and WT mice (controls) in the same C57Bl/6 genetic background and subjected to similar animal husbandry conditions are represented. The mice numbers included in the study for each model are indicated in brackets. Increased median lifespan extension is evident in all GHR female

mutants but only in GHR K4 male mutants.

The animals included in longevity studies were analysed for the cause of death initially based on gross morphology as indicated in figure 8.1D taken from 5 years of records. From the graph it is evident that the WT and GHR K1 males have higher incidences of macroscopic tumour as compared to other GHR male mutants. Interestingly, no death due to cancer was evident in GHR K4 male mice thus far. This was in striking contrast with unexpectedly high levels of tumour incidences observed in GHR K4 females even though they showed maximum lifespan extension (fig.8.1C). Other GHR female mutants had lower incidences of tumour-related deaths as compared to WT females.

D

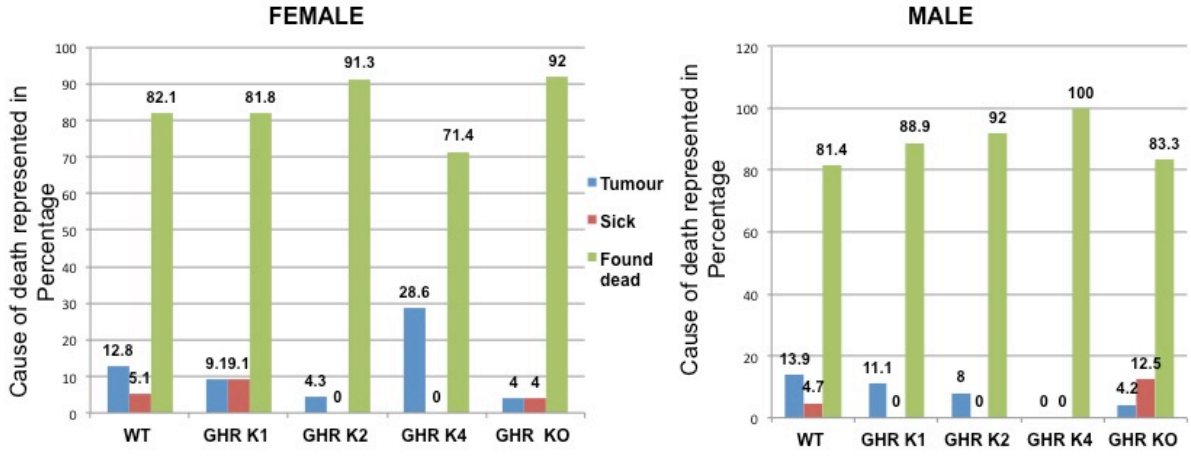

E

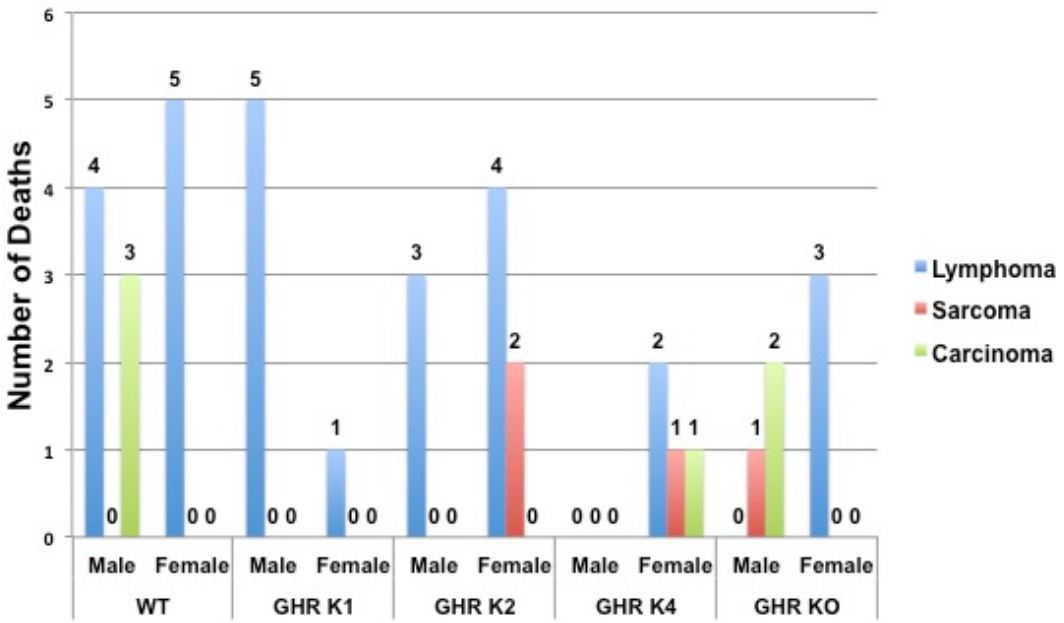

Figure 8.1: Attributes of GHR knockin and knockout mice mutants with regards to tumour and cancer incidences.

(D) Initial cause of death was classified as macroscopic tumour, sick (no evident tumour), found dead (no evident pathology) and is represented as percentage of total deaths. (E) Based on number of mice shown in histogram above, histopathology results of tumour incidences, GHR mutants are indicated with corresponding cancer modality.

After death (or euthanasia), all mice that were part of this study were sent for histopathologic evaluation for the exact cause of death. The chart in figure 8.1E represents the cancer modalities corresponding to the tumour-related cause of death. These results even though preliminary are indicative that lymphoma is the primary cause of death in most GHR male mutants (except GHR K4 males) and WT in C57Bl/6 genetic background. In the case of females, there is may be a reduction in lymphoma incidences across GHR KO and K2 mutants while GHR K4 are also prone to sarcoma and carcinoma as compared to WT mice. Since all GHR mutant females live longer than WT, this is suggestive of reduced lymphoma aggressiveness in female mice lacking GH-induced STAT5 activation.

In order to better understand the molecular mechanisms that may be associated with decreased cancer incidences and increased survival in some GHR mutant models indicated above, qPCR and immunoblotting experiments were carried out on metabolically active tissue(s) of young (12weeks) and old (78weeks) mice.

Gene expression profiles in young GHR mutant mice

The liver controls various metabolic processes including metabolite and xenobiotic detoxification, glucose production serum protein synthesis and bile production. It is composed of highly specialised tissues that regulate a wide variety of high-volume biochemical reactions, including the synthesis and breakdown of small and complex molecules, many of which are necessary for normal vital function. Since it is the primary target for GH action and therefore an endocrine organ that regulates IGF-1 levels it is important to determine the molecular elements that are altered in various GHR mutants that associate with increased protection against cancer and/or promote survival.

Elevated circulating GH levels in female GHR mutant mice

Growth Hormone was measured in the serum of 12weeks old female GHR mutant mice fed *ad libitum*. Serum GH was significantly elevated in these mice as evident from figure 8.2. GH-induced STAT5 is absent in these mutants (Rowland et al, 2005b), hence the circulating IGF-1 levels are dramatically low as evident from hepatic transcripts (fig.8.3). The elevated GH is a direct outcome of lack of IGF-1-mediated negative feedback on GH secretion in the hypothalamus and pituitary gland of these mice as compared to WT.

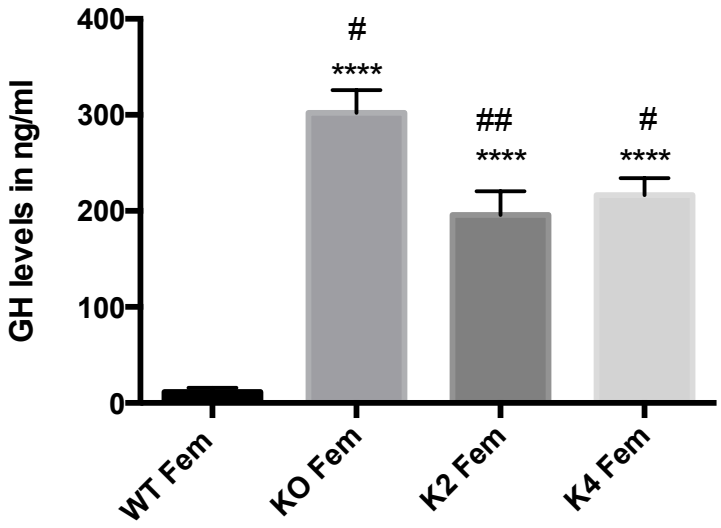

Figure 8.2: Circulating Growth Hormone levels in GHR mutant female mice fed *ad libitum*.
Circulating GH levels in are higher in all GHR mutant 12weeks old female mice compared to WT. K2 and K4 mice have lower GH levels than KO (n=6/genotype, mean ± SEM). ****, p<0.0001 compared to WT by ANOVA. #, p<0.05; ##, p<0.01 compared to KO by ANOVA.

In addition to the reduction in IGF-1 levels, IGF-2 transcript although present in low copy number was elevated in all the mutants and achieved significance in all KO mice and all GHR male mutants (fig.8.3). Other GH/IGF-1 axis parameters such as IGF binding proteins (IGFBPs) were differentially regulated in mice models. IGFBP-1 and 2 were significantly elevated in all GHR mutants independent of the gender. In addition, IGFBP-3 and 4 transcripts were also elevated in KO while IGFBP-2 and 3 were also sexually dimorphic in expression as shown in figure 8.3.

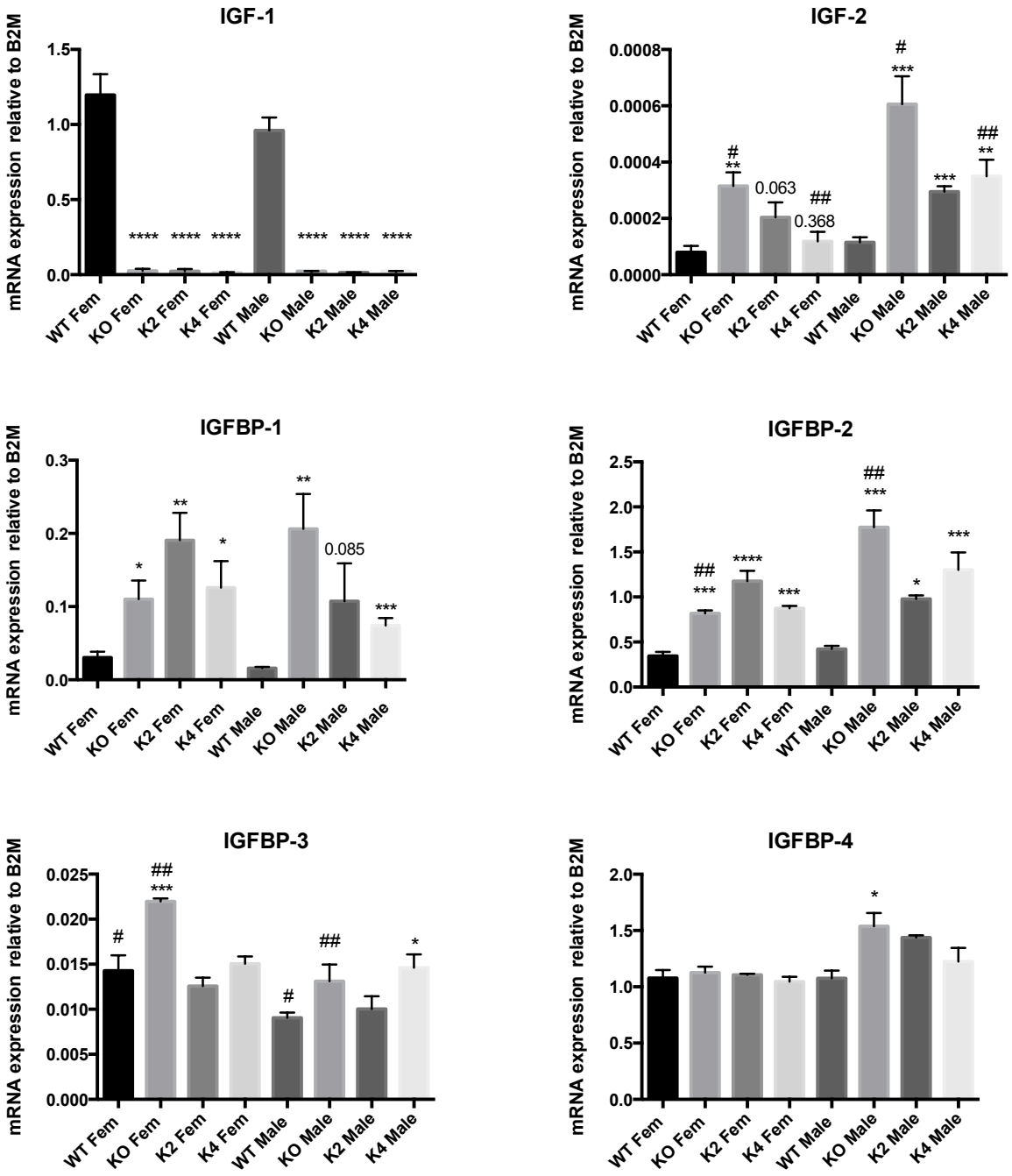

Figure 8.3: Altered hepatic transcripts of Insulin like growth factor and IGF binding protein in 12weeks old GHR mutant mice fed *ad libitum*.

Decrease in *IGF-1* and increase in *IGF-2* and *IGFBP-1 and 2* transcripts in 12weeks old male and female mice. Other IGFBPs were differentially regulated while being sexually dimorphic in its expression. Data represented as mean ± SEM (n=5mice/genotype). *, p<0.05; **, p<0.01; ***, p<0.001; ****,p<0.0001 compared to **WT of the same gender** by ANOVA. #, p<0.05; ##, p<0.01; ###, p<0.001; ####, p<0.0001 compared within the **same genotype of different gender** by student t-test.

Altered sirtuins and mitochondrial biogenesis regulator in mice models

The mitochondrial biogenesis and function regulator *pgc1α* (peroxisome proliferator-activated receptor gamma coactivator 1-alpha) transcript is significantly elevated in the liver of all GHR

mutant models. In contrast, *pgc1β* transcript was only elevated in the KO and K2 males (fig.8.4). However at the protein level PGC1 was elevated in KO and K4 male livers (fig.8.5).

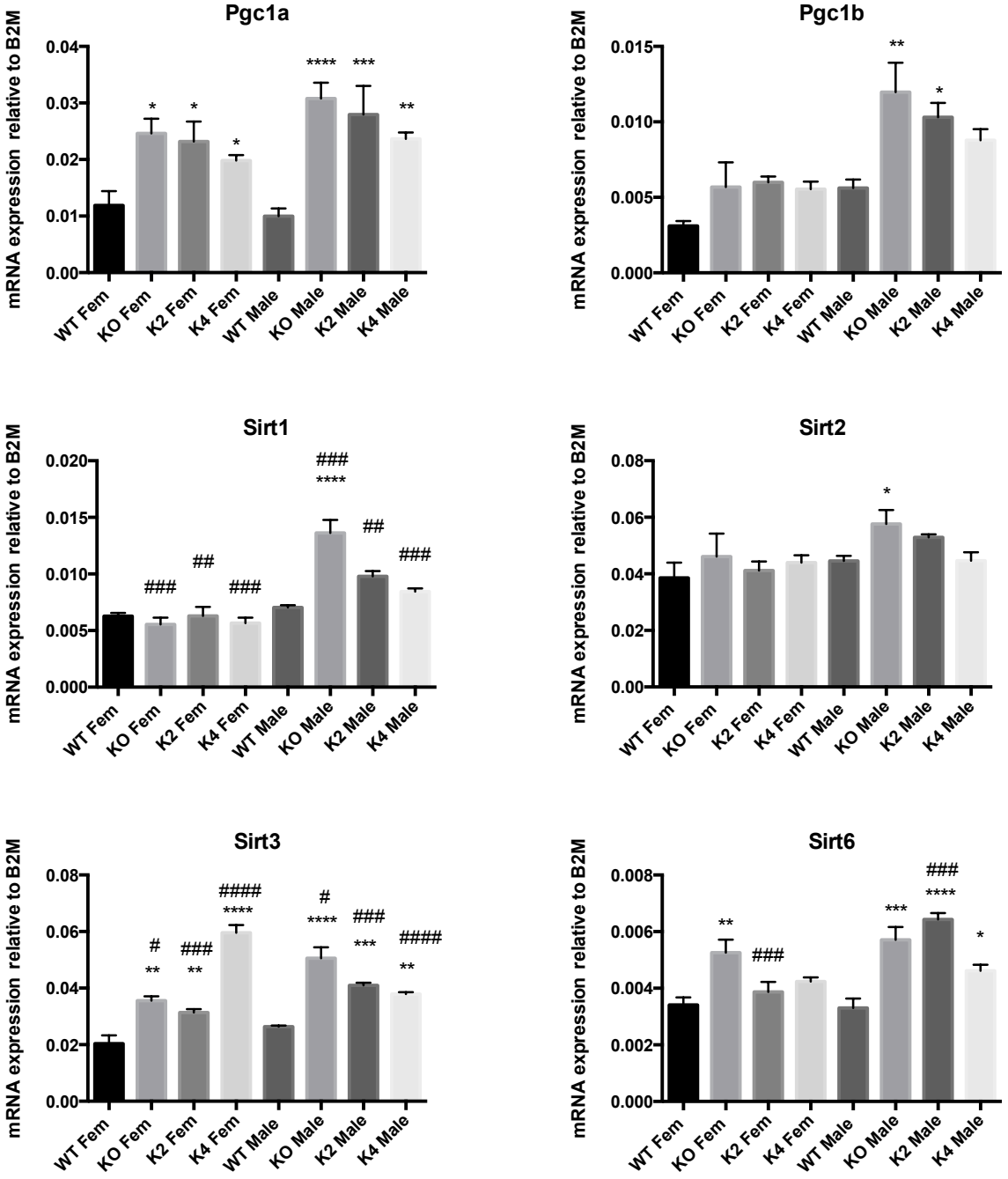

Figure 8.4: Altered mitochondrial biogenesis regulator and sirtuins transcripts in liver of 12weeks old GHR mutant mice fed *ad libitum*.

Mitochondrial biogenesis regulator *pgc1α* transcripts were significantly elevated in GHR mutants while *pgc1β* was upregulated in only GHR male mutants. Key mitochondrial sirtuin, *Sirt3* transcript was elevated in all the mutants independent of gender while Sirt1 and 2 were elevated mostly in KO males and Sirt6 in KO and K2 males. Data represented as mean ± SEM (n=5mice/genotype). *, p<0.05; **, p<0.01; ***, p<0.001; ****,p<0.0001 compared to **WT of the same gender** by ANOVA. #, p<0.05; ##, p<0.01; ###, p<0.001; ####, p<0.0001 compared within the **same genotype of different gender** by student t-test.

Mammalian homologs of Sir2, the sirtuins showed gender and genotype differences at the transcript level in these mice models. Sirt3 transcript was consistently elevated across all genotypes and this was also evident at the protein level (fig.8.5A and B). Sirt1 transcript was significantly elevated only in the KO male mice livers while the protein was elevated across all the genotypes in male mice as compared to WT (fig.8.4, 8.5A and B). Both Sirt1 and 3 transcripts were elevated in males more than females with the exception of Sirt3 in K4 females. Sirt2 showed only a slight increase in transcript in KO male whereas no change was observed at the protein level. Sirt6 transcripts were increased in both male and female in KO livers as well as K2 and K4 males (fig.8.4) but the protein level was not increased in KO and K4 male livers (fig.8.5A). Additionally, protein expression of GCN5 (KAT2A), a ubiquitous histone acetyltransferase that promotes acetylation and inactivation of PGC1α (Lerin et al, 2006) was also elevated in KO and K4 male mice liver. Another observation seen in the liver of all three male mutant models was increased levels of phosphorylated AMPK. AMPK besides being an energy sensor is an important player in mitochondrial biogenesis and ROS detoxification in conjunction with Sirt1 and 3 (Canto & Auwerx, 2009).

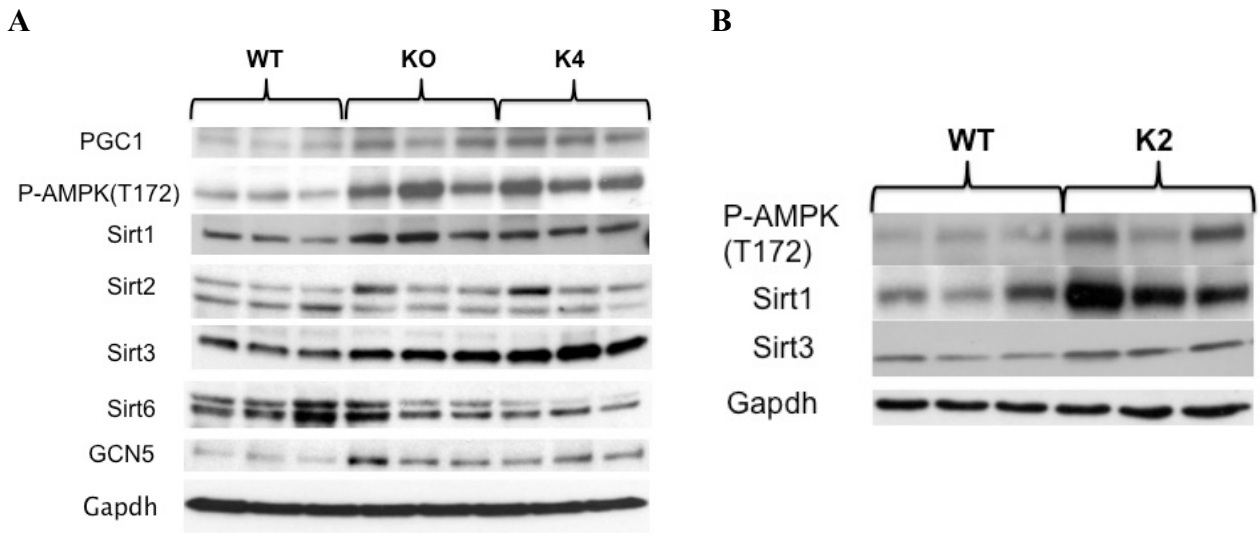

Figure 8.5: Protein levels of mitochondrial and key sirtuins in liver of 12weeks old male GHR mutant mice fed *ad libitum*.

(A) Increase in protein level of PGC1, phosphorylated-AMPK (T172), Sirt1 and 3 in KO and K4 GHR mutants. Sirt2 and 6 both have 2 isoforms and no change was observed in both mutants. GCN5 protein was elevated in KO and K4 mutant livers. Blots representative of n=5mice/genotype (B) Elevated phosphorylated-AMPK (T172) levels as well as Sirt1 and 3 protein in K2 male mutant mice as compared to WT. Blots representative of n=4mice/genotype.

Increased mitochondrial function in GHR mutants

In addition to the elevated mitochondrial biogenesis markers *pgc1α* and *pgc1β*, transcripts for mitochondrial oxidative phosphorylation enzymes were found to be elevated. These include *Sdhb*, *mt-CO1*, *Uqcrc2*, *ATP5a*, *Ndufa5* that were upregulated in most of the male mutants. In the case of female mutants, *ATP5a* was elevated across all the mutants while *Ndufa5* and *Uqcrc2* were

increased only in KO and *Sdhb* in KO and K4 females (fig.8.6). MFN2 (mitofusin2) involved in regulation of mitochondria morphology and function was elevated in all male GHR mutants but not in females at the transcript level. NAD(P)H dehydrogenase quinone 1, *Nqo1* transcript was significantly elevated in all the male GHR mutants, has been associated with promoting anti-carcinogenic and insulin sensitivity effects (Pearson et al, 2008).

It was important to address the question of whether the increase in mitochondrial OxPhos proteins observed was an outcome of increase in mitochondria number. Estimation of the ratio of mitochondrial DNA *vs* nuclear DNA by qPCR using genome-specific primers was performed to answer this question. It was clear that there was no change in mitochondria numbers in any of the GHR mutant female mice as compared to WT (fig.8.6).

Supporting these results, western blot analysis revealed elevated levels of oxidative phosphorylation enzymes ATP5a (complex V), Uqcrc2 (complex III), Ndufb8 (complex I) in KO, K4 and K2 and Sdhb (complex II) in both K4 and K2 (fig.8.7A and B). mt-CO-1 (Complex IV) could not be probed in these blots being heat labile as the liver lysates were boiled before gel electrophoresis. One of the nuclear encoded catalytic core subunits of mitochondria, cytochrome C oxidase IV (Cox IV) was elevated in KO and K4 mice liver while mTFAM (mitochondria transcription factor A) that aids in transcription of mitochondrial genome did not change (fig.8.7A). No change in levels of Sdha protein was observed in KO and K4 male mice.

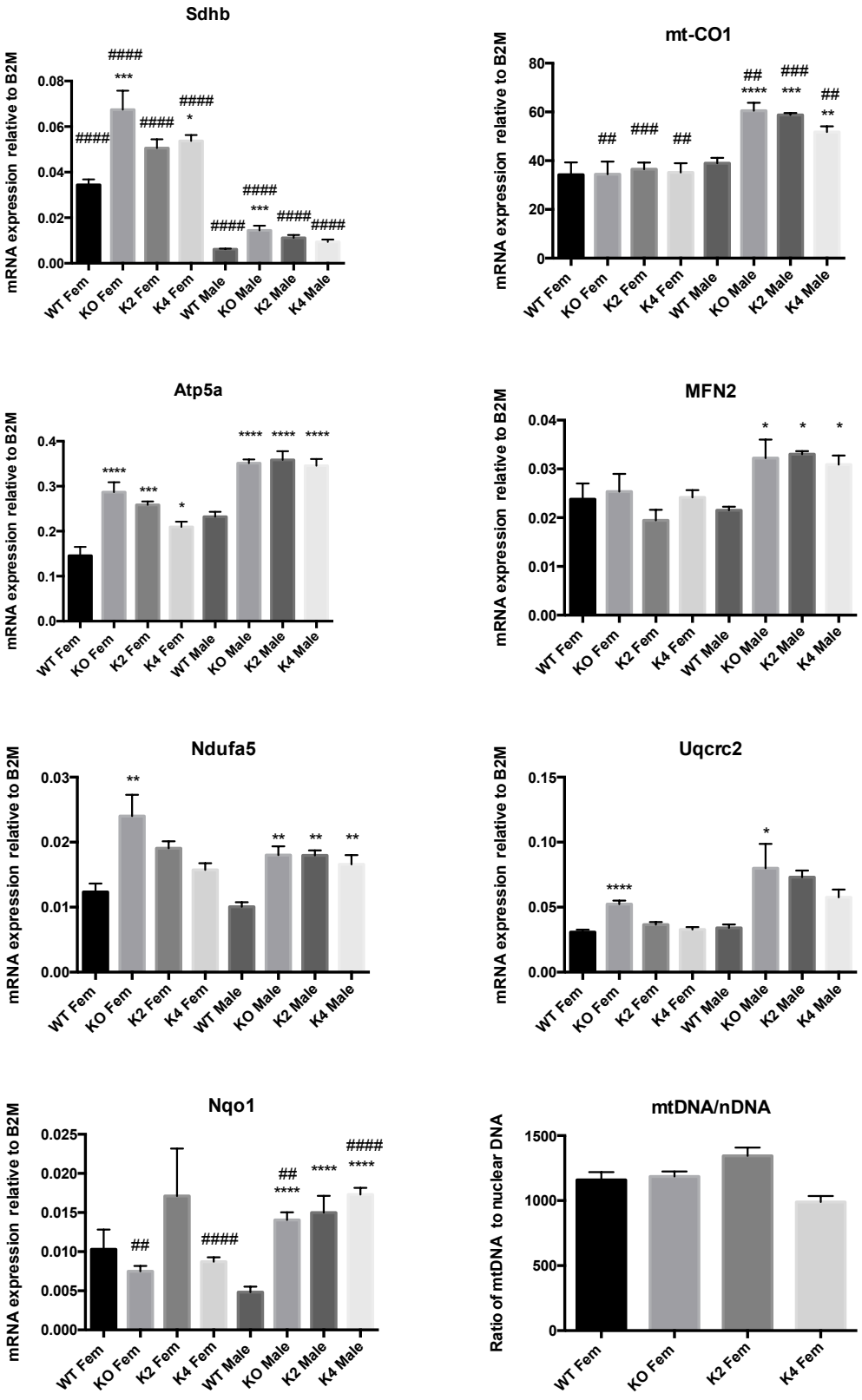

Figure 8.6: Altered mitochondrial oxidative phosphorylation enzymes transcripts and estimation of mitochondrial *vs* nuclear DNA in liver of 12weeks old GHR mutant mice fed *ad libitum*.

Hepatic ranscripts for enzymes involved in mitochondrial OxPhos complex *mt-CO1*, *Ndufa5* were elevated in GHR mutant males while *ATP5a* was elevated in all the mutant mice across both genders while *Uqcrc2* and *Sdhb* were elevated only in KO male and female mice. Other mitochondrial function regulator genes *mfn2* and *nqo1* were elevated only in GHR mutant males as compared to WT mice. No change in mitochondrial numbers was evident in GHR mutant females as evident from lack of differences in mitochondrial *vs* nuclear genome. Data represented as

mean ± SEM (n=5mice/genotype). *, p<0.05; **, p<0.01; ***, p<0.001; ****,p<0.0001 compared to **WT of the same gender** by ANOVA. #, p<0.05; ##, p<0.01; ###, p<0.001; ####, p<0.0001 compared within the **same genotype of different gender** by student t-test.

A

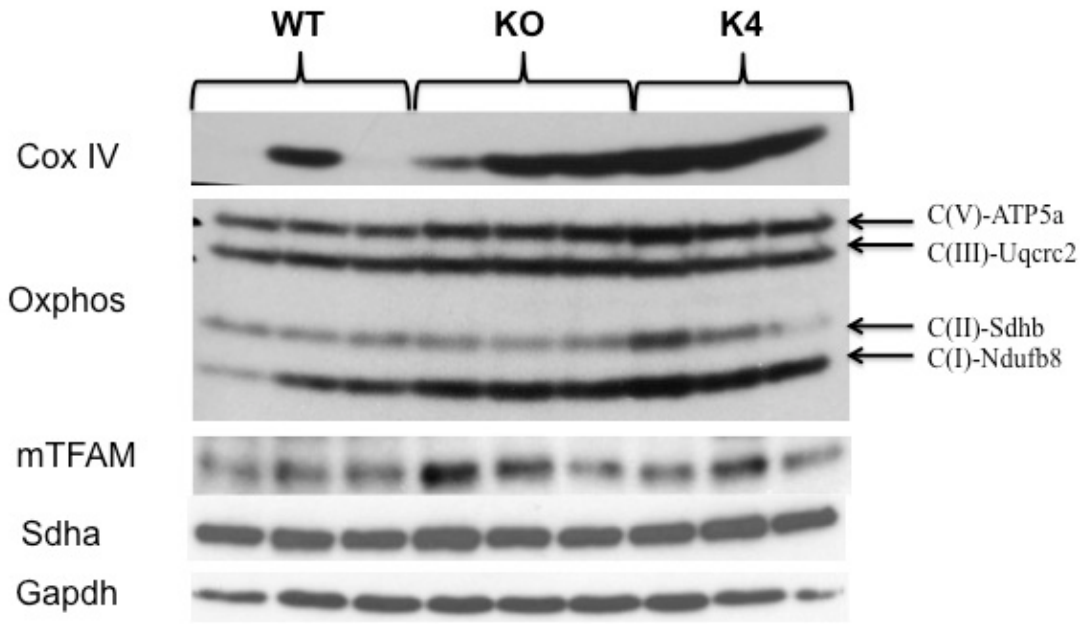

B

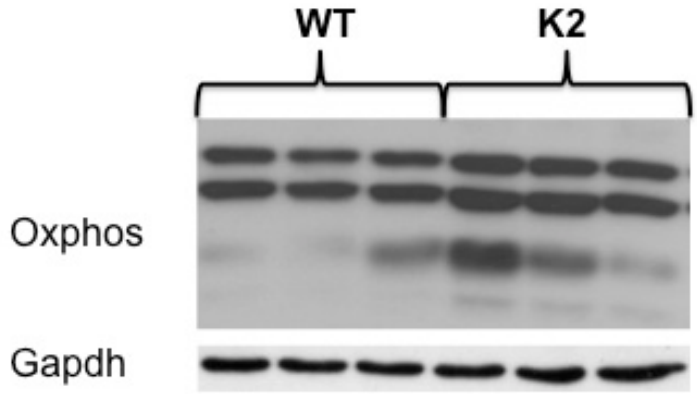

Figure 8.7: Protein levels of key mitochondria function regulator and oxidative phosphorylation complex enzymes in liver of 12weeks old male GHR mutant mice fed *ad libitum*.

(A) Male KO and K4 mutant mice livers have elevated levels of COX IV, mTFAM as well as OxPhos complexes I, III and V. Additionally complex II was elevated in K4 mice and no change was evident in Sdha levels. Blots representative of n=5mice/genotype. (B) Elevated OxPhos complex components I, II and III in K2 male mutant mice as compared to WT. Blot representative of n=4mice/genotype.

Increased insulin sensitivity in GHR mutants

The key downstream insulin receptor signalling molecules *IRS1* transcript was elevated in all male GHR mutants while *IRS2* transcript was elevated in male and female KO and male K4 mutant mice. The liver-specific glucose transporter *Glut2* transcript was elevated two-fold in all male GHR mutants and to a lesser extent in K2 female mice with significant sexual dimorphism across all the

GHR mutants. The phosphatase *PTP1B* that negatively regulates insulin signalling pathway was also elevated at transcript level in all the male GHR mutants and KO female livers. The fibroblast growth factor 21 (FGF21) is a hormone that is secreted by liver and is negatively regulated by PGC1α (Estall et al, 2009). The hepatic *FGF21* transcript was significantly downregulated in all the mutants across both genders with higher levels in mutant females than males (fig.8.8). The fatty acid translocase gene *CD36* was elevated in all the mutant GHR females and has been shown to play an important role in promoting tissue-specific insulin sensitivity in liver by hyperinsulinemic clamps (Goudriaan et al, 2003). Previous work from Waters' Group has reported elevated CD36 at both transcript and protein level in KO and K2 males (Barclay et al, 2011) as well increased insulin sensitivity (Nelson CN PhD thesis, 2013).

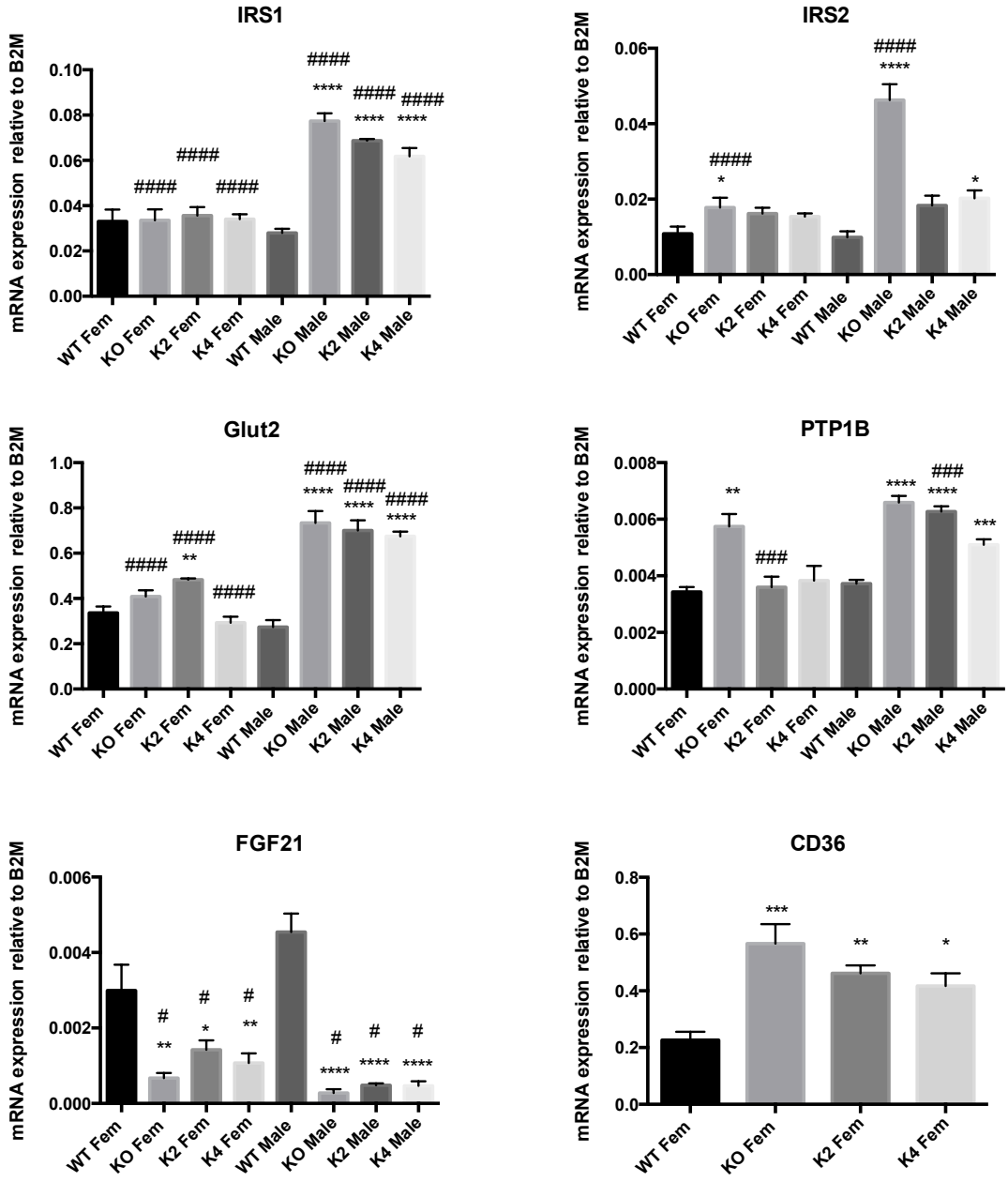

Figure 8.8: Altered hepatic transcripts involved in insulin signalling in liver of 12weeks old GHR mutant mice fed *ad libitum*.

Increase in *IRS1* and glucose transporter *Glut2* transcript in all male GHR mutants and *IRS2* transcript in KO male and female mutants while exhibiting sexual dimorphic expression. Negative regulator of insulin signalling, *PTP1B* is elevated in GHR mutants males and KO females specifically. *FGF21* was downregulated across all mutants in both genders while *CD36* was elevated in all female mutants with the former being sexually dimorphic. Data represented as mean ± SEM (n=5mice/genotype). *, p<0.05; **, p<0.01; ***, p<0.001; ****,p<0.0001 compared to **WT of the same gender** by ANOVA. #, p<0.05; ##, p<0.01; ###, p<0.001; ####, p<0.0001 compared within the **same genotype of different gender** by student t-test.

An important indicator of increased insulin sensitivity is the elevation of insulin receptor β subunit expression in male KO and K4 liver at the protein level (fig.8.9) with decrease in levels of downstream signalling adapter protein IRS1 and negative regulator of IRβ and IRS1/2, PTP1B in KO and K4 mutants in contrast to their transcript levels above. The FGF21 protein was in

accordance to transcript level while HNF4A was downregulated in the mutant livers in contrast to the unchanged transcript (fig.8.17).

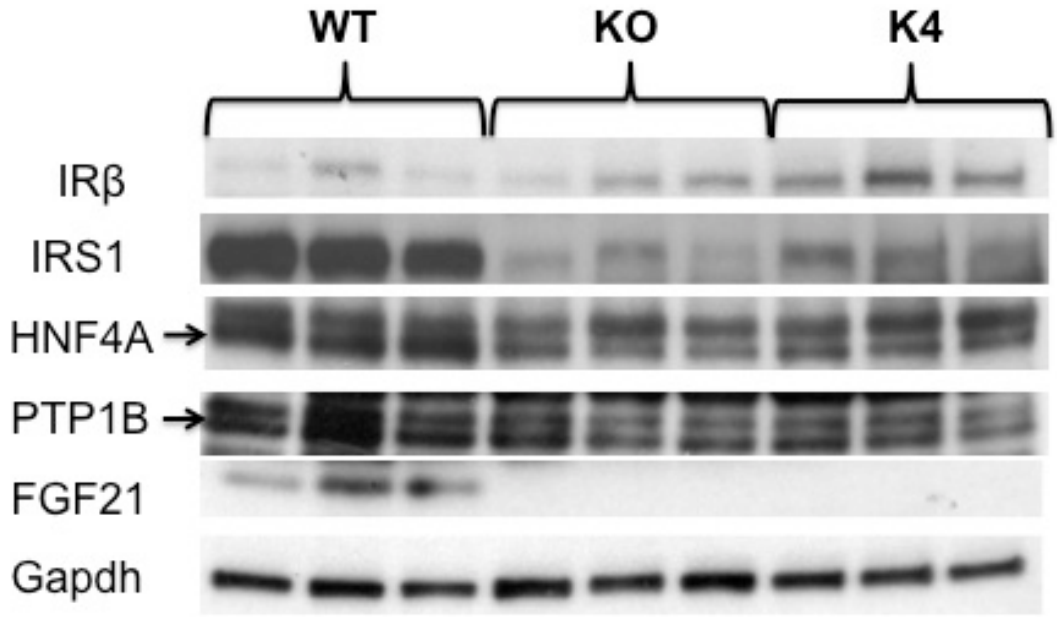

Figure 8.9: Altered protein levels of key insulin signalling molecules in liver of 12weeks old male GHR mutant mice fed *ad libitum*.

Increase in insulin receptor β protein levels in KO and K4 and reduction in insulin signalling molecule IRS-1 and hepatocyte nuclear factor4A in KO and K4. Negative regulator of insulin signalling, PTP1B is downregulated in KO and K4 as well as FGF21. Blots representative of n=5mice/genotype.

Increased Oxidative stress management and ROS detoxification in GHR mutant mice

The key antioxidant enzymes that catalyse the dismutation of superoxide radicals into oxygen and hydrogen peroxide are superoxide dismutase SOD1-3. *SOD2* and *SOD3* are elevated in all GHR mutant males while *SOD1* was increased only in KO males at mRNA and protein levels (fig.8.10 and 8.11A). In female GHR mutants *SOD2* was significantly elevated in all the mutants (fig.8.10). In addition, all the SOD genes were sexually dimorphic across all genotypes including WT. Sulfiredoxin encoded by *Srxn1* provides oxidative stress resistance by reducing cysteine-sulfinic acid formed under oxidant exposure. The *Srxn1* transcripts were significantly elevated in all the GHR mutants in both males and females with higher expression in males than females. The ubiquitous enzyme encoding Catalase gene, *CAT* was elevated in all the mutants but reached significance only in KO female mutant. The catalase enzyme is involved in decomposition of hydrogen peroxide to water and oxygen in turn protects the cell from oxidative damage. Apolipoprotein E (ApoE) transcript was elevated in most GHR mutants while the flavin containing monooxygenase, *FMO2* that catalyse oxidation of xenobiotics was elevated in all the GHR mutant males but downregulated in all GHR mutant females. Additionally, both male and female GHR KO

exhibited elevated *Mt1* (metallothionein1) transcript with 3 times higher levels in males than females.

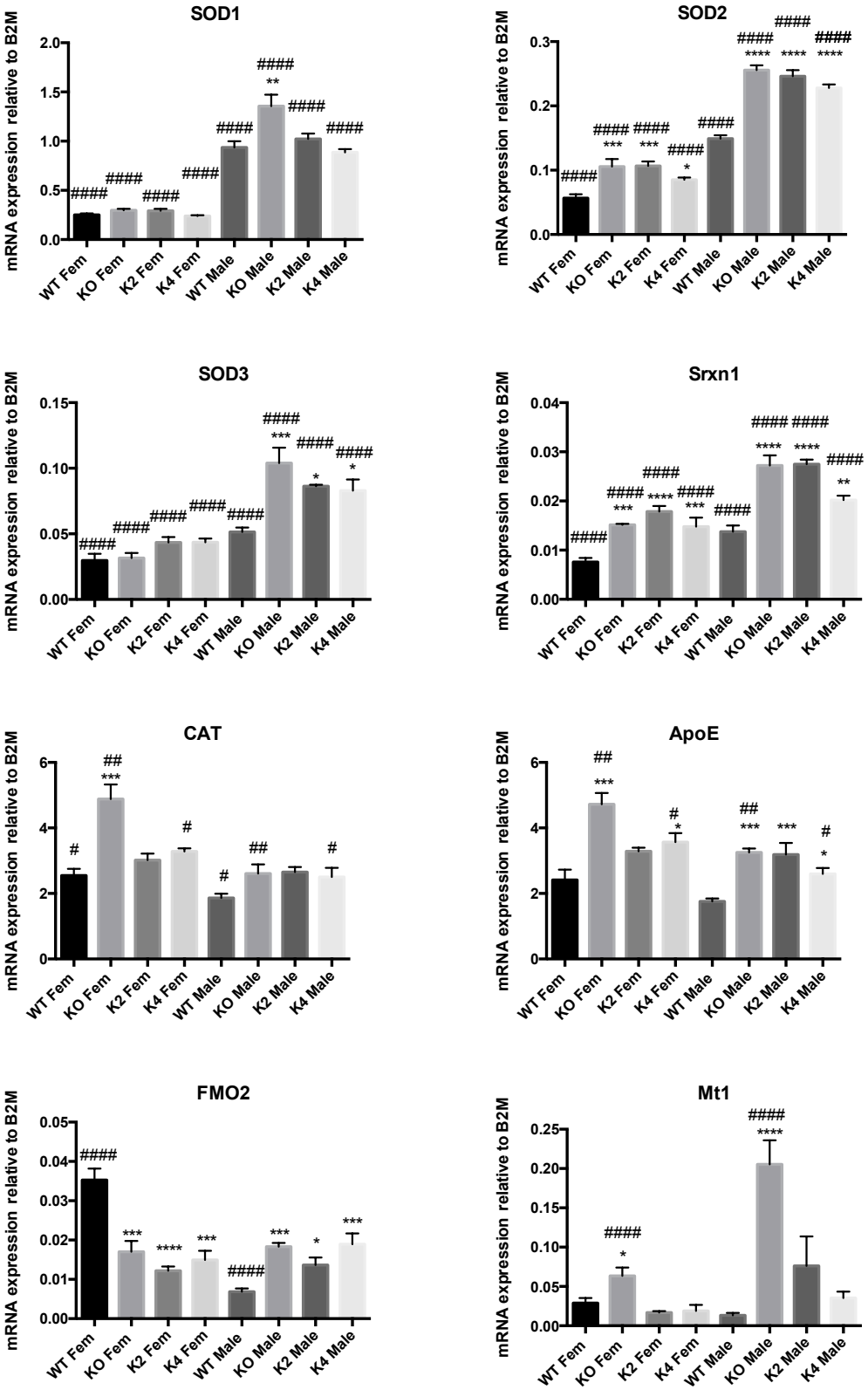

Figure 8.10: Altered hepatic transcripts involved in oxidative stress management in 12weeks old GHR mutant mice fed *ad libitum*.

Elevated transcripts of superoxide dismutase, *SOD1*, *SOD2*, *SOD3* in males and *SOD2* and *ApoE* in female GHR mutants. Increased *Srxn1*, *FMO2* and *ApoE* in male GHR mutants and *Mt1* and *CAT* in female GHR KO. Decrease in

expression of *FMO2* and increase in *Srxn1* in female GHR mutants. Data represented as mean ± SEM (n=5mice/genotype). *, p<0.05; **, p<0.01; ***, p<0.001; ****,p<0.0001 compared to **WT of the same gender** by ANOVA. #, p<0.05; ##, p<0.01; ###, p<0.001; ####, p<0.0001 compared within the **same genotype of different gender** by student t-test.

In addition to SOD's, liver of male GHR mutant mice have increased expression of nuclear factor erythroid 2-related factor respiratory factors, *Nrf1* and *Nrf2* at both transcript and protein levels (fig.8.11, 8.12A and B) with the latter being sexually dimorphic. Nrf's are important transcription factors that activate numerous metabolic genes regulating cellular growth and nuclear genes important in respiration, heme biosynthesis, and mtDNA transcription. In addition, Nrf's are responsible for mediating antioxidant response during stress and under the control of Keap1 (Kelch-like ECH-associated protein1) the transcript of which was increased specifically in KO male mutants. Interestingly there is a striking sexual dimorphic pattern between *Nrf2* and *Keap1* between male and female mice.

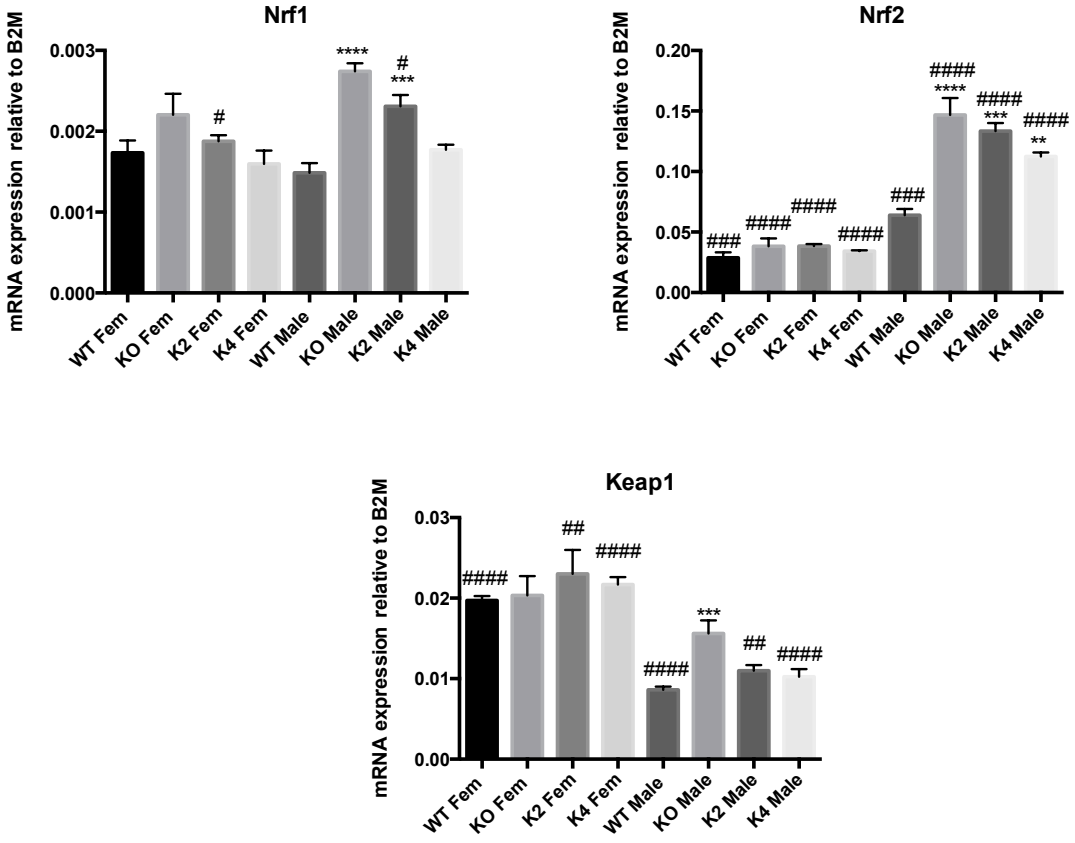

Figure 8.11: Altered hepatic transcripts associated with reactive oxygen species detoxification in 12weeks old GHR mutant mice fed *ad libitum*.

Elevated transcripts of *Nrf1* and *Nrf2* in male GHR mutants and *Keap1* specifically in GHR KO males with GHR mutants exhibiting sexual dimorphism in *Nrf2* and its inhibitor *Keap1*. Data represented as mean ± SEM (n=5mice/genotype). *, p<0.05; **, p<0.01; ***, p<0.001; ****,p<0.0001 compared to **WT of the same gender** by ANOVA. #, p<0.05; ##, p<0.01; ###, p<0.001; ####, p<0.0001 compared within the **same genotype of different gender** by student t-test.

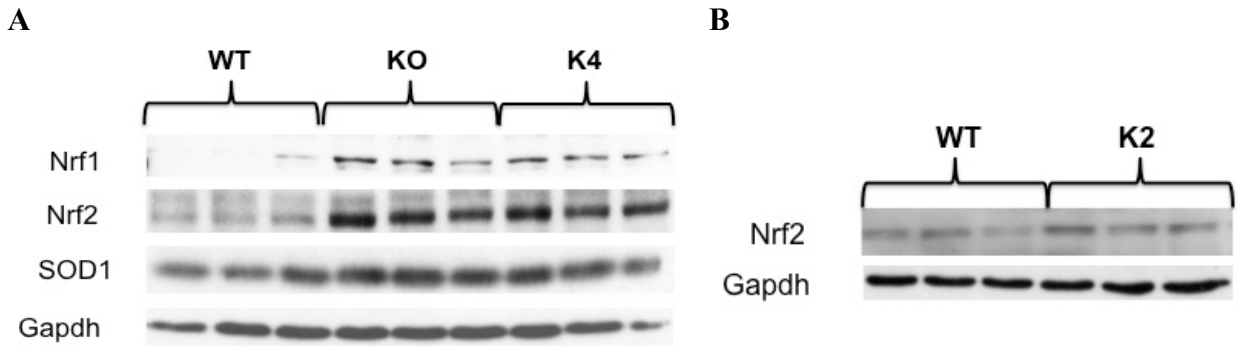

Figure 8.12: Elevated antioxidant transcription factors and enzyme in liver of 12weeks old GHR mutant mice fed *ad libitum*.

(A) Male KO and K4 mutant mice livers have elevated levels of Nrf1 and Nrf2 antioxidant transcription factors with KO liver also expressing higher SOD1 at protein level as compared to WT. Blots representative of n=5mice/genotype. (B) Elevated Nrf2 in K2 male mutant mice as compared to WT. Blot representative of n=4mice/genotype.

Dampening of signalling response in GHR mutant mice

The main outcome of the lack of GH-induced STAT5 signalling is evident from decreased mRNA levels of suppressors of cytokine signalling *SOCS2* and *CIS* across all GHR mutant mice (fig.8.13A). In contrast *SOCS3* levels were not significantly changed in all GHR mutants. Interestingly, *SOCS3* transcript levels were sex-dependent between males and females across all genotypes. The protein levels however were in complete contrast to the transcripts with higher levels of SOCS2, SOCS3 in KO and K4 male mutants and no change in CIS protein in comparison to WT (fig.8.13B) indicating a constant pool of these tumour suppressors in GHR mutant mice.

A

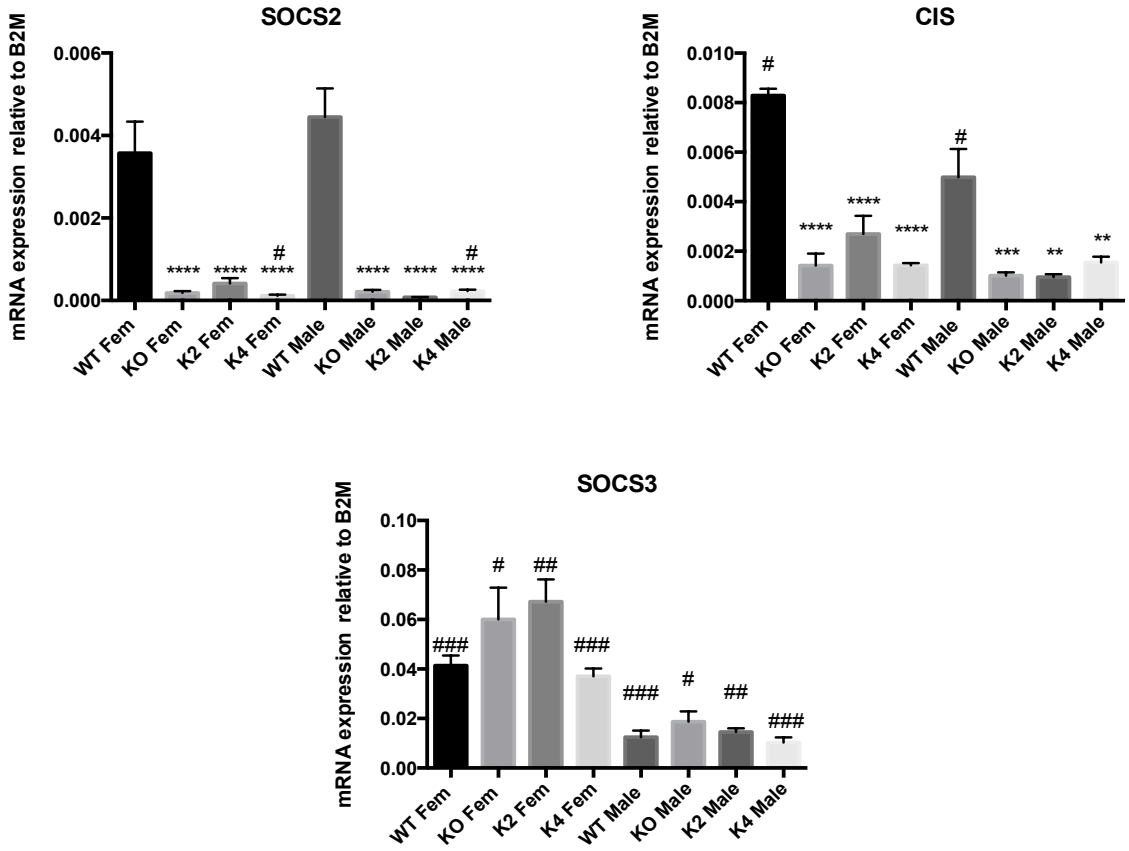

B

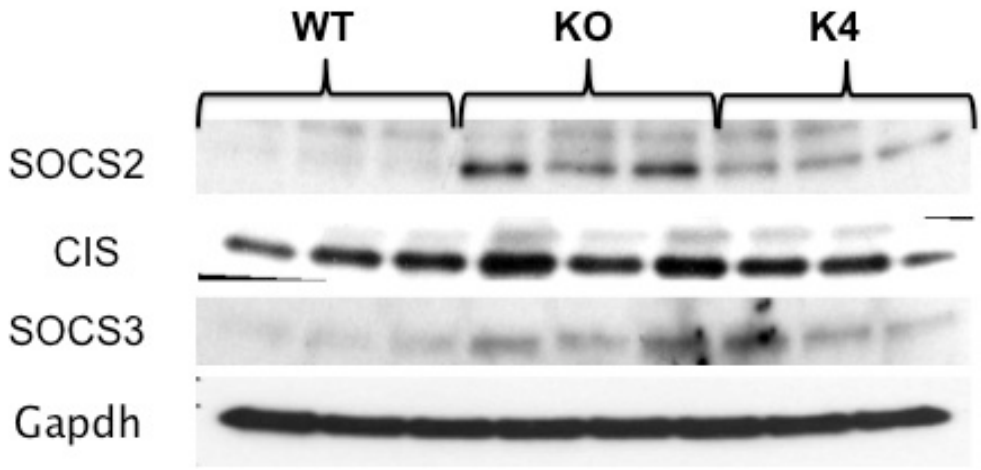

Figure 8.13: Altered hepatic transcripts and protein levels of suppressors of cytokine signalling molecules in 12weeks old mice fed *ad libitum*.

(A) Significant decline in SOCS2 and CIS transcripts in GHR mutant mice while SOCS3 remains unaltered but sexually dimorphic. Data represented as mean ± SEM (n=5mice/genotype). *, p<0.05; **, p<0.01; ***, p<0.001; ****,p<0.0001 compared to **WT of the same gender** by ANOVA. #, p<0.05; ##, p<0.01; ###, p<0.001; ####, p<0.0001 compared within the **same genotype of different gender** by student t-test. (B) Altered protein levels of suppressors of cytokine signalling molecules in liver of male GHR KO and K4 mice. Elevated SOCS2 and SOCS3 levels while CIS expression is unchanged in these mice. Blots representative of n=5mice/genotype.

Additionally, other key signalling elements that are elevated in cancers are downregulated at protein level in GHR mutant mice. Besides the decrease in *IGF-1* transcript, its receptor IGF-1R is also downregulated in the liver as well as its downstream signalling molecule Akt2, which is also a putative oncogene (fig.8.14). The most frequently mutated and elevated receptor EGFR was also downregulated in these mutants to undetectable levels. There was an increased expression and activation of STAT3 in the liver potentially due to the loss of GH-induced STAT5 activation. This is also reflected in increased SOCS3 level at transcript and protein level (fig.8.13A and B).

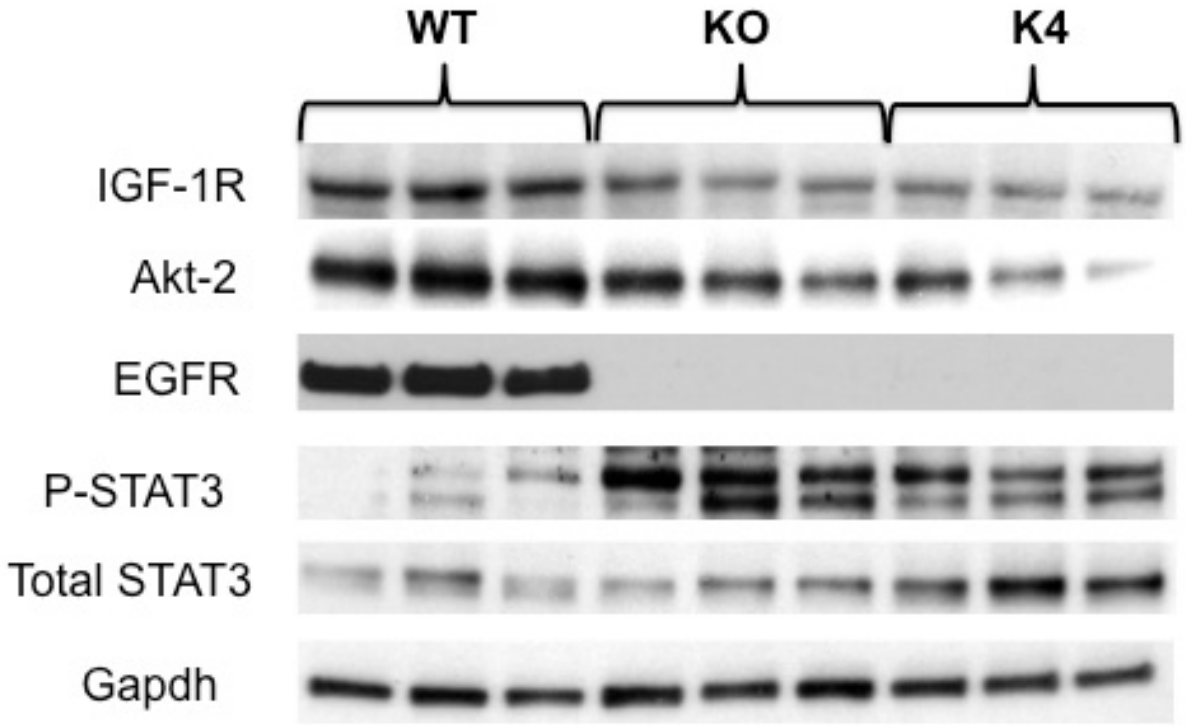

Figure 8.14: Altered protein levels of key factors involved in carcinogenesis in liver of 12weeks old male GHR mutant mice fed *ad libitum*.

Decrease in expression of IGF-1R, Akt2 and EGFR in GHR KO and K4 mice and increase in expression of active and total STAT3. Blots representative of n=5mice/genotype.

Decrease in pro-inflammatory factors in GHR mutant mice

The anti-inflammatory cytokine receptor genes *IL-10Rα* and *IL-10Rβ* transcripts were elevated in all male GHR mutants. In addition, while *IL-1β* pro-inflammatory messenger did not change but there was increase in IL-1 receptor antagonist (IL-1RA) messenger levels that has been shown to bind non-productively to IL-1 receptor and inhibit binding of IL-1 inflammatory cytokine and thereby decreasing inflammation. The IL-1RA had an overall increasing trend in all GHR mice but attained statistical significance in KO males and females and K2 males. Elevated *cdkn1a* in KO males and females is associated with decreased response to mitogenic stimuli and inflammatory cytokine (fig.8.15). The while *IL-1β* message needs to be evaluated in female GHR mutants.

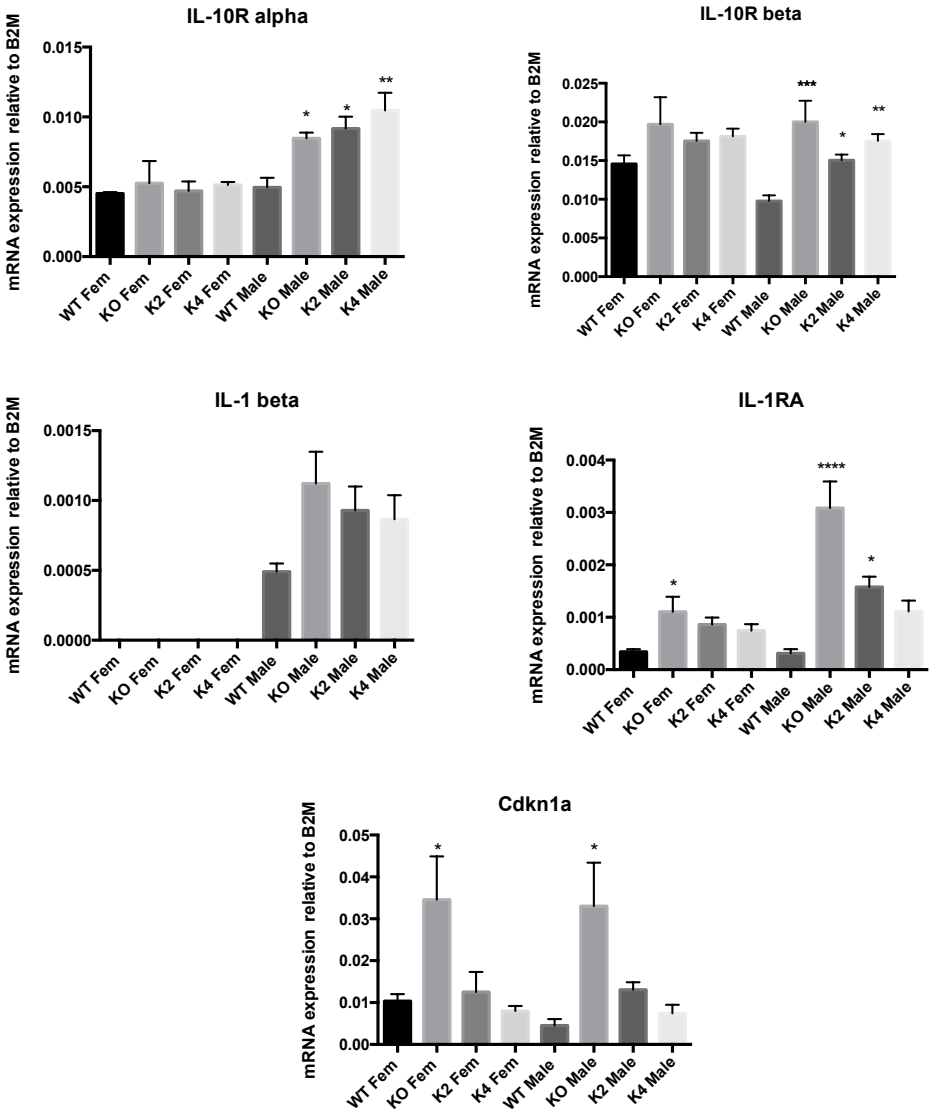

Figure 8.15: Altered hepatic transcripts of genes involved in inflammatory stimuli in 12weeks old GHR mutant mice fed *ad libitum*.

Elevated transcripts of *IL-10Rα* and *IL-10Rβ* in male GHR mutant and *IL-1RA, cdkn1a* in GHR KO males and females. No change was evident in *IL-1β* levels. Data represented as mean ± SEM (n=5mice/genotype). *, p<0.05; **, p<0.01; ***, p<0.001; ****,p<0.0001 compared to **WT of the same gender** by ANOVA. #, p<0.05; ##, p<0.01; ###, p<0.001; ####, p<0.0001 compared within the **same genotype of different gender** by student t-test.

The alterations in transcripts were accompanied by decrease of other pro-inflammatory signal modulators at the protein level (fig.8.16). There was decline in levels of acetylated tubulin, an anti-inflammatory signal (Wang et al, 2014) as well as that of active stress kinase p38 MAPK, indicative elevated stress in WT mice. This was also supported by reduction in NADPH oxidase4 (Nox4) expression along with p65 subunit of NF- κB, which is a potent inflammation and oxidative stress generator.

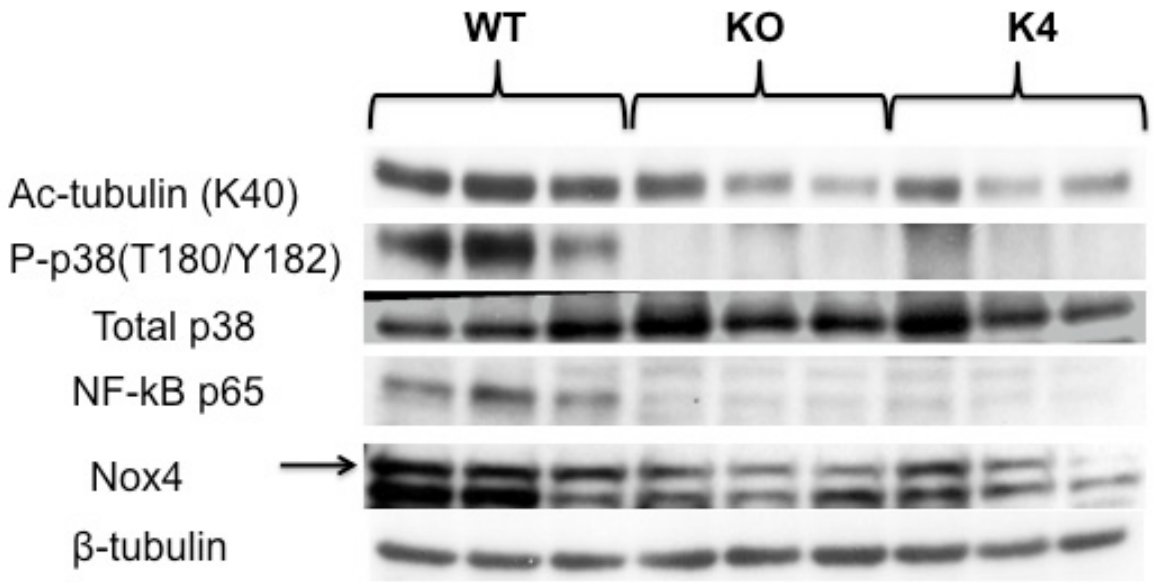

Figure 8.16: Decreased protein levels of inflammation modulators in livers of 12weeks old male GHR mutants fed *ad libitum*.

Decrease expression of acetylated tubulin (K40), phosphorylated p38 stress kinase as well as inflammatory and immune response modulator NF- κB p65 subunit and oxidative stress generator Nox4 in GHR KO and K4 mice. Blots representative of n=3mice/genotype.

Altered hepatic nuclear factors and receptor levels in GHR mutant mice

The GHR mutant mice were analysed for alterations in nuclear receptor and hepatocyte nuclear factor levels, both of which are key regulators of several aspects of hepatic physiology and pathophysiology. Nuclear receptors play a major role in metabolic processes, drug disposition, bile acid homeostasis, inflammation and tumourigenesis (Wagner et al, 2011). An important family of nuclear receptor comprises the peroxisome proliferator-activated receptors (PPAR). These receptors function as transcription factors regulating cellular differentiation, development and metabolism in a tissue-specific manner. The transcripts of *ppargamma1* were elevated in GHR mutant males and female GHR K2 mice while *ppargamma2* were significantly downregulated in most male mutants but elevated in K2 and K4 female GHR mutants. The level of *pparalpha* transcript was unaltered in any mutant mice but was dramatically sexually dimorphic like *ppardelta*, which was elevated in KO and K4 males and females (fig.8.17).

In addition, the hepatocyte nuclear factor *HNF1A* and *HNF3B* were elevated in all GHR mutant males while *HNF1A* was also elevated in KO and K2 females. The *HNF6* was drastically downregulated in both male and female GHR mutants (fig.8.17) and has been shown to be a GH-induced STAT5 dependent gene (Lahuna et al, 1997). These HNFs serve as transcription factors of diverse group of genes involved in glucose, cholesterol and fatty acid transport and metabolism.

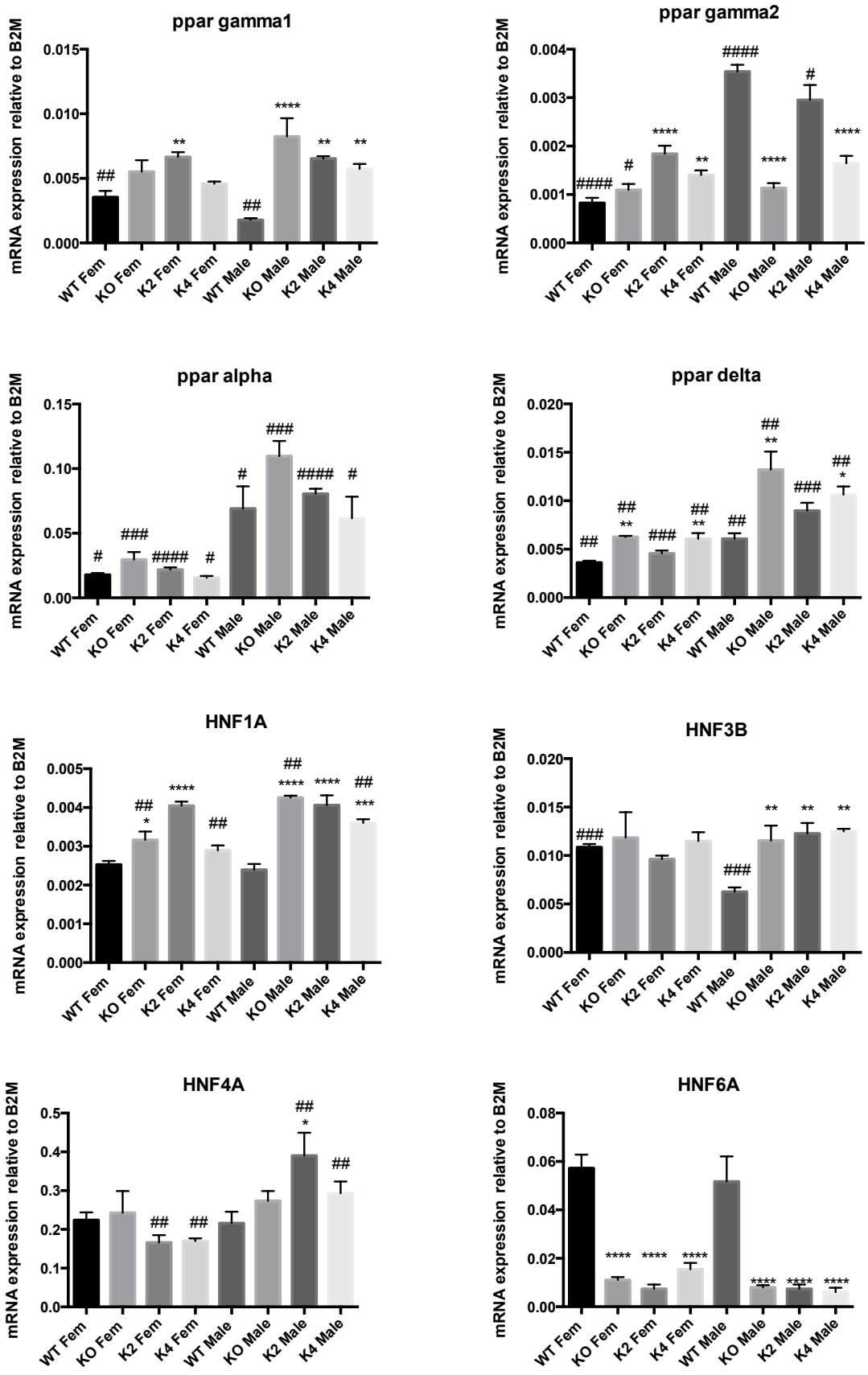

Figure 8.17: Altered hepatic transcript levels of nuclear receptors and hepatocyte nuclear factors in 12weeks old GHR mutant mice fed *ad libitum*.

Elevated levels of *ppargamma1* and *ppardelta* in male GHR mutants and some female mutants. The *ppargamma2*

transcript levels are downregulated in most male GHR mutants but elevated in female mutants. *HNF3B* and *HNF1A* levels are increased in male GHR mutants and few female mutants while *HNF6* is downregulated in all GHR mutant mice. Data represented as mean ± SEM (n=5mice/genotype). *, p<0.05; **, p<0.01; ***, p<0.001; ****,p<0.0001 compared to **WT of the same gender** by ANOVA. #, p<0.05; ##, p<0.01; ###, p<0.001; ####, p<0.0001 compared within the **same genotype of different gender** by student t-test.

Another family of nuclear receptor transcription factors are the liver X receptors (LXR) that are closely related to PPARs transcripts. The two isoforms *LXR alpha* and *LXR beta* were upregulated in all GHR male mutant mice and KO and K2 females respectively. The LXRs are important regulators of cholesterol, fatty acid, and glucose homeostasis. NCOR (nuclear receptor co-repressor) are transcriptional co-regulatory proteins that contain several nuclear receptor interacting domains and recruit histone deacetylases to DNA promoter regions resulting in downregulation of target gene expression. The *NCOR1* transcript was elevated in GHR KO males while *NCOR2* transcript was elevated in both GHR KO males and females (fig.8.18).

The RAR-related orphan receptors (RORs) are also members of the nuclear receptor family of intracellular transcription factors that are important for lipid, bile and steroid metabolism, inflammation response and importantly in the regulation of genes encoding several phase I and phase II metabolic enzymes (Kang et al, 2007). The GHR KO and K2 male and female mice exhibited elevated *ROR gamma* transcript and was sexually dimorphic in mutant mice. On the other hand *ROR alpha* was unaltered but was dramatically sexually dimorphic in all the mice. Finally, the two key transcriptional repressors Rev-Erb alpha and Rev-Erb beta that play an important role in circadian rhythm and metabolism were altered in GHR mutant mice. The levels of *Rev-Erb alpha* and *Rev-Erb beta* transcripts were drastically elevated and downregulated respectively in male GHR mutant mice. In addition, both the transcripts were sexually dimorphic in WT mice but not in the mutants indicating a feminising effect of lack of pulsatile GH-induced STAT5 signalling on GHR mutant males (fig.8.18).

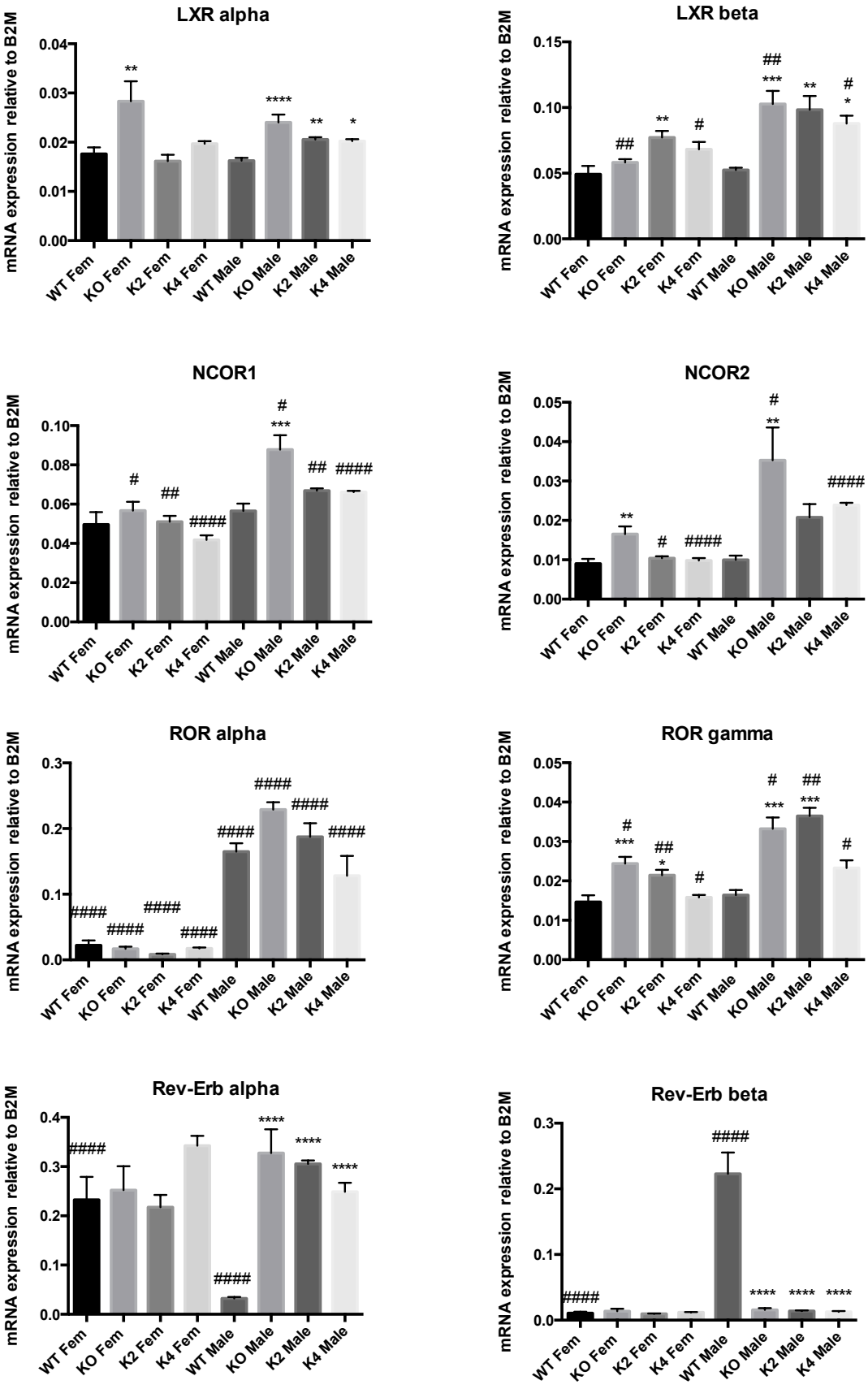

Figure 8.18: Altered hepatic transcript levels of nuclear receptors in 12weeks old GHR mutant mice fed *ad libitum*.

Elevated levels of *LXR alpha* and *LXR beta* in male GHR mutants and few female mutants. The *NCOR1*, *NCOR2* and *ROR gamma* transcript levels are upregulated in male GHR KO while *NCOR2* and *ROR gamma* levels are increased

in female GHR KO females. *Rev-Erb alpha* and *Rev-Erb beta* levels are differentially regulated in all male GHR mutant mice while WT mice are dramatically sexually dimorphic, indicating and overall feminising effect on GHR mutant. Data represented as mean ± SEM (n=5mice/genotype). *, p<0.05; **, p<0.01; ***, p<0.001; ****,p<0.0001 compared to **WT of the same gender** by ANOVA. #, p<0.05; ##, p<0.01; ###, p<0.001; ####, p<0.0001 compared within the **same genotype of different gender** by student t-test.

Gene expression profiles in old GHR mutant mice

Liver

Protein levels of key mitochondrial and antioxidant proteins altered in the liver of aged (78weeks old) mice exhibit striking sexual dimorphism. Increased levels of active AMPK and Sirt3 were observed only in female GHR K2 mice and these levels remained unchanged in males. Additionally, antioxidant transcription factor Nrf2 and anti-inflammatory IL-1RA appeared elevated in female K2 mice. Nrf2 protein was undetectable in aged male mice. Mitochondrial OxPhos components I, II and V were increased in females as was Cox IV and Sdha with no significant differences observed in males (fig.8.19). Cox IV has not yet been analysed in K2 males.

Lipid peroxide levels in the serum and liver tissue lysate were estimated as an indicator of free radical generation. No significant difference was determined as compared to WT mice.

A

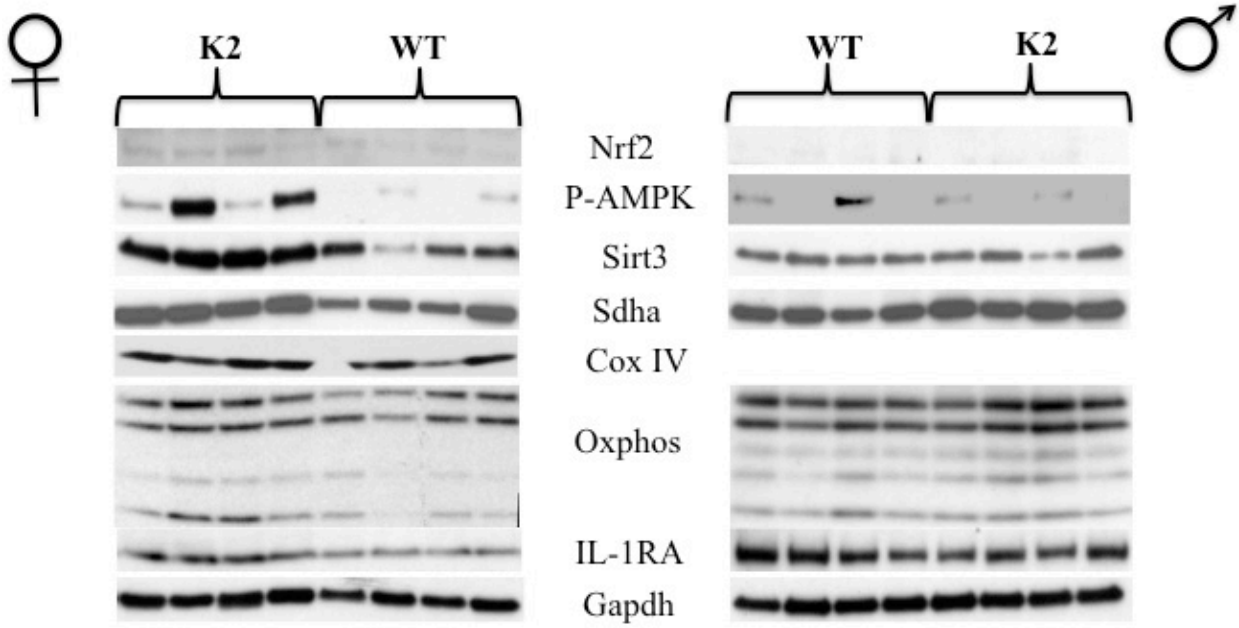

B

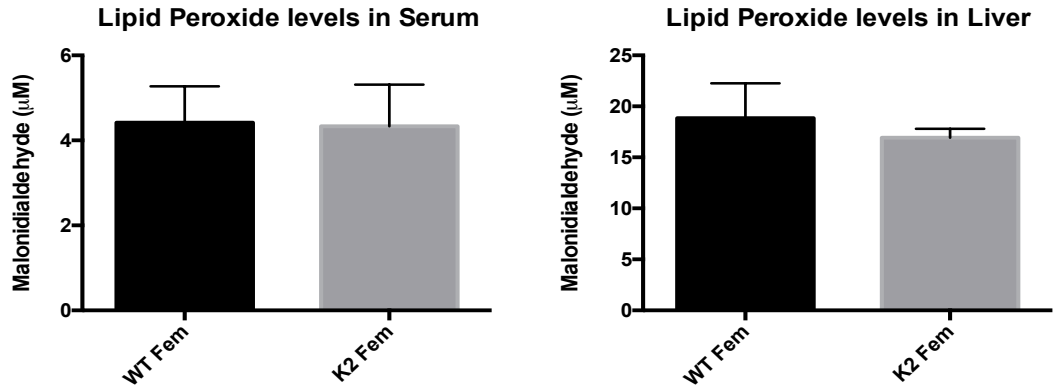

Figure 8.19: Altered hepatic levels of mitochondrial and antioxidant proteins and lipid peroxide levels in serum and liver of 78weeks old GHR K2 mice fed *ad libitum.*

(A) Increase in Nrf2, Sirt3, IL-1RA and active AMPK as well as mitochondrial proteins Cox IV, Sdha and OxPhos components in K2 GHR females specifically. Blots representative of n=4mice/genotype.

(B) Lipid peroxide levels measured as change in malonidialdehyde concentration (μM) in serum and liver tissue of aged female mice. Data represented as mean ± SEM (n=4mice/genotype) compared to WT by student t-test.

Heart

Similar to the trend observed in liver, there was increased expression of Sirt3 and phosphorylated AMPK and mitochondrial Cox IV and OxPhos components complex II, IV and V in female K2 GHR mutant with no significant change observed in males. Antioxidant proteins Bmi1 (B cell-specific moloney murine leukemia virus integration site1) and catalase were elevated in females while no catalase was detectable in males (fig.8.20). The mitochondrial uncoupling protein1 (UCP-1) was increased in cardiac tissue of aged female K2 mutants. The UCP-1 is normally found in brown adipose tissue (BAT) of mammals leading to thermogenesis. It has an important role in

increasing energy expenditure by returning the protons pumped by the respiratory chain to the mitochondrial matrix, bypassing the ATP-producing return pathway through the F_oF_1-ATP synthase (Hoerter et al, 2004). Another consequence of partial uncoupling is a reduction in the membrane potential that can lower the mitochondrial production of superoxide radicals. UCP-1, catalase, Cox IV and Bmi1 have not yet been analysed in male K2 mice.

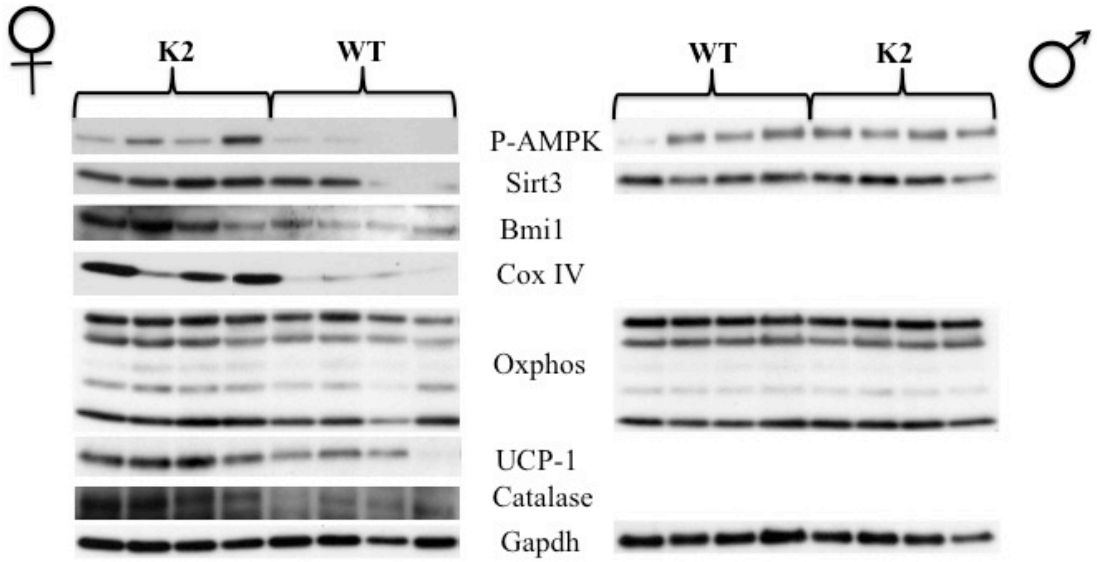

Figure 8.20: Altered levels of mitochondrial and antioxidant proteins in heart tissue of 78weeks old GHR K2 mice fed *ad libitum*.

Increase in Nrf2, Sirt3, Bmi1, catalase and active AMPK as well as mitochondrial proteins and OxPhos components in K2 GHR females with no change in K2 GHR males as compared to gender-matched WT. Blots representative of n=4mice/genotype.

Skeletal Muscle

The skeletal muscle of female K2 mutant mice showed elevation of mitochondrial Sirt3 and OxPhos components I, II, IV and III including cytochrome c, UCP-1 involved in electron transport chain, in female K2 mice specifically. The mitochondria biogenesis regulator PGC1 levels were unaltered in both male and female K2 mice as compared to gender-matched WT. Reactive oxygen detoxifying enzyme catalase was increased while SOD1 levels remained unaffected in both male and female K2 mutants (fig.8.21A). Other redox proteins thioredoxin1 (Trx1) and possibly sulfiredoxin1 (Srxn1) were elevated in K2 females as well (fig.8.21B). Antioxidant protein Nrf2 continued to be elevated in females and undetectable in male skeletal muscle tissue. IRβ as well as regulator of lipid biosynthesis regulator ACSL3 (Acyl-CoA synthetase long-chain family member 3) were increased in GHR K2 females selectively. Activated form of energy and ROS sensor AMPK was also elevated in K2 females. Finally activated STAT5 suppressor CIS levels were unaltered in K2 mice.

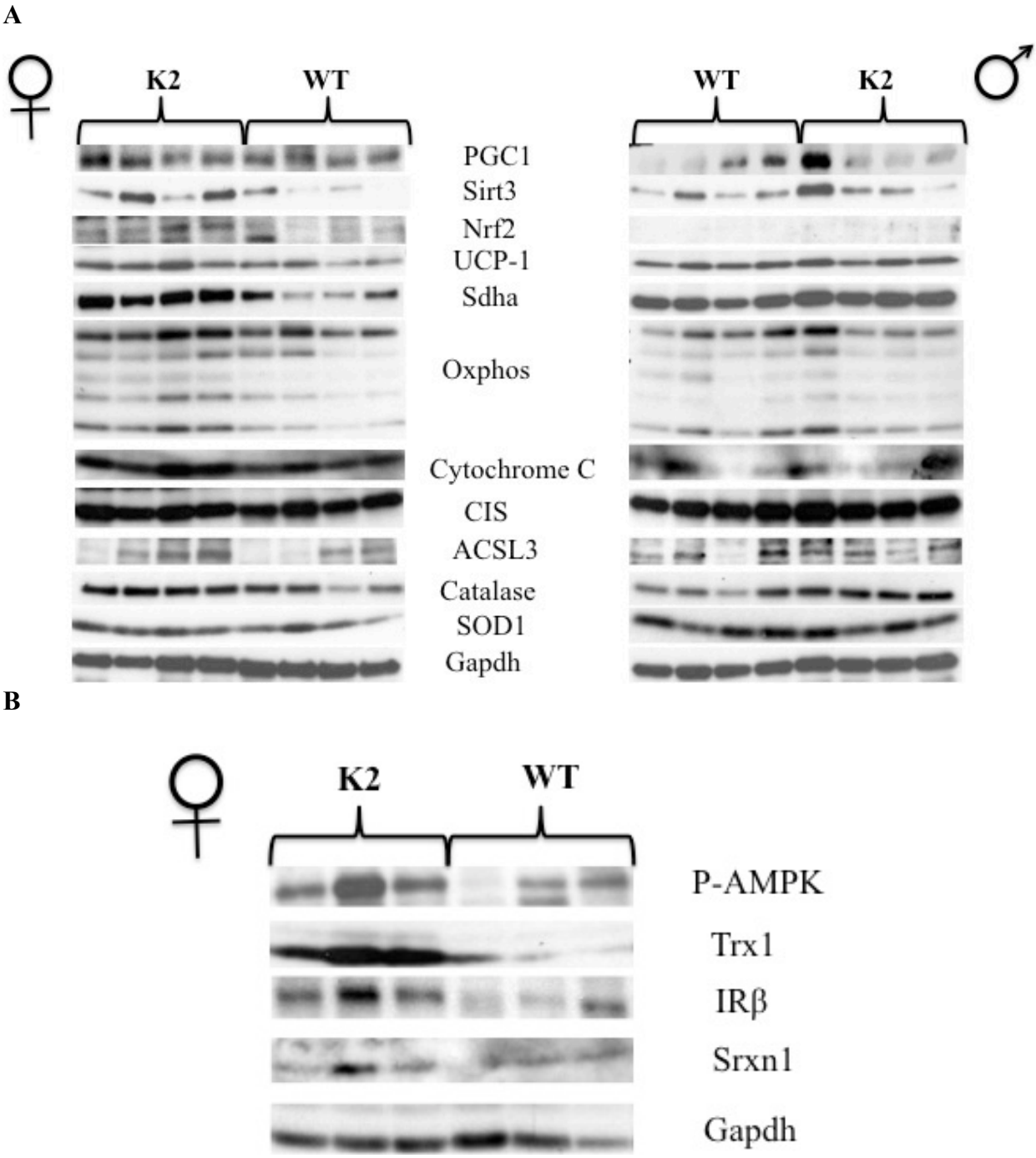

Figure 8.21: Altered levels of mitochondrial and antioxidant proteins in skeletal muscle tissue of 78weeks old GHR K2 mice fed *ad libitum.*

(A) Elevated levels of Sirt3, Nrf2 as well as mitochondrial UCP-1, Sdha and OxPhos components in K2 female mutants as opposed to K2 male. Increased amount of cytochrome c, ACSL3 in K2 females and catalase in K2 males and females. The level of PGC1, CIS and SOD1 was unaltered in mutants. Blots representative of n=4mice/genotype. (B) Increased activation of AMPK and elevation of redox enzyme Trx1 and IRβ in K2 females. Blots representative of n=3mice/genotype.

Kidney

The protein lysates from kidney of GHR K2 and KO female mutants were found to have elevated Sirt3 and Gapdh protein. The K2 females also have increased catalase expression while KO females

had higher level of antioxidant proteins endothelial nitric oxide synthase (eNOS), SOD2 and mitochondrial regulator PGC1 (fig.8.22).

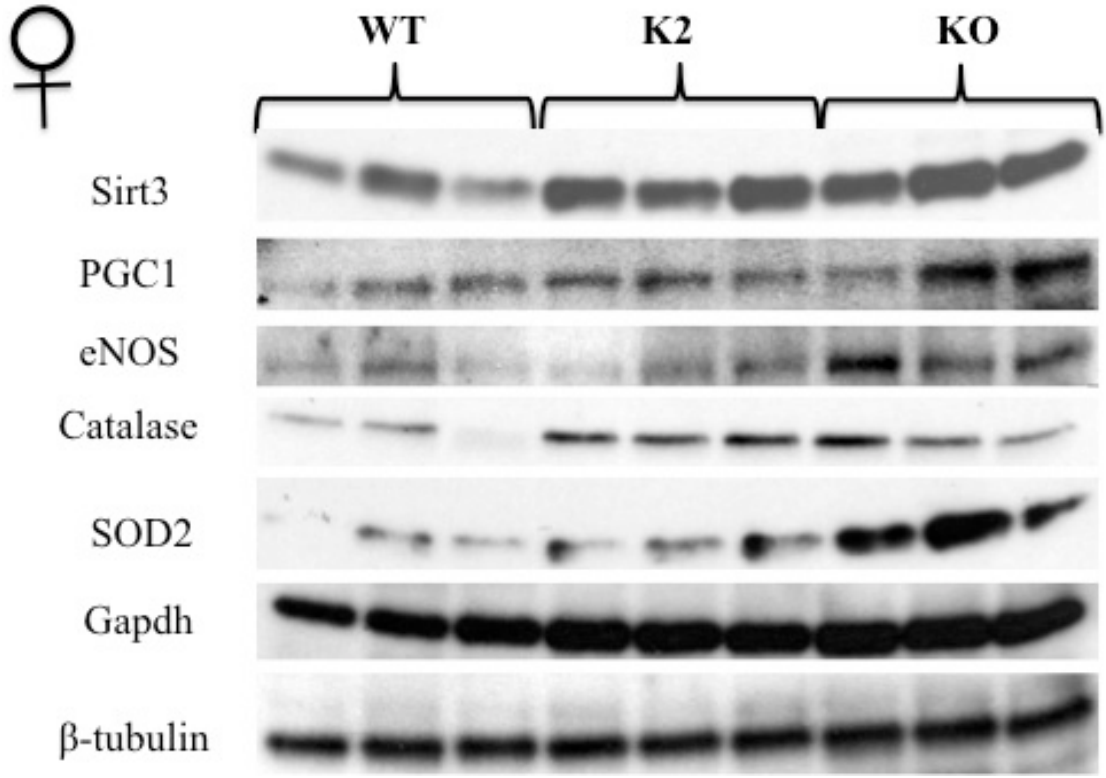

Figure 8.22: Altered protein levels in kidney of 78weeks old female GHR mutant mice fed *ad libitum*.
Increased expression of Sirt3, catalase and Gapdh in GHR K2 and KO female GHR mutant mice. Elevated levels of PGC1, SOD2 and eNOS in KO mutant mice selectively as compared to WT. Blots representative of n=3mice/genotype

Key sirtuins remain elevated in aged GHR mutant mice

In order to determine if the GHR mice retain elevated sirtuin levels with age, both young and aged mice livers were analysed in male GHR KO mice (fig.8.23). The GHR KO mutant mice exhibited a decline in the Sirt1 and 3 levels with age however their levels continued to be elevated when compared to age matched WT. The activated AMPK levels also remained elevated with age in GHR KO mice.

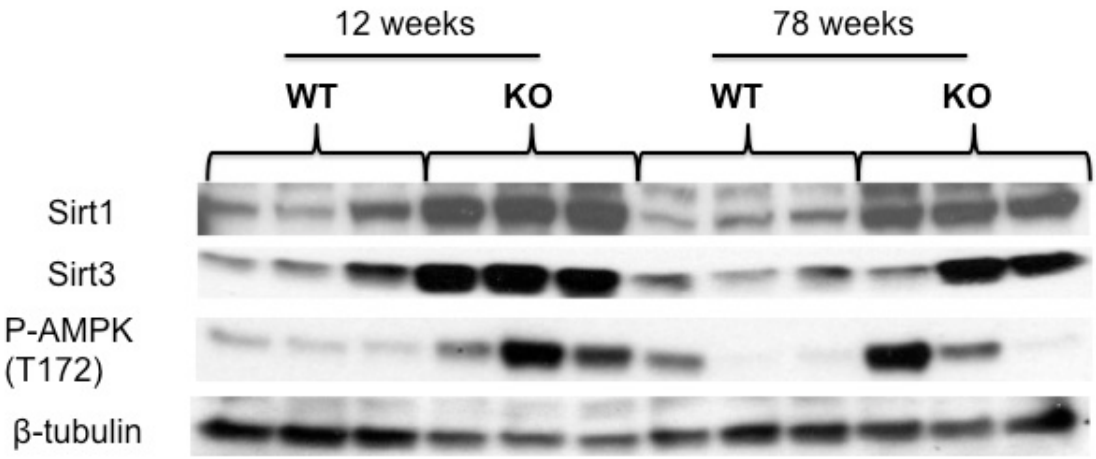

Figure 8.23: Retention of elevated expression of key sirtuins and activated AMPK in liver of GHR KO males fed *ad libitum* with age.

Increased level of Sirt1 and 3 and active AMPK observed in 12weeks old (young) is maintained with age as seen in 78weeks old (aged) GHR KO mice as compared to age-matched WT. Blots representative of n=3mice/genotype.

Increased circulating antioxidants in female GHR K2 mutant mice

The GHR K2 male and female mice were analysed for circulating levels of total antioxidant that was found to be dramatically elevated in females but no significance was attained in males (fig.8.24).

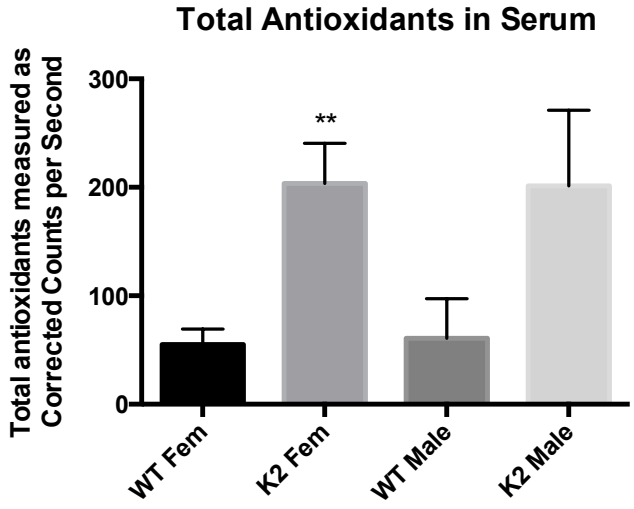

Figure 8.24: Lipid peroxidation and antioxidant capacity of 78weeks old GHR K2 mice fed *ad libitum*.

Total antioxidant capacity in female and male serum with significantly higher levels in female K2 mutant as compared to males. The antioxidant concentration is expressed as counts per second corrected for induction time and light production. Data represented as mean ± SEM (n=4mice/genotype). **, $p<0.01$ compared to gender-matched WT by student t-test.

Increased Src Family Kinase activation in the liver of GHR K4 female mice

There occurs a modest level of sexual dimorphism in the level of activation of SFK as evident from P-SFK (Y416) blot in the livers (fig.8.25A) of WT males and females. This dimorphism is however increased dramatically in the case of GHR K4 mice. In addition, K4 males had significantly lower level of SFK activation as compared to WT. In addition, the total c-Src (a ubiquitous SFK member) was modestly sexually dimorphic in GHR K4 and may further contribute to the decrease in the activation of SFK. The activation of ERK1/2 was unaltered between WT and K4 females but was increased in K4 males, although this increase was not statistically significant (fig.8.25B). This increase in active SFK levels in females could be responsible for reduction in lymphoma and increased sarcoma and carcinoma cancer modalities as indicated in figure 8.1E.

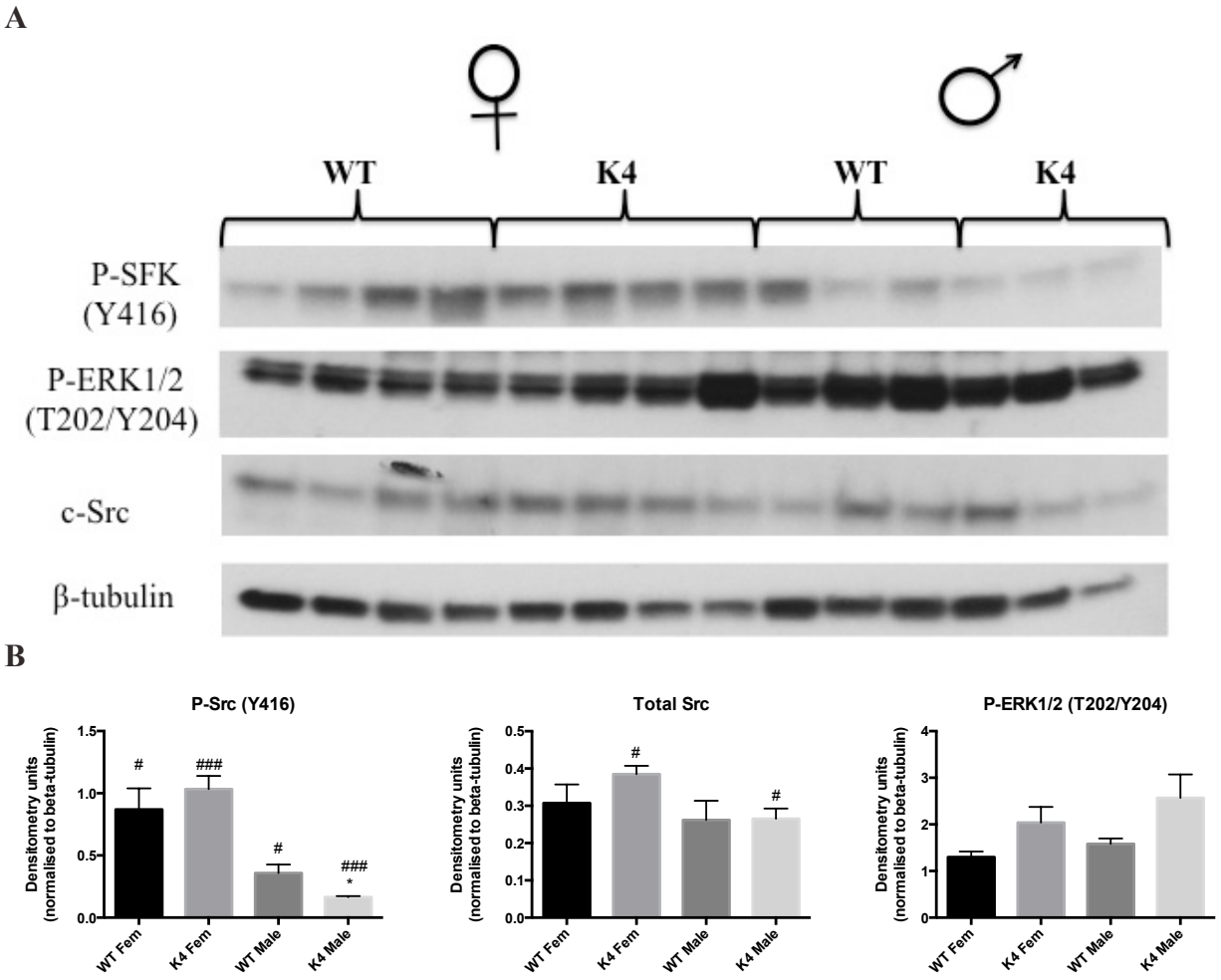

Figure 8.25: Altered protein levels of active ERK1/2 and sexually dimorphic levels of active SFK (Y416) and c-Src in liver of 12weeks old WT and GHR K4 mutant mice fed *ad libitum*.

(A) Western blot and (B) densitometry analysis of P-Src, P-ERK1/2 and total c-Src levels indicating enhanced sexual dimorphism in Src Family Kinase activation in GHR K4 as compared to WT mice. Blots representative of n=4mice for females and n=3mice for males. Data represented as mean ± SEM. *, p<0.05 compared to **WT of the same gender** by student t-test. #, p<0.05; ###, p<0.001 compared within the **same genotype of different gender** by student t-test.

Discussion

GH/IGF-1 axis in aging

Despite the numerous studies highlighting the importance of adequate levels of circulating GH and IGF-1 for healthy aging, the role of these potent anabolic hormones leading to aging phenotype remains highly controversial. Based on studies initially conducted in mutant and transgenic invertebrates (worms and flies), the corresponding data supports the conclusion that IGF-1 signalling is part of a "conserved mechanism of aging" with decreased level of GH/IGF-1 signalling delaying the aging process (Clancy et al, 2001; Kimura et al, 1997). In *C. elegans*, loss of function mutations in genes involved in IIS (Insulin-like-signalling) such as *daf-2* (homolog of mammalian insulin/IGF-1 receptor), *age-1* (encoding catalytic subunit of PI3-K), serine-threonine kinases Pdk-1, Sgk-1, Akt1, Akt2 as well as gain of function of *daf-16* (forkhead transcription factor) has been shown to increase lifespan (Berryman et al, 2008). Similarly in *D. melanogaster*, loss of function mutations in InR (insulin-like-receptor), Chico (insulin receptor substrate) and PI3-K/Akt/FOXO components of IIS can alter lifespan, sometimes in a tissue-specific manner (Berryman et al, 2008; Russell & Kahn, 2007).

Noteworthy was the expression and function of DAF-2 in a highly organ-specific manner in neuronal cells which was indicative of the central role of the nervous system in DAF-2–dependent regulation of animal longevity (Wolkow et al, 2000; Kimura et al, 2011) and surprisingly independent of the metabolic effects of insulin-like signalling in the gastrointestinal system and muscle tissue (Wolkow et al, 2000). However, the link between IGF-1 signalling in the brain and mammalian longevity had not been investigated until recently. IGF-1R levels in the brain were reported to be negatively associated with longevity in 16 rodent species (Azpurua et al, 2013). However, two disparate concepts exist; firstly the presence of normal levels of GH and IGF-1 accelerate aging and lack of these hormones or disruption of the signalling pathways driven by these hormones exert anti-aging effects (as indicated above) and secondly the age-related decline in GH and IGF-1 levels contribute to the deterioration of physiological function while replacement of these hormones delay or reverse the aging phenotype (Sonntag et al, 2012).

These conceptual differences have been exacerbated by numerous studies that draw conclusions about aging and lifespan based on a low number of experimental animals, suboptimal animal husbandry, and/or the absence of end-of-life pathology, generalisation of results from one gender to other and most importantly varied genetic backgrounds to corroborate the conclusions. This was evident in the case of reported longevity of IGF-$1^{+/-}$ mice which when corrected for genetic

background and animal husbandry conditions did not reach significance (Bokov et al, 2011). A similar outcome was evident in the case of GHR KO when the lifespan was analysed on C57Bl/6 background rather than on a mixed background (129Ola X BalbC). The most cited longevity study on GHR KO mice by Coschigano *et al.* was carried out in sample size of under 20 mice/genotype/gender on a mixed genetic background (Coschigano et al, 2003) when a minimum sample size of 30-40 mice per group (to be analysed) is required to accurately detect significant differences in mean lifespan (Liang et al, 2003). Therefore, using the existing GHR KO data in terms of longevity should be dealt with caution! Additionally, the subsequent study in C57Bl/6 indicates a percent increase in lifespan (in a small sample size) which if analysed as percentage median lifespan extension was estimated to be 20.2% in females and a modest 8.7% in males (Coschigano et al, 2003).

A later study from the same group has analysed lifespan extension this time with 37-43 mice per genotype but with genetic background not indicated (Bonkowski et al, 2006). This recent study has suggested a median lifespan extension of 28% in females and 18.8% in males as compared to WT. The main difference between Coschigano *et al.* (2003) and Bonkowski *et al.* (2006) is increase in mice numbers and also the protein content of the diet calculated as a percentage of total energy from proteins increased from 16% to 28.5% in the latter. In addition, the earlier (2003) study subjected the mice to a 14hr light/12hr dark cycle as opposed to 12hr light/12hr dark in the (2006) study. It is plausible that these changes increased median survival of GHR KO *vs* WT but remains inconclusive since the genetic background was not mentioned.

In contrast to the previous reports, our study found no evident lifespan extension in GHR KO males (n= 38 *vs* n= 54 in WT) but a 20% median lifespan extension in GHR KO females (n= 46 *vs* n= 69 in WT). Upon analysis of GHR knockin mutants with limited GH-mediated activity, the lifespan extension was evident selectively in females with the exception of GHR K4 where both males (15%) and females (45%) live longer. Yet, circulating IGF-1 levels are very low in both male and female mutants (Barclay et al, 2010; Rowland et al, 2005b). Therefore, our results are incompatible with the earlier concepts that reduction in GH/IGF-1 signalling always increases lifespan in mammals as was reported in invertebrate models (Kenyon et al, 1993). Therefore, it was of key importance to examine the pathological profile of these mutant mice by documenting their age-related cancer incidence and type.

It has been proposed that a common feature to the three models of GH/IGF-1 deficiency that consistently show increased lifespan across multiple studies: Ames, Snell, and GHR KO mice is the

resistance towards cancer (Junnila et al, 2013) (except Ames mice which only have delayed cancer occurrence but similar incidence and burden). The exact molecular basis of this has been unknown till date but credited mainly to reduced IGF-1 action. Human studies have been in accordance with this conclusion as in the case of Laron patients that have reduced IGF-1 levels and do not die from cancer compared to normal relatives (Guevara-Aguirre et al, 2011; Steuerman et al, 2011). However, these patients do not show lifespan extension, dying instead from convulsions, alcoholism and suicide.

GH/IGF-1 axis and cancer incidences

C57Bl/6 are the most commonly used strain in aging studies and are particularly prone to lymphomas and sarcoma (Blackwell et al, 1995; Ward, 2006; Ikeno et al, 2009) with higher incidences observed in females than males (Blackwell et al, 1995; Ward, 2006). In addition, overall spontaneous tumour incidences were reported to be double in females that also outlived males (Anisimov, 2001). Although calorie restriction (CR) has been shown to significantly reduce the lifetime tumour incidences in both and males and females, as compared to those fed *ad libitum*, there was increase in incidences of histiocytic sarcomas in females specifically (Blackwell et al, 1995). In our study all the animals utilised were of the C57Bl/6 genetic background, subjected to similar animal husbandry conditions and fed *ad libitum*. The common attribute to all GHR mutant mice was complete lack of GH-mediated STAT5 induction (Barclay et al, 2010; Rowland et al, 2005b). It is important to note here that no GH-induced STAT5 activation via SFK was observed in K4 mice *in vivo* (Barclay et al, 2010) in contrast to the *in vitro* studies with GH (Manabe et al, 2006) and EPO treatment (Okutani et al, 2001).

In on our studies we observed a similar percentage of spontaneous tumour-related deaths in WT males and females but the incidences of cancer in gender-matched mutants (GHR K2 and KO) were significantly reduced. In addition, no cancer death was evident for GHR K4 males which was in contrast with increased percentage of cancer-related deaths in K4 females. Further to this, we have sought to histologically evaluate the cancer modality as the cause of death in mice and from preliminary results it is evident that the major cause of death in these mice is lymphoma in most GHR mutants and WT mice.

No correlation was evident between lack of GH-mediated STAT5 activity (reduced circulating IGF-1 levels) and lymphoma *incidence* but there was either a delayed occurrence of cancer or reduction in severity of lymphoma in female mutants that allowed them to live for a longer period of time

especially with increase in median lifespan across all females. Even the GHR K4 female mutant that reported the highest level of total cancer-related deaths had reduced lymphoma but did harbour other cancer modalities (carcinoma and sarcoma). Excessive Jak/STAT5 signalling is well known to promote lymphoma in man (Marty et al, 2013).

All the GHR mutants exhibited drastically reduced hepatic IGF-1 transcripts and circulating levels resulting in small size and reduced body growth. These mice have significantly elevated GH due to absent IGF-1-mediated negative feedback on GH secretion at the hypothalamus and pituitary gland. In contrast, GH transgenic mice show a 'giant' phenotype due to increased circulating IGF-1. Given the lipolytic and β-oxidative actions of GH, the latter mice were extremely lean throughout life (Palmer et al, 2009). These mice have shortened lifespan due to pathological changes that arise as a result of GH excess such as insulin resistance, renal sclerosis, and hepatocellular carcinoma (Bartke, 2003). Although a negative correlation exists between body size/growth and longevity in rodents (Bartke, 2000), dogs (Li et al, 1996) and humans (Samaras & Elrick, 2002) there are a few exceptions. One such case is that of long living and stress resistant p66shc KO mice that have normal body size (as WT) (Migliaccio et al, 1999) with no data on cancer incidence reported. Additionally, 6 months of 25% CR has been shown to promote decrease in body weight as well as fat mass (similar to exercise) in humans (Redman et al, 2007) but it did not reduce GH or IGF-1 levels in humans (Redman et al, 2010) unless protein intake was also reduced, which was also protective against cancer (Fontana et al, 2008).

A more recent population-based study has revealed a relationship between circulating IGF-1 levels and mortality in the general population using random-effects meta-analysis and dose–response meta-regression (Burgers et al, 2011). Analysis of over 14,000 participants clearly demonstrated that in humans that there exists a U-shaped association between circulating IGF-1 levels and all-cause mortality (including cancer) and that low and high levels of IGF-1 translate into a significantly increased mortality risk in the general population, predominantly due to cardiovascular diseases and cancer (Burgers et al, 2011; Renehan et al, 2004).

Can such a U-shaped survival curve with regards to IGF-1 apply to rodents as well?

By using these genetic mouse models we aim to determine the factor(s) that affect cancer incidences and burden in GHR mutants while selectively increasing longevity in females. We chose to analyse tissues in these GHR mutants at two different ages; young (12weeks old) and aged (78weeks old) in order to determine some of the age-related alterations due to lack of or altered

GHR signalling. Our GHR mutant mice exhibited elevated *IGF-2* transcripts that have been linked to steatotic liver (Chiappini et al, 2006) and cancer progression (Malaguarnera & Belfiore, 2014). IGFBP-2 transcript was also elevated in all the mutants and its higher levels have been reported during liver cirrhosis (Wolf et al, 2000) due to decreased GH signalling caused by downregulation of GHR expression (Wang et al, 2003). Cirrhosis is the end outcome of non-alcoholic hepatic steatosis that has been reported in GHR mutant rodent models by our group (Barclay et al, 2011) and in adult Laron patients (Laron et al, 2008).

Reductions in GH-mediated STAT5 activation and Oxidative Stress

The current data from long-lived invertebrate and rodent genetic models is consistent with the observation that prolonged lifespan is associated with increased resistance to oxidative stress (Harper et al, 2006; Murakami, 2006). The 'oxidative stress theory of aging' hypothesises that free radicals and ROS cause cumulative damage of macromolecules, which accelerates aging (Kregel & Zhang, 2007). ROS are also by-products of normal metabolism generated by mitochondria that are necessary for cellular homeostasis at low levels. However as they accumulate with age they cause an increase in oxidative stress, presumably due to reduced defense against cellular stress with age. As a result they are closely associated with reprogramming of metabolism in cancer cells as well as tumour promoting inflammation, the key hallmarks of cancer (Hanahan & Weinberg, 2011). Wang *et al*. have shown that mitochondria in mammalian cells undergo quantal, stochastic bursts of superoxide production termed 'mitochondrial flashes' (mitoflashes). This mitoflash frequency is highly sensitive to oxidative stress and metabolic changes and can therefore be exploited as a readout of energy metabolism and free-radical production (Wang et al, 2008b). More importantly, they have demonstrated a strong coupling between mitochondrial function and ageing by *in vivo* visualization of these mitoflashes (Shen et al, 2014).

We have shown the mitochondrial Mn superoxide dismutase, SOD2 was elevated in all GHR mutant models with males selectively expressing higher level of the extracellular Cu-Zn SOD3 mRNA especially in KO. Mice lacking SOD2 were shown to die shortly after birth, indicating that unchecked levels of superoxide are incompatible with mammalian life (Li et al, 1995). However, mice 50% deficient in SOD2 exhibit a normal lifespan with minimal phenotypic defects but do suffer increased DNA damage and increased incidence of cancer (Van Remmen et al, 2003). Recently, CR has been shown to reduce oxidative stress by elevating SOD2 expression that is Sirt3-mediated (Qiu et al, 2010). In contrast to the earlier study, our GHR KO male mice had increased Cu-Zn SOD1 expression at transcript and protein levels. Studies in mice have also shown profound sex-specific differences in antioxidant responses with aging, with males showing low levels of

antioxidant enzymes such as superoxide dismutase, catalase, and glutathione reductase (Tomas-Zapico et al, 2006). The brains of female mice were reported to have lower oxidant and higher antioxidant capacity than those of males, mostly due to catalase enzyme activity (Sobocanec et al, 2003). In our study all SODs were expressed at higher levels in all male mice than females but this needs to be confirmed at protein level. In addition all the GHR mutants had elevated transcripts for sulfiredoxin (Srxn1), Nrf2 regulated gene. Sulfiredoxin1 belongs to an *in vivo* gene expression signature of oxidative stress in mice (Han et al, 2008) and shown to be critical for redox balance and survival of cells exposed to low steady-state levels of H_2O_2 (Baek et al, 2012). Catalase was exclusively elevated in KO females as compared to WT females, consistent with the earlier report (Al-Regaiey, 2013).

Based on these results it is clear that the liver of different GHR mutants may have altered gender-specific susceptibilities to oxidative damage even though they have a common feature of lack of GH-induced STAT5 activity.

In cancer cells unregulated cellular proliferation leads to formation of masses that extend beyond the resting vasculature, resulting in oxygen and nutrient deprivation. The resulting hypoxia triggers a number of critical adaptations that enable cancer cell survival, including apoptosis suppression, altered glucose metabolism, and an angiogenic phenotype with the activation of HIF-1α (Semenza, 2010). Because mitochondria are key organelles undergoing reprogramming during cancer induction, the relationship between mitochondria, ROS signalling, and dampening of pro-growth signalling pathways needs to be determined in these GHR mutants.

Reductions in GH-mediated STAT5 signalling and AMPK activation

AMPK activation controls numerous metabolic processes, including fatty acid synthesis, gluconeogenesis in the liver, and glucose uptake in muscle (Mihaylova & Shaw, 2011). Under conditions of stress (low glucose), ATP is depleted, leading to concomitant increase in cellular AMP and ADP that regulate AMPK function mainly by preventing its dephosphorylation and inactivation. However recent data has identified ADP rather than AMP as the predominant regulator of AMPK phosphorylation (Oakhill et al, 2012). The major upstream kinases that phosphorylate AMPK are liver kinase B1 (LKB1) (Woods et al, 2003) and Ca^{2+}/calmodulin-dependent protein kinase kinase beta (CaMKKβ) (Hawley et al, 2005). In addition to energy sensor role of AMPK, it can also be activated during cellular stress by non-canonical mechanisms that may not involve increases in AMP, ADP or Ca^{2+} levels. In cultured cells, AMPK was activated by reactive oxygen species (ROS) and reactive nitrogen species (RNS) (Fujita et al, 2010). It was also reported that at

high concentrations of free radicals, AMPK activation might be secondary to the inhibition of mitochondrial ATP synthesis, with consequent rises in AMP and ADP levels (Hawley et al, 2010). We have shown that all the male GHR mutant mice had elevated levels of active AMPK in their liver.

AMPK can act in coordination with NAD^+-dependent deacetylase Sirt1 by increasing cellular NAD^+ levels (Canto et al, 2009). One of the major Sirt1 targets is PGC1α, a master regulator of mitochondrial biogenesis (Canto & Auwerx, 2009). The biogenesis of mitochondria is a process that plays an essential role in energy homeostasis and metabolism, apoptosis regulation and cell viability (Hock & Kralli, 2009). Mitochondrial biogenesis is influenced by environmental stress such as exercise, caloric restriction, low temperature, oxidative stress, cell division and renewal and differentiation and is accompanied not only by variations in number, but also in size and mass. PGC1α/β are co-transcriptional regulation factors that induces mitochondrial biogenesis by activating Nrf1 and Nrf2, which promote the expression of mTFAM. NRFs are important contributors to the sequence of events leading to the increase in transcription of key mitochondrial enzymes, and have been shown to interact with mTFAM, which drives transcription and replication of mtDNA (Virbasius and Scarpulla, 1994). In the present study both *Pgc1α* and *Pgc1β* were elevated in the liver of most GHR mutants especially males at transcript and protein level confirming the earlier report in GHR KO males (Al-Regaiey et al, 2005). In contrast *Pgc1α* levels have been shown to decrease in GHtg mice (Al-Regaiey et al, 2005). Additionally, *MFN2* (mitofusin2) hepatic transcripts were also upregulated in all GHR males and are known to be indispensable in the maintenance and operation of the mitochondrial (Chan, 2006).

Reductions in GH-mediated STAT5 activation effects on mitochondrial parameters

Although the genes regulating mitochondrial biogenesis have been analysed in different tissues of GHR KO mice (Al-Regaiey et al, 2005; Gesing et al, 2011a; Gesing et al, 2011b), none have examined the OxPhos components in them. Most importantly, Cox IV, regarded as a measure of mitochondrial content was elevated in male GHR KO and K4 mutants at protein level. OxPhos components Ndufb8 (C(I)), Uqcrc2 (C(III)) and ATP5a (C(V)) were elevated in all male mutants while Sdhb (C(II)) was elevated only in GHR K4 and K2 male mice. Cytochrome c oxidase subunit I (mt-CO1) is one of three mtDNA encoded subunits of respiratory complex IV that was elevated in all male GHR mutants. These observations in GHR mutants were in contrast to the decrease in complex I, II and V reported in GHtg mice that have shortened lifespan (Brown-Borg & Bartke, 2012). Succinate dehydrogenase complex are involved in oxidation of succinate, a step where

electrons are generated. If its activity is inhibited electrons that would normally transfer through the Sdhb subunit to the ubiquinone pool are instead transferred to oxygen to create ROS that can stabilise the production of HIF-1α forming an active complex, in turn leading to the induction of tumourigenic genes (Selak et al, 2005) and inflammation (Mills & O'Neill, 2013). Sdha levels however remain unaltered in GHR KO and K4 males. In this study we have also shown *Sdhb* transcript was gender-specific while *mt-CO1* expression was sexually dimorphic only in the mutants and not WT. We also report that this increase in OxPhos complex protein or transcript was not due to change in mtDNA (possibly due to lack of change in mTFAM protein levels) as no statistically significant difference was evident in any of the female GHR mutants compared to WT, supporting a similar finding in Ames dwarf mice (Brown-Borg et al, 2012).

Disturbances in mitochondria biogenesis affect oxidative stress resistance, energy production and metabolism resulting in age-associated diseases (Reznick et al, 2007) that can be regulated by sirtuins. In this study we have analysed the expression of sirtuins at transcript and protein levels in GHR mutant livers. It has been reported that CR but not lack of GHR, resulted in increased Sirt1 protein levels in liver (Al-Regaiey et al, 2005). In contrast, our results show elevated *Sirt1* transcript in GHR KO males only but increased protein level was evident in all male GHR mutants. Interestingly, Sirt1 upregulation has been shown to have no detectable impact on longevity in two different mouse models but it did promote healthy aging (Herranz et al, 2010). However, increased Sirt1 levels (~3 fold) systemically were shown to be protective against physiological damage produced by high-fat diet (Pfluger et al, 2008), diabetes (Banks et al, 2008), and metabolic syndrome associated cancer (Herranz & Serrano, 2010).

Besides Sirt1, the transcript for mitochondria-localised sirtuin, *Sirt3*. was elevated in all GHR mutant mice and was confirmed at protein level in all males. Sirt3 expression is reported to be highest in metabolically active tissues including the brain, heart, liver, brown adipose tissue (BAT), and skeletal muscle (Lombard et al, 2007; Ahn et al, 2008; Gurd et al, 2012). Sirt3 is a crucial regulator of mitochondrial function and mTFAM targets, controlling global acetylation of the organelle and inducing activity of complex I and promoting oxidative phosphorylation. Sirt3 null mice show no obvious phenotypic changes, but succumb to age-linked diseases including metabolic syndrome, cancer, and cardiac failure (Hirschey et al, 2011). Sirt3 deletion in mice was shown to cause hyperacetylation of mitochondrial proteins and metabolic defects with 65% of all proteins in mitochondria having at least one lysine acetylated in liver tissue (Hebert et al, 2013). Therefore, loss of Sirt3 appears to decrease mitochondrial substrate oxidation and results in more intensive glycolysis and higher extracellular lactate levels (Finley et al, 2011a). The effect of Sirt3 deficiency

on ATP production is further aggravated by fasting, underlying its reliance on NAD^+ (Hirschey et al, 2011). Expression of Sirt3 in liver has been shown to be induced by PGC1α through a mechanism involving estrogen-related receptor alpha (ERRα) (Kong et al, 2010). Both PGC1α and ERRα are induced by fasting and consequently increase Sirt3 levels. In line with these observations, the increased expression of OxPhos components in GHR mutants may be the outcome of enhanced Sirt3 and/or PGC1α in liver as shown in myotubes (Kong et al, 2010). Succinate dehydrogenase enzymes have been shown to be direct targets of Sirt3 with hyperacetylated levels of Sdha and Sdhb reported in Sirt3 null mice thereby increasing succinate accumulation and HIF stabilisation (Finley et al, 2011b). In addition, Sirt3 was shown to oppose the reprogramming of breast cancer cells through destabilisation of HIF-1α (Finley et al, 2011a).

Sirt3 may also upregulate PGC1α and control mitochondrial biogenesis through a positive feedback mechanism by deacetylation and activation of liver kinase B1 (LKB1) as shown in cardiomyocytes (Pillai et al, 2010). Active LKB1 can phosphorylate and stimulate AMPK-mediated cyclic AMP response element binding protein (CREB) leading to increased PGC1α expression (Thomson et al, 2008). Moreover, AMPK has been shown to directly phosphorylate and activate PGC1α, adding additional stimulatory mechanisms to this pathway (Jager et al, 2007). It has been demonstrated that PGC1α is a suppressor of ROS generation in myotubes, hippocampus and endothelial cells by increasing the expression of GPx1 and SOD2 and reducing mitochondrial membrane potential (Kong et al, 2010; St-Pierre et al, 2006; Valle et al, 2005). Similarly, knockdown of endogenous Sirt3 expression led to an increase of cellular ROS level that was reversed by its overexpression, indicating that Sirt3, like PGC1α, acts as suppressor of ROS formation *in vivo* (Kong et al, 2010). Therefore, Sirt3 has the ability to integrate cellular energy metabolism and ROS generation Intriguingly, it has now been proposed that Sirt3 is a prominent regulator in CR adaptation by coordinately deacetylating proteins involved in diverse pathways of metabolism and mitochondrial maintenance (Hebert et al, 2013) and that these effects are distinct from those of Sirt1 (Tauriainen et al, 2011). Surprisingly whether Sirt3 transgenic mice (ubiquitous and/or tissue-specific) exhibit increased longevity is yet to be elucidated. Additionally, Sirt2 and 6 protein levels were not altered in the GHR mutants analysed. It is evident that by targeting numerous enzymes Sirt3 is perfectly positioned to orchestrate coordinated shifts in mitochondrial metabolism, with potential implications for diseases (especially cancer) that rely on mitochondrial metabolic activities.

It is important to note that key mechanism by which metformin inhibits cancer progression is by activation of AMPK via LKB1 (Shaw et al, 2005) which then inhibits the mammalian target of rapamycin complex 1 (mTORC1), a central mediator of cancer cell metabolism, growth and

proliferation (van Veelen et al, 2011). In addition, metformin has also been shown to act independently of AMPK by directly elevating AMP/ATP ratio in the liver restricting the supply of ATP for gluconeogenesis (Foretz et al, 2010). It is believed that mitochondria is the primary target of metformin action where it inhibits cellular respiration by directly decreasing oxygen consumption and mitochondrial membrane potential through inhibiting the OxPhos complex I to stop ATP synthesis without altering the downstream OxPhos machinery (Owen et al, 2000). Metformin has also been shown to reduce *Sirt3* levels as well as that of *ERRα* independently of AMPK (Buler et al, 2012).

Dampening of growth signalling owing to reduction in GH-mediated STAT5 activity.

Dampening of growth signalling by CR or by mutational inactivation of conserved GH/insulin/IGF-1 and mTOR signalling pathways has been shown to prolong the lifespans of eukaryotic organisms from yeasts to humans (Guevara-Aguirre et al, 2011). In complex eukaryotes, this inhibition of growth signalling also protects against age-related diseases, including cancer, cardiovascular disease and neurodegenerative disorders (Burhans & Weinberger, 2007). These lifespan-extending effects of reduced growth signalling occur in parallel with the induction of antioxidative stress responses that reduce levels of ROS. In line with these observations, a most striking result here was the contradictory levels of transcript and protein of two key suppressors of cytokine signalling; SOCS2 and CIS in GHR mutants. While the mRNA levels were dramatically downregulated the protein was upregulated, especially in the case of SOCS2, indicating that SOCS2's ubiquitin ligase activity is specific for GH-induced STAT5 inhibition and GHR degradation. On the other hand, CIS protein levels were unaltered in mutants whereas the transcript was downregulated in these mutants as compared to WT, indicating that hepatic CIS does not directly degrade GHR. Nevertheless, increased protein levels of both these tumour suppressors (Elliott et al, 2008) *in vivo* ensure dampening of pro-growth or inflammatory signalling via STAT5. In contrast to SOCS2 and CIS, the *SOCS3* mRNA remained unaltered but sexually dimorphic favouring the females while the protein was elevated in male mutants. Increased SOCS3 was in line with elevated STAT3 expression and activation observed in these mice due to lack of STAT5 activation reported here and elsewhere (Barclay et al, 2011). It would be worth determining if the STAT3 activation and/or expression is sexually dimorphic in liver as it has been shown to be in brain (Di Domenico et al, 2010).

GHR KO and K4 mutant mice have reduced IGF-1R and EGFR levels, which are commonly upregulated tyrosine kinase receptors in cancers. The decrease in IGF-1R level ensures not only

decreased IGF-1 signalling (which is already reduced to undetectable levels) but also of insulin (at elevated levels). In the presence of IGF-1, cells may accumulate more DNA damage and are protected from apoptosis, therefore increasing the likelihood of cancer cells proliferating. These results thus support the concept that reductions in GH and IGF-1 with aging may be important in protecting against the development of cancer, by altering cellular susceptibility to DNA damage and apoptosis (Guevara-Aguirre et al, 2011). A decrease in EGFR activation has been previously reported in GHR KO (Zerrad-Saadi et al, 2011). In addition, the downstream signalling molecule to IGF-1R and IR, Akt2 was reduced in GHR KO and K4 mice while its level has been reported to be upregulated in GHtg mice that have various hepatocellular abnormalities (Miquet et al, 2013). GHR KO males and females have increased transcript expression of *cdkn1a* that encodes for p21, inhibitory regulator of cell cycle progression.

Reductions in GH-mediated STAT5 activation and inflammation markers

CR has been shown to decrease inflammatory and endocrine markers that promote breast cancer (Harvie & Howell, 2012). A similar profile is evident in the case of GH-resistant and GH-deficient rodents where elevated adiponectin levels and AMPK activation reduce pro-inflammatory signals by inhibiting NF- κB signalling (Masternak & Bartke, 2012). This was evident by western blot analysis of GHR mutant liver where the protein level of p65(RelA) subunit of NF- κB were downregulated compared to WT. NF- κB is important in regulating cellular responses as it belongs to the category of "rapid-acting" primary transcription factors that are present in cells in an inactive state and do not require new protein synthesis in order to become activated. A few known inducers of NF- κB activity include ROS, TNFα, IL-1 beta. There is also antagonistic crosstalk between Sirt1 and NF- κB. Sirt1 has been shown to directly deacetylate p65RelA subunit of NF- κB complex while it stimulates oxidative energy production via the activation of AMPK, PPARα and PGC1α. Simultaneously, these factors inhibit NF- κB signalling and suppress inflammation. On the other hand, NF- κB signalling can downregulate Sirt1 activity through the expression of miR-34a, IFNγ, and ROS (Kauppinen et al, 2013).

Although, there was no change in the *IL-1beta* transcript levels in the male mutants there was increase in the mRNA levels of natural anti-inflammatory *IL-1RA* in both male and female GHR KO. Leptin, which is inherently higher in circulation in GHR KO (Al-Regaiey et al, 2005) has been shown to directly induce the expression of IL-1RA in monocytes (Gabay et al, 2001). Anti-inflammatory receptor *IL-10R alpha* and *IL-10R beta* were elevated in all male GHR mutants as well. The level of activated stress kinase p38 MAPK was reduced in the liver of GHR KO and K4 males and this, under physiological conditions has been shown to function as a mediator of ROS

signalling that can either activate or suppress cell cycle progression in hepatocytes depending on the level of ROS, as governed by the activation stimulus (Tormos et al, 2013). The NADPH oxidase 4 (Nox4) has recently been identified as a Janus-faced ROS generator having mostly detrimental but protective function in one report (Schmidt et al, 2012). The levels of Nox4 protein was down regulated in male GHR KO and K4 livers. Additionally the acetylated-tubulin (K40) levels (unknown pathological function) were downregulated in GHR mutant livers. Thus far there are two known deacetylases that act on tubulin; HDAC6 and Sirt2 (Janke & Bulinski, 2011) and since the level of latter are not changed in the livers this might imply that HDAC6 is elevated in the livers of these mice. This highlights the cancer resistance of the GHR mutants since HDAC6 has been identified as a tumour suppressor in liver cancers by promoting autophagic cell death (Jung et al, 2012).

Reductions in GH-mediated STAT5 and resistance against stress

Although stress resistance has been extensively studied in skin-derived fibroblasts from Ames, Snell and GHR KO mice (Wang & Miller, 2012; Murakami et al, 2003; Salmon et al, 2005) there is a lack of free radical scavenging reported *in vivo* in GHR KO liver and kidney with conflicting results from the same lab (Hauck et al, 2002; Al-Regaiey, 2013). This may be attributed to different genetic background of mice and the age group used between the two studies. The Laron dwarfs (Ecuadorian cohort) have reduced stress-induced signalling with their serum increasing *SOD2* and decreasing *mTOR* levels in human mammary epithelial cells (Guevara-Aguirre et al, 2011). Similarly, serum from individuals on long term CR has been shown to enhance stress resistance in primary fibroblasts in culture by elevating *SOD2* and *GPx1* (Omodei et al, 2013).

Transcriptional regulation of the antioxidant response element (ARE) by Nrf2 is important for the cellular adaptive response to toxic insults. Although there is no direct data of GH-mediated inhibition of Nrf2, recent data in skin-derived fibroblasts of Snell dwarf mouse indicates elevated levels of Nrf2 and of multiple Nrf2-regulated ARE genes (Leiser & Miller, 2010). Furthermore, mRNA levels for some Nrf2 regulated genes; *Mt1*, *Gclm*, *Txnrd*, *Hmox* were also elevated in at least some tissues of Snell dwarf mice. Sun *et al*. have shown elevated Nrf2 expression in cortex of long-lived GHRH KO mice (Sun et al, 2013). Intriguingly, it was also reported upon comparative microarray analysis that liver-specific Keap1 knockout mice have a similar hepatic gene expression pattern to GHRH KO mice (Sun et al, 2013). Our results have revealed an elevated expression of *Nrf1* and *Nrf2* in young GHR male mutants at transcript and protein level while the transcript levels remain unchanged in females for both genes. The Keap1 mRNA levels were elevated in GHR KO males and there was a strong sexual dimorphism evident in *Nrf2* and *Keapl* with levels of both

genes being inversely proportional.

NAD(P)H quinone oxidoreductase 1 (Nqo1) is a prototypical Nrf2 target gene that catalyses the reduction and detoxification of highly reactive quinones that can cause redox cycling and oxidative stress. *Nqo1* transcript was significantly elevated in all GHR male mutants. Additionally, the Nrf2 regulated antioxidant gene *Mt1* was dramatically elevated in GHR KO male and to a modest extent in KO female. Importantly, metallothionein is a negative regulator of oxidative stress-mediated apoptosis and buffers tissues against the initiation of inflammatory cascades following injury (Dutsch-Wicherek et al, 2008). *Mt1* is also a part of set of genes designated as a shared signature set of numerous mouse models with extended lifespan (Steinbaugh et al, 2012). Augmented activity of Nrf2 and ARE-responsive genes may therefore coordinate many of the stress resistance traits and cancer protection seen in cells from these long-lived mutant mice.

Despite the well-documented relationship between Nrf2 and protection from oxidative stress, relatively little is known about the role of Nrf2 in aging. Recent studies in *C. elegans* have suggested that the Nrf2 homologue, SKN-1, is necessary for the lifespan extension seen with dietary restriction (Bishop & Guarente, 2007) and insulin pathway disruption, and overexpression of SKN-1 can increase worm life span (Tullet et al, 2008). Further work has suggested that a Keap1 heterozygous loss of function mutation in *D. melanogaster* can increase Nrf2 activity, increasing both oxidative stress resistance and life span in male flies only (Sykiotis & Bohmann, 2008). Analogous studies in mice have been complicated by the lack of viability of the Keap1 knockout mouse (Wakabayashi et al, 2003) and have been mostly limited to observations of decreased Nrf2 signalling with increased age (Shih & Yen, 2007) and increased Nrf2 signalling with calorie restriction (Pearson et al, 2008).

Apolipoprotein E (ApoE) is a well-documented longevity gene in humans based on linkage studies of exceptionally long-lived families (Beekman et al, 2013; Brooks-Wilson, 2013). Considering liver is the primary organ involved in ApoE synthesis and lipid metabolism, elevated *ApoE* levels in most GHR mutants indicate decreased hepatic oxidative stress which is elevated in the case of $ApoE^{-/-}$ mice that contain increased oxidised DNA (Folkmann et al, 2007). In addition, $ApoE^{-/-}$ mice developed age-dependent morphological and biochemical alterations, including fibrosis (newly formed collagen), elevated pro-inflammatory cytokines (IL-6 and iNOS), and decrease of antioxidant enzymes (SOD and catalase) in several organs (kidney, liver and heart) thereby reducing survival (Bonomini et al, 2010).

Reductions in GH-mediated STAT5 activation and insulin signalling

It is well established that GH decreases insulin sensitivity (Dominici et al, 2005). Physiological bursts of GH have clear insulin antagonistic effects, rapidly decreasing glucose uptake, an effect that is sustained for several hours (Moller et al, 1990). Accordingly, excess GH signalling, as seen in acromegalics and bovine GH transgenic mice, results in insulin resistance (Coculescu et al, 2007; Olsson et al, 2005). Lack of GH signalling, despite its consequent obesity and NAFLD (conditions usually associated with insulin resistance), is associated with higher insulin sensitivity (Dominici et al, 2002). Additionally GHR KO and Ames dwarf mice have been shown to be insulin sensitive compared to respective WT mice (Masternak et al, 2009). Liu *et al*. have reported reduced insulin and glucose levels (increased insulin sensitivity) owing to significantly reduced pancreatic islet size in GHR KO mice (Liu et al, 2004). A similar low fasting glucose profile in other GHR mutants (Nelson CN PhD thesis, 2013) can explain the persistent activation of AMPK in these mice that are in a continuous state of starvation (as compared to WT) even in a fed condition.

Insulin release is stimulated by a rise in blood glucose and is instrumental in glucose regulation by stimulating its uptake into tissues. When blood glucose decreases, the opposing process of gluconeogenesis is stimulated by glucagon and other counter-regulatory hormones to maintain homeostasis by converting pyruvate to glucose. However, abnormal elevation of hepatic gluconeogenesis is central to the onset of hyperglycemia in patients with T2DM. The origin of insulin resistance has been difficult to elucidate in part due to diverse set of risk factors but the most reliable predictor is mitochondria generated superoxide radicals (Hoehn et al, 2009). Hence, genetic or pharmacologic strategies that can override the mitochondria generated radical can prevent insulin resistance. This is supported by selective induction of ROS by mitochondrial complex III antagonist antimycin A resulting in rapid insulin resistance that can be reversed by the mitochondrial specific SOD2 (Hoehn et al, 2009).

Several studies have reported that Sirt1 functions to activate gluconeogenesis in response to nutrient signalling by deacetylating PGC1α, thus permitting interaction between PGC1α, HNF4α and FOXO1 which leads to the induction of gluconeogenic genes (Caton et al, 2010). Interestingly, Sirt1-dependent gluconeogenesis was not regulated by classical gluconeogenic regulatory hormones such as glucagon or insulin, but was instead mediated by changes in the levels of NAD^+ and pyruvate (Rodgers et al, 2005). However, since HNF4A protein levels are downregulated in GHR mutants, gluconeogenesis is impaired in these mice. This was supported by pyruvate tolerance tests in these mutants (Nelson CN PhD thesis, 2013). In addition GCN5, an acetyl transferase, which is elevated in GHR KO and K4 male mutants, inhibits gluconeogenesis by acetylating and

deactivating PGC1α, also leading to the suppression of gluconeogenic gene expression (Lerin et al, 2006). Therefore, GCN5 inhibits gluconeogenesis and thereby promotes increased insulin sensitivity in GHR mutants. A similar mechanism is also used by metformin to suppress hepatic gluconeogenesis in diabetes by induction of Sirt1 and GCN5 (Caton et al, 2010). It is relevant that, reduction in age-enhanced gluconeogenesis has been shown to extend lifespan in yeasts (Hachinohe et al, 2013).

The elevated insulin sensitivity in GHR mutant mice was associated with increased insulin receptorβ and a decrease in phosphatase PTP1B protein. Additionally *IRS1* and *IRS2* mRNA were elevated in all male GHR mutants and male GHR KO respectively supporting the earlier literature in GHR KO males (Masternak et al, 2005). In contrast to their transcripts, IRS1 and PTP1B protein levels were reduced in GHR KO and K4 mutants. The decrease in hepatic PTP1B levels is associated with increased insulin sensitivity (Owen et al, 2013) and has been shown to be Sirt1-mediated (Sun et al, 2007). Insulin sensitivity is also consistent with elevated *Glut2* level in all male GHR mutants and female K2 mutants. In regards to longevity, CR diets apparently do not further increase lifespan in GHR KO mice (Bonkowski et al, 2006) possibly due to lack of increase in their insulin sensitivity (Masternak et al, 2009). However, there is evidence than reducing insulin sensitivity, provided that diabetes is not induced, has little effect on prolonging lifespan (Nelson et al, 2012). This is also evident in the case of long-living yet marginally insulin-resistant IGF-1R$^{+/-}$, IRS1$^{-/-}$ mouse models (Junnila et al, 2013).

FGF21 or starvation hormone plays an important role in eliciting and coordinating the adaptive fasting response and promotes similar physiological changes as CR, including decreased glucose levels, and increased insulin sensitivity (Potthoff et al, 2012). Overexpression of FGF21 has been shown to prolong lifespan in mice (Zhang et al, 2012b). Here, FGF21 transcript was downregulated in all GHR mutants. A plausible mechanism of low FGF21 expression is its negative regulation by PGC1α-mediated modulation of the heme/Rev-Erb alpha axis (Estall et al, 2009). The *Rev-Erb alpha* was elevated in all male GHR mutants, resembling a feminised pattern of expression which is sexually dimorphic and significantly higher in all females. Reduced FGF21 is associated with increased steatosis in these GHR mutants (Barclay et al, 2011) and more recently with brain circadian clock which coordinates nutrient homeostasis with reproduction (Bass, 2013).

Reductions in GH-mediated STAT5 activation and nuclear receptor expression

Nuclear receptors are the best-characterised regulators of Phase I xenobiotic metabolism genes (XMGs). Studies of GH regulation of xenobiotic metabolism have not been extensively carried out

except for Lit/Lit mice (Amador-Noguez et al, 2007). However, there is circumstantial evidence to suggest alterations of phase I XMGs expression by additional factors such as PPAR isoforms that are elevated in Ames and GHRKO (Masternak & Bartke, 2007). In this study we have analysed both isoforms of PPAR gamma and found elevated expression of *ppar gamma1* in K2 females and all male GHR mutant mice and decreased expression of *ppar gamma2* in GHR KO and K4 males. Both the isoforms were sexually dimorphic with *ppar gamma1* favouring females and *ppar gamma2* higher in the males indicating the feminised pattern in GHR mutant males. Additionally, *ppar alpha* expression was also gender-specific but elevation of its expression did not reach significance in GHR KO in our study. Besides influencing glucose homeostasis, suppression of GH signalling promotes β-oxidation of fatty acids in liver. Fatty acid oxidation is promoted by direct or indirect action of PPAR alpha, PGC1α, FGF21, adiponectin and AMPK while GH negatively regulates the expression or activation of each of these factors (Gesing et al, 2011b).

Differences in nuclear receptor expression were observed in LXR alpha and LXR beta with higher mRNA levels in GHR mutant males. These nuclear receptors are associated with cholesterol and lipid metabolism suggesting that they may influence the development of metabolic disorders. LXRs have been shown to regulate fatty acid synthesis and glucose metabolism by modulating the expression of sterol regulatory element binding protein-1c (SREBP-1c), which is also regulated by insulin (Repa et al, 2000). Elevated LXRs have been proposed to promote steatosis in GHR mice lacking STAT5 activity (Barclay et al, 2011).

Nuclear receptor co-repressors are key transcriptional co-regulatory proteins that contain several nuclear receptor interacting domains that have been shown to downregulate the DNA expression by recruiting HDACs to DNA promoter regions (Glass & Rosenfeld, 2000). Both NCOR1 and NCOR2 were elevated in GHR KO male and GHR KO male and female mutant mice respectively but their physiological relevance is yet unknown. Similarly, *ROR gamma* transcripts were elevated in both male and female GHR KO and K2 mutants while *ROR alpha* remained unchanged but highly sexually dimorphic. The RORs are involved in the regulation of circadian rhythms and shown to bind and activate the promoter of the *BMAL1* gene (Guillaumond et al, 2005), a transcription factor central to the generation of physiological circadian rhythms. Also, since the levels of RORs are rhythmic in some tissues (liver, kidney), they have been proposed to impose a circadian pattern of expression on a number of clock-controlled genes (Liu et al, 2008). These circadian rhythm functions of RORs are carried out in conjunction with another set of nuclear receptor family, Rev-Erb comprising of two forms alpha and beta. Intriguingly, both these forms were dramatically altered only in GHR male mutants with *Rev-Erb alpha* being elevated and *Rev-Erb beta*

downregulated to a level that is expressed in the females. It would be interesting to analyse the 'clock' genes in these mutants as well other genes that are bound by the circadian rhythms.

From out data there is clear feminisation of male GHR mutants owing to lack of GH-mediated STAT5 pulsatility. In support, long-lived Ames mice have been shown to lose the sexual dimorphic pattern associated of gene expression in male and female rodents (Amador-Noguez et al, 2005). A similar finding has been reported following calorie restriction (CR) where genome-wide mRNA profile in male mice was feminised (Estep et al, 2009) with alteration of 32 xenobiotic metabolising genes (XMG) (Fu & Klaassen, 2014). The CR-induced feminisation effects interestingly correlate with the phenomenon that females tend to have a longer life expectancy than males in humans (Vina et al, 2005) and rodents (Goodrick, 1975). Gender-divergent gene expression in rodent liver is determined in large part by GH secretory pattern, which is continuous in females but pulsatile in males (Waxman & O'Connor, 2006). The survival curves of GHR mutants in our group indicate a similar profile with all GHR mutant females outliving the genotype-matched males. CR was also reported to decrease plasma GH levels in male rats (Chacon et al, 2005). Therefore, the feminisation effects of many XMGs by CR in males may be due to the CR-induced decrease in GH levels in mice.

GHR knockout male mice retain key molecules with age

An important observation in this study was the retention of active AMPK, Sirt1 and Sirt3 protein levels in the liver of aged GHR KO males although there was an age-associated decline; it was clearly elevated as compared to age-matched WT males. Based on the existing literature this would imply that GHR KO males should exhibit cancer resistance and lifespan extension. The latter was not evident indicating that separate pathways exist for protection against cancer and for lifespan extension. This is in contrast to the earlier report suggesting reduction in AMPK activity and mitochondrial biogenesis as the cause for aging (Reznick et al, 2007). Similarly, Brown *et al.* have proposed that Sirt3 upregulation in hematopoietic stem cells (HSC) of aged mice can reverse the aging-associated degeneration by improving their regenerative capacity (Brown et al, 2013).

Why do female GHR mutants lacking GH-mediated STAT5 activation (reduced circulating IGF-1 levels) have lifespan extension, whereas males do not?

Sexism in GHR K2 mutants

In order to answer this question we had sought to determine changes in metabolically active tissue of old GHR K2 (lowest common denominator: both GH-mediated Jak2 and SFK activation but not of STAT5) male and female mice at the protein level. The results obtained in aged liver tissue were in complete contrast to ones observed in young mice with key antioxidants and mitochondrial proteins favouring only K2 female over males. The hepatic protein levels of Sirt3, Nrf2 and activated AMPK were upregulated in females and unaltered in males as compared to gender-matched WT. Expression of Nrf2 was surprisingly not detectable in males for the same amount of lysate even though Nrf2 was elevated in young K2 mice. In addition, it could be expected that inflammation is reduced in K2 females due to increase in IL-1RA, Sdha levels and key OxPhos components (I, II, V) in females. Cox IV levels were also elevated in K2 females. However, the lipid peroxide levels in serum and liver tissue of K2 females were unaltered while the males need to be tested.

A similar profile as liver was revealed in heart tissue as well, with elevated active AMPK, Sirt3, OxPhos components (II, IV and V) and Cox IV activity retained in K2 females and unaltered in males. In addition there was increased expression of antioxidant catalase in K2 females which was unaltered in K2 males. The antioxidant regulator specific to heart, Bmi1 was elevated in K2 females as compared to WT but undetectable in males in general. Uncoupling protein 1 levels were high indicating low ROS production and clearly better management due to elevated Sirt3 in K2 females. The skeletal muscle tissue of females revealed elevated levels of mitochondrial Sirt3 even though PGC1α were unaltered in both genders. Nrf2 and active AMPK were undetectable in males but were elevated in K2 females along with IRβ Sdha, Cox IV, UCP-1 and OxPhos components (I, II, III and IV). Numerous ROS quenchers and antioxidant enzymes such as sulfiredoxin1, thioredoxin1, cytochrome C were upregulated in K2 females as compared to WT. Catalase was upregulated in both male and female K2 mice. Interestingly, thioredoxin1 overexpression in mice (C57Bl/6) has been shown to prolong median lifespan by providing increased resistance against oxidative stress during the early part of life (Mitsui et al, 2002; Perez et al, 2011).

Kidney lysates of only female K2 and KO were analysed and revealed elevated Sirt3, catalase and Gapdh expression in both models. However PGC1, SOD2 and eNOS were selectively elevated in GHR KO indicating an inhibitory effect of GH-induced Jak2/STAT3 and SFK signalling on expression of these genes. The elevated Gapdh could possibly be due to increased renal gluconeogenesis that has been shown to occur during prolonged fasting or due to impaired hepatic gluconeogenesis (Mutel et al, 2011), which is clearly reduced in GHR mutants (Nelson CN PhD

thesis, 2013). Finally, a total antioxidant analysis revealed complimentary results with significantly higher levels in K2 females but not in K2 males. These results clearly highlight the molecular basis behind lifespan extension of K2 females that were absent in K2 males. However these findings did not aid in determining reasons for reduced cancer incidences that is independent of the gender. The common attribute of GHR mutant mice is lack of GH-induced STAT5 signalling and reduced IGF-1 levels. Hence, the Waters' Group is investigating the lifespan and cancer incidences in mice with liver expressing IGF-1 on a GHR K2 background to determine if the effects reported here are exclusive to GHR and independent of IGF-1 levels.

The feminisation of male-specific hepatic RNA expression as a consequence of lack of GH pulsatility involves not only differential regulation of XMGs but also other antioxidant and metabolism regulating genes that are differentially expressed in male and female mutant mice. In addition, the altered hepatic XMGs can generate different metabolites in mice on a particular diet that can be genotype and gender-specific (Steinbaugh et al, 2012; Waxman & O'Connor, 2006). With recent reports on impact of gut microbiota metabolism (Matsumoto et al, 2011), it is warranted that a mass spectroscopic or NMR analysis of the biological fluids (urine, stool) be carried out to generate a 'metabolic fingerprint' at different ages as shown previously by our group in GHR KO, K1 and K2 males (Schirra et al, 2008) as well as determine the gut flora in long-lived GHR mutants. In addition, the measurement of mitoflashes in metabolically active tissues at different ages of GHR mutants could provide information on the basis of lifespan extension in mice.

Role of SFK activation in cancer incidence and longevity

One possibility for increased cancer incidences in long-lived K4 females in comparison to WT females was elevated levels of GH and thereby increased GH-mediated SFK activation. However, this was not evident in the livers of these mice by immunoblot. On the contrary, SFK activation was reduced in K4 males as compared to WT, correlating with lack of tumour-related death. In addition, the SFK activation in liver tissue of K4 females was significantly higher than K4 males. The total Src levels were also reduced in K4 males further, enhancing the differential SFK activation. Thus far, there is only one study that has reported a sex-specific increased expression and activation of Src in kupffer cells of males over proestrus females following hypoxia (Zheng et al, 2006). In the light of existing literature and our own data it would be beneficial to determine if this sexual dimorphism also exists in other tissues and if certain SFK-regulated genes are differentially expressed (and activated) in females than males. SFKs have been shown to regulate nuclear export and degradation of Nrf2 to switch off antioxidant transcription (Niture et al, 2011). This could

explain high cancer incidences of cancer in K4 females over males even though both genders exhibit both median and maximal lifespan extension. Finally, the extent of sexual dimorphism in SFK activation in GHR KO (GH-independent) as well as GH-mediated SFK activation in male and female GHR K2 mutants (which can activate both Jak2 and SFK) remains to be evaluated.

Another aspect of reduced lymphoma but elevated sarcoma and carcinoma in GHR K4 females may be attributed to estrogen receptor (ER) signalling. Reports have suggested SFK as a critical upstream regulator of the estrogen-stimulated PI3-K/Akt pathway in endothelial cells (Haynes et al, 2003) while there is also amounting evidence for estrogen-mediated SFK activation in the same cells (Groten et al, 2005) indicating a complementary interaction between estrogen and SFK. Zhang *et al.* have reported that low concentrations of estrogen can activate SFK/ERK while high levels are inhibitory in breast cancer cells and proposed that Src acts as a switch in linking estrogen signalling with EGFR pathway (Zhang et al, 2012a). Estrogen receptor α (E2Rα)-mediated Src activation has been reported to promote proliferation in both E2R positive and negative cancer cells with positive crosstalk with EGFR (Fox et al, 2008). Importantly, estrogen regulates normal and pathophysiological processes differentially via its receptors E2Rα and E2Rβ (Yakimchuk et al, 2013). While estrogen-mediated signalling via E2Rα has been reported to promote proliferation of the breast (Fox et al, 2008), uterus and developing prostate (Yakimchuk et al, 2013), the E2Rβ activation results in suppression of proliferation and stimulation of differentiation of numerous tissues (Wada-Hiraike et al, 2006). This dichotomy of E2Rs in addition to the opposing effects of estrogen treatment reported earlier further increase the complexity of its role in promoting carcinogenesis and may therefore shift the balance from lymphoma (primarily STAT5 driven) in favour of carcinomas and sarcomas (SFK and Akt driven) in GHR K4 females.

Conclusion

The cancer resistance and lifespan extension in the GHR mutant mice lacking the full repertoire of GHR signalling is sexually dimorphic. In female mutants, reductions in GH-mediated STAT5 activation or circulating IGF-1 levels appear beneficial in mediating *median* and *maximal* lifespan extension and reducing tumour incidence and lymphoma aggressiveness. While in males, there was reduced cancer burden with the decrease in circulating IGF-1 levels, no effect was evident in lifespan extension. Therefore, instead of IGF-1, the delayed cancer occurrence or reduced cancer burden seen in GHR mutants could be the accumulative effect of multiple interacting mechanisms that include but are not limited to reduced activation of growth-promoting pathways, increased stress resistance, reduced inflammation markers, and increased insulin sensitivity. Interestingly

these changes are also common to calorie restriction mediated lifespan extension, at least in rodents and invertebrates. This multi-factorial involvement (illustrated in fig.8.26) is also evident in the recent use of the anti-diabetic drug metformin in cancer treatment (Pollak, 2012) where it has been shown to induce a dietary restriction-like state and protective oxidative stress response via AMPK and Nrf2 (Onken & Driscoll, 2010). Metformin also exerts CR-like genomic and metabolic responses, which were interpreted as induction of genes associated with longevity pathways in mice. Translation of the knowledge from these genetic models and CR may provide cancer prevention strategies in humans.

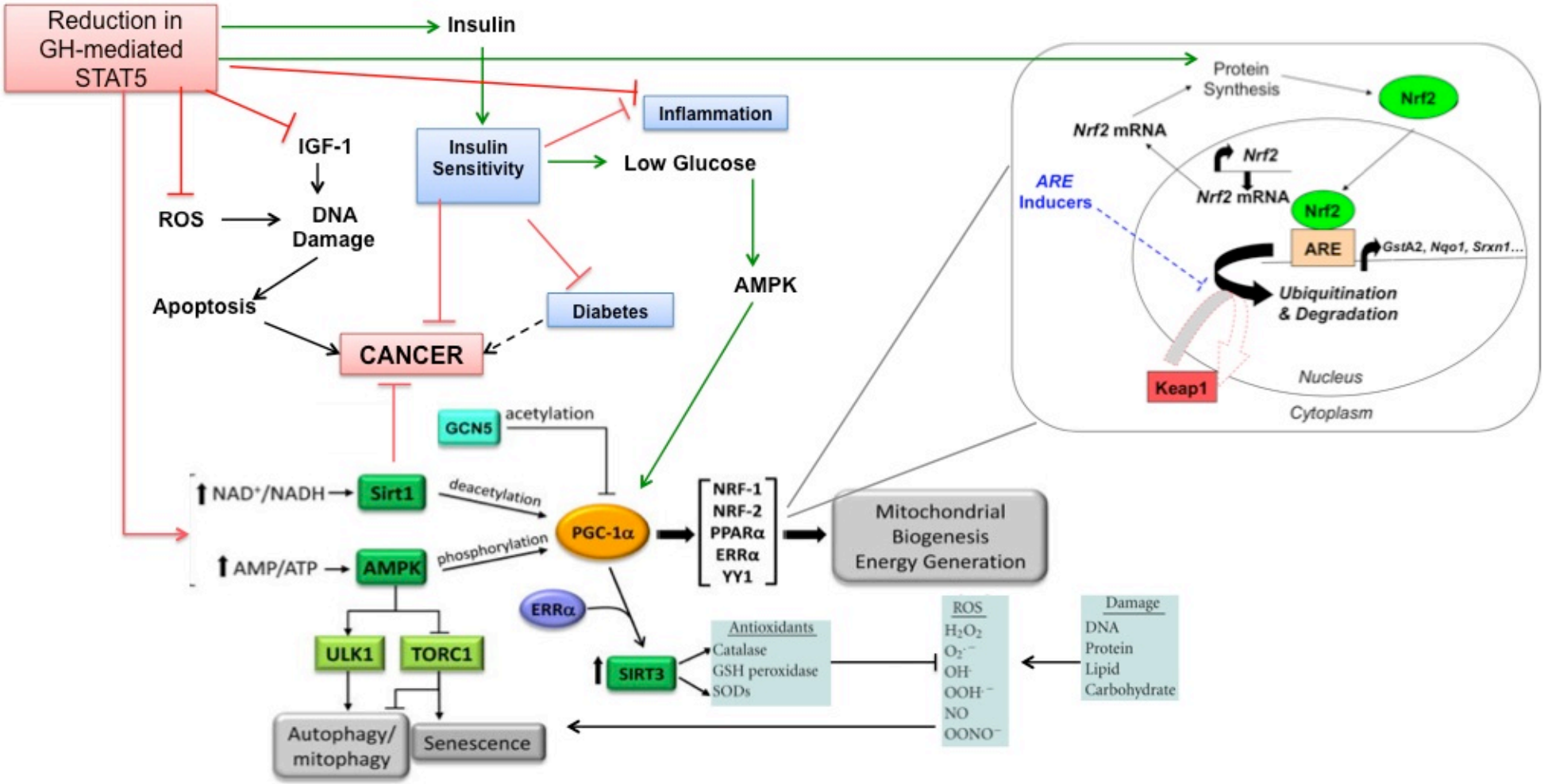

Figure 8.26: Cancer resistance pathways in GHR knockin and knockout mouse models.

The signalling pathways and molecules responsible for cancer resistance in form of reduced tumour incidence and/or aggressiveness in GHR mutants with lack of GH-mediated STAT5 activation are summarised.

Chapter 9
Final Discussion and Future Directions

Overview

The Growth Hormone Receptor is expressed in almost all cell types (Waters & Shang, 2002) and its transcript and protein and therefore its actions have been reported in every physiological system (Lichanska & Waters, 2008). It is the most widely studied member of its family of Class I cytokine receptors. At the cellular level, GHR has been implicated in proliferation, differentiation and survival and indeed GH acting on GHR has been reported to result in over 450 different actions in over 80 cell types (Waters & Shang, 2002). It is therefore no surprise that GH/GHR signalling is associated with each of the 'hallmarks of cancer' (fig.9.1) either directly or via IGF-1 induction, indicating that dysfunctional signalling emanating from overexpression of the hormone or its cognate receptor can promote cancer progression. The strongest evidence for this came from humans with dysfunctional GHR (Ecuadorian cohort) that have no reported deaths due to malignancy as compared to their relatives with functional receptor (Guevara-Aguirre et al, 2011). This finding supported a previous report from Shevah *et al.* (Shevah & Laron, 2007).

The risk of developing any cancer is determined by genetic elements and by environmental conditions including diet and lifestyle. Recent evidences have suggested that the GH/IGF-1 axis might provide a link between these factors and the disposition to cancer through its effects on normal cell proliferation, differentiation and apoptosis. The GH/IGF-1 axis influences several stages and aspects of cancer development and behaviour: cellular proliferation, cell survival, angiogenesis and metastasis, and even resistance to chemotherapy (Chhabra et al, 2011).

Figure 9.1: The hallmarks of cancer.

The complex nature of cancer has been reduced to a small number of underlying principles which dictates the common attributes ("hallmarks") that govern the transformation of normal cells to cancer (malignant or tumour) cells (Developed from (Hanahan & Weinberg, 2011)).

Major advances, both mechanistically and clinically, have been achieved over the past two decades in understanding the function of GH/IGF-1 axis. Many of its physiological roles, the genes it regulates and the signalling pathways used for this purpose are being determined. Moreover, a precise molecular understanding of how the hormone binds to its receptor and a new model for its activation is now available. In the last decade alone a considerable paradigm shift has occurred – from GH-induced dimerisation to constitutive homodimerisation, Jak-STAT specific signalling to recognition of additional Jak-independent pathways, receptor crosstalk signalling, autocrine mode of GH activation, and finally function of nuclear-localised receptor, yet much remains to be determined.

Structure-function aspects of GHR TMD

The GHR is a single pass constitutively dimerised receptor at the cell surface, and the existence of such dimers implies that a specific ligand-induced conformational change is required for signal transmission to the associated cytoplasmic Jak2 kinases (Brown et al, 2005). The conformational change/realignment in ECD induced by ligand binding activates Jak2 and these structural changes are transmitted through the TMD and intervening sequences from the ECD to the Box1 motif. However, unlike the ECD there has not been any direct structural information about the TMD and upper juxtamembrane linker or the ICD. GHR TMD interaction using ToxR assay have shown the importance of Pro266 and the first glycine (274) of the GxxG motif (both of which are highly conserved) in weakening the TMD helix interaction, since interaction increased on conversion of these residues to Ile. These results support the view that the GHR TMD helices do associate constitutively in a specific manner, but not so strongly as to preclude realignment as a result of ligand binding to the ECD (Brooks et al, 2014).

This chapter provided insights into the role of GHR TMD in ligand-induced activation, notably how proximity of ECD and separation of ICD upon ligand binding results in GHR activation. For this, we analysed the effect of cysteine scanning mutations (or SCAM) by individually mutating every residue across the upper juxtamembrane linker from L251 through the entire TMD to S288 with cysteine 259 mutated to serine to get a thiol-free background for analysis of the mutants. In addition, these mutants were made in full-length receptor or truncated (at 389) to analyse activation and dimerisation. The relation between TMD association and receptor dimerisation was evidenced by spontaneous cysteine crosslinking of the TMD and juxtamembrane residues. Earlier crosslinking studies using MTS in intact cells has revealed a helical periodicity in the TMD placements evident in dimer formation within the TMD and when crosslinked residues were plotted on a helix wheel projection, an interaction interface was apparent corresponding to the basal state. This included

I272/F273, I275/F276, and V280 with crosslinking just visible at F283. This interface correlates well with the basal state configuration predicted by molecular dynamics (MD) simulations (Brooks et al, 2014). It was indicated that MTS has limited accessibility to residues buried deep in the bilayer where little reactive thiolate anion is present, as a result of which low efficiency of dimer formation was observed towards the cytoplasmic side (Guan et al, 2002).

The truncated mutants were then subjected to Cu-o-phenanthroline (CuP) crosslinking to determine the extent of crosslinking in the presence or absence of GH using cell membrane extracts. We observed increased CuP-induced crosslinking of D262C, located in the JM region and decreased crosslinking of V284C and F287C, in the presence of GH, while other residues did not yield consistent results. This supports the view that ligand binding increases the proximity between JM residues in this conserved upper membrane proximal sequence while separating the lower juxtamembrane sequence. In addition, the observation of GH enhanced dimers at D262 is consistent with hGH-induced formation of disulfide dimers at the adjacent C259 residue in the native receptor as reported by others (Gent et al, 2003).

GHR dimerisation by disulfide bond formation at the extracellular juxtamembrane and upper TMD resulted in constitutively active receptors. GH, like its structural homologs EPO and PRL, has two asymmetrically placed receptor binding sites which would change the interaction geometry between the two receptor subunits on binding. In order to understand the nature of this change full-length cys mutants were utilised since we had observed that a minor fraction of cys mutants formed dimers spontaneously in the absence of ligand. To determine if this dimerisation resulted in GHR activation, transient expression in HEK293 cells revealed that constitutive crosslinking of the GHR with cysteine substitutions between E260 and L269 is accompanied by receptor activation (measured as STAT5 tyrosine phosphorylation), while above this dimer formation and activation (L251-T258) is weak. No significant dimer formation or signalling was seen with Cys259 converted to serine, i.e. when no JM or TMD free cysteines are present to crosslink. Evidently dimerisation within the upper TMD or the extracellular EED sequence can initiate signalling so that close apposition of the upper TMD is required for signalling. Accordingly, introducing two disulfide bonds by cysteine substitution at F263C and I270C resulted in the strongest receptor activation and this was confirmed in Ba/F3 stable lines showing constitutive proliferation and STAT5 activation in the absence of GH.

Finally, the CuP treatment on live cells transiently transfected with full-length upper TMD cys mutants has revealed that GHR undergoes relative rotation in the upper helices of TMD with L268

present on the interaction interphase while I270 is lies on the non-interacting side. When crosslinked at I270C with CuP, GH addition failed to induced GHR activation. These findings are suggestive that GHR activation involves both an optimum rotational position and the need to closely appose the upper JM sequences for activation, resulting in a "tilt and twist" movement of the TMDs. Such a mechanism may be common to other Class I cytokine receptors since the TMD and ICD of the G-CSFR and GHR, can be interchanged to produce signalling competent receptors (Ishizaka-Ikeda et al, 1993). These findings were supported by molecular dynamics modeling *in silico* to determine the 2 states of receptor TMD; basal and GH–induced (Brooks et al, 2014). This model of GHR activation (summarised in fig.9.2) will provide valuable insights into the design of new cytokine receptor therapeutics and facilitate understanding of a variety of relevant cytokine related genetic disorders.

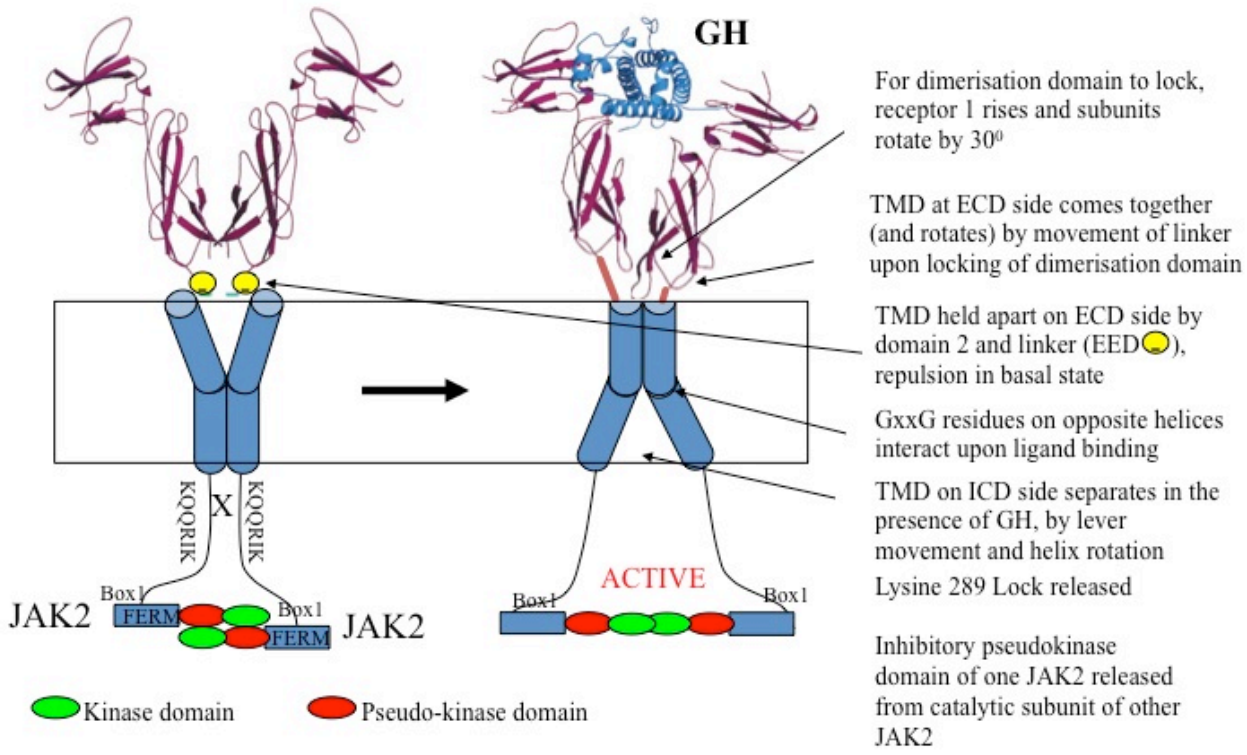

Figure 9.2: Proposed model of activation of GHR.

Refer Appendix VIII

Lyn (SFK member) interaction with GHR

The GH-induced Jak2 activation mechanism is now known but GHR has also been shown to activate other pathways independently of Jak2, and of these pathways have been associated with specific physiological roles in a cell line-dependent manner. One of these pathways is GH-induced SFK activation. Based on a previous study from our group there is solid evidence that GH activates SFK independently of Jak2 both *in vitro* and *in vivo* (Brooks & Waters, 2010) but the mechanism is unknown. In this study we employed truncated GHR constructs and determined a 23 residue conserved sequence between Box1 and Box2 motif as the Lyn binding region. The Lyn binding to GHR does not seem to be conventional in nature since no consensus SH2 and SH3 binding sites were evident in this region or for that matter within the entire GHR. The Lyn binding to GHR does not require a phosphorylated tyrosine since when the sole receptor tyrosine in the truncated receptor mutated to alanine (Y314A), the receptor was still able to bind Lyn. A similar interaction has been proposed in closely related PRLR where no receptor phosphorylation was evident in a Box1 mutant even though Src activation was reported after PRL stimulation. Another study has indicated that when WT GHR, Jak2 and Src were co-transfected together, this resulted in co-IP of Jak2 and Src with GHR and this association was also seen when non-catalytic Src mutants were used, indicating that Src association with GHR does not require SFK catalytic activity (Manabe et al, 2006).

In this study we have presented preliminary results indicating a reduction in Lyn binding to WT GHR following GH stimulation. It remains to be evaluated if this is a direct effect of Jak2 on Lyn or occurs due to rapid GH-induced degradation. In contrast, the Box1 mutant that cannot interact with Jak2 showed increased Lyn binding after GH stimulation. It may therefore be speculated that Lyn and GHR compete with each other for Jak2 binding and when Jak2 is unable to bind (as in Box1 mutant), it can facilitate the binding of Lyn to GHR either directly or via another molecule. Other studies have emerged reporting Jak2 inhibition can deactivate Lyn kinase (Samanta et al, 2009), further strengthening Jak2 and Lyn association. However, for GHR no Jak2 dependency of Lyn binding or activation to GHR was observed *in vitro* or *in vivo* (Rowlinson et al, 2008) (Barclay et al, 2010).

Determining the precise mechanism and cellular location of GHR-mediated SFK activation would be useful to determine its role in GH-mediated SFK activation in long-lived GHR K4 (all Box1 motif proline mutated to alanine) male and female mutants. In addition, GHR-mediated SFK activation has been implicated in mediating autocrine actions of GH (Tang et al, 2010a) with increased cancer cell 'hallmarks' associated with SFK signalling (Bougen et al, 2012).

Autocrine GH and GHR-mediated oncogenesis *in vitro*

The constitutively active constructs based on the structure and function studies of GHR along with the nuclear localised GHR (Conway-Campbell et al, 2007) were analysed in an androgen-independent prostate cancer cell line (DU145) to determine the direct role of GHR in promoting cancer progression. Although the jun zipper based, PM2/hGHR (F263C, I270C) and rGHR constructs (WT, NLS) were able to constitutively signal via STAT5 under normal growth conditions, no increase in proliferation or soft-agar growth was evident. However, the proliferation assay needs to be performed in serum-free media where STAT5 activity was clearly evident only for jun zipper construct. In addition, it is possible that instead of promoting proliferation, GHR can support cancer progression by reducing apoptosis, thereby increasing cell survival. This aspect of cancer progression is yet to be analysed. Several attempts to generate a NLS-GHR cancer model by sub-cutaneous inoculation of Ba/F3-NLS-GHR cells in athymic nude mice did not result in any tumour formation *in vivo* even when the injected cell numbers (based on (Conway-Campbell et al, 2007)) were doubled, raising the possibility of clonal artefact.

Based on the established role of autocrine GH and GHR signalling in MCF7 cells by Lobie's Group, we decided to investigate MCF-7 mammary cancer cell line instead. Forced expression of hGH has been shown to promote proliferation and phenotypic conversion of MCF-7 into a more invasive phenotype (Mukhina et al, 2004). However, these findings have been disputed by two separate groups indicating autocrine hGH to be growth-inhibitory (Nakonechnaya et al, 2013) and G120R-insensitive (van den Eijnden & Strous, 2007). We have utilised 2 model systems of autocrine hGH expression in order to bridge the gap between the conflicting studies from Strous's Group, Lobie's Group and Nakonechnaya *et al.* (2013). This was achieved by using two different promoter-driven expression models for hGH, namely strongly expressing CMV or the relatively weakly expressing MT promoter mainly used by Lobie's Group. From our studies it was evident that MT-driven hGH promoted proliferation in both complete growth media as well as serum-free media while CMV-driven hGH expression was inhibitory. In support of its cancer promoting effects, the lower expression of hGH (by MT promoter) also significantly increased the clonogenic ability of MCF-7 cells as well as the number of holoclones formed. Indeed, depending on the autocrine GH levels we were also able to show that the cell lines behaved differently phenotypically in a 2D-Matrigel assay with rapid stellate organisation of MT-driven hGH cells and only small colonies in CMV-hGH cells.

The immunoblot analysis of key downstream signalling pathways has indicated that the surface localisation of unbound GHR is reduced or non-functional in CMV-driven hGH MCF-7 stables as

no hGH-induced STAT5 or ERK activation was evident in contrast to MT-driven GH. This was indicative of the fact that lower levels of GH did not sequester all the available GHR and some unbound GHR was available at the surface to bind exogenous hGH, which could explain the inhibitory effects of autocrine hGH observed in LNCaP cell line (Nakonechnaya et al, 2013) and the inability to bind the G120R antagonist in the study by Strous's Group since both were driven by CMV promoter. In addition, no constitutive activation of STAT5 was evident in CMV-hGH, unlike MT-hGH. Importantly, MAPKs ERK1/2 and p38 activation were already higher in CMV-hGH cell lines independent of exogenous GH. A high level of ERK activation has been shown to be inhibitory for stem cell renewal (Binetruy et al, 2007) and even emergence (Zhang et al, 2014). This can be extrapolated to cancer stem cell renewal and emergence. In support of reduced proliferation in CMV-hGH MCF-7, these stables had reduced levels of CDK4 and high levels of p21 indicating cell cycle arrest. Active SFK levels were also higher in CMV-hGH as compared to MT-hGH cells that showed an exogenous GH response. It is possible that very high levels of GH can switch the pathway from Jak/STAT to SFK/ERK, and this shift may depend on the site where the signalling actually begins since the autocrine GH bound GHR complex has been shown to localise primarily in Golgi and ER in LNCaP cells where it is inhibitory (Nakonechnaya et al, 2013).

The Ba/F3-B2B2 proliferation assay for secreted/synthesised bioactive hGH in the media from the MCF-7 stables has indicated that the CMV-hGH cells secrete almost double the level of GH in comparison to MT-hGH stables. These levels, although higher than the levels reported in studies by Lobie's and Perry's Groups, have indicated that the lower GH levels are tumour promoting while higher levels are inhibitory and potentially apoptotic. A similar phenomenon was reported with high levels of prolactin shown to lower proliferation rate and reduce PRLR levels in forced autocrine PRL T47D cells (driven via a strong viral promoter), while the conditioned media was able to increase cell numbers of Nb2 cells and control T47D cells (Nitze et al, 2013).

The most encouraging support for the autocrine hGH in cancer hypothesis comes from the study by Lobie's Group (Wu et al, 2011), analysing expression of hGH in mammary carcinoma. These workers found autocrine hGH expression associated with lymph node metastasis, tumour stage and proliferative index, hence survival outcome. Hence, administering a suitable antagonist early on during disease progression should be clinically efficacious. Similar studies on larger population numbers are warranted which would allow one to establish a range for GH and also for PRL from cancer tissue biopsies (especially mammary and prostate of origin) and thence to compare the levels of these cytokine with the cancer modality and severity.

Molecular basis of P495TGHR associated cancer susceptibility

This chapter highlights the molecular basis of the lung cancer associated P495T polymorphism in GHR which has been associated with 2-12 fold increase in lung cancer susceptibility in two separate GWAS studies on different ethnic populations (Cao et al, 2008; Rudd et al, 2006). We have determined that GHR P495T signalling for this cytoplasmic domain variant was not constitutive but prolonged and in a cell-line dependent manner. Using two separate cell lines, a murine pro-B cell line and a human normal lung epithelial BEAS-2B line, we have shown that this polymorphism prolonged STAT5(tyr694) and Akt(thr308) activity respectively following an acute GH pulse, as compared to wildtype (P495). Both of these signalling proteins have been associated with neoplastic progression (Magkou et al, 2007; Mallette & Ferbeyre, 2007) and shown to converge into major downstream networks in lung cancer (Sordella et al, 2004). The role of the Akt pathway in cancer progression is still emerging but recent findings have implicated Akt not only in survival but also in the maintenance and meeting the metabolic requirements of cancer stem cells (Ito and Suda, 2014). In addition, activated Akt(thr308) serves as a prognostic indicator for non-small cell lung cancer (Vincent et al, 2011), the same modality associated with P495TGHR polymorphism in one of GWAS studies (Cao et al, 2008).

The stably transduced Ba/F3 cell lines for WT and P495TGHR differed significantly in level of receptor expression, with higher levels observed in latter owing to the polymorphism itself rather than being an artefact of the expression system. In addition, there was increased surface receptor level (mature glycosylated form) in BEAS-2B and DU145 lines evident at 45-60 minutes following a GH pulse. A GH-independent difference on GHR degradation was also evident in HEK293 cells stably expressing WT or P495TGHR. No degradation product was evident in P495TGHR and this was proteasome-independent. GHR-induced STAT5-mediated phosphatases and SOCS expression serves as a key negative feedback mechanism to suppress downstream signalling and in the process SOCS degrade GHR. Since binding of SOCS1 and 3 occurs either on Jak2 or on GHR tyrosine residues quite upstream to 495, we analysed the binding of P495T to SOCS2 and CIS since Y487 on GHR has been shown bind to SOCS2, an E3 ubiquitin ligase (Vesterlund et al, 2011), is in close proximity to the polymorphism. No direct interaction of GHR and CIS has been shown to date although Y595 has been predicted as a binding site based on MAPPIT studies (Uyttendaele et al, 2007).

Using a HEK293 system stably expressing WT and P495TGHR we found significant but equal induction of SOCS2 following acute GH stimulation. However, at low levels of SOCS2 expression, co-IP analysis revealed dramatically reduced binding of SOCS2 to P495TGHR as compared to WT

by transfecting small amount of SOCS2. In addition to SOCS2 we evaluated if a CIS interaction was impaired with P495T. However we could not detect any CIS interaction with GHR unlike SOCS2. Interestingly, we could confirm that the interaction of GHR was specific for SOCS2 but not CIS in the hepatic tissue of GHR KO since protein levels of SOCS were greater in the GHR KO. From the *in vivo* studies it was evident that GHR undergoes a continuous turnover owing to SOCS2. Extrapolating the current data it could be expected that P495TGHR *in vivo* would result in prolonged signal due to delayed degradation of GHR in both GH-dependent and independent manner and the choice of downstream signalling molecule would depend on the cell line harbouring the variant. This is the first time a 'gain of function' mutation in GHR has been linked with cancer development and highlights the importance of GHR turnover in cellular homeostasis.

Establishing the RCAS/TVA system

The RCAS/TVA system serves as an important tool for cell and developmental-stage specific delivery of the gene(s) of interest. ALSV viruses cannot infect mammalian cells efficiently because these cells lack the cognate receptors (TVA) that recognises the standard envelope subgroups expressed on the virus envelope. Even if the entry barrier is overcome by the virus it is incapable of producing infectious progeny, thereby making these ALSV viruses doubly-defective in mammalian cells (Young et al, 1993). We have successfully established the tissue-specific gene delivery system *in vitro* to deliver genes of interest using two different ALSV based viral particles by stably expressing the TVA receptor in cell lines or in a tissue-specific manner *in vivo* (using particular promoters).

The replication competent retrovirus generated from the chicken fibroblast cell line, DF-1 was generated at high titre but owing to insert size constraints and the obligatory requirement of dividing cells, these virus particles were not the ideal for *in vivo* utility. This limitation was overcome by using relatively safer replication defective EnvA-pseudotyped lentiviral particles, which allowed transduction of non-dividing cells as well as transduction with large inserts. The pseudotyped lentiviral virus was utilised for making stables in the prostate cancer cell line DU145 (Chapter 6). This system is a third generation lentiviral packaging system that makes it much safer, being *Tat*-independent and self-inactivating by virtue of a mutant promoter. By carrying out numerous standardisation experiments we have established a protocol that consistently provides high titre pseudotyped lentivirus that can be scaled up or down.

We then successfully demonstrated delivery of EnvA-pseudotyped lentivirus encoding GFP by qPCR and immunohistochemistry into muscle and liver tissue expressing TVA receptor. We were

unable to demonstrate the same by immunofluorescence due to a high level of autofluorescence in these adult tissues. Interestingly, autofluorescence is now used to analyse organ functionality during diseased states (Croce et al, 2014) yet many published studies have used this technique to show gene delivery without demonstrating valid controls (Pfeifer et al, 2001).

Using the TVA system we intend to introduce desired candidates that we have hypothesised to cause neoplasia from our *in vitro* studies by using the 2A peptide bridges. These peptide bridges have allowed expression of equimolar ratio of 2 or more heterologous genes driven via a single promoter (Mehta et al, 2009). The most pertinent study in this regard has shown that constitutive EGFR could induce gliomas only in combination with *cdk4* (cyclin dependent kinase 4) but not in conjunction with *p53* deficiency (Holland et al, 1998). Based on this strategy we intend to use the 2A peptide bridges to make constructs with combination of GHR (constitutively active full-length cys mutant (Chapter 3), gain of function variant P495TGHR (Chapter 4), nuclear localised GHR (Conway-Campbell et al, 2007), jun zipper construct (Behncken et al, 2000) (Brooks et al, 2014) in combination with previously established oncogenes (*cdk4*, *c-myc*, *Braf*, *Ras*, etc), transcription factors (STAT1/3/5) and signalling molecules (Src/lyn, Akt, Ras) to dissect the pathway of GHR-mediated oncogenesis *in vivo*.

To aid in this detection, we have generated TVA system in zebrafish for the first time and shown that these zebrafish were amenable to EnvA-pseudotyped lentiviral infections and anticipate that similar to TVA mouse models, tissue specific *tva*-zebrafish can also be generated and used in future.

Cancer incidences and longevity in GHR knockin and knockout mouse models

Phenotypic and genotypic characteristics of all living organisms are determined by the interplay of genetic and environmental influences, and this applies to the control of aging and cancer development. There is solid evidence that the endocrine system plays an important role in mediating the impact of genetic and environmental factors on physiological processes. Mice with mutations causing a deficiency of GH or resistance to its actions are long-lived (Ikeno et al, 2009) (Junnila et al, 2013), and humans with similar mutations are protected from cancer, diabetes and other diseases (Guevara-Aguirre et al, 2011). A series of key observations have led to a growing convergence between the biology of ageing and the mechanisms that underlie cancer. It is not yet clear as to how and where these two processes merge and where their mechanisms diverge. However, the last few decades have witnessed an increase in identification of hundreds of potential cancer-related targets

for therapeutic development. Of note is the observation that selective anti-cancer drugs can prolong lifespan in Drosophila (Danilov et al, 2013).

In this chapter we have explored the pathways and evaluated molecules that may provide protection against cancer and/or promote lifespan extension in GHR mouse models lacking the full repertoire of GHR signalling. For our study all animals in the same genetic background (C57Bl/6) were subjected to similar husbandry conditions and the common attribute to all these mutant mice was lack of GH-induced STAT5 activation and therefore reduced IGF-1 and high GH serum levels. We observed that while female mice lacking GHR-STAT5 activation have substantial lifespan extension (20-26%), males did not, despite having similarly low plasma IGF-1 levels. However, in mice with targeted mutation to the Box1 motif, hence unable to activate Jak2 but able to activate Src family kinases (SFK), life extension was evident in both male and females (females 45%, males 15%).

In the same study we also analysed the cause of death initially based on gross morphology, which was indicative of reduced macroscopic tumour incidences in most GHR mutant males and females with no cancer-related death in GHR K4 male and strikingly high levels in K4 females. While both GHR K4 mutants are long lived, the contrasting cancer incidences can be attributed to sexual dimorphic SFK activation evident in age-matched hepatic tissue. This finding needs to be evaluated on other metabolically active tissues and to determine the downstream genes that may be regulated/activated and responsible for common lifespan extension and differential cancer modalities evident in GHR K4 males and females.

While no correlation was evident between lack of GH-induced STAT5 activation (reduced IGF-1 levels in the circulation) and lymphoma incidence upon histopathological analysis of tumours, there was reduction in lymphoma aggressiveness in females that could therefore be responsible for increased median and maximal lifespan. Interestingly, increased SFK activation in GHR K4 females could be attributed to other cancer modalities evident in these mice. In males however, reduced IGF-1 levels were not responsible to lifespan but could be credited for reduced cancer incidences in most mutants.

Upon analysis of young male mutants for determining reduced cancer incidence, we found that GHR mutant models have increased mitochondrial protein levels for the OxPhos complex, which may be the direct outcome of persistently active energy sensor kinase, AMPK, even in fed conditions, to maintain steady ATP levels. The elevated AMPK activity implies a continuous

energy deprivation state also observed during calorie restriction (Canto & Auwerx, 2009) and metformin administration for cancer treatment (Shaw et al, 2005). In support of elevated AMPK activity, these mutant models have reduced serum glucose levels and increased insulin sensitivity when analysed at 12weeks of age. The elevated insulin sensitivity was also associated with increased insulin receptor and decreased PTP1B and IRS1 protein levels.

Dampening of growth signalling has been shown to protect against age-related diseases including cancer (Burhans & Weinberger, 2007). This was consistent with increased levels of SOCS proteins and reduced levels of EGFR, Akt2, and IGF-1R in hepatic tissue of GHR mutants. The elevated levels of total and active STAT3 as a result of reduced GH-mediated STAT5 activation has been associated with increased hepatic steatosis (Barclay et al, 2011) rather than cancer. During cancer progression, transformed cells shift their metabolism from aerobic respiration to glycolysis to meet increased energy requirements and create a hypoxic environment in the core, which in turn increases inflammation and modulates metabolic reprogramming (Semenza, 2010). The HIF-1α generated during hypoxia has been shown to be stabilised by ROS/RNS (Chandel et al, 2000). In cultured cells, AMPK was shown to be activated by ROS and RNS (Fujita et al, 2010) which might be secondary to inhibition of mitochondrial ATP synthesis, with consequent rises in AMP and ADP levels (Hawley et al, 2010). In the GHR mutants, however, while there is increased mitochondrial activity and AMPK activation there are also increased enzymes to reduce unwanted ROS/RNS.

The GHR mutants appear able to manage oxidative stress by detoxification of ROS generated during physiological processes. Most young mutant mice express elevated levels of antioxidative enzymes SOD1 and SOD2 while all young and old GHR K2 female mutants expressed increased levels of Nrf2, the master regulator of antioxidant responses as well numerous Nrf2 regulated genes.

While there is increased expression of mitochondrial progenitor (PGC1α) in mutants there was no evident increase in mitochondrial numbers. Mitochondrial Sirt3 and nuclear Sirt1 were also elevated in all young male mutants. The sirtuins are implicated in positive regulation of mitochondrial pathways as well as in stress responses and longevity (Haigis & Sinclair, 2010) where they deacetylate proteins to control protein-protein interaction, protein stability, cellular localisation or modulate enzymatic activity. Sirt3 has the ability to integrate cellular energy metabolism and ROS generation and has been proposed to be a prominent regulator in CR adaptation by coordinately deacetylating proteins involved in diverse pathways of metabolism and mitochondrial maintenance (Hebert et al, 2013). Moreover, GHR mutants are expected to have reduced inflammation based on upregulation of anti-inflammatory cytokine receptors (IL-10R) and

pro-inflammatory receptor antagonist (IL-1RA) as well reduced activity of p38 stress kinase in young male mutants.

In order to determine why GHR mutants lacking GH-mediated STAT5 activation exhibit sexually dimorphic effects in lifespan extension, we have analysed metabolically active tissues of 78weeks old GHR K2 males and females with age and gender-matched WT. We have obtained contrasting results in comparison to young mice with key antioxidants and mitochondrial proteins favouring only females over males along with higher plasma antioxidant levels in female mutants only. Another important observation in this study was the retention of active AMPK, Sirt1 and Sirt3 protein levels in the liver of aged GHR KO males, and although there was an age-associated decline, levels were clearly elevated as compared to age-matched WT males. Based on the existing literature this would imply that GHR KO males should exhibit cancer resistance and lifespan extension. The latter was not evident indicating that separate pathways exist for protection against cancer and lifespan extension. This is in contrast to the earlier report suggesting reduction in AMPK activity and mitochondrial biogenesis as the cause for aging (Reznick et al, 2007).

This study suggests a universal role for IGF-1 deficiency in cancer resistance or aggressiveness but not in longevity. While resistance against cancer seems to be a combination of multiple factors (fig.9.3) such as increased insulin sensitivity, increased mitochondrial function, increased stress resistance, reduced inflammation markers and reduced growth-promoting pathways, none of these individually or in combination support the increased lifespan extension we observe in the GHR mutants, and we are seeking the molecular basis for this differential effect.

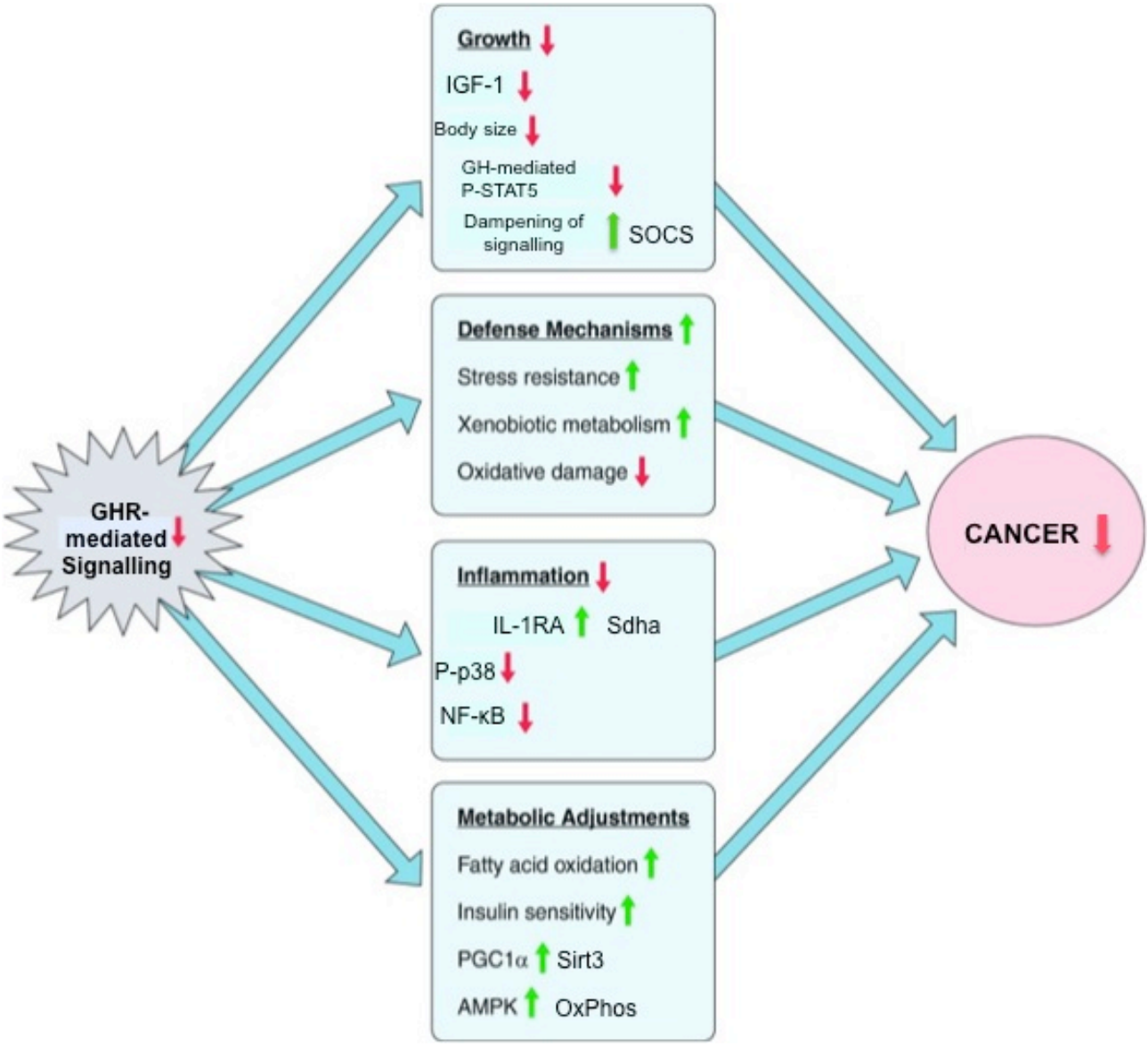

Figure 9.3: Mechanisms involved in resistance towards cancer owing to reduced/lack of GHR-mediated signalling

Developed from (Bartke et al, 2013).

Future Directions

Given the animal and human data supporting critical involvement of the GH/IGF-1 axis in cancer incidence and progression, the development of GH antagonists for use alone or in conjunction with IGF-1R blockers, is of key importance. While pegvisomant is partially effective in suppressing cancer in animal models and autocrine cancers, it is disadvantaged by high cost and likely impairment of its action by elevated plasma GH resulting from lowered IGF-1 feedback. Therefore, other means of limiting GH action are needed and would require the knowledge of the mechanism of activation of GHR we have provided. However, the recently proposed model of GHR-mediated Jak2 activation by our group has a much broader relevance and could be extended to other Class I cytokine receptors. Using the cysteine crosslinking analysis, we were able to make the first constitutively active full-length GHR constructs that will be analysed in *tva*-zebrafish model to show their effect *in vivo* in a tissue-specific or ubiquitous manner. In addition, it remains to be seen if these cysteine mutants have the ability to activate other GH-mediated pathways such as SFK. Simultaneously, there is a gap in determining the precise mechanism of SFK activation and role of Lyn binding to Jak2 at physiological levels. More research is warranted to determine:

1) If Lyn binding to GHR truncations can activate signalling pathways upon GH stimulation or requires the full downstream cytosolic region on GHR to trigger activation.
2) If Lyn activate can phosphorylate the GHR in a Jak2-deficient (γ2A fibrosarcoma) cell line and stably transduced FDC-P1 cell line.
3) The subcellular localisation where Lyn and GHR binding occurs? Is it only at the surface due to myristoylation of Lyn.
4) If Lyn binds to Jak2 and the effect of GH/GHR on this binding as well as its kinase activity.
5) If Lyn binding mediates STAT5 activation via GHR and if this is cell-line dependent.
6) If GHR binding to other SFK members follows similar attributes to that of Lyn.

Recent emerging findings on GHR polymorphisms in relation to GH responsiveness and disease susceptibilities have given significant attention on *in vitro* receptor signalling outcomes. Although over 60 loss of function mutations in GHR have been associated with deficient post-natal growth, to date no constitutively active GHR mutation has been reported. Our study currently in progress is aimed at identifying novel mutations in GHR, STAT5, Jak2, and GH in clinical prostate cancer tissues. In addition, we seek to determine the basis of the GH-independent receptor fragments observed in WT GHR lysates as compared to P495TGHR. There is also a possibility of lysosomal rather than proteasomal-mediated degradation that may be involved in the control of basal level of GHR degradation. This will be analysed by pre-treatment of the HEK293 stables with specific

inhibitors such as chloroquine, and leupeptin. Based on the P495 adjacent sequence analogy to the cdc4 recognition sequence, a physical interaction of cdc4 and GHR remains to be evaluated by co-IP. Finally, to confirm the role of SOCS2 in decreased GH-mediated P495TGHR degradation, SOCS2 co-IP in Ba/F3 and Beas-2B stables at 60minutes time point (when the difference in receptor level is quite apparent) would be beneficial. In support of the same, surface GHR degradation in P495TGHR needs to be analysed using BFA in the presence of SOCS2.

Although substantial evidence supports a causal role for the GH/IGF-1 axis in cancer, important questions remain unanswered with respect to the utility of GH antagonism in cancer. While we were able to show a differential effect of the level of autocrine hGH *in vitro*, this needs to be substantiated using GH antagonists in both MCF-7 stables (CMV *vs* MT) as well as by xenograft and autocrine models *in vivo*. In addition, cell survival assays and other typical cancer 'hallmark' assays such as invasion, migration and spheroid assays need to be performed at the differential autocrine GH levels. An important goal would be to determine the signalling pathways and the cellular localisation of signal in both these models as well as any miRNA that may be involved in modulating differential effects of autocrine GH or as a consequence of it.

A Tet-regulated system would serve as a suitable model to confirm the 'cancer like' effects of low levels of autocrine GH, although this time the expression will be driven via the same promoter to reduce further variables. This would allow one to control the relative levels of GH and GHR and determine a threshold level of GH, beyond which it is non-tumourigenic. Finally, these experiments need to be performed in the other cancer cells such as LNCaP to confirm a broader applicability of our hypothesis and bridge the gap in knowledge between published studies. Based on our preliminary and anticipated future results, we would be able to explain the ineffectiveness of pegvisomant in treatment of certain tumours and also draw much needed attention towards the design and use of more antisense oligonucleotide inhibitors specific to GHR per se. These would directly control GHR availability as opposed to G120R-mediated reduced signalling that is actually dependent on unbound GHR availability in the first place.

The direct oncogenic potential of GHR needs to be evaluated in different cancer models. Physiologically, it may involve gene amplification, activating mutations in GHR or downstream molecule that requires GHR for signalling (similar to Jak2V617F). While the former will be analysed from prostate cancer slides, we intend to evaluate the latter using constitutively active and nuclear-localised GHR starting with prostate cancer model (LNCaP) cell lines and extend it *in vivo* using the RCAS/TVA system that we have established.

Using the GHR mutant models we plan to continue the determination of cancer incidences, burden and modality in comparison to WT for both genders (increasing mouse number as and when available), in conjunction with the histopathologist. A considerable amount of work also needs to be done to determine the sexually dimorphic pattern of lifespan extension in GHR KO and K2 mutants and in contrast the sex-independent longevity observed in GHR K4. Such a task would require microarray analysis to determine differentially expressed transcripts (and miRNA) and protein as well as pertinent antioxidants and stress assays (*in vivo* or on fibroblasts extracted from mice). Specific mitochondrial activity assays and acetylation status to evaluate the role of sirtuins will be undertaken in metabolically active tissues from both young and old mice. In addition, the GHR K4 mutant females will be studied in detail to determine if increased SFK activation is prevalent in other tissues and the probable cause of cancer modalities not common to C57Bl/6 strain. Based on current literature, the role of estrogen-mediated signalling will be further explored.

Nevertheless, clinical trials of pegvisomant in cancer in conjunction with other adjuvant therapies appear warranted. The ability of GH and IGF-1 to confer resistance to radiotherapy and chemotherapy is a further reason for use of GH antagonists. Given the potential role of GH in promoting stem cell activation, one can expect to see translational studies relating GH action to cancer stem cells and GH. In the near future, we can expect small molecule agonists and antagonists, tissue-specific deletion of the receptor and many surprises to provide novel understandings of the physiological actions of this pleiotropic cytokine.

References

REFERENCES

Aalbers AM, Chin D, Pratt KL, Little BM, Frank SJ, Hwa V, Rosenfeld RG (2009) Extreme elevation of serum growth hormone-binding protein concentrations resulting from a novel heterozygous splice site mutation of the growth hormone receptor gene. *Hormone research* **71:** 276-284

Adams TE, Hansen JA, Starr R, Nicola NA, Hilton DJ, Billestrup N (1998) Growth hormone preferentially induces the rapid, transient expression of SOCS-3, a novel inhibitor of cytokine receptor signaling. *The Journal of biological chemistry* **273:** 1285-1287

Adkins HB, Brojatsch J, Young JA (2000) Identification and characterization of a shared TNFR-related receptor for subgroup B, D, and E avian leukosis viruses reveal cysteine residues required specifically for subgroup E viral entry. *Journal of virology* **74:** 3572-3578

Aguirre-Ghiso JA, Estrada Y, Liu D, Ossowski L (2003) ERK(MAPK) activity as a determinant of tumor growth and dormancy; regulation by p38(SAPK). *Cancer research* **63:** 1684-1695

Ahmad A, Banerjee S, Wang Z, Kong D, Majumdar AP, Sarkar FH (2009) Aging and inflammation: etiological culprits of cancer. *Current aging science* **2:** 174-186

Ahn BH, Kim HS, Song S, Lee IH, Liu J, Vassilopoulos A, Deng CX, Finkel T (2008) A role for the mitochondrial deacetylase Sirt3 in regulating energy homeostasis. *Proceedings of the National Academy of Sciences of the United States of America* **105:** 14447-14452

Ahonen TJ, Xie J, LeBaron MJ, Zhu J, Nurmi M, Alanen K, Rui H, Nevalainen MT (2003) Inhibition of transcription factor Stat5 induces cell death of human prostate cancer cells. *The Journal of biological chemistry* **278:** 27287-27292

Ajo R, Cacicedo L, Navarro C, Sanchez-Franco F (2003) Growth hormone action on proliferation and differentiation of cerebral cortical cells from fetal rat. *Endocrinology* **144:** 1086-1097

Al-Regaiey KA (2013) Effect of Growth Hormone and Calorie Restriction on the Expression of Antioxidant Enzymes in the Liver and Kidney of Growth Hormone Receptor Knockout Mice. *Atlas Journal of Biology* **2:** 136-141

Al-Regaiey KA, Masternak MM, Bonkowski M, Sun L, Bartke A (2005) Long-lived growth hormone receptor knockout mice: interaction of reduced insulin-like growth factor i/insulin signaling and caloric restriction. *Endocrinology* **146:** 851-860

Alderman JM, Flurkey K, Brooks NL, Naik SB, Gutierrez JM, Srinivas U, Ziara KB, Jing L, Boysen G, Bronson R, Klebanov S, Chen X, Swenberg JA, Stridsberg M, Parker CE, Harrison DE, Combs TP (2009) Neuroendocrine inhibition of glucose production and resistance to cancer in dwarf mice. *Experimental gerontology* **44:** 26-33

Allevato G, Billestrup N, Goujon L, Galsgaard ED, Norstedt G, Postel-Vinay MC, Kelly PA, Nielsen JH (1995) Identification of phenylalanine 346 in the rat growth hormone receptor as being critical for ligand-mediated internalization and down-regulation. *The Journal of biological chemistry* **270:** 17210-17214

Alsat E, Guibourdenche J, Couturier A, Evain-Brion D (1998) Physiological role of human placental growth hormone. *Molecular and cellular endocrinology* **140:** 121-127

Alves dos Santos CM, ten Broeke T, Strous GJ (2001) Growth hormone receptor ubiquitination, endocytosis, and degradation are independent of signal transduction via Janus kinase 2. *The Journal of biological chemistry* **276:** 32635-32641

Amador-Noguez D, Dean A, Huang W, Setchell K, Moore D, Darlington G (2007) Alterations in xenobiotic metabolism in the long-lived Little mice. *Aging cell* **6:** 453-470

Amador-Noguez D, Zimmerman J, Venable S, Darlington G (2005) Gender-specific alterations in gene expression and loss of liver sexual dimorphism in the long-lived Ames dwarf mice. *Biochemical and biophysical research communications* **332:** 1086-1100

Amit T, Bergman T, Dastot F, Youdim MB, Amselem S, Hochberg Z (1997) A membrane-fixed, truncated isoform of the human growth hormone receptor. *The Journal of clinical endocrinology and metabolism* **82:** 3813-3817

Andersen M (2014) Management of endocrine disease: GH excess: diagnosis and medical therapy. *European journal of endocrinology / European Federation of Endocrine Societies* **170:** R31-41

Andersson H, Baechi T, Hoechl M, Richter C (1998) Autofluorescence of living cells. *J Microsc* **191:** 1-7

Andreassen M, Frystyk J, Faber J, Kristensen LO (2012) GH activity and markers of inflammation: a crossover study in healthy volunteers treated with GH and a GH receptor antagonist. *European journal of endocrinology / European Federation of Endocrine Societies* **166:** 811-819

Anisimov VN (2001) Mutant and genetically modified mice as models for studying the relationship between aging and carcinogenesis. *Mechanisms of ageing and development* **122:** 1221-1255

Aoki N, Matsuda T (2000) A cytosolic protein-tyrosine phosphatase PTP1B specifically dephosphorylates and deactivates prolactin-activated STAT5a and STAT5b. *The Journal of biological chemistry* **275:** 39718-39726

Arbet-Engels C, Tartare-Deckert S, Eckhart W (1999) C-terminal Src kinase associates with ligand-stimulated insulin-like growth factor-I receptor. *The Journal of biological chemistry* **274:** 5422-5428

Argetsinger LS, Campbell GS, Yang X, Witthuhn BA, Silvennoinen O, Ihle JN, Carter-Su C (1993) Identification of JAK2 as a growth hormone receptor-associated tyrosine kinase. *Cell* **74:** 237-244

Argetsinger LS, Carter-Su C (1996) Growth hormone signalling mechanisms: involvement of the tyrosine kinase JAK2. *Hormone research* **45 Suppl 1:** 22-24

Argetsinger LS, Kouadio JL, Steen H, Stensballe A, Jensen ON, Carter-Su C (2004) Autophosphorylation of JAK2 on tyrosines 221 and 570 regulates its activity. *Molecular and cellular biology* **24:** 4955-4967

Argetsinger LS, Stuckey JA, Robertson SA, Koleva RI, Cline JM, Marto JA, Myers MG, Jr., Carter-Su C (2010) Tyrosines 868, 966, and 972 in the kinase domain of JAK2 are

autophosphorylated and required for maximal JAK2 kinase activity. *Molecular endocrinology* **24:** 1062-1076

Arnold RE, Weigent DA (2003) The inhibition of superoxide production in EL4 lymphoma cells overexpressing growth hormone. *Immunopharmacology and immunotoxicology* **25:** 159-177

Asakawa K, Hizuka N, Takano K, Horikawa R, Sukegawa I, Toyoda C, Shizume K (1989) Human growth hormone stimulates liver regeneration in rats. *Journal of endocrinological investigation* **12:** 343-347

Ashraf N, Zino S, Macintyre A, Kingsmore D, Payne AP, George WD, Shiels PG (2006) Altered sirtuin expression is associated with node-positive breast cancer. *British journal of cancer* **95:** 1056-1061

Auboeuf D, Dowhan DH, Li X, Larkin K, Ko L, Berget SM, O'Malley BW (2004) CoAA, a nuclear receptor coactivator protein at the interface of transcriptional coactivation and RNA splicing. *Molecular and cellular biology* **24:** 442-453

Ayling RM, Ross RJ, Towner P, Von Laue S, Finidori J, Moutoussamy S, Buchanan CR, Clayton PE, Norman MR (1999) New growth hormone receptor exon 9 mutation causes genetic short stature. *Acta Paediatr Suppl* **88:** 168-172; discussion 173

Azpurua J, Yang JN, Van Meter M, Liu Z, Kim J, Lobo Ladd AA, Coppi AA, Gorbunova V, Seluanov A (2013) IGF1R levels in the brain negatively correlate with longevity in 16 rodent species. *Aging* **5:** 304-314

Baek JY, Han SH, Sung SH, Lee HE, Kim YM, Noh YH, Bae SH, Rhee SG, Chang TS (2012) Sulfiredoxin protein is critical for redox balance and survival of cells exposed to low steady-state levels of H2O2. *The Journal of biological chemistry* **287:** 81-89

Balciunas D, Wangensteen KJ, Wilber A, Bell J, Geurts A, Sivasubbu S, Wang X, Hackett PB, Largaespada DA, McIvor RS, Ekker SC (2006) Harnessing a high cargo-capacity transposon for genetic applications in vertebrates. *PLoS genetics* **2:** e169

Baldys-Waligorska A, Krzentowska A, Golkowski F, Sokolowski G, Hubalewska-Dydejczyk A (2010) The prevalence of benign and malignant neoplasms in acromegalic patients. *Endokrynologia Polska* **61:** 29-34

Ballesteros M, Leung KC, Ross RJ, Iismaa TP, Ho KK (2000) Distribution and abundance of messenger ribonucleic acid for growth hormone receptor isoforms in human tissues. *The Journal of clinical endocrinology and metabolism* **85:** 2865-2871

Bandaranayake RM, Ungureanu D, Shan Y, Shaw DE, Silvennoinen O, Hubbard SR (2012) Crystal structures of the JAK2 pseudokinase domain and the pathogenic mutant V617F. *Nature structural & molecular biology* **19:** 754-759

Banks AS, Kon N, Knight C, Matsumoto M, Gutierrez-Juarez R, Rossetti L, Gu W, Accili D (2008) SirT1 gain of function increases energy efficiency and prevents diabetes in mice. *Cell metabolism* **8:** 333-341

Barabutis N, Schally AV (2008) Antioxidant activity of growth hormone-releasing hormone antagonists in LNCaP human prostate cancer line. *Proceedings of the National Academy of Sciences of the United States of America* **105:** 20470-20475

Barber MF, Michishita-Kioi E, Xi Y, Tasselli L, Kioi M, Moqtaderi Z, Tennen RI, Paredes S, Young NL, Chen K, Struhl K, Garcia BA, Gozani O, Li W, Chua KF (2012) SIRT7 links H3K18 deacetylation to maintenance of oncogenic transformation. *Nature* **487:** 114-118

Barbour LA, Mizanoor Rahman S, Gurevich I, Leitner JW, Fischer SJ, Roper MD, Knotts TA, Vo Y, McCurdy CE, Yakar S, Leroith D, Kahn CR, Cantley LC, Friedman JE, Draznin B (2005) Increased P85alpha is a potent negative regulator of skeletal muscle insulin signaling and induces in vivo insulin resistance associated with growth hormone excess. *The Journal of biological chemistry* **280:** 37489-37494

Barclay JL, Kerr LM, Arthur L, Rowland JE, Nelson CN, Ishikawa M, d'Aniello EM, White M, Noakes PG, Waters MJ (2010) In vivo targeting of the growth hormone receptor (GHR) Box1 sequence demonstrates that the GHR does not signal exclusively through JAK2. *Molecular endocrinology* **24:** 204-217

Barclay JL, Nelson CN, Ishikawa M, Murray LA, Kerr LM, McPhee TR, Powell EE, Waters MJ (2011) GH-dependent STAT5 signaling plays an important role in hepatic lipid metabolism. *Endocrinology* **152:** 181-192

Barretina J, Caponigro G, Stransky N, Venkatesan K, Margolin AA, Kim S, Wilson CJ, Lehar J, Kryukov GV, Sonkin D, Reddy A, Liu M, Murray L, Berger MF, Monahan JE, Morais P, Meltzer J, Korejwa A, Jane-Valbuena J, Mapa FA, Thibault J, Bric-Furlong E, Raman P, Shipway A, Engels IH, Cheng J, Yu GK, Yu J, Aspesi P, Jr., de Silva M, Jagtap K, Jones MD, Wang L, Hatton C, Palescandolo E, Gupta S, Mahan S, Sougnez C, Onofrio RC, Liefeld T, MacConaill L, Winckler W, Reich M, Li N, Mesirov JP, Gabriel SB, Getz G, Ardlie K, Chan V, Myer VE, Weber BL, Porter J, Warmuth M, Finan P, Harris JL, Meyerson M, Golub TR, Morrissey MP, Sellers WR, Schlegel R, Garraway LA (2012) The Cancer Cell Line Encyclopedia enables predictive modelling of anticancer drug sensitivity. *Nature* **483:** 603-607

Barsov EV, Huber WE, Marcotrigiano J, Clark PK, Clark AD, Arnold E, Hughes SH (1996) Inhibition of human immunodeficiency virus type 1 integrase by the Fab fragment of a specific monoclonal antibody suggests that different multimerization states are required for different enzymatic functions. *Journal of virology* **70:** 4484-4494

Barsov EV, Payne WS, Hughes SH (2001) Adaptation of chimeric retroviruses in vitro and in vivo: isolation of avian retroviral vectors with extended host range. *Journal of virology* **75:** 4973-4983

Bartke A (2000) Delayed aging in Ames dwarf mice. Relationships to endocrine function and body size. *Results and problems in cell differentiation* **29:** 181-202

Bartke A (2003) Can growth hormone (GH) accelerate aging? Evidence from GH-transgenic mice. *Neuroendocrinology* **78:** 210-216

Bartke A, Sun LY, Longo V (2013) Somatotropic signaling: trade-offs between growth, reproductive development, and longevity. *Physiological reviews* **93:** 571-598

Bartke A, Westbrook R (2012) Metabolic characteristics of long-lived mice. *Frontiers in genetics* **3:** 288

Bass J (2013) Forever (FGF) 21. *Nature medicine* **19:** 1090-1092

Bates P, Young JA, Varmus HE (1993) A receptor for subgroup A Rous sarcoma virus is related to the low density lipoprotein receptor. *Cell* **74:** 1043-1051

Baumann G (2001) Growth hormone binding protein 2001. *Journal of pediatric endocrinology & metabolism : JPEM* **14:** 355-375

Baumann G, Frank SJ (2002) Metalloproteinases and the modulation of GH signaling. *The Journal of endocrinology* **174:** 361-368

Baumgartner JW, Wells CA, Chen CM, Waters MJ (1994) The role of the WSXWS equivalent motif in growth hormone receptor function. *The Journal of biological chemistry* **269:** 29094-29101

Bazan JF (1990) Structural design and molecular evolution of a cytokine receptor superfamily. *Proceedings of the National Academy of Sciences of the United States of America* **87:** 6934-6938

Beaver CM, Ahmed A, Masters JR (2014) Clonogenicity: holoclones and meroclones contain stem cells. *PloS one* **9:** e89834

Beekman M, Blanche H, Perola M, Hervonen A, Bezrukov V, Sikora E, Flachsbart F, Christiansen L, De Craen AJ, Kirkwood TB, Rea IM, Poulain M, Robine JM, Valensin S, Stazi MA, Passarino G, Deiana L, Gonos ES, Paternoster L, Sorensen TI, Tan Q, Helmer Q, van den Akker EB, Deelen J, Martella F, Cordell HJ, Ayers KL, Vaupel JW, Tornwall O, Johnson TE, Schreiber S, Lathrop M, Skytthe A, Westendorp RG, Christensen K, Gampe J, Nebel A, Houwing-Duistermaat JJ, Slagboom PE, Franceschi C, consortium G (2013) Genome-wide linkage analysis for human longevity: Genetics of Healthy Aging Study. *Aging cell* **12:** 184-193

Behncken SN, Billestrup N, Brown R, Amstrup J, Conway-Campbell B, Waters MJ (2000) Growth hormone (GH)-independent dimerization of GH receptor by a leucine zipper results in constitutive activation. *The Journal of biological chemistry* **275:** 17000-17007

Behncken SN, Rowlinson SW, Rowland JE, Conway-Campbell BL, Monks TA, Waters MJ (1997) Aspartate 171 is the major primate-specific determinant of human growth hormone. Engineering porcine growth hormone to activate the human receptor. *The Journal of biological chemistry* **272:** 27077-27083

Behncken SN, Waters MJ (1999) Molecular recognition events involved in the activation of the growth hormone receptor by growth hormone. *Journal of molecular recognition : JMR* **12:** 355-362

Bell EL, Emerling BM, Ricoult SJ, Guarente L (2011) SirT3 suppresses hypoxia inducible factor 1alpha and tumor growth by inhibiting mitochondrial ROS production. *Oncogene* **30:** 2986-2996

Bell J, Parker KL, Swinford RD, Hoffman AR, Maneatis T, Lippe B (2010) Long-term safety of recombinant human growth hormone in children. *The Journal of clinical endocrinology and metabolism* **95:** 167-177

Benavente CA, Schnell SA, Jacobson EL (2012) Effects of niacin restriction on sirtuin and PARP responses to photodamage in human skin. *PloS one* **7:** e42276

Berg AH, Combs TP, Du X, Brownlee M, Scherer PE (2001) The adipocyte-secreted protein Acrp30 enhances hepatic insulin action. *Nature medicine* **7:** 947-953

Bergad PL, Shih HM, Towle HC, Schwarzenberg SJ, Berry SA (1995) Growth hormone induction of hepatic serine protease inhibitor 2.1 transcription is mediated by a Stat5-related factor binding synergistically to two gamma-activated sites. *The Journal of biological chemistry* **270:** 24903-24910

Bergan HE, Kittilson JD, Sheridan MA (2013) PKC and ERK mediate GH-stimulated lipolysis. *Journal of molecular endocrinology* **51:** 213-224

Bergeron JJ, Posner BI, Josefsberg Z, Sikstrom R (1978) Intracellular polypeptide hormone receptors. The demonstration of specific binding sites for insulin and human growth hormone in Golgi fractions isolated from the liver of female rats. *The Journal of biological chemistry* **253:** 4058-4066

Bernat B, Pal G, Sun M, Kossiakoff AA (2003) Determination of the energetics governing the regulatory step in growth hormone-induced receptor homodimerization. *Proceedings of the National Academy of Sciences of the United States of America* **100:** 952-957

Berryman DE, Christiansen JS, Johannsson G, Thorner MO, Kopchick JJ (2008) Role of the GH/IGF-1 axis in lifespan and healthspan: lessons from animal models. *Growth hormone & IGF research : official journal of the Growth Hormone Research Society and the International IGF Research Society* **18:** 455-471

Berryman DE, List EO, Coschigano KT, Behar K, Kim JK, Kopchick JJ (2004) Comparing adiposity profiles in three mouse models with altered GH signaling. *Growth hormone & IGF research : official journal of the Growth Hormone Research Society and the International IGF Research Society* **14:** 309-318

Beyea JA, Sawicki G, Olson DM, List E, Kopchick JJ, Harvey S (2006) Growth hormone (GH) receptor knockout mice reveal actions of GH in lung development. *Proteomics* **6:** 341-348

Bidosee M, Karry R, Weiss-Messer E, Barkey RJ (2011) Growth hormone affects gene expression and proliferation in human prostate cancer cells. *International journal of andrology* **34:** 124-137

Biener E, Martin C, Daniel N, Frank SJ, Centonze VE, Herman B, Djiane J, Gertler A (2003) Ovine placental lactogen-induced heterodimerization of ovine growth hormone and prolactin receptors in living cells is demonstrated by fluorescence resonance energy transfer microscopy and leads to prolonged phosphorylation of signal transducer and activator of transcription (STAT)1 and STAT3. *Endocrinology* **144:** 3532-3540

Biener-Ramanujan E, Ramanujan VK, Herman B, Gertler A (2006) Spatio-temporal kinetics of growth hormone receptor signaling in single cells using FRET microscopy. *Growth hormone & IGF research : official journal of the Growth Hormone Research Society and the International IGF Research Society* **16:** 247-257

Biller BM, Ji HJ, Ahn H, Savoy C, Siepl EC, Popovic V, Coculescu M, Roemmler J, Gavrila C, Cook DM, Strasburger CJ (2011) Effects of once-weekly sustained-release growth hormone: a double-blind, placebo-controlled study in adult growth hormone deficiency. *The Journal of clinical endocrinology and metabolism* **96:** 1718-1726

Billestrup N, Bouchelouche P, Allevato G, Ilondo M, Nielsen JH (1995) Growth hormone receptor C-terminal domains required for growth hormone-induced intracellular free Ca2+ oscillations and gene transcription. *Proceedings of the National Academy of Sciences of the United States of America* **92:** 2725-2729

Billestrup N, Nielsen JH (1991) The stimulatory effect of growth hormone, prolactin, and placental lactogen on beta-cell proliferation is not mediated by insulin-like growth factor-I. *Endocrinology* **129:** 883-888

Billinton N, Knight AW (2001) Seeing the wood through the trees: a review of techniques for distinguishing green fluorescent protein from endogenous autofluorescence. *Anal Biochem* **291:** 175-197

Binetruy B, Heasley L, Bost F, Caron L, Aouadi M (2007) Concise review: regulation of embryonic stem cell lineage commitment by mitogen-activated protein kinases. *Stem cells* **25:** 1090-1095

Bishop NA, Guarente L (2007) Two neurons mediate diet-restriction-induced longevity in C. elegans. *Nature* **447:** 545-549

Bjelakovic G, Nikolova D, Gluud C (2014) Antioxidant supplements and mortality. *Current opinion in clinical nutrition and metabolic care* **17:** 40-44

Bjorge JD, Jakymiw A, Fujita DJ (2000) Selected glimpses into the activation and function of Src kinase. *Oncogene* **19:** 5620-5635

Blackmore DG, Golmohammadi MG, Large B, Waters MJ, Rietze RL (2009) Exercise increases neural stem cell number in a growth hormone-dependent manner, augmenting the regenerative response in aged mice. *Stem cells* **27:** 2044-2052

Blackmore DG, Reynolds BA, Golmohammadi MG, Large B, Aguilar RM, Haro L, Waters MJ, Rietze RL (2012) Growth hormone responsive neural precursor cells reside within the adult mammalian brain. *Scientific reports* **2:** 250

Blackwell BN, Bucci TJ, Hart RW, Turturro A (1995) Longevity, body weight, and neoplasia in ad libitum-fed and diet-restricted C57BL6 mice fed NIH-31 open formula diet. *Toxicologic pathology* **23:** 570-582

Blott S, Kim JJ, Moisio S, Schmidt-Kuntzel A, Cornet A, Berzi P, Cambisano N, Ford C, Grisart B, Johnson D, Karim L, Simon P, Snell R, Spelman R, Wong J, Vilkki J, Georges M, Farnir F, Coppieters W (2003) Molecular dissection of a quantitative trait locus: a phenylalanine-to-tyrosine substitution in the transmembrane domain of the bovine growth hormone receptor is associated with a major effect on milk yield and composition. *Genetics* **163:** 253-266

Bluher M, Kahn BB, Kahn CR (2003) Extended longevity in mice lacking the insulin receptor in adipose tissue. *Science* **299:** 572-574

Bodzin AS, Wei Z, Hurtt R, Gu T, Doria C (2012) Gefitinib resistance in HCC mahlavu cells: upregulation of CD133 expression, activation of IGF-1R signaling pathway, and enhancement of IGF-1R nuclear translocation. *Journal of cellular physiology* **227:** 2947-2952

Boggon TJ, Eck MJ (2004) Structure and regulation of Src family kinases. *Oncogene* **23:** 7918-7927

Bokov AF, Garg N, Ikeno Y, Thakur S, Musi N, DeFronzo RA, Zhang N, Erickson RC, Gelfond J, Hubbard GB, Adamo ML, Richardson A (2011) Does reduced IGF-1R signaling in Igf1r+/- mice alter aging? *PloS one* **6:** e26891

Bonkowski MS, Rocha JS, Masternak MM, Al Regaiey KA, Bartke A (2006) Targeted disruption of growth hormone receptor interferes with the beneficial actions of calorie restriction. *Proceedings of the National Academy of Sciences of the United States of America* **103:** 7901-7905

Bonomini F, Filippini F, Hayek T, Aviram M, Keidar S, Rodella LF, Coleman R, Rezzani R (2010) Apolipoprotein E and its role in aging and survival. *Experimental gerontology* **45:** 149-157

Borges S, Moudilou E, Vouyovitch C, Chiesa J, Lobie P, Mertani H, Raccurt M (2008) Involvement of a JAK/STAT pathway inhibitor: cytokine inducible SH2 containing protein in breast cancer. *Advances in experimental medicine and biology* **617:** 321-329

Bosch-Presegue L, Vaquero A (2013) Sirtuins in stress response: guardians of the genome. *Oncogene*

Boudot C, Dasse E, Lambert E, Kadri Z, Mayeux P, Chretien S, Haye B, Billat C, Petitfrere E (2003) Involvement of the Src kinase Lyn in phospholipase C-gamma 2 phosphorylation and phosphatidylinositol 3-kinase activation in Epo signalling. *Biochemical and biophysical research communications* **300:** 437-442

Bougen NM, Steiner M, Pertziger M, Banerjee A, Brunet-Dunand SE, Zhu T, Lobie PE, Perry JK (2012) Autocrine human GH promotes radioresistance in mammary and endometrial carcinoma cells. *Endocrine-related cancer* **19:** 625-644

Bougen NM, Yang T, Chen H, Lobie PE, Perry JK (2011) Autocrine human growth hormone reduces mammary and endometrial carcinoma cell sensitivity to mitomycin C. *Oncology reports* **26:** 487-493

Bourgeais J, Gouilleux-Gruart V, Gouilleux F (2013) Oxidative metabolism in cancer: A STAT affair? *Jak-Stat* **2:** e25764

Bramnert M, Segerlantz M, Laurila E, Daugaard JR, Manhem P, Groop L (2003) Growth hormone replacement therapy induces insulin resistance by activating the glucose-fatty acid cycle. *The Journal of clinical endocrinology and metabolism* **88:** 1455-1463

Brodsky JL (2012) Cleaning up: ER-associated degradation to the rescue. *Cell* **151:** 1163-1167

Brojatsch J, Naughton J, Rolls MM, Zingler K, Young JA (1996) CAR1, a TNFR-related protein, is a cellular receptor for cytopathic avian leukosis-sarcoma viruses and mediates apoptosis. *Cell* **87:** 845-855

Bronson RT, Lipman RD (1991) Reduction in rate of occurrence of age related lesions in dietary restricted laboratory mice. *Growth, development, and aging : GDA* **55:** 169-184

Brooks AJ, Dai W, O'Mara ML, Abankwa D, Chhabra Y, Pelekanos RA, Gardon O, Tunny KA, Blucher KM, Morton CJ, Parker MW, Sierecki E, Gambin Y, Gomez GA, Alexandrov K, Wilson IA, Doxastakis M, Mark AE, Waters MJ (2014) A new cytokine receptor activation paradigm: activation of JAK2 by the Growth Hormone Receptor. *Science* **In press**

Brooks AJ, Waters MJ (2010) The growth hormone receptor: mechanism of activation and clinical implications. *Nature reviews Endocrinology* **6:** 515-525

Brooks AJ, Wooh JW, Tunny KA, Waters MJ (2008) Growth hormone receptor; mechanism of action. *The international journal of biochemistry & cell biology* **40:** 1984-1989

Brooks AR, Harkins RN, Wang P, Qian HS, Liu P, Rubanyi GM (2004) Transcriptional silencing is associated with extensive methylation of the CMV promoter following adenoviral gene delivery to muscle. *J Gene Med* **6:** 395-404

Brooks NL, Trent CM, Raetzsch CF, Flurkey K, Boysen G, Perfetti MT, Jeong YC, Klebanov S, Patel KB, Khodush VR, Kupper LL, Carling D, Swenberg JA, Harrison DE, Combs TP (2007) Low utilization of circulating glucose after food withdrawal in Snell dwarf mice. *The Journal of biological chemistry* **282:** 35069-35077

Brooks-Wilson AR (2013) Genetics of healthy aging and longevity. *Human genetics* **132:** 1323-1338

Brown K, Xie S, Qiu X, Mohrin M, Shin J, Liu Y, Zhang D, Scadden DT, Chen D (2013) SIRT3 reverses aging-associated degeneration. *Cell reports* **3:** 319-327

Brown MT, Cooper JA (1996) Regulation, substrates and functions of src. *Biochimica et biophysica acta* **1287:** 121-149

Brown RJ, Adams JJ, Pelekanos RA, Wan Y, McKinstry WJ, Palethorpe K, Seeber RM, Monks TA, Eidne KA, Parker MW, Waters MJ (2005) Model for growth hormone receptor activation based on subunit rotation within a receptor dimer. *Nature structural & molecular biology* **12:** 814-821

Brown-Borg HM, Bartke A (2012) GH and IGF1: roles in energy metabolism of long-living GH mutant mice. *The journals of gerontology Series A, Biological sciences and medical sciences* **67:** 652-660

Brown-Borg HM, Bode AM, Bartke A (1999) Antioxidative mechanisms and plasma growth hormone levels: potential relationship in the aging process. *Endocrine* **11:** 41-48

Brown-Borg HM, Johnson WT, Rakoczy SG (2012) Expression of oxidative phosphorylation components in mitochondria of long-living Ames dwarf mice. *Age* **34:** 43-57

Brown-Borg HM, Rakoczy SG (2000) Catalase expression in delayed and premature aging mouse models. *Experimental gerontology* **35:** 199-212

Brown-Borg HM, Rakoczy SG (2003) Growth hormone administration to long-living dwarf mice alters multiple components of the antioxidative defense system. *Mechanisms of ageing and development* **124:** 1013-1024

Brunet-Dunand SE, Vouyovitch C, Araneda S, Pandey V, Vidal LJ, Print C, Mertani HC, Lobie PE, Perry JK (2009) Autocrine human growth hormone promotes tumor angiogenesis in mammary carcinoma. *Endocrinology* **150:** 1341-1352

Bryksin A, Matsumura I (2013) Overlap extension PCR cloning. *Methods in molecular biology* **1073:** 31-42

Buler M, Aatsinki SM, Izzi V, Hakkola J (2012) Metformin reduces hepatic expression of SIRT3, the mitochondrial deacetylase controlling energy metabolism. *PloS one* **7:** e49863

Burdon RH (1995) Superoxide and hydrogen peroxide in relation to mammalian cell proliferation. *Free radical biology & medicine* **18:** 775-794

Burgers AM, Biermasz NR, Schoones JW, Pereira AM, Renehan AG, Zwahlen M, Egger M, Dekkers OM (2011) Meta-analysis and dose-response metaregression: circulating insulin-like growth factor I (IGF-I) and mortality. *The Journal of clinical endocrinology and metabolism* **96:** 2912-2920

Burhans WC, Weinberger M (2007) DNA replication stress, genome instability and aging. *Nucleic acids research* **35:** 7545-7556

Bussmann J, Schulte-Merker S (2011) Rapid BAC selection for tol2-mediated transgenesis in zebrafish. *Development* **138:** 4327-4332

Butler SL, Johnson EP, Bushman FD (2002) Human immunodeficiency virus cDNA metabolism: notable stability of two-long terminal repeat circles. *Journal of virology* **76:** 3739-3747

Calle EE, Kaaks R (2004) Overweight, obesity and cancer: epidemiological evidence and proposed mechanisms. *Nature reviews Cancer* **4:** 579-591

Campbell GS, Christian LJ, Carter-Su C (1993) Evidence for involvement of the growth hormone receptor-associated tyrosine kinase in actions of growth hormone. *The Journal of biological chemistry* **268:** 7427-7434

Campbell RA, Bhat-Nakshatri P, Patel NM, Constantinidou D, Ali S, Nakshatri H (2001) Phosphatidylinositol 3-kinase/AKT-mediated activation of estrogen receptor alpha: a new model for anti-estrogen resistance. *The Journal of biological chemistry* **276:** 9817-9824

Campeau E, Ruhl VE, Rodier F, Smith CL, Rahmberg BL, Fuss JO, Campisi J, Yaswen P, Cooper PK, Kaufman PD (2009) A versatile viral system for expression and depletion of proteins in mammalian cells. *PloS one* **4:** e6529

Cannata D, Fierz Y, Vijayakumar A, LeRoith D (2010) Type 2 diabetes and cancer: what is the connection? *The Mount Sinai journal of medicine, New York* **77:** 197-213

Canto C, Auwerx J (2009) PGC-1alpha, SIRT1 and AMPK, an energy sensing network that controls energy expenditure. *Current opinion in lipidology* **20:** 98-105

Canto C, Gerhart-Hines Z, Feige JN, Lagouge M, Noriega L, Milne JC, Elliott PJ, Puigserver P, Auwerx J (2009) AMPK regulates energy expenditure by modulating NAD+ metabolism and SIRT1 activity. *Nature* **458:** 1056-1060

Cao G, Lu H, Feng J, Shu J, Zheng D, Hou Y (2008) Lung cancer risk associated with Thr495Pro polymorphism of GHR in Chinese population. *Japanese journal of clinical oncology* **38:** 308-316

Caro JF, Poulos J, Ittoop O, Pories WJ, Flickinger EG, Sinha MK (1988) Insulin-like growth factor I binding in hepatocytes from human liver, human hepatoma, and normal, regenerating, and fetal rat liver. *The Journal of clinical investigation* **81:** 976-981

Carter-Su C, Argetsinger LS, Campbell GS, Wang X, Ihle J, Witthuhn B (1994) The identification of JAK2 tyrosine kinase as a signaling molecule for growth hormone. *Proc Soc Exp Biol Med* **206:** 210-215

Carter-Su C, Stubbart JR, Wang XY, Stred SE, Argetsinger LS, Shafer JA (1989) Phosphorylation of highly purified growth hormone receptors by a growth hormone receptor-associated tyrosine kinase. *The Journal of biological chemistry* **264:** 18654-18661

Casanueva FF (1992) Physiology of growth hormone secretion and action. *Endocrinology and metabolism clinics of North America* **21:** 483-517

Castro JR, Costoya JA, Gallego R, Prieto A, Arce VM, Senaris R (2000) Expression of growth hormone receptor in the human brain. *Neuroscience letters* **281:** 147-150

Caton PW, Nayuni NK, Kieswich J, Khan NQ, Yaqoob MM, Corder R (2010) Metformin suppresses hepatic gluconeogenesis through induction of SIRT1 and GCN5. *The Journal of endocrinology* **205:** 97-106

Cecchini G (2003) Function and structure of complex II of the respiratory chain. *Annual review of biochemistry* **72:** 77-109

Ceda GP, Davis RG, Rosenfeld RG, Hoffman AR (1987) The growth hormone (GH)-releasing hormone (GHRH)-GH-somatomedin axis: evidence for rapid inhibition of GHRH-elicited GH release by insulin-like growth factors I and II. *Endocrinology* **120:** 1658-1662

Chacon F, Esquifino AI, Perello M, Cardinali DP, Spinedi E, Alvarez MP (2005) 24-hour changes in ACTH, corticosterone, growth hormone, and leptin levels in young male rats subjected to calorie restriction. *Chronobiology international* **22:** 253-265

Chalkiadaki A, Guarente L (2012) Sirtuins mediate mammalian metabolic responses to nutrient availability. *Nature reviews Endocrinology* **8:** 287-296

Chan DC (2006) Mitochondria: dynamic organelles in disease, aging, and development. *Cell* **125:** 1241-1252

Chandel NS, McClintock DS, Feliciano CE, Wood TM, Melendez JA, Rodriguez AM, Schumacker PT (2000) Reactive oxygen species generated at mitochondrial complex III stabilize hypoxia-inducible factor-1alpha during hypoxia: a mechanism of O2 sensing. *The Journal of biological chemistry* **275:** 25130-25138

Chandrashekar V, Dawson CR, Martin ER, Rocha JS, Bartke A, Kopchick JJ (2007) Age-related alterations in pituitary and testicular functions in long-lived growth hormone receptor gene-disrupted mice. *Endocrinology* **148:** 6019-6025

Chatterjee-Kishore M, van den Akker F, Stark GR (2000) Association of STATs with relatives and friends. *Trends in cell biology* **10:** 106-111

Cheatham B, Vlahos CJ, Cheatham L, Wang L, Blenis J, Kahn CR (1994) Phosphatidylinositol 3-kinase activation is required for insulin stimulation of pp70 S6 kinase, DNA synthesis, and glucose transporter translocation. *Molecular and cellular biology* **14:** 4902-4911

Chen C, Brinkworth R, Waters MJ (1997) The role of receptor dimerization domain residues in growth hormone signaling. *The Journal of biological chemistry* **272:** 5133-5140

Chen HC, Appeddu PA, Isoda H, Guan JL (1996) Phosphorylation of tyrosine 397 in focal adhesion kinase is required for binding phosphatidylinositol 3-kinase. *The Journal of biological chemistry* **271:** 26329-26334

Chen WY, Wang DH, Yen RC, Luo J, Gu W, Baylin SB (2005) Tumor suppressor HIC1 directly regulates SIRT1 to modulate p53-dependent DNA-damage responses. *Cell* **123:** 437-448

Chen WY, Wight DC, Mehta BV, Wagner TE, Kopchick JJ (1991) Glycine 119 of bovine growth hormone is critical for growth-promoting activity. *Molecular endocrinology* **5:** 1845-1852

Cheng L, Ziegelhoffer PR, Yang NS (1993) In vivo promoter activity and transgene expression in mammalian somatic tissues evaluated by using particle bombardment. *Proceedings of the National Academy of Sciences of the United States of America* **90:** 4455-4459

Chhabra Y, Waters MJ, Brooks AJ (2011) Role of the growth hormone-IGF-1 axis in cancer. *Expert Review of Endocrinology and Metabolism* **6:** 71-84

Chia DJ, Ono M, Woelfle J, Schlesinger-Massart M, Jiang H, Rotwein P (2006a) Characterization of distinct Stat5b binding sites that mediate growth hormone-stimulated IGF-I gene transcription. *The Journal of biological chemistry* **281:** 3190-3197

Chia DJ, Subbian E, Buck TM, Hwa V, Rosenfeld RG, Skach WR, Shinde U, Rotwein P (2006b) Aberrant folding of a mutant Stat5b causes growth hormone insensitivity and proteasomal dysfunction. *The Journal of biological chemistry* **281:** 6552-6558

Chiappini F, Barrier A, Saffroy R, Domart MC, Dagues N, Azoulay D, Sebagh M, Franc B, Chevalier S, Debuire B, Dudoit S, Lemoine A (2006) Exploration of global gene expression in human liver steatosis by high-density oligonucleotide microarray. *Laboratory investigation; a journal of technical methods and pathology* **86:** 154-165

Chiesa J, Ferrer C, Arnould C, Vouyovitch CM, Diaz JJ, Gonzalez S, Mares P, Morel G, Wu ZS, Zhu T, Lobie PE, Mertani HC (2011) Autocrine proliferative effects of hGH are maintained in primary cultures of human mammary carcinoma cells. *The Journal of clinical endocrinology and metabolism* **96:** E1418-1426

Chin E, Zhou J, Bondy CA (1992) Renal growth hormone receptor gene expression: relationship to renal insulin-like growth factor system. *Endocrinology* **131:** 3061-3066

Chin H, Arai A, Wakao H, Kamiyama R, Miyasaka N, Miura O (1998) Lyn physically associates with the erythropoietin receptor and may play a role in activation of the Stat5 pathway. *Blood* **91:** 3734-3745

Choi J, Joseph L, Pilote L (2013) Obesity and C-reactive protein in various populations: a systematic review and meta-analysis. *Obesity reviews : an official journal of the International Association for the Study of Obesity* **14:** 232-244

Choi JH, Kim HS, Kim SH, Yang YR, Bae YS, Chang JS, Kwon HM, Ryu SH, Suh PG (2006) Phospholipase Cgamma1 negatively regulates growth hormone signalling by forming a ternary complex with Jak2 and protein tyrosine phosphatase-1B. *Nature cell biology* **8:** 1389-1397

Chopin LK, Veveris-Lowe TL, Philipps AF, Herington AC (2002) Co-expression of GH and GHR isoforms in prostate cancer cell lines. *Growth hormone & IGF research : official journal of the Growth Hormone Research Society and the International IGF Research Society* **12:** 126-136

Clackson T, Ultsch MH, Wells JA, de Vos AM (1998) Structural and functional analysis of the 1:1 growth hormone:receptor complex reveals the molecular basis for receptor affinity. *Journal of molecular biology* **277:** 1111-1128

Clancy DJ, Gems D, Harshman LG, Oldham S, Stocker H, Hafen E, Leevers SJ, Partridge L (2001) Extension of life-span by loss of CHICO, a Drosophila insulin receptor substrate protein. *Science* **292:** 104-106

Clark R, Olson K, Fuh G, Marian M, Mortensen D, Teshima G, Chang S, Chu H, Mukku V, Canova-Davis E, Somers T, Cronin M, Winkler M, Wells JA (1996) Long-acting growth hormones produced by conjugation with polyethylene glycol. *The Journal of biological chemistry* **271:** 21969-21977

Clarkson RW, Shang CA, Levitt LK, Howard T, Waters MJ (1999) Ternary complex factors Elk-1 and Sap-1a mediate growth hormone-induced transcription of egr-1 (early growth response factor-1) in 3T3-F442A preadipocytes. *Molecular endocrinology* **13:** 619-631

Claustres M, Chatelain P, Sultan C (1987) Insulin-like growth factor I stimulates human erythroid colony formation in vitro. *The Journal of clinical endocrinology and metabolism* **65:** 78-82

Clayton PE, Freeth JS, Whatmore AJ, Ayling RM, Norman MR, Silva CM (1999) Signal transduction defects in growth hormone insensitivity. *Acta Paediatr Suppl* **88:** 174-178; discussion 179

Clemmons DR (2002) Roles of insulin-like growth factor-I and growth hormone in mediating insulin resistance in acromegaly. *Pituitary* **5:** 181-183

Clevenger CV, Chang WP, Ngo W, Pasha TL, Montone KT, Tomaszewski JE (1995) Expression of prolactin and prolactin receptor in human breast carcinoma. Evidence for an autocrine/paracrine loop. *The American journal of pathology* **146:** 695-705

Cobb MH, Goldsmith EJ (1995) How MAP kinases are regulated. *The Journal of biological chemistry* **270:** 14843-14846

Cocca C, Martin G, Rivera E, Davio C, Cricco G, Lemos B, Fitzsimons C, Gutierrez A, Levin E, Levin R, Croci M, Bergoc RM (1998) An experimental model of diabetes and cancer in rats. *European journal of cancer* **34:** 889-894

Coculescu M, Niculescu D, Lichiardopol R, Purice M (2007) Insulin resistance and insulin secretion in non-diabetic acromegalic patients. *Experimental and clinical endocrinology & diabetes : official journal, German Society of Endocrinology [and] German Diabetes Association* **115:** 308-316

Colosi P, Wong K, Leong SR, Wood WI (1993) Mutational analysis of the intracellular domain of the human growth hormone receptor. *The Journal of biological chemistry* **268:** 12617-12623

Consortium GT (2013) The Genotype-Tissue Expression (GTEx) project. *Nature genetics* **45:** 580-585

Constantinescu SN, Girardot M, Pecquet C (2008) Mining for JAK-STAT mutations in cancer. *Trends in biochemical sciences* **33:** 122-131

Constantinescu SN, Keren T, Socolovsky M, Nam H, Henis YI, Lodish HF (2001) Ligand-independent oligomerization of cell-surface erythropoietin receptor is mediated by the transmembrane domain. *Proceedings of the National Academy of Sciences of the United States of America* **98:** 4379-4384

Conway-Campbell BL, Brooks AJ, Robinson PJ, Perani M, Waters MJ (2008) The extracellular domain of the growth hormone receptor interacts with coactivator activator to promote cell proliferation. *Molecular endocrinology* **22:** 2190-2202

Conway-Campbell BL, Wooh JW, Brooks AJ, Gordon D, Brown RJ, Lichanska AM, Chin HS, Barton CL, Boyle GM, Parsons PG, Jans DA, Waters MJ (2007) Nuclear targeting of the growth hormone receptor results in dysregulation of cell proliferation and tumorigenesis. *Proceedings of the National Academy of Sciences of the United States of America* **104:** 13331-13336

Coschigano KT, Clemmons D, Bellush LL, Kopchick JJ (2000) Assessment of growth parameters and life span of GHR/BP gene-disrupted mice. *Endocrinology* **141:** 2608-2613

Coschigano KT, Holland AN, Riders ME, List EO, Flyvbjerg A, Kopchick JJ (2003) Deletion, but not antagonism, of the mouse growth hormone receptor results in severely decreased body weights, insulin, and insulin-like growth factor I levels and increased life span. *Endocrinology* **144:** 3799-3810

Cousin SP, Hugl SR, Myers MG, Jr., White MF, Reifel-Miller A, Rhodes CJ (1999) Stimulation of pancreatic beta-cell proliferation by growth hormone is glucose-dependent: signal transduction via janus kinase 2 (JAK2)/signal transducer and activator of transcription 5 (STAT5) with no crosstalk to insulin receptor substrate-mediated mitogenic signalling. *The Biochemical journal* **344 Pt 3:** 649-658

Cowan JW, Wang X, Guan R, He K, Jiang J, Baumann G, Black RA, Wolfe MS, Frank SJ (2005) Growth hormone receptor is a target for presenilin-dependent gamma-secretase cleavage. *The Journal of biological chemistry* **280:** 19331-19342

Croce AC, Ferrigno A, Santin G, Piccolini VM, Bottiroli G, Vairetti M (2014) Autofluorescence of liver tissue and bile: Organ functionality monitoring during ischemia and reoxygenation. *Lasers in surgery and medicine*

Croker BA, Krebs DL, Zhang JG, Wormald S, Willson TA, Stanley EG, Robb L, Greenhalgh CJ, Forster I, Clausen BE, Nicola NA, Metcalf D, Hilton DJ, Roberts AW, Alexander WS (2003) SOCS3 negatively regulates IL-6 signaling in vivo. *Nature immunology* **4:** 540-545

Cummings DE, Merriam GR (1999) Age-related changes in growth hormone secretion: should the somatopause be treated? *Seminars in reproductive endocrinology* **17:** 311-325

Cunningham BC, Wells JA (1991) Rational design of receptor-specific variants of human growth hormone. *Proceedings of the National Academy of Sciences of the United States of America* **88:** 3407-3411

Currie RA, Walker KS, Gray A, Deak M, Casamayor A, Downes CP, Cohen P, Alessi DR, Lucocq J (1999) Role of phosphatidylinositol 3,4,5-trisphosphate in regulating the activity and localization of 3-phosphoinositide-dependent protein kinase-1. *The Biochemical journal* **337 (Pt 3):** 575-583

da Silva Almeida AC, Hocking HG, Boelens R, Strous GJ, van Rossum AG (2013) betaTrCP interacts with the ubiquitin-dependent endocytosis motif of the GH receptor in an unconventional manner. *The Biochemical journal* **453:** 291-301

da Silva Almeida AC, Strous GJ, van Rossum AG (2012) betaTrCP controls GH receptor degradation via two different motifs. *Molecular endocrinology* **26:** 165-177

Dagnaes-Hansen F, Duan H, Rasmussen LM, Friend KE, Flyvbjerg A (2004) Growth hormone receptor antagonist administration inhibits growth of human colorectal carcinoma in nude mice. *Anticancer research* **24:** 3735-3742

Dagvadorj A, Collins S, Jomain JB, Abdulghani J, Karras J, Zellweger T, Li H, Nurmi M, Alanen K, Mirtti T, Visakorpi T, Bubendorf L, Goffin V, Nevalainen MT (2007) Autocrine prolactin promotes prostate cancer cell growth via Janus kinase-2-signal transducer and activator of transcription-5a/b signaling pathway. *Endocrinology* **148:** 3089-3101

Dallas NA, Xia L, Fan F, Gray MJ, Gaur P, van Buren G, 2nd, Samuel S, Kim MP, Lim SJ, Ellis LM (2009) Chemoresistant colorectal cancer cells, the cancer stem cell phenotype, and increased sensitivity to insulin-like growth factor-I receptor inhibition. *Cancer research* **69:** 1951-1957

Dan L, Klimenkova O, Klimiankou M, Klusman JH, van den Heuvel-Eibrink MM, Reinhardt D, Welte K, Skokowa J (2012) The role of sirtuin 2 activation by nicotinamide phosphoribosyltransferase in the aberrant proliferation and survival of myeloid leukemia cells. *Haematologica* **97:** 551-559

Danilov A, Shaposhnikov M, Plyusnina E, Kogan V, Fedichev P, Moskalev A (2013) Selective anticancer agents suppress aging in Drosophila. *Oncotarget* **4:** 1507-1526

Danilovich N, Wernsing D, Coschigano KT, Kopchick JJ, Bartke A (1999) Deficits in female reproductive function in GH-R-KO mice; role of IGF-I. *Endocrinology* **140:** 2637-2640

Das C, Lucia MS, Hansen KC, Tyler JK (2009) CBP/p300-mediated acetylation of histone H3 on lysine 56. *Nature* **459:** 113-117

Dastot F, Sobrier ML, Duquesnoy P, Duriez B, Goossens M, Amselem S (1996) Alternatively spliced forms in the cytoplasmic domain of the human growth hormone (GH) receptor regulate its ability to generate a soluble GH-binding protein. *Proceedings of the National Academy of Sciences of the United States of America* **93:** 10723-10728

Davey HW, Xie T, McLachlan MJ, Wilkins RJ, Waxman DJ, Grattan DR (2001) STAT5b is required for GH-induced liver IGF-I gene expression. *Endocrinology* **142:** 3836-3841

Davidson MB (1987) Effect of growth hormone on carbohydrate and lipid metabolism. *Endocrine reviews* **8:** 115-131

de Benedictis G, Carrieri G, Varcasia O, Bonafe M, Franceschi C (2000) Inherited variability of the mitochondrial genome and successful aging in humans. *Annals of the New York Academy of Sciences* **908:** 208-218

de Ostrovich KK, Lambertz I, Colby JK, Tian J, Rundhaug JE, Johnston D, Conti CJ, DiGiovanni J, Fuchs-Young R (2008) Paracrine overexpression of insulin-like growth factor-1 enhances mammary tumorigenesis in vivo. *The American journal of pathology* **173:** 824-834

de Schepper J, Rasmussen MH, Gucev Z, Eliakim A, Battelino T (2011) Long-acting pegylated human GH in children with GH deficiency: a single-dose, dose-escalation trial investigating safety, tolerability, pharmacokinetics and pharmacodynamics. *European journal of endocrinology / European Federation of Endocrine Societies* **165:** 401-409

de Vos AM, Ultsch M, Kossiakoff AA (1992) Human growth hormone and extracellular domain of its receptor: crystal structure of the complex. *Science* **255:** 306-312

Dehari R, Nakamura Y, Okamoto N, Nakayama H (2008) Increased nuclear expression of growth hormone receptor in uterine cervical neoplasms of women under 40 years old. *The Tohoku journal of experimental medicine* **216:** 165-172

Deitel K, Dantzer D, Ferguson P, Pollak M, Beamer W, Andrulis I, Bell R (2002) Reduced growth of human sarcoma xenografts in hosts homozygous for the lit mutation. *Journal of surgical oncology* **81:** 75-79

Delenda C (2004) Lentiviral vectors: optimization of packaging, transduction and gene expression. *J Gene Med* **6 Suppl 1:** S125-138

Deng L, He K, Wang X, Yang N, Thangavel C, Jiang J, Fuchs SY, Frank SJ (2007) Determinants of growth hormone receptor down-regulation. *Molecular endocrinology* **21:** 1537-1551

Deng L, Jiang J, Frank SJ (2012) Growth hormone-induced JAK2 signaling and GH receptor down-regulation: role of GH receptor intracellular domain tyrosine residues. *Endocrinology* **153:** 2311-2322

Dey BR, Furlanetto RW, Nissley SP (1998a) Cloning of human p55 gamma, a regulatory subunit of phosphatidylinositol 3-kinase, by a yeast two-hybrid library screen with the insulin-like growth factor-I receptor. *Gene* **209:** 175-183

Dey BR, Spence SL, Nissley P, Furlanetto RW (1998b) Interaction of human suppressor of cytokine signaling (SOCS)-2 with the insulin-like growth factor-I receptor. *The Journal of biological chemistry* **273:** 24095-24101

Di Domenico F, Casalena G, Sultana R, Cai J, Pierce WM, Perluigi M, Cini C, Baracca A, Solaini G, Lenaz G, Jia J, Dziennis S, Murphy SJ, Alkayed NJ, Butterfield DA (2010) Involvement of Stat3 in mouse brain development and sexual dimorphism: a proteomics approach. *Brain research* **1362:** 1-12

Dinerstein H, Lago F, Goujon L, Ferrag F, Esposito N, Finidori J, Kelly PA, Postel-Vinay MC (1995) The proline-rich region of the GH receptor is essential for JAK2 phosphorylation, activation of cell proliferation, and gene transcription. *Molecular endocrinology* **9:** 1701-1707

Ding J, Berryman DE, Jara A, Kopchick JJ (2012) Age- and sex-associated plasma proteomic changes in growth hormone receptor gene-disrupted mice. *The journals of gerontology Series A, Biological sciences and medical sciences* **67:** 830-840

Ding J, Berryman DE, Kopchick JJ (2011) Plasma proteomic profiles of bovine growth hormone transgenic mice as they age. *Transgenic research* **20:** 1305-1320

Ding J, Komatsu H, Iida S, Yano H, Kusumoto S, Inagaki A, Mori F, Ri M, Ito A, Wakita A, Ishida T, Nitta M, Ueda R (2009) The Asn505 mutation of the c-MPL gene, which causes familial essential thrombocythemia, induces autonomous homodimerization of the c-Mpl protein due to strong amino acid polarity. *Blood* **114:** 3325-3328

Divisova J, Kuiatse I, Lazard Z, Weiss H, Vreeland F, Hadsell DL, Schiff R, Osborne CK, Lee AV (2006) The growth hormone receptor antagonist pegvisomant blocks both mammary gland development and MCF-7 breast cancer xenograft growth. *Breast cancer research and treatment* **98:** 315-327

Doetsch F, Petreanu L, Caille I, Garcia-Verdugo JM, Alvarez-Buylla A (2002) EGF converts transit-amplifying neurogenic precursors in the adult brain into multipotent stem cells. *Neuron* **36:** 1021-1034

Doi T, Striker LJ, Quaife C, Conti FG, Palmiter R, Behringer R, Brinster R, Striker GE (1988) Progressive glomerulosclerosis develops in transgenic mice chronically expressing growth hormone and growth hormone releasing factor but not in those expressing insulinlike growth factor-1. *The American journal of pathology* **131:** 398-403

Dominici FP, Argentino DP, Munoz MC, Miquet JG, Sotelo AI, Turyn D (2005) Influence of the crosstalk between growth hormone and insulin signalling on the modulation of insulin sensitivity. *Growth hormone & IGF research : official journal of the Growth Hormone Research Society and the International IGF Research Society* **15:** 324-336

Dominici FP, Cifone D, Bartke A, Turyn D (1999) Loss of sensitivity to insulin at early events of the insulin signaling pathway in the liver of growth hormone-transgenic mice. *The Journal of endocrinology* **161:** 383-392

Dominici FP, Hauck S, Argentino DP, Bartke A, Turyn D (2002) Increased insulin sensitivity and upregulation of insulin receptor, insulin receptor substrate (IRS)-1 and IRS-2 in liver of Ames dwarf mice. *The Journal of endocrinology* **173:** 81-94

Donaghy AJ, Delhanty PJ, Ho KK, Williams R, Baxter RC (2002) Regulation of the growth hormone receptor/binding protein, insulin-like growth factor ternary complex system in human cirrhosis. *Journal of hepatology* **36:** 751-758

Donnelly ML, Luke G, Mehrotra A, Li X, Hughes LE, Gani D, Ryan MD (2001) Analysis of the aphthovirus 2A/2B polyprotein 'cleavage' mechanism indicates not a proteolytic reaction, but a novel translational effect: a putative ribosomal 'skip'. *The Journal of general virology* **82:** 1013-1025

Dos Santos C, Essioux L, Teinturier C, Tauber M, Goffin V, Bougneres P (2004) A common polymorphism of the growth hormone receptor is associated with increased responsiveness to growth hormone. *Nature genetics* **36:** 720-724

Dryden SC, Nahhas FA, Nowak JE, Goustin AS, Tainsky MA (2003) Role for human SIRT2 NAD-dependent deacetylase activity in control of mitotic exit in the cell cycle. *Molecular and cellular biology* **23:** 3173-3185

Du J, Zhou Y, Su X, Yu JJ, Khan S, Jiang H, Kim J, Woo J, Kim JH, Choi BH, He B, Chen W, Zhang S, Cerione RA, Auwerx J, Hao Q, Lin H (2011) Sirt5 is a NAD-dependent protein lysine demalonylase and desuccinylase. *Science* **334:** 806-809

Du YC, Lewis BC, Hanahan D, Varmus H (2007) Assessing tumor progression factors by somatic gene transfer into a mouse model: Bcl-xL promotes islet tumor cell invasion. *PLoS Biol* **5:** e276

Du Z, Li Y (2007) RCAS-TVA in the mammary gland: an in vivo oncogene screen and a high fidelity model for breast transformation? *Cell cycle* **6:** 823-826

Dull T, Zufferey R, Kelly M, Mandel RJ, Nguyen M, Trono D, Naldini L (1998) A third-generation lentivirus vector with a conditional packaging system. *Journal of virology* **72:** 8463-8471

Dunn KJ, Williams BO, Li Y, Pavan WJ (2000) Neural crest-directed gene transfer demonstrates Wnt1 role in melanocyte expansion and differentiation during mouse development. *Proceedings of the National Academy of Sciences of the United States of America* **97:** 10050-10055

Duquesnoy P, Sobrier ML, Duriez B, Dastot F, Buchanan CR, Savage MO, Preece MA, Craescu CT, Blouquit Y, Goossens M, et al. (1994) A single amino acid substitution in the exoplasmic domain of the human growth hormone (GH) receptor confers familial GH resistance (Laron syndrome) with positive GH-binding activity by abolishing receptor homodimerization. *The EMBO journal* **13:** 1386-1395

Dutsch-Wicherek M, Sikora J, Tomaszewska R (2008) The possible biological role of metallothionein in apoptosis. *Frontiers in bioscience : a journal and virtual library* **13:** 4029-4038

Edens A, Southard JN, Talamantes F (1994) Mouse growth hormone-binding protein and growth hormone receptor transcripts are produced from a single gene by alternative splicing. *Endocrinology* **135:** 2802-2805

Edens A, Talamantes F (1998) Alternative processing of growth hormone receptor transcripts. *Endocrine reviews* **19:** 559-582

Egecioglu E, Bjursell M, Ljungberg A, Dickson SL, Kopchick JJ, Bergstrom G, Svensson L, Oscarsson J, Tornell J, Bohlooly YM (2006) Growth hormone receptor deficiency results in blunted ghrelin feeding response, obesity, and hypolipidemia in mice. *American journal of physiology Endocrinology and metabolism* **290:** E317-325

Ekberg S, Luther M, Nakamura T, Jansson JO (1992) Growth hormone promotes early initiation of hepatocyte growth factor gene expression in the liver of hypophysectomized rats after partial hepatectomy. *The Journal of endocrinology* **135:** 59-67

El Mjiyad N, Caro-Maldonado A, Ramirez-Peinado S, Munoz-Pinedo C (2011) Sugar-free approaches to cancer cell killing. *Oncogene* **30:** 253-264

Elliott J, Hookham MB, Johnston JA (2008) The suppressors of cytokine signalling E3 ligases behave as tumour suppressors. *Biochemical Society transactions* **36:** 464-468

Emerald BS, Chen Y, Zhu T, Zhu Z, Lee KO, Gluckman PD, Lobie PE (2007) AlphaCP1 mediates stabilization of hTERT mRNA by autocrine human growth hormone. *The Journal of biological chemistry* **282:** 680-690

Emerman JT, Leahy M, Gout PW, Bruchovsky N (1985) Elevated growth hormone levels in sera from breast cancer patients. *Hormone and metabolic research = Hormon- und Stoffwechselforschung = Hormones et metabolisme* **17:** 421-424

Endo TA, Masuhara M, Yokouchi M, Suzuki R, Sakamoto H, Mitsui K, Matsumoto A, Tanimura S, Ohtsubo M, Misawa H, Miyazaki T, Leonor N, Taniguchi T, Fujita T, Kanakura Y, Komiya S, Yoshimura A (1997) A new protein containing an SH2 domain that inhibits JAK kinases. *Nature* **387:** 921-924

Esposito N, Wojcik J, Chomilier J, Martini JF, Kelly PA, Finidori J, Postel-Vinay MC (1998) The D152H mutation found in growth hormone insensitivity syndrome impairs expression and function of human growth hormone receptor but is silent in rat receptor. *Journal of molecular endocrinology* **21:** 61-72

Estall JL, Ruas JL, Choi CS, Laznik D, Badman M, Maratos-Flier E, Shulman GI, Spiegelman BM (2009) PGC-1alpha negatively regulates hepatic FGF21 expression by modulating the heme/Rev-Erb(alpha) axis. *Proceedings of the National Academy of Sciences of the United States of America* **106:** 22510-22515

Estep PW, 3rd, Warner JB, Bulyk ML (2009) Short-term calorie restriction in male mice feminizes gene expression and alters key regulators of conserved aging regulatory pathways. *PloS one* **4:** e5242

Evrard-Todeschi N, Pons J, Gharbi-Benarous J, Bertho G, Benarous R, Girault JP (2008) Structure of the complex between phosphorylated substrates and the SCF beta-TrCP ubiquitin ligase receptor: a combined NMR, molecular modeling, and docking approach. *Journal of chemical information and modeling* **48:** 2350-2361

Faglia G, Arosio M, Spada A (1996) GS protein mutations and pituitary tumors: functional correlates and possible therapeutic implications. *Metabolism: clinical and experimental* **45:** 117-119

Fang P, Kofoed EM, Little BM, Wang X, Ross RJ, Frank SJ, Hwa V, Rosenfeld RG (2006) A mutant signal transducer and activator of transcription 5b, associated with growth hormone insensitivity and insulin-like growth factor-I deficiency, cannot function as a signal transducer or transcription factor. *The Journal of clinical endocrinology and metabolism* **91:** 1526-1534

Federspiel MJ, Bates P, Young JA, Varmus HE, Hughes SH (1994) A system for tissue-specific gene targeting: transgenic mice susceptible to subgroup A avian leukosis virus-based retroviral vectors. *Proceedings of the National Academy of Sciences of the United States of America* **91:** 11241-11245

Federspiel MJ, Swing DA, Eagleson B, Reid SW, Hughes SH (1996) Expression of transduced genes in mice generated by infecting blastocysts with avian leukosis virus-based retroviral vectors. *Proceedings of the National Academy of Sciences of the United States of America* **93:** 4931-4936

Feelders RA, Hofland LJ, van Aken MO, Neggers SJ, Lamberts SW, de Herder WW, van der Lely AJ (2009) Medical therapy of acromegaly: efficacy and safety of somatostatin analogues. *Drugs* **69:** 2207-2226

Feigerlova E, Swinyard M, Derr MA, Farnsworth J, Andrew SF, Rosenfeld RG, Hwa V (2013) A Novel GHR Intronic Variant, c.266+83G>T , Activates a Cryptic 5' Splice Site Causing Severe GHR Deficiency and Classical GH Insensitivity Syndrome. *Hormone research in paediatrics*

Feldman BJ, Feldman D (2001) The development of androgen-independent prostate cancer. *Nature reviews Cancer* **1:** 34-45

Feldman M, Ruan W, Cunningham BC, Wells JA, Kleinberg DL (1993) Evidence that the growth hormone receptor mediates differentiation and development of the mammary gland. *Endocrinology* **133:** 1602-1608

Felice DL, El-Shennawy L, Zhao S, Lantvit DL, Shen Q, Unterman TG, Swanson SM, Frasor J (2013) Growth hormone potentiates 17beta-estradiol-dependent breast cancer cell proliferation independently of IGF-I receptor signaling. *Endocrinology* **154:** 3219-3227

Feng J, Witthuhn BA, Matsuda T, Kohlhuber F, Kerr IM, Ihle JN (1997) Activation of Jak2 catalytic activity requires phosphorylation of Y1007 in the kinase activation loop. *Molecular and cellular biology* **17:** 2497-2501

Fernandes G, Venkatraman JT, Turturro A, Attwood VG, Hart RW (1997) Effect of food restriction on life span and immune functions in long-lived Fischer-344 x Brown Norway F1 rats. *Journal of clinical immunology* **17:** 85-95

Fernandez-Perez L, Guerra B, Diaz-Chico JC, Flores-Morales A (2013) Estrogens regulate the hepatic effects of growth hormone, a hormonal interplay with multiple fates. *Frontiers in endocrinology* **4:** 66

Filopanti M, Giavoli C, Grottoli S, Bianchi A, De Marinis L, Ghigo E, Spada A (2011) The exon 3-deleted growth hormone receptor: molecular and functional characterization and impact on GH/IGF-I axis in physiological and pathological conditions. *Journal of endocrinological investigation* **34:** 861-868

Finley LW, Carracedo A, Lee J, Souza A, Egia A, Zhang J, Teruya-Feldstein J, Moreira PI, Cardoso SM, Clish CB, Pandolfi PP, Haigis MC (2011a) SIRT3 opposes reprogramming of cancer cell metabolism through HIF1alpha destabilization. *Cancer cell* **19:** 416-428

Finley LW, Haas W, Desquiret-Dumas V, Wallace DC, Procaccio V, Gygi SP, Haigis MC (2011b) Succinate dehydrogenase is a direct target of sirtuin 3 deacetylase activity. *PloS one* **6:** e23295

Fisher GH, Orsulic S, Holland E, Hively WP, Li Y, Lewis BC, Williams BO, Varmus HE (1999) Development of a flexible and specific gene delivery system for production of murine tumor models. *Oncogene* **18:** 5253-5260

Flores-Morales A, Greenhalgh CJ, Norstedt G, Rico-Bautista E (2006) Negative regulation of growth hormone receptor signaling. *Molecular endocrinology* **20:** 241-253

Flurkey K, Papaconstantinou J, Harrison DE (2002) The Snell dwarf mutation Pit1(dw) can increase life span in mice. *Mechanisms of ageing and development* **123:** 121-130

Flurkey K, Papaconstantinou J, Miller RA, Harrison DE (2001) Lifespan extension and delayed immune and collagen aging in mutant mice with defects in growth hormone production. *Proceedings of the National Academy of Sciences of the United States of America* **98:** 6736-6741

Folkmann JK, Loft S, Moller P (2007) Oxidatively damaged DNA in aging dyslipidemic ApoE-/- and wild-type mice. *Mutagenesis* **22:** 105-110

Fontana L, Weiss EP, Villareal DT, Klein S, Holloszy JO (2008) Long-term effects of calorie or protein restriction on serum IGF-1 and IGFBP-3 concentration in humans. *Aging cell* **7:** 681-687

Foppiano S, Hu D, Marcucio RS (2007) Signaling by bone morphogenetic proteins directs formation of an ectodermal signaling center that regulates craniofacial development. *Developmental biology* **312:** 103-114

Foretz M, Hebrard S, Leclerc J, Zarrinpashneh E, Soty M, Mithieux G, Sakamoto K, Andreelli F, Viollet B (2010) Metformin inhibits hepatic gluconeogenesis in mice independently of the LKB1/AMPK pathway via a decrease in hepatic energy state. *The Journal of clinical investigation* **120:** 2355-2369

Foster CM, Shafer JA, Rozsa FW, Wang XY, Lewis SD, Renken DA, Natale JE, Schwartz J, Carter-Su C (1988) Growth hormone promoted tyrosyl phosphorylation of growth hormone receptors in murine 3T3-F442A fibroblasts and adipocytes. *Biochemistry* **27:** 326-334

Fox EM, Bernaciak TM, Wen J, Weaver AM, Shupnik MA, Silva CM (2008) Signal transducer and activator of transcription 5b, c-Src, and epidermal growth factor receptor signaling play integral roles in estrogen-stimulated proliferation of estrogen receptor-positive breast cancer cells. *Molecular endocrinology* **22:** 1781-1796

Frank SJ (2001) Growth hormone signalling and its regulation: preventing too much of a good thing. *Growth hormone & IGF research : official journal of the Growth Hormone Research Society and the International IGF Research Society* **11:** 201-212

Frank SJ (2008) Mechanistic aspects of crosstalk between GH and PRL and ErbB receptor family signaling. *Journal of mammary gland biology and neoplasia* **13:** 119-129

Frank SJ, Fuchs SY (2008) Modulation of growth hormone receptor abundance and function: roles for the ubiquitin-proteasome system. *Biochimica et biophysica acta* **1782:** 785-794

Frank SJ, Yi W, Zhao Y, Goldsmith JF, Gilliland G, Jiang J, Sakai I, Kraft AS (1995) Regions of the JAK2 tyrosine kinase required for coupling to the growth hormone receptor. *The Journal of biological chemistry* **270:** 14776-14785

Fresno Vara JA, Carretero MV, Geronimo H, Ballmer-Hofer K, Martin-Perez J (2000) Stimulation of c-Src by prolactin is independent of Jak2. *The Biochemical journal* **345 Pt 1:** 17-24

Frick F, Bohlooly YM, Linden D, Olsson B, Tornell J, Eden S, Oscarsson J (2001) Long-term growth hormone excess induces marked alterations in lipoprotein metabolism in mice. *American journal of physiology Endocrinology and metabolism* **281:** E1230-1239

Friedbichler K, Hoelbl A, Li G, Bunting KD, Sexl V, Gouilleux F, Moriggl R (2011) Serine phosphorylation of the Stat5a C-terminus is a driving force for transformation. *Frontiers in bioscience* **16:** 3043-3056

Friend KE, Khandwala HM, Flyvbjerg A, Hill H, Li J, McCutcheon IE (2001) Growth hormone and insulin-like growth factor-I: effects on the growth of glioma cell lines. *Growth hormone & IGF research : official journal of the Growth Hormone Research Society and the International IGF Research Society* **11:** 84-91

Fu ZD, Klaassen CD (2014) Short-term calorie restriction feminizes the mRNA profiles of drug metabolizing enzymes and transporters in livers of mice. *Toxicology and applied pharmacology* **274:** 137-146

Fuchs SY, Spiegelman VS, Kumar KG (2004) The many faces of beta-TrCP E3 ubiquitin ligases: reflections in the magic mirror of cancer. *Oncogene* **23:** 2028-2036

Fuh G, Cunningham BC, Fukunaga R, Nagata S, Goeddel DV, Wells JA (1992) Rational design of potent antagonists to the human growth hormone receptor. *Science* **256:** 1677-1680

Fuh G, Mulkerrin MG, Bass S, McFarland N, Brochier M, Bourell JH, Light DR, Wells JA (1990) The human growth hormone receptor. Secretion from Escherichia coli and disulfide bonding pattern of the extracellular binding domain. *The Journal of biological chemistry* **265:** 3111-3115

Fuhrman B, Barba M, Schunemann HJ, Hurd T, Quattrin T, Cartagena R, Carruba G, Muti P (2005) Basal growth hormone concentrations in blood and the risk for prostate cancer: a case-control study. *The Prostate* **64:** 109-115

Fujimoto M, Naka T (2003) Regulation of cytokine signaling by SOCS family molecules. *Trends in immunology* **24:** 659-666

Fujita Y, Hosokawa M, Fujimoto S, Mukai E, Abudukadier A, Obara A, Ogura M, Nakamura Y, Toyoda K, Nagashima K, Seino Y, Inagaki N (2010) Metformin suppresses hepatic gluconeogenesis and lowers fasting blood glucose levels through reactive nitrogen species in mice. *Diabetologia* **53:** 1472-1481

Funakoshi-Tago M, Tago K, Kasahara T, Parganas E, Ihle JN (2008) Negative regulation of Jak2 by its auto-phosphorylation at tyrosine 913 via the Epo signaling pathway. *Cellular signalling* **20:** 1995-2001

Gabay C, Dreyer M, Pellegrinelli N, Chicheportiche R, Meier CA (2001) Leptin directly induces the secretion of interleukin 1 receptor antagonist in human monocytes. *The Journal of clinical endocrinology and metabolism* **86:** 783-791

Gadd SL, Clevenger CV (2006) Ligand-independent dimerization of the human prolactin receptor isoforms: functional implications. *Molecular endocrinology* **20:** 2734-2746

Galvao DA, Nosaka K, Taaffe DR, Peake J, Spry N, Suzuki K, Yamaya K, McGuigan MR, Kristjanson LJ, Newton RU (2008) Endocrine and immune responses to resistance training in prostate cancer patients. *Prostate cancer and prostatic diseases* **11:** 160-165

Gan Y, Paterson AJ, Zhang Y, Jiang J, Frank SJ (2013) Functional collaboration of Insulin-like Growth Factor-1 Receptor (IGF-1R), but not insulin receptor (IR), with acute GH signaling in mouse calvarial cells. *Endocrinology***:** en20131732

Gan Y, Zhang Y, Digirolamo DJ, Jiang J, Wang X, Cao X, Zinn KR, Carbone DP, Clemens TL, Frank SJ (2010) Deletion of IGF-I receptor (IGF-IR) in primary osteoblasts reduces GH-induced STAT5 signaling. *Molecular endocrinology* **24:** 644-656

Garcia-Aragon J, Lobie PE, Muscat GE, Gobius KS, Norstedt G, Waters MJ (1992) Prenatal expression of the growth hormone (GH) receptor/binding protein in the rat: a role for GH in embryonic and fetal development? *Development* **114:** 869-876

Garcia-Caballero T, Mertani HM, Lambert A, Gallego R, Fraga M, Pintos E, Forteza J, Chevallier M, Lobie PE, Vonderhaar BK, Beiras A, Morel G (2000) Increased expression of growth hormone and prolactin receptors in hepatocellular carcinomas. *Endocrine* **12:** 265-271

Garcia-Martinez JM, Calcabrini A, Gonzalez L, Martin-Forero E, Agullo-Ortuno MT, Simon V, Watkin H, Anderson SM, Roche S, Martin-Perez J (2010) A non-catalytic function of the Src family tyrosine kinases controls prolactin-induced Jak2 signaling. *Cellular signalling* **22:** 415-426

Gebre-Medhin M, Kindblom LG, Wennbo H, Tornell J, Meis-Kindblom JM (2001) Growth hormone receptor is expressed in human breast cancer. *The American journal of pathology* **158:** 1217-1222

Gent J, Van Den Eijnden M, Van Kerkhof P, Strous GJ (2003) Dimerization and signal transduction of the growth hormone receptor. *Molecular endocrinology* **17:** 967-975

Gent J, van Kerkhof P, Roza M, Bu G, Strous GJ (2002) Ligand-independent growth hormone receptor dimerization occurs in the endoplasmic reticulum and is required for ubiquitin system-dependent endocytosis. *Proceedings of the National Academy of Sciences of the United States of America* **99:** 9858-9863

Gesing A, Bartke A, Wang F, Karbownik-Lewinska M, Masternak MM (2011a) Key regulators of mitochondrial biogenesis are increased in kidneys of growth hormone receptor knockout (GHRKO) mice. *Cell biochemistry and function* **29:** 459-467

Gesing A, Masternak MM, Wang F, Joseph AM, Leeuwenburgh C, Westbrook R, Lewinski A, Karbownik-Lewinska M, Bartke A (2011b) Expression of key regulators of mitochondrial biogenesis in growth hormone receptor knockout (GHRKO) mice is enhanced but is not further improved by other potential life-extending interventions. *The journals of gerontology Series A, Biological sciences and medical sciences* **66:** 1062-1076

Gevers EF, van der Eerden BC, Karperien M, Raap AK, Robinson IC, Wit JM (2002) Localization and regulation of the growth hormone receptor and growth hormone-binding protein in the rat growth plate. *Journal of bone and mineral research : the official journal of the American Society for Bone and Mineral Research* **17:** 1408-1419

Gil-Puig C, Seoane S, Blanco M, Macia M, Garcia-Caballero T, Segura C, Perez-Fernandez R (2005) Pit-1 is expressed in normal and tumorous human breast and regulates GH secretion and cell proliferation. *European journal of endocrinology / European Federation of Endocrine Societies* **153:** 335-344

Gilbert JM, Bates P, Varmus HE, White JM (1994) The receptor for the subgroup A avian leukosis-sarcoma viruses binds to subgroup A but not to subgroup C envelope glycoprotein. *Journal of virology* **68:** 5623-5628

Giri DK, Ali-Seyed M, Li LY, Lee DF, Ling P, Bartholomeusz G, Wang SC, Hung MC (2005) Endosomal transport of ErbB-2: mechanism for nuclear entry of the cell surface receptor. *Molecular and cellular biology* **25:** 11005-11018

Glass CK, Rosenfeld MG (2000) The coregulator exchange in transcriptional functions of nuclear receptors. *Genes & development* **14:** 121-141

Glimm DR, Baracos VE, Kennelly JJ (1990) Molecular evidence for the presence of growth hormone receptors in the bovine mammary gland. *The Journal of endocrinology* **126:** R5-8

Gobeil F, Fortier A, Zhu T, Bossolasco M, Leduc M, Grandbois M, Heveker N, Bkaily G, Chemtob S, Barbaz D (2006) G-protein-coupled receptors signalling at the cell nucleus: an emerging paradigm. *Canadian journal of physiology and pharmacology* **84:** 287-297

Gobius KS, Rowlinson SW, Barnard R, Mattick JS, Waters MJ (1992) The first disulphide loop of the rabbit growth hormone receptor is required for binding to the hormone. *Journal of molecular endocrinology* **9:** 213-220

Godowski PJ, Leung DW, Meacham LR, Galgani JP, Hellmiss R, Keret R, Rotwein PS, Parks JS, Laron Z, Wood WI (1989) Characterization of the human growth hormone receptor gene and demonstration of a partial gene deletion in two patients with Laron-type dwarfism. *Proceedings of the National Academy of Sciences of the United States of America* **86:** 8083-8087

Goffin V, Shiverick KT, Kelly PA, Martial JA (1996) Sequence-function relationships within the expanding family of prolactin, growth hormone, placental lactogen, and related proteins in mammals. *Endocrine reviews* **17:** 385-410

Goodrick CL (1975) Life-span and the inheritance of longevity of inbred mice. *Journal of gerontology* **30:** 257-263

Gorin E, Goodman HM (1985) Turnover of growth hormone receptors in rat adipocytes. *Endocrinology* **116:** 1796-1805

Gorin E, Grichting G, Goodman HM (1984) Binding and degradation of [125I]human growth hormone in rat adipocytes. *Endocrinology* **115:** 467-475

Goudriaan JR, Dahlmans VE, Teusink B, Ouwens DM, Febbraio M, Maassen JA, Romijn JA, Havekes LM, Voshol PJ (2003) CD36 deficiency increases insulin sensitivity in muscle, but induces insulin resistance in the liver in mice. *Journal of lipid research* **44:** 2270-2277

Govers R, ten Broeke T, van Kerkhof P, Schwartz AL, Strous GJ (1999) Identification of a novel ubiquitin conjugation motif, required for ligand-induced internalization of the growth hormone receptor. *The EMBO journal* **18:** 28-36

Govers R, van Kerkhof P, Schwartz AL, Strous GJ (1997) Linkage of the ubiquitin-conjugating system and the endocytic pathway in ligand-induced internalization of the growth hormone receptor. *The EMBO journal* **16:** 4851-4858

Govers R, van Kerkhof P, Schwartz AL, Strous GJ (1998) Di-leucine-mediated internalization of ligand by a truncated growth hormone receptor is independent of the ubiquitin conjugation system. *The Journal of biological chemistry* **273:** 16426-16433

Graham TR, Zhau HE, Odero-Marah VA, Osunkoya AO, Kimbro KS, Tighiouart M, Liu T, Simons JW, O'Regan RM (2008) Insulin-like growth factor-I-dependent up-regulation of ZEB1 drives epithelial-to-mesenchymal transition in human prostate cancer cells. *Cancer research* **68:** 2479-2488

Graichen R, Liu D, Sun Y, Lee KO, Lobie PE (2002) Autocrine human growth hormone inhibits placental transforming growth factor-beta gene transcription to prevent apoptosis and allow cell cycle progression of human mammary carcinoma cells. *The Journal of biological chemistry* **277:** 26662-26672

Graichen R, Sandstedt J, Goh EL, Isaksson OG, Tornell J, Lobie PE (2003) The growth hormone-binding protein is a location-dependent cytokine receptor transcriptional enhancer. *The Journal of biological chemistry* **278:** 6346-6354

Greenhalgh CJ, Bertolino P, Asa SL, Metcalf D, Corbin JE, Adams TE, Davey HW, Nicola NA, Hilton DJ, Alexander WS (2002) Growth enhancement in suppressor of cytokine signaling 2 (SOCS-2)-deficient mice is dependent on signal transducer and activator of transcription 5b (STAT5b). *Molecular endocrinology* **16:** 1394-1406

Greenhalgh CJ, Rico-Bautista E, Lorentzon M, Thaus AL, Morgan PO, Willson TA, Zervoudakis P, Metcalf D, Street I, Nicola NA, Nash AD, Fabri LJ, Norstedt G, Ohlsson C, Flores-Morales A, Alexander WS, Hilton DJ (2005) SOCS2 negatively regulates growth hormone action in vitro and in vivo. *The Journal of clinical investigation* **115:** 397-406

Greenhouse JJ, Petropoulos CJ, Crittenden LB, Hughes SH (1988) Helper-independent retrovirus vectors with Rous-associated virus type O long terminal repeats. *Journal of virology* **62:** 4809-4812

Gregoraszczuk EL, Milewicz T, Kolodziejczyk J, Krzysiek J, Basta A, Sztefko K, Kurek S, Stachura J (2001) Progesterone-induced secretion of growth hormone, insulin-like growth factor I and prolactin by human breast cancer explants. *Gynecological endocrinology : the official journal of the International Society of Gynecological Endocrinology* **15:** 251-258

Groten T, Pierce AA, Huen AC, Schnaper HW (2005) 17 beta-estradiol transiently disrupts adherens junctions in endothelial cells. *FASEB journal : official publication of the Federation of American Societies for Experimental Biology* **19:** 1368-1370

Grotzinger J (2002) Molecular mechanisms of cytokine receptor activation. *Biochimica et biophysica acta* **1592:** 215-223

Gu F, Dube N, Kim JW, Cheng A, Ibarra-Sanchez Mde J, Tremblay ML, Boisclair YR (2003) Protein tyrosine phosphatase 1B attenuates growth hormone-mediated JAK2-STAT signaling. *Molecular and cellular biology* **23:** 3753-3762

Gu L, Dagvadorj A, Lutz J, Leiby B, Bonuccelli G, Lisanti MP, Addya S, Fortina P, Dasgupta A, Hyslop T, Bubendorf L, Nevalainen MT (2010) Transcription factor Stat3 stimulates metastatic behavior of human prostate cancer cells in vivo, whereas Stat5b has a preferential role in the promotion of prostate cancer cell viability and tumor growth. *The American journal of pathology* **176:** 1959-1972

Guan L, Murphy FD, Kaback HR (2002) Surface-exposed positions in the transmembrane helices of the lactose permease of Escherichia coli determined by intermolecular thiol cross-linking. *Proceedings of the National Academy of Sciences of the United States of America* **99:** 3475-3480

Guesdon F, Kaabi Y, Riley AH, Wilkinson IR, Gray C, James DC, Artymiuk PJ, Sayers JR, Ross RJ (2012) Expression of a glycosylphosphatidylinositol-anchored ligand, growth hormone, blocks receptor signalling. *Bioscience reports* **32:** 653-660

Guevara-Aguirre J, Balasubramanian P, Guevara-Aguirre M, Wei M, Madia F, Cheng CW, Hwang D, Martin-Montalvo A, Saavedra J, Ingles S, de Cabo R, Cohen P, Longo VD (2011) Growth hormone receptor deficiency is associated with a major reduction in pro-aging signaling, cancer, and diabetes in humans. *Science translational medicine* **3:** 70ra13

Guillaumond F, Dardente H, Giguere V, Cermakian N (2005) Differential control of Bmal1 circadian transcription by REV-ERB and ROR nuclear receptors. *Journal of biological rhythms* **20:** 391-403

Gunnell D, May M, Ben-Shlomo Y, Yarnell J, Smith GD (2003) Height, leg length, and cancer: the Caerphilly Study. *Nutrition and cancer* **47:** 34-39

Gunnell D, Okasha M, Smith GD, Oliver SE, Sandhu J, Holly JM (2001) Height, leg length, and cancer risk: a systematic review. *Epidemiologic reviews* **23:** 313-342

Guo Y, Lu Y, Houle D, Robertson K, Tang Z, Kopchick JJ, Liu YL, Liu JL (2005) Pancreatic islet-specific expression of an insulin-like growth factor-I transgene compensates islet cell growth in growth hormone receptor gene-deficient mice. *Endocrinology* **146:** 2602-2609

Gurd BJ, Holloway GP, Yoshida Y, Bonen A (2012) In mammalian muscle, SIRT3 is present in mitochondria and not in the nucleus; and SIRT3 is upregulated by chronic muscle contraction in an adenosine monophosphate-activated protein kinase-independent manner. *Metabolism: clinical and experimental* **61:** 733-741

Guren TK, Odegard J, Abrahamsen H, Thoresen GH, Susa M, Andersson Y, Ostby E, Christoffersen T (2003) EGF receptor-mediated, c-Src-dependent, activation of Stat5b is downregulated in mitogenically responsive hepatocytes. *Journal of cellular physiology* **196:** 113-123

Hachinohe M, Yamane M, Akazawa D, Ohsawa K, Ohno M, Terashita Y, Masumoto H (2013) A reduction in age-enhanced gluconeogenesis extends lifespan. *PloS one* **8:** e54011

Hackett RH, Wang YD, Sweitzer S, Feldman G, Wood WI, Larner AC (1997) Mapping of a cytoplasmic domain of the human growth hormone receptor that regulates rates of inactivation of Jak2 and Stat proteins. *The Journal of biological chemistry* **272:** 11128-11132

Haddad BR, Gu L, Mirtti T, Dagvadorj A, Vogiatzi P, Hoang DT, Bajaj R, Leiby B, Ellsworth E, Blackmon S, Ruiz C, Curtis M, Fortina P, Ertel A, Liu C, Rui H, Visakorpi T, Bubendorf L, Lallas CD, Trabulsi EJ, McCue P, Gomella L, Nevalainen MT (2013) STAT5A/B gene locus undergoes amplification during human prostate cancer progression. *The American journal of pathology* **182:** 2264-2275

Hadjantonakis AK, Cox LL, Tam PP, Nagy A (2001) An X-linked GFP transgene reveals unexpected paternal X-chromosome activity in trophoblastic giant cells of the mouse placenta. *Genesis* **29:** 133-140

Hadjantonakis AK, Gertsenstein M, Ikawa M, Okabe M, Nagy A (1998) Generating green fluorescent mice by germline transmission of green fluorescent ES cells. *Mech Dev* **76:** 79-90

Haigis MC, Mostoslavsky R, Haigis KM, Fahie K, Christodoulou DC, Murphy AJ, Valenzuela DM, Yancopoulos GD, Karow M, Blander G, Wolberger C, Prolla TA, Weindruch R, Alt FW, Guarente L (2006) SIRT4 inhibits glutamate dehydrogenase and opposes the effects of calorie restriction in pancreatic beta cells. *Cell* **126:** 941-954

Haigis MC, Sinclair DA (2010) Mammalian sirtuins: biological insights and disease relevance. *Annual review of pathology* **5:** 253-295

Hamanaka RB, Chandel NS (2010) Mitochondrial reactive oxygen species regulate cellular signaling and dictate biological outcomes. *Trends in biochemical sciences* **35:** 505-513

Han ES, Muller FL, Perez VI, Qi W, Liang H, Xi L, Fu C, Doyle E, Hickey M, Cornell J, Epstein CJ, Roberts LJ, Van Remmen H, Richardson A (2008) The in vivo gene expression signature of oxidative stress. *Physiological genomics* **34:** 112-126

Hanada M, Feng J, Hemmings BA (2004) Structure, regulation and function of PKB/AKT--a major therapeutic target. *Biochimica et biophysica acta* **1697:** 3-16

Hanahan D, Weinberg RA (2000) The hallmarks of cancer. *Cell* **100:** 57-70

Hanahan D, Weinberg RA (2011) Hallmarks of cancer: the next generation. *Cell* **144:** 646-674

Hansen LH, Wang X, Kopchick JJ, Bouchelouche P, Nielsen JH, Galsgaard ED, Billestrup N (1996) Identification of tyrosine residues in the intracellular domain of the growth hormone receptor required for transcriptional signaling and Stat5 activation. *The Journal of biological chemistry* **271:** 12669-12673

Harding PA, Wang XZ, Kelder B, Souza S, Okada S, Kopchick JJ (1994) In vitro mutagenesis of growth hormone receptor Asn-linked glycosylation sites. *Molecular and cellular endocrinology* **106:** 171-180

Harper JM, Durkee SJ, Dysko RC, Austad SN, Miller RA (2006) Genetic modulation of hormone levels and life span in hybrids between laboratory and wild-derived mice. *The journals of gerontology Series A, Biological sciences and medical sciences* **61:** 1019-1029

Harpur AG, Andres AC, Ziemiecki A, Aston RR, Wilks AF (1992) JAK2, a third member of the JAK family of protein tyrosine kinases. *Oncogene* **7:** 1347-1353

Harvey S (2010) Extrapituitary growth hormone. *Endocrine* **38:** 335-359

Harvey S, Azumaya Y, Hull KL (2000) Pituitary and extrapituitary growth hormone: Pit-1 dependence? *Canadian journal of physiology and pharmacology* **78:** 1013-1028

Harvey S, Hull K (2003) Neural growth hormone: an update. *Journal of molecular neuroscience : MN* **20:** 1-14

Harvey S, Kakebeeke M, Sanders EJ (2004) Growth hormone localization in the neural retina and retinal pigmented epithelium of embryonic chicks. *Journal of molecular neuroscience : MN* **22:** 139-145

Harvie M, Howell A (2012) Energy restriction and the prevention of breast cancer. *The Proceedings of the Nutrition Society* **71:** 263-275

Hasskarl J, Kaufmann M, Schmid HA (2011) Somatostatin receptors in non-neuroendocrine malignancies: the potential role of somatostatin analogs in solid tumors. *Future oncology* **7:** 895-913

Hattori N (2009) Expression, regulation and biological actions of growth hormone (GH) and ghrelin in the immune system. *Growth hormone & IGF research : official journal of the Growth Hormone Research Society and the International IGF Research Society* **19:** 187-197

Hattori N, Saito T, Yagyu T, Jiang BH, Kitagawa K, Inagaki C (2001) GH, GH receptor, GH secretagogue receptor, and ghrelin expression in human T cells, B cells, and neutrophils. *The Journal of clinical endocrinology and metabolism* **86:** 4284-4291

Hauck SJ, Aaron JM, Wright C, Kopchick JJ, Bartke A (2002) Antioxidant enzymes, free-radical damage, and response to paraquat in liver and kidney of long-living growth hormone receptor/binding protein gene-disrupted mice. *Hormone and metabolic research = Hormon- und Stoffwechselforschung = Hormones et metabolisme* **34:** 481-486

Hauck SJ, Hunter WS, Danilovich N, Kopchick JJ, Bartke A (2001) Reduced levels of thyroid hormones, insulin, and glucose, and lower body core temperature in the growth hormone receptor/binding protein knockout mouse. *Experimental biology and medicine* **226:** 552-558

Hawley SA, Pan DA, Mustard KJ, Ross L, Bain J, Edelman AM, Frenguelli BG, Hardie DG (2005) Calmodulin-dependent protein kinase kinase-beta is an alternative upstream kinase for AMP-activated protein kinase. *Cell metabolism* **2:** 9-19

Hawley SA, Ross FA, Chevtzoff C, Green KA, Evans A, Fogarty S, Towler MC, Brown LJ, Ogunbayo OA, Evans AM, Hardie DG (2010) Use of cells expressing gamma subunit variants to identify diverse mechanisms of AMPK activation. *Cell metabolism* **11:** 554-565

Haynes MP, Li L, Sinha D, Russell KS, Hisamoto K, Baron R, Collinge M, Sessa WC, Bender JR (2003) Src kinase mediates phosphatidylinositol 3-kinase/Akt-dependent rapid endothelial nitric-oxide synthase activation by estrogen. *The Journal of biological chemistry* **278:** 2118-2123

He K, Loesch K, Cowan JW, Li X, Deng L, Wang X, Jiang J, Frank SJ (2005) Janus kinase 2 enhances the stability of the mature growth hormone receptor. *Endocrinology* **146:** 4755-4765

He K, Wang X, Jiang J, Guan R, Bernstein KE, Sayeski PP, Frank SJ (2003) Janus kinase 2 determinants for growth hormone receptor association, surface assembly, and signaling. *Molecular endocrinology* **17:** 2211-2227

Hebert AS, Dittenhafer-Reed KE, Yu W, Bailey DJ, Selen ES, Boersma MD, Carson JJ, Tonelli M, Balloon AJ, Higbee AJ, Westphall MS, Pagliarini DJ, Prolla TA, Assadi-Porter F, Roy S, Denu JM, Coon JJ (2013) Calorie restriction and SIRT3 trigger global reprogramming of the mitochondrial protein acetylome. *Molecular cell* **49:** 186-199

Herman A, Bignon C, Daniel N, Grosclaude J, Gertler A, Djiane J (2000) Functional heterodimerization of prolactin and growth hormone receptors by ovine placental lactogen. *The Journal of biological chemistry* **275:** 6295-6301

Hernandez-Gordillo D, Ortega-Gomez Mdel R, Galicia-Polo L, Castorena-Maldonado A, Vergara-Lopez A, Guillen-Gonzalez MA, Torre-Bouscoulet L (2012) Sleep apnea in patients with acromegaly. Frequency, characterization and positive pressure titration. *The open respiratory medicine journal* **6:** 28-33

Herranz D, Munoz-Martin M, Canamero M, Mulero F, Martinez-Pastor B, Fernandez-Capetillo O, Serrano M (2010) Sirt1 improves healthy ageing and protects from metabolic syndrome-associated cancer. *Nature communications* **1:** 3

Herranz D, Serrano M (2010) SIRT1: recent lessons from mouse models. *Nature reviews Cancer* **10:** 819-823

Herrington J, Carter-Su C (2001) Signaling pathways activated by the growth hormone receptor. *Trends in endocrinology and metabolism: TEM* **12:** 252-257

Herrington J, Diakonova M, Rui L, Gunter DR, Carter-Su C (2000a) SH2-B is required for growth hormone-induced actin reorganization. *The Journal of biological chemistry* **275:** 13126-13133

Herrington J, Smit LS, Schwartz J, Carter-Su C (2000b) The role of STAT proteins in growth hormone signaling. *Oncogene* **19:** 2585-2597

Himly M, Foster DN, Bottoli I, Iacovoni JS, Vogt PK (1998) The DF-1 chicken fibroblast cell line: transformation induced by diverse oncogenes and cell death resulting from infection by avian leukosis viruses. *Virology* **248:** 295-304

Hiratsuka M, Inoue T, Toda T, Kimura N, Shirayoshi Y, Kamitani H, Watanabe T, Ohama E, Tahimic CG, Kurimasa A, Oshimura M (2003) Proteomics-based identification of differentially expressed genes in human gliomas: down-regulation of SIRT2 gene. *Biochemical and biophysical research communications* **309:** 558-566

Hirschey MD, Shimazu T, Jing E, Grueter CA, Collins AM, Aouizerat B, Stancakova A, Goetzman E, Lam MM, Schwer B, Stevens RD, Muehlbauer MJ, Kakar S, Bass NM, Kuusisto J, Laakso M, Alt FW, Newgard CB, Farese RV, Jr., Kahn CR, Verdin E (2011) SIRT3 deficiency and mitochondrial protein hyperacetylation accelerate the development of the metabolic syndrome. *Molecular cell* **44:** 177-190

Hock MB, Kralli A (2009) Transcriptional control of mitochondrial biogenesis and function. *Annual review of physiology* **71:** 177-203

Hoehn KL, Salmon AB, Hohnen-Behrens C, Turner N, Hoy AJ, Maghzal GJ, Stocker R, Van Remmen H, Kraegen EW, Cooney GJ, Richardson AR, James DE (2009) Insulin resistance is a cellular antioxidant defense mechanism. *Proceedings of the National Academy of Sciences of the United States of America* **106:** 17787-17792

Hoerter J, Gonzalez-Barroso MD, Couplan E, Mateo P, Gelly C, Cassard-Doulcier AM, Diolez P, Bouillaud F (2004) Mitochondrial uncoupling protein 1 expressed in the heart of transgenic mice protects against ischemic-reperfusion damage. *Circulation* **110:** 528-533

Holland EC (2000) A mouse model for glioma: biology, pathology, and therapeutic opportunities. *Toxicologic pathology* **28:** 171-177

Holland EC, Hively WP, DePinho RA, Varmus HE (1998) A constitutively active epidermal growth factor receptor cooperates with disruption of G1 cell-cycle arrest pathways to induce glioma-like lesions in mice. *Genes & development* **12:** 3675-3685

Holland EC, Varmus HE (1998) Basic fibroblast growth factor induces cell migration and proliferation after glia-specific gene transfer in mice. *Proceedings of the National Academy of Sciences of the United States of America* **95:** 1218-1223

Holzenberger M, Dupont J, Ducos B, Leneuve P, Geloen A, Even PC, Cervera P, Le Bouc Y (2003) IGF-1 receptor regulates lifespan and resistance to oxidative stress in mice. *Nature* **421:** 182-187

Hooghe R, Merchav S, Gaidano G, Naessens F, Matera L (1998) A role for growth hormone and prolactin in leukaemia and lymphoma? *Cellular and molecular life sciences : CMLS* **54:** 1095-1101

Hotamisligil GS, Shargill NS, Spiegelman BM (1993) Adipose expression of tumor necrosis factor-alpha: direct role in obesity-linked insulin resistance. *Science* **259:** 87-91

Hou X, Xu S, Maitland-Toolan KA, Sato K, Jiang B, Ido Y, Lan F, Walsh K, Wierzbicki M, Verbeuren TJ, Cohen RA, Zang M (2008) SIRT1 regulates hepatocyte lipid metabolism through activating AMP-activated protein kinase. *The Journal of biological chemistry* **283:** 20015-20026

Houtkooper RH, Pirinen E, Auwerx J (2012) Sirtuins as regulators of metabolism and healthspan. *Nature reviews Molecular cell biology* **13:** 225-238

Huang Y, Kim SO, Yang N, Jiang J, Frank SJ (2004) Physical and functional interaction of growth hormone and insulin-like growth factor-I signaling elements. *Molecular endocrinology* **18:** 1471-1485

Hubbard SR, Till JH (2000) Protein tyrosine kinase structure and function. *Annual review of biochemistry* **69:** 373-398

Hughes S, Kosik E (1984) Mutagenesis of the region between env and src of the SR-A strain of Rous sarcoma virus for the purpose of constructing helper-independent vectors. *Virology* **136:** 89-99

Hughes SH (2004) The RCAS vector system. *Folia Biol (Praha)* **50:** 107-119

Hughes SH, Greenhouse JJ, Petropoulos CJ, Sutrave P (1987) Adaptor plasmids simplify the insertion of foreign DNA into helper-independent retroviral vectors. *Journal of virology* **61:** 3004-3012

Huttemann M, Lee I, Grossman LI, Doan JW, Sanderson TH (2012) Phosphorylation of mammalian cytochrome c and cytochrome c oxidase in the regulation of cell destiny: respiration, apoptosis, and human disease. *Advances in experimental medicine and biology* **748:** 237-264

Hwa V, Little B, Adiyaman P, Kofoed EM, Pratt KL, Ocal G, Berberoglu M, Rosenfeld RG (2005) Severe growth hormone insensitivity resulting from total absence of signal transducer and activator of transcription 5b. *The Journal of clinical endocrinology and metabolism* **90:** 4260-4266

Hwang SJ, Cheng LS, Lozano G, Amos CI, Gu X, Strong LC (2003) Lung cancer risk in germline p53 mutation carriers: association between an inherited cancer predisposition, cigarette smoking, and cancer risk. *Human genetics* **113:** 238-243

Iavnilovitch E, Cardiff RD, Groner B, Barash I (2004) Deregulation of Stat5 expression and activation causes mammary tumors in transgenic mice. *International journal of cancer Journal international du cancer* **112:** 607-619

Iglesias-Gato D, Chuan YC, Wikstrom P, Augsten S, Jiang N, Niu Y, Seipel A, Danneman D, Vermeij M, Fernandez-Perez L, Jenster G, Egevad L, Norstedt G, Flores-Morales A (2014) SOCS2 mediates the cross talk between androgen and growth hormone signaling in prostate cancer. *Carcinogenesis* **35:** 24-33

Ikeno Y, Bronson RT, Hubbard GB, Lee S, Bartke A (2003) Delayed occurrence of fatal neoplastic diseases in ames dwarf mice: correlation to extended longevity. *The journals of gerontology Series A, Biological sciences and medical sciences* **58:** 291-296

Ikeno Y, Hubbard GB, Lee S, Cortez LA, Lew CM, Webb CR, Berryman DE, List EO, Kopchick JJ, Bartke A (2009) Reduced incidence and delayed occurrence of fatal neoplastic diseases in growth hormone receptor/binding protein knockout mice. *The journals of gerontology Series A, Biological sciences and medical sciences* **64:** 522-529

Ilkbahar YN, Wu K, Thordarson G, Talamantes F (1995) Expression and distribution of messenger ribonucleic acids for growth hormone (GH) receptor and GH-binding protein in mice during pregnancy. *Endocrinology* **136:** 386-392

Ilondo MM, Damholt AB, Cunningham BA, Wells JA, De Meyts P, Shymko RM (1994) Receptor dimerization determines the effects of growth hormone in primary rat adipocytes and cultured human IM-9 lymphocytes. *Endocrinology* **134:** 2397-2403

Ishida-Takahashi R, Rosario F, Gong Y, Kopp K, Stancheva Z, Chen X, Feener EP, Myers MG, Jr. (2006) Phosphorylation of Jak2 on Ser(523) inhibits Jak2-dependent leptin receptor signaling. *Molecular and cellular biology* **26:** 4063-4073

Ishizaka-Ikeda E, Fukunaga R, Wood WI, Goeddel DV, Nagata S (1993) Signal transduction mediated by growth hormone receptor and its chimeric molecules with the granulocyte colony-stimulating factor receptor. *Proceedings of the National Academy of Sciences of the United States of America* **90:** 123-127

Ishtiaq Ahmed AS, Xiong F, Pang SC, He MD, Waters MJ, Zhu ZY, Sun YH (2010) Activation of GH signaling and GH-independent stimulation of growth in zebrafish by introduction of a constitutively activated GHR construct. *Transgenic research*

Iyer J, Reich NC (2008) Constitutive nuclear import of latent and activated STAT5a by its coiled coil domain. *FASEB journal : official publication of the Federation of American Societies for Experimental Biology* **22:** 391-400

Izzard AS, Emerson M, Prehar S, Neyses L, Trainer P, List EO, Kopchick JJ, Heagerty AM (2009) The cardiovascular phenotype of a mouse model of acromegaly. *Growth hormone & IGF research : official journal of the Growth Hormone Research Society and the International IGF Research Society* **19:** 413-419

Jackson KA, Snyder DS, Goodell MA (2004) Skeletal muscle fiber-specific green autofluorescence: potential for stem cell engraftment artifacts. *Stem cells* **22:** 180-187

Jaffe CA, Turgeon DK, Lown K, Demott-Friberg R, Watkins PB (2002) Growth hormone secretion pattern is an independent regulator of growth hormone actions in humans. *American journal of physiology Endocrinology and metabolism* **283:** E1008-1015

Jager S, Handschin C, St-Pierre J, Spiegelman BM (2007) AMP-activated protein kinase (AMPK) action in skeletal muscle via direct phosphorylation of PGC-1alpha. *Proceedings of the National Academy of Sciences of the United States of America* **104:** 12017-12022

Janke C, Bulinski JC (2011) Post-translational regulation of the microtubule cytoskeleton: mechanisms and functions. *Nature reviews Molecular cell biology* **12:** 773-786

Jans DA, Hassan G (1998) Nuclear targeting by growth factors, cytokines, and their receptors: a role in signaling? *BioEssays : news and reviews in molecular, cellular and developmental biology* **20:** 400-411

Jansson JO, Eden S, Isaksson O (1985) Sexual dimorphism in the control of growth hormone secretion. *Endocrine reviews* **6:** 128-150

Jansson JO, Ekberg S, Hoath SB, Beamer WG, Frohman LA (1988) Growth hormone enhances hepatic epidermal growth factor receptor concentration in mice. *The Journal of clinical investigation* **82:** 1871-1876

Jansson JO, Frohman LA (1987) Differential effects of neonatal and adult androgen exposure on the growth hormone secretory pattern in male rats. *Endocrinology* **120:** 1551-1557

Jeay S, Sonenshein GE, Kelly PA, Postel-Vinay MC, Baixeras E (2001) Growth hormone exerts antiapoptotic and proliferative effects through two different pathways involving nuclear factor-kappaB and phosphatidylinositol 3-kinase. *Endocrinology* **142:** 147-156

Jeay S, Sonenshein GE, Postel-Vinay MC, Baixeras E (2000) Growth hormone prevents apoptosis through activation of nuclear factor-kappaB in interleukin-3-dependent Ba/F3 cell line. *Molecular endocrinology* **14:** 650-661

Jeay S, Sonenshein GE, Postel-Vinay MC, Kelly PA, Baixeras E (2002) Growth hormone can act as a cytokine controlling survival and proliferation of immune cells: new insights into signaling pathways. *Molecular and cellular endocrinology* **188:** 1-7

Jenkins PJ (2004) Acromegaly and cancer. *Hormone research* **62 Suppl 1:** 108-115

Jenkins PJ, Besser M (2001) Clinical perspective: acromegaly and cancer: a problem. *The Journal of clinical endocrinology and metabolism* **86:** 2935-2941

Jenkins PJ, Bustin SA (2004) Evidence for a link between IGF-I and cancer. *European journal of endocrinology / European Federation of Endocrine Societies* **151 Suppl 1:** S17-22

Jiang J, Wan Y, Wang X, Xu J, Harris JM, Lobie PE, Zhang Y, Zinn KR, Waters MJ, Frank SJ (2011) Inhibitory GH receptor extracellular domain monoclonal antibodies: three-dimensional epitope mapping. *Endocrinology* **152:** 4777-4788

Jin H, Lanning NJ, Carter-Su C (2008) JAK2, but not Src family kinases, is required for STAT, ERK, and Akt signaling in response to growth hormone in preadipocytes and hepatoma cells. *Molecular endocrinology* **22:** 1825-1841

Johnson HM, Subramaniam PS, Olsnes S, Jans DA (2004) Trafficking and signaling pathways of nuclear localizing protein ligands and their receptors. *BioEssays : news and reviews in molecular, cellular and developmental biology* **26:** 993-1004

Jonckheere AI, Huigsloot M, Lammens M, Jansen J, van den Heuvel LP, Spiekerkoetter U, von Kleist-Retzow JC, Forkink M, Koopman WJ, Szklarczyk R, Huynen MA, Fransen JA, Smeitink JA, Rodenburg RJ (2011) Restoration of complex V deficiency caused by a novel deletion in the human TMEM70 gene normalizes mitochondrial morphology. *Mitochondrion* **11:** 954-963

Jostel A, Mukherjee A, Alenfall J, Smethurst L, Shalet SM (2005) A new sustained-release preparation of human growth hormone and its pharmacokinetic, pharmacodynamic and safety profile. *Clinical endocrinology* **62:** 623-627

Jung KH, Noh JH, Kim JK, Eun JW, Bae HJ, Chang YG, Kim MG, Park WS, Lee JY, Lee SY, Chu IS, Nam SW (2012) Histone deacetylase 6 functions as a tumor suppressor by activating c-Jun NH2-terminal kinase-mediated beclin 1-dependent autophagic cell death in liver cancer. *Hepatology* **56:** 644-657

Junnila RK, List EO, Berryman DE, Murrey JW, Kopchick JJ (2013) The GH/IGF-1 axis in ageing and longevity. *Nature reviews Endocrinology* **9:** 366-376

Kaidi A, Weinert BT, Choudhary C, Jackson SP (2010) Human SIRT6 promotes DNA end resection through CtIP deacetylation. *Science* **329:** 1348-1353

Kamura T, Maenaka K, Kotoshiba S, Matsumoto M, Kohda D, Conaway RC, Conaway JW, Nakayama KI (2004) VHL-box and SOCS-box domains determine binding specificity for Cul2-Rbx1 and Cul5-Rbx2 modules of ubiquitin ligases. *Genes & development* **18:** 3055-3065

Kanfi Y, Naiman S, Amir G, Peshti V, Zinman G, Nahum L, Bar-Joseph Z, Cohen HY (2012) The sirtuin SIRT6 regulates lifespan in male mice. *Nature* **483:** 218-221

Kang H, Freund C, Duke-Cohan JS, Musacchio A, Wagner G, Rudd CE (2000) SH3 domain recognition of a proline-independent tyrosine-based RKxxYxxY motif in immune cell adaptor SKAP55. *The EMBO journal* **19:** 2889-2899

Kang HS, Angers M, Beak JY, Wu X, Gimble JM, Wada T, Xie W, Collins JB, Grissom SF, Jetten AM (2007) Gene expression profiling reveals a regulatory role for ROR alpha and ROR gamma in phase I and phase II metabolism. *Physiological genomics* **31:** 281-294

Karolewski BA, Watson DJ, Parente MK, Wolfe JH (2003) Comparison of transfection conditions for a lentivirus vector produced in large volumes. *Hum Gene Ther* **14:** 1287-1296

Kassem M (1997) Cellular and molecular effects of growth hormone and estrogen on human bone cells. *APMIS Supplementum* **71:** 1-30

Kaulsay KK, Mertani HC, Lee KO, Lobie PE (2000) Autocrine human growth hormone enhancement of human mammary carcinoma cell spreading is Jak2 dependent. *Endocrinology* **141:** 1571-1584

Kaulsay KK, Mertani HC, Tornell J, Morel G, Lee KO, Lobie PE (1999) Autocrine stimulation of human mammary carcinoma cell proliferation by human growth hormone. *Experimental cell research* **250:** 35-50

Kaulsay KK, Zhu T, Bennett W, Lee KO, Lobie PE (2001) The effects of autocrine human growth hormone (hGH) on human mammary carcinoma cell behavior are mediated via the hGH receptor. *Endocrinology* **142:** 767-777

Kauppinen A, Suuronen T, Ojala J, Kaarniranta K, Salminen A (2013) Antagonistic crosstalk between NF-kappaB and SIRT1 in the regulation of inflammation and metabolic disorders. *Cellular signalling* **25:** 1939-1948

Keith B, Simon MC (2007) Hypoxia-inducible factors, stem cells, and cancer. *Cell* **129:** 465-472

Kemp SF, Fielder PJ, Attie KM, Blethen SL, Reiter EO, Ford KM, Marian M, Dao LN, Lee HJ, Saenger P (2004) Pharmacokinetic and pharmacodynamic characteristics of a long-acting growth hormone (GH) preparation (nutropin depot) in GH-deficient children. *The Journal of clinical endocrinology and metabolism* **89:** 3234-3240

Kensler TW, Wakabayashi N, Biswal S (2007) Cell survival responses to environmental stresses via the Keap1-Nrf2-ARE pathway. *Annual review of pharmacology and toxicology* **47:** 89-116

Kenyon C, Chang J, Gensch E, Rudner A, Tabtiang R (1993) A C. elegans mutant that lives twice as long as wild type. *Nature* **366:** 461-464

Kern PA, Saghizadeh M, Ong JM, Bosch RJ, Deem R, Simsolo RB (1995) The expression of tumor necrosis factor in human adipose tissue. Regulation by obesity, weight loss, and relationship to lipoprotein lipase. *The Journal of clinical investigation* **95:** 2111-2119

Kershaw NJ, Murphy JM, Liau NP, Varghese LN, Laktyushin A, Whitlock EL, Lucet IS, Nicola NA, Babon JJ (2013) SOCS3 binds specific receptor-JAK complexes to control cytokine signaling by direct kinase inhibition. *Nature structural & molecular biology* **20:** 469-476

Khandwala HM, McCutcheon IE, Flyvbjerg A, Friend KE (2000) The effects of insulin-like growth factors on tumorigenesis and neoplastic growth. *Endocrine reviews* **21:** 215-244

Kim HS, Patel K, Muldoon-Jacobs K, Bisht KS, Aykin-Burns N, Pennington JD, van der Meer R, Nguyen P, Savage J, Owens KM, Vassilopoulos A, Ozden O, Park SH, Singh KK, Abdulkadir SA, Spitz DR, Deng CX, Gius D (2010) SIRT3 is a mitochondria-localized tumor suppressor required for maintenance of mitochondrial integrity and metabolism during stress. *Cancer cell* **17:** 41-52

Kim HS, Vassilopoulos A, Wang RH, Lahusen T, Xiao Z, Xu X, Li C, Veenstra TD, Li B, Yu H, Ji J, Wang XW, Park SH, Cha YI, Gius D, Deng CX (2011) SIRT2 maintains genome integrity and suppresses tumorigenesis through regulating APC/C activity. *Cancer cell* **20:** 487-499

Kim SC, Sprung R, Chen Y, Xu Y, Ball H, Pei J, Cheng T, Kho Y, Xiao H, Xiao L, Grishin NV, White M, Yang XJ, Zhao Y (2006) Substrate and functional diversity of lysine acetylation revealed by a proteomics survey. *Molecular cell* **23:** 607-618

Kim SO, Houtman JC, Jiang J, Ruppert JM, Bertics PJ, Frank SJ (1999) Growth hormone-induced alteration in ErbB-2 phosphorylation status in 3T3-F442A fibroblasts. *The Journal of biological chemistry* **274:** 36015-36024

Kim SO, Jiang J, Yi W, Feng GS, Frank SJ (1998) Involvement of the Src homology 2-containing tyrosine phosphatase SHP-2 in growth hormone signaling. *The Journal of biological chemistry* **273:** 2344-2354

Kimata H, Yoshida A (1994) Differential effect of growth hormone and insulin-like growth factor-I, insulin-like growth factor-II, and insulin on Ig production and growth in human plasma cells. *Blood* **83:** 1569-1574

Kimura KD, Riddle DL, Ruvkun G (2011) The C. elegans DAF-2 insulin-like receptor is abundantly expressed in the nervous system and regulated by nutritional status. *Cold Spring Harbor symposia on quantitative biology* **76:** 113-120

Kimura KD, Tissenbaum HA, Liu Y, Ruvkun G (1997) daf-2, an insulin receptor-like gene that regulates longevity and diapause in Caenorhabditis elegans. *Science* **277:** 942-946

Kinzler KW, Vogelstein B (1996) Lessons from hereditary colorectal cancer. *Cell* **87:** 159-170

Kirpensteijn J, Timmermans-Sprang EP, van Garderen E, Rutteman GR, Lantinga-van Leeuwen IS, Mol JA (2002) Growth hormone gene expression in canine normal growth plates and spontaneous osteosarcoma. *Molecular and cellular endocrinology* **197:** 179-185

Klaassen CD, Liu L, Dunn RT, 2nd (1998) Regulation of sulfotransferase mRNA expression in male and female rats of various ages. *Chemico-biological interactions* **109:** 299-313

Klages N, Zufferey R, Trono D (2000) A stable system for the high-titer production of multiply attenuated lentiviral vectors. *Molecular therapy : the journal of the American Society of Gene Therapy* **2:** 170-176

Klaman LD, Boss O, Peroni OD, Kim JK, Martino JL, Zabolotny JM, Moghal N, Lubkin M, Kim YB, Sharpe AH, Stricker-Krongrad A, Shulman GI, Neel BG, Kahn BB (2000) Increased energy expenditure, decreased adiposity, and tissue-specific insulin sensitivity in protein-tyrosine phosphatase 1B-deficient mice. *Molecular and cellular biology* **20:** 5479-5489

Kleinberg DL, Wood TL, Furth PA, Lee AV (2009) Growth hormone and insulin-like growth factor-I in the transition from normal mammary development to preneoplastic mammary lesions. *Endocrine reviews* **30:** 51-74

Kloth MT, Catling AD, Silva CM (2002) Novel activation of STAT5b in response to epidermal growth factor. *The Journal of biological chemistry* **277:** 8693-8701

Knobil E GR (1959) The physiology of growth hormone with particular reference to its action in the rhesus monkey and the “species specificity” problem. *Recent Prog Horm Res* **15:** 1–69

Ko C, Chaudhry S (2002) The need for a multidisciplinary approach to cancer care. *The Journal of surgical research* **105:** 53-57

Kofoed EM, Hwa V, Little B, Woods KA, Buckway CK, Tsubaki J, Pratt KL, Bezrodnik L, Jasper H, Tepper A, Heinrich JJ, Rosenfeld RG (2003) Growth hormone insensitivity associated with a STAT5b mutation. *The New England journal of medicine* **349:** 1139-1147

Kolle S, Sinowatz F, Boie G, Temmim-Baker L, Lincoln D (1999) Expression of growth hormone receptor in human prostatic carcinoma and hyperplasia. *International journal of oncology* **14:** 911-916

Kolle S, Stojkovic M, Prelle K, Waters M, Wolf E, Sinowatz F (2001) Growth hormone (GH)/GH receptor expression and GH-mediated effects during early bovine embryogenesis. *Biology of reproduction* **64:** 1826-1834

Kong X, Wang R, Xue Y, Liu X, Zhang H, Chen Y, Fang F, Chang Y (2010) Sirtuin 3, a new target of PGC-1alpha, plays an important role in the suppression of ROS and mitochondrial biogenesis. *PloS one* **5:** e11707

Kotenko SV, Langer JA (2004) Full house: 12 receptors for 27 cytokines. *International immunopharmacology* **4:** 593-608

Kotzmann H, Riedl M, Clodi M, Barnas U, Kaider A, Hocker P, Luger A (1996) The influence of growth hormone substitution therapy on erythroid and myeloid progenitor cells and on peripheral blood cells in adult patients with growth hormone deficiency. *European journal of clinical investigation* **26:** 1175-1181

Kregel KC, Zhang HJ (2007) An integrated view of oxidative stress in aging: basic mechanisms, functional effects, and pathological considerations. *American journal of physiology Regulatory, integrative and comparative physiology* **292:** R18-36

Kubatzky KF, Ruan W, Gurezka R, Cohen J, Ketteler R, Watowich SS, Neumann D, Langosch D, Klingmuller U (2001) Self assembly of the transmembrane domain promotes signal transduction through the erythropoietin receptor. *Current biology : CB* **11:** 110-115

Kurmasheva RT, Houghton PJ (2006) IGF-I mediated survival pathways in normal and malignant cells. *Biochimica et biophysica acta* **1766:** 1-22

Kurosu H, Yamamoto M, Clark JD, Pastor JV, Nandi A, Gurnani P, McGuinness OP, Chikuda H, Yamaguchi M, Kawaguchi H, Shimomura I, Takayama Y, Herz J, Kahn CR, Rosenblatt KP, Kuro-o M (2005) Suppression of aging in mice by the hormone Klotho. *Science* **309:** 1829-1833

Kuter DJ (2009) Thrombopoietin and thrombopoietin mimetics in the treatment of thrombocytopenia. *Annual review of medicine* **60:** 193-206

Kwan KM, Fujimoto E, Grabher C, Mangum BD, Hardy ME, Campbell DS, Parant JM, Yost HJ, Kanki JP, Chien CB (2007) The Tol2kit: a multisite gateway-based construction kit for Tol2 transposon transgenesis constructs. *Developmental dynamics : an official publication of the American Association of Anatomists* **236:** 3088-3099

Lacroix MC, Guibourdenche J, Frendo JL, Muller F, Evain-Brion D (2002) Human placental growth hormone--a review. *Placenta* **23 Suppl A:** S87-94

Lahuna O, Fernandez L, Karlsson H, Maiter D, Lemaigre FP, Rousseau GG, Gustafsson J, Mode A (1997) Expression of hepatocyte nuclear factor 6 in rat liver is sex-dependent and regulated by

growth hormone. *Proceedings of the National Academy of Sciences of the United States of America* **94:** 12309-12313

Lange M, Thulesen J, Feldt-Rasmussen U, Skakkebaek NE, Vahl N, Jorgensen JO, Christiansen JS, Poulsen SS, Sneppen SB, Juul A (2001) Skin morphological changes in growth hormone deficiency and acromegaly. *European journal of endocrinology / European Federation of Endocrine Societies* **145:** 147-153

Lannutti BJ, Drachman JG (2004) Lyn tyrosine kinase regulates thrombopoietin-induced proliferation of hematopoietic cell lines and primary megakaryocytic progenitors. *Blood* **103:** 3736-3743

Lantinga van Leeuwen IS, Teske E, van Garderen E, Mol JA (2000) Growth hormone gene expression in normal lymph nodes and lymphomas of the dog. *Anticancer research* **20:** 2371-2376

Lantinga-van Leeuwen IS, Oudshoorn M, Mol JA (1999) Canine mammary growth hormone gene transcription initiates at the pituitary-specific start site in the absence of Pit-1. *Molecular and cellular endocrinology* **150:** 121-128

Laron Z (1972) The role of growth hormone on fetal development in utero. *Advances in experimental medicine and biology* **27:** 391-398

Laron Z (2002) Growth hormone insensitivity (Laron syndrome). *Reviews in endocrine & metabolic disorders* **3:** 347-355

Laron Z, Ginsberg S, Webb M (2008) Nonalcoholic fatty liver in patients with Laron syndrome and GH gene deletion - preliminary report. *Growth hormone & IGF research : official journal of the Growth Hormone Research Society and the International IGF Research Society* **18:** 434-438

Laron Z, Pertzelan A, Mannheimer S (1966) Genetic pituitary dwarfism with high serum concentation of growth hormone--a new inborn error of metabolism? *Israel journal of medical sciences* **2:** 152-155

Latres E, Chiaur DS, Pagano M (1999) The human F box protein beta-Trcp associates with the Cul1/Skp1 complex and regulates the stability of beta-catenin. *Oncogene* **18:** 849-854

Law JH, Habibi G, Hu K, Masoudi H, Wang MY, Stratford AL, Park E, Gee JM, Finlay P, Jones HE, Nicholson RI, Carboni J, Gottardis M, Pollak M, Dunn SE (2008) Phosphorylated insulin-like growth factor-i/insulin receptor is present in all breast cancer subtypes and is related to poor survival. *Cancer research* **68:** 10238-10246

Le MN, Kohanski RA, Wang LH, Sadowski HB (2002) Dual mechanism of signal transducer and activator of transcription 5 activation by the insulin receptor. *Molecular endocrinology* **16:** 2764-2779

Lea MA, Randolph VM (1998) Induction of reporter gene expression by inhibitors of histone deacetylase. *Anticancer research* **18:** 2717-2722

Legraverend C, Mode A, Wells T, Robinson I, Gustafsson JA (1992) Hepatic steroid hydroxylating enzymes are controlled by the sexually dimorphic pattern of growth hormone secretion in normal and dwarf rats. *FASEB journal : official publication of the Federation of American Societies for Experimental Biology* **6:** 711-718

Leiser SF, Miller RA (2010) Nrf2 signaling, a mechanism for cellular stress resistance in long-lived mice. *Molecular and cellular biology* **30:** 871-884

Lempereur L, Brambilla D, Scoto GM, D'Alcamo M, Goffin V, Crosta L, Palmucci T, Rampello L, Bernardini R, Cantarella G (2003) Growth hormone protects human lymphocytes from irradiation-induced cell death. *British journal of pharmacology* **138:** 1411-1416

Lennerz V, Fatho M, Gentilini C, Frye RA, Lifke A, Ferel D, Wolfel C, Huber C, Wolfel T (2005) The response of autologous T cells to a human melanoma is dominated by mutated neoantigens. *Proceedings of the National Academy of Sciences of the United States of America* **102:** 16013-16018

Leong GM, Moverare S, Brce J, Doyle N, Sjogren K, Dahlman-Wright K, Gustafsson JA, Ho KK, Ohlsson C, Leung KC (2004) Estrogen up-regulates hepatic expression of suppressors of cytokine signaling-2 and -3 in vivo and in vitro. *Endocrinology* **145:** 5525-5531

Lerin C, Rodgers JT, Kalume DE, Kim SH, Pandey A, Puigserver P (2006) GCN5 acetyltransferase complex controls glucose metabolism through transcriptional repression of PGC-1alpha. *Cell metabolism* **3:** 429-438

Leung DW, Spencer SA, Cachianes G, Hammonds RG, Collins C, Henzel WJ, Barnard R, Waters MJ, Wood WI (1987) Growth hormone receptor and serum binding protein: purification, cloning and expression. *Nature* **330:** 537-543

Lewis BC, Chinnasamy N, Morgan RA, Varmus HE (2001) Development of an avian leukosis-sarcoma virus subgroup A pseudotyped lentiviral vector. *Journal of virology* **75:** 9339-9344

Lewis BC, Klimstra DS, Socci ND, Xu S, Koutcher JA, Varmus HE (2005) The absence of p53 promotes metastasis in a novel somatic mouse model for hepatocellular carcinoma. *Molecular and cellular biology* **25:** 1228-1237

Lewis MD, Horan M, Millar DS, Newsway V, Easter TE, Fryklund L, Gregory JW, Norin M, Del Valle CJ, Lopez-Siguero JP, Canete R, Lopez-Canti LF, Diaz-Torrado N, Espino R, Ulied A, Scanlon MF, Procter AM, Cooper DN (2004) A novel dysfunctional growth hormone variant (Ile179Met) exhibits a decreased ability to activate the extracellular signal-regulated kinase pathway. *The Journal of clinical endocrinology and metabolism* **89:** 1068-1075

Li H, Bartold PM, Young WG, Xiao Y, Waters MJ (2001) Growth hormone induces bone morphogenetic proteins and bone-related proteins in the developing rat periodontium. *Journal of bone and mineral research : the official journal of the American Society for Bone and Mineral Research* **16:** 1068-1076

Li X, Huang Y, Jiang J, Frank SJ (2011) Synergy in ERK activation by cytokine receptors and tyrosine kinase growth factor receptors. *Cellular signalling* **23:** 417-424

Li Y, Clevenger CV, Minkovsky N, Kumar KG, Raghunath PN, Tomaszewski JE, Spiegelman VS, Fuchs SY (2006) Stabilization of prolactin receptor in breast cancer cells. *Oncogene* **25:** 1896-1902

Li Y, Deeb B, Pendergrass W, Wolf N (1996) Cellular proliferative capacity and life span in small and large dogs. *The journals of gerontology Series A, Biological sciences and medical sciences* **51:** B403-408

Li Y, Huang TT, Carlson EJ, Melov S, Ursell PC, Olson JL, Noble LJ, Yoshimura MP, Berger C, Chan PH, Wallace DC, Epstein CJ (1995) Dilated cardiomyopathy and neonatal lethality in mutant mice lacking manganese superoxide dismutase. *Nature genetics* **11:** 376-381

Li Y, Kumar KG, Tang W, Spiegelman VS, Fuchs SY (2004) Negative regulation of prolactin receptor stability and signaling mediated by SCF(beta-TrCP) E3 ubiquitin ligase. *Molecular and cellular biology* **24:** 4038-4048

Liang H, Masoro EJ, Nelson JF, Strong R, McMahan CA, Richardson A (2003) Genetic mouse models of extended lifespan. *Experimental gerontology* **38:** 1353-1364

Lichanska AM, Waters MJ (2008) New insights into growth hormone receptor function and clinical implications. *Hormone research* **69:** 138-145

Lim JH, Lee YM, Chun YS, Chen J, Kim JE, Park JW (2010) Sirtuin 1 modulates cellular responses to hypoxia by deacetylating hypoxia-inducible factor 1alpha. *Molecular cell* **38:** 864-878

Lim L, Spencer SA, McKay P, Waters MJ (1990) Regulation of growth hormone (GH) bioactivity by a recombinant human GH-binding protein. *Endocrinology* **127:** 1287-1291

Lim WA, Richards FM, Fox RO (1994) Structural determinants of peptide-binding orientation and of sequence specificity in SH3 domains. *Nature* **372:** 375-379

Lin SC, Lin CR, Gukovsky I, Lusis AJ, Sawchenko PE, Rosenfeld MG (1993) Molecular basis of the little mouse phenotype and implications for cell type-specific growth. *Nature* **364:** 208-213

Lin SY, Makino K, Xia W, Matin A, Wen Y, Kwong KY, Bourguignon L, Hung MC (2001) Nuclear localization of EGF receptor and its potential new role as a transcription factor. *Nature cell biology* **3:** 802-808

Lin Y, Li S, Cao P, Cheng L, Quan M, Jiang S (2011) The effects of recombinant human GH on promoting tumor growth depend on the expression of GH receptor in vivo. *The Journal of endocrinology* **211:** 249-256

Lincoln DT, Kaiser HE, Raju GP, Waters MJ (2000) Growth hormone and colorectal carcinoma: localization of receptors. *In vivo* **14:** 41-49

Lincoln DT, Sinowatz F, Kolle S, Takahashi H, Parsons P, Waters M (1999) Up-regulation of growth hormone receptor immunoreactivity in human melanoma. *Anticancer research* **19:** 1919-1931

Lincoln DT, Sinowatz F, Temmim-Baker L, Baker HI, Kolle S, Waters MJ (1998) Growth hormone receptor expression in the nucleus and cytoplasm of normal and neoplastic cells. *Histochemistry and cell biology* **109:** 141-159

Lincoln DT, Water MJ, Breipohl W, Sinowatz F, Lobie PE (1990) Growth hormone receptors expression in the proliferating rat mammary gland. *Acta histochemica Supplementband* **40:** 47-49

Ling L, Zhu T, Lobie PE (2003) Src-CrkII-C3G-dependent activation of Rap1 switches growth hormone-stimulated p44/42 MAP kinase and JNK/SAPK activities. *The Journal of biological chemistry* **278:** 27301-27311

Liu AC, Tran HG, Zhang EE, Priest AA, Welsh DK, Kay SA (2008) Redundant function of REV-ERBalpha and beta and non-essential role for Bmal1 cycling in transcriptional regulation of intracellular circadian rhythms. *PLoS genetics* **4:** e1000023

Liu JC, Makova KD, Adkins RM, Gibson S, Li WH (2001) Episodic evolution of growth hormone in primates and emergence of the species specificity of human growth hormone receptor. *Molecular biology and evolution* **18:** 945-953

Liu JL, Coschigano KT, Robertson K, Lipsett M, Guo Y, Kopchick JJ, Kumar U, Liu YL (2004) Disruption of growth hormone receptor gene causes diminished pancreatic islet size and increased insulin sensitivity in mice. *American journal of physiology Endocrinology and metabolism* **287:** E405-413

Liu L, Russell SM, Nicoll CS (1987) Growth and differentiation of transplanted rat embryos in intact, diabetic and hypophysectomized hosts: comparison with their growth in situ. *Biology of the neonate* **52:** 307-316

Liu N, Mertani HC, Norstedt G, Tornell J, Lobie PE (1997) Mode of the autocrine/paracrine mechanism of growth hormone action. *Experimental cell research* **237:** 196-206

Liu W, Kawahara M, Ueda H, Nagamune T (2009) The influence of domain structures on the signal transduction of chimeric receptors derived from the erythropoietin receptor. *Journal of biochemistry* **145:** 575-584

Lo HW, Ali-Seyed M, Wu Y, Bartholomeusz G, Hsu SC, Hung MC (2006) Nuclear-cytoplasmic transport of EGFR involves receptor endocytosis, importin beta1 and CRM1. *Journal of cellular biochemistry* **98:** 1570-1583

Lobie PE, Barnard R, Waters MJ (1991) The nuclear growth hormone receptor binding protein. Antigenic and physicochemical characterization. *The Journal of biological chemistry* **266:** 22645-22652

Lobie PE, Breipohl W, Lincoln DT, Garcia-Aragon J, Waters MJ (1990a) Localization of the growth hormone receptor/binding protein in skin. *The Journal of endocrinology* **126:** 467-471

Lobie PE, Breipohl W, Waters MJ (1990b) Growth hormone receptor expression in the rat gastrointestinal tract. *Endocrinology* **126:** 299-306

Lobie PE, Garcia-Aragon J, Lincoln DT, Barnard R, Wilcox JN, Waters MJ (1993) Localization and ontogeny of growth hormone receptor gene expression in the central nervous system. *Brain research Developmental brain research* **74:** 225-233

Lobie PE, Garcia-Aragon J, Wang BS, Baumbach WR, Waters MJ (1992) Cellular localization of the growth hormone binding protein in the rat. *Endocrinology* **130:** 3057-3065

Lobie PE, Mertani H, Morel G, Morales-Bustos O, Norstedt G, Waters MJ (1994a) Receptor-mediated nuclear translocation of growth hormone. *The Journal of biological chemistry* **269:** 21330-21339

Lobie PE, Sadir R, Graichen R, Mertani HC, Morel G (1999) Caveolar internalization of growth hormone. *Experimental cell research* **246:** 47-55

Lobie PE, Wood TJ, Chen CM, Waters MJ, Norstedt G (1994b) Nuclear translocation and anchorage of the growth hormone receptor. *The Journal of biological chemistry* **269:** 31735-31746

Loesch K, Deng L, Cowan JW, Wang X, He K, Jiang J, Black RA, Frank SJ (2006) Janus kinase 2 influences growth hormone receptor metalloproteolysis. *Endocrinology* **147:** 2839-2849

Loesch K, Deng L, Wang X, He K, Jiang J, Frank SJ (2007) Endoplasmic reticulum-associated degradation of growth hormone receptor in Janus kinase 2-deficient cells. *Endocrinology* **148:** 5955-5965

Loftus SK, Larson DM, Watkins-Chow D, Church DM, Pavan WJ (2001) Generation of RCAS vectors useful for functional genomic analyses. *DNA Res* **8:** 221-226

Lombard DB, Alt FW, Cheng HL, Bunkenborg J, Streeper RS, Mostoslavsky R, Kim J, Yancopoulos G, Valenzuela D, Murphy A, Yang Y, Chen Y, Hirschey MD, Bronson RT, Haigis M, Guarente LP, Farese RV, Jr., Weissman S, Verdin E, Schwer B (2007) Mammalian Sir2 homolog SIRT3 regulates global mitochondrial lysine acetylation. *Molecular and cellular biology* **27:** 8807-8814

Longhi SA, Cortes MM, Retegui LA (2003) 22- and 20 kDa-human growth hormones bind to different sites within certain cellular receptors. *Growth hormone & IGF research : official journal of the Growth Hormone Research Society and the International IGF Research Society* **13:** 353-360

Loser P, Jennings GS, Strauss M, Sandig V (1998) Reactivation of the previously silenced cytomegalovirus major immediate-early promoter in the mouse liver: involvement of NFkappaB. *Journal of virology* **72:** 180-190

Lu C, Kumar PA, Fan Y, Sperling MA, Menon RK (2010) A novel effect of growth hormone on macrophage modulates macrophage-dependent adipocyte differentiation. *Endocrinology* **151:** 2189-2199

Lu X, Gross AW, Lodish HF (2006) Active conformation of the erythropoietin receptor: random and cysteine-scanning mutagenesis of the extracellular juxtamembrane and transmembrane domains. *The Journal of biological chemistry* **281:** 7002-7011

Lu X, Huang LJ, Lodish HF (2008) Dimerization by a cytokine receptor is necessary for constitutive activation of JAK2V617F. *The Journal of biological chemistry* **283:** 5258-5266

Lubbers ER, List EO, Jara A, Sackman-Sala L, Cordoba-Chacon J, Gahete MD, Kineman RD, Boparai R, Bartke A, Kopchick JJ, Berryman DE (2013) Adiponectin in mice with altered GH action: links to insulin sensitivity and longevity? *The Journal of endocrinology* **216:** 363-374

Lucet IS, Fantino E, Styles M, Bamert R, Patel O, Broughton SE, Walter M, Burns CJ, Treutlein H, Wilks AF, Rossjohn J (2006) The structural basis of Janus kinase 2 inhibition by a potent and specific pan-Janus kinase inhibitor. *Blood* **107:** 176-183

Ludovini V, Bellezza G, Pistola L, Bianconi F, Di Carlo L, Sidoni A, Semeraro A, Del Sordo R, Tofanetti FR, Mameli MG, Daddi G, Cavaliere A, Tonato M, Crino L (2009) High coexpression of both insulin-like growth factor receptor-1 (IGFR-1) and epidermal growth factor receptor (EGFR) is associated with shorter disease-free survival in resected non-small-cell lung cancer patients. *Annals of oncology : official journal of the European Society for Medical Oncology / ESMO* **20:** 842-849

Lukanova A, Zeleniuch-Jacquotte A, Lundin E, Micheli A, Arslan AA, Rinaldi S, Muti P, Lenner P, Koenig KL, Biessy C, Krogh V, Riboli E, Shore RE, Stattin P, Berrino F, Hallmans G, Toniolo P, Kaaks R (2004) Prediagnostic levels of C-peptide, IGF-I, IGFBP -1, -2 and -3 and risk of endometrial cancer. *International journal of cancer Journal international du cancer* **108:** 262-268

Luo J, Nikolaev AY, Imai S, Chen D, Su F, Shiloh A, Guarente L, Gu W (2001) Negative control of p53 by Sir2alpha promotes cell survival under stress. *Cell* **107:** 137-148

Lupu F, Terwilliger JD, Lee K, Segre GV, Efstratiadis A (2001) Roles of growth hormone and insulin-like growth factor 1 in mouse postnatal growth. *Developmental biology* **229:** 141-162

Ma F, Wei Z, Shi C, Gan Y, Lu J, Frank SJ, Balducci J, Huang Y (2011) Signaling cross talk between growth hormone (GH) and insulin-like growth factor-I (IGF-I) in pancreatic islet beta-cells. *Molecular endocrinology* **25:** 2119-2133

Maamra M, Milward A, Esfahani HZ, Abbott LP, Metherell LA, Savage MO, Clark AJ, Ross RJ (2006) A 36 residues insertion in the dimerization domain of the growth hormone receptor results in defective trafficking rather than impaired signaling. *The Journal of endocrinology* **188:** 251-261

Madsen MA, Hsieh CC, Boylston WH, Flurkey K, Harrison D, Papaconstantinou J (2004) Altered oxidative stress response of the long-lived Snell dwarf mouse. *Biochemical and biophysical research communications* **318:** 998-1005

Magkou C, Mylona E, Theohari I, Giannopoulou I, Papanikolaou E, Markaki S, Nakopoulou L (2007) An immunohistochemical evaluation of phosphorylated Akt at threonine 308 [pAkt(Thr308)] in invasive breast cancer. *In vivo* **21:** 967-972

Magnani E, Bartling L, Hake S (2006) From Gateway to MultiSite Gateway in one recombination event. *BMC Mol Biol* **7:** 46

Makki K, Froguel P, Wolowczuk I (2013) Adipose Tissue in Obesity-Related Inflammation and Insulin Resistance: Cells, Cytokines, and Chemokines. *ISRN inflammation* **2013:** 139239

Malaguarnera R, Belfiore A (2014) The Emerging Role of Insulin and Insulin-Like Growth Factor Signaling in Cancer Stem Cells. *Frontiers in endocrinology* **5:** 10

Malin A, Matthews CE, Shu XO, Cai H, Dai Q, Jin F, Gao YT, Zheng W (2005) Energy balance and breast cancer risk. *Cancer epidemiology, biomarkers & prevention : a publication of the American Association for Cancer Research, cosponsored by the American Society of Preventive Oncology* **14:** 1496-1501

Mallette FA, Ferbeyre G (2007) The DNA damage signaling pathway connects oncogenic stress to cellular senescence. *Cell cycle* **6:** 1831-1836

Manabe N, Kubota Y, Kitanaka A, Ohnishi H, Taminato T, Tanaka T (2006) Src transduces signaling via growth hormone (GH)-activated GH receptor (GHR) tyrosine-phosphorylating GHR and STAT5 in human leukemia cells. *Leukemia research* **30:** 1391-1398

Manhes C, Kayser C, Bertheau P, Kelder B, Kopchick JJ, Kelly PA, Touraine P, Goffin V (2006) Local over-expression of prolactin in differentiating mouse mammary gland induces functional defects and benign lesions, but no carcinoma. *The Journal of endocrinology* **190:** 271-285

Marques RB, Dits NF, Erkens-Schulze S, van Weerden WM, Jenster G (2010) Bypass mechanisms of the androgen receptor pathway in therapy-resistant prostate cancer cell models. *PloS one* **5:** e13500

Martin-Montalvo A, Villalba JM, Navas P, de Cabo R (2011) NRF2, cancer and calorie restriction. *Oncogene* **30:** 505-520

Martinez-Redondo P, Santos-Barriopedro I, Vaquero A (2012) A big step for SIRT7, one giant leap for Sirtuins... in cancer. *Cancer cell* **21:** 719-721

Marty C, Lacout C, Droin N, Le Couedic JP, Ribrag V, Solary E, Vainchenker W, Villeval JL, Plo I (2013) A role for reactive oxygen species in JAK2 V617F myeloproliferative neoplasm progression. *Leukemia* **27:** 2187-2195

Masternak MM, Al-Regaiey KA, Del Rosario Lim MM, Jimenez-Ortega V, Panici JA, Bonkowski MS, Bartke A (2005) Effects of caloric restriction on insulin pathway gene expression in the skeletal muscle and liver of normal and long-lived GHR-KO mice. *Experimental gerontology* **40:** 679-684

Masternak MM, Bartke A (2007) PPARs in Calorie Restricted and Genetically Long-Lived Mice. *PPAR research* **2007:** 28436

Masternak MM, Bartke A (2012) Growth hormone, inflammation and aging. *Pathobiology of aging & age related diseases* **2**

Masternak MM, Panici JA, Bonkowski MS, Hughes LF, Bartke A (2009) Insulin sensitivity as a key mediator of growth hormone actions on longevity. *The journals of gerontology Series A, Biological sciences and medical sciences* **64:** 516-521

Matakidou A, Eisen T, Houlston RS (2005) Systematic review of the relationship between family history and lung cancer risk. *British journal of cancer* **93:** 825-833

Matoba S, Kang JG, Patino WD, Wragg A, Boehm M, Gavrilova O, Hurley PJ, Bunz F, Hwang PM (2006) p53 regulates mitochondrial respiration. *Science* **312:** 1650-1653

Matsumoto M, Kurihara S, Kibe R, Ashida H, Benno Y (2011) Longevity in mice is promoted by probiotic-induced suppression of colonic senescence dependent on upregulation of gut bacterial polyamine production. *PloS one* **6:** e23652

Matthews EE, Thevenin D, Rogers JM, Gotow L, Lira PD, Reiter LA, Brissette WH, Engelman DM (2011) Thrombopoietin receptor activation: transmembrane helix dimerization, rotation, and allosteric modulation. *FASEB journal : official publication of the Federation of American Societies for Experimental Biology* **25:** 2234-2244

Mayr U, von Werder A, Seidler B, Reindl W, Bajbouj M, Schmid RM, Schneider G, Saur D (2008) RCAS-mediated Retroviral Gene Delivery - A Versatile Tool to Study Gene Function in a Mouse Model of Pancreatic Cancer. *Hum Gene Ther*

Mazurkiewicz-Munoz AM, Argetsinger LS, Kouadio JL, Stensballe A, Jensen ON, Cline JM, Carter-Su C (2006) Phosphorylation of JAK2 at serine 523: a negative regulator of JAK2 that is

stimulated by growth hormone and epidermal growth factor. *Molecular and cellular biology* **26:** 4052-4062

McCann JP, Altszuler N, Hampshire J, Concannon PW (1987) Growth hormone, insulin, glucose, cortisol, luteinizing hormone, and diabetes in beagle bitches treated with medroxyprogesterone acetate. *Acta endocrinologica* **116:** 73-80

McCarter R, Mejia W, Ikeno Y, Monnier V, Kewitt K, Gibbs M, McMahan A, Strong R (2007) Plasma glucose and the action of calorie restriction on aging. *The journals of gerontology Series A, Biological sciences and medical sciences* **62:** 1059-1070

McLenachan S, Lum MG, Waters MJ, Turnley AM (2009) Growth hormone promotes proliferation of adult neurosphere cultures. *Growth hormone & IGF research : official journal of the Growth Hormone Research Society and the International IGF Research Society* **19:** 212-218

Meazza C, Elsedfy HH, Pagani S, Bozzola E, El Kholy M, Bozzola M (2013) Metabolic Parameters and Adipokine Profile in Growth Hormone Deficient (GHD) Children Before and After 12-Month GH Treatment. *Hormone and metabolic research = Hormon- und Stoffwechselforschung = Hormones et metabolisme*

Mehta AK, Majumdar SS, Alam P, Gulati N, Brahmachari V (2009) Epigenetic regulation of cytomegalovirus major immediate-early promoter activity in transgenic mice. *Gene* **428:** 20-24

Melikyan GB, Barnard RJ, Markosyan RM, Young JA, Cohen FS (2004) Low pH is required for avian sarcoma and leukosis virus Env-induced hemifusion and fusion pore formation but not for pore growth. *Journal of virology* **78:** 3753-3762

Meng J, Tsai-Morris CH, Dufau ML (2004) Human prolactin receptor variants in breast cancer: low ratio of short forms to the long-form human prolactin receptor associated with mammary carcinoma. *Cancer research* **64:** 5677-5682

Mercado M, DaVila N, McLeod JF, Baumann G (1994) Distribution of growth hormone receptor messenger ribonucleic acid containing and lacking exon 3 in human tissues. *The Journal of clinical endocrinology and metabolism* **78:** 731-735

Mertani HC, Garcia-Caballero T, Lambert A, Gerard F, Palayer C, Boutin JM, Vonderhaar BK, Waters MJ, Lobie PE, Morel G (1998) Cellular expression of growth hormone and prolactin receptors in human breast disorders. *International journal of cancer Journal international du cancer* **79:** 202-211

Mertani HC, Morel G, Lobie PE (1999) Cytoplasmic and nuclear cytokine receptor complexes. *Vitamins and hormones* **57:** 79-121

Mertani HC, Waters MJ, Morel G (1996) Cellular trafficking of exogenous growth hormone in dwarf rat pituitary. *Neuroendocrinology* **63:** 257-268

Mertani HC, Zhu T, Goh EL, Lee KO, Morel G, Lobie PE (2001) Autocrine human growth hormone (hGH) regulation of human mammary carcinoma cell gene expression. Identification of CHOP as a mediator of hGH-stimulated human mammary carcinoma cell survival. *The Journal of biological chemistry* **276:** 21464-21475

Metcalf D, Greenhalgh CJ, Viney E, Willson TA, Starr R, Nicola NA, Hilton DJ, Alexander WS (2000) Gigantism in mice lacking suppressor of cytokine signalling-2. *Nature* **405:** 1069-1073

Meton I, Boot EP, Sussenbach JS, Steenbergh PH (1999) Growth hormone induces insulin-like growth factor-I gene transcription by a synergistic action of STAT5 and HNF-1alpha. *FEBS letters* **444:** 155-159

Meyer L, Deau B, Forejtnikova H, Dumenil D, Margottin-Goguet F, Lacombe C, Mayeux P, Verdier F (2007) beta-Trcp mediates ubiquitination and degradation of the erythropoietin receptor and controls cell proliferation. *Blood* **109:** 5215-5222

Michishita E, McCord RA, Berber E, Kioi M, Padilla-Nash H, Damian M, Cheung P, Kusumoto R, Kawahara TL, Barrett JC, Chang HY, Bohr VA, Ried T, Gozani O, Chua KF (2008) SIRT6 is a histone H3 lysine 9 deacetylase that modulates telomeric chromatin. *Nature* **452:** 492-496

Michishita E, McCord RA, Boxer LD, Barber MF, Hong T, Gozani O, Chua KF (2009) Cell cycle-dependent deacetylation of telomeric histone H3 lysine K56 by human SIRT6. *Cell cycle* **8:** 2664-2666

Michishita E, Park JY, Burneskis JM, Barrett JC, Horikawa I (2005) Evolutionarily conserved and nonconserved cellular localizations and functions of human SIRT proteins. *Molecular biology of the cell* **16:** 4623-4635

Migliaccio E, Giorgio M, Mele S, Pelicci G, Reboldi P, Pandolfi PP, Lanfrancone L, Pelicci PG (1999) The p66shc adaptor protein controls oxidative stress response and life span in mammals. *Nature* **402:** 309-313

Mihaylova MM, Shaw RJ (2011) The AMPK signalling pathway coordinates cell growth, autophagy and metabolism. *Nature cell biology* **13:** 1016-1023

Milewicz T, Rys J, Wojtowicz A, Stochmal E, Jach R, Krzysiek J, Gregoraszczuk E, Huras H, Dziadek O (2011) Overexpression of P53 protein and local hGH, IGF-I, IGFBP-3, IGFBP-2 and PRL secretion by human breast cancer explants. *Neuro endocrinology letters* **32:** 328-333

Miller WL, Eberhardt NL (1983) Structure and evolution of the growth hormone gene family. *Endocrine reviews* **4:** 97-130

Mills E, O'Neill LA (2013) Succinate: a metabolic signal in inflammation. *Trends in cell biology*

Milward A, Metherell L, Maamra M, Barahona MJ, Wilkinson IR, Camacho-Hubner C, Savage MO, Bidlingmaier M, Clark AJ, Ross RJ, Webb SM (2004) Growth hormone (GH) insensitivity syndrome due to a GH receptor truncated after Box1, resulting in isolated failure of STAT 5 signal transduction. *The Journal of clinical endocrinology and metabolism* **89:** 1259-1266

Minamitani K (2002) [Truncated growth hormone receptor mutations function as dominant-negative inhibitors of the full-length receptor and cause genetic short stature]. *Nihon rinsho Japanese journal of clinical medicine* **60:** 313-318

Minoia M, Gentilin E, Mole D, Rossi M, Filieri C, Tagliati F, Baroni A, Ambrosio MR, degli Uberti E, Zatelli MC (2012) Growth hormone receptor blockade inhibits growth hormone-induced chemoresistance by restoring cytotoxic-induced apoptosis in breast cancer cells independently of estrogen receptor expression. *The Journal of clinical endocrinology and metabolism* **97:** E907-916

Miquet JG, Freund T, Martinez CS, Gonzalez L, Diaz ME, Micucci GP, Zotta E, Boparai RK, Bartke A, Turyn D, Sotelo AI (2013) Hepatocellular alterations and dysregulation of oncogenic pathways in the liver of transgenic mice overexpressing growth hormone. *Cell cycle* **12:** 1042-1057

Miquet JG, Giani JF, Martinez CS, Munoz MC, Gonzalez L, Sotelo AI, Boparai RK, Masternak MM, Bartke A, Dominici FP, Turyn D (2011) Prolonged exposure to GH impairs insulin signaling in the heart. *Journal of molecular endocrinology* **47:** 167-177

Miquet JG, Gonzalez L, Matos MN, Hansen CE, Louis A, Bartke A, Turyn D, Sotelo AI (2008) Transgenic mice overexpressing GH exhibit hepatic upregulation of GH-signaling mediators involved in cell proliferation. *The Journal of endocrinology* **198:** 317-330

Mishra DK, Chen Z, Wu Y, Sarkissyan M, Koeffler HP, Vadgama JV (2010) Global methylation pattern of genes in androgen-sensitive and androgen-independent prostate cancer cells. *Molecular cancer therapeutics* **9:** 33-45

Mitsui A, Hamuro J, Nakamura H, Kondo N, Hirabayashi Y, Ishizaki-Koizumi S, Hirakawa T, Inoue T, Yodoi J (2002) Overexpression of human thioredoxin in transgenic mice controls oxidative stress and life span. *Antioxidants & redox signaling* **4:** 693-696

Miyoshi H, Blomer U, Takahashi M, Gage FH, Verma IM (1998) Development of a self-inactivating lentivirus vector. *Journal of virology* **72:** 8150-8157

Mol JA, Henzen-Logmans SC, Hageman P, Misdorp W, Blankenstein MA, Rijnberk A (1995a) Expression of the gene encoding growth hormone in the human mammary gland. *The Journal of clinical endocrinology and metabolism* **80:** 3094-3096

Mol JA, van Garderen E, Selman PJ, Wolfswinkel J, Rijinberk A, Rutteman GR (1995b) Growth hormone mRNA in mammary gland tumors of dogs and cats. *The Journal of clinical investigation* **95:** 2028-2034

Moller N, Jorgensen JO, Schmitz O, Moller J, Christiansen J, Alberti KG, Orskov H (1990) Effects of a growth hormone pulse on total and forearm substrate fluxes in humans. *The American journal of physiology* **258:** E86-91

Morita S, Kojima T, Kitamura T (2000) Plat-E: an efficient and stable system for transient packaging of retroviruses. *Gene Ther* **7:** 1063-1066

Morris BJ (2013) Seven sirtuins for seven deadly diseases of aging. *Free radical biology & medicine* **56:** 133-171

Mothes W, Boerger AL, Narayan S, Cunningham JM, Young JA (2000) Retroviral entry mediated by receptor priming and low pH triggering of an envelope glycoprotein. *Cell* **103:** 679-689

Mukhina S, Mertani HC, Guo K, Lee KO, Gluckman PD, Lobie PE (2004) Phenotypic conversion of human mammary carcinoma cells by autocrine human growth hormone. *Proceedings of the National Academy of Sciences of the United States of America* **101:** 15166-15171

Murakami S (2006) Stress resistance in long-lived mouse models. *Experimental gerontology* **41:** 1014-1019

Murakami S, Salmon A, Miller RA (2003) Multiplex stress resistance in cells from long-lived dwarf mice. *FASEB journal : official publication of the Federation of American Societies for Experimental Biology* **17:** 1565-1566

Murphy GJ, Leavitt AD (1999) A model for studying megakaryocyte development and biology. *Proceedings of the National Academy of Sciences of the United States of America* **96:** 3065-3070

Murphy LJ, Lazarus L (1984) The mouse fibroblast growth hormone receptor: ligand processing and receptor modulation and turnover. *Endocrinology* **115:** 1625-1632

Mutel E, Gautier-Stein A, Abdul-Wahed A, Amigo-Correig M, Zitoun C, Stefanutti A, Houberdon I, Tourette JA, Mithieux G, Rajas F (2011) Control of blood glucose in the absence of hepatic glucose production during prolonged fasting in mice: induction of renal and intestinal gluconeogenesis by glucagon. *Diabetes* **60:** 3121-3131

Myers MG, Jr., Mendez R, Shi P, Pierce JH, Rhoads R, White MF (1998) The COOH-terminal tyrosine phosphorylation sites on IRS-1 bind SHP-2 and negatively regulate insulin signaling. *The Journal of biological chemistry* **273:** 26908-26914

Nabarro JD (1987) Acromegaly. *Clinical endocrinology* **26:** 481-512

Nabi IR, Le PU (2003) Caveolae/raft-dependent endocytosis. *The Journal of cell biology* **161:** 673-677

Nakonechnaya AO, Jefferson HS, Chen X, Shewchuk BM (2013) Differential effects of exogenous and autocrine growth hormone on LNCaP prostate cancer cell proliferation and survival. *Journal of cellular biochemistry* **114:** 1322-1335

Naldini L (1999) In vivo gene delivery by lentiviral vectors. *Thromb Haemost* **82:** 552-554

Naldini L, Blomer U, Gage FH, Trono D, Verma IM (1996) Efficient transfer, integration, and sustained long-term expression of the transgene in adult rat brains injected with a lentiviral vector. *Proceedings of the National Academy of Sciences of the United States of America* **93:** 11382-11388

Napolitano LA, Schmidt D, Gotway MB, Ameli N, Filbert EL, Ng MM, Clor JL, Epling L, Sinclair E, Baum PD, Li K, Killian ML, Bacchetti P, McCune JM (2008) Growth hormone enhances thymic function in HIV-1-infected adults. *The Journal of clinical investigation* **118:** 1085-1098

Neggers SJ, van der Lely AJ (2011) Pegvisomant and improvement of quality of life in acromegalic patients. *Hormone research in paediatrics* **76 Suppl 1:** 102-105

Nelson JF, Strong R, Bokov A, Diaz V, Ward W (2012) Probing the relationship between insulin sensitivity and longevity using genetically modified mice. *The journals of gerontology Series A, Biological sciences and medical sciences* **67:** 1332-1338

Nelson RF, Glenn KA, Miller VM, Wen H, Paulson HL (2006) A novel route for F-box protein-mediated ubiquitination links CHIP to glycoprotein quality control. *The Journal of biological chemistry* **281:** 20242-20251

Nemoto S, Fergusson MM, Finkel T (2004) Nutrient availability regulates SIRT1 through a forkhead-dependent pathway. *Science* **306:** 2105-2108

Nguyen AP, Chandorkar A, Gupta C (1996) The role of growth hormone in fetal mouse reproductive tract differentiation. *Endocrinology* **137:** 3659-3666

Nicholson SE, Willson TA, Farley A, Starr R, Zhang JG, Baca M, Alexander WS, Metcalf D, Hilton DJ, Nicola NA (1999) Mutational analyses of the SOCS proteins suggest a dual domain requirement but distinct mechanisms for inhibition of LIF and IL-6 signal transduction. *The EMBO journal* **18:** 375-385

Nilsson O, Marino R, De Luca F, Phillip M, Baron J (2005) Endocrine regulation of the growth plate. *Hormone research* **64:** 157-165

Nishizawa H, Handayaningsih AE, Iguchi G, Cho Y, Takahashi M, Yamamoto M, Suda K, Kasahara K, Hakuno F, Yamanouchi K, Nishihara M, Seino S, Takahashi S, Takahashi Y (2012) Enhanced oxidative stress in GH-transgenic rat and acromegaly in humans. *Growth hormone & IGF research : official journal of the Growth Hormone Research Society and the International IGF Research Society* **22:** 64-68

Niture SK, Jain AK, Shelton PM, Jaiswal AK (2011) Src subfamily kinases regulate nuclear export and degradation of transcription factor Nrf2 to switch off Nrf2-mediated antioxidant activation of cytoprotective gene expression. *The Journal of biological chemistry* **286:** 28821-28832

Nitze LM, Galsgaard ED, Din N, Lund VL, Rasmussen BB, Berchtold MW, Christensen L, Panina S (2013) Reevaluation of the proposed autocrine proliferative function of prolactin in breast cancer. *Breast cancer research and treatment* **142:** 31-44

Noble ME, Musacchio A, Saraste M, Courtneidge SA, Wierenga RK (1993) Crystal structure of the SH3 domain in human Fyn; comparison of the three-dimensional structures of SH3 domains in tyrosine kinases and spectrin. *The EMBO journal* **12:** 2617-2624

Noto H, Tsujimoto T, Sasazuki T, Noda M (2011) Significantly increased risk of cancer in patients with diabetes mellitus: a systematic review and meta-analysis. *Endocrine practice : official journal of the American College of Endocrinology and the American Association of Clinical Endocrinologists* **17:** 616-628

Oakhill JS, Scott JW, Kemp BE (2012) AMPK functions as an adenylate charge-regulated protein kinase. *Trends in endocrinology and metabolism: TEM* **23:** 125-132

Ocaranza P, Morales F, Roman R, Iniguez G, Fernando C (2012) Expression of SOCS1, SOCS2, and SOCS3 in growth hormone-stimulated skin fibroblasts from children with idiopathic short stature. *Journal of pediatric endocrinology & metabolism : JPEM* **25:** 273-278

Ohlsson C, Lovstedt K, Holmes PV, Nilsson A, Carlsson L, Tornell J (1993) Embryonic stem cells express growth hormone receptors: regulation by retinoic acid. *Endocrinology* **133:** 2897-2903

Ohlsson C, Mohan S, Sjogren K, Tivesten A, Isgaard J, Isaksson O, Jansson JO, Svensson J (2009) The role of liver-derived insulin-like growth factor-I. *Endocrine reviews* **30:** 494-535

Okada S, Kopchick JJ (2001) Biological effects of growth hormone and its antagonist. *Trends in molecular medicine* **7:** 126-132

Okutani Y, Kitanaka A, Tanaka T, Kamano H, Ohnishi H, Kubota Y, Ishida T, Takahara J (2001) Src directly tyrosine-phosphorylates STAT5 on its activation site and is involved in erythropoietin-induced signaling pathway. *Oncogene* **20:** 6643-6650

Olefsky JM, Glass CK (2010) Macrophages, inflammation, and insulin resistance. *Annual review of physiology* **72:** 219-246

Olivo-Marston SE, Hursting SD, Lavigne J, Perkins SN, Maarouf RS, Yakar S, Harris CC (2009) Genetic reduction of circulating insulin-like growth factor-1 inhibits azoxymethane-induced colon tumorigenesis in mice. *Molecular carcinogenesis* **48:** 1071-1076

Olney RC (2003) Regulation of bone mass by growth hormone. *Medical and pediatric oncology* **41:** 228-234

Olsson B, Bohlooly YM, Fitzgerald SM, Frick F, Ljungberg A, Ahren B, Tornell J, Bergstrom G, Oscarsson J (2005) Bovine growth hormone transgenic mice are resistant to diet-induced obesity but develop hyperphagia, dyslipidemia, and diabetes on a high-fat diet. *Endocrinology* **146:** 920-930

Omodei D, Licastro D, Salvatore F, Crosby SD, Fontana L (2013) Serum from humans on long-term calorie restriction enhances stress resistance in cell culture. *Aging* **5:** 599-606

Onishi M, Mui AL, Morikawa Y, Cho L, Kinoshita S, Nolan GP, Gorman DM, Miyajima A, Kitamura T (1996) Identification of an oncogenic form of the thrombopoietin receptor MPL using retrovirus-mediated gene transfer. *Blood* **88:** 1399-1406

Onken B, Driscoll M (2010) Metformin induces a dietary restriction-like state and the oxidative stress response to extend C. elegans Healthspan via AMPK, LKB1, and SKN-1. *PloS one* **5:** e8758

Onyango P, Celic I, McCaffery JM, Boeke JD, Feinberg AP (2002) SIRT3, a human SIR2 homologue, is an NAD-dependent deacetylase localized to mitochondria. *Proceedings of the National Academy of Sciences of the United States of America* **99:** 13653-13658

Orlicky S, Tang X, Willems A, Tyers M, Sicheri F (2003) Structural basis for phosphodependent substrate selection and orientation by the SCFCdc4 ubiquitin ligase. *Cell* **112:** 243-256

Orme SM, McNally RJ, Cartwright RA, Belchetz PE (1998) Mortality and cancer incidence in acromegaly: a retrospective cohort study. United Kingdom Acromegaly Study Group. *The Journal of clinical endocrinology and metabolism* **83:** 2730-2734

Orsulic S (2002) An RCAS-TVA-based approach to designer mouse models. *Mamm Genome* **13:** 543-547

Owen C, Lees EK, Grant L, Zimmer DJ, Mody N, Bence KK, Delibegovic M (2013) Inducible liver-specific knockdown of protein tyrosine phosphatase 1B improves glucose and lipid homeostasis in adult mice. *Diabetologia* **56:** 2286-2296

Owen MR, Doran E, Halestrap AP (2000) Evidence that metformin exerts its anti-diabetic effects through inhibition of complex 1 of the mitochondrial respiratory chain. *The Biochemical journal* **348 Pt 3:** 607-614

Owens KM, Kulawiec M, Desouki MM, Vanniarajan A, Singh KK (2011) Impaired OXPHOS complex III in breast cancer. *PloS one* **6:** e23846

Ozkan EE (2011) Plasma and tissue insulin-like growth factor-I receptor (IGF-IR) as a prognostic marker for prostate cancer and anti-IGF-IR agents as novel therapeutic strategy for refractory cases: a review. *Molecular and cellular endocrinology* **344:** 1-24

Palacios OM, Carmona JJ, Michan S, Chen KY, Manabe Y, Ward JL, 3rd, Goodyear LJ, Tong Q (2009) Diet and exercise signals regulate SIRT3 and activate AMPK and PGC-1alpha in skeletal muscle. *Aging* **1:** 771-783

Palmeiro CR, Anand R, Dardi IK, Balasubramaniyam N, Schwarcz MD, Weiss IA (2012) Growth hormone and the cardiovascular system. *Cardiology in review* **20:** 197-207

Palmer AJ, Chung MY, List EO, Walker J, Okada S, Kopchick JJ, Berryman DE (2009) Age-related changes in body composition of bovine growth hormone transgenic mice. *Endocrinology* **150:** 1353-1360

Pandey V, Perry JK, Mohankumar KM, Kong XJ, Liu SM, Wu ZS, Mitchell MD, Zhu T, Lobie PE (2008) Autocrine human growth hormone stimulates oncogenicity of endometrial carcinoma cells. *Endocrinology* **149:** 3909-3919

Pantaleon M, Whiteside EJ, Harvey MB, Barnard RT, Waters MJ, Kaye PL (1997) Functional growth hormone (GH) receptors and GH are expressed by preimplantation mouse embryos: a role for GH in early embryogenesis? *Proceedings of the National Academy of Sciences of the United States of America* **94:** 5125-5130

Pao W, Klimstra DS, Fisher GH, Varmus HE (2003) Use of avian retroviral vectors to introduce transcriptional regulators into mammalian cells for analyses of tumor maintenance. *Proceedings of the National Academy of Sciences of the United States of America* **100:** 8764-8769

Park PH, Huang H, McMullen MR, Mandal P, Sun L, Nagy LE (2008) Suppression of lipopolysaccharide-stimulated tumor necrosis factor-alpha production by adiponectin is mediated by transcriptional and post-transcriptional mechanisms. *The Journal of biological chemistry* **283:** 26850-26858

Park S, Kim M, Paik JK, Jang YJ, Lee SH, Lee JH (2013) Oxidative stress is associated with C-reactive protein in nondiabetic postmenopausal women, independent of obesity and insulin resistance. *Clinical endocrinology* **79:** 65-70

Parsons JA, Bartke A, Sorenson RL (1995) Number and size of islets of Langerhans in pregnant, human growth hormone-expressing transgenic, and pituitary dwarf mice: effect of lactogenic hormones. *Endocrinology* **136:** 2013-2021

Parsons SJ, Parsons JT (2004) Src family kinases, key regulators of signal transduction. *Oncogene* **23:** 7906-7909

Pasquali C, Curchod ML, Walchli S, Espanel X, Guerrier M, Arigoni F, Strous G, Hooft van Huijsduijnen R (2003) Identification of protein tyrosine phosphatases with specificity for the ligand-activated growth hormone receptor. *Molecular endocrinology* **17:** 2228-2239

Paul C, Seiliez I, Thissen JP, Le Cam A (2000) Regulation of expression of the rat SOCS-3 gene in hepatocytes by growth hormone, interleukin-6 and glucocorticoids mRNA analysis and promoter characterization. *European journal of biochemistry / FEBS* **267:** 5849-5857

Pazaitou-Panayiotou K, Kelesidis T, Kelesidis I, Kaprara A, Blakeman J, Vainas I, Mpousoulegas A, Williams CJ, Mantzoros C (2007) Growth hormone-binding protein is directly and IGFBP-3 is inversely associated with risk of female breast cancer. *European journal of endocrinology / European Federation of Endocrine Societies* **156:** 187-194

Pearson KJ, Lewis KN, Price NL, Chang JW, Perez E, Cascajo MV, Tamashiro KL, Poosala S, Csiszar A, Ungvari Z, Kensler TW, Yamamoto M, Egan JM, Longo DL, Ingram DK, Navas P, de Cabo R (2008) Nrf2 mediates cancer protection but not prolongevity induced by caloric restriction. *Proceedings of the National Academy of Sciences of the United States of America* **105:** 2325-2330

Pekic S, Popovic V (2013) GH therapy and cancer risk in hypopituitarism: what we know from human studies. *European journal of endocrinology / European Federation of Endocrine Societies* **169:** R89-97

Peng C, Lu Z, Xie Z, Cheng Z, Chen Y, Tan M, Luo H, Zhang Y, He W, Yang K, Zwaans BM, Tishkoff D, Ho L, Lombard D, He TC, Dai J, Verdin E, Ye Y, Zhao Y (2011) The first identification of lysine malonylation substrates and its regulatory enzyme. *Molecular & cellular proteomics : MCP* **10:** M111 012658

Pennisi PA, Kopchick JJ, Thorgeirsson S, LeRoith D, Yakar S (2004) Role of growth hormone (GH) in liver regeneration. *Endocrinology* **145:** 4748-4755

Perez VI, Cortez LA, Lew CM, Rodriguez M, Webb CR, Van Remmen H, Chaudhuri A, Qi W, Lee S, Bokov A, Fok W, Jones D, Richardson A, Yodoi J, Zhang Y, Tominaga K, Hubbard GB, Ikeno Y (2011) Thioredoxin 1 overexpression extends mainly the earlier part of life span in mice. *The journals of gerontology Series A, Biological sciences and medical sciences* **66:** 1286-1299

Perez-Ibave DC, Rodriguez-Sanchez IP, Garza-Rodriguez MD, Barrera-Saldana HA (2014) Extrapituitary growth hormone synthesis in humans. *Growth hormone & IGF research : official journal of the Growth Hormone Research Society and the International IGF Research Society*

Perret-Vivancos C, Abbate A, Ardail D, Raccurt M, Usson Y, Lobie PE, Morel G (2006) Growth hormone activity in mitochondria depends on GH receptor Box 1 and involves caveolar pathway targeting. *Experimental cell research* **312:** 215-232

Perry JK, Emerald BS, Mertani HC, Lobie PE (2006) The oncogenic potential of growth hormone. *Growth hormone & IGF research : official journal of the Growth Hormone Research Society and the International IGF Research Society* **16:** 277-289

Perry JK, Liu DX, Wu ZS, Zhu T, Lobie PE (2013) Growth hormone and cancer: an update on progress. *Current opinion in endocrinology, diabetes, and obesity* **20:** 307-313

Perry JK, Mohankumar KM, Emerald BS, Mertani HC, Lobie PE (2008) The contribution of growth hormone to mammary neoplasia. *Journal of mammary gland biology and neoplasia* **13:** 131-145

Peters CJ, Rees JR, Hardwick RH, Hardwick JS, Vowler SL, Ong CA, Zhang C, Save V, O'Donovan M, Rassl D, Alderson D, Caldas C, Fitzgerald RC, Oesophageal Cancer C, Molecular

Stratification Study G (2010) A 4-gene signature predicts survival of patients with resected adenocarcinoma of the esophagus, junction, and gastric cardia. *Gastroenterology* **139:** 1995-2004 e1915

Petropoulos CJ, Hughes SH (1991) Replication-competent retrovirus vectors for the transfer and expression of gene cassettes in avian cells. *Journal of virology* **65:** 3728-3737

Petropoulos CJ, Payne W, Salter DW, Hughes SH (1992) Appropriate in vivo expression of a muscle-specific promoter by using avian retroviral vectors for gene transfer [corrected]. *Journal of virology* **66:** 3391-3397

Pfeifer A, Kessler T, Yang M, Baranov E, Kootstra N, Cheresh DA, Hoffman RM, Verma IM (2001) Transduction of liver cells by lentiviral vectors: analysis in living animals by fluorescence imaging. *Molecular therapy : the journal of the American Society of Gene Therapy* **3:** 319-322

Pfluger PT, Herranz D, Velasco-Miguel S, Serrano M, Tschop MH (2008) Sirt1 protects against high-fat diet-induced metabolic damage. *Proceedings of the National Academy of Sciences of the United States of America* **105:** 9793-9798

Pilecka I, Patrignani C, Pescini R, Curchod ML, Perrin D, Xue Y, Yasenchak J, Clark A, Magnone MC, Zaratin P, Valenzuela D, Rommel C, Hooft van Huijsduijnen R (2007) Protein-tyrosine phosphatase H1 controls growth hormone receptor signaling and systemic growth. *The Journal of biological chemistry* **282:** 35405-35415

Pillai VB, Sundaresan NR, Kim G, Gupta M, Rajamohan SB, Pillai JB, Samant S, Ravindra PV, Isbatan A, Gupta MP (2010) Exogenous NAD blocks cardiac hypertrophic response via activation of the SIRT3-LKB1-AMP-activated kinase pathway. *The Journal of biological chemistry* **285:** 3133-3144

Pinto VB, Prasad S, Yewdell J, Bennink J, Hughes SH (2000) Restricting expression prolongs expression of foreign genes introduced into animals by retroviruses. *Journal of virology* **74:** 10202-10206

Pircher TJ, Petersen H, Gustafsson JA, Haldosen LA (1999) Extracellular signal-regulated kinase (ERK) interacts with signal transducer and activator of transcription (STAT) 5a. *Molecular endocrinology* **13:** 555-565

Piwien Pilipuk G, Galigniana MD, Schwartz J (2003) Subnuclear localization of C/EBP beta is regulated by growth hormone and dependent on MAPK. *The Journal of biological chemistry* **278:** 35668-35677

Piwien-Pilipuk G, Huo JS, Schwartz J (2002) Growth hormone signal transduction. *Journal of pediatric endocrinology & metabolism : JPEM* **15:** 771-786

Plotnikov A, Li Y, Tran TH, Tang W, Palazzo JP, Rui H, Fuchs SY (2008) Oncogene-mediated inhibition of glycogen synthase kinase 3 beta impairs degradation of prolactin receptor. *Cancer research* **68:** 1354-1361

Poger D, Mark AE (2010) Turning the growth hormone receptor on: evidence that hormone binding induces subunit rotation. *Proteins* **78:** 1163-1174

Politi K, Pao W (2011) How Genetically Engineered Mouse Tumor Models Provide Insights Into Human Cancers. *J Clin Oncol*

Pollak M (2008) Insulin and insulin-like growth factor signalling in neoplasia. *Nature reviews Cancer* **8:** 915-928

Pollak MN (2012) Investigating metformin for cancer prevention and treatment: the end of the beginning. *Cancer discovery* **2:** 778-790

Postel-Vinay MC, Finidori J (1995) Growth hormone receptor: structure and signal transduction. *European journal of endocrinology / European Federation of Endocrine Societies* **133:** 654-659

Postel-Vinay MC, Kayser C, Desbuquois B (1982) Fate of injected human growth hormone in the female rat liver in vivo. *Endocrinology* **111:** 244-251

Potthoff MJ, Kliewer SA, Mangelsdorf DJ (2012) Endocrine fibroblast growth factors 15/19 and 21: from feast to famine. *Genes & development* **26:** 312-324

Price NL, Gomes AP, Ling AJ, Duarte FV, Martin-Montalvo A, North BJ, Agarwal B, Ye L, Ramadori G, Teodoro JS, Hubbard BP, Varela AT, Davis JG, Varamini B, Hafner A, Moaddel R, Rolo AP, Coppari R, Palmeira CM, de Cabo R, Baur JA, Sinclair DA (2012) SIRT1 is required for AMPK activation and the beneficial effects of resveratrol on mitochondrial function. *Cell metabolism* **15:** 675-690

Putters J, da Silva Almeida AC, van Kerkhof P, van Rossum AG, Gracanin A, Strous GJ (2011) Jak2 is a negative regulator of ubiquitin-dependent endocytosis of the growth hormone receptor. *PloS one* **6:** e14676

Qazi AM, Tsai-Morris CH, Dufau ML (2006) Ligand-independent homo- and heterodimerization of human prolactin receptor variants: inhibitory action of the short forms by heterodimerization. *Molecular endocrinology* **20:** 1912-1923

Qin JY, Zhang L, Clift KL, Hulur I, Xiang AP, Ren BZ, Lahn BT (2010) Systematic comparison of constitutive promoters and the doxycycline-inducible promoter. *PloS one* **5:** e10611

Qiu X, Brown K, Hirschey MD, Verdin E, Chen D (2010) Calorie restriction reduces oxidative stress by SIRT3-mediated SOD2 activation. *Cell metabolism* **12:** 662-667

Queiroga FL, Perez-Alenza D, Silvan G, Pena L, Lopes CS, Illera JC (2010) Serum and intratumoural GH and IGF-I concentrations: prognostic factors in the outcome of canine mammary cancer. *Research in veterinary science* **89:** 396-403

Queiroga FL, Raposo T, Carvalho MI, Prada J, Pires I (2011) Canine mammary tumours as a model to study human breast cancer: most recent findings. *In vivo* **25:** 455-465

Raccurt M, Lobie PE, Moudilou E, Garcia-Caballero T, Frappart L, Morel G, Mertani HC (2002) High stromal and epithelial human gh gene expression is associated with proliferative disorders of the mammary gland. *The Journal of endocrinology* **175:** 307-318

Raccurt M, Tam SP, Lau P, Mertani HC, Lambert A, Garcia-Caballero T, Li H, Brown RJ, McGuckin MA, Morel G, Waters MJ (2003) Suppressor of cytokine signalling gene expression is elevated in breast carcinoma. *British journal of cancer* **89:** 524-532

Railo MJ, von Smitten K, Pekonen F (1994) The prognostic value of insulin-like growth factor-I in breast cancer patients. Results of a follow-up study on 126 patients. *European journal of cancer* **30A:** 307-311

Ralph SJ, Rodriguez-Enriquez S, Neuzil J, Saavedra E, Moreno-Sanchez R (2010) The causes of cancer revisited: "mitochondrial malignancy" and ROS-induced oncogenic transformation - why mitochondria are targets for cancer therapy. *Molecular aspects of medicine* **31:** 145-170

Ram PA, Park SH, Choi HK, Waxman DJ (1996) Growth hormone activation of Stat 1, Stat 3, and Stat 5 in rat liver. Differential kinetics of hormone desensitization and growth hormone stimulation of both tyrosine phosphorylation and serine/threonine phosphorylation. *The Journal of biological chemistry* **271:** 5929-5940

Ram PA, Waxman DJ (1999) SOCS/CIS protein inhibition of growth hormone-stimulated STAT5 signaling by multiple mechanisms. *The Journal of biological chemistry* **274:** 35553-35561

Ransome MI, Goldshmit Y, Bartlett PF, Waters MJ, Turnley AM (2004) Comparative analysis of CNS populations in knockout mice with altered growth hormone responsiveness. *The European journal of neuroscience* **19:** 2069-2079

Rao G, Pedone CA, Del Valle L, Reiss K, Holland EC, Fults DW (2004) Sonic hedgehog and insulin-like growth factor signaling synergize to induce medulloblastoma formation from nestin-expressing neural progenitors in mice. *Oncogene* **23:** 6156-6162

Redman LM, Heilbronn LK, Martin CK, Alfonso A, Smith SR, Ravussin E, Pennington CT (2007) Effect of calorie restriction with or without exercise on body composition and fat distribution. *The Journal of clinical endocrinology and metabolism* **92:** 865-872

Redman LM, Veldhuis JD, Rood J, Smith SR, Williamson D, Ravussin E, Pennington CT (2010) The effect of caloric restriction interventions on growth hormone secretion in nonobese men and women. *Aging cell* **9:** 32-39

Reilly JF, Maher PA (2001) Importin beta-mediated nuclear import of fibroblast growth factor receptor: role in cell proliferation. *The Journal of cell biology* **152:** 1307-1312

Reiser J (2000) Production and concentration of pseudotyped HIV-1-based gene transfer vectors. *Gene Ther* **7:** 910-913

Renehan AG, O'Connell J, O'Halloran D, Shanahan F, Potten CS, O'Dwyer ST, Shalet SM (2003) Acromegaly and colorectal cancer: a comprehensive review of epidemiology, biological mechanisms, and clinical implications. *Hormone and metabolic research = Hormon- und Stoffwechselforschung = Hormones et metabolisme* **35:** 712-725

Renehan AG, Zwahlen M, Minder C, O'Dwyer ST, Shalet SM, Egger M (2004) Insulin-like growth factor (IGF)-I, IGF binding protein-3, and cancer risk: systematic review and meta-regression analysis. *Lancet* **363:** 1346-1353

Repa JJ, Liang G, Ou J, Bashmakov Y, Lobaccaro JM, Shimomura I, Shan B, Brown MS, Goldstein JL, Mangelsdorf DJ (2000) Regulation of mouse sterol regulatory element-binding protein-1c gene (SREBP-1c) by oxysterol receptors, LXRalpha and LXRbeta. *Genes & development* **14:** 2819-2830

Resh MD (1999) Fatty acylation of proteins: new insights into membrane targeting of myristoylated and palmitoylated proteins. *Biochimica et biophysica acta* **1451:** 1-16

Reznick RM, Zong H, Li J, Morino K, Moore IK, Yu HJ, Liu ZX, Dong J, Mustard KJ, Hawley SA, Befroy D, Pypaert M, Hardie DG, Young LH, Shulman GI (2007) Aging-associated reductions in AMP-activated protein kinase activity and mitochondrial biogenesis. *Cell metabolism* **5:** 151-156

Rico-Bautista E, Flores-Morales A, Fernandez-Perez L (2006) Suppressor of cytokine signaling (SOCS) 2, a protein with multiple functions. *Cytokine & growth factor reviews* **17:** 431-439

Rico-Bautista E, Greenhalgh CJ, Tollet-Egnell P, Hilton DJ, Alexander WS, Norstedt G, Flores-Morales A (2005) Suppressor of cytokine signaling-2 deficiency induces molecular and metabolic changes that partially overlap with growth hormone-dependent effects. *Molecular endocrinology* **19:** 781-793

Rijnberk A, Kooistra HS, Mol JA (2003) Endocrine diseases in dogs and cats: similarities and differences with endocrine diseases in humans. *Growth hormone & IGF research : official journal of the Growth Hormone Research Society and the International IGF Research Society* **13 Suppl A:** S158-164

Robinson JP, VanBrocklin MW, Guilbeault AR, Signorelli DL, Brandner S, Holmen SL (2010) Activated BRAF induces gliomas in mice when combined with Ink4a/Arf loss or Akt activation. *Oncogene* **29:** 335-344

Robinson JP, Vanbrocklin MW, Lastwika KJ, McKinney AJ, Brandner S, Holmen SL (2011) Activated MEK cooperates with Ink4a/Arf loss or Akt activation to induce gliomas in vivo. *Oncogene* **30:** 1341-1350

Rodgers JT, Lerin C, Haas W, Gygi SP, Spiegelman BM, Puigserver P (2005) Nutrient control of glucose homeostasis through a complex of PGC-1alpha and SIRT1. *Nature* **434:** 113-118

Rondini EA, Harvey AE, Steibel JP, Hursting SD, Fenton JI (2011) Energy balance modulates colon tumor growth: Interactive roles of insulin and estrogen. *Molecular carcinogenesis* **50:** 370-382

Rong L, Bates P (1995) Analysis of the subgroup A avian sarcoma and leukosis virus receptor: the 40-residue, cysteine-rich, low-density lipoprotein receptor repeat motif of Tva is sufficient to mediate viral entry. *Journal of virology* **69:** 4847-4853

Rosen T, Johannsson G, Johansson JO, Bengtsson BA (1995) Consequences of growth hormone deficiency in adults and the benefits and risks of recombinant human growth hormone treatment. A review paper. *Hormone research* **43:** 93-99

Rosenfeld RG, Kofoed E, Buckway C, Little B, Woods KA, Tsubaki J, Pratt KA, Bezrodnik L, Jasper H, Tepper A, Heinrich JJ, Hwa V (2005) Identification of the first patient with a confirmed mutation of the JAK-STAT system. *Pediatric nephrology* **20:** 303-305

Ross RJ, Esposito N, Shen XY, Von Laue S, Chew SL, Dobson PR, Postel-Vinay MC, Finidori J (1997) A short isoform of the human growth hormone receptor functions as a dominant negative inhibitor of the full-length receptor and generates large amounts of binding protein. *Molecular endocrinology* **11:** 265-273

Ross RJ, Leung KC, Maamra M, Bennett W, Doyle N, Waters MJ, Ho KK (2001) Binding and functional studies with the growth hormone receptor antagonist, B2036-PEG (pegvisomant), reveal effects of pegylation and evidence that it binds to a receptor dimer. *The Journal of clinical endocrinology and metabolism* **86:** 1716-1723

Rowland JE, Kerr LM, White M, Noakes PG, Waters MJ (2005a) Heterozygote effects in mice with partial truncations in the growth hormone receptor cytoplasmic domain: assessment of growth parameters and phenotype. *Endocrinology* **146:** 5278-5286

Rowland JE, Lichanska AM, Kerr LM, White M, d'Aniello EM, Maher SL, Brown R, Teasdale RD, Noakes PG, Waters MJ (2005b) In vivo analysis of growth hormone receptor signaling domains and their associated transcripts. *Molecular and cellular biology* **25:** 66-77

Rowland JE, Marshall NJ, Leung KC, Ho KK, Cotterill AM, Rowlinson SW, Waters MJ (2002) A novel bioassay for human somatogenic activity in serum samples supports the clinical reliability of immunoassays. *Clinical endocrinology* **56:** 475-485

Rowlinson SW, Barnard R, Bastiras S, Robins AJ, Senn C, Wells JR, Brinkworth R, Waters MJ (1994) Evidence for involvement of the carboxy terminus of helix 1 of growth hormone in receptor binding: use of charge reversal mutagenesis to account for calcium dependence of binding and for design of higher affinity analogues. *Biochemistry* **33:** 11724-11733

Rowlinson SW, Behncken SN, Rowland JE, Clarkson RW, Strasburger CJ, Wu Z, Baumbach W, Waters MJ (1998) Activation of chimeric and full-length growth hormone receptors by growth hormone receptor monoclonal antibodies. A specific conformational change may be required for full-length receptor signaling. *The Journal of biological chemistry* **273:** 5307-5314

Rowlinson SW, Yoshizato H, Barclay JL, Brooks AJ, Behncken SN, Kerr LM, Millard K, Palethorpe K, Nielsen K, Clyde-Smith J, Hancock JF, Waters MJ (2008) An agonist-induced conformational change in the growth hormone receptor determines the choice of signalling pathway. *Nature cell biology* **10:** 740-747

Rudd MF, Webb EL, Matakidou A, Sellick GS, Williams RD, Bridle H, Eisen T, Houlston RS (2006) Variants in the GH-IGF axis confer susceptibility to lung cancer. *Genome research* **16:** 693-701

Ruderman NB, Xu XJ, Nelson L, Cacicedo JM, Saha AK, Lan F, Ido Y (2010) AMPK and SIRT1: a long-standing partnership? *American journal of physiology Endocrinology and metabolism* **298:** E751-760

Rui L, Carter-Su C (1999) Identification of SH2-bbeta as a potent cytoplasmic activator of the tyrosine kinase Janus kinase 2. *Proceedings of the National Academy of Sciences of the United States of America* **96:** 7172-7177

Russell SJ, Kahn CR (2007) Endocrine regulation of ageing. *Nature reviews Molecular cell biology* **8:** 681-691

Ryan MD, King AM, Thomas GP (1991) Cleavage of foot-and-mouth disease virus polyprotein is mediated by residues located within a 19 amino acid sequence. *The Journal of general virology* **72 (Pt 11):** 2727-2732

Rycyzyn MA, Reilly SC, O'Malley K, Clevenger CV (2000) Role of cyclophilin B in prolactin signal transduction and nuclear retrotranslocation. *Molecular endocrinology* **14:** 1175-1186

Sachse M, Ramm G, Strous G, Klumperman J (2002a) Endosomes: multipurpose designs for integrating housekeeping and specialized tasks. *Histochemistry and cell biology* **117:** 91-104

Sachse M, Urbe S, Oorschot V, Strous GJ, Klumperman J (2002b) Bilayered clathrin coats on endosomal vacuoles are involved in protein sorting toward lysosomes. *Molecular biology of the cell* **13:** 1313-1328

Saglam S, Wilson CB, Seymour RJ (1970) Indications for hypophysectomy in diabetic retinopathy and cancer of the breast and prostate. *California medicine* **113:** 1-6

Saito H (1998) Anabolic agents in trauma and sepsis: repleting body mass and function. *Nutrition* **14:** 554-556

Sakalian M, Hunter E (1998) Molecular events in the assembly of retrovirus particles. *Advances in experimental medicine and biology* **440:** 329-339

Sakoda T, Kasahara N, Hamamori Y, Kedes L (1999) A high-titer lentiviral production system mediates efficient transduction of differentiated cells including beating cardiac myocytes. *J Mol Cell Cardiol* **31:** 2037-2047

Salminen A, Hyttinen JM, Kaarniranta K (2011) AMP-activated protein kinase inhibits NF-kappaB signaling and inflammation: impact on healthspan and lifespan. *Journal of molecular medicine* **89:** 667-676

Salmon AB, Murakami S, Bartke A, Kopchick J, Yasumura K, Miller RA (2005) Fibroblast cell lines from young adult mice of long-lived mutant strains are resistant to multiple forms of stress. *American journal of physiology Endocrinology and metabolism* **289:** E23-29

Salvioli S, Bonafe M, Capri M, Monti D, Franceschi C (2001) Mitochondria, aging and longevity--a new perspective. *FEBS letters* **492:** 9-13

Samani AA, Yakar S, LeRoith D, Brodt P (2007) The role of the IGF system in cancer growth and metastasis: overview and recent insights. *Endocrine reviews* **28:** 20-47

Samanta AK, Chakraborty SN, Wang Y, Kantarjian H, Sun X, Hood J, Perrotti D, Arlinghaus RB (2009) Jak2 inhibition deactivates Lyn kinase through the SET-PP2A-SHP1 pathway, causing apoptosis in drug-resistant cells from chronic myelogenous leukemia patients. *Oncogene* **28:** 1669-1681

Samaras TT, Elrick H (2002) Height, body size, and longevity: is smaller better for the human body? *The Western journal of medicine* **176:** 206-208

Sanders BM, Jay M, Draper GJ, Roberts EM (1989) Non-ocular cancer in relatives of retinoblastoma patients. *British journal of cancer* **60:** 358-365

Sanders EJ, Harvey S (2004) Growth hormone as an early embryonic growth and differentiation factor. *Anat Embryol (Berl)* **209:** 1-9

Sarfstein R, Pasmanik-Chor M, Yeheskel A, Edry L, Shomron N, Warman N, Wertheimer E, Maor S, Shochat L, Werner H (2012) Insulin-like growth factor-I receptor (IGF-IR) translocates to nucleus and autoregulates IGF-IR gene expression in breast cancer cells. *The Journal of biological chemistry* **287:** 2766-2776

Sausville J, Molinolo AA, Cheng X, Frampton J, Takebe N, Gutkind JS, Feldman RA (2008) RCAS/SCL-TVA animal model allows targeted delivery of polyoma middle T oncogene to vascular endothelial progenitors in vivo and results in hemangioma development. *Clinical cancer research : an official journal of the American Association for Cancer Research* **14:** 3948-3955

Savine R, Sonksen P (2000) Growth hormone - hormone replacement for the somatopause? *Hormone research* **53 Suppl 3:** 37-41

Savino W, Smaniotto S, Binart N, Postel-Vinay MC, Dardenne M (2003) In vivo effects of growth hormone on thymic cells. *Annals of the New York Academy of Sciences* **992:** 179-185

Sbracia M, Scarpellini F, Poverini R, Alo PL, Rossi G, Di Tondo U (2004) Immunohistochemical localization of the growth hormone in human endometrium and decidua. *American journal of reproductive immunology* **51:** 112-116

Schaefer-Klein J, Givol I, Barsov EV, Whitcomb JM, VanBrocklin M, Foster DN, Federspiel MJ, Hughes SH (1998) The EV-O-derived cell line DF-1 supports the efficient replication of avian leukosis-sarcoma viruses and vectors. *Virology* **248:** 305-311

Scheepens A, Moderscheim TA, Gluckman PD (2005) The role of growth hormone in neural development. *Hormone research* **64 Suppl 3:** 66-72

Schirra HJ, Anderson CG, Wilson WJ, Kerr L, Craik DJ, Waters MJ, Lichanska AM (2008) Altered metabolism of growth hormone receptor mutant mice: a combined NMR metabonomics and microarray study. *PloS one* **3:** e2764

Schlaepfer DD, Jones KC, Hunter T (1998) Multiple Grb2-mediated integrin-stimulated signaling pathways to ERK2/mitogen-activated protein kinase: summation of both c-Src- and focal adhesion kinase-initiated tyrosine phosphorylation events. *Molecular and cellular biology* **18:** 2571-2585

Schmidt D, Muller S (2003) PIAS/SUMO: new partners in transcriptional regulation. *Cellular and molecular life sciences : CMLS* **60:** 2561-2574

Schmidt HH, Wingler K, Kleinschnitz C, Dusting G (2012) NOX4 is a Janus-faced reactive oxygen species generating NADPH oxidase. *Circulation research* **111:** e15-16; author reply e17-18

Schwartzbauer G, Menon RK (1998) Regulation of growth hormone receptor gene expression. *Molecular genetics and metabolism* **63:** 243-253

Schwer B, Eckersdorff M, Li Y, Silva JC, Fermin D, Kurtev MV, Giallourakis C, Comb MJ, Alt FW, Lombard DB (2009) Calorie restriction alters mitochondrial protein acetylation. *Aging cell* **8:** 604-606

Sclimenti CR, Thyagarajan B, Calos MP (2001) Directed evolution of a recombinase for improved genomic integration at a native human sequence. *Nucleic acids research* **29:** 5044-5051

Segard HB, Moulin S, Boumard S, Augier de Cremiers C, Kelly PA, Finidori J (2003) Autocrine growth hormone production prevents apoptosis and inhibits differentiation in C2C12 myoblasts. *Cellular signalling* **15:** 615-623

Seidler B, Schmidt A, Mayr U, Nakhai H, Schmid RM, Schneider G, Saur D (2008) A Cre-loxP-based mouse model for conditional somatic gene expression and knockdown in vivo by using avian retroviral vectors. *Proceedings of the National Academy of Sciences of the United States of America* **105:** 10137-10142

Selak MA, Armour SM, MacKenzie ED, Boulahbel H, Watson DG, Mansfield KD, Pan Y, Simon MC, Thompson CB, Gottlieb E (2005) Succinate links TCA cycle dysfunction to oncogenesis by inhibiting HIF-alpha prolyl hydroxylase. *Cancer cell* **7:** 77-85

Selman C, Lingard S, Choudhury AI, Batterham RL, Claret M, Clements M, Ramadani F, Okkenhaug K, Schuster E, Blanc E, Piper MD, Al-Qassab H, Speakman JR, Carmignac D, Robinson IC, Thornton JM, Gems D, Partridge L, Withers DJ (2008) Evidence for lifespan extension and delayed age-related biomarkers in insulin receptor substrate 1 null mice. *FASEB journal : official publication of the Federation of American Societies for Experimental Biology* **22:** 807-818

Selman C, Partridge L, Withers DJ (2011) Replication of extended lifespan phenotype in mice with deletion of insulin receptor substrate 1. *PloS one* **6:** e16144

Selman C, Tullet JM, Wieser D, Irvine E, Lingard SJ, Choudhury AI, Claret M, Al-Qassab H, Carmignac D, Ramadani F, Woods A, Robinson IC, Schuster E, Batterham RL, Kozma SC, Thomas G, Carling D, Okkenhaug K, Thornton JM, Partridge L, Gems D, Withers DJ (2009) Ribosomal protein S6 kinase 1 signaling regulates mammalian life span. *Science* **326:** 140-144

Semenza GL (2010) Defining the role of hypoxia-inducible factor 1 in cancer biology and therapeutics. *Oncogene* **29:** 625-634

Seoane S, Alonso M, Segura C, Perez-Fernandez R (2002) Localization of a negative vitamin D response sequence in the human growth hormone gene. *Biochemical and biophysical research communications* **292:** 250-255

Seoane S, Perez-Fernandez R (2006) The vitamin D receptor represses transcription of the pituitary transcription factor Pit-1 gene without involvement of the retinoid X receptor. *Molecular endocrinology* **20:** 735-748

Shang CA, Waters MJ (2003) Constitutively active signal transducer and activator of transcription 5 can replace the requirement for growth hormone in adipogenesis of 3T3-F442A preadipocytes. *Molecular endocrinology* **17:** 2494-2508

Shapiro BH, Agrawal AK, Pampori NA (1995) Gender differences in drug metabolism regulated by growth hormone. *The international journal of biochemistry & cell biology* **27:** 9-20

Shaw RJ, Lamia KA, Vasquez D, Koo SH, Bardeesy N, Depinho RA, Montminy M, Cantley LC (2005) The kinase LKB1 mediates glucose homeostasis in liver and therapeutic effects of metformin. *Science* **310:** 1642-1646

Shchelkunova A, Ermolinsky B, Boyle M, Mendez I, Lehker M, Martirosyan KS, Kazansky AV (2013) Tuning of alternative splicing--switch from proto-oncogene to tumor suppressor. *International journal of biological sciences* **9:** 45-54

Shen EZ, Song CQ, Lin Y, Zhang WH, Su PF, Liu WY, Zhang P, Xu J, Lin N, Zhan C, Wang X, Shyr Y, Cheng H, Dong MQ (2014) Mitoflash frequency in early adulthood predicts lifespan in Caenorhabditis elegans. *Nature*

Shevah O, Laron Z (2007) Patients with congenital deficiency of IGF-I seem protected from the development of malignancies: a preliminary report. *Growth hormone & IGF research : official journal of the Growth Hormone Research Society and the International IGF Research Society* **17:** 54-57

Shih PH, Yen GC (2007) Differential expressions of antioxidant status in aging rats: the role of transcriptional factor Nrf2 and MAPK signaling pathway. *Biogerontology* **8:** 71-80

Shim H, Chun YS, Lewis BC, Dang CV (1998) A unique glucose-dependent apoptotic pathway induced by c-Myc. *Proceedings of the National Academy of Sciences of the United States of America* **95:** 1511-1516

Silverman BL, Blethen SL, Reiter EO, Attie KM, Neuwirth RB, Ford KM (2002) A long-acting human growth hormone (Nutropin Depot): efficacy and safety following two years of treatment in children with growth hormone deficiency. *Journal of pediatric endocrinology & metabolism : JPEM* **15 Suppl 2:** 715-722

Siwko SK, Bu W, Gutierrez C, Lewis B, Jechlinger M, Schaffhausen B, Li Y (2008) Lentivirus-mediated oncogene introduction into mammary cells in vivo induces tumors. *Neoplasia* **10:** 653-662, 651 p following 662

Sjoholm A, Zhang Q, Welsh N, Hansson A, Larsson O, Tally M, Berggren PO (2000) Rapid Ca2+ influx and diacylglycerol synthesis in growth hormone-mediated islet beta -cell mitogenesis. *The Journal of biological chemistry* **275:** 21033-21040

Slater M, Cooper M, Murphy CR (2006) Human growth hormone and interleukin-6 are upregulated in endometriosis and endometrioid adenocarcinoma. *Acta histochemica* **108:** 13-18

Slater MD, Murphy CR (2006) Co-expression of interleukin-6 and human growth hormone in apparently normal prostate biopsies that ultimately progress to prostate cancer using low pH, high temperature antigen retrieval. *Journal of molecular histology* **37:** 37-41

Slotman JA, da Silva Almeida AC, Hassink GC, van de Ven RH, van Kerkhof P, Kuiken HJ, Strous GJ (2012) Ubc13 and COOH terminus of Hsp70-interacting protein (CHIP) are required for growth hormone receptor endocytosis. *The Journal of biological chemistry* **287:** 15533-15543

Smith DW (1996) Cancer mortality at very old ages. *Cancer* **77:** 1367-1372

Sobiczewska E, Szmigielski S (1997) [The role of selected cell growth factors in the wound healing process]. *Przeglad lekarski* **54:** 634-638

Sobocanec S, Balog T, Sverko V, Marotti T (2003) Sex-dependent antioxidant enzyme activities and lipid peroxidation in ageing mouse brain. *Free radical research* **37:** 743-748

Sondergaard E, Klose M, Hansen M, Hansen BS, Andersen M, Feldt-Rasmussen U, Laursen T, Rasmussen MH, Christiansen JS (2011) Pegylated long-acting human growth hormone possesses a promising once-weekly treatment profile, and multiple dosing is well tolerated in adult patients with growth hormone deficiency. *The Journal of clinical endocrinology and metabolism* **96:** 681-688

Songyang Z, Baltimore D, Cantley LC, Kaplan DR, Franke TF (1997) Interleukin 3-dependent survival by the Akt protein kinase. *Proceedings of the National Academy of Sciences of the United States of America* **94:** 11345-11350

Songyang Z, Shoelson SE, Chaudhuri M, Gish G, Pawson T, Haser WG, King F, Roberts T, Ratnofsky S, Lechleider RJ, et al. (1993) SH2 domains recognize specific phosphopeptide sequences. *Cell* **72:** 767-778

Sonntag WE, Csiszar A, deCabo R, Ferrucci L, Ungvari Z (2012) Diverse roles of growth hormone and insulin-like growth factor-1 in mammalian aging: progress and controversies. *The journals of gerontology Series A, Biological sciences and medical sciences* **67:** 587-598

Sordella R, Bell DW, Haber DA, Settleman J (2004) Gefitinib-sensitizing EGFR mutations in lung cancer activate anti-apoptotic pathways. *Science* **305:** 1163-1167

Sorge J, Hughes SH (1982) Splicing of intervening sequences introduced into an infectious retroviral vector. *J Mol Appl Genet* **1:** 547-559

Sornson MW, Wu W, Dasen JS, Flynn SE, Norman DJ, O'Connell SM, Gukovsky I, Carriere C, Ryan AK, Miller AP, Zuo L, Gleiberman AS, Andersen B, Beamer WG, Rosenfeld MG (1996) Pituitary lineage determination by the Prophet of Pit-1 homeodomain factor defective in Ames dwarfism. *Nature* **384:** 327-333

Sotiropoulos A, Goujon L, Simonin G, Kelly PA, Postel-Vinay MC, Finidori J (1993) Evidence for generation of the growth hormone-binding protein through proteolysis of the growth hormone membrane receptor. *Endocrinology* **132:** 1863-1865

Sotiropoulos A, Moutoussamy S, Binart N, Kelly PA, Finidori J (1995) The membrane proximal region of the cytoplasmic domain of the growth hormone receptor is involved in the activation of Stat 3. *FEBS letters* **369:** 169-172

St-Pierre J, Drori S, Uldry M, Silvaggi JM, Rhee J, Jager S, Handschin C, Zheng K, Lin J, Yang W, Simon DK, Bachoo R, Spiegelman BM (2006) Suppression of reactive oxygen species and neurodegeneration by the PGC-1 transcriptional coactivators. *Cell* **127:** 397-408

Stachowiak EK, Maher PA, Tucholski J, Mordechai E, Joy A, Moffett J, Coons S, Stachowiak MK (1997) Nuclear accumulation of fibroblast growth factor receptors in human glial cells--association with cell proliferation. *Oncogene* **14:** 2201-2211

Staerk J, Lacout C, Sato T, Smith SO, Vainchenker W, Constantinescu SN (2006) An amphipathic motif at the transmembrane-cytoplasmic junction prevents autonomous activation of the thrombopoietin receptor. *Blood* **107:** 1864-1871

Stafler P, Wallis C (2008) Prader-Willi syndrome: who can have growth hormone? *Archives of disease in childhood* **93:** 341-345

Stallings-Mann ML, Ludwiczak RL, Klinger KW, Rottman F (1996) Alternative splicing of exon 3 of the human growth hormone receptor is the result of an unusual genetic polymorphism. *Proceedings of the National Academy of Sciences of the United States of America* **93:** 12394-12399

Starr R, Metcalf D, Elefanty AG, Brysha M, Willson TA, Nicola NA, Hilton DJ, Alexander WS (1998) Liver degeneration and lymphoid deficiencies in mice lacking suppressor of cytokine signaling-1. *Proceedings of the National Academy of Sciences of the United States of America* **95:** 14395-14399

Stattin P, Bjor O, Ferrari P, Lukanova A, Lenner P, Lindahl B, Hallmans G, Kaaks R (2007) Prospective study of hyperglycemia and cancer risk. *Diabetes care* **30:** 561-567

Steinbaugh MJ, Sun LY, Bartke A, Miller RA (2012) Activation of genes involved in xenobiotic metabolism is a shared signature of mouse models with extended lifespan. *American journal of physiology Endocrinology and metabolism* **303:** E488-495

Steuerman R, Shevah O, Laron Z (2011) Congenital IGF1 deficiency tends to confer protection against post-natal development of malignancies. *European journal of endocrinology / European Federation of Endocrine Societies* **164:** 485-489

Stewart SA, Dykxhoorn DM, Palliser D, Mizuno H, Yu EY, An DS, Sabatini DM, Chen IS, Hahn WC, Sharp PA, Weinberg RA, Novina CD (2003) Lentivirus-delivered stable gene silencing by RNAi in primary cells. *RNA* **9:** 493-501

Steyn FJ, Huang L, Ngo ST, Leong JW, Tan HY, Xie TY, Parlow AF, Veldhuis JD, Waters MJ, Chen C (2011) Development of a method for the determination of pulsatile growth hormone secretion in mice. *Endocrinology* **152:** 3165-3171

Stofega MR, Herrington J, Billestrup N, Carter-Su C (2000) Mutation of the SHP-2 binding site in growth hormone (GH) receptor prolongs GH-promoted tyrosyl phosphorylation of GH receptor, JAK2, and STAT5B. *Molecular endocrinology* **14:** 1338-1350

Stokoe D, Stephens LR, Copeland T, Gaffney PR, Reese CB, Painter GF, Holmes AB, McCormick F, Hawkins PT (1997) Dual role of phosphatidylinositol-3,4,5-trisphosphate in the activation of protein kinase B. *Science* **277:** 567-570

Strous GJ, dos Santos CA, Gent J, Govers R, Sachse M, Schantl J, van Kerkhof P (2004) Ubiquitin system-dependent regulation of growth hormone receptor signal transduction. *Current topics in microbiology and immunology* **286:** 81-118

Strous GJ, Govers R (1999) The ubiquitin-proteasome system and endocytosis. *Journal of cell science* **112 (Pt 10):** 1417-1423

Strous GJ, van Kerkhof P (2002) The ubiquitin-proteasome pathway and the regulation of growth hormone receptor availability. *Molecular and cellular endocrinology* **197:** 143-151

Strous GJ, van Kerkhof P, Govers R, Ciechanover A, Schwartz AL (1996) The ubiquitin conjugation system is required for ligand-induced endocytosis and degradation of the growth hormone receptor. *The EMBO journal* **15:** 3806-3812

Sui Y, Yang Z, Xiong S, Zhang L, Blanchard KL, Peiper SC, Dynan WS, Tuan D, Ko L (2007) Gene amplification and associated loss of 5' regulatory sequences of CoAA in human cancers. *Oncogene* **26:** 822-835

Sun C, Zhang F, Ge X, Yan T, Chen X, Shi X, Zhai Q (2007) SIRT1 improves insulin sensitivity under insulin-resistant conditions by repressing PTP1B. *Cell metabolism* **6:** 307-319

Sun LY, Spong A, Swindell WR, Fang Y, Hill C, Huber JA, Boehm JD, Westbrook R, Salvatori R, Bartke A (2013) Growth hormone-releasing hormone disruption extends lifespan and regulates response to caloric restriction in mice. *eLife* **2:** e01098

Sustarsic EG, Junnila RK, Kopchick JJ (2013) Human metastatic melanoma cell lines express high levels of growth hormone receptor and respond to GH treatment. *Biochemical and biophysical research communications* **441:** 144-150

Svensson J, Sjogren K, Faldt J, Andersson N, Isaksson O, Jansson JO, Ohlsson C (2011) Liver-derived IGF-I regulates mean life span in mice. *PloS one* **6:** e22640

Sykiotis GP, Bohmann D (2008) Keap1/Nrf2 signaling regulates oxidative stress tolerance and lifespan in Drosophila. *Developmental cell* **14:** 76-85

Szendroedi J, Phielix E, Roden M (2012) The role of mitochondria in insulin resistance and type 2 diabetes mellitus. *Nature reviews Endocrinology* **8:** 92-103

Tachas G, Lofthouse S, Wraight CJ, Baker BF, Sioufi NB, Jarres RA, Berdeja A, Rao AM, Kerr LM, d'Aniello EM, Waters MJ (2006) A GH receptor antisense oligonucleotide inhibits hepatic GH receptor expression, IGF-I production and body weight gain in normal mice. *The Journal of endocrinology* **189:** 147-154

Takada Y, Bando H, Miyamoto Y, Kosaka M, Sano T (1991) [Effect of growth hormone on immune function in normal and hypophysectomised rats]. *Nihon Naibunpi Gakkai zasshi* **67:** 1162-1177

Takahara K, Tearle H, Ghaffari M, Gleave ME, Pollak M, Cox ME (2011) Human prostate cancer xenografts in lit/lit mice exhibit reduced growth and androgen-independent progression. *The Prostate* **71:** 525-537

Takahashi MO, Takahashi Y, Iida K, Okimura Y, Kaji H, Abe H, Chihara K (1999) Growth hormone stimulates tyrosine phosphorylation of focal adhesion kinase (p125(FAK)) and actin stress fiber formation in human osteoblast-like cells, Saos2. *Biochemical and biophysical research communications* **263:** 100-106

Takeuchi A, Shiota M, Beraldi E, Thaper D, Takahara K, Ibuki N, Pollak M, Cox ME, Naito S, Gleave ME, Zoubeidi A (2014) Insulin-like growth factor-I induces CLU expression through Twist1 to promote prostate cancer growth. *Molecular and cellular endocrinology* **384:** 117-125

Tallet E, Rouet V, Jomain JB, Kelly PA, Bernichtein S, Goffin V (2008) Rational design of competitive prolactin/growth hormone receptor antagonists. *Journal of mammary gland biology and neoplasia* **13:** 105-117

Tan SH, Dagvadorj A, Shen F, Gu L, Liao Z, Abdulghani J, Zhang Y, Gelmann EP, Zellweger T, Culig Z, Visakorpi T, Bubendorf L, Kirken RA, Karras J, Nevalainen MT (2008) Transcription

factor Stat5 synergizes with androgen receptor in prostate cancer cells. *Cancer research* **68:** 236-248

Tanaka M, Gong JS, Zhang J, Yoneda M, Yagi K (1998) Mitochondrial genotype associated with longevity. *Lancet* **351:** 185-186

Tang JZ, Kong XJ, Banerjee A, Muniraj N, Pandey V, Steiner M, Perry JK, Zhu T, Liu DX, Lobie PE (2010a) STAT3alpha is oncogenic for endometrial carcinoma cells and mediates the oncogenic effects of autocrine human growth hormone. *Endocrinology* **151:** 4133-4145

Tang JZ, Zuo ZH, Kong XJ, Steiner M, Yin Z, Perry JK, Zhu T, Liu DX, Lobie PE (2010b) Signal transducer and activator of transcription (STAT)-5A and STAT5B differentially regulate human mammary carcinoma cell behavior. *Endocrinology* **151:** 43-55

Tang W, Ehrlich I, Wolff SB, Michalski AM, Wolfl S, Hasan MT, Luthi A, Sprengel R (2009) Faithful expression of multiple proteins via 2A-peptide self-processing: a versatile and reliable method for manipulating brain circuits. *The Journal of neuroscience : the official journal of the Society for Neuroscience* **29:** 8621-8629

Tanner JW, Chen W, Young RL, Longmore GD, Shaw AS (1995) The conserved box 1 motif of cytokine receptors is required for association with JAK kinases. *The Journal of biological chemistry* **270:** 6523-6530

Tatar M, Bartke A, Antebi A (2003) The endocrine regulation of aging by insulin-like signals. *Science* **299:** 1346-1351

Tauriainen E, Luostarinen M, Martonen E, Finckenberg P, Kovalainen M, Huotari A, Herzig KH, Lecklin A, Mervaala E (2011) Distinct effects of calorie restriction and resveratrol on diet-induced obesity and Fatty liver formation. *Journal of nutrition and metabolism* **2011:** 525094

Taylor SS, Knighton DR, Zheng J, Ten Eyck LF, Sowadski JM (1992) Structural framework for the protein kinase family. *Annual review of cell biology* **8:** 429-462

Teglund S, McKay C, Schuetz E, van Deursen JM, Stravopodis D, Wang D, Brown M, Bodner S, Grosveld G, Ihle JN (1998) Stat5a and Stat5b proteins have essential and nonessential, or redundant, roles in cytokine responses. *Cell* **93:** 841-850

Teng CL, Hsieh YC, Phan L, Shin J, Gully C, Velazquez-Torres G, Skerl S, Yeung SC, Hsu SL, Lee MH (2012) FBXW7 is involved in Aurora B degradation. *Cell cycle* **11:** 4059-4068

Terzolo M, Reimondo G, Gasperi M, Cozzi R, Pivonello R, Vitale G, Scillitani A, Attanasio R, Cecconi E, Daffara F, Gaia E, Martino E, Lombardi G, Angeli A, Colao A (2005) Colonoscopic screening and follow-up in patients with acromegaly: a multicenter study in Italy. *The Journal of clinical endocrinology and metabolism* **90:** 84-90

Thirone AC, Carvalho CR, Saad MJ (1999) Growth hormone stimulates the tyrosine kinase activity of JAK2 and induces tyrosine phosphorylation of insulin receptor substrates and Shc in rat tissues. *Endocrinology* **140:** 55-62

Thomas C, Zoubeidi A, Kuruma H, Fazli L, Lamoureux F, Beraldi E, Monia BP, MacLeod AR, Thuroff JW, Gleave ME (2011) Transcription factor Stat5 knockdown enhances androgen receptor

degradation and delays castration-resistant prostate cancer progression in vivo. *Molecular cancer therapeutics* **10:** 347-359

Thompson BJ, Shang CA, Waters MJ (2000) Identification of genes induced by growth hormone in rat liver using cDNA arrays. *Endocrinology* **141:** 4321-4324

Thomson DM, Herway ST, Fillmore N, Kim H, Brown JD, Barrow JR, Winder WW (2008) AMP-activated protein kinase phosphorylates transcription factors of the CREB family. *Journal of applied physiology* **104:** 429-438

Tilbrook PA, Ingley E, Williams JH, Hibbs ML, Klinken SP (1997) Lyn tyrosine kinase is essential for erythropoietin-induced differentiation of J2E erythroid cells. *The EMBO journal* **16:** 1610-1619

Tiscornia G, Singer O, Verma IM (2006) Production and purification of lentiviral vectors. *Nature protocols* **1:** 241-245

Tiulpakov A, Rubtsov P, Dedov I, Peterkova V, Bezlepkina O, Chrousos GP, Hochberg Z (2005) A novel C-terminal growth hormone receptor (GHR) mutation results in impaired GHR-STAT5 but normal STAT-3 signaling. *The Journal of clinical endocrinology and metabolism* **90:** 542-547

Tognon M, Cattozzo EM, Bianchi S, Romanelli MG (1996) Enhancement of HSV-DNA infectivity, in Vero and RS cells, by a modified calcium-phosphate transfection technique. *Virus Genes* **12:** 193-197

Tollet-Egnell P, Flores-Morales A, Stavreus-Evers A, Sahlin L, Norstedt G (1999) Growth hormone regulation of SOCS-2, SOCS-3, and CIS messenger ribonucleic acid expression in the rat. *Endocrinology* **140:** 3693-3704

Tomas-Zapico C, Alvarez-Garcia O, Sierra V, Vega-Naredo I, Caballero B, Joaquin Garcia J, Acuna-Castroviejo D, Rodriguez MI, Tolivia D, Rodriguez-Colunga MJ, Coto-Montes A (2006) Oxidative damage in the livers of senescence-accelerated mice: a gender-related response. *Canadian journal of physiology and pharmacology* **84:** 213-220

Tormos AM, Talens-Visconti R, Nebreda AR, Sastre J (2013) p38 MAPK: a dual role in hepatocyte proliferation through reactive oxygen species. *Free radical research* **47:** 905-916

Tornell J, Carlsson B, Pohjanen P, Wennbo H, Rymo L, Isaksson O (1992) High frequency of mammary adenocarcinomas in metallothionein promoter-human growth hormone transgenic mice created from two different strains of mice. *J Steroid Biochem Mol Biol* **43:** 237-242

Touraine P, Martini JF, Zafrani B, Durand JC, Labaille F, Malet C, Nicolas A, Trivin C, Postel-Vinay MC, Kuttenn F, Kelly PA (1998) Increased expression of prolactin receptor gene assessed by quantitative polymerase chain reaction in human breast tumors versus normal breast tissues. *The Journal of clinical endocrinology and metabolism* **83:** 667-674

Tripaldi R, Stuppia L, Alberti S (2013) Human height genes and cancer. *Biochimica et biophysica acta* **1836:** 27-41

Trono D (2002) *Lentiviral Vectors*, Hardbound edn.: Springer Berlin Heidelberg.

Truett GE, Heeger P, Mynatt RL, Truett AA, Walker JA, Warman ML (2000) Preparation of PCR-quality mouse genomic DNA with hot sodium hydroxide and tris (HotSHOT). *BioTechniques* **29:** 52, 54

Tsunematsu R, Nakayama K, Oike Y, Nishiyama M, Ishida N, Hatakeyama S, Bessho Y, Kageyama R, Suda T, Nakayama KI (2004) Mouse Fbw7/Sel-10/Cdc4 is required for notch degradation during vascular development. *The Journal of biological chemistry* **279:** 9417-9423

Tsushima T, Friesen HG (1973) Radioreceptor assay for growth hormone. *The Journal of clinical endocrinology and metabolism* **37:** 334-337

Tullet JM, Hertweck M, An JH, Baker J, Hwang JY, Liu S, Oliveira RP, Baumeister R, Blackwell TK (2008) Direct inhibition of the longevity-promoting factor SKN-1 by insulin-like signaling in C. elegans. *Cell* **132:** 1025-1038

Turnley AM, Faux CH, Rietze RL, Coonan JR, Bartlett PF (2002) Suppressor of cytokine signaling 2 regulates neuronal differentiation by inhibiting growth hormone signaling. *Nature neuroscience* **5:** 1155-1162

Uddin S, Sher DA, Alsayed Y, Pons S, Colamonici OR, Fish EN, White MF, Platanias LC (1997) Interaction of p59fyn with interferon-activated Jak kinases. *Biochemical and biophysical research communications* **235:** 83-88

Udy GB, Towers RP, Snell RG, Wilkins RJ, Park SH, Ram PA, Waxman DJ, Davey HW (1997) Requirement of STAT5b for sexual dimorphism of body growth rates and liver gene expression. *Proceedings of the National Academy of Sciences of the United States of America* **94:** 7239-7244

Ungureanu D, Saharinen P, Junttila I, Hilton DJ, Silvennoinen O (2002) Regulation of Jak2 through the ubiquitin-proteasome pathway involves phosphorylation of Jak2 on Y1007 and interaction with SOCS-1. *Molecular and cellular biology* **22:** 3316-3326

Ungureanu D, Wu J, Pekkala T, Niranjan Y, Young C, Jensen ON, Xu CF, Neubert TA, Skoda RC, Hubbard SR, Silvennoinen O (2011) The pseudokinase domain of JAK2 is a dual-specificity protein kinase that negatively regulates cytokine signaling. *Nature structural & molecular biology* **18:** 971-976

Untergasser G, Rumpold H, Hermann M, Dirnhofer S, Jilg G, Berger P (1999) Proliferative disorders of the aging human prostate: involvement of protein hormones and their receptors. *Experimental gerontology* **34:** 275-287

Urbanek M, MacLeod JN, Cooke NE, Liebhaber SA (1992) Expression of a human growth hormone (hGH) receptor isoform is predicted by tissue-specific alternative splicing of exon 3 of the hGH receptor gene transcript. *Molecular endocrinology* **6:** 279-287

Uyttendaele I, Lemmens I, Verhee A, De Smet AS, Vandekerckhove J, Lavens D, Peelman F, Tavernier J (2007) Mammalian protein-protein interaction trap (MAPPIT) analysis of STAT5, CIS, and SOCS2 interactions with the growth hormone receptor. *Molecular endocrinology* **21:** 2821-2831

Vakhrusheva O, Braeuer D, Liu Z, Braun T, Bober E (2008) Sirt7-dependent inhibition of cell growth and proliferation might be instrumental to mediate tissue integrity during aging. *Journal of*

physiology and pharmacology : an official journal of the Polish Physiological Society **59 Suppl 9:** 201-212

Valle I, Alvarez-Barrientos A, Arza E, Lamas S, Monsalve M (2005) PGC-1alpha regulates the mitochondrial antioxidant defense system in vascular endothelial cells. *Cardiovascular research* **66:** 562-573

van den Eijnden MJ, Strous GJ (2007) Autocrine growth hormone: effects on growth hormone receptor trafficking and signaling. *Molecular endocrinology* **21:** 2832-2846

van der Eerden BC, Karperien M, Wit JM (2003) Systemic and local regulation of the growth plate. *Endocrine reviews* **24:** 782-801

van Garderen E, de Wit M, Voorhout WF, Rutteman GR, Mol JA, Nederbragt H, Misdorp W (1997) Expression of growth hormone in canine mammary tissue and mammary tumors. Evidence for a potential autocrine/paracrine stimulatory loop. *The American journal of pathology* **150:** 1037-1047

van Garderen E, Schalken JA (2002) Morphogenic and tumorigenic potentials of the mammary growth hormone/growth hormone receptor system. *Molecular and cellular endocrinology* **197:** 153-165

van Kerkhof P, Govers R, Alves dos Santos CM, Strous GJ (2000) Endocytosis and degradation of the growth hormone receptor are proteasome-dependent. *The Journal of biological chemistry* **275:** 1575-1580

van Kerkhof P, Putters J, Strous GJ (2007) The ubiquitin ligase SCF(betaTrCP) regulates the degradation of the growth hormone receptor. *The Journal of biological chemistry* **282:** 20475-20483

van Kerkhof P, Smeets M, Strous GJ (2002) The ubiquitin-proteasome pathway regulates the availability of the GH receptor. *Endocrinology* **143:** 1243-1252

van Kerkhof P, Strous GJ (2001) The ubiquitin-proteasome pathway regulates lysosomal degradation of the growth hormone receptor and its ligand. *Biochemical Society transactions* **29:** 488-493

van Kerkhof P, Vallon E, Strous GJ (2003) A method to increase the number of growth hormone receptors at the surface of cells. *Molecular and cellular endocrinology* **201:** 57-62

Van Meter M, Mao Z, Gorbunova V, Seluanov A (2011) SIRT6 overexpression induces massive apoptosis in cancer cells but not in normal cells. *Cell cycle* **10:** 3153-3158

van Neck JW, Dits NF, Cingel V, Hoppenbrouwers IA, Drop SL, Flyvbjerg A (2000) Dose-response effects of a new growth hormone receptor antagonist (B2036-PEG) on circulating, hepatic and renal expression of the growth hormone/insulin-like growth factor system in adult mice. *The Journal of endocrinology* **167:** 295-303

Van Remmen H, Ikeno Y, Hamilton M, Pahlavani M, Wolf N, Thorpe SR, Alderson NL, Baynes JW, Epstein CJ, Huang TT, Nelson J, Strong R, Richardson A (2003) Life-long reduction in MnSOD activity results in increased DNA damage and higher incidence of cancer but does not accelerate aging. *Physiological genomics* **16:** 29-37

van Veelen W, Korsse SE, van de Laar L, Peppelenbosch MP (2011) The long and winding road to rational treatment of cancer associated with LKB1/AMPK/TSC/mTORC1 signaling. *Oncogene* **30:** 2289-2303

VanBrocklin MW, Robinson JP, Lastwika KJ, Khoury JD, Holmen SL (2010) Targeted delivery of NRASQ61R and Cre-recombinase to post-natal melanocytes induces melanoma in Ink4a/Arflox/lox mice. *Pigment Cell Melanoma Res* **23:** 531-541

Vanderkuur JA, Butch ER, Waters SB, Pessin JE, Guan KL, Carter-Su C (1997) Signaling molecules involved in coupling growth hormone receptor to mitogen-activated protein kinase activation. *Endocrinology* **138:** 4301-4307

Vansaun MN (2013) Molecular pathways: adiponectin and leptin signaling in cancer. *Clinical cancer research : an official journal of the American Association for Cancer Research* **19:** 1926-1932

Varghese LN, Ungureanu D, Liau NP, Young SN, Laktyushin A, Hammaren H, Lucet IS, Nicola NA, Silvennoinen O, Babon JJ, Murphy JM (2014) Mechanistic insights into activation and SOCS3-mediated inhibition of myeloproliferative neoplasm-associated JAK2 mutants from biochemical and structural analyses. *The Biochemical journal* **458:** 395-405

Vasto S, Candore G, Balistreri CR, Caruso M, Colonna-Romano G, Grimaldi MP, Listi F, Nuzzo D, Lio D, Caruso C (2007) Inflammatory networks in ageing, age-related diseases and longevity. *Mechanisms of ageing and development* **128:** 83-91

Veldhuis JD, Anderson SM, Shah N, Bray M, Vick T, Gentili A, Mulligan T, Johnson ML, Weltman A, Evans WS, Iranmanesh A (2001) Neurophysiological regulation and target-tissue impact of the pulsatile mode of growth hormone secretion in the human. *Growth hormone & IGF research : official journal of the Growth Hormone Research Society and the International IGF Research Society* **11 Suppl A:** S25-37

Ventura B, Genova ML, Bovina C, Formiggini G, Lenaz G (2002) Control of oxidative phosphorylation by Complex I in rat liver mitochondria: implications for aging. *Biochimica et biophysica acta* **1553:** 249-260

Vesterlund M, Zadjali F, Persson T, Nielsen ML, Kessler BM, Norstedt G, Flores-Morales A (2011) The SOCS2 ubiquitin ligase complex regulates growth hormone receptor levels. *PloS one* **6:** e25358

Vickers MH, Gilmour S, Gertler A, Breier BH, Tunny K, Waters MJ, Gluckman PD (2009) 20-kDa placental hGH-V has diminished diabetogenic and lactogenic activities compared with 22-kDa hGH-N while retaining antilipogenic activity. *American journal of physiology Endocrinology and metabolism* **297:** E629-637

Vidarsdottir S, Walenkamp MJ, Pereira AM, Karperien M, van Doorn J, van Duyvenvoorde HA, White S, Breuning MH, Roelfsema F, Kruithof MF, van Dissel J, Janssen R, Wit JM, Romijn JA (2006) Clinical and biochemical characteristics of a male patient with a novel homozygous STAT5b mutation. *The Journal of clinical endocrinology and metabolism* **91:** 3482-3485

Viegas MS, Martins TC, Seco F, do Carmo A (2007) An improved and cost-effective methodology for the reduction of autofluorescence in direct immunofluorescence studies on formalin-fixed paraffin-embedded tissues. *Eur J Histochem* **51:** 59-66

Vielma SA, Klein RL, Levingston CA, Young MR (2013) Adipocytes as immune regulatory cells. *International immunopharmacology* **16:** 224-231

Vigneri P, Frasca F, Sciacca L, Pandini G, Vigneri R (2009) Diabetes and cancer. *Endocrine-related cancer* **16:** 1103-1123

Villares R, Kakabadse D, Juarranz Y, Gomariz RP, Martinez AC, Mellado M (2013) Growth hormone prevents the development of autoimmune diabetes. *Proceedings of the National Academy of Sciences of the United States of America* **110:** E4619-4627

Vina J, Borras C, Gambini J, Sastre J, Pallardo FV (2005) Why females live longer than males: control of longevity by sex hormones. *Science of aging knowledge environment : SAGE KE* **2005:** pe17

Vincent EE, Elder DJ, Thomas EC, Phillips L, Morgan C, Pawade J, Sohail M, May MT, Hetzel MR, Tavare JM (2011) Akt phosphorylation on Thr308 but not on Ser473 correlates with Akt protein kinase activity in human non-small cell lung cancer. *British journal of cancer* **104:** 1755-1761

von Horn H, Ekstrom C, Ellis E, Olivecrona H, Einarsson C, Tally M, Ekstrom TJ (2002) GH is a regulator of IGF2 promoter-specific transcription in human liver. *The Journal of endocrinology* **172:** 457-465

von Werder A, Seidler B, Schmid RM, Schneider G, Saur D (2012) Production of avian retroviruses and tissue-specific somatic retroviral gene transfer in vivo using the RCAS/TVA system. *Nature protocols* **7:** 1167-1183

Vonderhaar BK (1998) Prolactin: the forgotten hormone of human breast cancer. *Pharmacology & therapeutics* **79:** 169-178

Vouyovitch CM, Vidal L, Borges S, Raccurt M, Arnould C, Chiesa J, Lobie PE, Lachuer J, Mertani HC (2008) Proteomic analysis of autocrine/paracrine effects of human growth hormone in human mammary carcinoma cells. *Advances in experimental medicine and biology* **617:** 493-500

Wada-Hiraike O, Hiraike H, Okinaga H, Imamov O, Barros RP, Morani A, Omoto Y, Warner M, Gustafsson JA (2006) Role of estrogen receptor beta in uterine stroma and epithelium: Insights from estrogen receptor beta-/- mice. *Proceedings of the National Academy of Sciences of the United States of America* **103:** 18350-18355

Wagner M, Zollner G, Trauner M (2011) Nuclear receptors in liver disease. *Hepatology* **53:** 1023-1034

Wakabayashi N, Itoh K, Wakabayashi J, Motohashi H, Noda S, Takahashi S, Imakado S, Kotsuji T, Otsuka F, Roop DR, Harada T, Engel JD, Yamamoto M (2003) Keap1-null mutation leads to postnatal lethality due to constitutive Nrf2 activation. *Nature genetics* **35:** 238-245

Wakai K, Tsushima T, Murakami H, Isozaki O, Demura H, Nozoe Y, Yamada H (1998) Protein kinase C (PKC)-mediated growth hormone (GH) actions. *Endocrine journal* **45 Suppl:** S97-99

Waksman G, Shoelson SE, Pant N, Cowburn D, Kuriyan J (1993) Binding of a high affinity phosphotyrosyl peptide to the Src SH2 domain: crystal structures of the complexed and peptide-free forms. *Cell* **72:** 779-790

Wallace DC (2012) Mitochondria and cancer. *Nature reviews Cancer* **12:** 685-698

Walsh ST, Jevitts LM, Sylvester JE, Kossiakoff AA (2003) Site2 binding energetics of the regulatory step of growth hormone-induced receptor homodimerization. *Protein science : a publication of the Protein Society* **12:** 1960-1970

Wan Y, McDevitt A, Shen B, Smythe ML, Waters MJ (2004) Increased site 1 affinity improves biopotency of porcine growth hormone. Evidence against diffusion dependent receptor dimerization. *The Journal of biological chemistry* **279:** 44775-44784

Wan Y, Zheng YZ, Harris JM, Brown R, Waters MJ (2003) Epitope map for a growth hormone receptor agonist monoclonal antibody, MAb 263. *Molecular endocrinology* **17:** 2240-2250

Wang B, Rao YH, Inoue M, Hao R, Lai CH, Chen D, McDonald SL, Choi MC, Wang Q, Shinohara ML, Yao TP (2014) Microtubule acetylation amplifies p38 kinase signalling and anti-inflammatory IL-10 production. *Nature communications* **5:** 3479

Wang H, Pevsner J (1999) Detection of endogenous biotin in various tissues: novel functions in the hippocampus and implications for its use in avidin-biotin technology. *Cell Tissue Res* **296:** 511-516

Wang HT, Chen S, Wang J, Ou QJ, Liu C, Zheng SS, Deng MH, Liu XP (2003) Expression of growth hormone receptor and its mRNA in hepatic cirrhosis. *World journal of gastroenterology : WJG* **9:** 765-770

Wang L, Kurosaki T, Corey SJ (2007) Engagement of the B-cell antigen receptor activates STAT through Lyn in a Jak-independent pathway. *Oncogene* **26:** 2851-2859

Wang M, Miller RA (2012) Fibroblasts from long-lived mutant mice exhibit increased autophagy and lower TOR activity after nutrient deprivation or oxidative stress. *Aging cell* **11:** 668-674

Wang RH, Zheng Y, Kim HS, Xu X, Cao L, Luhasen T, Lee MH, Xiao C, Vassilopoulos A, Chen W, Gardner K, Man YG, Hung MC, Finkel T, Deng CX (2008a) Interplay among BRCA1, SIRT1, and Survivin during BRCA1-associated tumorigenesis. *Molecular cell* **32:** 11-20

Wang S, Zhang M, Liang B, Xu J, Xie Z, Liu C, Viollet B, Yan D, Zou MH (2010a) AMPKalpha2 deletion causes aberrant expression and activation of NAD(P)H oxidase and consequent endothelial dysfunction in vivo: role of 26S proteasomes. *Circulation research* **106:** 1117-1128

Wang W, Fang H, Groom L, Cheng A, Zhang W, Liu J, Wang X, Li K, Han P, Zheng M, Yin J, Wang W, Mattson MP, Kao JP, Lakatta EG, Sheu SS, Ouyang K, Chen J, Dirksen RT, Cheng H (2008b) Superoxide flashes in single mitochondria. *Cell* **134:** 279-290

Wang X, Darus CJ, Xu BC, Kopchick JJ (1996) Identification of growth hormone receptor (GHR) tyrosine residues required for GHR phosphorylation and JAK2 and STAT5 activation. *Molecular endocrinology* **10:** 1249-1260

Wang X, He K, Gerhart M, Huang Y, Jiang J, Paxton RJ, Yang S, Lu C, Menon RK, Black RA, Baumann G, Frank SJ (2002) Metalloprotease-mediated GH receptor proteolysis and GHBP shedding. Determination of extracellular domain stem region cleavage site. *The Journal of biological chemistry* **277:** 50510-50519

Wang YN, Yamaguchi H, Huo L, Du Y, Lee HJ, Lee HH, Wang H, Hsu JM, Hung MC (2010b) The translocon Sec61beta localized in the inner nuclear membrane transports membrane-embedded EGF receptor to the nucleus. *The Journal of biological chemistry* **285:** 38720-38729

Wang Z, Wang Z, Liang Z, Liu J, Shi W, Bai P, Lin X, Magaye R, Zhao J (2013) Expression and clinical significance of IGF-1, IGFBP-3, and IGFBP-7 in serum and lung cancer tissues from patients with non-small cell lung cancer. *OncoTargets and therapy* **6:** 1437-1444

Wanke R, Hermanns W, Folger S, Wolf E, Brem G (1991) Accelerated growth and visceral lesions in transgenic mice expressing foreign genes of the growth hormone family: an overview. *Pediatric nephrology* **5:** 513-521

Ward JM (2006) Lymphomas and leukemias in mice. *Experimental and toxicologic pathology : official journal of the Gesellschaft fur Toxikologische Pathologie* **57:** 377-381

Wass JA, Turner HE, Adams CB (1999) The importance of locating a good pituitary surgeon. *Pituitary* **2:** 51-54

Wassenaar MJ, Dekkers OM, Pereira AM, Wit JM, Smit JW, Biermasz NR, Romijn JA (2009) Impact of the exon 3-deleted growth hormone (GH) receptor polymorphism on baseline height and the growth response to recombinant human GH therapy in GH-deficient (GHD) and non-GHD children with short stature: a systematic review and meta-analysis. *The Journal of clinical endocrinology and metabolism* **94:** 3721-3730

Waters MJ (1999) *Handbook of Physiology- Section 7*, New York: Oxford University.

Waters MJ, Barclay JL (2007) Does growth hormone drive breast and other cancers? *Endocrinology* **148:** 4533-4535

Waters MJ, Brooks AJ (2011) Growth hormone receptor: structure function relationships. *Hormone research in paediatrics* **76 Suppl 1:** 12-16

Waters MJ, Conway-Campbell BL (2004) The oncogenic potential of autocrine human growth hormone in breast cancer. *Proceedings of the National Academy of Sciences of the United States of America* **101:** 14992-14993

Waters MJ, Hoang HN, Fairlie DP, Pelekanos RA, Brown RJ (2006) New insights into growth hormone action. *Journal of molecular endocrinology* **36:** 1-7

Waters MJ, Kaye PL (2002) The role of growth hormone in fetal development. *Growth hormone & IGF research : official journal of the Growth Hormone Research Society and the International IGF Research Society* **12:** 137-146

Waters MJ, Shang CA (2002) Physiology of normal growth hormone receptor function. *Journal of pediatric endocrinology & metabolism : JPEM* **15 Suppl 5:** 1443-1446

Waxman DJ, Holloway MG (2009) Sex differences in the expression of hepatic drug metabolizing enzymes. *Molecular pharmacology* **76:** 215-228

Waxman DJ, O'Connor C (2006) Growth hormone regulation of sex-dependent liver gene expression. *Molecular endocrinology* **20:** 2613-2629

Weaver AM, Silva CM (2007) S731 in the transactivation domain modulates STAT5b activity. *Biochemical and biophysical research communications* **362:** 1026-1030

Wei Y, Rhani Z, Goodyer CG (2006) Characterization of growth hormone receptor messenger ribonucleic acid variants in human adipocytes. *The Journal of clinical endocrinology and metabolism* **91:** 1901-1908

Weigent DA, Arnold RE (2005) Expression of insulin-like growth factor-1 and insulin-like growth factor-1 receptors in EL4 lymphoma cells overexpressing growth hormone. *Cellular immunology* **234:** 54-66

Weinberg F, Chandel NS (2009) Mitochondrial metabolism and cancer. *Annals of the New York Academy of Sciences* **1177:** 66-73

Weiss-Messer E, Merom O, Adi A, Karry R, Bidosee M, Ber R, Kaploun A, Stein A, Barkey RJ (2004) Growth hormone (GH) receptors in prostate cancer: gene expression in human tissues and cell lines and characterization, GH signaling and androgen receptor regulation in LNCaP cells. *Molecular and cellular endocrinology* **220:** 109-123

Wells JA (1996) Binding in the growth hormone receptor complex. *Proceedings of the National Academy of Sciences of the United States of America* **93:** 1-6

Wen Z, Zhong Z, Darnell JE, Jr. (1995) Maximal activation of transcription by Stat1 and Stat3 requires both tyrosine and serine phosphorylation. *Cell* **82:** 241-250

Wennbo H, Gebre-Medhin M, Gritli-Linde A, Ohlsson C, Isaksson OG, Tornell J (1997) Activation of the prolactin receptor but not the growth hormone receptor is important for induction of mammary tumors in transgenic mice. *The Journal of clinical investigation* **100:** 2744-2751

Wickelgren RB, Landin KL, Ohlsson C, Carlsson LM (1995) Expression of exon 3-retaining and exon 3-excluding isoforms of the human growth hormone-receptor is regulated in an interindividual, rather than a tissue-specific, manner. *The Journal of clinical endocrinology and metabolism* **80:** 2154-2157

Wilkinson IR, Ferrandis E, Artymiuk PJ, Teillot M, Soulard C, Touvay C, Pradhananga SL, Justice S, Wu Z, Leung KC, Strasburger CJ, Sayers JR, Ross RJ (2007) A ligand-receptor fusion of growth hormone forms a dimer and is a potent long-acting agonist. *Nature medicine* **13:** 1108-1113

Wilkinson-Berka JL, Lofthouse S, Jaworski K, Ninkovic S, Tachas G, Wraight CJ (2007) An antisense oligonucleotide targeting the growth hormone receptor inhibits neovascularization in a mouse model of retinopathy. *Molecular vision* **13:** 1529-1538

Wilson VJ, Rattray M, Thomas CR, Moreland BH, Schulster D (1995) Growth hormone increases IGF-I, collagen I and collagen III gene expression in dwarf rat skeletal muscle. *Molecular and cellular endocrinology* **115:** 187-197

Winston JT, Strack P, Beer-Romero P, Chu CY, Elledge SJ, Harper JW (1999) The SCFbeta-TRCP-ubiquitin ligase complex associates specifically with phosphorylated destruction motifs in IkappaBalpha and beta-catenin and stimulates IkappaBalpha ubiquitination in vitro. *Genes & development* **13:** 270-283

Winston LA, Bertics PJ (1992) Growth hormone stimulates the tyrosine phosphorylation of 42- and 45-kDa ERK-related proteins. *The Journal of biological chemistry* **267:** 4747-4751

Wojcik J, Berg MA, Esposito N, Geffner ME, Sakati N, Reiter EO, Dower S, Francke U, Postel-Vinay MC, Finidori J (1998) Four contiguous amino acid substitutions, identified in patients with Laron syndrome, differently affect the binding affinity and intracellular trafficking of the growth hormone receptor. *The Journal of clinical endocrinology and metabolism* **83:** 4481-4489

Wolf E, Kahnt E, Ehrlein J, Hermanns W, Brem G, Wanke R (1993) Effects of long-term elevated serum levels of growth hormone on life expectancy of mice: lessons from transgenic animal models. *Mechanisms of ageing and development* **68:** 71-87

Wolf E, Lahm H, Wu M, Wanke R, Hoeflich A (2000) Effects of IGFBP-2 overexpression in vitro and in vivo. *Pediatric nephrology* **14:** 572-578

Wolinski K, Czarnywojtek A, Ruchala M (2014) Risk of thyroid nodular disease and thyroid cancer in patients with acromegaly - meta-analysis and systematic review. *PloS one* **9:** e88787

Wolkow CA, Kimura KD, Lee MS, Ruvkun G (2000) Regulation of C. elegans life-span by insulinlike signaling in the nervous system. *Science* **290:** 147-150

Wood TJ, Sliva D, Lobie PE, Goullieux F, Mui AL, Groner B, Norstedt G, Haldosen LA (1997) Specificity of transcription enhancement via the STAT responsive element in the serine protease inhibitor 2.1 promoter. *Molecular and cellular endocrinology* **130:** 69-81

Woods A, Johnstone SR, Dickerson K, Leiper FC, Fryer LG, Neumann D, Schlattner U, Wallimann T, Carlson M, Carling D (2003) LKB1 is the upstream kinase in the AMP-activated protein kinase cascade. *Current biology : CB* **13:** 2004-2008

Woods KA, Fraser NC, Postel-Vinay MC, Savage MO, Clark AJ (1996) A homozygous splice site mutation affecting the intracellular domain of the growth hormone (GH) receptor resulting in Laron syndrome with elevated GH-binding protein. *The Journal of clinical endocrinology and metabolism* **81:** 1686-1690

Workman JL, Kingston RE (1998) Alteration of nucleosome structure as a mechanism of transcriptional regulation. *Annual review of biochemistry* **67:** 545-579

Wormald S, Hilton DJ (2004) Inhibitors of cytokine signal transduction. *The Journal of biological chemistry* **279:** 821-824

Wu X, Zang W, Cui S, Wang M (2012) Bioinformatics analysis of two microarray gene-expression data sets to select lung adenocarcinoma marker genes. *European review for medical and pharmacological sciences* **16:** 1582-1587

Wu Y, Cui K, Miyoshi K, Hennighausen L, Green JE, Setser J, LeRoith D, Yakar S (2003) Reduced circulating insulin-like growth factor I levels delay the onset of chemically and genetically induced mammary tumors. *Cancer research* **63:** 4384-4388

Wu Y, Yakar S, Zhao L, Hennighausen L, LeRoith D (2002) Circulating insulin-like growth factor-I levels regulate colon cancer growth and metastasis. *Cancer research* **62:** 1030-1035

Wu Z, Puigserver P, Andersson U, Zhang C, Adelmant G, Mootha V, Troy A, Cinti S, Lowell B, Scarpulla RC, Spiegelman BM (1999) Mechanisms controlling mitochondrial biogenesis and respiration through the thermogenic coactivator PGC-1. *Cell* **98:** 115-124

Wu ZS, Yang K, Wan Y, Qian PX, Perry JK, Chiesa J, Mertani HC, Zhu T, Lobie PE (2011) Tumor expression of human growth hormone and human prolactin predict a worse survival outcome in patients with mammary or endometrial carcinoma. *The Journal of clinical endocrinology and metabolism* **96:** E1619-1629

Xing Z, Chen HC, Nowlen JK, Taylor SJ, Shalloway D, Guan JL (1994) Direct interaction of v-Src with the focal adhesion kinase mediated by the Src SH2 domain. *Molecular biology of the cell* **5:** 413-421

Xiong H, Chen ZF, Liang QC, Du W, Chen HM, Su WY, Chen GQ, Han ZG, Fang JY (2009) Inhibition of DNA methyltransferase induces G2 cell cycle arrest and apoptosis in human colorectal cancer cells via inhibition of JAK2/STAT3/STAT5 signalling. *Journal of cellular and molecular medicine* **13:** 3668-3679

Xu J, Gontier G, Chaker Z, Lacube P, Dupont J, Holzenberger M (2014) Longevity effect of IGF-1R(+/-) mutation depends on genetic background-specific receptor activation. *Aging cell* **13:** 19-28

Xu J, Messina JL (2009) Crosstalk between growth hormone and insulin signaling. *Vitamins and hormones* **80:** 125-153

Xu J, Sun D, Jiang J, Deng L, Zhang Y, Yu H, Bahl D, Langenheim JF, Chen WY, Fuchs SY, Frank SJ (2013) The role of prolactin receptor in GH signaling in breast cancer cells. *Molecular endocrinology* **27:** 266-279

Xu J, Zhang Y, Berry PA, Jiang J, Lobie PE, Langenheim JF, Chen WY, Frank SJ (2011) Growth hormone signaling in human T47D breast cancer cells: potential role for a growth hormone receptor-prolactin receptor complex. *Molecular endocrinology* **25:** 597-610

Xu XQ, Emerald BS, Goh EL, Kannan N, Miller LD, Gluckman PD, Liu ET, Lobie PE (2005) Gene expression profiling to identify oncogenic determinants of autocrine human growth hormone in human mammary carcinoma. *The Journal of biological chemistry* **280:** 23987-24003

Yakimchuk K, Jondal M, Okret S (2013) Estrogen receptor alpha and beta in the normal immune system and in lymphoid malignancies. *Molecular and cellular endocrinology* **375:** 121-129

Yamauchi T, Kaburagi Y, Ueki K, Tsuji Y, Stark GR, Kerr IM, Tsushima T, Akanuma Y, Komuro I, Tobe K, Yazaki Y, Kadowaki T (1998a) Growth hormone and prolactin stimulate tyrosine phosphorylation of insulin receptor substrate-1, -2, and -3, their association with p85 phosphatidylinositol 3-kinase (PI3-kinase), and concomitantly PI3-kinase activation via JAK2 kinase. *The Journal of biological chemistry* **273:** 15719-15726

Yamauchi T, Kamon J, Minokoshi Y, Ito Y, Waki H, Uchida S, Yamashita S, Noda M, Kita S, Ueki K, Eto K, Akanuma Y, Froguel P, Foufelle F, Ferre P, Carling D, Kimura S, Nagai R, Kahn BB,

Kadowaki T (2002) Adiponectin stimulates glucose utilization and fatty-acid oxidation by activating AMP-activated protein kinase. *Nature medicine* **8:** 1288-1295

Yamauchi T, Ueki K, Tobe K, Tamemoto H, Sekine N, Wada M, Honjo M, Takahashi M, Takahashi T, Hirai H, Tsushima T, Akanuma Y, Fujita T, Komuro I, Yazaki Y, Kadowaki T (1998b) Growth hormone-induced tyrosine phosphorylation of EGF receptor as an essential element leading to MAP kinase activation and gene expression. *Endocrine journal* **45 Suppl:** S27-31

Yamauchi T, Ueki K, Tobe K, Tamemoto H, Sekine N, Wada M, Honjo M, Takahashi M, Takahashi T, Hirai H, Tushima T, Akanuma Y, Fujita T, Komuro I, Yazaki Y, Kadowaki T (1997) Tyrosine phosphorylation of the EGF receptor by the kinase Jak2 is induced by growth hormone. *Nature* **390:** 91-96

Yang N, Huang Y, Jiang J, Frank SJ (2004) Caveolar and lipid raft localization of the growth hormone receptor and its signaling elements: impact on growth hormone signaling. *The Journal of biological chemistry* **279:** 20898-20905

Yang N, Wang X, Jiang J, Frank SJ (2007) Role of the growth hormone (GH) receptor transmembrane domain in receptor predimerization and GH-induced activation. *Molecular endocrinology* **21:** 1642-1655

Yang XF, Beamer WG, Huynh H, Pollak M (1996) Reduced growth of human breast cancer xenografts in hosts homozygous for the lit mutation. *Cancer research* **56:** 1509-1511

Yankovskaya V, Horsefield R, Tornroth S, Luna-Chavez C, Miyoshi H, Leger C, Byrne B, Cecchini G, Iwata S (2003) Architecture of succinate dehydrogenase and reactive oxygen species generation. *Science* **299:** 700-704

Yeung F, Hoberg JE, Ramsey CS, Keller MD, Jones DR, Frye RA, Mayo MW (2004) Modulation of NF-kappaB-dependent transcription and cell survival by the SIRT1 deacetylase. *The EMBO journal* **23:** 2369-2380

Yoshida M, Muneyuki E, Hisabori T (2001) ATP synthase--a marvellous rotary engine of the cell. *Nature reviews Molecular cell biology* **2:** 669-677

Young JA, Bates P, Varmus HE (1993) Isolation of a chicken gene that confers susceptibility to infection by subgroup A avian leukosis and sarcoma viruses. *Journal of virology* **67:** 1811-1816

Yu DH, Qu CK, Henegariu O, Lu X, Feng GS (1998) Protein-tyrosine phosphatase Shp-2 regulates cell spreading, migration, and focal adhesion. *The Journal of biological chemistry* **273:** 21125-21131

Yu W, Dittenhafer-Reed KE, Denu JM (2012) SIRT3 protein deacetylates isocitrate dehydrogenase 2 (IDH2) and regulates mitochondrial redox status. *The Journal of biological chemistry* **287:** 14078-14086

Yurkovetsky Z, Ta'asan S, Skates S, Rand A, Lomakin A, Linkov F, Marrangoni A, Velikokhatnaya L, Winans M, Gorelik E, Maxwell GL, Lu K, Lokshin A (2007) Development of multimarker panel for early detection of endometrial cancer. High diagnostic power of prolactin. *Gynecologic oncology* **107:** 58-65

Zatelli MC, Minoia M, Mole D, Cason V, Tagliati F, Margutti A, Bondanelli M, Ambrosio MR, degli Uberti E (2009) Growth hormone excess promotes breast cancer chemoresistance. *The Journal of clinical endocrinology and metabolism* **94:** 3931-3938

Zekri A, Ghaffari SH, Yousefi M, Ghanizadeh-Vesali S, Mojarrad M, Alimoghaddam K, Ghavamzadeh A (2013) Autocrine human growth hormone increases sensitivity of mammary carcinoma cell to arsenic trioxide-induced apoptosis. *Molecular and cellular endocrinology* **377:** 84-92

Zennou V, Petit C, Guetard D, Nerhbass U, Montagnier L, Charneau P (2000) HIV-1 genome nuclear import is mediated by a central DNA flap. *Cell* **101:** 173-185

Zerrad-Saadi A, Lambert-Blot M, Mitchell C, Bretes H, Collin de l'Hortet A, Baud V, Chereau F, Sotiropoulos A, Kopchick JJ, Liao L, Xu J, Gilgenkrantz H, Guidotti JE (2011) GH receptor plays a major role in liver regeneration through the control of EGFR and ERK1/2 activation. *Endocrinology* **152:** 2731-2741

Zhang C, Lv J, He Q, Wang S, Gao Y, Meng A, Yang X, Liu F (2014) Inhibition of endothelial ERK signalling by Smad1/5 is essential for haematopoietic stem cell emergence. *Nature communications* **5:** 3431

Zhang F, Zhang Q, Tengholm A, Sjoholm A (2006) Involvement of JAK2 and Src kinase tyrosine phosphorylation in human growth hormone-stimulated increases in cytosolic free Ca2+ and insulin secretion. *American journal of physiology Cell physiology* **291:** C466-475

Zhang X, Meng J, Wang ZY (2012a) A switch role of Src in the biphasic EGF signaling of ER-negative breast cancer cells. *PloS one* **7:** e41613

Zhang X, Zhu T, Chen Y, Mertani HC, Lee KO, Lobie PE (2003) Human growth hormone-regulated HOXA1 is a human mammary epithelial oncogene. *The Journal of biological chemistry* **278:** 7580-7590

Zhang Y, Jiang J, Black RA, Baumann G, Frank SJ (2000) Tumor necrosis factor-alpha converting enzyme (TACE) is a growth hormone binding protein (GHBP) sheddase: the metalloprotease TACE/ADAM-17 is critical for (PMA-induced) GH receptor proteolysis and GHBP generation. *Endocrinology* **141:** 4342-4348

Zhang Y, Jiang J, Kopchick JJ, Frank SJ (1999) Disulfide linkage of growth hormone (GH) receptors (GHR) reflects GH-induced GHR dimerization. Association of JAK2 with the GHR is enhanced by receptor dimerization. *The Journal of biological chemistry* **274:** 33072-33084

Zhang Y, Xie Y, Berglund ED, Coate KC, He TT, Katafuchi T, Xiao G, Potthoff MJ, Wei W, Wan Y, Yu RT, Evans RM, Kliewer SA, Mangelsdorf DJ (2012b) The starvation hormone, fibroblast growth factor-21, extends lifespan in mice. *eLife* **1:** e00065

Zhang YY, Zhou LM (2012) Sirt3 inhibits hepatocellular carcinoma cell growth through reducing Mdm2-mediated p53 degradation. *Biochemical and biophysical research communications* **423:** 26-31

Zheng R, Pan G, Thobe BM, Choudhry MA, Matsutani T, Samy TS, Kang SC, Bland KI, Chaudry IH (2006) MyD88 and Src are differentially regulated in Kupffer cells of males and proestrus females following hypoxia. *Molecular medicine* **12:** 65-73

Zhong L, D'Urso A, Toiber D, Sebastian C, Henry RE, Vadysirisack DD, Guimaraes A, Marinelli B, Wikstrom JD, Nir T, Clish CB, Vaitheesvaran B, Iliopoulos O, Kurland I, Dor Y, Weissleder R, Shirihai OS, Ellisen LW, Espinosa JM, Mostoslavsky R (2010) The histone deacetylase Sirt6 regulates glucose homeostasis via Hif1alpha. *Cell* **140:** 280-293

Zhou D, Yang J, Huang WD, Wang J, Zhang Q (2013) siRNA-targeted inhibition of growth hormone receptor in human colon cancer SW480 cells. *World journal of gastroenterology : WJG* **19:** 8108-8113

Zhou Y, He L, Baumann G, Kopchick JJ (1997a) Deletion of the mouse GH-binding protein (mGHBP) mRNA polyadenylation and splicing sites does not abolish production of mGHBP. *Journal of molecular endocrinology* **19:** 1-13

Zhou Y, Jiang H (2006) Short communication: A milk trait-associated polymorphism in the bovine growth hormone receptor gene does not affect receptor signaling. *Journal of dairy science* **89:** 1761-1764

Zhou Y, Xu BC, Maheshwari HG, He L, Reed M, Lozykowski M, Okada S, Cataldo L, Coschigamo K, Wagner TE, Baumann G, Kopchick JJ (1997b) A mammalian model for Laron syndrome produced by targeted disruption of the mouse growth hormone receptor/binding protein gene (the Laron mouse). *Proceedings of the National Academy of Sciences of the United States of America* **94:** 13215-13220

Zhu T, Goh EL, Graichen R, Ling L, Lobie PE (2001) Signal transduction via the growth hormone receptor. *Cellular signalling* **13:** 599-616

Zhu T, Goh EL, LeRoith D, Lobie PE (1998a) Growth hormone stimulates the formation of a multiprotein signaling complex involving p130(Cas) and CrkII. Resultant activation of c-Jun N-terminal kinase/stress-activated protein kinase (JNK/SAPK). *The Journal of biological chemistry* **273:** 33864-33875

Zhu T, Goh EL, Lobie PE (1998b) Growth hormone stimulates the tyrosine phosphorylation and association of p125 focal adhesion kinase (FAK) with JAK2. Fak is not required for stat-mediated transcription. *The Journal of biological chemistry* **273:** 10682-10689

Zhu T, Ling L, Lobie PE (2002) Identification of a JAK2-independent pathway regulating growth hormone (GH)-stimulated p44/42 mitogen-activated protein kinase activity. GH activation of Ral and phospholipase D is Src-dependent. *The Journal of biological chemistry* **277:** 45592-45603

Zhu T, Lobie PE (2000) Janus kinase 2-dependent activation of p38 mitogen-activated protein kinase by growth hormone. Resultant transcriptional activation of ATF-2 and CHOP, cytoskeletal re-organization and mitogenesis. *The Journal of biological chemistry* **275:** 2103-2114

Zhu T, Starling-Emerald B, Zhang X, Lee KO, Gluckman PD, Mertani HC, Lobie PE (2005) Oncogenic transformation of human mammary epithelial cells by autocrine human growth hormone. *Cancer research* **65:** 317-324

Zufferey R, Dull T, Mandel RJ, Bukovsky A, Quiroz D, Naldini L, Trono D (1998) Self-inactivating lentivirus vector for safe and efficient in vivo gene delivery. *Journal of virology* **72:** 9873-9880

Appendices

Appendix I: List of primers designed for making hGHR cys mutants

Primer	Sequence
L251C Rvs	5'CATCTGAGGACATGTTACATAGAGCACCTCACTGAACTCGCC
P252C Fwd	5'TGTCAGATGAGCCAATTTACATCTGAAGAAGATTTCTACTTTC
P252C Rvs	5'AAGTGTTACATAGAGCACCTCACTGAACTCGCC
Q253C Fwd	5'TGCATGAGCCAATTTACATCTGAAGAAGATTTCTACTTTCC
Q253C Rvs	5'AGGAAGTGTTACATAGAGCACCTCACTGAACTCG
M254C Rvs	5'ACACTGAGGAAGTGTTACATAGAGCACCTCACTGAACTCG
S255C Rvs	5'TGTAAATTGGCACATCTGAGGAAGTGTTACATAGAGCACCTC
Q256C Rvs	5'TGTAAAGCAGCTCATCTGAGGAAGTGTTACATAGAGCACCTC
F257C Rvs	5'TGTACATTGGCTCATCTGAGGAAGTGTTACATAGAGCAC
T258C Rvs	5'GCAAAATTGGCTCATCTGAGGAAGTGTTACATAGAGC
Fwd a (From S255) USED FOR L251 to M254)	5'AGCCAATTTACATCTGAAGAAGATTTCTACTTTCCATG
Fwd b (From C259S) USED FOR S255 to T258)	5'TCTGAAGAAGATTTCTACTTTCCATGGCTCTTAATTATTATC
Fwd A (Common for all)	5'CTGGAGTCTGCAAAGTGTTAATCCAGGCC
Rvs A (Common for all)	5'GATCGATTCCTTTAATCTTTGGAACTGGAACTGG

Primer	Sequence
C259S Fwd	5'GATGAGCCAATTTACATCTGAAGAAGATTTCTAC
C259S Rvs	5'GTAGAAATCTTCTTCAGATGTAAATTGGCTCATC
E260C Fwd	5'GAGCCAATTTACATCTTGTGAAGATTTCTACTTT
E260C Rvs	5'AAAGTAGAAATCTTCACAAGATGTAAATTGGCTC
E261C Fwd	5'CCAATTTACATCTGAATGTGATTTCTACTTTCCA
E261C Rvs	5'TGGAAAGTAGAAATCACATTCAGATGTAAATTGG
D262C Fwd	5'ATTTACATCTGAAGAATGTTTCTACTTTCCATGG
D262C Rvs	5'CCATGGAAAGTAGAAACATTCTTCAGATGTAAAT
F263C Fwd	5'TACATCTGAAGAAGATTGCTACTTTCCATGGCTC
F263C Rvs	5'GAGCCATGGAAAGTAGCAATCTTCTTCAGATGTA
Y264C Fwd	5'ATCTGAAGAAGATTTCTGCTTTCCATGGCTCTTA
Y264C Rvs	5'TAAGAGCCATGGAAAGCAGAAATCTTCTTCAGAT
F265C Fwd	5'TGAAGAAGATTTCTACTGTCCATGGCTCTTAATT
F265C Rvs	5'AATTAAGAGCCATGGACAGTAGAAATCTTCTTCA
P266C Fwd	5'AGAAGATTTCTACTTTTGTTGGCTCTTAATTATT
P266C Rvs	5'AATAATTAAGAGCCAACAAAAGTAGAAATCTTCT
W267C Fwd	5'AGATTTCTACTTTCCATGTCTCTTAATTATTATC
W267C Rvs	5'GATAATAATTAAGAGACATGGAAAGTAGAAATCT
L268C Fwd	5'TTTCTACTTTCCATGGTGCTTAATTATTATCTTT
L268C Rvs	5'AAAGATAATAATTAAGCACCATGGAAAGTAGAAA
L269C Fwd	5'CTACTTTCCATGGCTCTGTATTATTATCTTTGGA
L269C Rvs	5'TCCAAAGATAATAATACAGAGCCATGGAAAGTAG
I270C Fwd	5'CTTTCCATGGCTCTTATGTATTATCTTTGGAATA
I270C Rvs	5'TATTCCAAAGATAATACATAAGAGCCATGGAAAG
I271C Fwd	5'TCCATGGCTCTTAATTTGTATCTTTGGAATATTT
I271C Rvs	5'AAATATTCCAAAGATACAAATTAAGAGCCATGGA
I272C Fwd	5'ATGGCTCTTAATTATTTGCTTTGGAATATTTGGG
I272C Rvs	5'CCCAAATATTCCAAAGCAAATAATTAAGAGCCAT
F273C Fwd	5'GCTCTTAATTATTATCTGTGGAATATTTGGGCTA
F273C Rvs	5'TAGCCCAAATATTCCACAGATAATAATTAAGAGC
G274C Fwd	5'CTTAATTATTATCTTTTGTATATTTGGGCTAACA
G274C Rvs	5'TGTTAGCCCAAATATACAAAAGATAATAATTAAG

I275C Fwd	5’AATTATTATCTTTGGATGTTTTGGGCTAACAGTG
I275C Rvs	5’CACTGTTAGCCCAAAACATCCAAAGATAATAATT
F276C Fwd	5’TATTATCTTTGGAATATGTGGGCTAACAGTGATG
F276C Rvs	5’CATCACTGTTAGCCCACATATTCCAAAGATAATA
G277C Fwd	5’TATCTTTGGAATATTTTGCCTAACAGTGATGCTA
G277C Rvs	5’TAGCATCACTGTTAGGCAAAATATTCCAAAGATA
L278C Fwd	5’CTTTGGAATATTTGGGTGTACAGTGATGCTATTT
L278C Rvs	5’AAATAGCATCACTGTACACCCAAATATTCCAAAG
T279C Fwd	5’TGGAATATTTGGGCTATGTGTGATGCTATTTGTA
T279C Rvs	5’TACAAATAGCATCACACATAGCCCAAATATTCCA
V280C Fwd	5’AATATTTGGGCTAACATGCATGCTATTTGTATTC
V280C Rvs	5’GAATACAAATAGCATGCATGTTAGCCCAAATATT
M281C Fwd	5’ATTTGGGCTAACAGTGTGCCTATTTGTATTCTTA
M281C Rvs	5’TAAGAATACAAATAGGCACACTGTTAGCCCAAAT
L282C Fwd	5’TGGGCTAACAGTGATGTGTTTTGTATTCTTATTT
L282C Rvs	5’AAATAAGAATACAAAACACATCACTGTTAGCCCA
F283C Fwd	5’GCTAACAGTGATGCTATGTGTATTCTTATTTTCT
F283C Rvs	5’AGAAAATAAGAATACACATAGCATCACTGTTAGC
V284C Fwd	5’AACAGTGATGCTATTTTGTTTCTTATTTTCTAAA
V284C Rvs	5’TTTAGAAAATAAGAAACAAAATAGCATCACTGTT
F285C Fwd	5’AGTGATGCTATTTGTATGCTTATTTTCTAAACAG
F285C Rvs	5’CTGTTTAGAAAATAAGCATACAAATAGCATCACT
L286C Fwd	5’GATGCTATTTGTATTCTGTTTTTCTAAACAGCAA
L286C Rvs	5’TTGCTGTTTAGAAAAACAGAATACAAATAGCATC
F289Fwd	5’GCTATTTGTATTCTTATGTTCTAAACAGCAAAGG
F287 Rvs	5’CCTTTGCTGTTTAGAACATAAGAATACAAATAGC
S288C Fwd	5’ATTTGTATTCTTATTTTGTAAACAGCAAAGGATT
S288C Rvs	5’AATCCTTTGCTGTTTACAAAATAAGAATACAAAT
C389Stop Fwd	5’CTCTGGACGTACCAGCTGATGTGAACCTGACATT
C389Stop Rvs	5’AATGTCAGGTTCACATCAGCTGGTACGTCCAGAG

Appendix II: List of sequencing primers

Primer	Sequence
hGHR426 Fwd	5'GCAGCTATCCTTAGCAGAGC
hGHR827 Fwd	5'CTGAACGTCAGTTTAACTGG
hGHR1439 Fwd	5'CAGACTTCTAAGCAGTGACC
hGHR1815 Fwd	5'CAGGTGAGCGACATTACACC
hGHR2091 Fwd	5'ACAGGAGAACATGTTCCAGG
hGHRintron Rvs	5'CTTCAGGTGTTAATTAGTACTAGC
hGHR709 Rvs	5'ACAATAAGGTATCCAGATGG
hGHR1014 Rvs	5'ACTTCATATTCCTTATCCAC
hGHR1381 Rvs	5'TCAACCCAAGAGTCATCACTG
hGHR1706 Rvs	5'CTCTGCTTGGATAACACTGG
hGHR2053 Rvs	5'AGTGGTAAGGCTTTCTGTGG

Primer	Sequence
rGHR102 Fwd	5'ATTCACCAAGTGCCGTTCACC
rGHR499 Fwd	5'AAGGGATGGATAGTCTTGGAG
rGHR908 Fwd	5'GAGGTGAACACAATCTTAGCC
rGHR1299 Fwd	5'AGAGGAAGACAAACCGCGACC
rGHR1700 Fwd	5'CCCCAGGTTCTGAGATGCCTG
rGHR1501 Rvs	5'CTGGATGCGCATCACACTGAG
rGHR1098 Rvs	5'AGAGTCGTCATCCTTTGCTGC
rGHR701 Rvs	5'GGAAGGGTTACATAGAGCACC
rGHR199 Rvs	5'ACAGCTGCACAGATCCTGGGC

Appendix III: List of primers designed for plasmid construction, gene expression and genotyping in the RCAS/TVA system

Primer	Sequence	Utility
hGHR-AclI Rvs	TATCAACGTTCTGGCATGATTTTGTTCAGTTGGT CTGTG	HA-hGHR HA-NLS-hGHR
GFP-AclI-Rvs	TATCAACGTTACTTGTACAGCTCGTCCATGCCG AGAG	HA-NLS-GFP
AclI-HA Fwd	TACTAACGTTATGGGATATCCATATGATGTTCC AGATTACGC	HA-NLS-GFP
rGHR-AclI Rvs	GATCAACGTTCTATGGCAAGATTTTGTTGGTCTG TG	HA-rGHR HA-NLS-rGHR
AclI-pGHRsig Fwd	TACTAACGTTATGGATCTCTGGCAGCTTCTGTTG ACC	HA-hGHR HA-NLS-hGHR HA-rGHR HA-NLS-rGHR
attB1-pGHRsig Fwd	GGGGACAAGTTTGTACAAAAAAGCAGGCTATG GATCTCTGGCAGCTTCTGTTGACC	HA-hGHR HA-NLS-hGHR HA-rGHR HA-NLS-rGHR HA-Jun-3A-rGHR
rGHR-attB2 Rvs	GGGGACCACTTTGTACAAGAAAGCTGGGTCTAT GGCAAGATTTTGTTCAGTTGGTCTGTG	HA-rGHR HA-NLS-rGHR HA-Jun-3A-rGHR
attB1-HA Fwd	GGGGACAAGTTTGTACAAAAAAGCAGGCTATG GGATATCCATATGATGTTCCAGATTACGC	HA-NLS-GFP
GFP-attB2 Rvs	GGGGACCACTTTGTACAAGAAAGCTGGGTTTAC TTGTACAGCTCGTCCATGCCGAGAG	HA-NLS-GFP
hGHR-attB2 Rvs	GGGGACCACTTTGTACAAGAAAGCTGGGTCTAA GGCATGATTTTGTTCAGTTGGTCTGTG	HA-hGHR HA-NLS-hGHR
mGAPDH Fwd	AGCCTCGTCCCGTAGACAAAA	qPCR
mGAPDH Rvs	TGGCAACAATCTCCACTTTGC	qPCR
tva Fwd	GAGTGTTACCCGCAGGACTGG	Genotyping
TVA Rvs	GAGTCAGGTTCCGTGGTGAGC	Genotyping
GFP Fwd	CAGAAGAACGGCATCAAGGTG	qPCR
GFP Rvs	GGACTGGGTGCTCAGGTAGTG	qPCR
zfTVA Fwd	CACGGACAACGGCACAGA	qPCR
zfTVA Rvs	AGCAAAAGATCCCTGCAGTGA	qPCR
ZfHPRT Fwd	ATCAGCGAAACAGGAAAGGAG	qPCR
ZfHPRT Rvs	CTGCGGTGAGCTGCACTACT	qPCR

Appendix IV: List of primers designed for making constructs comprising 2A peptide bridges

Primer	Sequence
attB1-psig Fwd	5'GGGGACAAGTTTGTACAAAAAAGCAGGCTATGGATCTCTGGCAGCT TCTGTTGACC
hGHR-2Ac1 Rvs	5'GTTTTCCTCCACGTCGCCGCAGGTGAGCAGGCTTCCCCTGCCCTCAG GCATGATTTTGTTCAGTTGGTCTGTGCTC
rGHR-2Ac1 Rvs	5'GTTTTCCTCCACGTCGCCGCAGGTGAGCAGGCTTCCCCTGCCCTCTG GCAAGATTTTGTTCAGTTGGTCTGTGCT
2AC1-CDK4 Fwd	5'ACCTGCGGCGACGTGGAGGAAAACCCTGGCCCCGCCCCAGGATCCA TGGCTACCTCTCGATATGAGCCAGTGGC
CDK4-2Ac2 Rvs	5'GGGATTCTCTTCGACATCTCCACATGTCAGGAGGCTTCCCCTGCCCT CCTCCGGATTACCTTCATCCTTATGTAGATAAGAGTGC
2AC1-c-myc Fwd	5'ACCTGCGGCGACGTGGAGGAAAACCCTGGCCCCGCCCCAGGATCCA TGCCCCTCAACGTTAGCTTCACCAAC
c-Myc-2Ac2 Rvs	5'GGGATTCTCTTCGACATCTCCACATGTCAGGAGGCTTCCCCTGCCCT CCGCACAAGAGTTCCGTAGCTGTTCAAGTTT
2AC2-GFP Fwd	5'CTGACATGTGGAGATGTCGAAGAGAATCCCGGCCCTGCCCCAGGAT CCATGGTGAGCAAGGGCGAGGAGCTG
GFP-attB2 Rvs	5'GGGGACCACTTTGTACAAGAAAGCTGGGTTTACTTGTACAGCTCGTC CATGCCGAGAG
attB1-CDK4 Fwd	5'GGGGACAAGTTTGTACAAAAAAGCAGGCTATGGCTACCTCTCGATA TGAGCCAGTGGC
CDK4-2AC1 Rvs	5'GTTTTCCTCCACGTCGCCGCAGGTGAGCAGGCTTCCCCTGCCCTCCT CCGGATTACCTTCATCCTTATGTAGATAAGAGTGC
attB1 c-Myc Fwd	5'GGGGACAAGTTTGTACAAAAAAGCAGGCTATGCCCCTCAACGTTAG CTTCACCAAC
c-Myc-2Ac1 Rvs	5'GTTTTCCTCCACGTCGCCGCAGGTGAGCAGGCTTCCCCTGCCCTCCG CACAAGAGTTCCGTAGCTGTTCAAGTTT
2AC1-GFP Fwd	5'ACCTGCGGCGACGTGGAGGAAAACCCTGGCCCCGCCCCAGGATCCA TGGTGAGCAAGGGCGAGGAGCTG
2Ac1 mKate2 Fwd	5'ACCTGCGGCGACGTGGAGGAAAACCCTGGCCCCGCCCCAGGATCCA TGGTGAGCGAGCTGATTAAGGAGAACATG
mKate2-attB2 Rvs	5'GGGGACCACTTTGTACAAGAAAGCTGGGTTCATCTGTGCCCCAGTTT GCTAGGG

Primer	Fwd	Rvs
GH1/2	5'GCAGTGCCTTCCCAACCA	5'ATGGGCGCGGAGCAT
SOCS2	5'CCCGGAACGGCACTGTT	5'CTACAGAGATGCTGCAGAGATGGT
B2M	5'CATTCGG5'GCCGAGATGTCT	5'CTCCAGGCCAGAAAGAGAGAGTAG
GusB	5'TTCCCTCCAGCTTCAATGACA	5'CCACACCCAGCCGACAA
GAPDH	5'GCCCCCGGTTTCTATAAATTG	5'GTCGAACAGGAGGAGCAGAGA

Appendix V: List of primers designed for qPCR analysis on mouse tissues

Primer	Sequence
m16S Fwd (for genomic DNA)	CCGAAACCAAACGAGCTACCT
m16S Rvs (for genomic DNA)	CTCGTTAGGCTTTTCACCTCTACCT
mApoE Fwd	TGGCTACCAACCCCATCATC
mApoE Rvs	TGCAGGACAGGAGAAGGATACTC
mAtp5a Fwd	CAACAAAGGATGACCCCAAA
mAtp5a Rvs	AAGCTGCAAGGATGCTGTCT
mB2M Fwd	ACTGATACATACGCCTGCAGAGTT
mB2M Rvs	CTCGATCCCAGTAGACGGTCTT
mCAT Fwd	TGGCTTTTGACCCAAGCAAT
mCAT Rvs	CGGCCCTGAAGCATTTTGT
mCD36 Fwd	TGTGTGGAGCAACTGGTGGAT
mCD36 Rvs	CGTGGCCCGGTTCTACTAATT
mCdkn1a Fwd	GAAACACCAGCACTATGATTGGA
mCdkn1a Rvs	ATTCCCGTAAACTCCCCTGTG
mCIS Fwd	TACAACATCTGTGTCGGCTAAGTCA
mCIS Rvs	TCGGAGGTAGTCGGCCATAC
mFGF21 Fwd	ATGGAATGGATGAGATCTAGAGTTGG
mFGF21 Rvs	TCTTGGTGGTCATCTGTGTAGAGG
mFMO2 Fwd	GATTTAGCTCCATGCTCCGAAA
mFMO2 Rvs	TCTGTTGTTCCATCATCCACTTG
mGlut2 Fwd	CGGAATGGTCGCCTCATT
mGlut2 Rvs	ACATTGCTTTGATCCTTCCAAGTT
mHNF1A Fwd	AAAGAGCTGGAGAACCTCAGC
mHNF1A Rvs	GACAGGTGGGACTGGTTGA
mHNF3B Fwd	TCATGTTGCTCACGGAAGAG
mHNF3B Rvs	TAAAGTATGCTGGGAGCCGT
mHNF4A Fwd	GCTGTCCTCGTAGCTTGACC
mHNF4A Rvs	TTAAGAAGTGCTTCCGGGCT
mHNF6A Fwd	TCCTTCCCATGTTCTTGCTC
mHNF6A Rvs	GGAGGATGTGGAAGTGGCT
mIGF-1 Fwd	CACTCATCCACAATGCCTGT
mIGF-1 Rvs	TGGATGCTCTTCAGTTCGTG
mIGF-2 Fwd	TGTGTGACCAGGCTGCTAGTTC
mIGF-2 Rvs	ACCATGTGGACAGGTGCTTAGA
mIGFBP-1 Fwd	TGGACAGCTTCCACCTGATG
mIGFBP-1 Rvs	TGATGGCGTTCCACAGGAT
mIGFBP-2 Fwd	CAGCAGGTTGCAGACAGTGATG
mIGFBP-2 Rvs	GCTCCTTCATGCCTGACTTGAG
mIGFBP-3 Fwd	GCTGGTGTGTGGACAAGTATGG
mIGFBP-3 Rvs	GGCAATGTACGTCGTCTTTCC
mIGFBP-4 Fwd	GCCCATCTTTGGTCAGGGTAT
mIGFBP-4 Rvs	TTTCCCACAGCAGAGATCTACCT
mIL-10beta Fwd	TGTCAAATTCATTCATGGCCT
mIL-10heta Rvs	ATCGATTTCTCCCCTGTGAA

mIL-10R alpha Fwd	TGAGCCTAGAATTCATTGCATACG
mIL-10R alpha Rvs	GGAAAAATCTGGCTTCAAACCA
mIL-10R beta Fwd	TTCGGAGTGGGTCAATGTCA
mIL-10R beta Rvs	TGCATCTCAGGAGGTCCAATG
mIL-1RA Fwd	GCATCTTGCAGGGTCTTTTC
mIL-1RA Rvs	GTGAGACGTTGGAAGGCAGT
mIRS1 Fwd	GGAGGATTTGCTGAGGTCAT
mIRS1 Rvs	CTATGCCAGCATCAGCTTCC
mIRS2 Fwd	CCCCAGTGTCCCCATCCT
mIRS2 Rvs	TTTCCTGAGAGAGACGTTTTCCA
mKeap1 Fwd	CATCCACCCTAAGGTCATGGA
mKeap1 Rvs	CATCACGTGCAGGACACACTT
mLXR alpha Fwd	TGGAGAACTCAAAGATGGGG
mLXR alpha Rvs	TGAGAGCATCACCTTCCTCA
mLXR beta Fwd	AGAACTTGTGGGGGAAGACA
mLXR beta Rvs	GGTGCAGTCATGAGCCCC
mMFN2 Fwd	TGAAAGTCACTGTGCATTTGATAAAGT
mMFN2 Rvs	GGCGCCCATCAGTCATTC
mMt1 Fwd	GCTGTGCCTGATGTGACGAA
mMt1 Rvs	AGGAAGACGCTGGGTTGGT
mNCOR1 Fwd	CCTATTAAACCAAACCCATTGGAT
mNCOR1 Rvs	CATGGAGTGCAAGAAACCATTG
mNCOR2 Fwd	CCTTCCGTGAGAAGTTTATGCA
mNCOR2 Rvs	CACACTCAGCGACCGTCTTTC
mNdufa5 Fwd	TGGAAGAGCCGCCTGCTA
mNdufa5 Rvs	TTCCCATCCACCATCTGACA
mNqo1 Fwd	GGGTCGTCTTGGCAACCA
mNqo1 Rvs	CAGATGTTGAGGGAGGATCGTAA
mNrf1 Fwd	TCCAGTCTCTGTGGACAAAATGA
mNrf1 Rvs	CGACCTGTGGAATACTTGAGCAT
mNrf2 Fwd	TCCTTAGACTCAAATCCCACCTTAA
mNrf2 Rvs	GGGCTCTGCTATGAAAGCAGAA
mPgc1α Fwd	AGCGCCGTGTGATTTACGTT
mPgc1α Rvs	GTCTCCATCATCCCGCAGATT
mPgc1β Fwd	TCCTGTAAAAGCCCGGAGTAT
mPgc1β Rvs	GCTCTGGTAGGGGCAGTGA
mPolg2 Fwd (for genomic DNA)	CGCAGCCGAGGGACAGT
mPolg2 Rvs (for genomic DNA)	AAGAAATGCCACTAGCTGTTCCTT
mPpar alpha Fwd	AGTGCCCTGAACATCGAGTGT
mPpar alpha Rvs	CCGAATAGTTCGCCGAAAGA
mPpar delta Fwd	GGTCATAGCTCTGCCACCAT
mPpar delta Rvs	ACTCAGAGGCTCCTGCTCAC
mPpar gamma1 Fwd	GCGGCTGAGAAATCACGTTC
mPpar gamma1 Rvs	GAATATCAGTGGTTCACCGCTTC
mPpar gamma2 Fwd	AACTCTGGGAGATTCTCCTGTTGA
mPpar gamma2 Rvs	GAAGTGCTCATAGGCAGTGCAT
mPparγ Fwd	GCATCAGGCTTCCACTATGGA
mPparγ Rvs	TCCGGCAGTTAAGATCACACC

mPtp1B Fwd	GGCGGCCCAAAGAGTGA
mPtp1B Rvs	GGAGATGCATAGCCTGAAAAGG
mRev-Erb alpha Fwd	ACGGCAAGGCAACACCAA
mRev-Erb alpha Rvs	CTTCCCAGATCTCCTGCACAGT
mRev-Erb beta Fwd	CTGTGATGCCAACGGCAAT
mRev-Erb beta Rvs	CTGTGCGGTCACTCTTCAGAAC
mRORalpha Fwd	TGACGCCCACCTACAACATC
mRORalpha Rvs	CATCCATATAGGTGCTGAGGTCAT
mRORgamma Fwd	GCTCATCAGCTCCATATTTGACTTT
mRORgamma Rvs	AGGGCAATCTCATCCTCAGAAA
mSdhb Fwd	TCTGGGTCCCATCGGTAAAT
mSdhb Rvs	GCCGTTCTCGGCAGAGTC
mSIRT1 Fwd	GACACAGAGACGGCTGGAAC
mSIRT1 Rvs	CAGACCCTCAAGCCATGTTT
mSIRT2 Fwd	CCGCGGGTATCCCTGACT
mSIRT2 Rvs	GGTACTTCTCCAGGTTTGCATAGAG
mSIRT3 Fwd	GGTTTCACAACGCCAGTACA
mSIRT3 Rvs	CAGCTACATGCACGGTCTGT
mSIRT6 Fwd	ACCTGCCCCTTGCCACTAA
mSIRT6 Rvs	TGGGTTGCAGGTTGACAATG
mSOCS2 Fwd	CGCGTCTGGCGAAAGC
mSOCS2 Rvs	TTCATTAACAGTCATACTTCCCCAGTA
mSOCS3 Fwd	AACTTGCTGTGGGTGACCAT
mSOCS3 Rvs	AAGGCCGGAGATTTCGCT
mSOD1 Fwd	TTTTTTGCGCGGTCCTTTC
mSOD1 Rvs	GACCAGAGAGAGCAAGACGAGAAG
mSOD2 Fwd	TCACTCACGGCCACATTGAG
mSOD2 Rvs	CAGTCATAGTGCTGCAATGCTCTA
mSOD3 Fwd	CATGCAATCTGCAGGGTACAA
mSOD3 Rvs	AGAACCAAGCCGGTGATCTG
mSrxn1 Fwd	GCATCCACACCAGACTTGCA
mSrxn1 Rvs	CCGGGTAGTGGTGCTGATGT
mt-CO1 Fwd	TGCTAGCCGCAGGCATTAC
mt-CO1 Rvs	GGGTGCCCAAAGAATCAGAAC
mUqcrc2 Fwd	GCGCTTCACTCTCAGGTCAAA
mUqcrc2 Rvs	CCAGCCACTTGCTTGATGCT

Appendix VI: List of antibodies used for immunoblotting and immunoprecipitation

Antibody	Vendor	Dilution	Antibody dilution Buffer
Acetylated tubulin (K40)	Cell Signaling Technology (MA, USA)	1:1000	5% BSA/TBST
Akt	Cell Signaling Technology (MA, USA)	1:1000	5% BSA/TBST
Akt2	Cell Signaling Technology (MA, USA)	1:1000	5% BSA/TBST
ASCL3	Santa Cruz (CA, USA)	1:1000	5% BSA/TBST
Bmi1	Cell Signaling Technology (MA, USA)	1:1000	5% BSA/TBST
Catalase	Cell Signaling Technology (MA, USA)	1:1000	5% BSA/TBST
CDK4	Cell Signaling Technology (MA, USA)	1:2000	5% Skim milk/TBST
CIS	Cell Signaling Technology (MA, USA)	1:1000 WB 1:100 IP	5% BSA/TBST
Cox IV	Cell Signaling Technology (MA, USA)	1:1000	5% BSA/TBST
Cytochrome C	Abcam Inc (MA, USA)	1:1000	5% Skim milk/TBST
E-cadherin	Cell Signaling Technology (MA, USA)	1:1000	5% BSA/TBST
EGFR	Cell Signaling Technology (MA, USA)	1:1000	5% BSA/TBST
eNOS	Cell Signaling Technology (MA, USA)	1:1000	5% BSA/TBST
ERK1/2	Santa Cruz (CA, USA)	1:1000	5% BSA/TBST
FGF21	Abcam Inc (MA, USA)	1:1000	5% BSA/TBST
GAPDH	Cell Signaling Technology (MA, USA)	1:1000	5% BSA/TBST
GCN5	Abcam Inc (MA, USA)	1:1000	5% BSA/TBST
GFP	Abcam Inc (MA, USA)	1:2000	5% BSA/TBST
GH1/2	Santa Cruz (CA, USA)	1:500	5% BSA/TBST
Haemagglutinin (HA) antibody	Covance (NJ, USA)	1:1000 WB 1:100 IP	5% Skim milk/TBST
HNF4A	Santa Cruz (CA, USA)	1:1000	5% BSA/TBST
IGF-1R	Santa Cruz (CA, USA)	1:1000	5% BSA/TBST
IL-1RA	Abcam Inc (MA, USA)	1:5000	5% BSA/TBST
IRS1	Santa Cruz (CA, USA)	1:1000	5% BSA/TBST
IRβ	Santa Cruz (CA, USA)	1:1000	5% BSA/TBST
Jak2	Cell Signaling Technology (MA, USA)	1:1000 WB 1:100 IP	5% BSA/TBST
Lyn	Cell Signaling Technology (MA, USA)	1:1000 WB 1:50 IP	5% BSA/TBST
mTFAM	Abcam Inc (MA, USA)	1:500	5% BSA/TBST
Myc-tag	Cell Signaling Technology (MA, USA)	1:1000 WB 1:100 IP	5% BSA/TBST
NF-κB p65	Cell Signaling Technology (MA, USA)	1:1000	5% BSA/TBST
Nox4	Santa Cruz (CA, USA)	1:500	5% BSA/TBST
Nrf1	Cell Signaling Technology	1:1000	5% BSA/TBST

	(MA, USA)		
Nrf2	Cell Signaling Technology (MA, USA)	1:1000	5% BSA/TBST
OxPhos cocktail	Abcam Inc (MA, USA)	1:2000	5% Skim milk/TBST
P-Akt (Ser473)	Cell Signaling Technology (MA, USA)	1:1000	5% BSA/TBST
P-Akt (Thr308)	Cell Signaling Technology (MA, USA)	1:1000	5% BSA/TBST
P-AMPK (Thr172)	Cell Signaling Technology (MA, USA)	1:1000	5% BSA/TBST
P-ERK p42/p44 (Thr202/Tyr204)	Cell Signaling Technology (MA, USA)	1:1000	5% BSA/TBST
P-Jak2 (Tyr1007/1008)	Cell Signaling Technology (MA, USA)	1:1000	5% BSA/TBST5
P-p38 (Thr180/Tyr182)	Cell Signaling Technology (MA, USA)	1:1000	5% BSA/TBST
P-Src (Tyr416)	Cell Signaling Technology (MA, USA)	1:1000	5% BSA/TBST
P-STAT3 (Tyr705)	Cell Signaling Technology (MA, USA)	1:1000	5% Skim milk/TBST
P-STAT5 (Tyr694)	Cell Signaling Technology (MA, USA)	1:1000	5% BSA/TBST
p21	Cell Signaling Technology (MA, USA)	1:1000	5% BSA/TBST
p38	Cell Signaling Technology (MA, USA)	1:1000	5% BSA/TBST
PGC1	Abcam Inc (MA, USA)	1:1000	5% BSA/TBST
PTEN	Cell Signaling Technology (MA, USA)	1:2000	5% BSA/TBST
PTP1B	Abcam Inc (MA, USA)	1:1000	5% BSA/TBST
Sdha	Cell Signaling Technology (MA, USA)	1:2500	5% BSA/TBST
Sirt1	Cell Signaling Technology (MA, USA)	1:1000	5% BSA/TBST
Sirt2	Cell Signaling Technology (MA, USA)	1:1000	5% BSA/TBST
Sirt3	Cell Signaling Technology (MA, USA)	1:1000	5% BSA/TBST
Sirt6	Cell Signaling Technology (MA, USA)	1:1000	5% BSA/TBST
SOCS2	Cell Signaling Technology (MA, USA)	1:1000 WB 1:100 IP	5% BSA/TBST
SOCS3	Santa Cruz (CA, USA)	1:1000	5% BSA/TBST
SOD1	Abcam Inc (MA, USA)	1:10000	5% BSA/TBST
SOD2	Abcam Inc (MA, USA)	1:10000	5% BSA/TBST
Srnx1	Santa Cruz (CA, USA)	1:1000	5% BSA/TBST
STAT3	Cell Signaling Technology (MA, USA)	1:1000	5% BSA/TBST
STAT5	Santa Cruz (CA, USA)	1:5000	5% BSA/TBST
Trx1	Cell Signaling Technology (MA, USA)	1:1000	5% BSA/TBST
UCP-1	Abcam Inc (MA, USA)	1:1000	5% BSA/TBST
Vimentin	Cell Signaling Technology (MA, USA)	1:1000	5% BSA/TBST
β-tubulin	Cell Signaling Technology (MA, USA)	1:1000	5% Skim milk/TBST

Sheep Horseradish peroxidase-conjugated anti-goat IgG	Santa Cruz (CA, USA)	1:10000	5% BSA/TBST
Donkey Horseradish peroxidase-conjugated anti-mouse IgG	GE Healthcare Life Sciences (Dusseldorf, Germany)	1:10000	5% Skim milk/TBST
Donkey Horseradish peroxidase-conjugated anti-rabbit IgG	Santa Cruz (CA, USA)	1:10000	5% BSA/TBST

Appendix VII: Gene expression analysis of key GH/IGF-1 axis molecules in cancerous and normal tissues

Figure S.1. Expression of *GHR (A), PRLR* (B), *GH1* (C), *GH2* (D), *PRL* (E), IGF- 1 (F) and IGF-1R (G) from Cancer Cell Line Encyclopedia (CCLE).

CCLE *GHR* mRNA expression levels from 947 cell lines in 36 tumour classifications. Expression levels are represented as box-and-whisker plots with median expression level indicated by a line, the inter-quartile range by a box, and bars represent 1.5x the inter-quartile range. The number of samples for each cancer type (n) is shown in parentheses. Gene expression data was extracted from CCLE_Expression_Entrez_2012-10-18.res and is presented as gene-centric Robust Multi-array Average-normalised mRNA expression levels. This data was extracted from the publicly accessible CCLE database (Barretina et al, 2012).

A

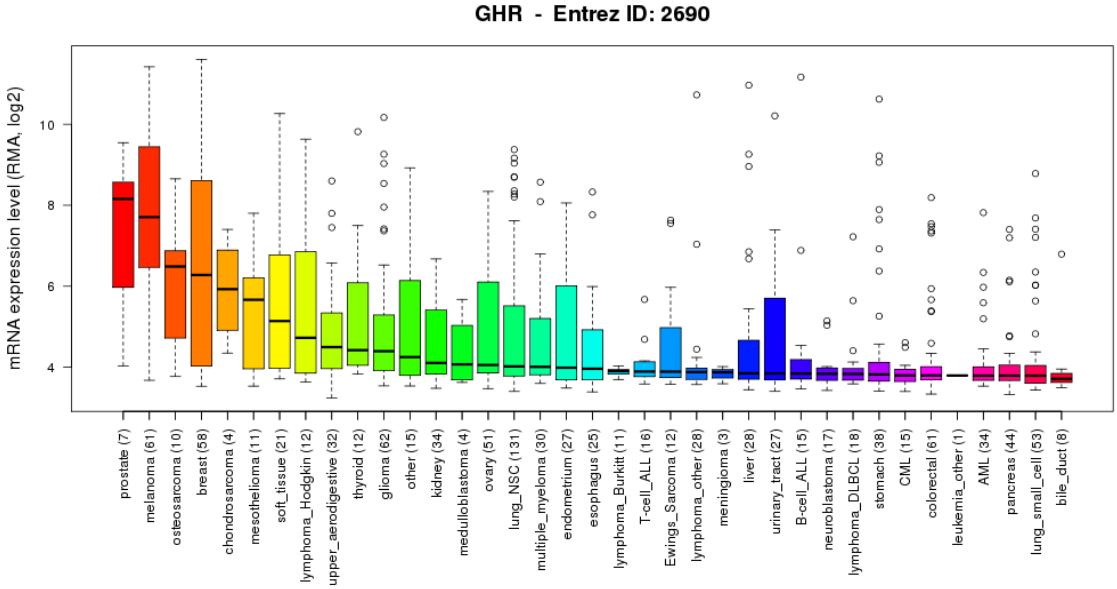

B

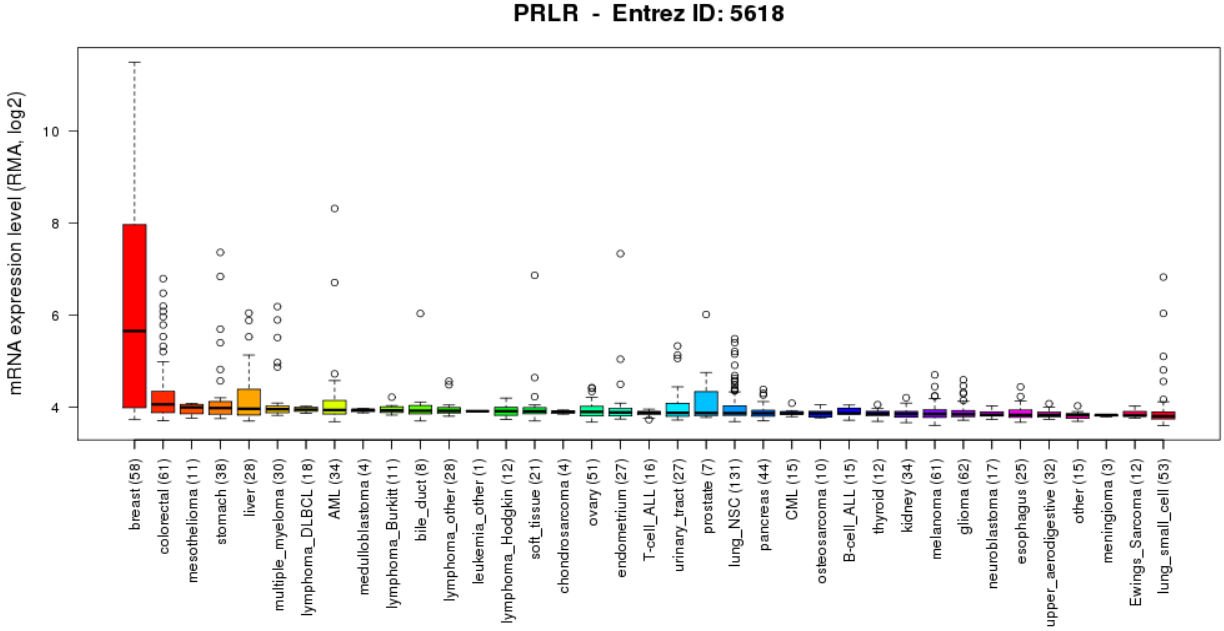

C

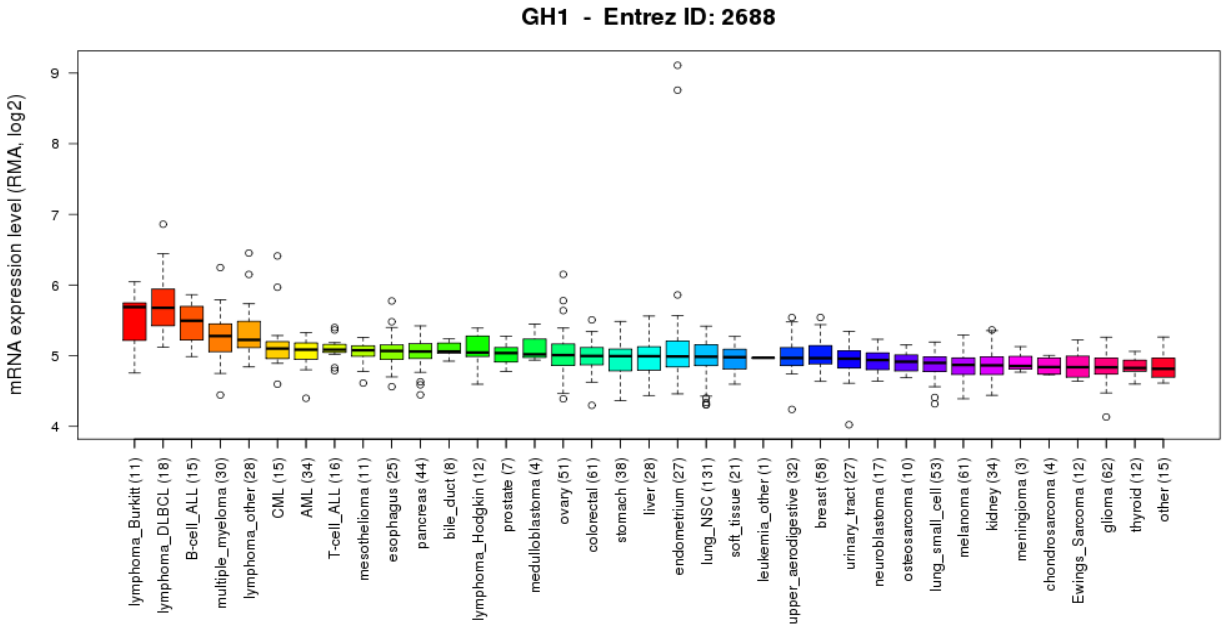
GH1 - Entrez ID: 2688
mRNA expression level (RMA, log2)
9
8
7
6
5
4
lymphoma_Burkitt (11)
lymphoma_DLBCL (18)
B-cell_ALL (15)
multiple_myeloma (30)
lymphoma_other (28)
CML (15)
AML (34)
T-cell_ALL (16)
mesothelioma (11)
esophagus (25)
pancreas (44)
bile_duct (8)
lymphoma_Hodgkin (12)
prostate (7)
medulloblastoma (4)
ovary (51)
colorectal (61)
stomach (38)
liver (28)
endometrium (27)
lung_NSC (131)
soft_tissue (21)
leukemia_other (1)
upper_aerodigestive (32)
breast (58)
urinary_tract (27)
neuroblastoma (17)
osteosarcoma (10)
lung_small_cell (53)
melanoma (61)
kidney (34)
meningioma (3)
chondrosarcoma (4)
Ewings_Sarcoma (12)
glioma (62)
thyroid (12)
other (15)

D

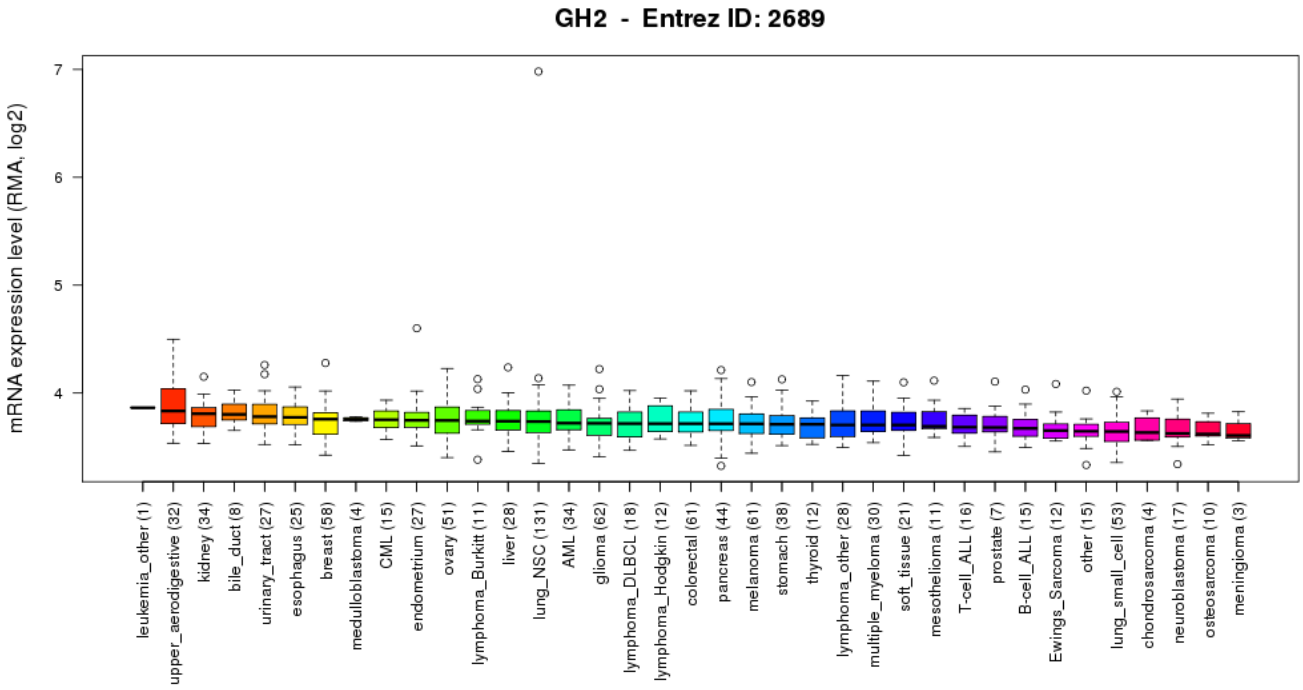
GH2 - Entrez ID: 2689
mRNA expression level (RMA, log2)
7
6
5
4
leukemia_other (1)
upper_aerodigestive (32)
kidney (34)
bile_duct (8)
urinary_tract (27)
esophagus (25)
breast (58)
medulloblastoma (4)
CML (15)
endometrium (27)
ovary (51)
lymphoma_Burkitt (11)
liver (28)
lung_NSC (131)
AML (34)
glioma (62)
lymphoma_DLBCL (18)
lymphoma_Hodgkin (12)
colorectal (61)
pancreas (44)
melanoma (61)
stomach (38)
thyroid (12)
lymphoma_other (28)
multiple_myeloma (30)
soft_tissue (21)
mesothelioma (11)
T-cell_ALL (16)
prostate (7)
B-cell_ALL (15)
Ewings_Sarcoma (12)
other (15)
lung_small_cell (53)
chondrosarcoma (4)
neuroblastoma (17)
osteosarcoma (10)
meningioma (3)

E

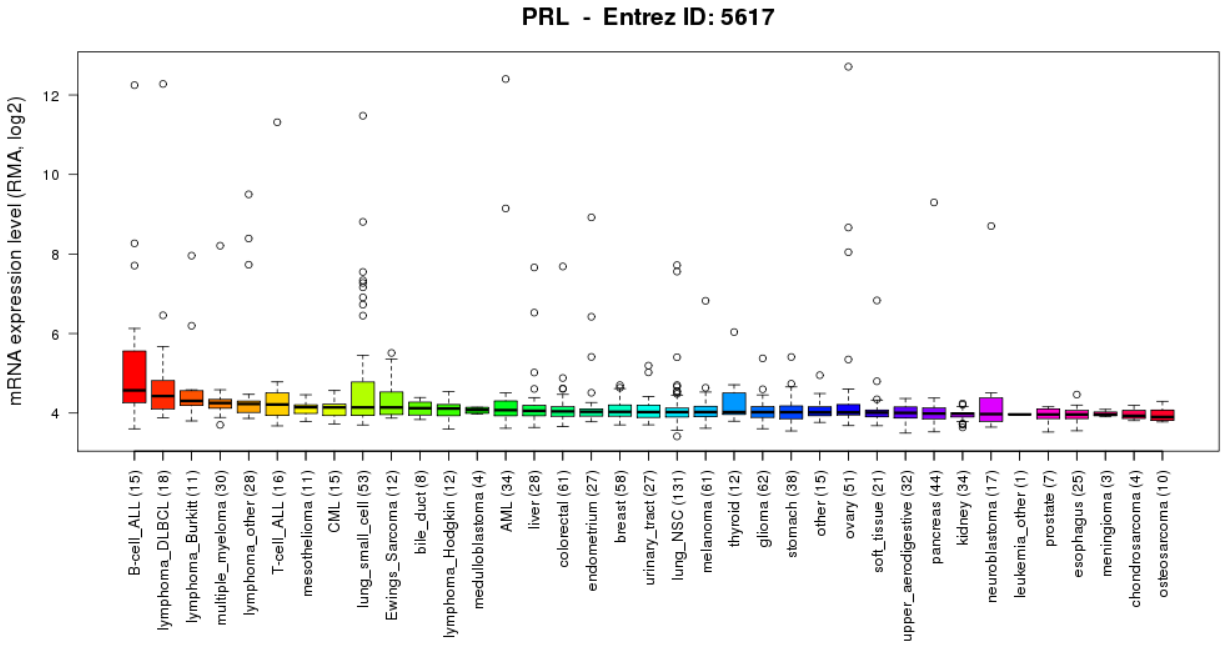
PRL - Entrez ID: 5617
mRNA expression level (RMA, log2)
B-cell_ALL (15)
lymphoma_DLBCL (18)
lymphoma_Burkitt (11)
multiple_myeloma (30)
lymphoma_other (28)
T-cell_ALL (16)
mesothelioma (11)
CML (15)
lung_small_cell (53)
Ewings_Sarcoma (12)
bile_duct (8)
lymphoma_Hodgkin (12)
medulloblastoma (4)
AML (34)
liver (28)
colorectal (61)
endometrium (27)
breast (58)
urinary_tract (27)
lung_NSC (131)
melanoma (61)
thyroid (12)
glioma (62)
stomach (38)
other (15)
ovary (51)
soft_tissue (21)
upper_aerodigestive (32)
pancreas (44)
kidney (34)
neuroblastoma (17)
leukemia_other (1)
prostate (7)
esophagus (25)
meningioma (3)
chondrosarcoma (4)
osteosarcoma (10)

F

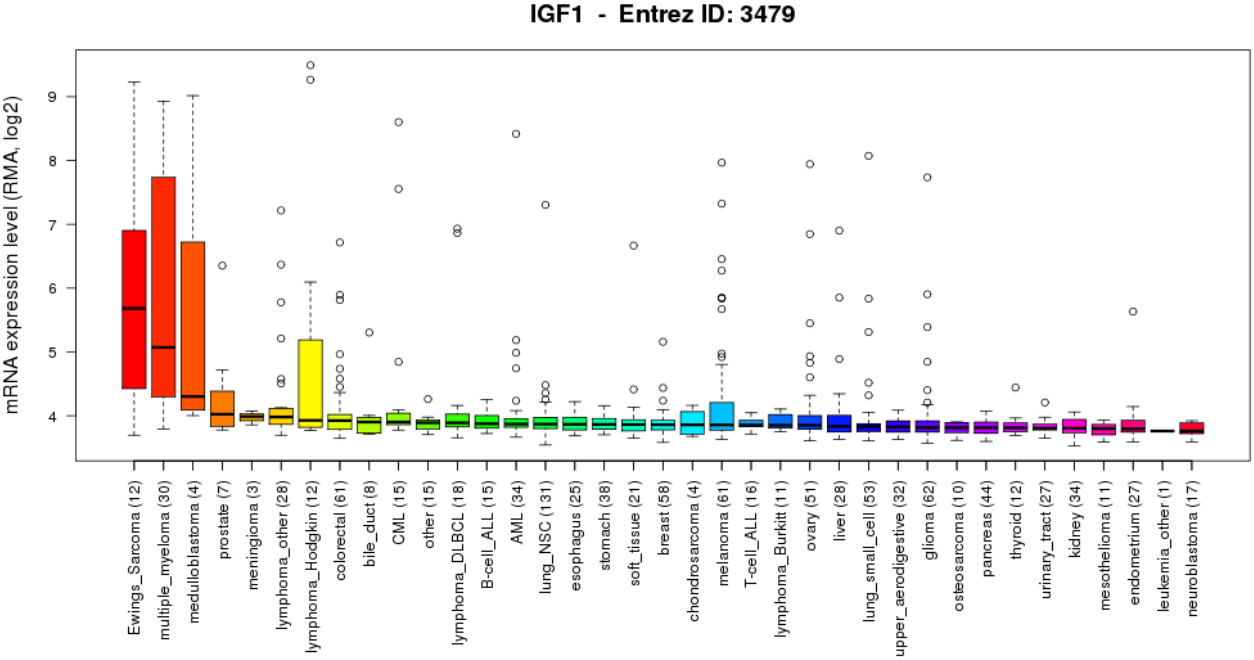
IGF1 - Entrez ID: 3479
mRNA expression level (RMA, log2)
Ewings_Sarcoma (12)
multiple_myeloma (30)
medulloblastoma (4)
prostate (7)
meningioma (3)
lymphoma_other (28)
lymphoma_Hodgkin (12)
colorectal (61)
bile_duct (8)
CML (15)
other (15)
lymphoma_DLBCL (18)
B-cell_ALL (15)
AML (34)
lung_NSC (131)
esophagus (25)
stomach (38)
soft_tissue (21)
breast (58)
chondrosarcoma (4)
melanoma (61)
T-cell_ALL (16)
lymphoma_Burkitt (11)
ovary (51)
liver (28)
lung_small_cell (53)
upper_aerodigestive (32)
glioma (62)
osteosarcoma (10)
pancreas (44)
thyroid (12)
urinary_tract (27)
kidney (34)
mesothelioma (11)
endometrium (27)
leukemia_other (1)
neuroblastoma (17)

G

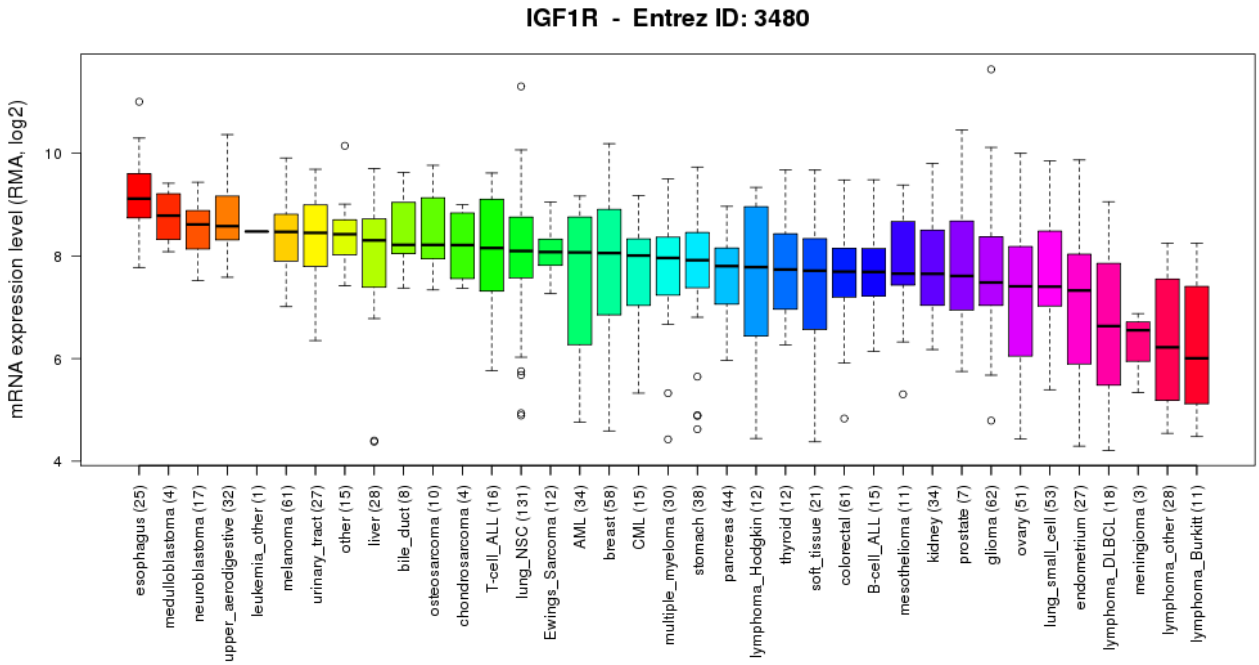

Figure S.2. Expression of *GHR (A), PRLR* (B), *GH1* (C), *GH2* (D), *PRL* (E), IGF-1 (F) and IGF-1R (G) from Genotype-Tissue Expression (GTEx) database (Consortium, 2013).

A

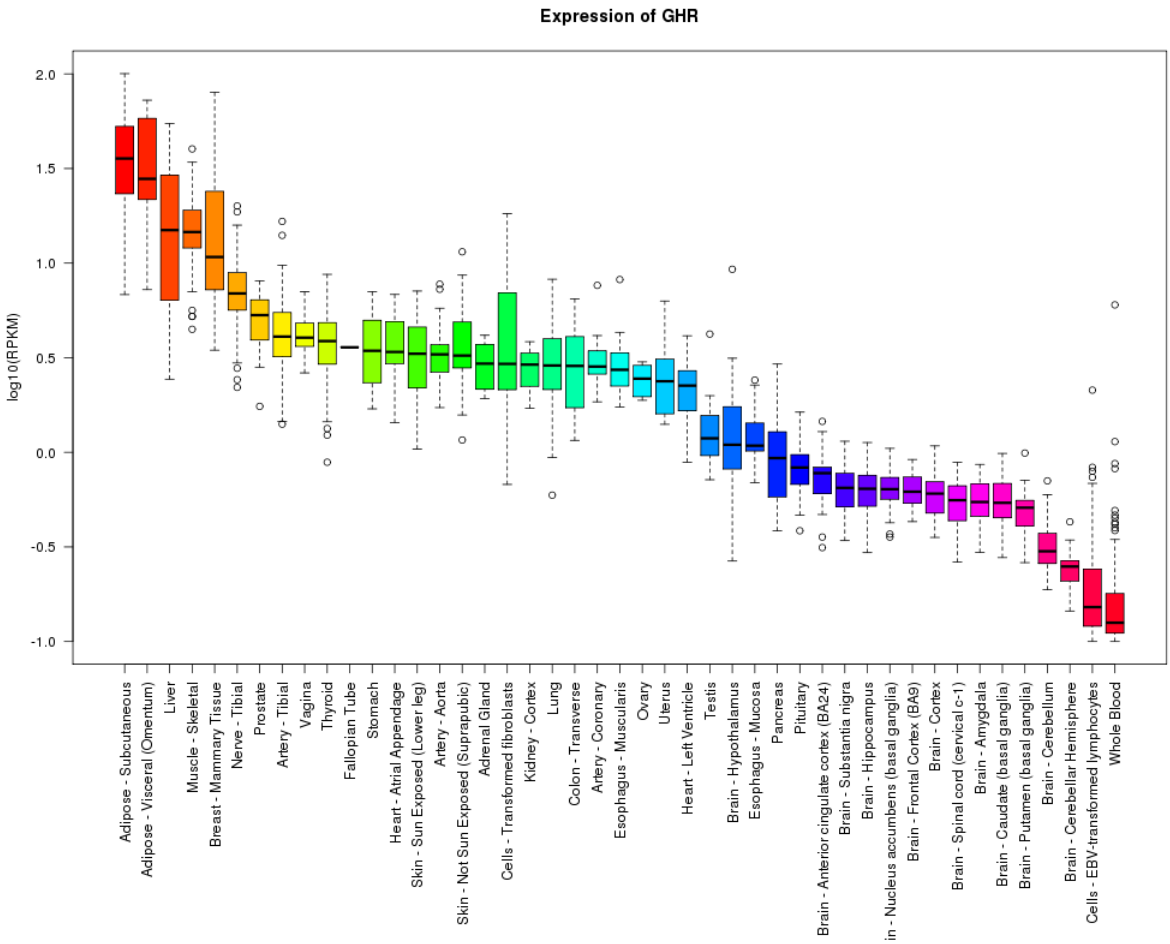
Expression of GHR
log10(RPKM)
2.0
1.5
1.0
0.5
0.0
-0.5
-1.0
Adipose - Subcutaneous
Adipose - Visceral (Omentum)
Liver
Muscle - Skeletal
Breast - Mammary Tissue
Nerve - Tibial
Prostate
Artery - Tibial
Vagina
Thyroid
Fallopian Tube
Stomach
Heart - Atrial Appendage
Skin - Sun Exposed (Lower leg)
Artery - Aorta
Skin - Not Sun Exposed (Suprapubic)
Adrenal Gland
Cells - Transformed fibroblasts
Kidney - Cortex
Lung
Colon - Transverse
Artery - Coronary
Esophagus - Muscularis
Ovary
Uterus
Heart - Left Ventricle
Testis
Brain - Hypothalamus
Esophagus - Mucosa
Pancreas
Pituitary
Brain - Anterior cingulate cortex (BA24)
Brain - Substantia nigra
Brain - Hippocampus
in - Nucleus accumbens (basal ganglia)
Brain - Frontal Cortex (BA9)
Brain - Cortex
Brain - Spinal cord (cervical c-1)
Brain - Amygdala
Brain - Caudate (basal ganglia)
Brain - Putamen (basal ganglia)
Brain - Cerebellum
Brain - Cerebellar Hemisphere
Cells - EBV-transformed lymphocytes
Whole Blood

B

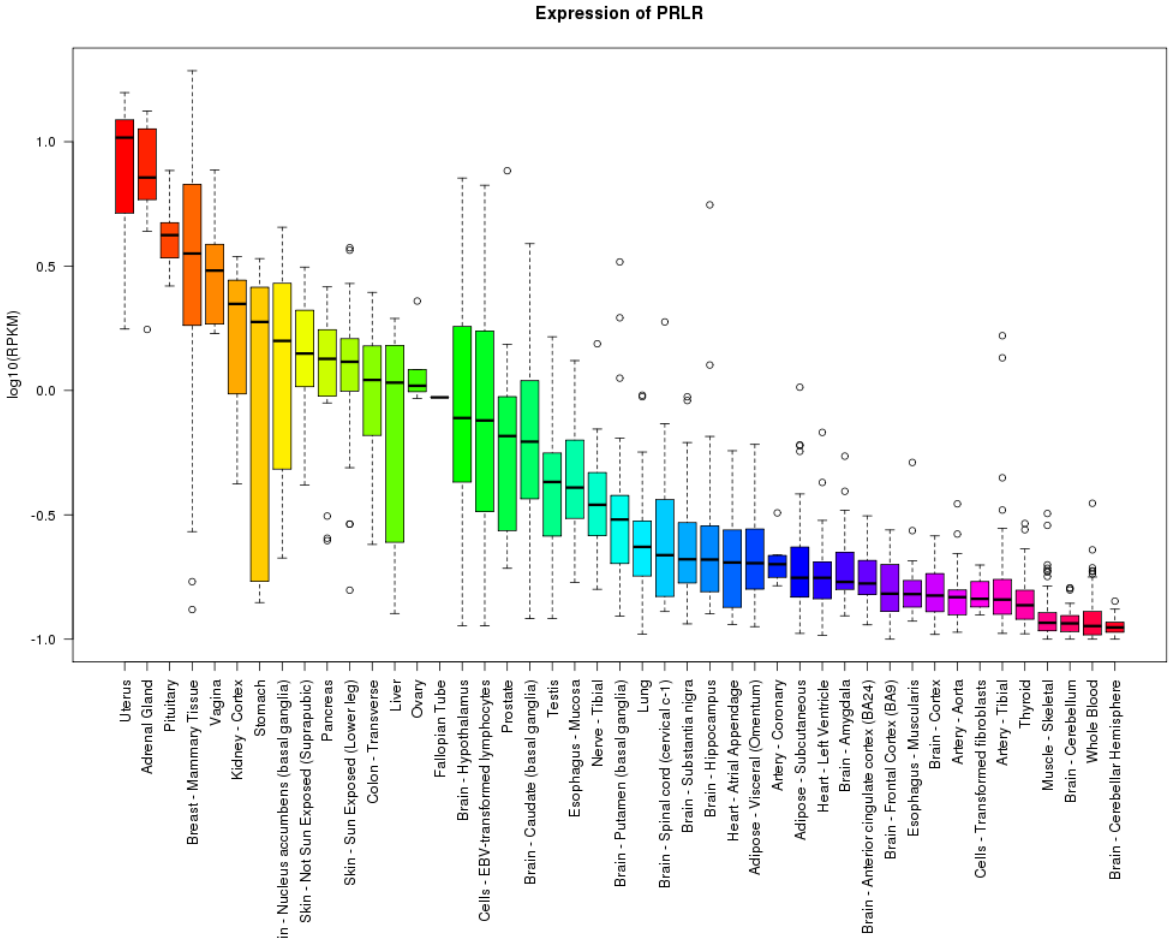
Expression of PRLR
log10(RPKM)
1.0
0.5
0.0
-0.5
-1.0
Uterus
Adrenal Gland
Pituitary
Breast - Mammary Tissue
Vagina
Kidney - Cortex
Stomach
in - Nucleus accumbens (basal ganglia)
Skin - Not Sun Exposed (Suprapubic)
Pancreas
Skin - Sun Exposed (Lower leg)
Colon - Transverse
Liver
Ovary
Fallopian Tube
Brain - Hypothalamus
Cells - EBV-transformed lymphocytes
Prostate
Brain - Caudate (basal ganglia)
Testis
Esophagus - Mucosa
Nerve - Tibial
Brain - Putamen (basal ganglia)
Lung
Brain - Spinal cord (cervical c-1)
Brain - Substantia nigra
Brain - Hippocampus
Heart - Atrial Appendage
Adipose - Visceral (Omentum)
Artery - Coronary
Adipose - Subcutaneous
Heart - Left Ventricle
Brain - Amygdala
Brain - Anterior cingulate cortex (BA24)
Brain - Frontal Cortex (BA9)
Esophagus - Muscularis
Brain - Cortex
Artery - Aorta
Cells - Transformed fibroblasts
Artery - Tibial
Thyroid
Muscle - Skeletal
Brain - Cerebellum
Whole Blood
Brain - Cerebellar Hemisphere

C

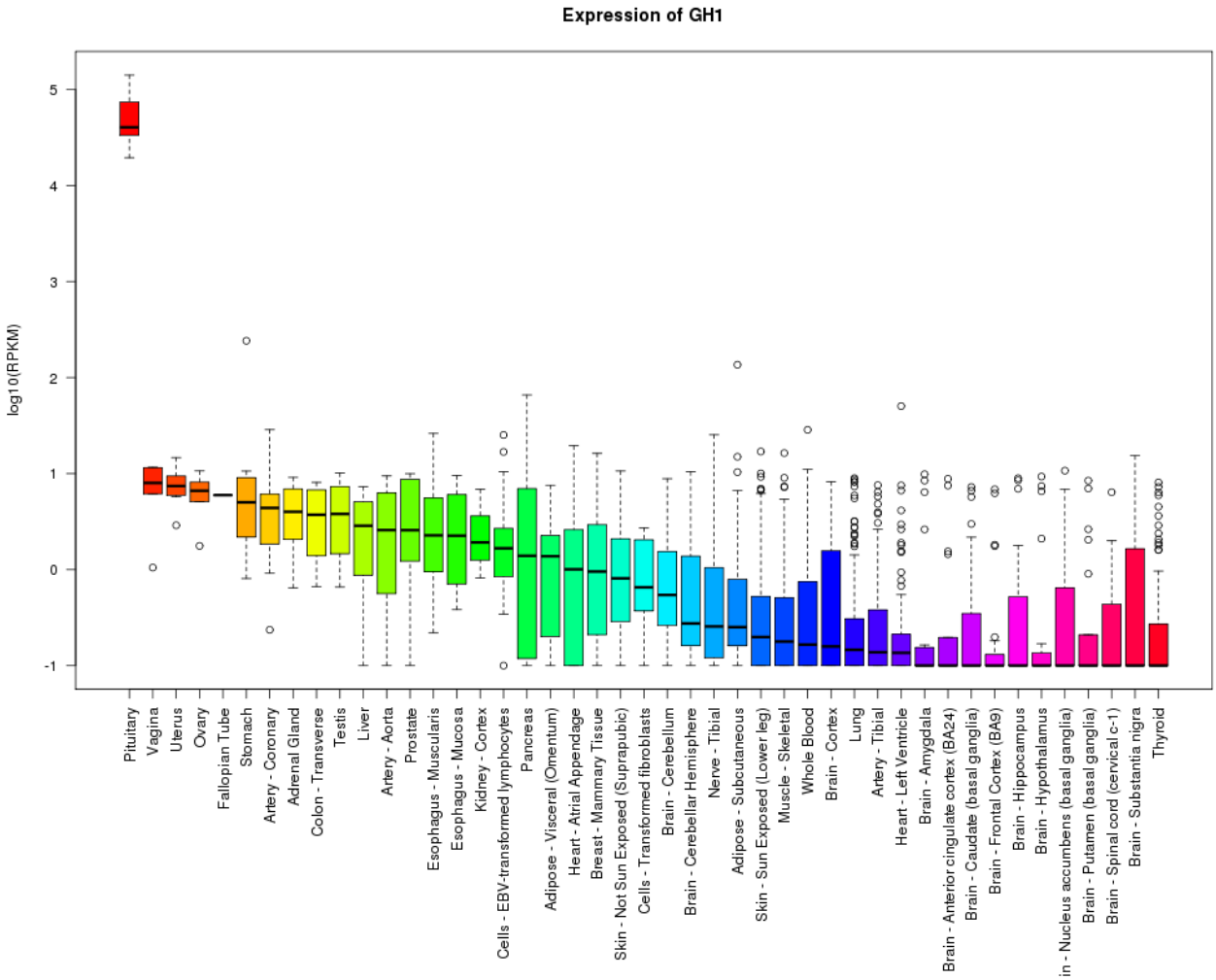
Expression of GH1
log10(RPKM)
5
4
3
2
1
0
-1
Pituitary
Vagina
Uterus
Ovary
Fallopian Tube
Stomach
Artery - Coronary
Adrenal Gland
Colon - Transverse
Testis
Liver
Artery - Aorta
Prostate
Esophagus - Muscularis
Esophagus - Mucosa
Kidney - Cortex
Cells - EBV-transformed lymphocytes
Pancreas
Adipose - Visceral (Omentum)
Heart - Atrial Appendage
Breast - Mammary Tissue
Skin - Not Sun Exposed (Suprapubic)
Cells - Transformed fibroblasts
Brain - Cerebellum
Brain - Cerebellar Hemisphere
Nerve - Tibial
Adipose - Subcutaneous
Skin - Sun Exposed (Lower leg)
Muscle - Skeletal
Whole Blood
Brain - Cortex
Lung
Artery - Tibial
Heart - Left Ventricle
Brain - Amygdala
Brain - Anterior cingulate cortex (BA24)
Brain - Caudate (basal ganglia)
Brain - Frontal Cortex (BA9)
Brain - Hippocampus
Brain - Hypothalamus
in - Nucleus accumbens (basal ganglia)
Brain - Putamen (basal ganglia)
Brain - Spinal cord (cervical c-1)
Brain - Substantia nigra
Thyroid

D

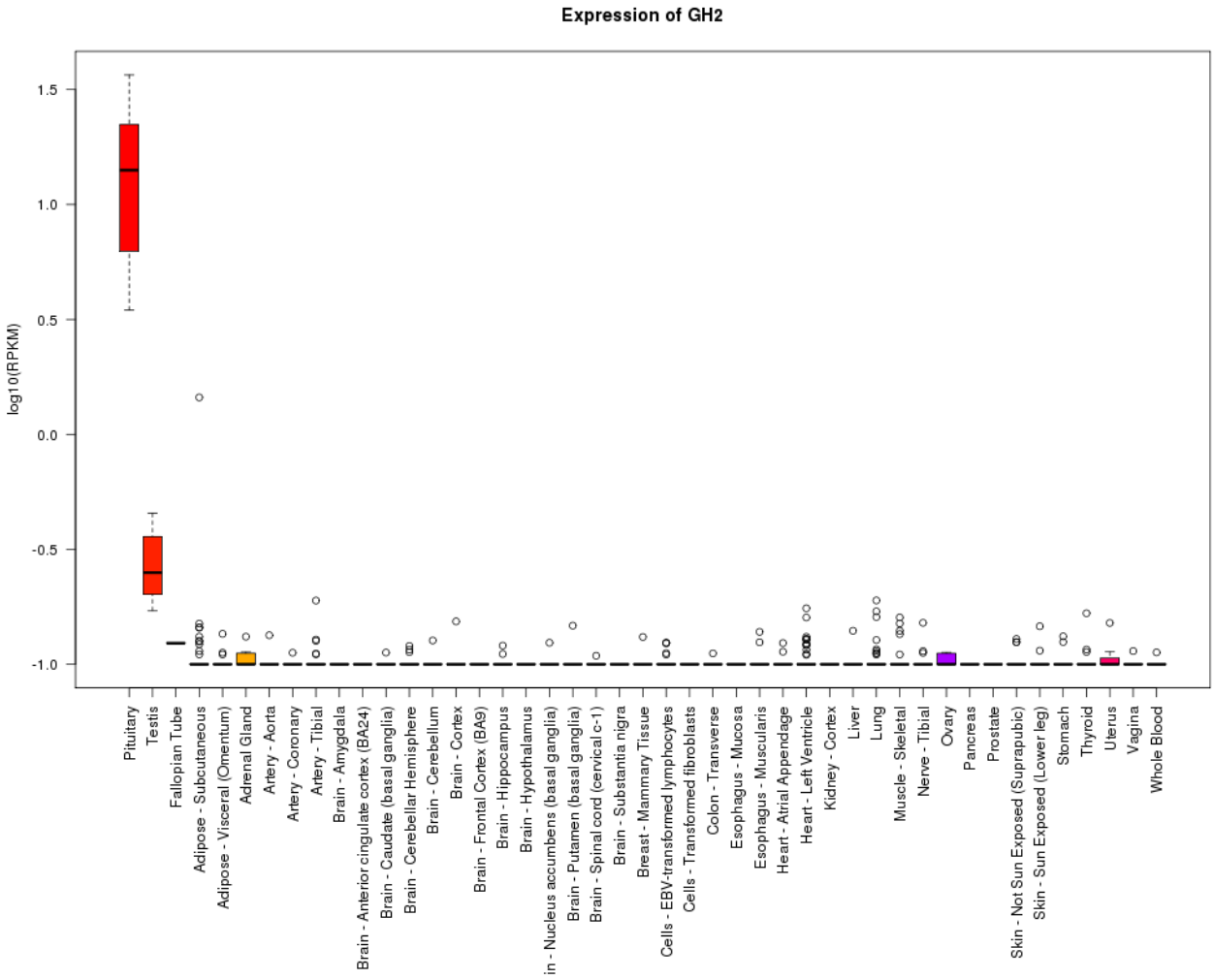
Expression of GH2
log10(RPKM)
1.5
1.0
0.5
0.0
-0.5
-1.0
Pituitary
Testis
Fallopian Tube
Adipose - Subcutaneous
Adipose - Visceral (Omentum)
Adrenal Gland
Artery - Aorta
Artery - Coronary
Artery - Tibial
Brain - Amygdala
Brain - Anterior cingulate cortex (BA24)
Brain - Caudate (basal ganglia)
Brain - Cerebellar Hemisphere
Brain - Cerebellum
Brain - Cortex
Brain - Frontal Cortex (BA9)
Brain - Hippocampus
Brain - Hypothalamus
in - Nucleus accumbens (basal ganglia)
Brain - Putamen (basal ganglia)
Brain - Spinal cord (cervical c-1)
Brain - Substantia nigra
Breast - Mammary Tissue
Cells - EBV-transformed lymphocytes
Cells - Transformed fibroblasts
Colon - Transverse
Esophagus - Mucosa
Esophagus - Muscularis
Heart - Atrial Appendage
Heart - Left Ventricle
Kidney - Cortex
Liver
Lung
Muscle - Skeletal
Nerve - Tibial
Ovary
Pancreas
Prostate
Skin - Not Sun Exposed (Suprapubic)
Skin - Sun Exposed (Lower leg)
Stomach
Thyroid
Uterus
Vagina
Whole Blood

E

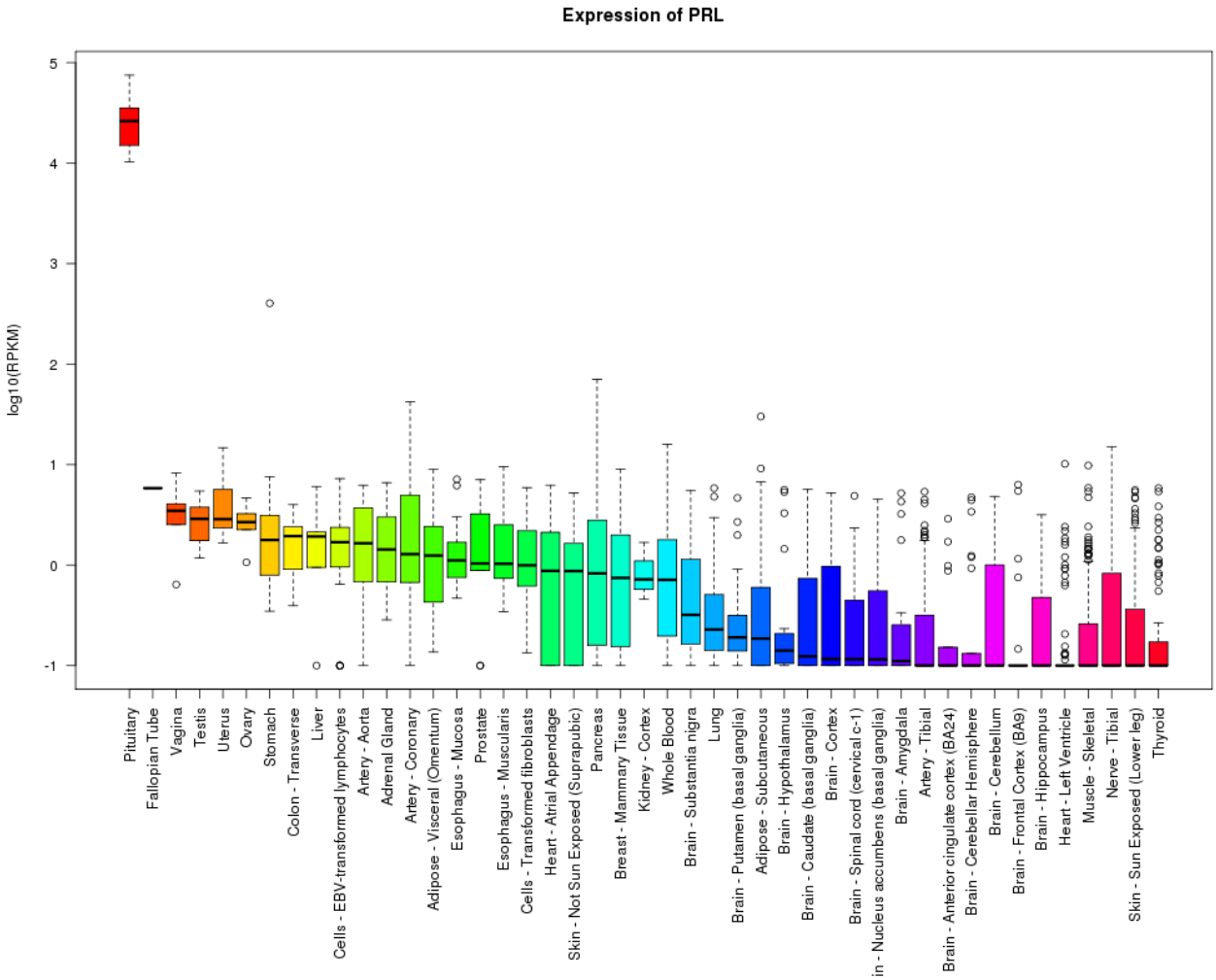
Expression of PRL
log10(RPKM)
5
4
3
2
1
0
-1
Pituitary
Fallopian Tube
Vagina
Testis
Uterus
Ovary
Stomach
Colon - Transverse
Liver
Cells - EBV-transformed lymphocytes
Artery - Aorta
Adrenal Gland
Artery - Coronary
Adipose - Visceral (Omentum)
Esophagus - Mucosa
Prostate
Esophagus - Muscularis
Cells - Transformed fibroblasts
Heart - Atrial Appendage
Skin - Not Sun Exposed (Suprapubic)
Pancreas
Breast - Mammary Tissue
Kidney - Cortex
Whole Blood
Brain - Substantia nigra
Lung
Brain - Putamen (basal ganglia)
Adipose - Subcutaneous
Brain - Hypothalamus
Brain - Caudate (basal ganglia)
Brain - Cortex
Brain - Spinal cord (cervical c-1)
in - Nucleus accumbens (basal ganglia)
Brain - Amygdala
Artery - Tibial
Brain - Anterior cingulate cortex (BA24)
Brain - Cerebellar Hemisphere
Brain - Cerebellum
Brain - Frontal Cortex (BA9)
Brain - Hippocampus
Heart - Left Ventricle
Muscle - Skeletal
Nerve - Tibial
Skin - Sun Exposed (Lower leg)
Thyroid

F

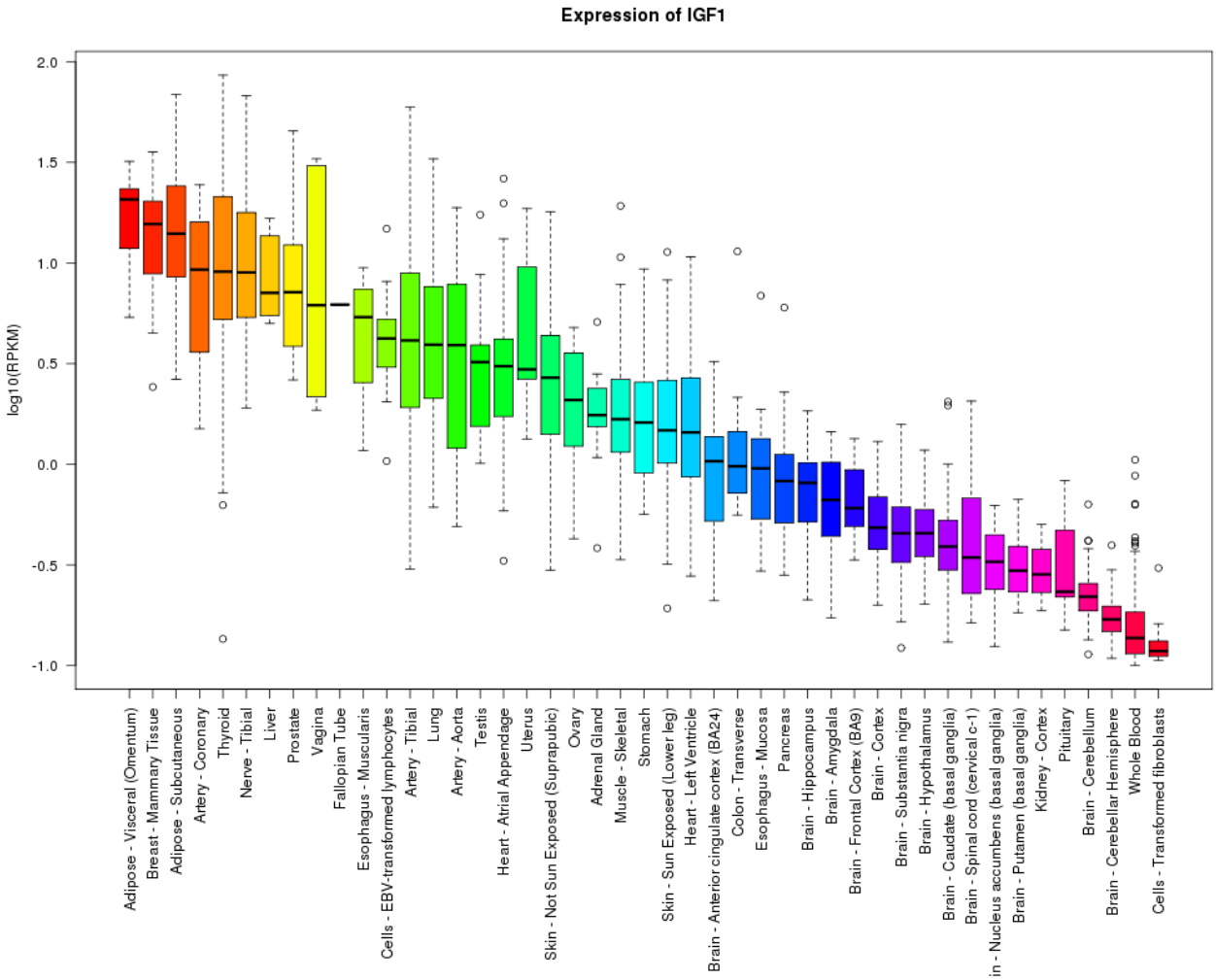
Expression of IGF1
log10(RPKM)
2.0
1.5
1.0
0.5
0.0
-0.5
-1.0
Adipose - Visceral (Omentum)
Breast - Mammary Tissue
Adipose - Subcutaneous
Artery - Coronary
Thyroid
Nerve - Tibial
Liver
Prostate
Vagina
Fallopian Tube
Esophagus - Muscularis
Cells - EBV-transformed lymphocytes
Artery - Tibial
Lung
Artery - Aorta
Testis
Heart - Atrial Appendage
Uterus
Skin - Not Sun Exposed (Suprapubic)
Ovary
Adrenal Gland
Muscle - Skeletal
Stomach
Skin - Sun Exposed (Lower leg)
Heart - Left Ventricle
Brain - Anterior cingulate cortex (BA24)
Colon - Transverse
Esophagus - Mucosa
Pancreas
Brain - Hippocampus
Brain - Amygdala
Brain - Frontal Cortex (BA9)
Brain - Cortex
Brain - Substantia nigra
Brain - Hypothalamus
Brain - Caudate (basal ganglia)
Brain - Spinal cord (cervical c-1)
in - Nucleus accumbens (basal ganglia)
Brain - Putamen (basal ganglia)
Kidney - Cortex
Pituitary
Brain - Cerebellum
Brain - Cerebellar Hemisphere
Whole Blood
Cells - Transformed fibroblasts

G

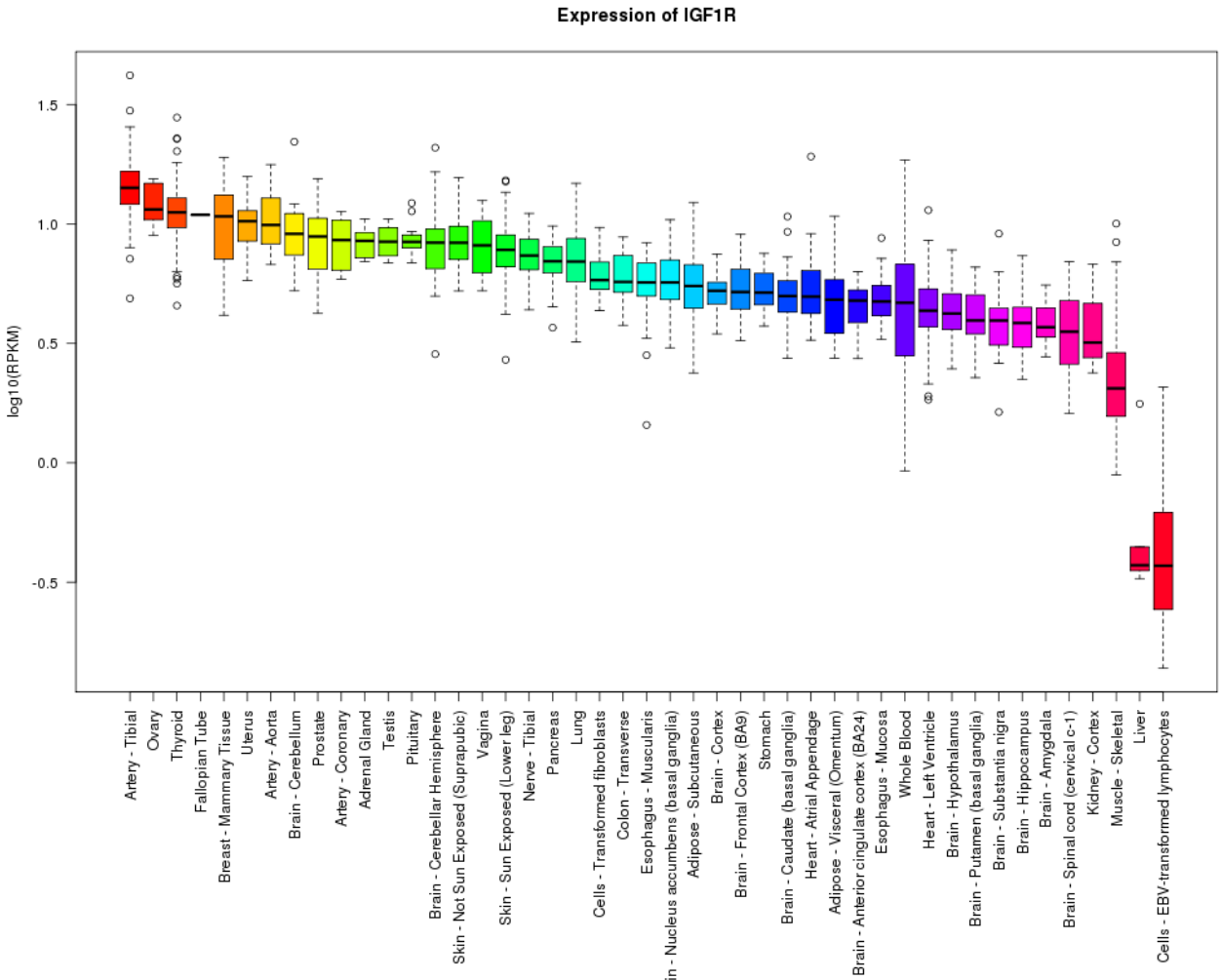
Expression of IGF1R
log10(RPKM)
1.5
1.0
0.5
0.0
-0.5
Artery - Tibial
Ovary
Thyroid
Fallopian Tube
Breast - Mammary Tissue
Uterus
Artery - Aorta
Brain - Cerebellum
Prostate
Artery - Coronary
Adrenal Gland
Testis
Pituitary
Brain - Cerebellar Hemisphere
Skin - Not Sun Exposed (Suprapubic)
Vagina
Skin - Sun Exposed (Lower leg)
Nerve - Tibial
Pancreas
Lung
Cells - Transformed fibroblasts
Colon - Transverse
Esophagus - Muscularis
in - Nucleus accumbens (basal ganglia)
Adipose - Subcutaneous
Brain - Cortex
Brain - Frontal Cortex (BA9)
Stomach
Brain - Caudate (basal ganglia)
Heart - Atrial Appendage
Adipose - Visceral (Omentum)
Brain - Anterior cingulate cortex (BA24)
Esophagus - Mucosa
Whole Blood
Heart - Left Ventricle
Brain - Hypothalamus
Brain - Putamen (basal ganglia)
Brain - Substantia nigra
Brain - Hippocampus
Brain - Amygdala
Brain - Spinal cord (cervical c-1)
Kidney - Cortex
Muscle - Skeletal
Liver
Cells - EBV-transformed lymphocytes

Appendix VIII: Human Growth Hormone Receptor cDNA sequence

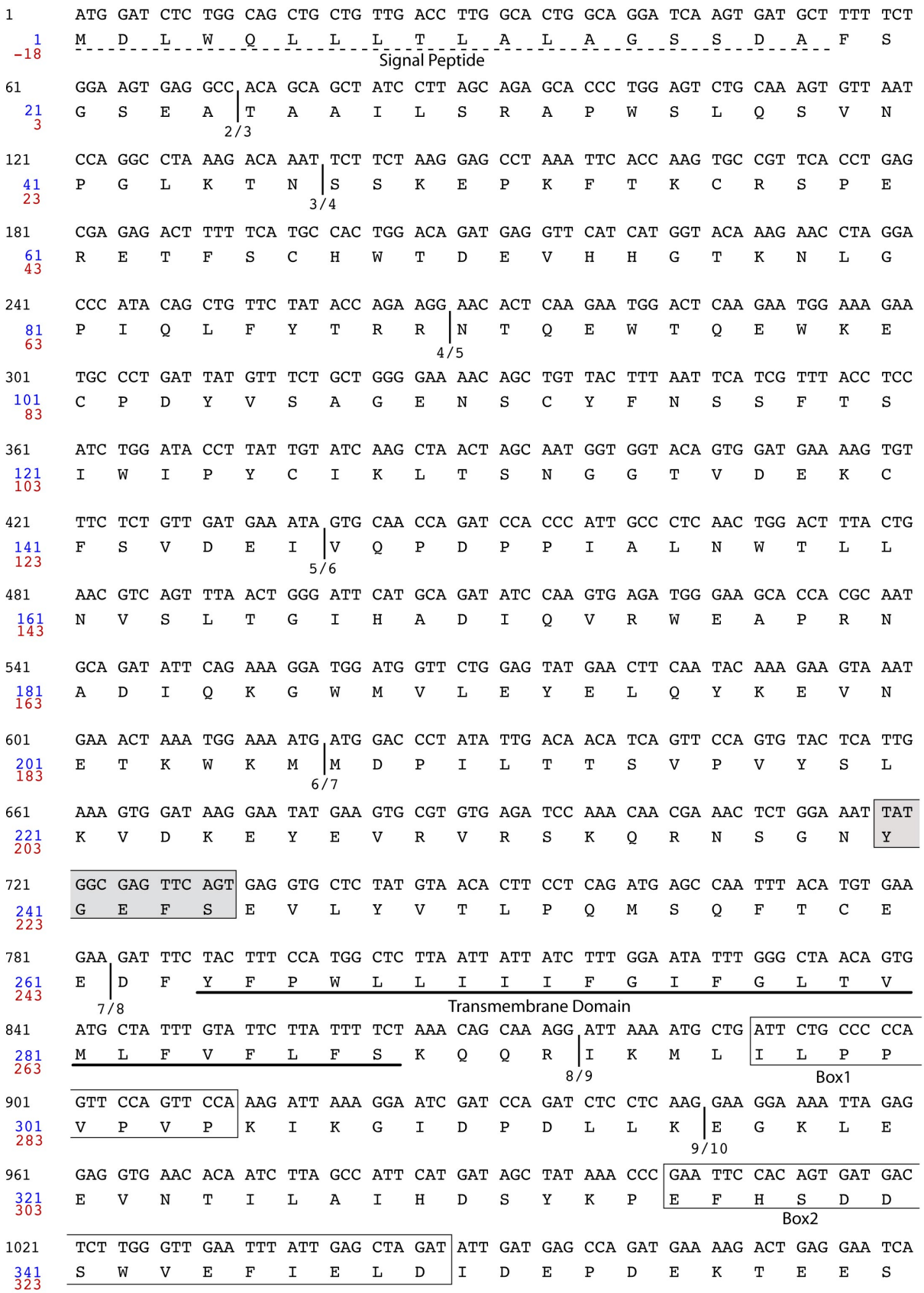

```
1081   GAC ACA GAC AGA CTT CTA AGC AGT GAC CAT GAG AAA TCA CAT AGT AAC CTA GGG GTG AAG
 361   D   T   D   R   L   L   S   S   D   H   E   K   S   H   S   N   L   G   V   K
 343

1141   GAT GGC GAC TCT GGA CGT ACC AGC TGT TGT GAA CCT GAC ATT CTG GAG ACT GAT TTC AAT
 381   D   G   D   S   G   R   T   S   C   C   E   P   D   I   L   E   T   D   F   N
 363

1201   GCC AAT GAC ATA CAT GAG GGT ACC TCA GAG GTT GCT CAG CCA CAG AGG TTA AAA GGG GAA
 401   A   N   D   I   H   E   G   T   S   E   V   A   Q   P   Q   R   L   K   G   E
 383

1261   GCA GAT CTC TTA TGC CTT GAC CAG AAG AAT CAA AAT AAC TCA CCT TAT CAT GAT GCT TGC
 421   A   D   L   L   C   L   D   Q   K   N   Q   N   N   S   P   Y   H   D   A   C
 403

1321   CCT GCT ACT CAG CAG CCC AGT GTT ATC CAA GCA GAG AAA AAC AAA CCA CAA CCA CTT CCT
 441   P   A   T   Q   Q   P   S   V   I   Q   A   E   K   N   K   P   Q   P   L   P
 423

1381   ACT GAA GGA GCT GAG TCA ACT CAC CAA GCT GCC CAT ATT CAG CTA AGC AAT CCA AGT TCA
 461   T   E   G   A   E   S   T   H   Q   A   A   H   I   Q   L   S   N   P   S   S
 443

1441   CTG TCA AAC ATC GAC TTT TAT GCC CAG GTG AGC GAC ATT ACA CCA GCA GGT AGT GTG GTC
 481   L   S   N   I   D   F   Y   A   Q   V   S   D   I   T   P   A   G   S   V   V
 463

1501   CTT TCC CCG GGC CAA AAG AAT AAG GCA GGG ATG TCC CAA TGT GAC ATG CAC CCG GAA ATG
 501   L   S   P   G   Q   K   N   K   A   G   M   S   Q   C   D   M   H   P   E   M
 483

1561   GTC TCA CTC TGC CAA GAA AAC TTC CTT ATG GAC AAT GCC TAC TTC TGT GAG GCA GAT GCC
 521   V   S   L   C   Q   E   N   F   L   M   D   N   A   Y   F   C   E   A   D   A
 503

1621   AAA AAG TGC ATC CCT GTG GCT CCT CAC ATC AAG GTT GAA TCA CAC ATA CAG CCA AGC TTA
 541   K   K   C   I   P   V   A   P   H   I   K   V   E   S   H   I   Q   P   S   L
 523

1681   AAC CAA GAG GAC ATT TAC ATC ACC ACA GAA AGC CTT ACC ACT GCT GCT GGG AGG CCT GGG
 561   N   Q   E   D   I   Y   I   T   T   E   S   L   T   T   A   A   G   R   P   G
 543

1741   ACA GGA GAA CAT GTT CCA GGT TCT GAG ATG CCT GTC CCA GAC TAT ACC TCC ATT CAT ATA
 581   T   G   E   H   V   P   G   S   E   M   P   V   P   D   Y   T   S   I   H   I
 563

1801   GTA CAG TCC CCA CAG GGC CTC ATA CTC AAT GCG ACT GCC TTG CCC TTG CCT GAC AAA GAG
 601   V   Q   S   P   Q   G   L   I   L   N   A   T   A   L   P   L   P   D   K   E
 583

1861   TTT CTC TCA TCA TGT GGC TAT GTG AGC ACA GAC CAA CTG AAC AAA ATC ATG CCT TAG
 621   F   L   S   S   C   G   Y   V   S   T   D   Q   L   N   K   I   M   P   .
 603
```

This figure outlines the nucleotide (upper line) and amino acid (lower line) sequences of the full-length hGHR. Nucleotide numbering is in black, blue numbers correspond to amino acids of the full-length transcribed protein or immature receptor (from M at the signal peptide being 1), and red numbers correspond to the mature protein (excluding 18 amino acids of the putative signal peptide sequence, M is residue number -18). Exon boundaries are indicated by arrows and numbering, eg 5/6 indicates the boundary between exon 5 and exon 6. The residues that make up the putative signal peptide are indicated by a dashed underline and the putative TMD is indicated by a solid underline. The WSxWS like motif (YGEFS in hGHR) is indicated by the grey box, and the Box1 and Box2 motifs are indicated by white boxes. Figure developed from (Waters, 1999).

Appendix IX: A new cytokine receptor activation paradigm: activation of Jak2 by GHR

Accepted manuscript comprising part of Chapter 3.

A new cytokine receptor activation paradigm: activation of JAK2 by the Growth Hormone Receptor

Authors: Andrew J. Brooks[1]*, Wei Dai[3], Megan L. O'Mara[2], Daniel Abankwa[1], Yash Chhabra[1], Rebecca A. Pelekanos[1], Olivier Gardon[1], Kathryn A. Tunny[1], Kristopher M. Blucher[1], Craig J. Morton[4], Michael W. Parker[4,5], Emma Sierecki[1], Yann Gambin[1], Guillermo A. Gomez[1], Kirill Alexandrov[1], Ian A Wilson[6], Manolis Doxastakis[3], Alan E. Mark[1,2], Michael J. Waters[1]*

Affiliations:

[1]The University of Queensland, Institute for Molecular Bioscience, Qld 4072, Australia. [2]The University of Queensland, School of Chemistry and Molecular Biosciences, Qld 4072, Australia. [3]Department of Chemical and Biomolecular Engineering, University of Houston, Houston, Texas. [4]Biota Structural Biology Laboratory and ACRF Rational Drug Discovery Centre, St Vincent's Institute of Medical Research, Fitzroy, VIC 3065, Australia. [5]Department of Biochemistry and Molecular Biology and Bio21 Institute, University of Melbourne, Parkville, VIC 3052, Australia. [6]Scripps Research Institute La Jolla, California.

*Corresponding authors: m.waters@uq.edu.au, a.brooks@uq.edu.au

Abstract:

JAK-STAT signaling is key to many aspects of biology and medicine, yet the mechanism used by cytokine receptors to initiate signaling is enigmatic. We present the first complete mechanistic model for JAK2 activation based on an archetypal cytokine receptor, the growth hormone receptor. To formulate this model we have used FRET to monitor positioning of the JAK2 binding motif, Jun-zipper receptor constructs to control receptor transmembrane (TM) helix position, atomistic modeling of TM helix interactions and docking of JAK2 kinase and inhibitory pseudokinase crystal structures with an opposing pair in *trans*. Surprisingly, we find that activation of the receptor dimer induces a separation of its JAK2 binding motifs, driven by a ligand-induced transition from a parallel TM helix pair to a left handed crossover arrangement. This mechanism leads to removal of the pseudokinase domain from the kinase domain of the partner JAK2 and pairing of the two kinase domains, facilitating *trans*-activation. This model may generalize to other class I cytokine receptors.

One Sentence Summary:

We present a novel mechanism for activation of JAK2 tyrosine kinase by a typical cytokine receptor, the growth hormone receptor, and the molecular movements involved.

Dedication: Dedicated to Professor Henry G Friesen

Main Text:

Class I cytokine receptors are key regulators of many processes including postnatal growth, erythropoiesis, myelopoiesis, lactation, and metabolism. These receptors utilize the JAK-STAT signaling pathway, which when deregulated becomes an important oncogenic pathway (*1*). Despite this, the molecular process responsible for activation of JAK2 tyrosine kinase by class I cytokine receptors has remained elusive.

The first class I cytokine to be cloned was growth hormone (GH), as was its receptor. These have been mechanistic exemplars for class I signaling molecules since publication of the crystal structure of the 2:1 complex of GH receptor (GHR) extracellular domains (ECDs) with the hormone (*2*). That structure led to a model of receptor activation wherein hormone-induced receptor dimerization resulted in close proximity of the receptor intracellular domains (ICDs) and apposition of the activation loops within the catalytic domains of a pair of receptor-bound JAK2 kinases, resulting in kinase activation (*3*). However, for the GHR and other related cytokine receptors such as the erythropoietin (EPO), prolactin, and thrombopoietin receptors, this model was superseded with the demonstration that these receptors exists largely as an inactive dimer in the absence of ligand (*4-9*). It was found that the transmembrane domain (TMD) of these single pass cytokine receptors play an important role in the constitutive dimerization through use of the ToxCAT/ToxR assay for the EPO Receptor (EPOR), and FRET and Co-IP studies with the GH and prolactin receptors. The existence of such dimers implies that a specific ligand-induced conformational change is required for signal transmission to the associated cytoplasmic JAK2 kinases.

Comparison of receptor subunit 1 in the 2:1 complex of the GHR with our unliganded crystal structure showed only minor conformational differences, implying that the signal is initiated by subunit realignment as a result of the asymmetric placement of the receptor binding sites on GH (*5*). How this realignment is used to bring the dimeric receptor-associated JAK2 pair into productive interaction has remained elusive, despite the obvious importance of JAK-STAT signaling in biology. Single particle electron microscopic imaging of homologous JAK1 has not thus far been able to resolve this issue, while the full crystal structure of JAK2 itself is not yet resolved (*10*). An appropriate model for JAK2 activation by its associated cytokine receptor should provide a means of removing the inhibitory pseudokinase domain from the kinase domain of JAK2, and then align the kinase domains for their transactivation and signal initiation. This model should also account for the observation that mutations V617F and Y613E, which result in constitutively active JAK2 mutants, are only active at physiological expression levels in the presence of receptor dimers (*11, 12*). It should also encompass the finding that JAK2 binds to the juxtamembrane (JM) Box1 sequence of GHR via residues close to the end of the N-terminal FERM domain (*13*).

We present here a model for activation of JAK2 by GH and the molecular movements of its receptor which bring about this activation, based on experimentation and molecular modeling (view animation at http://web-services.imb.uq.edu.au/waters/hgh.html). We anticipate this has application to other class I cytokine receptors.

Results

GHR TMD interaction supports the role of the TMD in constitutive dimer formation and the importance of key residues in TMD helix packing

Previous data have indicated a key role for the GHR TMD in ligand-independent receptor association (*5*). To characterize which interactions within the TMD contribute to constitutive GHR dimerization, the ToxR assay (*14*) was used. This assay provides a colorimetric measure of TMD interactions using isolated TMDs expressed in the inner cell membrane of *E. coli* (fig. S2), and has been used to demonstrate TMD association for the homologous EPOR and TpoR (*8, 15*). The ToxR assay showed that the GHR TMDs self-associate (Fig. 2A), although less strongly than the homodimeric EPOR or the leucine zipper control, but strongly compared to the non-

interacting poly-alanine (Alanine 16) control. The N-, C-terminal and central portions of the GHR TMD were all shown to interact in this assay. Pro266 and the first glycine (274) of the GxxG motif (both of which are highly conserved, fig. S1) appear to weaken the TMD helix interaction, since interaction increased on conversion of these residues to Ile (Fig. 2B and 2C). Substitution of individual residues within the TMD with alanine is known to have negligible effect on helix interactions for these cytokine receptors (*15*), so we introduced disruptive Gly-Pro double substitutions at ^{272}IF and ^{282}LF. These substitutions significantly decreased helix interaction (as they do for the EPOR TMD interaction, where they are thought to introduce a kink (*6*). Conversely, substitution of ^{280}VM with GP has the opposite action, increasing GHR TMD helix interaction (Fig. 2C). These results support the view that the GHR TMD helices do associate constitutively in a specific manner, but not so strongly as to preclude realignment as a result of ligand binding to the ECD.

Verification of constitutive dimer formation of GHR in mammalian cells was obtained by homo-FRET using confocal microscopy anisotropy analysis at the cell surface (*16, 17*) (Fig. 2D). As controls for these experiments we determined the FRET efficiency measured by fluorescence anisotropy of constitutive monomeric and dimeric versions of the Receptor-type tyrosine-protein phosphatase alpha (RTPTα) transmembrane protein and compared with that of the GHR fused to mCitrine (mCit) after residue 341, 37 residues after the Box1 sequence. For the monomeric RTPTα construct the TMD was exchanged for the monomeric LDL receptor (*18*), while the dimeric RTPTα construct a constitutive disulfide bond was introduced in the extracellular domain adjacent to the TMD (*19-21*) (see Supplementary Materials). This data shows that it is evident that the GHR receptor exists primarily as a dimer at the surface of live cells.

Cysteine scanning analysis of GHR TMD interactions indicates relative orientation of helices in the receptor dimer

TMD association was verified using cysteine crosslinking of the TMD and juxtamembrane (JM) residues. For these studies a receptor construct was truncated in the intracellular domain after residue 388 and Cys259 was converted to Ser, resulting in a receptor that was absent of cysteines C-terminal of the lower cytokine domain. Within this construct each amino acid from the top of the JM linker that joins the lower cytokine domain to the TMD, down to the end of the TMD (Leu251 to Ser288) was individually mutated to cysteine, and crosslinking between receptors was examined. For these experiments both intact cells and cell membranes were used. We crosslinked with either a cell-permeable 5Å linker (MTS) or through the formation of a disulfide bond using Cu-phenanthroline. Crosslinking with MTS in intact cells revealed dimeric and monomeric forms, with all of the N-terminal JM residues (Cys259-Phe265) crosslinking similarly, presumably reflecting flexibility in the absence of ligand. However, within the bulk of the TMD there was a helical periodicity evident in dimer formation, and when crosslinked residues were plotted on a helix wheel projection, an interaction interface was apparent, which included Ileu272/Phe273, Ile275/Phe276, and Val280 with crosslinking just visible at Phe283 (Fig. 3A and 3B). It should be noted that MTS has limited accessibility to residues buried deep in the bilayer where little reactive thiolate anion is present (*22*), which is presumably the reason for the low efficiency of dimer formation towards the cytoplasmic side. This interface correlates well with the basal state configuration predicted by molecular dynamics (MD) simulations (Fig. 6). Notably, the conserved GxxG motif is not involved in the TMD interaction in the basal state. Crosslinking of cell membranes with Cu-phenanthroline, though less able to penetrate the cell

membranes, did show crosslinks could form from Thr258 to Ileu268, and again from Thr280 to Leu286 at the lower TMD boundary.

The extent of crosslinking in the presence or absence of human GH (hGH) was next investigated in cell membrane preparations. We observed increased Cu-phenanthroline-induced crosslinking of Asp262Cys, located in the JM region, in the presence of hGH (Fig. 3C), although other residues did not yield consistent results. This supports the view that ligand binding increases the proximity between JM residues in this conserved membrane proximal sequence, and is consistent with hGH-induced formation of disulfide dimers at the adjacent Cys259 residue in the native receptor as reported by others (*23*).

GHR dimerization by disulfide bond formation at the extracellular JM and TMD results in constitutively active receptors

GH, like its structural homologs EPO and Prolactin, has two asymmetrically placed receptor binding sites which would change the interaction geometry between the two receptor subunits on binding. To understand the nature of this change we began with the observation that a minor fraction of the cysteine-substituted receptors described above form crosslinked dimers spontaneously in the absence of ligand (fig. S3). Hence, we could observe the activity of full length dimerized receptor in the absence of ligand through cysteine substitution at crosslinked residues within the JM linker and upper TMD helix regions. For these experiments we also mutated wild type (WT) Cys259 to serine. Transient expression in HEK293 cells revealed that constitutive crosslinking of the GHR with cysteine substitutions between Glu260 and Leu269 is accompanied by receptor activation (measured as STAT5 Y694 phosphorylation), while above this the dimer formation and activation is weak. No significant dimer formation or signaling was seen with Cys259 converted to serine, *ie* when no JM or TMD free cysteines are present (Fig. 3D). Evidently dimerization within the upper TMD or the extracellular EED sequence can initiate signaling, *ie* only close apposition of the upper TMD is required for signaling. Accordingly, introducing two disulfide bonds by cysteine substitution at E260C and I270C resulted in even stronger receptor activation (Fig. 3D).

Controlled dimerization of GHR using Jun zipper-receptor chimeras combined with FRET analysis reveals that increased receptor activation correlates with an increase in separation of the Box1 motifs

To better understand the steric requirements for receptor activation we substituted the GHR ECD with a leucine zipper from c-Jun. This allowed us to control the positioning of the TMD without compensatory movements by the ECDs. The positioning of the cytoplasmic JAK2-binding Box1 motif was then monitored by placing C-terminal FRET reporters (mCit or mCFP) 37 residues below the Box1 sequence. The receptor truncation and addition of FRET reporters did not prevent JAK2 binding, and GH addition was able to activate JAK2 with these receptor constructs (fig. S4 and S5).

We first positioned the Jun zipper 12 residues above the presumed TMD boundary, where the GHR linker joins to the lower cytokine receptor domain. We had previously shown that this construct results in constitutive activation (*24*). Shortening the linker by 4 residues at a time revealed that the closer the Jun zipper came to the TMD, the stronger was the signal that was generated, as measured by cell proliferation (Fig. 4A and 4B). Surprisingly, strength of signal correlated ***inversely*** with FRET ratio, *ie* signal activation was associated with ***separation*** of the Box1 sequences (Fig. 4C to 4E). Next the Jun zipper was placed at the upper TMD boundary and

the helices were rotated by inserting 1-4 alanines sequentially at the junction with the TMD. There was an optimum rotational position for signal activation, with the active and inactive positions adjacent. Again, the FRET ratio indicated that separation of the Box1 sequences occurs in the active rotational position (Fig. 4F to 4H). In order to exclude the possibility that the changes in FRET ratio resulted from reorientation of the fluorophores rather than their separation, the comparison of the 3Ala and 4Ala Jun insertion constructs was repeated using a flexible linker RSIAT (*25*) between the fluorophores and residue 341 of the receptor. This did not influence the FRET ratio comparison, from which we conclude that the decreased FRET ratio in the active states is due to an increased distance and not a result of fluorophore rotation (fig. S6).

Because clamping the receptors together at the upper TMD interface, either by use of the Jun zipper (Fig. 4A to 4E) or through disulfide bond formation (Fig. 3D) resulted in receptor activation, the role of the conserved EED acidic sequence (fig. S1) positioned therein was examined. It seemed likely that like-charge repulsion could maintain separation of the receptors here and play a role as a gating mechanism to maintain the receptor in an inactive state in the absence of ligand. Repulsion could then be overcome by ligand binding inducing closer apposition of the receptors within the constitutive dimer. This hypothesis was explored by comparing the Jun-3Ala construct with an equivalent construct where the three alanines were reverted to the WT ^{260}EED sequence. As shown in Fig. 5A, this showed the presence of the AAA sequence compared to EED substantially increased the proliferative activity and again decreased the FRET ratio at the Box1 domain, again indicating that when the receptor dimer is clamped tighter together at the upper TMD interface, the Box1 motifs separate.

We then asked if this phenomenon applied to the full length receptor and could act as a gate for receptor activation. We introduced the charge reversal mutations KKR in place of the EED sequence and co-transduced the full length KKR construct together with the WT construct, or separately, into Ba/F3 cells and looked for constitutive activity. Electrostatic attraction at this position was found to partially activate the full length receptor (Fig. 5B). This activation was again shown to be associated with separation of the Box1 sequences below the membrane by using GHR constructs that contained the full ECD with mCFP/mCit reporters placed after the Box1 motif in the same manner as the Jun zipper constructs (Fig. 5C). Expression of WT-GHR or KKR-GHR individually gave similar FRET values, while co-expression of both constructs gave a significantly lower FRET value, again demonstrating the inverse correlation between activation and separation of the Box1 motif.

Importantly, by using the full ECD WT-GHR FRET constructs we verified that the binding of hormone alone to the receptor on intact cells also resulted in a significantly decreased FRET ratio with membrane extracts from these cells (Fig. 5D). The GHR D170H mutation (often referred to as D152H using numbering of the mature protein) which results in GH insensitive Laron dwarfism (*26*) was then introduced into these FRET constructs and was found to prevent the decrease in FRET seen with WT receptor in response to GH binding (Fig. 5D). Finally, the decrease in FRET ratio induced by WT GH was not seen with the clinical GH antagonist G120R hGH, and this blocked the decrease in FRET ratio induced by WT GH (Fig. 5D).

We believe that a previous observation that hormone binding to GHR produced a transient increase in FRET signal (*27*) is a result of their FRET reporters being placed at the C-terminus. Given the relative immobilization of receptor-bound JAKs below the TMD, the lower cytoplasmic domains must move toward the JAKs for tyrosine phosphorylation to occur. This

would be facilitated by an unstructured cytoplasmic domain as is known to occur in the JAK1-gp130 couple (*28*).

Lysine 289 at the GHR TMD-ICD boundary plays a critical role in receptor activation

The data presented above are consistent with a gating mechanism at the upper TMD boundary that holds the receptors apart, minimizing activation in the absence of ligand. We then investigated whether there are residues which hold the submembrane sequences together in the inactive state similar to the TPO receptor (TpoR or c-Mpl), where mutations within the conserved sequence above the Box1 domain results in constitutive activation and myeloproliferative neoplasms (*29*). As shown in Fig. 5E and 5F alanine substitution within the equivalent conserved SKQQRIK sequence (fig. S1) in the GH receptor revealed conversion of the first lysine residue (289) to alanine resulted in increased signaling. This finding parallels the result of Staerk et al (2006) (*29*) showing increased activation for the equivalent K507A mutant in TpoR. Again, for K289A GHR, the submembrane FRET reporters indicate increased separation of the Box1 sequences (Fig. 5E) through movement of the JM α-helical sequence (*30*).

Molecular simulations of GHR TMDs identify active and inactive dimer orientations.

In order to understand the above experimental data in terms of a molecular model, extensive *in silico* modeling of the hGHR TMD helix dimers was undertaken, initially *in vacuo*. As shown in fig. S7, searches *in vacuo* of helix rotation angles for both right and left handed crossing angles predicted a helix alignment corresponding to crosslink data (Fig. 3A), with interactions between Phe276 and Phe283 (lowest free energy, Cluster 1, fig. S7A). The rather different chicken GHR sequence was predicted to give a similar alignment (fig. S7C).

To understand the dynamics of receptor activation, we then used MD simulations to model the behavior of the TMDs in a lipid bilayer (Fig. 6A, B and Supplementary Materials). A coarse grained (CG) representation of the peptide, lipids and solvent (*31*) was used to obtain the free energy profile as a function of distance (PMF) between two TMD by exhaustive Monte Carlo simulations using 128 replica pairs for a range of separations between the centers of mass of the helices (*32*). The fact that the PMF has a deep minimum at a separation of 0.7-0.8nm with a predicted free energy of binding around 10 kcal/mol supports the finding that two TMDs interact strongly with minimal free monomer present (Fig. 6B).

We next sought measures to characterize our modeling data such as the crossing angle Ω between the helix axes, the helix tilt angles τ, and contact maps between specific amino acids within the two TMDs. Fig. 6C shows the maps of the contacts between the two helices as they approach within a lipid bilayer. Helices tilt and interact first when the lateral separation of the centers of mass is ~2nm. Repulsive interactions at the N-termini result in formation of an initial contact at the C-termini. Subsequently, the TMDs follow a path that maximizes interactions between the Phe residues and Thr-Thr hydrogen bonding. This initially leads to an essentially parallel dimer (State 1 in Fig. 6D) with a low Ω value but with many interactions. Closer approach of the helices (as could result from hormone binding) leads to a close-packed structure (State 2 in Fig. 6E) with increased tilting and Ω, resulting in a left handed cross over dimer with increased separation at the C-terminus (see below). Both State 1 and 2 lie within the energy minimum shown in Fig. 6B, indicating a relatively facile State1-State2 transition. This transition has been observed for other TMDs using coarse-grained and atomistic simulations in simpler environments (*33, 34*). GHR TMDs form the left handed dimer by rotating Phe276 and 283 out

of the interface. Importantly, right handed essentially parallel dimers at close separation readily rearrange to left handed dimers (State 2) by substitution of disulfide bonds at Glu260 and Ile270 (Fig. 7A and 7B) which correlates with the constitutive receptor activation seen in Fig. 3D with such dimers.

To better identify structures correlated to activity we needed to compare our predictions with mutation and crosslinking experiments. Therefore, atomistic models of helical TMDs were superimposed onto the structures from the CG simulations and subjected to MD in large lipid-bilayer systems for several months of CPU time. For State 1, three structures were each simulated for 0.3μs. Fig. 6D shows a snapshot of one such dimer (State 1) together with an analysis of the separation between specific residues for which cysteine substitutions had been performed for each of the three trajectories. All three dimers fluctuated significantly but maintained a separation of between 0.9-1.2nm, slightly tilted relative to the normal of the bilayer and in a parallel arrangement with low Ω. These dimers are characterized by extensive interactions between Phe residues and appear to be stabilized by Lys289 that anchors the lower C-termini at the water-hydrophobic region boundary. The predicted sulfur-sulfur separation distances closely resemble the experimental crosslink pattern seen with cysteine-crosslinking experiments in the absence of ligand, supporting State 1 as the inactive state. Note that Gly274 is far from the helix interface in the absence of hormone.

Fig. 6E presents the results of a 0.7μs full atomistic simulation for the most stable dimer predicted by the simpler coarse-grain CG model (State 2), which remained helical throughout the 0.7μs simulation. Backbone atoms presented small fluctuations with an overall lateral separation of 0.8nm. Helices tilt, rotate and pack against Gly274 with a separation of substituted cysteines distinctively different from the experimental data obtained for the inactive receptor. Importantly, when the inactive state (Fig. 6D) is compared with the left handed crossover form in Fig. 6E, separation between the C-termini has increased substantially (evident in the Cys substitution sulfur-sulfur distances). The increased separation parallels our finding that activity correlates with higher separation of the C-termini as monitored by FRET. Moreover, in the proposed active State2 form the N-terminal Trp267 sits favorably at the membrane interface, facing outward to favor association, while the C-terminal Lys289 is in an unfavorable configuration for helix interaction (*ie* allowing greater separation), consistent with NMR studies using model peptides (*35*). Thus the model can explain how alanine substitution of Lys289 promotes the left handed dimer form, correlating with the increased activation seen on conversion of Lys289 to alanine (Fig. 5E and 5F).

Finally, a chimeric model was constructed in which the proposed TMD dimer configurations were joined to the crystal structure of the human GH:ECD receptor complex (PDBid:3HHR). Missing residues were generated using Modeller (http://salilab.org/modeller/about_modeller.html). The overall best configuration based on Modeller's objective function for the linking amino acids is shown in Fig. 7C. This shows a good fit between the ECD positioning and the State2 configuration and places the two Cys259 residues in close enough proximity to form a disulfide bond, as previously shown experimentally after GH addition (*23*). We could also identify potential inter-receptor hydrogen bonds in the linker that could assist in stabilizing the active configuration, between Glu260 of receptor 1 and the amide of Trp267 in receptor 2, as well as between the backbone carbonyl of Phe257 and amide of Glu260 in receptor 2. The ECDs without the hormone were then attached to the parallel TMD (State1). This simulation produced rotation of the ECDs, as described previously for isolated

ECDs (*36*). Interestingly, in these simulations the linker region sat on the membrane, although the ECD domains did not separate. This observation is consistent with our inability to crosslink receptors above Cys259 efficiently in the basal state. Potentially this is related to repulsion between the acidic EED sequences.

A new model for GHR activation

The above findings are consistent with a receptor activation model wherein binding of the GH through its asymmetrically placed binding sites (*2*) would realign the two receptors by relative rotation as evident in MD simulations (*36*), and together with elevation of receptor 1, lock the two dimerization domains in the ECD closely together. This locking is necessary for signal transduction (*37, 38*), and brings the upper TMD sequences close together by overcoming the electrostatic repulsion of the EED gate. Closer apposition of the adjacent juxtamembrane sequences is presumably the reason for resistance to proteolytic attack on the receptor when GH is bound, in contrast to its sensitivity when the G120R hGH antagonist is bound (*39*). Closure of the upper TMD would promote the transition to the left handed TMD form, with increased separation of the Box1 sequences.

A new model for JAK2 activation by GH

Separation of the JAK2 binding Box1 sequences as a mechanism for JAK2 activation is novel. We have considered how such a separation might occur within a receptor dimer containing a JAK2 molecule bound to each receptor, given the finding that even constitutively activated oncogenic JAK2 mutants V617F, L611S, and Y613E require the presence of receptor for significant activity (*11, 12*), *ie* the receptors need to be present to correctly appose the kinase domains for efficient transactivation. We hypothesized that if the kinase domain of the first JAK2 was inhibited by the complimentary pseudokinase domain of the second JAK2, and vice versa, then moving the JAK2 molecules apart in a sliding motion would remove the pseudokinase domain inhibitions, and bring the kinase domains into productive proximity (Fig. 7D and animation at http://web-services.imb.uq.edu.au/waters/hgh.html).

Activation of JAK2 by GH involves removal of trans inhibition

To provide experimental evidence for this model we placed FRET reporters (mCFP or mCit) at strategic locations within JAK2, then compared the FRET ratios when cells were co-transduced with WT rGHR (rabbit GHR) or rGHR that had the EED/KKR substitution either individually (inactive) or together (providing a subset of active receptors). This strategy allowed measurement of FRET ratios when all receptors were fixed in an inactive basal state in comparison to having a subset of receptors fixed in an active orientation. FRET reporters were placed at the C-terminus of JAK2 to monitor movement of the catalytic domains, or C-terminal to the SH2 domain at Asn533, in place of the pseudokinase domain. Reporter pairs were co-transfected (or transfected separately for FRET calculations) into HEK293T cells with the rGHR expression plasmids. Washed membrane preparations were then prepared from these cells (to reduce the background signal from free JAK2) and FRET ratios were determined. While FRET ratio changes were modest (Fig. 7E and 7F), they were consistent. The modest changes in FRET would be due in part to FRET observed between three receptor interaction possibilities when the KKR mutant is expressed with the WT receptor, *ie* WT-WT (inactive), KKR-KKR (inactive), and WT-KKR (active). The significant increase in FRET ratio for the C-terminal reporters (Fig. 7E) is consistent with the requirement for the kinase domains to transactivate, while the reporters

positioned in the location of the pseudokinase domain (*ie* C-terminal to the SH2 domain, Fig. 7F) showed a *decreased* FRET ratio in accord with the model in Fig. 7D and the animation.

To further substantiate our JAK2 activation model, the kinase and pseudokinase domains were swapped (JAK2-KP), then co-transfected together with a WT JAK2 construct and the GH receptor into JAK2 deficient γ2A cells. Our model would predict constitutive JAK2 activity only when these two JAK2 constructs are together, but not for either alone. This result is evident in Fig. 8A where STAT5 phosphorylation by JAK2 is significantly increased when WT JAK2 and JAK2-KP are present, noting that in each experiment the total amount of JAK2 transfected was the same. Overexpression of JAK2 is known to lead to constitutive activation (*40*), which explains why some activated STAT5 is detectable when each JAK2 construct is transfected separately.

Molecular modeling of the JAK2 kinase/pseudokinase domain dimer interaction

Currently only the crystal structures of individual JAK2 kinase and pseudokinase domains are known (*41, 42*). To test if the proposed model is compatible with these structures the pseudokinase and kinase domain structures were docked using HADDOCK. The resulting equilibrated dimer after 40ns of unrestrained MD simulations (Fig. 8B) represents the interaction between the kinase of one molecule and the pseudokinase domain of another. In particular, the docked structures predict a close complementary interaction between the opposing kinase and pseudokinase domains. Importantly, the structure shows a close relationship between the activation loops and V617 in the pseudokinase domain which, when mutated, results in constitutive activation and oncogenesis. To make a model of the complete complex, docked kinase and pseudokinase pairs were placed in alternative orientations with another pair, and the cognate domains of each JAK2 were joined with their 30 residue interdomain linker. Fig. 8C and 7D show two orientations and their movements that are consistent with our experimental results.

We then verified that the pseudokinase-kinase pair can associate with a second such pair using AlphaScreen (fig. S9A to C) based on cell free expression of N-terminal eGFP or C-terminal mCherry-Myc tagged pairs. We supported this with single molecule brightness coincidence results consistent with dimerization of pseudokinase-kinase pairs using cell free expressed GFP tagged proteins (fig. S9D). As is evident in fig. S9F while the separate kinase domains do not associate under these conditions, the pseudokinase-kinase pairs do associate effectively *in trans*.

Discussion

This study has allowed us to propose a novel mechanism for activation of JAK2 by the growth hormone receptor, an archetypal class I homomeric cytokine receptor. We have shown that the receptor exists as a constitutive dimer with its TMDs held in an inactive orientation in the absence of hormone (with the caveat that some monomer is likely present). The central observation on which our model is based is that activation of the receptor is associated with the separation of the membrane proximal signaling domains below the TMD, as assessed by FRET, and consistent with MD modeling of the TMD.

In formulating a model to explain the increased separation of Box1 sequences on ligand binding, we were cognizant of our earlier finding that locking together of the ECD "dimerization domains" of the membrane proximal cytokine receptor module by specific hydrogen bonds and electrostatic bonds is essential for GH signaling (*37*). Based on MD modeling (*36*) this locking requires a relative rotation of receptor subunits of around 40°, and disruption of this lock with the

D170H mutation results in GH insensitive (Laron) dwarfism (*1*). We previously proposed that this locking resulted in activation of the receptor by relative rotation of the TMDs that was transmitted to the JAK2 binding Box1 sequence to allow contact of their catalytic kinase domains (*5*). However, when we introduced alanine insertions in the upper TMD of full-length receptor we observed only weak receptor activation, indicating some other ligand-induced movement was necessary for robust activation.

We explored the geometry of activation by clamping the receptor signaling units (TMD and cytoplasmic domain) together in defined ways, and observed that bringing a Jun zipper clamp down to the membrane surface gave the strongest activation, although concurrent insertion of alanines at the upper TMD boundary did show an optimum rotational position within the clamped receptor. Support for this model was provided by cysteine crosslink scanning of the upper linker and TMD residues, which showed that crosslinking at the EEDF sequence just above the TMD could activate the receptor in an analogous manner to the Jun zipper clamp. Similar crosslinking results have been reported for the full length EPOR (*43*), and an optimum rotational position for activation has been reported for both EPOR (*44*) and TpoR (*45*). These findings suggest a common mechanism within related class I receptors involving both an optimum rotational position and the need to closely appose the upper JM sequences for activation, resulting in a "tilt and twist" movement of the TMDs. This is supported by the finding that the TMD and ICD of the G-CSFR and GHR, both class I cytokine receptors, can be interchanged to produce signaling competent receptors (*46*). This result implies that the conserved GxxG sequence of the GHR TMD is not necessary for receptor activation, and indeed, we have found that substituting either Gly, or both, with bulky Ile residue does not have a significant effect on proliferative signaling or STAT5 activation (not shown).

Our activation model requires separation of the Box1 motifs. Given that, how could separation result in activation of JAK2 bound by its FERM domain to the lower JM segment of each receptor? Current models of JAK2 assume that it exists as a monomer, where each JAK2 is autoinhibited by its own pseudokinase domain in the basal state (*47*). However, other studies (*11, 12*) show that constitutively active JAK2 point mutations require a receptor dimer to manifest at physiologic expression. Clearly a new model is needed to account for this finding and our FRET observations. The original JAK2 structural model (*48*) has been superseded by the recent elucidation of the JAK2 kinase and pseudokinase domain crystal structures. We used these to determine if two kinase domains and two pseudokinase domains could pair in a complementary fashion such that an increased distance between the receptors and their attached JAK2 would slide the pseudokinase domains away from the kinase domains of their opposing counterpart, and bring the two kinase domains together for *trans*-activation. Indeed, we found optimized docked solutions which allowed this interaction, and also located key residues known to be associated with constitutive activation of JAK2 (*eg* in myeloproliferative disorders) in the interface between the inhibitory pseudokinase domain and its kinase domain complement in the basal state. By placing FRET reporters either at the C-teminus (kinase domain) or in place of the pseudokinase domain, we were able to show experimentally that the FRET ratio for the pseudokinase domains decreased on receptor activation (as predicted), while the ratio for the catalytic domains increased, supporting a model in which the domains slide apart. Further, by exchanging the kinase and pseudokinase domains we were able to obtain strong experimental support for our model, since when this domain reversal mutant was expressed together with WT JAK2, constitutive activity was evident. Finally, we could show with single molecule fluorescence

brightness and AlphaScreen that the pseudokinase-kinase domain pair can indeed associate *in trans* with another such pair.

We anticipate that these findings will provide valuable insights into the design of new cytokine receptor therapeutics and will facilitate understanding of a variety of relevant cytokine-related genetic disorders.

Methods:

ToxR Assay of TMD Interaction

This well validated assay provides a means for testing the interaction of TM helices that are placed in the inner membrane of bacteria. ToxR assays were performed essentially as previously described (*14*) using regions of the GHR TMD described in the Results. See fig S2 for the principle of this assay.

Cysteine Crosslinking Studies

A series of N-terminal HA-tagged hGHR mutants in pcDNA3.1 was constructed using Quickchange mutagenesis where every residue from Pro252 to Ser288 was converted to a cysteine after converting Cys259 to serine. Two sets of these mutants were used: either truncated at residue 389 (for crosslinking studies) or full length GHR (for STAT5 activation studies). These mutants were used for crosslinking according to (*49*) and immunoblotting or signal activation studies as detailed in Supplementary Materials.

Analysis of Proliferative Signal from GHR Constructs

The strength of constitutive proliferation signal from GHR constructs was assessed by starving Ba/F3 cells overnight in Ba/F3 starve media (see Supplementary Materials). Cultures were then counted using a Scepter with 40 μM sensors (Millipore) and seeded at equal concentrations into three flasks for each sample and cultured in starve media. Cell concentration was subsequently counted on following days and plotted as shown.

FRET Analysis

FRET measurements, using expression constructs detailed in Supplementary Materials, were performed on single cells by confocal microscopy and flow cytometry essentially as previously described (*50*). Membrane extracts and FRET analysis with a fluorescence plate reader was essentially as described previously and detailed in Supplementary Materials. Live cell membrane Homo-FRET methods are described in the Supplementary Materials.

Signaling Analysis of JAK2 Co-transfected with Kinase-Pseudokinase Domain Swap JAK2

Expression constructs for WT murine JAK2 and for JAK2 with the kinase domain and pseudokinase domain swapped (referred to as JAK2-KP corresponding to: (Met1-Ile540)-(Asp840-Ala1132)-(Gly831-Arg839)-(Asn542-Gly834)) were constructed as described in Supplementary Materials. JAK2 deficient (and STAT5 deficient) γ2A cells (a gift from G. Stark, ICRF, London), were transfected with expression plasmids for hGHR, STAT5B, and either WT-JAK2 or JAK2-KP separately, or WT-JAK2 and JAK2-KP co-transfected. In each set of experiments where P-STAT5 signal from co-transfected WT-JAK2 and JAK2-KP was compared with each JAK2 construct transfected separately, the total amount of JAK2 transfected was identical. Details are given in Supplementary Materials.

JAK2 Interface Model

To construct a model of the interface between the pseudokinase and kinase domains of neighboring subunits the crystal structures of the JAK2 pseudokinase (PDB id: 4FVP) and kinase (PDB id: 2B7A) domains were docked using the HADDOCK webserver with distance constraints between Tyr1007 of the kinase domain and both Phe595 and Val617 of the pseudokinase domain. The docked model was then refined by simulating it for 40 ns in water. Full details are given in the Supplementary Materials. The actual interface between the two consecutive kinase-pseudokinase pairs is not known. To generate possible arrangements of JAK2 dimers that are consistent both with the 30 amino acid linker sequence and with our experimental data, a second copy of the MD conformation of the pseudokinase−kinase domain dimer was positioned adjacent to original pair. That this arrangement was possible was confirmed by modelling in the missing linker region. Note, while the proposed arrangement is possible the model does not preclude the possibility other arrangements being consistent with the data.

Statistics

One way ANOVA was undertaken with Tukey's multiple comparison test, while for comparisons of two groups only unpaired Student's *t* test was used. Significance shown as *P< 0.05, **P<0.01, ***P<0.001, with SEM.

References and Notes:

1. A. J. Brooks, M. J. Waters, The growth hormone receptor: mechanism of activation and clinical implications. *Nat Rev Endocrinol* **6**, 515 (Sep, 2010).

2. A. M. de Vos, M. Ultsch, A. A. Kossiakoff, Human growth hormone and extracellular domain of its receptor: crystal structure of the complex. *Science* **255**, 306 (Jan 17, 1992).

3. J. A. Wells, Binding in the growth hormone receptor complex. *Proc Natl Acad Sci U S A* **93**, 1 (Jan 9, 1996).

4. J. Gent, P. van Kerkhof, M. Roza, G. Bu, G. J. Strous, Ligand-independent growth hormone receptor dimerization occurs in the endoplasmic reticulum and is required for ubiquitin system-dependent endocytosis. *Proc Natl Acad Sci U S A* **99**, 9858 (Jul 23, 2002).

5. R. J. Brown *et al.*, Model for growth hormone receptor activation based on subunit rotation within a receptor dimer. *Nat Struct Mol Biol* **12**, 814 (Sep, 2005).

6. K. F. Kubatzky *et al.*, Self assembly of the transmembrane domain promotes signal transduction through the erythropoietin receptor. *Curr Biol* **11**, 110 (Jan 23, 2001).

7. S. L. Gadd, C. V. Clevenger, Ligand-independent dimerization of the human prolactin receptor isoforms: functional implications. *Mol Endocrinol* **20**, 2734 (Nov, 2006).

8. E. E. Matthews *et al.*, Thrombopoietin receptor activation: transmembrane helix dimerization, rotation, and allosteric modulation. *FASEB J* **25**, 2234 (Jul, 2011).

9. O. Livnah *et al.*, An antagonist peptide-EPO receptor complex suggests that receptor dimerization is not sufficient for activation. *Nat Struct Biol* **5**, 993 (Nov, 1998).

10. P. J. Lupardus *et al.*, Structural snapshots of full-length Jak1, a transmembrane gp130/IL-6/IL-6Ralpha cytokine receptor complex, and the receptor-Jak1 holocomplex. *Structure* **19**, 45 (Jan 12, 2011).

11. M. Funakoshi-Tago, S. Pelletier, H. Moritake, E. Parganas, J. N. Ihle, Jak2 FERM domain interaction with the erythropoietin receptor regulates Jak2 kinase activity. *Mol Cell Biol* **28**, 1792 (Mar, 2008).

12. X. Lu, L. J. Huang, H. F. Lodish, Dimerization by a cytokine receptor is necessary for constitutive activation of JAK2V617F. *J Biol Chem* **283**, 5258 (Feb 29, 2008).

13. K. He *et al.*, Janus kinase 2 determinants for growth hormone receptor association, surface assembly, and signaling. *Mol Endocrinol* **17**, 2211 (Nov, 2003).

14. D. Langosch, B. Brosig, H. Kolmar, H. J. Fritz, Dimerisation of the glycophorin A transmembrane segment in membranes probed with the ToxR transcription activator. *J Mol Biol* **263**, 525 (Nov 8, 1996).

15. W. Ruan, V. Becker, U. Klingmuller, D. Langosch, The interface between self-assembling erythropoietin receptor transmembrane segments corresponds to a membrane-spanning leucine zipper. *J Biol Chem* **279**, 3273 (Jan 30, 2004).

16. A. N. Bader *et al.*, Homo-FRET imaging as a tool to quantify protein and lipid clustering. *Chemphyschem : a European journal of chemical physics and physical chemistry* **12**, 475 (Feb 25, 2011).

17. S. Ghosh, S. Saha, D. Goswami, S. Bilgrami, S. Mayor, Dynamic imaging of homo-FRET in live cells by fluorescence anisotropy microscopy. *Methods in enzymology* **505**, 291 (2012).

18. R. S. Kasai *et al.*, Full characterization of GPCR monomer-dimer dynamic equilibrium by single molecule imaging. *J Cell Biol* **192**, 463 (Feb 7, 2011).

19. L. G. Tertoolen *et al.*, Dimerization of receptor protein-tyrosine phosphatase alpha in living cells. *BMC Cell Biol* **2**, 8 (2001).

20. G. Jiang *et al.*, Dimerization inhibits the activity of receptor-like protein-tyrosine phosphatase-alpha. *Nature* **401**, 606 (Oct 7, 1999).

21. G. Jiang, J. den Hertog, T. Hunter, Receptor-like protein tyrosine phosphatase alpha homodimerizes on the cell surface. *Mol Cell Biol* **20**, 5917 (Aug, 2000).

22. L. Guan, F. D. Murphy, H. R. Kaback, Surface-exposed positions in the transmembrane helices of the lactose permease of Escherichia coli determined by intermolecular thiol cross-linking. *Proc Natl Acad Sci U S A* **99**, 3475 (Mar 19, 2002).

23. Y. Zhang, J. Jiang, J. J. Kopchick, S. J. Frank, Disulfide linkage of growth hormone (GH) receptors (GHR) reflects GH-induced GHR dimerization. Association of JAK2 with the GHR is enhanced by receptor dimerization. *J Biol Chem* **274**, 33072 (Nov 12, 1999).

24. S. N. Behncken *et al.*, Growth hormone (GH)-independent dimerization of GH receptor by a leucine zipper results in constitutive activation. *J Biol Chem* **275**, 17000 (Jun 2, 2000).

25. T. K. Kerppola, Design and implementation of bimolecular fluorescence complementation (BiFC) assays for the visualization of protein interactions in living cells. *Nature Protocols* **1**, 1278 (2006).

26. P. Duquesnoy *et al.*, A single amino acid substitution in the exoplasmic domain of the human growth hormone (GH) receptor confers familial GH resistance (Laron syndrome) with positive GH-binding activity by abolishing receptor homodimerization. *EMBO J* **13**, 1386 (Mar 15, 1994).

27. E. Biener-Ramanujan, V. K. Ramanujan, B. Herman, A. Gertler, Spatio-temporal kinetics of growth hormone receptor signaling in single cells using FRET microscopy. *Growth Horm IGF Res* **16**, 247 (Aug, 2006).

28. G. Skiniotis, P. J. Lupardus, M. Martick, T. Walz, K. C. Garcia, Structural organization of a full-length gp130/LIF-R cytokine receptor transmembrane complex. *Mol Cell* **31**, 737 (Sep 5, 2008).

29. J. Staerk *et al.*, An amphipathic motif at the transmembrane-cytoplasmic junction prevents autonomous activation of the thrombopoietin receptor. *Blood* **107**, 1864 (Mar 1, 2006).

30. M. J. Waters, H. N. Hoang, D. P. Fairlie, R. A. Pelekanos, R. J. Brown, New insights into growth hormone action. *J Mol Endocrinol* **36**, 1 (Feb, 2006).

31. L. Monticelli *et al.*, The MARTINI coarse-grained force field: Extension to proteins. *J Chem Theory Comput* **4**, 819 (May, 2008).

32. L. Janosi, A. Prakash, M. Doxastakis, Lipid-modulated sequence-specific association of glycophorin A in membranes. *Biophysical journal* **99**, 284 (Jul 7, 2010).

33. J. Henin, A. Pohorille, C. Chipot, Insights into the recognition and association of transmembrane alpha-helices. The free energy of alpha-helix dimerization in glycophorin A. *J Am Chem Soc* **127**, 8478 (Jun 15, 2005).

34. A. Prakash, L. Janosi, M. Doxastakis, GxxxG motifs, phenylalanine, and cholesterol guide the self-association of transmembrane domains of ErbB2 receptors. *Biophysical journal* **101**, 1949 (Oct 19, 2011).

35. S. Ozdirekcan, D. T. Rijkers, R. M. Liskamp, J. A. Killian, Influence of flanking residues on tilt and rotation angles of transmembrane peptides in lipid bilayers. A solid-state 2H NMR study. *Biochemistry* **44**, 1004 (Jan 25, 2005).

36. D. Poger, A. E. Mark, Turning the growth hormone receptor on: evidence that hormone binding induces subunit rotation. *Proteins* **78**, 1163 (Apr, 2010).

37. C. Chen, R. Brinkworth, M. J. Waters, The role of receptor dimerization domain residues in growth hormone signaling. *J Biol Chem* **272**, 5133 (Feb 21, 1997).

38. B. Bernat, G. Pal, M. Sun, A. A. Kossiakoff, Determination of the energetics governing the regulatory step in growth hormone-induced receptor homodimerization. *Proc Natl Acad Sci U S A* **100**, 952 (Feb 4, 2003).

39. P. van Kerkhof, M. Smeets, G. J. Strous, The ubiquitin-proteasome pathway regulates the availability of the GH receptor. *Endocrinology* **143**, 1243 (Apr, 2002).

40. O. Silvennoinen, J. N. Ihle, J. Schlessinger, D. E. Levy, Interferon-induced nuclear signalling by Jak protein tyrosine kinases. *Nature* **366**, 583 (Dec 9, 1993).

41. I. S. Lucet *et al.*, The structural basis of Janus kinase 2 inhibition by a potent and specific pan-Janus kinase inhibitor. *Blood* **107**, 176 (Jan 1, 2006).

42. R. M. Bandaranayake *et al.*, Crystal structures of the JAK2 pseudokinase domain and the pathogenic mutant V617F. *Nat Struct Mol Biol* **19**, 754 (Aug, 2012).

43. X. Lu, A. W. Gross, H. F. Lodish, Active conformation of the erythropoietin receptor: random and cysteine-scanning mutagenesis of the extracellular juxtamembrane and transmembrane domains. *J Biol Chem* **281**, 7002 (Mar 17, 2006).

44. N. Seubert *et al.*, Active and inactive orientations of the transmembrane and cytosolic domains of the erythropoietin receptor dimer. *Mol Cell* **12**, 1239 (Nov, 2003).

45. J. Staerk *et al.*, Orientation-specific signalling by thrombopoietin receptor dimers. *EMBO J* **30**, 4398 (Nov 2, 2011).

46. E. Ishizaka-Ikeda, R. Fukunaga, W. I. Wood, D. V. Goeddel, S. Nagata, Signal transduction mediated by growth hormone receptor and its chimeric molecules with the granulocyte colony-stimulating factor receptor. *Proc Natl Acad Sci U S A* **90**, 123 (Jan 1, 1993).

47. P. Saharinen, O. Silvennoinen, The pseudokinase domain is required for suppression of basal activity of Jak2 and Jak3 tyrosine kinases and for cytokine-inducible activation of signal transduction. *J Biol Chem* **277**, 47954 (Dec 6, 2002).

48. F. Giordanetto, R. T. Kroemer, Prediction of the structure of human Janus kinase 2 (JAK2) comprising JAK homology domains 1 through 7. *Protein Eng* **15**, 727 (Sep, 2002).

49. W. Guo, L. Shi, M. Filizola, H. Weinstein, J. A. Javitch, Crosstalk in G protein-coupled receptors: changes at the transmembrane homodimer interface determine activation. *Proc Natl Acad Sci U S A* **102**, 17495 (Nov 29, 2005).

50. D. Abankwa, H. Vogel, A FRET map of membrane anchors suggests distinct microdomains of heterotrimeric G proteins. *J Cell Sci* **120**, 2953 (Aug 15, 2007).

51. P. D. Adams, D. M. Engelman, A. T. Brunger, Improved prediction for the structure of the dimeric transmembrane domain of glycophorin A obtained through global searching. *Proteins* **26**, 257 (Nov, 1996).

52. L. Janosi, M. Doxastakis, Accelerating flat-histogram methods for potential of mean force calculations. *The Journal of chemical physics* **131**, 054105 (Aug 7, 2009).

53. A. Prakash, L. Janosi, M. Doxastakis, Self-association of models of transmembrane domains of ErbB receptors in a lipid bilayer. *Biophysical journal* **99**, 3657 (Dec 1, 2010).

54. C. Oostenbrink, A. Villa, A. E. Mark, W. F. van Gunsteren, A biomolecular force field based on the free enthalpy of hydration and solvation: the GROMOS force-field parameter sets 53A5 and 53A6. *J Comput Chem* **25**, 1656 (Oct, 2004).

55. A. J. Beevers, A. Kukol, Systematic molecular dynamics searching in a lipid bilayer: application to the glycophorin A and oncogenic ErbB-2 transmembrane domains. *Journal of molecular graphics & modelling* **25**, 226 (Oct, 2006).

56. S. Pronk *et al.*, GROMACS 4.5: a high-throughput and highly parallel open source molecular simulation toolkit. *Bioinformatics*, (Feb 21, 2013).

57. H. J. C. Berendsen, J. P. M. Postma, W. F. Vangunsteren, A. Dinola, J. R. Haak, Molecular-Dynamics with Coupling to an External Bath. *Journal of Chemical Physics* **81**, 3684 (1984).

58. B. Hess, H. Bekker, H. J. C. Berendsen, J. G. E. M. Fraaije, LINCS: A linear constraint solver for molecular simulations. *J Comput Chem* **18**, 1463 (Sep, 1997).

59. D. P. Tieleman, S. J. Marrink, H. J. Berendsen, A computer perspective of membranes: molecular dynamics studies of lipid bilayer systems. *Biochimica et biophysica acta* **1331**, 235 (Nov 21, 1997).

60. X. Liu *et al.*, Generation of mammalian cells stably expressing multiple genes at predetermined levels. *Anal Biochem* **280**, 20 (Apr 10, 2000).

61. E. Campeau *et al.*, A versatile viral system for expression and depletion of proteins in mammalian cells. *PLoS ONE* **4**, e6529 (2009).

62. J. Quan, J. Tian, Circular polymerase extension cloning of complex gene libraries and pathways. *PLoS ONE* **4**, e6441 (2009).

63. S. Morita, T. Kojima, T. Kitamura, Plat-E: an efficient and stable system for transient packaging of retroviruses. *Gene therapy* **7**, 1063 (Jun, 2000).

64. L. Galili, K. Herz, O. Dym, E. Padan, Unraveling functional and structural interactions between transmembrane domains IV and XI of NhaA Na+/H+ antiporter of Escherichia coli. *J Biol Chem* **279**, 23104 (May 28, 2004).

65. G. W. Gordon, G. Berry, X. H. Liang, B. Levine, B. Herman, Quantitative fluorescence resonance energy transfer measurements using fluorescence microscopy. *Biophysical journal* **74**, 2702 (May, 1998).

66. P. K. Wolber, B. S. Hudson, An analytic solution to the Forster energy transfer problem in two dimensions. *Biophysical journal* **28**, 197 (Nov, 1979).

67. S. J. Han *et al.*, Pronounced conformational changes following agonist activation of the M(3) muscarinic acetylcholine receptor. *J Biol Chem* **280**, 24870 (Jul 1, 2005).

68. Y. Wan, A. McDevitt, B. Shen, M. L. Smythe, M. J. Waters, Increased site 1 affinity improves biopotency of porcine growth hormone. Evidence against diffusion dependent receptor dimerization. *J Biol Chem* **279**, 44775 (Oct 22, 2004).

69. A. A. Heikal, S. T. Hess, G. S. Baird, R. Y. Tsien, W. W. Webb, Molecular spectroscopy and dynamics of intrinsically fluorescent proteins: coral red (dsRed) and yellow (Citrine). *Proc Natl Acad Sci U S A* **97**, 11996 (Oct 24, 2000).

70. D. Watling *et al.*, Complementation by the protein tyrosine kinase JAK2 of a mutant cell line defective in the interferon-gamma signal transduction pathway. *Nature* **366**, 166 (Nov 11, 1993).

71. S. J. de Vries *et al.*, HADDOCK versus HADDOCK: new features and performance of HADDOCK2.0 on the CAPRI targets. *Proteins* **69**, 726 (Dec 1, 2007).

72. C. Dominguez, R. Boelens, A. M. Bonvin, HADDOCK: a protein-protein docking approach based on biochemical or biophysical information. *J Am Chem Soc* **125**, 1731 (Feb 19, 2003).

73. D. van der Spoel, P. J. van Maaren, C. Caleman, GROMACS molecule & liquid database. *Bioinformatics* **28**, 752 (Mar 1, 2012).

74. N. Schmid *et al.*, Definition and testing of the GROMOS force-field versions 54A7 and 54B7. *European biophysics journal : EBJ* **40**, 843 (Jul, 2011).

75. W. F. van Gunsteren, H. J. Berendsen, J. Hermans, W. G. Hol, J. P. Postma, Computer simulation of the dynamics of hydrated protein crystals and its comparison with x-ray data. *Proc Natl Acad Sci U S A* **80**, 4315 (Jul, 1983).

76. I. G. Tironi, R. Sperb, P. E. Smith, W. F. Vangunsteren, A Generalized Reaction Field Method for Molecular-Dynamics Simulations. *Journal of Chemical Physics* **102**, 5451 (Apr 1, 1995).

77. S. Miyamoto, P. A. Kollman, Settle - an Analytical Version of the Shake and Rattle Algorithm for Rigid Water Models. *J Comput Chem* **13**, 952 (Oct, 1992).

78. K. A. Feenstra, B. Hess, H. J. C. Berendsen, Improving efficiency of large time-scale molecular dynamics simulations of hydrogen-rich systems. *J Comput Chem* **20**, 786 (Jun, 1999).

79. W. Humphrey, A. Dalke, K. Schulten, VMD: Visual molecular dynamics. *Journal of molecular graphics & modelling* **14**, 33 (Feb, 1996).

80. S. Mureev, O. Kovtun, U. T. Nguyen, K. Alexandrov, Species-independent translational leaders facilitate cell-free expression. *Nat Biotechnol* **27**, 747 (Aug, 2009).

81. Y. Gambin *et al.*, Direct single-molecule observation of a protein living in two opposed native structures. *Proc Natl Acad Sci U S A* **106**, 10153 (Jun 23, 2009).

82. Y. Gambin *et al.*, Visualizing a one-way protein encounter complex by ultrafast single-molecule mixing. *Nature methods* **8**, 239 (Mar, 2011).

Acknowledgments:
Supported by grants from National Health and Medical Research Council of Australia (Grants 511120, 1002893 and 102082) and the Australian Research Council to M.J.W., A.J.B, A.E.M. and M.W.P. Infrastructure funding from the Victorian Government to St Vincent's Institute is gratefully acknowledged. WD and MD acknowledge financial support by the NSF (USA) CBET No. 1067356 and CPU time by the University of Houston Research Computing Center. G.A.G acknowledge financial support by the Kids Cancer Project of the Oncology Research Foundation. We thank Dr Wayne A. Johnston, for optimizing the *Leishmania* based cell-free

lysate expression system used in the single-molecule and alpha screen interaction studies. Confocal imaging was performed at the IMB/ACRF Cancer Biology Imaging Facility, established with the support of the Australian Cancer Research Foundation

Figure Captions

Fig. 1. Cartoon of GHR showing key features with residue numbers.

Fig. 2. GHR exists primarily as dimers in cell surface membranes. (**A**-**C**) GHR TMD association shown by ToxR assay (**A**) ToxR assay showing self association of GHR and EPOR TMDs with controls showing amino acid sequences used for each transmembrane domain (TMD) construct together with a Maltose Binding Protein (MBP) immunoblot of the ToxR-TMD-MBP chimeric proteins expressed in FHK12 *E. coli* which was used to normalize the β-galactosidase values in Miller units (see fig S2 for detail). (**B**-**C**) GHR TMD sequences showing mutations introduced to perturb TMD association as monitored in the ToxR assay (n= 4-17 independent experiments in triplicate, values expressed as % L-16 value after normalization of β-galactosidase activity to MBP expression). Average ± SEM, with one-way ANOVA and Tukey's multiple comparison post-test (*= $P<0.05$, **= $P<0.01$, ***= $P<0.001$ compared to test constructs). Data shows that the GHR TMD associates with itself and that the first glycine (G274) of the GxxG motif and Pro266 inhibit helix association, as shown by replacement with Ile and that introduction of helix disrupting GP mutations into the TMD helix disrupt TMD association. (**D**) homo-FRET using confocal microscopy anisotropy analysis at the surface of live mammalian cells shows GHR is essentially dimeric in comparison to constitutive monomeric and dimeric versions of the Receptor-type tyrosine-protein phosphatase alpha (RTPTα) transmembrane protein.

Fig. 3. Crosslinking of cysteine substituted GHR TMD residues shows interacting residues together with crosslinked residues that can induce constitutive activation. (**A**) Cysteine scan of TMD with crosslinking of transiently expressed GHR by MTS crosslinker in intact cells as described in Supplementary Materials. No evident orientation constraints are seen within the upper JM linker, but crosslinking within the TMD is periodic, and plots to one side of a helix wheel projection shown in (**B**). (**C**) Addition of 2 nM hGH promotes disulfide dimer formation at D262C in the JM linker using cell membrane preparations. Three independent experiments are shown with Cu-o-phenanthroline crosslinking (*49*). (**D**) Constitutive activation of spontaneously crosslinked cysteine substituted receptors, evident as STAT5 tyrosine phosphorylation in transiently transfected HEK293 cells. Level of receptor expression is shown by corresponding HA-blot for hGHR, and histogram shows pSTAT5 level normalized to receptor protein expression for three replicate experiments (mean +/- SEM).

Fig. 4. Replacement of ECD with Jun zippers enables analysis of orientational constraints in constitutive signaling by GHR. Activation of proliferative signaling correlates with increased separation of FRET reporters placed below Box1 of the intracellular domain (ICD). (**A**) Shortening of the linker between the Jun zipper and the TMD results in (**B**) increased receptor activation in Ba/F3 cells stably expressing Jun fusion constructs. (**C** and **D**) FRET analysis by FACS and live cell confocal microscopy shows an inverse relation between cell proliferation (shown for day 8 from Fig. 4B for illustrative purposes) and FRET ratio for these constructs (**E**). (**F**) Rotation of the Jun clamped TMD by insertion of 1-4 alanines into the HA-

JUN-0aa-rGHR construct reveals an optimum orientation of the TMD helix for signaling (**G**), and this correlates with decreased FRET reporter signal below the TMD (**H**).

Fig. 5. The GHR upper and lower JM sequences act as a signaling gates. Validation of FRET movement with WT receptor ECD and GH addition. (**A**) Replacement of the WT acidic EED linker sequence with 3Ala promotes proliferative signaling by Jun-GHR in stable Ba/F3 cells (shown for proliferation assay at day 8), and decreases FRET signal in the ICD with membrane preparations. (**B**) Expression of full length GHR in transduced Ba/F3 cells with WT GHR, or GHR with the ^{260}EED residues substituted to AAA or KKR reveals that charge complementation of linker EED sequence by co-expression WT GHR with GHR-KKR results in constitutive activation. (**C**) When FRET reporters are placed below Box1, this activation correlates with decreased FRET. (**D**) Addition of 5 nM hGH to rGHR with FRET reporters below Box1 induces a decrease in FRET ratio in membrane preparations from transiently expressed constructs in HEK293T cells while no significant change is observed with addition of 500 nM G120R hGH. Incubation of 500 nM G120R hGH for 10 min prior to 5nM hGH impairs the GH induced decrease in FRET. GHR D170H Laron mutant shows no FRET change upon GH addition. (**E** and **F**) Substitution of Lys289 with Ala promotes proliferative signaling in stably expressing Jun GHR Ba/F3 cells (shown for proliferation assay at day 3), and this correlates with decreased FRET from reporters placed below Box1.

Fig. 6. Coarse Grain and Atomistic simulations of GHR TMDs. (**A**) Single helix showing predicted helicity between Phe265 and Lys289, and positioning of Trp267 at upper membrane boundary, with Lys289 at lower membrane boundary (see Supplementary Materials). (**B**) Free energy profiles for approach of helices showing different energetic contributions of lipid and protein. Note that there is only a modest total free energy difference (black line) between the parallel form at 11Å separation and the left handed crossover form at 8Å separation. (**C**) The three stages of helix interaction – firstly contact at the C-terminus, then the parallel form with interactions between Phe276 and Phe283 (**D**), State1, and finally the left handed crossover form (**E**), State2, after rotation to bring the GxxG motif (green spheres) in close packing. S-S separation distances are modeled for the latter two states, with 3 simulations for the parallel form, which corresponds to the pattern seen in the absence of hormone by crosslinking (Fig. 3).

Fig. 7. Validation of the GHR homology model. Repositioning of JAK2 observed by FRET. (**A**) Disulfide bonding between cysteines substituted at Glu260 and Ile270 rapidly converts State 1 to State 2 in MD simulations, correlating with constitutive activation seen experimentally. (**B**) Separations of backbone residues from MD of the active disulfide dimer overlay closely on those for State 2 calculated by MD simulation for 0.5-0.9 nM separations. (**C**) Full length simulations. The best model of the JM linker joined to the hGH:ECD receptor complex crystal structure (PDB id:3HHR) is shown. Note the proximity of Cys259s, which form a disulfide bond on addition of ligand. There are also two potential hydrogen bonds between linkers which could stabilize this conformation (see text). (**D**) Diagram of JAK2 dimer showing proposed movement of kinase and pseudokinase domains following receptor TMD separation in State 2. (**E** and **F**) FRET ratio measurements with activated receptor (WT + KKR charge reversal mutant as in Fig. 5B and 5C) and KKR or WT receptor alone, showing convergence of kinase domains and separation of pseudokinase domains on activation.

Fig. 8. JAK2 kinase domain swap and modeling studies support the new activation model. (**A**) Diagram of JAK2 domain swap construct. Immunoblots showing constitutive activation of JAK2 when kinase and pseudokinase domains are swapped, and the domain swap is co-

transfected with WT JAK2. Result of 3 independent experiments shown with total JAK2 plasmid quantity identical. (**B**) The pseudokinase-kinase domain interface in the inactivated state after 40ns of MD. The pseudokinase and kinase domains are shown in grey and blue ribbons, respectively. The following key residues are shown in spacefill representation: F595 (pink: required for V617F constitutive activation), V617 (red: mutation causing constitutive activation), substrate binding site D976 (blue). Activation loop phosphorylation residues Y1007 (yellow), and Y1008 (orange). The ATP binding site and catalytic K882 are shown in purple ribbons and spacefill, respectively. View of the dimer interface from below shows the ATP binding site is located in the center of residues implicated in constitutive activation. The dimer conformation derived from MD simulations can be used to construct two tetrameric orientations that fulfill the experimental data: (**C**) a stacked tetramer, (**D**) or an inverse stacked tetramer, with each JAK2 circled. Arrows show proposed direction of movement induced by receptor separation below TMD, removing pseudokinase domain inhibition and bringing the kinase domains in proximity.

Fig. 1

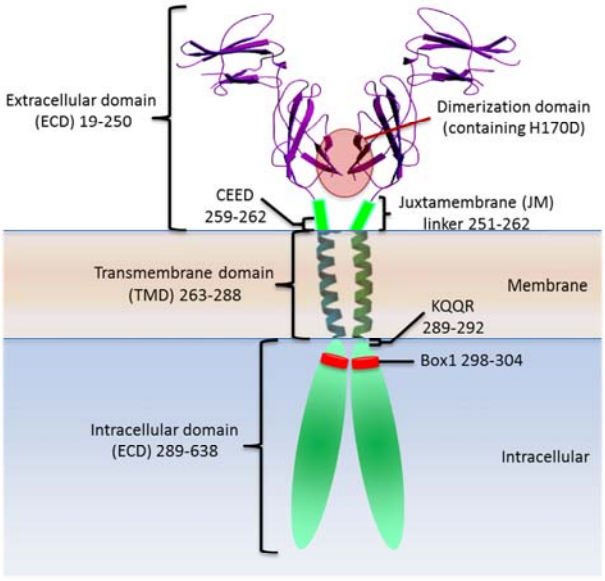
Extracellular domain
(ECD) 19-250
Dimerization domain
(containing H170D)
CEED
259-262
Juxtamembrane (JM)
linker 251-262
Transmembrane domain
(TMD) 263-288
Membrane
KQQR
289-292
Box1 298-304
Intracellular domain
(ECD) 289-638
Intracellular

Fig. 2

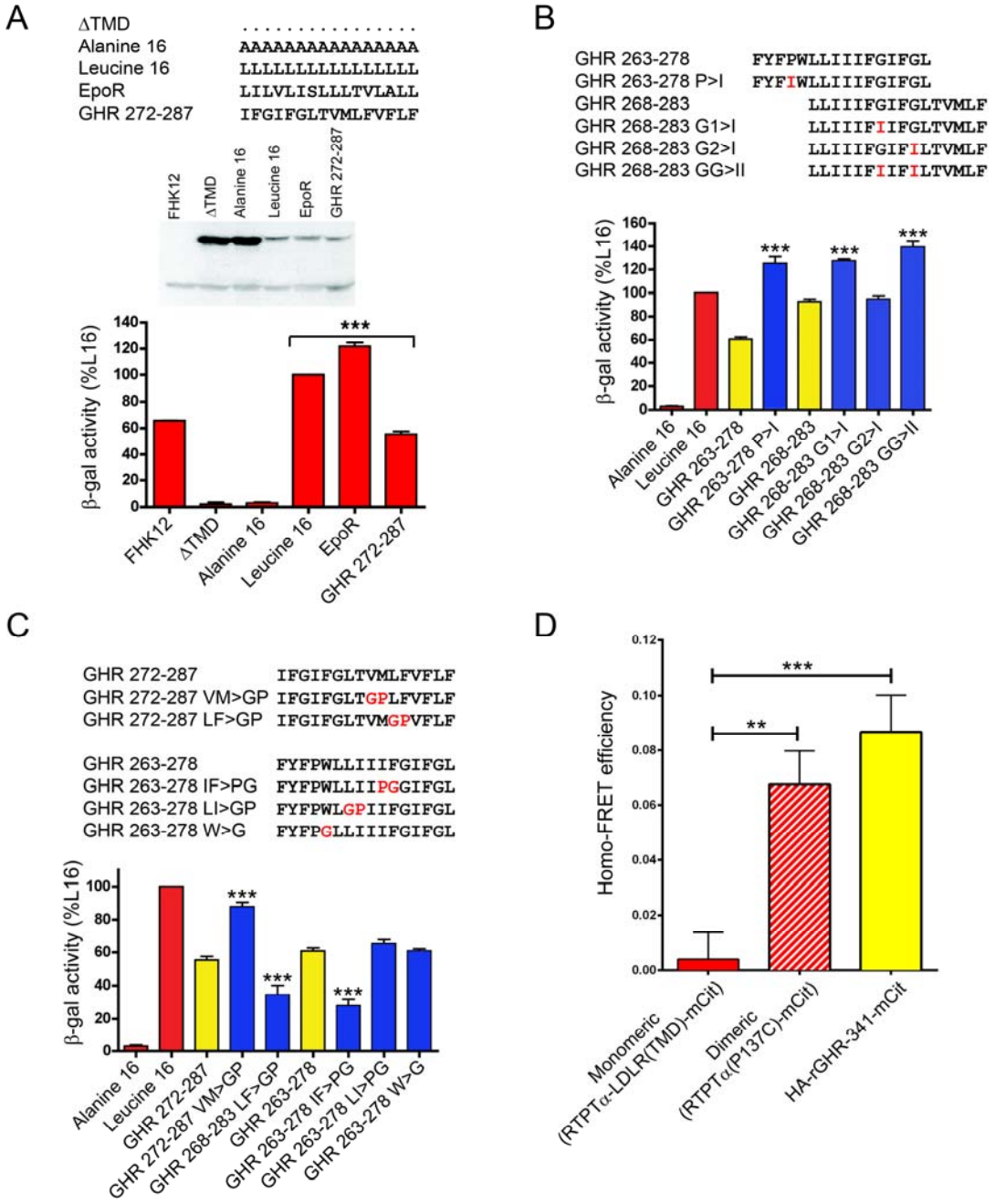
A
ΔTMD .....
Alanine 16 AAAAAAAAAAAAAAAA
Leucine 16 LLLLLLLLLLLLLLLL
EpoR LILVLISLLLTVLALL
GHR 272-287 IFGIFGLTVMLFVFLF
FHK12
ΔTMD
Alanine 16
Leucine 16
EpoR
GHR 272-287
β-gal activity (%L16)
***
B
GHR 263-278 FYFPWLLIIIFGIFGL
GHR 263-278 P>I FYFIWLLIIIFGIFGL
GHR 268-283 LLIIIFGIFGLTVMLF
GHR 268-283 G1>I LLIIIFIIFGLTVMLF
GHR 268-283 G2>I LLIIIFGIFILTVMLF
GHR 268-283 GG>II LLIIIFIIFILTVMLF
β-gal activity (%L16)
Alanine 16
Leucine 16
GHR 263-278
GHR 263-278 P>I
GHR 268-283
GHR 268-283 G1>I
GHR 268-283 G2>I
GHR 268-283 GG>II
C
GHR 272-287 IFGIFGLTVMLFVFLF
GHR 272-287 VM>GP IFGIFGLTGPLFVFLF
GHR 272-287 LF>GP IFGIFGLTVMGPVFLF
GHR 263-278 FYFPWLLIIIFGIFGL
GHR 263-278 IF>PG FYFPWLLIIPGGIFGL
GHR 263-278 LI>GP FYFPWLGPIIFGIFGL
GHR 263-278 W>G FYFPGLLIIIFGIFGL
β-gal activity (%L16)
Alanine 16
Leucine 16
GHR 272-287
GHR 272-287 VM>GP
GHR 268-283 LF>GP
GHR 263-278
GHR 263-278 IF>PG
GHR 263-278 LI>PG
GHR 263-278 W>G
D
Homo-FRET efficiency
Monomeric (RTPTα-LDLR(TMD)-mCit)
Dimeric (RTPTα(P137C)-mCit)
HA-rGHR-341-mCit

Fig. 3

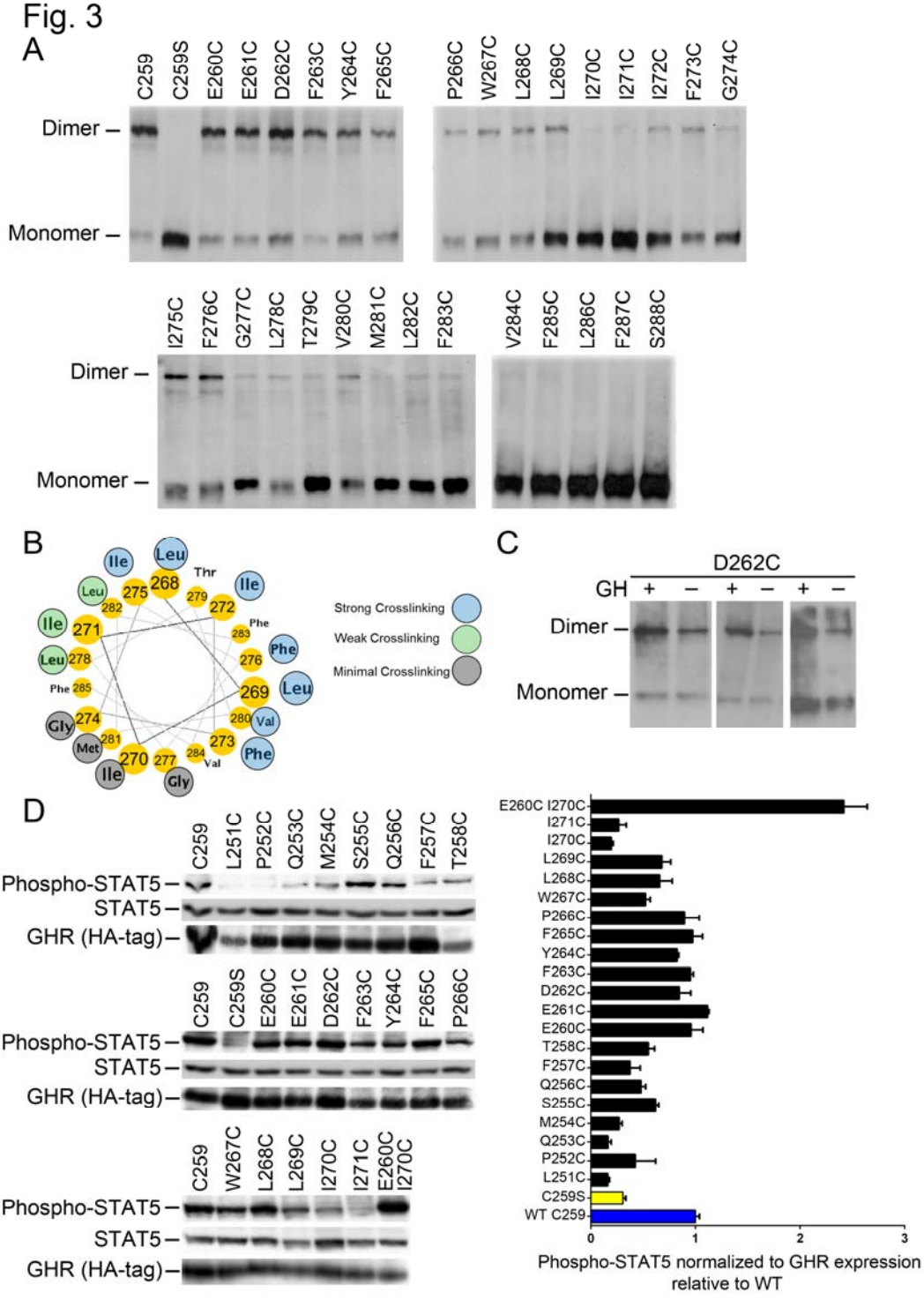
A
C259
C259S
E260C
E261C
D262C
F263C
Y264C
F265C
P266C
W267C
L268C
L269C
I270C
I271C
I272C
F273C
G274C
Dimer
Monomer
I275C
F276C
G277C
L278C
T279C
V280C
M281C
L282C
F283C
V284C
F285C
L286C
F287C
S288C
B
Strong Crosslinking
Weak Crosslinking
Minimal Crosslinking
C
D262C
GH
D
Phospho-STAT5
STAT5
GHR (HA-tag)
C259
L251C
P252C
Q253C
M254C
S255C
Q256C
F257C
T258C
C259S
E260C
E261C
D262C
F263C
Y264C
F265C
P266C
W267C
L268C
L269C
I270C
I271C
E260C I270C
WT C259
Phospho-STAT5 normalized to GHR expression relative to WT

Fig. 4

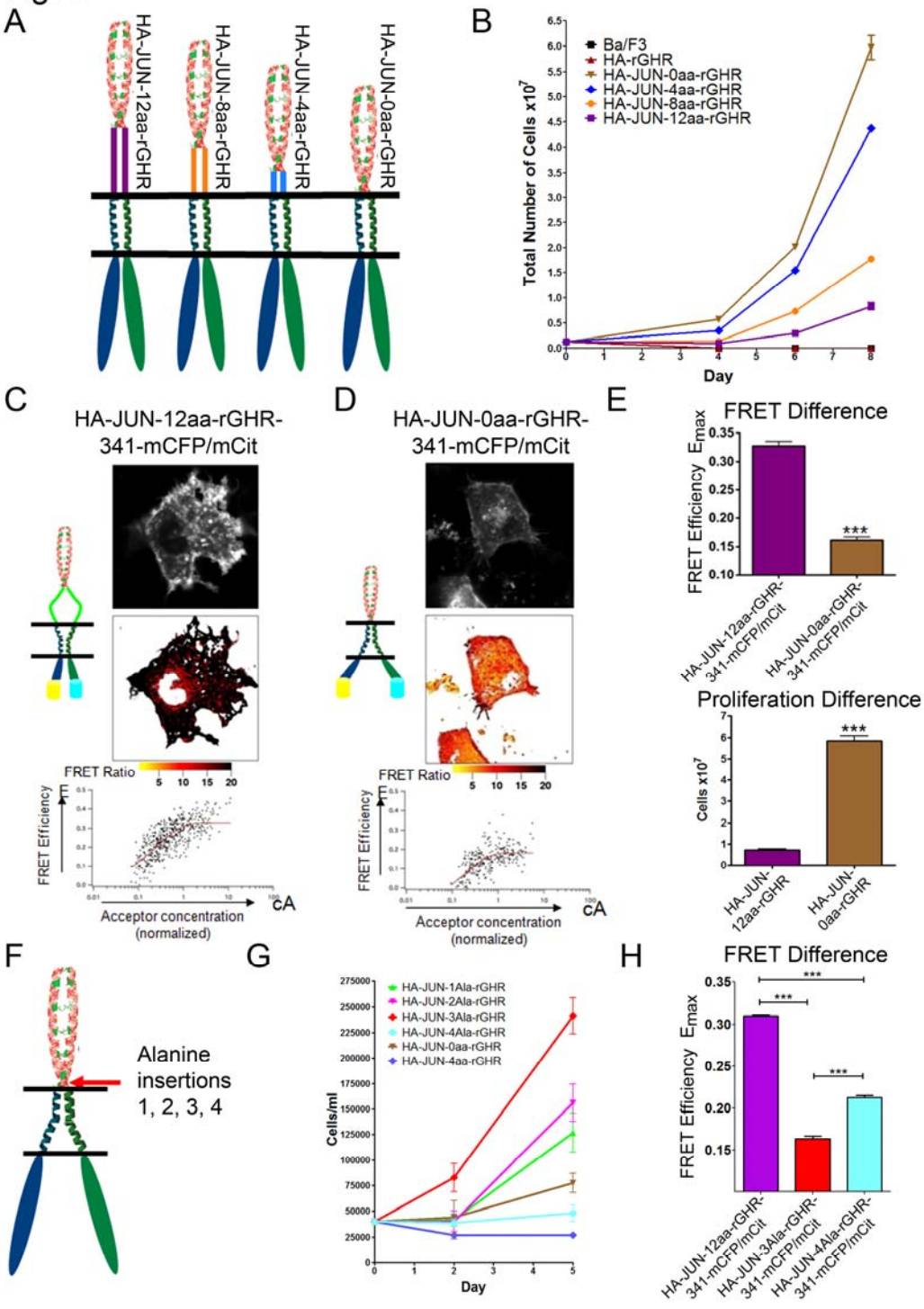
A
HA-JUN-12aa-rGHR
HA-JUN-8aa-rGHR
HA-JUN-4aa-rGHR
HA-JUN-0aa-rGHR
B
Ba/F3
HA-rGHR
HA-JUN-0aa-rGHR
HA-JUN-4aa-rGHR
HA-JUN-8aa-rGHR
HA-JUN-12aa-rGHR
Total Number of Cells x10^7
Day
C
HA-JUN-12aa-rGHR-341-mCFP/mCit
FRET Ratio
FRET Efficiency
Acceptor concentration (normalized)
cA
D
HA-JUN-0aa-rGHR-341-mCFP/mCit
FRET Ratio
FRET Efficiency
Acceptor concentration (normalized)
cA
E
FRET Difference
FRET Efficiency Emax
***
HA-JUN-12aa-rGHR-341-mCFP/mCit
HA-JUN-0aa-rGHR-341-mCFP/mCit
Proliferation Difference
Cells x10^7
***
HA-JUN-12aa-rGHR
HA-JUN-0aa-rGHR
F
Alanine insertions 1, 2, 3, 4
G
HA-JUN-1Ala-rGHR
HA-JUN-2Ala-rGHR
HA-JUN-3Ala-rGHR
HA-JUN-4Ala-rGHR
HA-JUN-0aa-rGHR
HA-JUN-4aa-rGHR
Cells/ml
Day
H
FRET Difference
FRET Efficiency Emax
***
***
***
HA-JUN-12aa-rGHR-341-mCFP/mCit
HA-JUN-3Ala-rGHR-341-mCFP/mCit
HA-JUN-4Ala-rGHR-341-mCFP/mCit

Fig. 5

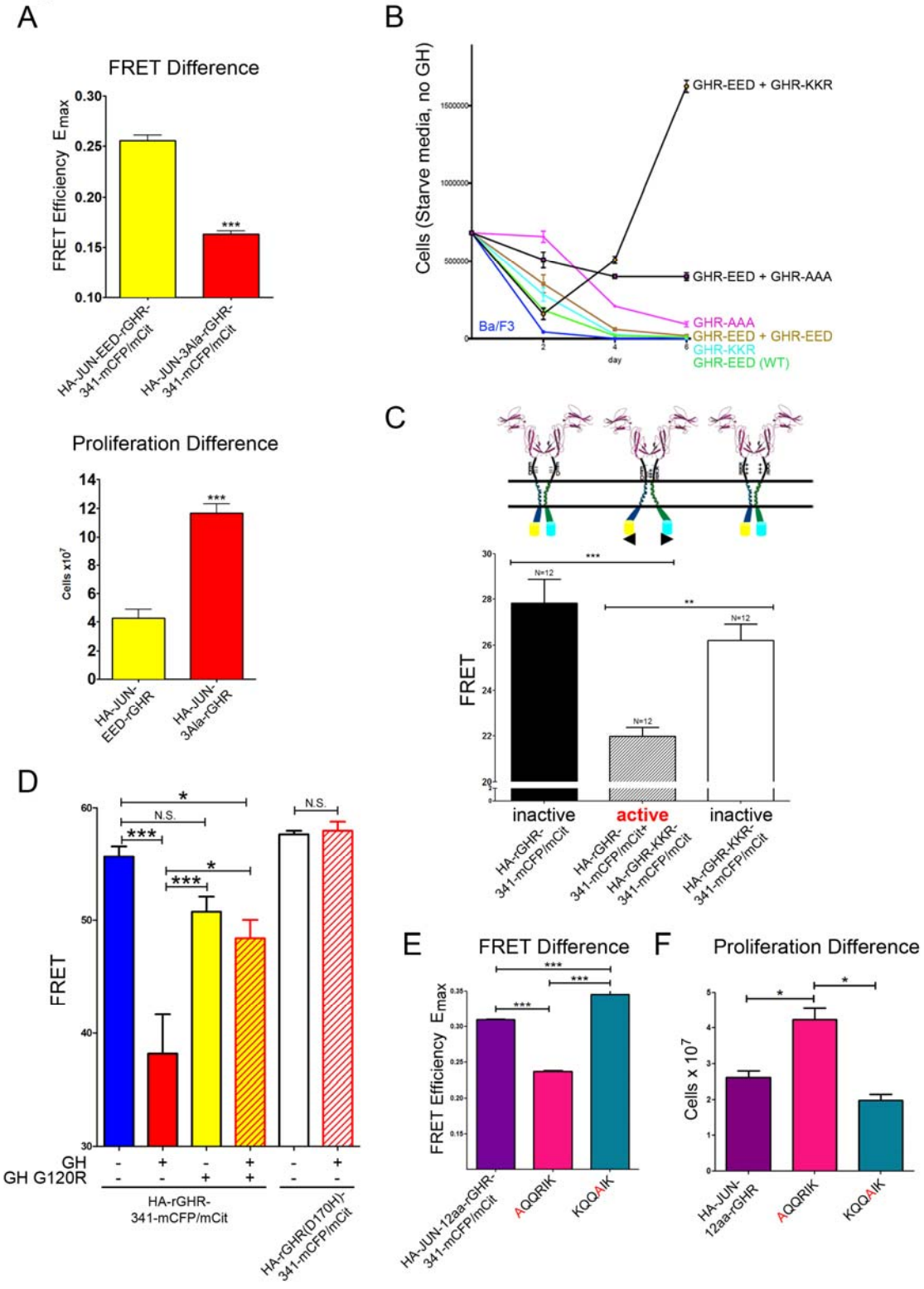
A
FRET Difference
FRET Efficiency Emax
0.30
0.25
0.20
0.15
0.10
***
HA-JUN-EED-rGHR-341-mCFP/mCit
HA-JUN-3Ala-rGHR-341-mCFP/mCit
Proliferation Difference
Cells x10^7
14
12
10
8
6
4
2
0
***
HA-JUN-EED-rGHR
HA-JUN-3Ala-rGHR
B
Cells (Starve media, no GH)
1500000
1000000
500000
0
2
4
6
day
GHR-EED + GHR-KKR
GHR-EED + GHR-AAA
GHR-AAA
GHR-EED + GHR-EED
GHR-KKR
GHR-EED (WT)
Ba/F3
C
FRET
30
28
26
24
22
20
***
**
N=12
N=12
N=12
inactive
active
inactive
HA-rGHR-341-mCFP/mCit
HA-rGHR-341-mCFP/mCit+ HA-rGHR-KKR-341-mCFP/mCit
HA-rGHR-KKR-341-mCFP/mCit
D
FRET
60
50
40
30
*
N.S.
***
*
***
N.S.
GH
GH G120R
HA-rGHR-341-mCFP/mCit
HA-rGHR(D170H)-341-mCFP/mCit
E
FRET Difference
FRET Efficiency Emax
***
***
***
HA-JUN-12aa-rGHR-341-mCFP/mCit
AQQRIK
KQQAIK
F
Proliferation Difference
Cells x 10^7
*
*
HA-JUN-12aa-rGHR
AQQRIK
KQQAIK

Fig. 6

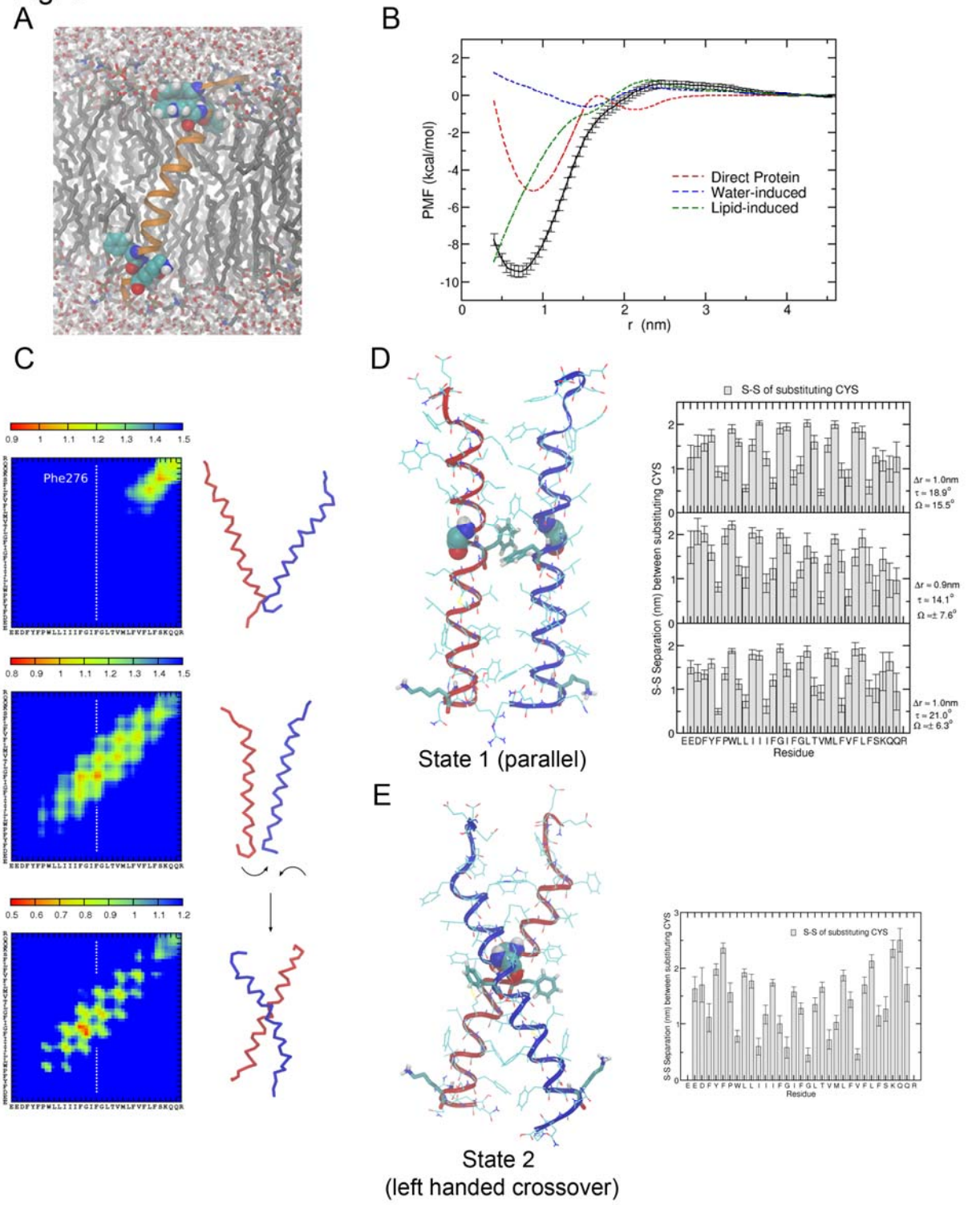
A
B
PMF (kcal/mol)
r (nm)
Direct Protein
Water-induced
Lipid-induced
C
Phe276
D
State 1 (parallel)
S-S of substituting CYS
S-S Separation (nm) between substituting CYS
Residue
Δr = 1.0nm
τ = 18.9°
Ω = 15.5°
Δr = 0.9nm
τ = 14.1°
Ω = ± 7.6°
Δr = 1.0nm
τ = 21.0°
Ω = ± 6.3°
E
State 2
(left handed crossover)

Fig. 7

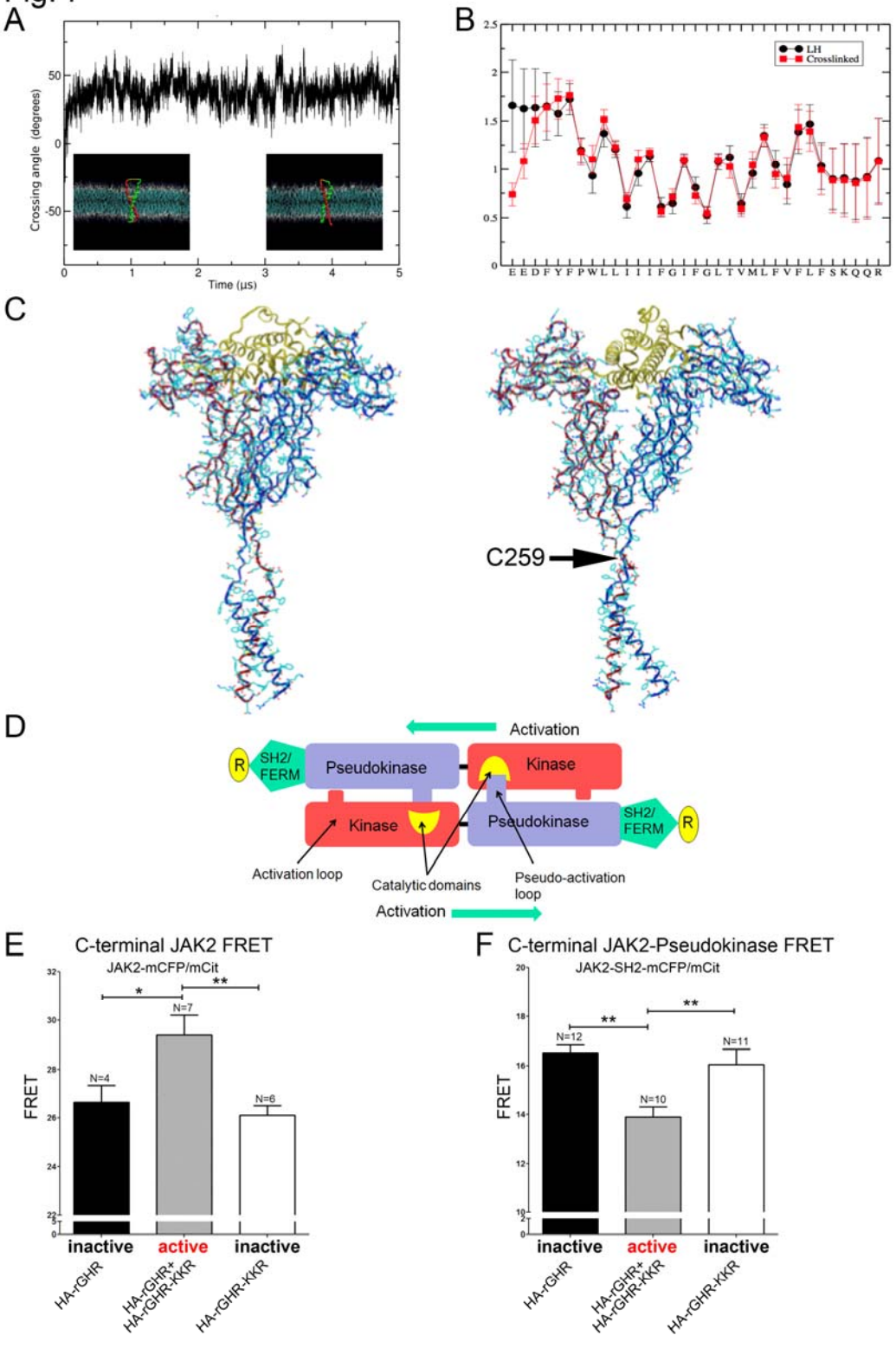
A
Crossing angle (degrees)
Time (μs)
B
LH
Crosslinked
E E D F Y F P W L L I I I F G I F G L T V M L F V F L F S K Q Q R
C
C259
D
Activation
R
SH2/
FERM
Pseudokinase
Kinase
Kinase
Pseudokinase
SH2/
FERM
R
Activation loop
Catalytic domains
Pseudo-activation
loop
Activation
E
C-terminal JAK2 FRET
JAK2-mCFP/mCit
FRET
N=4
N=7
N=6
inactive
active
inactive
HA-rGHR
HA-rGHR*
HA-rGHR-KKR
HA-rGHR-KKR
F
C-terminal JAK2-Pseudokinase FRET
JAK2-SH2-mCFP/mCit
FRET
N=12
N=10
N=11
inactive
active
inactive
HA-rGHR
HA-rGHR*
HA-rGHR-KKR
HA-rGHR-KKR

Fig. 8

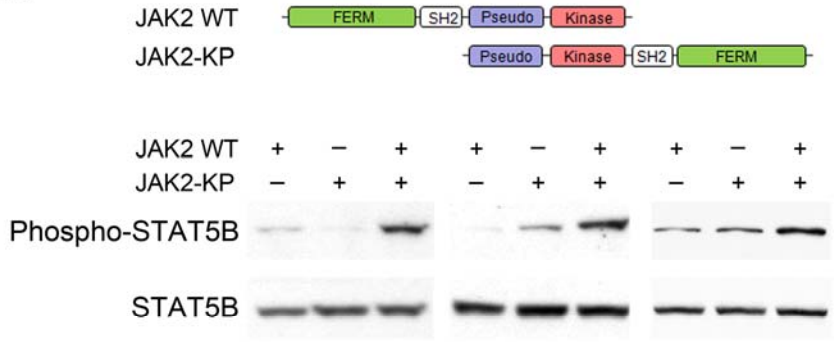
A
JAK2 WT
FERM
SH2
Pseudo
Kinase
JAK2-KP
Pseudo
Kinase
SH2
FERM
JAK2 WT + − + + − + + − +
JAK2-KP − + + − + + − + +
Phospho-STAT5B
STAT5B

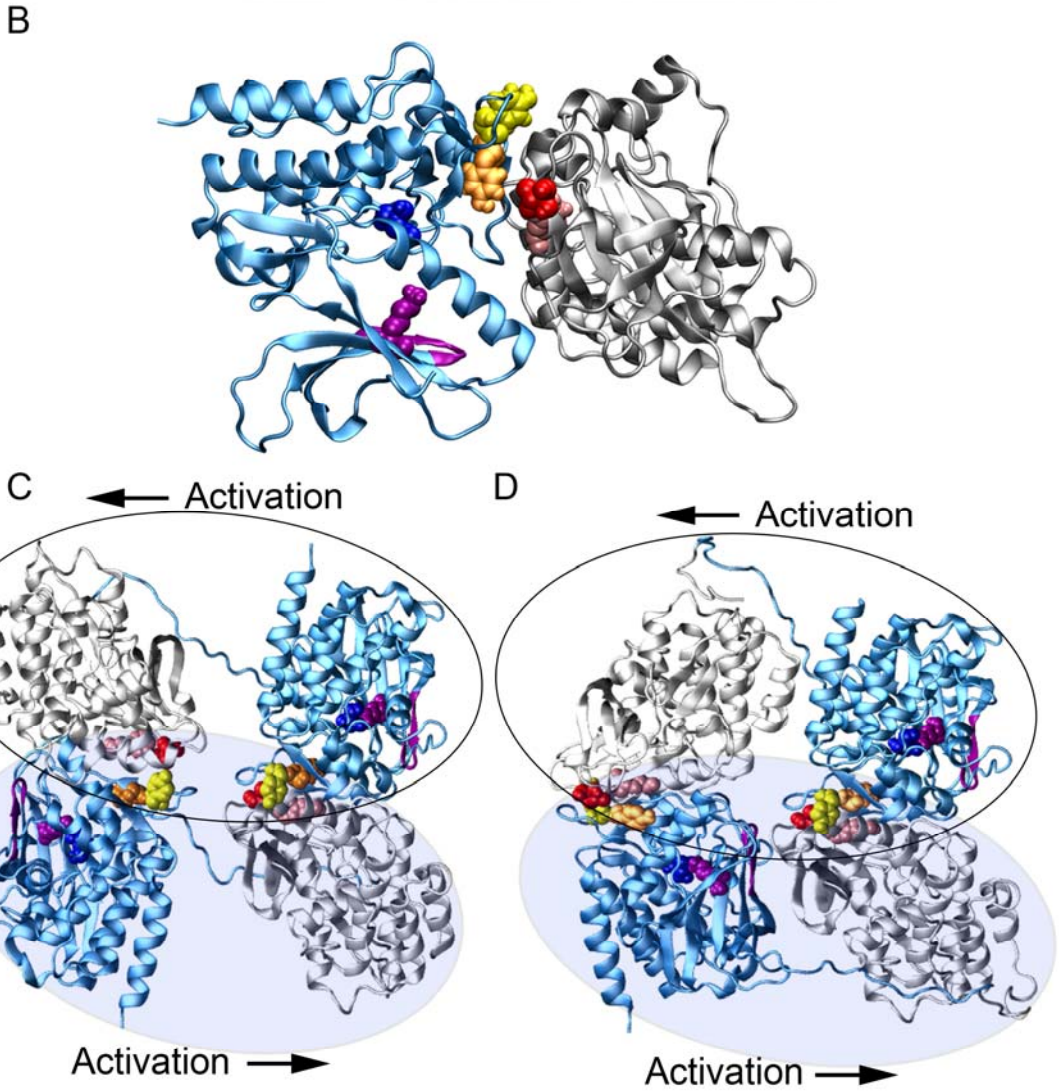
B
C
Activation
Activation
D
Activation
Activation

Supplementary Materials:

Supplementary Text

In vacuo molecular dynamics modeling of TMD interactions predicts a minimum free energy dimer orientation

Molecular modeling was undertaken to identify residues likely to interact in the unliganded state. Computational searches were carried out on a pair of human GHR transmembrane helices, (residues 265 to 288) *in vacuo* using CHI (*51*). The packing of the helix dimers was explored with helical rotation angles from 0° to 360° for each helix and both left and right handed crossing angles of 25° and -25° respectively. The step size was 45° with four trials carried out for each conformation, using a molecular dynamics (MD) simulation of all atomic coordinates allowing rotation- and crossing-angles to vary. These calculations used a non-bonded cutoff of 13Å with a switching function for van der Waals and electrostatic terms between 10Å to 12Å. The resulting structures were analyzed to determine the final crossing angle and rotation angles of both helices.

Clustering the dimers identified seven significant left handed clusters (defined as a minimum of 8 structures within a 1Å cut off, see fig. S7A) and another three right handed clusters (data not shown). Of all clusters, Cluster 1 has the lowest average non-bonded interaction energy of -69.3kcal/mol, making it the "best" cluster overall. Unlike other clusters, Cluster1 has the helices packed in a two-fold symmetric orientation. The average molecular structure from cluster 1 is shown in fig. S7B. The dimer interface is lined by predominantly hydrophobic residues including Leu269, Ile272, Phe276, Phe283 and Leu286. Although there are two polar residues in the sequence (Thr279 and Ser288) theoretically capable of stabilizing the dimer through hydrogen bonding, these do not contribute to inter-helix bonding. The closest approach between the two helices is at Val280, where the axes of the helices are separated by 8.3Å. This brings two phenylalanines, Phe276 and Phe283, into close proximity as pairs in the dimer interface. This stacking of the Phe rings explains the two substantial contributions to the interaction energy seen in fig. S7D at these positions in the helix, Phe276 and Phe283. These residues provide most of the observed binding energy.

We carried out the same analysis with the chicken GHR TMD helix, which differs substantially in its sequence (fig. S7C). For the chicken GHR, there are four left handed clusters and two right handed clusters, with the best result being left handed Cluster4. When the average structure from Cluster4 was superimposed onto the best cluster from human GHR, the backbone RMSD was found to be 1.54Å, with the symmetry of the transmembrane helices unchanged (fig. S7C). From the average interaction energy plot (not shown), the residues that contribute to the dimer stability are similar to those in human GHR. The closest approach between the two helices is at Val253, equivalent to Val280 in human GHR.

Coarse Grain Simulations in Lipid Bilayers

The model for the GHR TMD was composed of a sequence of 33 amino acids that included the transmembrane domain EEDFYFPWLLIIIFGIFGLTVMLFVFLFSKQQR in di-palmitoyl phosphatidylcholine using the coarse-grain MARTINI model (*31*) imposing a helical structure between Phe265 and Phe287 based on input from atomistic simulations (Fig. 6A). The protonation state of interfacial amino acids in the coarse-grain and atomistic models was assigned according to neutral pH conditions. To drastically sample all accessible configurations at 323K we employed the multiple-walkers, multiple-windows expanded density of states

$(MW)^2$-XDOS method (*32, 52*), an efficient Monte Carlo algorithm that allows continuous uniform sampling of lateral centers of mass separations without a priori knowledge of the free energy profile. Simulations were performed over 16 windows with 8 pairs in each window; all 128 pairs were capable of forming dimers or sample large separations where no correlations persist through replica exchanges between different processors. Free energy profiles and characteristics of the association process were extracted as described in the literature (*32, 34, 53*) (fig. S8).

Atomistic Molecular Dynamics in Lipid bilayers

Atomistic simulations in di-palmitoyl phosphatidylcholine bilayers were performed using the GROMOS 53a6 force field (*54, 55*) and GROMACS 4.5.1 and 4.5.4 (*56*) at 323K. We employed semi-isotropic pressure coupling at 1atm, a time-step of 2 s by constraining all bonds with LINCS, a twin range-cutoff for van der Waals interactions (0.9 and 1.4nm) and particle mesh Ewald for electrostatics (*57-59*). A single helical GHR TMD was inserted in a lipid bilayer. Removing overlapping molecules resulted in 110 lipid and 6364 water molecules being added with necessary ions included to maintain charge neutrality (counterbalancing E, E, D, K and R of the GHR TMD). For the single TMD simulation, after a pre-equilibration period the total simulations consisted of 0.4μs. For dimers, helices were first superimposed to the maintained helical domain of the coarse-grain model. Then after a similar insertion procedure starting with a larger bilayer of 256 lipids was followed, this resulted in structures with approximately 230 lipids and total of 50,000 atoms subjected to simulations of 0.3-0.7μs. All mutations of TMDs were performed with Modeller and loop-refining protocols a posteriori on hundreds of snapshots from the trajectories created.

Linking the GHR TMDs to ECD Structure

The hGH:ECD hGH receptor crystal structure (PDB id: 3HHR structure; (*2*)) was retrieved from the Protein Data Bank and connected to the predicted left handed dimer using an iterative procedure. The two structures were aligned with their main axis parallel and five different separations along this axis were selected (2 to 4.5nm between Pro234 of the membrane-proximal domain in GHR and Glu260 of the TMD). For each separation 12 different rotations of the TMD dimer were performed (by 30°). For each TMD, missing residues were constructed with Modeller and a standard loop-refining protocol that included a series of energy minimization and MD steps with simulated annealing. The optimal structure out of the 600 constructed totally based on Modeller's standard objective function is shown in Fig. 6C.

Supplementary Materials and Methods

Cell Culture

Ba/F3 cells were cultured in Ba/F3 growth media: RPMI medium 1640 with 2 mM L-glutamine (Life Technologies), 10% Serum Supreme (Lonza), and IL-3 (supplemented to provide 1 × maximum growth determined by MMT assay on Ba/F3 cells; IL-3 produced from supernatant from baculovirus expression of SF9 cells, UQ Protein Expression Facility). Ba/F3 cells were starved in Ba/F3 starve media without IL-3 or GH (RPMI medium 1640 with 2 mM L-glutamine (Life Technologies), and 10% of Serum Supreme (Lonza) for Jun zipper fusions or 2.5% Serum Supreme for full length GHR proliferation assays). HEK293, HEK293T, COS-1, Plat-E, γ2A, and BHK-21 cells were cultured in DMEM 10% FBS (Life Technologies).

Expression Plasmid Constructs

Expression constructs for retroviral transduction of Ba/F3 cells were cloned into pMX-IRES-GFP (*60*) by exchanging the stuffer fragment with (human) hGHR or (rabbit) rGHR genes. The chimeric Jun leucine zipper GHR constructs were based on the previously described pcDNA3.1-Jun-pGHR (comprising pGHR signal peptide, HA-tag, c-Jun leucine zipper (residues 277-315), porcine GHR (residues 251-638)) (*24*). The pGHR sequence coding for resides 251-638 was exchanged for the coding sequence for the same residues from either rGHR or hGHR. The GHR residues 251-638 include the ECD 12 amino acid linker; therefore constructs that were created without the linker comprise residues 263-638. The different length linkers, alanine insertions, and substitutions were made by restriction digestion and ligation of restriction digested annealed oligonucleotides or PCR mediated site-directed mutagenesis. Point mutations in full length constructs were created by PCR mediated site-directed mutagenesis (details including primers used are available upon request). The constructs containing the ^{260}EED mutations to AAA or KKR in full length rGHR were moved into both pQCXP CMV/TO DEST and pQCXIH CMV/TO DEST (Addgene plasmid 17386 and 17394 (*61*)) by Gateway cloning. Expression constructs for HA-tagged hGHR and Box1 mutant GHR (299P, 300P, 302P, 304P all converted to alanine) were also moved into pQCXP CMV/TO DEST as above. The Box1 mutant (HA-hGHR-Box1) was created by PCR mediated site-directed mutagenesis and overlap extension. All constructs were verified by DNA sequencing.

Rabbit GHR (rGHR) FRET reporter constructs were created based on the previously described hGHR322Δ-FP (*5*). This previous construct was numbered according to first residue after signal peptide cleavage. For consistency with this manuscript 322 is equivalent to 340 when numbering from the first translated residue. Jun zipper-rGHR constructs and full-length GHR constructs (described above) were amplified by PCR to include the N-terminal signal peptide and HA-tag and were cloned into pmCFP-N1 or pmCit-N1 so that the coding sequence following residue 341 of rGHR (fusion resulted in restoration of an extra GHR residue) was fused to the N-terminus of mCFP or mCit using standard cloning techniques. The D170H mutation was introduced using overlapping oligonucleotides incorporating the mutation, PCR generating two fragments which were subsequently used in overlap extension and the mutant sequence was exchanged with the wild type sequence by restriction enzyme digestion and ligation. pJAK2 FRET reporter constructs were created by amplifying full length murine JAK2 or truncated after residue 533 by PCR from pBSK-JAK2 (kindly provided by J. N. Ihle, St. Jude Children's Research Hospital, TN, USA). Full length JAK2 was fused N-terminal or C-terminal to mCFP or mCit by cloning into the vectors pmCFP-N1, pmCFP-C1, pmCit-N1 and pmCit-C1. In order to place FRET reporters in a similar position to the pseudokinase domain of JAK2, the JAK2 coding sequence corresponding to the FERM and SH2 domains (amino acids 1-533) was fused to the N-terminus of mCFP and mCit as described above. All constructs were verified by DNA sequencing (primers and cloning details available upon request). Constructs used for cysteine crosslinking studies are detailed below.

A JAK2 expression construct was made via PCR using primers incorporating *Nhe*I and *Not*I sites and pBSK-JAK2 as template, and subsequently cloned into the same sites of pJAK2-mCFP. An expression construct for JAK2 with the kinase domain and pseudokinase domain swapped (referred to as JAK2-KP) was created by circular polymerase extension cloning (CPEC) based on the previously described method (*62*). Briefly, three PCR products were created using KOD Hot Start DNA Polymerase (Merck) following the manufacture's protocol in a 50µl

reaction with pJAK2-mCFP as template and the following primer pairs (Jak2 Kinase-C-N-Pseudo R: CCCTGTCTTCAAAAGCACCAGAAAACCCCGCAGCTATACTGTCCCGGATTTGATCC and Jak2 KinaseN-SH2-F: GCATAATAATGTGAATCAAATGGTGTTTCACAAAATCGACCCTACACAGTTTGAAGA GAGACACTTGAAGTTTC), Jak2 Kinase-C-N-Pseudo F: GGGGTTTTCTGGTGCTTTTGAAGACAGGAATGAAGATTTAATATTTAATGAAAGTCT TGGCCAAGGT and Jak2 PseudoEndstop-vec-R: CAAATGTGGTATGGCTGATTATGATCTAGAGTCGCTCAACCAGAAAACCCTAGGGC ACCTATTCTCATG), and (Vect3'F : GCGACTCTAGATCATAATCAGCCATACCACATTTG and Jak2 SH2 R: GATTTTGTGAAACACCATTTGATTCACATTATTATGC). Each amplified product was purified using a PureLink PCR purification Kit (Invitrogen). An equal molar amount of each product was used in a single 50µl reaction containing 1× Phusion HF Buffer, 0.5 µl Phusion Hot Start II DNA Polymerase (Finnzymes), and 200 µM each dNTPs. The reaction mixture was denatured at 98°C for 30 sec, 20 cycles of 98°C for 10 sec, 70°C for 30 sec, and 72°C for 155 sec, followed by a final incubation of 72°C for 5 min. DH5α cells were transformed using 1µl of the CPEC reaction and single colonies were isolated and correct constructs were verified by DNA sequencing. The resulting construct for JAK2-KP corresponds to: FERM-SH2 (Met1-Ile540) kinase (Asp840-Ala1132) -kinase-pseudokinase linker (Gly831-Arg839) pseudokinase (Asn542-Gly834).

Retroviral transduction

Retroviral expression vectors were transfected into Plate-E cells (*63*) using Lipofectamine 2000. Plat-E cells were kindly provided by Dr. Kitamura (Tokyo Univ., Tokyo, Japan). Supernatant from transfected Plat-E cells was used to transduce Ba/F3 cells in the presence of 8µg/ml polybrene and IL-3. Transduced cells were cultured as normal in Ba/F3 growth media and were sorted for GFP positive cells by FACS.

Cysteine Crosslinking Studies

Cells were transfected with a series of N-terminal HA-tagged hGHR mutants in pcDNA3.1 truncated at residue 389 where each residue from Pro252 to Ser288 was converted to a cysteine after converting Cys259 to serine. Receptor constructs were titered to give a mimimal level for clear detection *ie* 100 ng/well (6 well plate). Crosslinking was performed 16-20 hours after transfection. Cells underwent cross-linking treatment with MTS-2-MTS (1,2-ethanediyl bismethanethiosulfonate; Toronto Research Chemical) or direct disulfide bond formation with Cu-o-phenanthroline. For cross-linking with MTS-2-MTS (*64*), COS-1 cells were transfected and MTS-2-MTS was added to intact cells at a 1mM final concentration in PBS 0.1mM $CaCl_2$, 1mM $MgCl_2$, 0.015% saponin in DMEM pH 8.0 and incubated for 10 min. Samples were lysed in homogenizing buffer (1% NP-40, 10% glycerol, 150mM NaCl, 50mM Tris-HCl pH 7.6, 50mM NaF, 1mM $ZnCl_2$, 1mM Na_3VO_4, 2% β-mercaptoethanol) containing 1 × Complete Protease Inhibitor Cocktail (Roche)), 12µl of cleared lysate was mixed with 6µl of 3× sodium dodecyl sulphate (SDS) sample buffer (20% SDS, 10% glycerol, +/- 1 M DTT, bromophenol blue), boiled and run on non-reducing SDS-PAGE gels, then immunoblotted and probed with HA.11-antibody (Covance). For direct disulfide bond formation with Cu-o-phenanthroline, transiently transfected HEK293 cell membranes were crosslinked essentially as previously described (*49*) with 0.40mM $CuSO_4$ and 1.60mM o-phenanthroline for 10 min at 37°C after

addition of 2 nM hGH. The reaction was terminated with 10 mM EDTA prior to SDS-PAGE. Samples were lysed in RIPA buffer and run on non-reducing SDS-PAGE gels as above, immunoblotted and probed with HA.11-antibody (Covance).

For signaling analysis, HEK293 cells were transfected with full length hGHR expression constructs coding for the same cysteine mutations from Pro252 to Ser288 as above with Cys259 to serine, together with 30 ng *stat5* cDNA in pcDNA3.1. STAT5 phosphorylation was analyzed by resolving extracts using reducing SDS-PAGE, western blotting and probing with anti-phospho-STAT5-tyrosine694 antibody (Cell Signaling Technology, cat 9351) and with total STAT5 antibody (SantaCruz C-17).

FRET Analysis

FRET analysis by live cell imaging was performed using confocal microscopy of BHK cells 24 hours post-transfection. For live cell imaging 2×10^4 BHK-21 cells were seeded in 2 ml DMEM medium in a 35 mm glass bottom dish and transfected after 24 hours. Co-transfection was performed with 1μg of each plasmid. Confocal microscopy was carried out 48 hours after transfection. Using filter-settings for donor-channel, acceptor-channel and FRET-channel, three images were recorded and FRET calculated afterwards. All confocal images were acquired using a Zeiss LSM-510 META inverted laser scanning confocal microscope (Carl Zeiss GmbH, Oberkochen, Germany). As objective a 63× oil immersion plan apochromat with numerical apertures of 1.4 was used. Images were recorded at 12 bit depth and a size of 512 × 512 pixels. During measurements, regions of too high intensity (outside of the dynamic range) were excluded. All settings for detector gain and laser power were made at the beginning of imaging and not changed during FRET sample measurements. Zeiss LSM-510 software package was used to adjust settings and save pictures. Image editing and conversion was performed with Fiji (based on ImageJA 1.42I) with LSM-Toolbox (Patrick Pirrotte, v4.0b). The imaging raw data were exported and for each sample three images (donor-channel, acceptor-channel and FRET-channel) were imported into IgorPro (v6.05, WaveMetrics Inc., Lake Oswego, USA). Background correction was done by defining and averaging a region-of-interest (ROI) outside of the cell and excluding all pixels below this value plus 3-fold its standard deviation. Areas which showed overexpression (signal out-of-range) were excluded as well. Cross-talk factors were calculated by setting and averaging a ROI within cells, which expressed donor and acceptor only. The G-factor, relating the loss of donor emission due to FRET in the donor-filter-set and the gain of acceptor emission due to FRET in the FRET-filter-set, was determined by calibration, using a cell expressing the covalently fused mCFP-mCitrine. The G-factor was adjusted to reach a FRET-efficiency of 0.35 ±0.03 (35% ±3%). FRET efficiencies were then calculated pixel wise in a batch procedure for all images, as previously described (*65*) and FRET efficiency images of cells were graphed.

FRET analysis by flow cytometry was performed on transfected BHK cells (as described above) using a BD FACS CantoII flow cytometer (BD Biosciences) to measure fluorescence of cells in donor- (405 nm excitation, 450/50 nm emission), acceptor- (488 nm excitation, 530/30 nm emission) and FRET-channels (405 nm excitation, 585/42 nm emission). Doublet discrimination was carried out to measure signals of single cells. FRET analysis of flow cytometer data was carried out as previously described with a custom written algorithms in IgorPro5 (Wavemetrics) (*50*). Calibration for normalized acceptor surface concentration cA was carried out essentially as described (*50*) using: $cA=N_{Ac}/A_{cell}R_0^2$, where N_{Ac}, the number of mCit fluorophores per cell, A_{cell} is the surface area of a model spherical BHK cell and R_0=4.7 nm, the

Försters radius of mCFP/mCit, calculated using spectroscopic data. Fluorescent beads (#1139, Bangs Laboratories) with defined fluorescein loading and size were used to determine N_{Ac} and A_{cell}. A fusion protein of mCFP-mCit was used to calibrate donor-acceptor ratio and FRET-efficiency. The FRET-efficiency was calculated per cell by using an adapted sensitized acceptor emission method. Only cells with a donor-mole fraction x_D=0.5±0.1, corresponding to a ~1:1 donor-acceptor ratio, were analyzed. The characteristic E_{max} value was determined using the equation $E=E_{max}-(A_1\ e^{-k1\ a\ (cA+cA_0)} + A_2\ e^{-k2\ a\ (cA+cA_0)})$ as previously described (*50*) where A_1=0.6322, k_1=3.1871, A_2=0.3678, k_2=0.7515, for R_c/R_0=0.7 (*66*), using R_c, the closest approach distance of the fluorescent proteins (=3.4 nm) (*50*). Curve fitting was carried out using IgorPro5 software by iterative minimization of χ^2 with the Levenberg-Marquardt algorithm. Standard errors in the fitting of E_{max} were calculated based on the residuals.

FRET analysis of membrane extracts from transfected HEK293T cells were performed on a fluorescence plate reader. For each sample 4×10^5 HEK293T cells were seeded into a well of a 6-well cell culture plate at an even distribution and incubated for 24 hours, then transfected with relevant constructs using 7µl Lipofectamine 2000. For analysis of HA-rGHR341Δ-mCFP/mCit and HA-rGHR(EED-KKR)341Δ-mCFP 1µg of each construct was used for transfection. Analysis of C-terminal or N-terminal mCFP/mCit labeled JAK2 was performed with 5 µg of each construct per transfection with 2 µg of pQCXP-rGHR, or 2 µg pQCXP-rGHR(EED-KKR), or 1 µg each of pQCXP-rGHR and pQCXP-rGHR(EED-KKR). Cells were treated, 24 hours after transfection, with 10mM sodium butyrate overnight and membrane extracts based on the method described by Han et al. (2005) (*67*) were performed. Briefly, cells were removed by quickly aspirating with a pipette, transferred to a centrifuge tube, centrifuged at 600*g* and washed with 1.5 ml ice-cold phosphate-buffered saline (pH7.4) containing 2mM Na_3VO_4. Cells were resuspended in 1ml of ice-cold buffer A (25mM sodium phosphate, 5mM $MgCl_2$, 2mM Na_3VO_4, pH 7.4 with 1× Complete Protease Inhibitor Cocktail (Roche)) and subjected to three rounds of freezing and thawing using a dry ice ethanol bath and 37ºC water bath with mixing between each thaw. Subsequently lysed cells were centrifuged at 17 000g for 20 min, resuspended in buffer A and centrifuged again for 20 min followed by resuspension in 100 µl of buffer A and stored at -80ºC. Each suspension was thawed and placed in a well of a black bottom 96 well plate (OptiPlate-96F, PerkinElmer) and fluorescence readouts were performed on a Synergy4-platereader (BioTek Instruments).

For experiments with addition of GH transfection conditions were optimized to determine the most GH responsive conditions by titration of HA-rGHR341Δ-mCFP/mCit. The minimal amount of GH required to give significant FRET responses was determined by titration of GH. Subsequent experiments used 10 ng of each plasmid for transfection with 6 µl Lipofectamine as above and 5 nM GH was added to cells in culture for 1 min prior to harvesting. For experiments using the antagonist G120R hGH cells were incubated for 10 min with 500 nM G120R hGH prior to addition of GH. G120R human GH (hGH) was expressed and purified as previously described (*68*). Cells were harvested in a similar manner as described above except ice-cold buffer B (25 mM Tris-HCl and 10 mM $MgCl_2$, 2 mM Na_3VO_4, pH 7.4 with 1 × Complete Protease Inhibitor Cocktail (Roche)) was used in place of buffer A and membrane extracts were not frozen and read immediately on a Synergy4-platereader. Appropriate filter settings were used to record intensities of donor-channel (excitation 420/50 nm, emission 485/20 nm), acceptor-channel (excitation 500/27 nm, emission 540/35 nm) and FRET-channel (excitation 420/50 nm, emission 540/35 nm). Background correction was performed by subtracting the intensity of a well with untransfected cells (background) from all other fluorescence intensities. Then cross-

talk factors were calculated with the donor-only and acceptor-only samples as described before. Using these cross-talk factors and the background-corrected FRET-samples in all three channels, the FRET-efficiency was calculated as previously described (*65*).

Homo-FRET anisotropy analysis of live cell surface transmembrane receptors

Construction of monomeric and dimeric homo-FRET controls were created by CPEC essentially as described above where primer sequences can be provided on request. The monomeric construct comprised the extracellular residues 1-142 of mouse RTPTα fused to the TMD of the LDL receptor (ALSIVLPIVLLVFLCLGVFLLW) and intracellular residues KNWRLKNINS followed by fusion to mCit resulting in RPTPα-LDLR(TMD)-mCit. The dimeric construct comprised the RTPTα residues 1-249 including the mutation P137C and fused at the C-terminus to mCit to give RPTPα(P137C)-mCit

HEK293 cells were transiently transfected with mCit, RPTPα(P137C)-mCit, RPTPα-LDLR(TMD)-mCit, and HA-rGHR341Δ-mCit. Cells were imaged live at 37°C by confocal microscopy and images acquired on a LSM710 Zeiss confocal microscope equipped with a 40× oil immersion objective (Plan Apochromat 40× 1.4 NA, Zeiss, Jena, GER). Images were acquired by using a 514 nm laser excitation line and collecting the corresponding emissions in the range 530-560 nm using band pass emission filters. Fluorescence emissions parallel (Ipar) and perpendicular (Iper) to the plane of excitation were acquired by splitting the emission light path using a polarized beam splitter. The fluorescence anisotropy was determined by measuring average values of Ipar and Iper on regions of interest at the plasma membrane in ImageJ and using the following equation:$r = \frac{Ipar - G \cdot Iper}{Ipar + 2 \cdot G \cdot Iper}$. where the correction factor G was estimated using r_0=0.39 of soluble mCitrine as reference (*16, 69*). Then, anisotropy values were then converted to homo-FRET efficiency values using the following equation (*17*) $E = 1 - \frac{r}{r_{mCit}}$. Data presented are mean efficiency values calculated across the different images (~50 cells per conditions) and their standard errors.

Analysis of GH stimulated JAK2 activation by rGHR341Δ FRET constructs

GH stimulated JAK2 activation was analyzed by expression of GHR constructs in HEK293 cells, immunoprecipitation (IP) of JAK2 and western blotting. Initially, small scale tests for expression of GHR constructs was performed in order to achieve similar expression levels for each GHR construct. For each experiment 3.8×10^5 HEK293 cells were seeded into a $25cm^2$ cell culture flask and transfected 6 hours later with 40 ng pHA-rGHRΔ-mCit or 300 ng pQCXP-HA-rGHR with Lipofectamine 2000, incubated in DMEM 10% FBS for 24 hours, then starved overnight by incubation in DMEM 0.5% FBS. Cells were stimulated with 5 nM hGH for 10 min at 37°C. Cells were harvested after washing in ice-cold PBS containing 2 mM Na_3VO_4, centrifuged at 400*g* for 5 min at 4°C, washed again in ice-cold PBS containing 2 mM Na_3VO_4 and cell pellet resuspended in ice-cold extraction buffer (50 mM Tris pH7.5, 150 mM NaCl, 5 mM EDTA, 0.5% Triton X-100, 2 mM Na_3VO_4, 30 mM NaF, 10 mM $Na_4P_2O_7$, and 1× Complete Protease Inhibitor Cocktail EDTA-free (Roche)). Protein concentrations for each lysate were determined by BCA protein assay (Pierce). 2.5 µl of anti-Jak2 (D2E12) XP antibody (Cell Signaling Technology, cat 3230) was then added to an equal amount of protein for each sample in a final volume of 200 µl of extraction buffer and incubated for 1 hour at 4°C on a rotating wheel. Protein G Sepharose 4 Fast Flow (GE Healthcare Life Sciences) was washed in extraction buffer and 60 µl of a 50% resuspended sepharose solution was then added to each protein-antibody mix

and incubated for a further hour at 4°C on a rotating wheel. Sepharose was pelleted by centrifugation at 5000*g* and washed twice with IP wash buffer (50 mM Tris pH7.5, 150 mM NaCl, 5 mM EDTA, 2 mM Na_3VO_4, 30 mM NaF, 10 mM $Na_4P_2O_7$, and 1× Complete Protease Inhibitor Cocktail EDTA-free (Roche)). Sepharose pellets were resuspended in 15 µl of 6 × SDS sample buffer (containing 100 mM DTT), incubated at 98°C for 5 min, centrifuged at 17 000*g* for 1 min and the supernatant was analysed on 7% SDS-PAGE gels with transfer to PDVF and immunoblot using anti-Phospho-Jak2 (Tyr1007/1008) (Cell Signaling Technology, cat 3771), anti-Jak2 (D2E12) XP. Expression of HA-tagged GHR was analysed from cell lysates using equalised amounts of protein on SDS-PAGE and western blotting using anti-HA (HA.11), and β-tubulin antibodies (Cell Signaling Technology, cat 21461).

Signaling analysis of JAK2 co-transfected with kinase pseudokinase domain swap JAK2

JAK2 deficient (and STAT5 deficient) γ2A cells (*70*), a gift from G. Stark (Imperial Cancer Research Fund, London), were seeded into 6 well plates at 1.5×10^5 cells per well and cultured overnight. Cells were then transfected with 3µl of Lipofectamine 2000, 100 ng pcDNA3.1-STAT5B, 150 ng pQCXP-hGHR (constructed as described above for rGHR), and the JAK2 expression construct. As overexpression of JAK2 leads to constitutive phosphorylation of STAT5, the amount of JAK2 required to give minimal background P-STAT5 while still give strong P-STAT5 signal upon GH stimulation was regularly determined as the amount required varied over time likely due to passage number of cells or batch variation in reagents such as Lipofectamine. The suitable amount of JAK2 expression plasmid used for transfection ranged between 10-0.1 ng DNA. Following transfection cells were incubated overnight and culture media was replaced with fresh media. Cells were cultured for another day and cells were starved overnight in DMEM with 0.5% FBS. Cells were washed in ice-cold PBS containing 1 mM Na_3VO_4, and harvested in ice-cold PBS containing 1 mM Na_3VO_4 using a cell scraper and centrifuged at 600*g*. Cells were lysed in RIPA buffer (50 mM Tris pH 7.4, 150 mM NaCl, 1% NP-40, 0.5% sodium deoxycholate, 0.1% SDS) containing Na_3VO_4, 10 mM $Na_4P_2O_7$, 30 mM NaF, and 1× Complete Protease Inhibitor Cocktail EDTA-free (Roche), and snap frozen in dry ice. JAK2 signaling was subsequently analysed by western blot for P-STAT5 signaling.

Analysis of interaction of JAK2 with GHR341Δ FRET constructs and kinase-pseudokinase domain swap JAK2 with GHR

The interaction of JAK2-KP with GHR and WT JAK with rGHR341Δ FRET constructs was determined by Co-IP. For each experiment, HEK293 cells at approximately 60% confluent in a $75cm^2$ cell culture flask were transfected with 3 µg HA-hGHR, 3µg HA-hGHR-Box1, or 400 ng HA-rGHR341Δ-mCit were co-transfected with 400 ng JAK2 or 400 ng JAK2-KP expression constructs with Lipofectamine 2000, incubated in DMEM 10% FBS for 24 hours, then starved overnight by incubation in DMEM 0.5% FBS. Immunoprecipitation of JAK2 was performed essentially as above except 6 µl anti-Jak2 antibody was used in each sample and each IP was incubated in a final volume of 600 µl of extraction buffer. Following SDS-PAGE and transfer, western blots were probed with anti-HA (HA.11) and anti-Jak2 (D2E12) XP. Expression of HA-tagged GHR was analysed from cell lysates using equalised amounts of protein on SDS-PAGE and western blotting using anti-HA (HA.11). Note that the HA-rGHR341Δ-mCit expression plasmid is much smaller than the retroviral pQCXP-HA-hGHR expression plasmid and the HA-rGHR341Δ protein lacks the FIELD internalization motif involved in ubiquitination and receptor degradation. Together these contribute to the difference expression levels observed when transfecting equal amounts of plasmid for the different GHR expression constructs.

JAK 2 Pseudokinase-Kinase Docking Studies

Janus kinase 2 (JAK2) consists of seven homologous subdomains, numbered from N-terminus to C-terminus as JH7 to JH1. Interactions between the JH1 (kinase) and JH2 (pseudokinase) subdomains are important for signal transduction in the growth hormone receptor. The pseudokinase domain spans residue 541 to 839 of JAK2, while the kinase domain spans residue 840 to 1132. While crystal structures of the JAK2 kinase domain were first published in 2006 (*41*) the structure of the JAK2 pseudokinase domain was only recently resolved (*42*). This crystal structure shows significant structural differences to previous homology models used to interpret functional and mechanistic aspects of JAK2 pseudokinase-kinase interactions.

To facilitate modeling of the pseudokinase−kinase domain interface, two lines of approach were taken. Firstly, the molecular docking program HADDOCK (*71, 72*) was used to generate physiologically plausible relative orientation of the kinase and pseudokinase domains. Here we imposed the distance constraints between Tyr1007 of the kinase domain and both Phe595 and Val617 of the pseudokinase domain. Co-mutation of these two residues, which lie in close proximity to each other, are required for constitutive activation. The second approach used the crystallographic symmetry of the JAK2 pseudokinase crystal structure (PDBID: 4FVP) to provide the relative orientation of domain pairs in the crystal structure. In this approach we hypothesized that exploiting the crystallographic packing of the individual domain structures may help identify a stable interface between the kinase and pseudokinase domain. The symmetry operator of 4FVP (P 1 21 1) was chosen over that of 2B7A (P 41) as it provided a greater number of possible interfaces. Starting from the crystallographic coordinates of 4FVP, the kinase domain (PDB id: 2B7A) was superimposed onto each of the pseudokinase domain crystal contacts to provide a possible relative orientation of the kinase-pseudokinase domains, using the protocol outlined below.

Molecular dynamics (MD) simulations were performed using the GROMACS (Groningen Machine for Chemical Simulation) package version 3.3.3 (*73*) in conjunction with the GROMOS 54A7 (*74*) force field for proteins. The simple point charge (SPC) water model (*75*) was used to describe the solvent water. The dimensions of the box were chosen such that the minimum distance between the protein and the box wall was at least 1.0nm. The non-bonded interactions were evaluated using a twin-range method. Interactions within the short-range cutoff of 0.9nm were updated every step. Interactions within the long-range cutoff of 1.4nm were updated every 3 steps together with the pair list. To minimize the effect of truncating the electrostatic interactions beyond the 1.4 nm long range cutoff, a reaction field correction was applied using a relative dielectric constant of ε_r = 78.5 (*76*). Neutral pH was assumed. The SHAKE algorithm (*58*) was used to constrain the lengths of the covalent bonds. The SETTLE algorithm (*77*) was used to constrain the geometry of the water molecules. In order to extend the timescale that could be simulated, explicit hydrogen atoms in the protein were replaced with dummy atoms, the positions of which were calculated each step based on the positions of the heavy atoms to which they were attached. This eliminates high frequency degrees of freedom associated with the bond angle vibrations involving hydrogens, allowing a time step of 4fs to be used to integrate the equations of motion without affecting thermodynamic properties of the system significantly (*78*). The simulations were carried out in the NPT ensemble at T = 300 K and P = 1 bar. The temperature and pressure were maintained close to the reference values by weakly coupling the system to an external temperature and pressure bath using a relaxation time constant of 0.1 ps (*57*) and 0.5 ps, respectively. The compressibility was 4.5×10^{-5} bar. The

pressure coupling was semi-isotropic in the case of the membrane simulation and fully isotropic in the case of the simulations in water. Configurations were saved every 40ps for analysis. Images were produced using VMD (*79*).

Six individual conformations of the pseudokinase-kinase domain dimer were set up in MD simulations: five of these were derived from the crystallographic symmetry approach and one was derived from docking studies described above. All simulations were performed under periodic boundary conditions in a rectangular box. To equilibrate the system, 500 steps of steepest descent energy minimization were performed to relax the solvent while the conformation of the protein was restrained using a harmonic potential with a force constant of $1000 kJ \cdot mol^{-1} \cdot nm^{-1}$. Then a series of 2 ns simulations were performed in which the force constant was progressively reduced (500, 100, 50 and $10 kJ \cdot mol^{-1}$ nm^{-1}). Position restraints were then removed from all domains. New velocities were then assigned and unrestrained simulations were performed on each system for 40 ns. In each of the conformations derived from crystallographic symmetry, the interface between the pseudokinase and kinase domain was not stable in MD simulations and the domains adopted a random orientation throughout the simulations. In contrast, in the docked conformation, the contact interface between the domains associated more closely in simulations to form a stable pseudokinase-kinase domain conformation that was maintained throughout the 40 ns simulation.

Analysis of JAK2 Pseudokinase-Kinase domain interaction

We applied a unique combination of cell-free protein expression, AlphaScreen and single molecule fluorescence analysis to dissect the interaction between the Pseudokinase and Kinase domains of JAK2. We expressed fluorescently-tagged Pseudokinase-Kinase, Pseudokinase or Kinase truncations in the eukaryotic *in vitro* translation system derived from *Leishmania tarentolae* (*80*). This system is suitable for co-expression of multiple exogenous cDNAs and allows production of large multidomain proteins in active form.

AlphaScreen cMyc detection and Proxiplate-384 Plus 384-wells plates were purchased from Perkin Elmer. Proteins (one bearing a N-terminal eGFP tag, the other labeled with C-terminal mCherry-Myc) were co-expressed in the cell-free system by adding mixed DNA vectors in 10 µL of the *Leishmania tarentolae*-based cell-free system (to a final DNA concentration of 30 nM for the GFP-vector and 60 nM for the Cherry-vector) The mixture was incubated for 3.5h at 27°C. Four serial dilutions of the proteins of ¼ were made in buffer A (25 mM HEPES, 50 mM NaCl). The AlphaScreen Assay was performed in 384-well plates. Per well, 0.4 µg of the Anti-Myc coated Acceptor Beads (PerkinElmer) was added in 12.5 µL reaction buffer B (25 mM HEPES, 50 mM NaCl, 0.001% NP40, 0.001% casein). 2 µL of the diluted proteins and 2 µL of biotin labeled GFP-nanotrap (diluted in reaction buffer A to a concentration of 45 nM) were added to the acceptor beads, followed by incubation for 45 min at RT. Then 0.4 µg of Streptavidin coated Donor Beads diluted in 2 µL buffer A was added, followed by an incubation in the dark for 45 min at RT. AlphaScreen signal was recorded on a PE Envision Multilabel Platereader, using the manufacturer's recommended settings (excitation: 680/30nm for 0.18 s, emission: 570/100nm after 37 ms). The signals were then averaged and normalized to background.

Single molecule spectroscopy was performed based on the previously described methods (*81, 82*). The method is based on a simple principle: on a confocal microscope, an excitation laser creates a very small observation volume (~1 fL). The proteins are tagged with genetically-

encoded GFP fluorophores (fig. S9D). Proteins diffuse freely by Brownian motion, and they enter and exit the confocal volume constantly. For single-molecule brightness analysis, the samples were diluted to approximately 100 pM concentration, so that only single proteins are present in the confocal volume. The fluorescence intensity was binned in 1 ms intervals, *ie* we calculate the number of photons collected in 1 ms. When a protein goes through the focal volume, a fluorescent burst is detected, and its brightness is analyzed to access the number of proteins in possible oligomers. In case of a dimer, the burst size will be approximately twice as high as in case of a monomer. Samples were reduced to a volume of 20 µl and placed into a custom-made silicone 192-well plate equipped with a 70 × 80 mm glass coverslip (ProSciTech). Plates were analyzed on a Zeiss LSM710 microscope with a Confocor3 module, at room temperature. A 488 nm laser focused in solution using a 40× 1.2 NA water immersion objective (Zeiss); fluorescence was collected and filtered by a 505-540 band pass filter. The experiment was calibrated using GFP expressed in the same cell-free extracts.

In fig. S9E, the brightness of the bursts is plotted against the number of bursts of that brightness. Due to random diffusion, most of the events are incomplete transfer through the focal volume, and few bursts represent the maximal number of photons that the GFP-tagged proteins can emit. For GFP, we obtained a profile of burst sizes that rapidly decreases and shows that the largest burst we observed was about 100-110 photons.

The Jak2 Pseudokinase-Kinase domains were analyzed in the same conditions. The data in fig. S9E show a different slope of distribution of brightness, with a maximal value of 220-230 photons, suggesting that this truncated domain can form stable dimers. The analysis of binding of the PseudoKinase and Kinase domains separately reveals that the PseudoKinase domain but not the Kinase domain can form dimers at single-molecule concentration (fig. S9F). In case of larger oligomerization of the GFP- labeled Jak2 domains, multiple proteins and their fluorescent labels would pass the confocal volume at the same time, resulting in an even higher photon count. The data show clearly that the Jak2 truncated domains do not form non-specific aggregates.

Supplementary Figure Captions

Fig. S1. Sequence conservation of the GHR TMD and JM residues. Sequence alignments of GHR TMDs and JMs showing key conserved residues including the GxxG motif and Lys 289.

Fig. **S2**. **A diagrammatic representation of the ToxR assay.** The chimeric protein consisting of the N-terminal domain of the maltose binding protein (MBP, in red) was fused to the cytoplasmic domain of the ToxR transcriptional activator (in blue) via a transmembrane domain (TMD) of interest (in orange). The MBP is then located in the periplasmic space, between the inner and outer membranes of *E. coli*. TMD mediated homodimerization of this chimera leads to the ToxR dimer binding to the cholera toxin promoter, *ctx* (in light green) and activating transcription of the lacZ gene (in dark green) followed by translation of the β-galactosidase protein (β-gal), the activity of which is determined and expressed in Miller units, corrected for protein expression by MBP immunoblot. Adapted from Langosch *et al.* (*14*).

Fig. S3. Extent of dimer formation of GHR cysteine mutants in the absence of crosslinker shown as a HA-immunoblot of a non-reducing Laemelli gel. Samples run in parallel to experiment shown in Fig. 3D as described in Supplementary Materials. Note correlation of dimer formation with constitutive signaling shown in Fig. 3D and absence of dimer in C259S mutant.

Fig. S4. The JAK2-KP construct is able to effectively bind GHR, and the GHR truncated FRET constructs are able to bind JAK2 effectively. The full length HA-GHR or HA-GHR-341-mCit construct were co-transfected with the WT JAK2 or the domain reversed JAK2-KP expression plasmid into HEK293 cells as described in the Supplementary Materials, and after immunoprecipitaion with a JAK2 antibody, the subsequent immunoblot was probed for HA. As a control, a Box1 mutated construct was used which does not bind JAK2. Representative blot shown from three independent experiments.

Fig. S5. Construct used for FRET studies (rGHR341-mCit) is able to activate JAK2 in response to GH addition in HEK293 cells. Cells were stimulated with 5 nM hGH for 10 min as detailed in the Supplementary Materials, and activation of JAK2 was demonstrated by immunoblot for Y1007/1008 in the activation loop of JAK2. Note that the mature form of the rGHR341-mCit at the cell surface would be the GH responsive form, with similar expression to the HA-GHR control. Representative blot shown from three independent experiments.

Fig. S6. The decreased FRET in the ICD seen with 3Ala insertions for JUN-3Ala-rGHR-341-mCFP/mCit insertions is not a consequence of FRET fluorophore orientation, since the decrease is seen when a flexible linker (RSIAT) attaches the reporter to the ICD.

Fig. S7. *In vacuo* modeling of the hGHR TMD helices using CHI software (*51*). (**A**) Plot of the f1 and f2 helical rotation values for the left handed dimer clusters. The capital 'A' indicates the orientation of the average structure in each cluster. (**B**) Dimer structure of the hGHR TMD helices for Cluster 1. Residues contributing most to the interaction energy as indicated in (**D**) are shown as rods colored by atom type. (**C**) Sequence alignment of human and chicken GHR TMD sequences highlighting non-conserved residues in blue. Superimposition of the best cluster TMD helix backbone alignment of chicken GHR (blue) on to the Cluster 1 human GHR backbone alignment (yellow) showing close similarity (RMSD 1.54Å). The helices share the same symmetry, although the register of the helices is shifted by about 1.6Å. (**D**) Graph showing calculated helix interaction energy contributed by each residue in the Cluster 1 model of the helix dimer.

Fig. S8. Atomistic MD modelling of GHR TMD in DPPC lipid bilayer shows helix from Phe265 to Lys289, and stable tilt angle relative to bilayer normal of around 20 degrees after only 0.2 µsec. The tilt of the helix is promoted by a hydrophobic mismatch and flanking residues that are on the same face of the helix but favor tilting in different directions. Specifically, Tyr264 and Trp267 are located at the interface of the hydrophilic/hydrophobic domain with the Trp inducing helix tilting towards the opposite direction than Lys289 (see also Fig 6).

Fig. S9. The JAK2 Pseudokinase-Kinase domain for dimers as determined by AlphaScreen and single-molecule brightness analysis. (**A**) JAK2 domain diagram illustrating positions of domains used for analysis. (**B**) Diagram illustrating set up used for AlphaScreen. (**C**) Domain interaction analysis by AlphaScreen shows Pseudokinase-Kinase domain formation. (**D**) Schematic of the focal volume and free diffusion of the GFP-tagged JAK2 domains. (**E**) Calibration of the brightness of GFP used for single molecule brightness analysis. Single-molecule brightness analysis of truncated JAK2 reveals formation of dimers driven by the PseudoKinase-PseudoKinase (PK-PK) interaction (F). Distribution of bursts obtained for PseudoKinase-Kinase (PK-K), Pseudokinase (PK), and Kinase (K) respectively. Maximal burst size obtained for the different constructs, with the GFP calibrating the number of photons expected for a monomeric protein.

Fig. S1

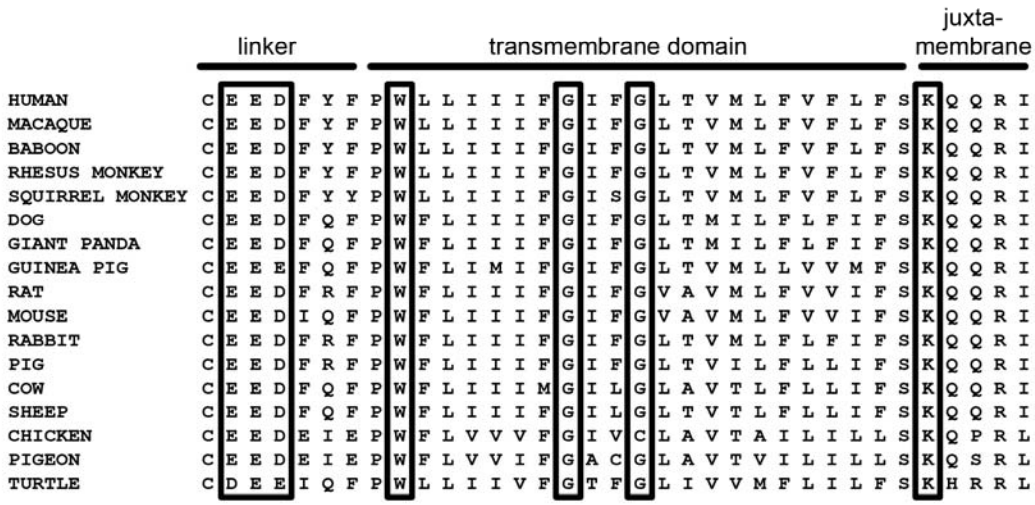
linker
transmembrane domain
juxta-membrane
HUMAN C E E D F Y F P W L L I I I F G I F G L T V M L F V F L F S K Q Q R I
MACAQUE C E E D F Y F P W L L I I I F G I F G L T V M L F V F L F S K Q Q R I
BABOON C E E D F Y F P W L L I I I F G I F G L T V M L F V F L F S K Q Q R I
RHESUS MONKEY C E E D F Y F P W L L I I I F G I F G L T V M L F V F L F S K Q Q R I
SQUIRREL MONKEY C E E D F Y Y P W L L I I I F G I S G L T V M L F V F L F S K Q Q R I
DOG C E E D F Q F P W F L I I I F G I F G L T M I L F L F I F S K Q Q R I
GIANT PANDA C E E D F Q F P W F L I I I F G I F G L T M I L F L F I F S K Q Q R I
GUINEA PIG C E E E F Q F P W F L I M I F G I F G L T V M L L V V M F S K Q Q R I
RAT C E E D F R F P W F L I I I F G I F G V A V M L F V V I F S K Q Q R I
MOUSE C E E D I Q F P W F L I I I F G I F G V A V M L F V V I F S K Q Q R I
RABBIT C E E D F R F P W F L I I I F G I F G L T V M L F L F I F S K Q Q R I
PIG C E E D F R F P W F L I I I F G I F G L T V I L F L L I F S K Q Q R I
COW C E E D F Q F P W F L I I I M G I L G L A V T L F L L I F S K Q Q R I
SHEEP C E E D F Q F P W F L I I I F G I L G L T V T L F L L I F S K Q Q R I
CHICKEN C E E D E I E P W F L V V V F G I V C L A V T A I L I L L S K Q P R L
PIGEON C E E D E I E P W F L V V I F G A C G L A V T V I L I L L S K Q S R L
TURTLE C D E E I Q F P W L L I I V F G T F G L I V V M F L I L F S K H R R L

Fig. S2

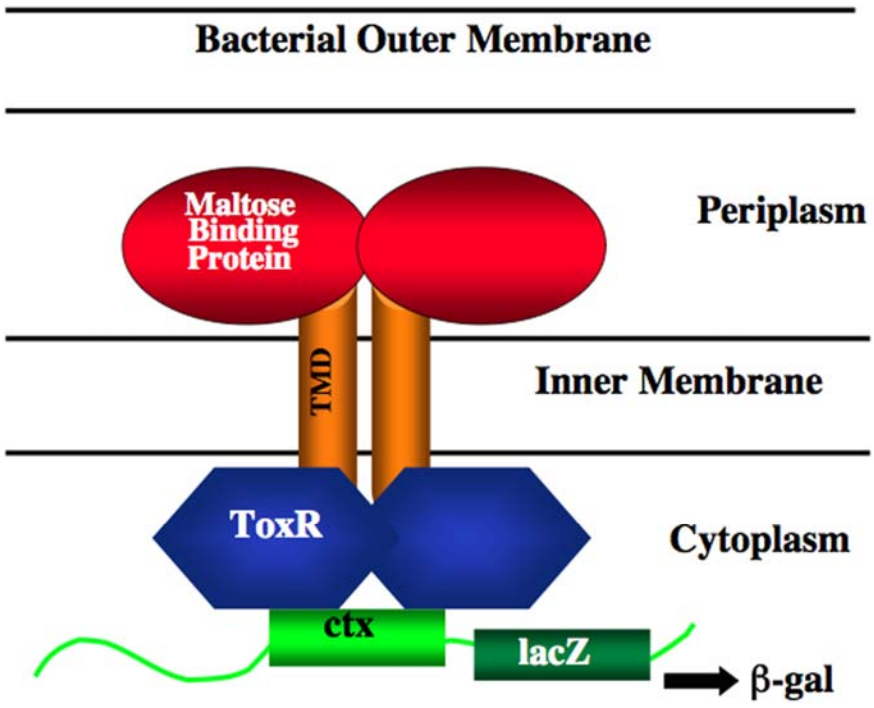
Bacterial Outer Membrane
Maltose Binding Protein
Periplasm
TMD
Inner Membrane
ToxR
Cytoplasm
ctx
lacZ
β-gal

Fig. S3

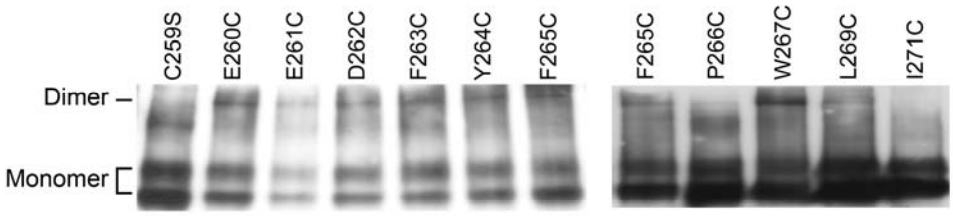
C259S
E260C
E261C
D262C
F263C
Y264C
F265C
F265C
P266C
W267C
L269C
I271C
Dimer
Monomer

Fig. S4

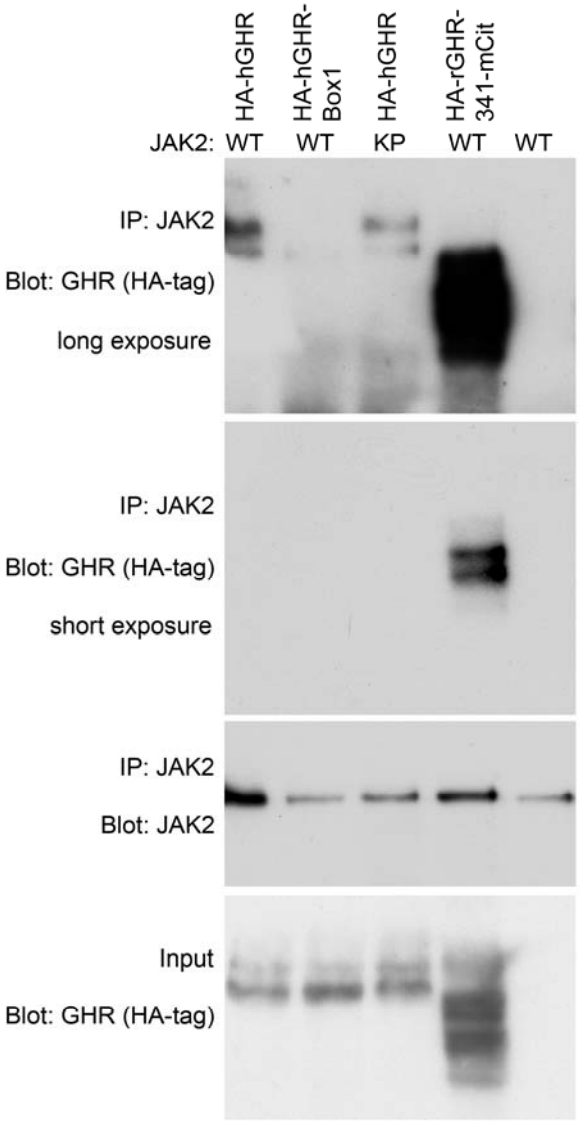
HA-hGHR
HA-hGHR-Box1
HA-hGHR
HA-rGHR-341-mCit
JAK2: WT WT KP WT WT
IP: JAK2
Blot: GHR (HA-tag)
long exposure
IP: JAK2
Blot: GHR (HA-tag)
short exposure
IP: JAK2
Blot: JAK2
Input
Blot: GHR (HA-tag)

Fig. S5

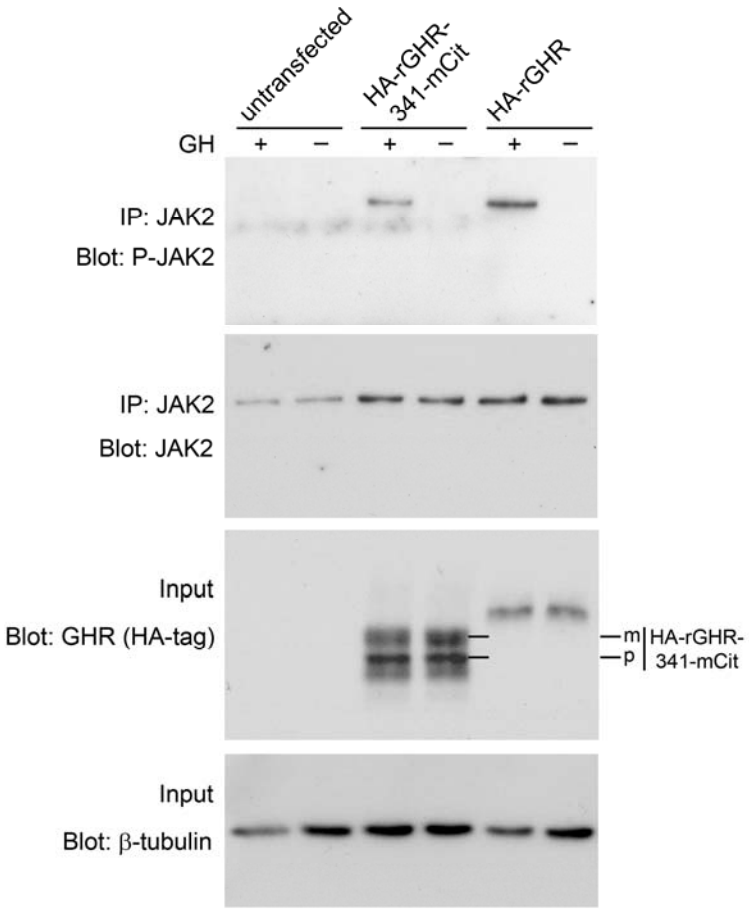
untransfected
HA-rGHR-341-mCit
HA-rGHR
GH
+
−
+
−
+
−
IP: JAK2
Blot: P-JAK2
IP: JAK2
Blot: JAK2
Input
Blot: GHR (HA-tag)
m
p
HA-rGHR-341-mCit
Input
Blot: β-tubulin

Fig. S6

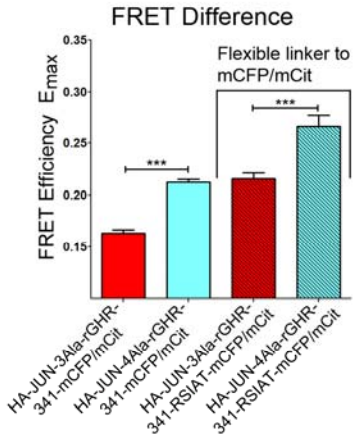
FRET Difference
FRET Efficiency Emax
0.35
0.30
0.25
0.20
0.15
Flexible linker to mCFP/mCit
***
***
HA-JUN-3Ala-rGHR-341-mCFP/mCit
HA-JUN-4Ala-rGHR-341-mCFP/mCit
HA-JUN-3Ala-rGHR-341-RSIAT-mCFP/mCit
HA-JUN-4Ala-rGHR-341-RSIAT-mCFP/mCit

Fig. S7

A

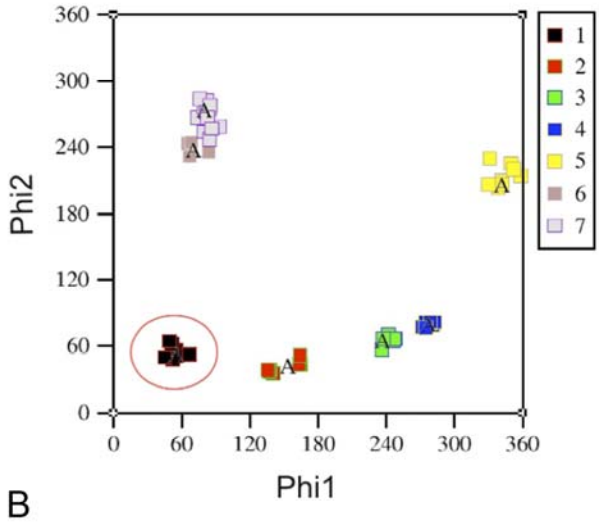
360
300
240
180
120
60
0
Phi2
0
60
120
180
240
300
360
Phi1
1
2
3
4
5
6
7

B

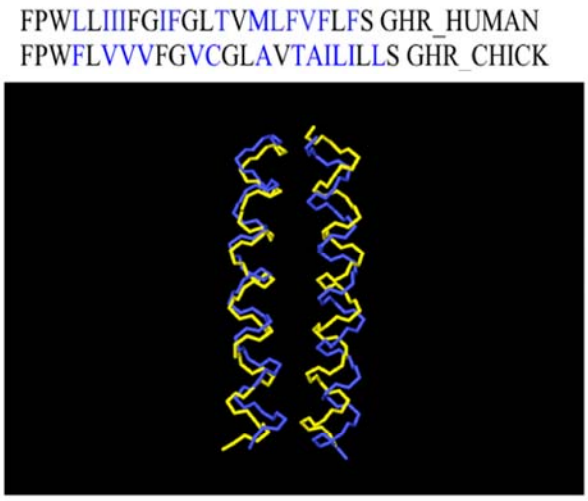
FPWLLIIIFGIFGLTVMLFVFLFS GHR_HUMAN
FPWFLVVVFGVCGLAVTAILILLS GHR_CHICK

C

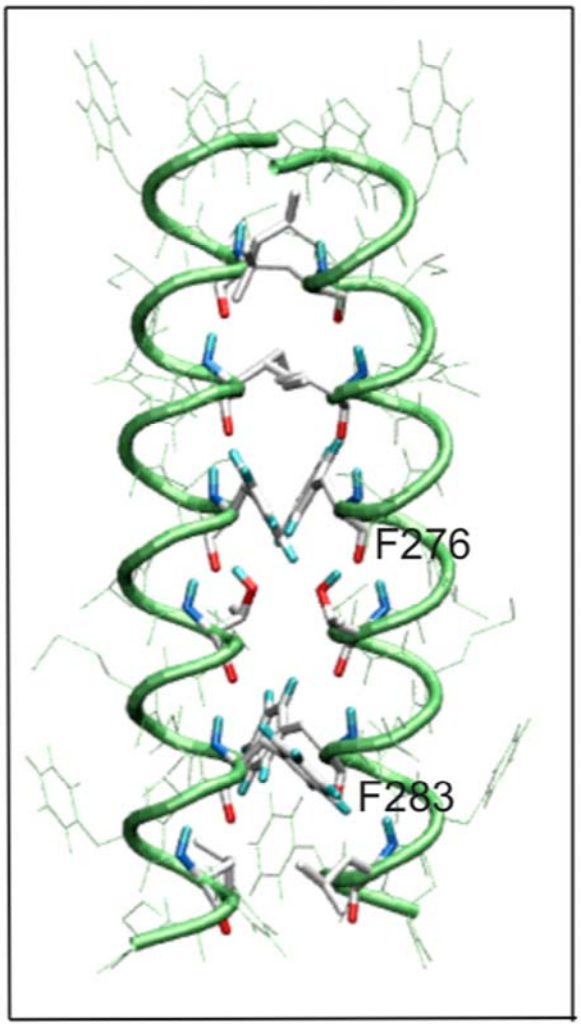
F276
F283

D

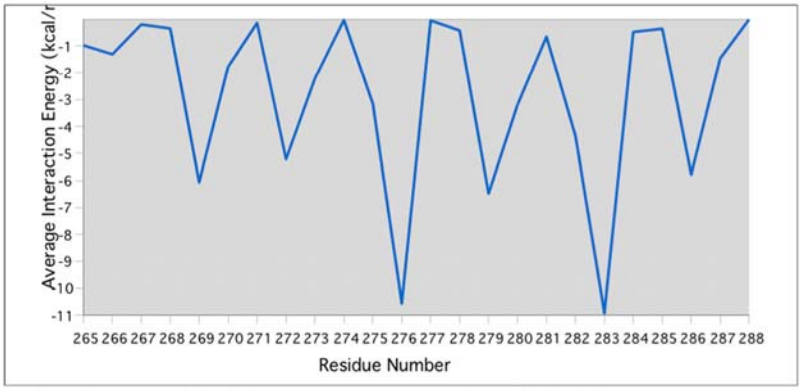
Average Interaction Energy (kcal/
-1
-2
-3
-4
-5
-6
-7
-8
-9
-10
-11
265 266 267 268 269 270 271 272 273 274 275 276 277 278 279 280 281 282 283 284 285 286 287 288
Residue Number

Fig. S8

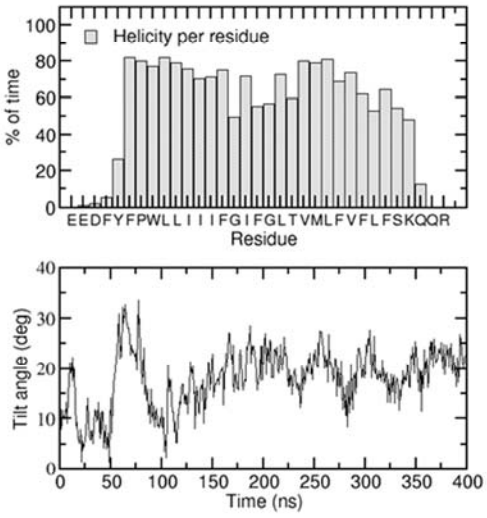
Helicity per residue
% of time
100
80
60
40
20
0
EEDFYFPWLLIIIFGIFGLTVMLFVFLFSKQQR
Residue
Tilt angle (deg)
40
30
20
10
0
0
50
100
150
200
250
300
350
400
Time (ns)

Fig. S9

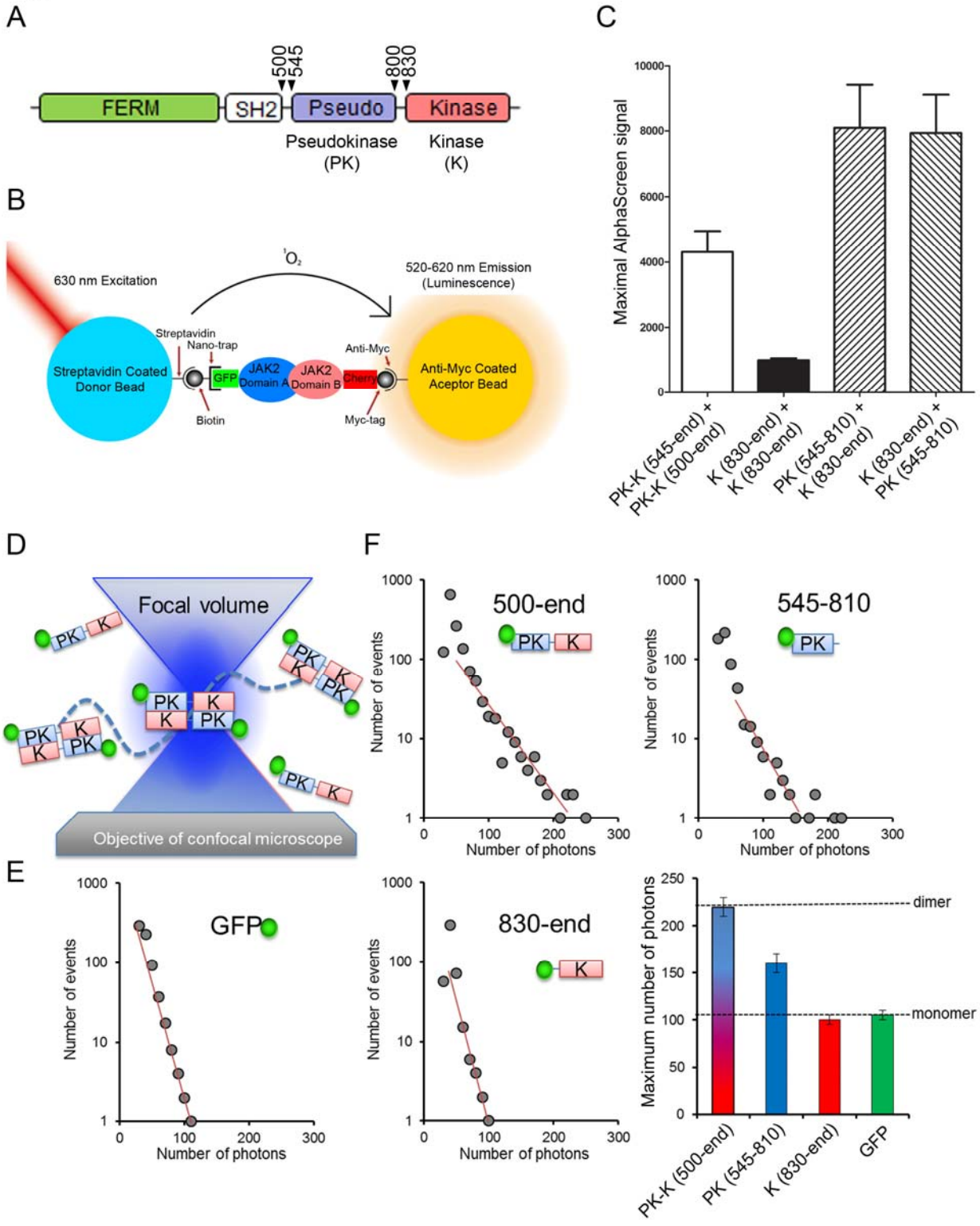
A
500
545
800
830
FERM
SH2
Pseudo
Kinase
Pseudokinase (PK)
Kinase (K)
B
630 nm Excitation
$^1O_2$
520-620 nm Emission (Luminescence)
Streptavidin Coated Donor Bead
Streptavidin
Nano-trap
Biotin
GFP
JAK2 Domain A
JAK2 Domain B
Anti-Myc
Cherry
Myc-tag
Anti-Myc Coated Aceptor Bead
C
Maximal AlphaScreen signal
10000
8000
6000
4000
2000
0
PK-K (545-end) + PK-K (500-end)
K (830-end) + K (830-end)
PK (545-810) + K (830-end)
K (830-end) + PK (545-810)
D
Focal volume
PK
K
Objective of confocal microscope
E
GFP
Number of events
Number of photons
F
500-end
545-810
830-end
Maximum number of photons
dimer
monomer
PK-K (500-end)
PK (545-810)
K (830-end)
GFP

Appendix X: Role of GH/IGF-1 Axis in Cancer (Review Article)

EXPERT REVIEWS

Role of the growth hormone–IGF-1 axis in cancer

Expert Rev. Endocrinol. Metab. 6(1), 71–84 (2011)

Yash Chhabra[1*], Michael J Waters[†1*] and Andrew J Brooks[1]

[1]*The University of Queensland, Institute for Molecular Bioscience, Brisbane, Qld 4072, Australia*
[†]*Author for correspondence:*
Tel.: +61 733 462 037
Fax: +61 733 462 101
m.waters@uq.edu.au

**These authors contributed equally to this article*

A substantial body of evidence supports a role for the growth hormone (GH)–IGF-1 axis in cancer incidence and progression. This includes epidemiological evidence relating elevated plasma IGF-1 to cancer incidence as well as a lack of cancers in GH/IGF-1 deficiency. Rodent models lacking GH or its receptor are strikingly resistant to the induction of a wide range of cancers, and treatment with the GH antagonist pegvisomant slows tumor progression. While GH receptor expression is elevated in many cancers, autocrine GH is present in several types, and overexpression of autocrine GH can induce cell transformation. While the mechanism of autocrine action is not clear, it does involve both STAT5 and STAT3 activation, and probably nuclear translocation of the GH receptor. Development of a more potent GH receptor antagonist or secretion inhibitor is warranted for cancer therapy.

Keywords: autocrine GH • breast cancer • colon cancer • epidemiology • GH receptor • growth hormone • insulin-like growth factor-1 • nuclear GH receptor • prolactin • prostate cancer • signal transducer and activator of transcription-5

Six decades of research have established that growth hormone (GH) plays a crucial role in promoting proportionate postnatal growth, and that this is largely mediated through the induction of IGF-1. This action is supported by important roles of GH in the regulation of metabolism, and of cardiovascular, renal, reproductive and immune functions. These roles are accomplished through ubiquitously expressed GH receptors (GHRs) which, similar to receptors for many other growth factors, signal through a tyrosine kinase (JAK2) able to activate STAT, Ras/ERK and PI3K/Akt pathways. The ability of GH to also induce IGF-1, both locally in a paracrine/autocrine manner [1,2] and in an endocrine manner via action on the liver, results in a particularly potent growth stimulus that requires tight control. This comprises feedback inhibition of GH secretion by pituitary somatotropes by hepatic (endocrine) IGF-1, as well as a set of negative regulators common to other growth factor/cytokine signaling factors: suppressors of cytokine signaling (SOCS), protein inhibitors of activated STAT (PIAS) proteins, phosphatases, receptor downregulation, and transcriptional regulation of receptor expression. Given the ability of GH and IGF-1 to promote cell proliferation, cell movement and angiogenesis, and to suppress apoptosis, it is not surprising that dysregulation of the tightly controlled GH–IGF-1 axis promotes neoplasia. As discussed here, converging data from recent epidemiologic, animal and *in vitro* studies indicate that the state of the GH–IGF-1 axis has important influences on cancer biology, cancer risk and carcinogenesis.

Actions of the GH–IGF-1 axis in relation to cancer

The risk of developing cancer is determined by genetic elements and by environmental conditions including diet and lifestyle. Recent evidence suggests that the GH–IGF-1 axis might provide a link between these factors and the disposition to cancer through its effects on normal cell proliferation, differentiation and apoptosis. The GH–IGF-1 axis influences several stages and aspects of cancer development and behaviour: cellular proliferation, cell survival, angiogenesis and metastasis, and even resistance to chemotherapy [3]. Being a potent and ubiquitous mitogen, IGF-1 can act on many cell types to bring about increased proliferation via the MAPK signaling pathway. Its anti-apoptotic actions are mediated via the PI3K/Akt pathway and can disrupt the tight control between cell proliferation and death leading to hyper-proliferation [4]. Carcinogenesis is a multistep process which involves accumulation of a number of genomic 'hits' leading to complete transformation and/or survival of partially transformed

 10.1586/EEM.10.73 ISSN 1744-6651

cells with one or a few hits [5]. In such a case, IGF-1 would increase the pool of transformed/damaged cells that are available for undergoing subsequent hits. This implies that higher levels of IGF-1 can bring about increased proliferation and survival and hence promote carcinogenesis even though not being directly responsible for initiating cancer development. Hence, individuals with relatively high levels of IGF-1 may be at an increased risk as the anti-apoptotic actions of IGF supports partially transformed cells to provide an increased pool of cells for subsequent damaging hits. It is important to note that the IGF-1 activity in a given tissue is not merely a function of its circulating levels but also the local expression of genes encoding for IGFs, IGF-1 receptor (IGF-1R), IGFBPs and proteases that cleave the IGFBPs to regulate the release of IGF-1 (particularly for IGFBP-3). There is considerable heterogeneity in the levels of IGF-1 and IGFBP-3 between normal individuals as a result of genetic and non-genetic determinants [6,7].

Recent evidence suggests a complex cross-talk between the GH–IGF-1 axis and estrogen receptor signaling that can stimulate mammary epithelial proliferation under normal conditions and increase the risk of breast cancer [8], as well as positive cross-talk with the ErbB1 receptor [9]. The latter also undergoes direct tyrosine phosphorylation by the GHR [10], which itself is able to activate the classic oncogenic pathways directly through JAK2 and Src [11]. Thus, the combination of GH and IGF-1 signaling, together with their interactions with other potentially oncogenic signaling proteins such as estrogen receptor and ErbB1 would lead one to expect involvement in cancer initiation or progression for this key growth-promoting axis (Figure 1).

Epidemiological studies

Numerous epidemiological studies have provided evidence that GH/IGF-1 is likely to be a driver of major human cancers. First, there is a link between tall stature, cancer risk and GH/IGF-1 levels. With the use of final height as a marker for GH and IGF-1 action, a review of over 300 case–control and cohort studies [12] found that taller individuals have a higher incidence of breast cancer (22% increase), prostate cancer (20% increase) and colon cancer (20–60% increase) relative to shorter individuals. A Danish study of 14-year-old children in the top quintile of height showed that they have an adjusted relative risk of over 1.5 for breast cancer, which surpasses other risk factors examined including BMI and age of first menarche [13]. A carefully controlled twin study from Scandinavia also found that tallness associates with increased breast cancer risk [14]. An anthropometric analysis revealed an association between rapid childhood growth during adolescence with the risk of developing several cancers, particularly of the breast, prostate and colon [3]. For breast cancer risk, a major prospective meta-analysis of patients in 12 countries concluded that not only are serum IGF-1 concentrations positively associated with height, but they are also positively associated with breast cancer risk in women (high vs low serum IGF-1; OR: 1.28), but only in estrogen receptor-positive tumors [15]. Moreover, higher levels of free and total plasma IGF-1 have been reported in breast cancer patients [16]. In relation to the restriction of risk to estrogen receptor-positive women, synergistic interaction between estrogen action and IGF-1 action has been shown *in vitro* for epithelial cell proliferation [17]. IGF-1 levels are also positively related to high mammographic density, which is an indicator of increased breast cancer risk [18]. Of further relevance, loss of BRCA1 function associates with overactivation of the IGF-1 signaling axis [19].

There have been reports that genetic variants in the GH–IGF system can determine relative tumor risk. A genome-wide association study (GWAS) in UK Caucasians has identified 64 SNPs that influence susceptibility for lung cancer, of which 11 were mapped to genes of the GH–IGF-1 axis, including GH1, GHR, GH-releasing hormone (GHRH) and IGFBP5 [20], and genetic variation at many genes in the GH–IGF pathway have been shown to associate with a variety of cancers [20,21]. A recent GWAS of over 1000 breast cancer cases matched with a similar number of controls concluded that the GH signaling pathway was the third most highly enriched pathway in breast cancer, but found insulin signaling intermediates rather than IGF-1 intermediates to co-associate with GH/JAK2 signaling in this analysis [22]. However, polymorphisms in the *IGF-1* gene or in the GH synthesis pathway were not significantly associated with breast cancer [23]. Four *IGFBP-3* SNPs have been reported to be associated with IGF-1 and IGFBP-3 levels in one study [24], and a strong association between a specific BP-3 promoter polymorphism and mammographic density, a known risk factor for breast cancer development, in another study [25]. However a larger cohort and a recent multi-ethnic cohort study reported no direct association of BP3 with breast cancer [23,26]. While *IGFBP-3* polymorphic alleles were modestly associated with risk of colorectal cancer [27], there were contrasting associations between *IGFBP-3* polymorphisms and the risk of prostate cancer in other studies [28,29]. It remains to be seen if these genetic variations could determine a higher cancer risk in susceptible individuals receiving GH treatment.

Elevated levels of IGF-1 have also been shown to confer an increased risk for other cancers such as colorectal cancer and prostate cancer. A recent systematic review of 42 published studies concluded that raised circulating IGF-1 is positively associated with prostate cancer risk, with little evidence for a role of IGF-2, IGFBP-1, IGFBP-2, and inconclusive evidence for involvement of IGFBP-3 [30]. For colon cancer, the relative risk for IGF-1 (RR: 1.07; 95% CI: 1.01–1.14) is modest compared with that seen in acromegaly [31]. This may be a consequence of the elevated insulin levels associated with acromegaly acting together with elevated IGF-1 and, of course, GH itself [31–33].

Acromegaly & cancer risk

Acromegaly is an important disease state for assessment of cancer risk because of the presence of persistently elevated levels of IGF-1. This is a result of hypersecretion of GH by pituitary somatotropes, particularly as a result of activating mutations in the GHRH signaling cascade. A number of studies have been carried out to assess whether this condition is associated with cancer risk. The most recent meta-analysis by Renehan and Brennan across three population studies concluded that acromegaly is associated with a 2.46-fold (95% CI: 1.79–3.38) increased risk of colon cancer [34]. Adenomatous lesions tend to be larger

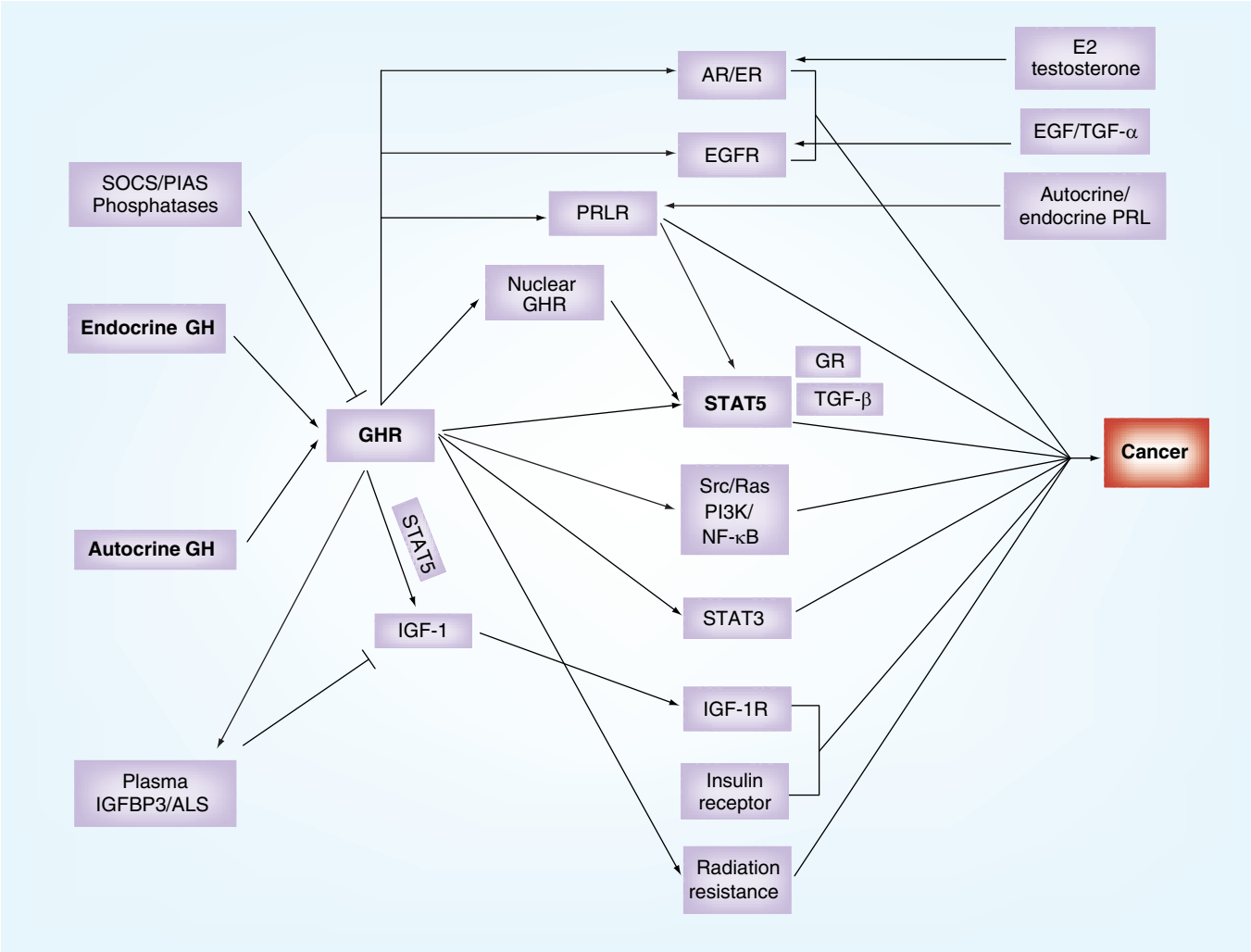

Figure 1. The major factors contributing to growth hormone-induced oncogenesis. GH receptor activation by endocrine or autocrine GH is feedback regulated by SOCS, phosphatases and PIAS. Receptor activation induces transcription of IGF-1, and the receptors for prolactin, EGF, estrogen and androgen, as well as promoting insulin synthesis and secretion. While GH receptor activation results in activation of oncogenic Src, Ras/ERK, PI3-kinase and NF-κB pathways, it also activates oncogenic STATs, STAT3 and particularly STAT5. The latter complexes with glucocorticoid receptors and TGF-β, and is necessary for the transforming actions of nuclear localized GHR. Finally, IGF-1 produced as a result of GHR activation and regulated by GH-dependent IGFBP3/ALS is a key element in tumor promotion. Text in bold shows standard abbreviaitons.
ALS: Acid labile subunit; AR: Androgen receptor; EGFR: EGF receptor; ER: Estrogen receptor; GH: Growth hormone; GHR: Growth hormone receptor; GR: Glucocorticoid receptor; IGFBP3: Insulin-like growth factor-binding protein 3; PIAS: Protein inhibitors of activated signal transducer and activator of transcription; PRL: Pituitary hormone prolactin; PRLR: Pituitary hormone prolactin receptor; SOCS: Suppressor of cytokine signaling proteins; STAT: Signal transducer and activator of transcription.

and more dysplastic in acromegaly, and are often multiple [35]. Acromegaly was also associated with an increased risk for thyroid cancer (3.64-fold; 95% CI: 1.63–8.11) in this meta-analysis. However, there is no statistical association between serum IGF-1 and presence of colorectal neoplasia in the three existing studies [34], so one is left with the possibility of direct GH action on the colon, or elevated plasma insulin as a driving factor, consequent to the diabetogenic action of elevated GH [36]. In relation to the other cancers, which showed a relationship to circulating IGF-1 in large population studies, in acromegaly there has been no confirmed association with breast cancer, although the limited sample number of untreated female acromegalics may have prevented small effects being observed [35]. This could also be a consequence of impaired ovulation in acromegalic women; hence, a lack of progesterone and estrogen, which together can promote breast cancer. Likewise, prostatic cancer shows no evident association with acromegaly, although benign prostatic hyperplasia with calcifications is evident across different studies [35]. A number of other cancers have been reported to be associated with acromegaly, but insufficient numbers are available for definite conclusions. These include various lympho-hematopoietic neoplasms (e.g., lymphoma, multiple myeloma, chronic myeloid or lymphocytic leukemia), brain tumors including meningiomas, adrenal tumors and melanomas [35].

These studies indicate a low but significant risk for certain cancers, particularly of epithelial origin, in relation to elevated circulating IGF-1. What of the converse situation, that is, GH and/or IGF-1 deficiency? In the sole published study to date, a worldwide survey of 222 individuals with GHR mutation or isolated GH deficiency, not a single case of malignancy was reported. Conversely, 338 first- and second-degree relatives reported a 10–24% incidence of a range of malignancies [37]. The difference in average age between the two groups (32 vs 55 years, respectively) probably contributed to this disparity, but the apparent resistance of GH-deficient and/or IGF-1-deficient individuals to cancer is supported by extensive animal studies. These will be discussed in the following sections, but at face value, the above findings imply that IGF-1–GH signaling is permissive for cancer but that beyond its essential role at low IGF-1 concentrations, has only modest effects in cancer promotion.

Children treated with GH & cancer risk

The administration of recombinant human GH was approved for the treatment of children with GH deficiency in 1985 and GH was one of the first therapeutic drugs to be produced by recombinant DNA technology. Over the past few years, several concerns have been raised in regard to its diabetogenic effects, adverse effects on skeletal growth, or increased risk of new or recurrent cancers [38]. A recent report by Bell *et al.* recorded findings generated from a study of 54,996 children treated with recombinant GH, corresponding to nearly 195,000 patient-years of monitoring [39]. This study found very low adverse effects of GH administration and no additional cancer cases in children without other risk factors for malignancy. However, in children with hypothyroidism, the risk of second neoplasm was increased, suggesting that GH could aggravate neoplastic tendencies resulting from underlying genetic abnormalities or radiotherapy. Another independent study by Ergun-Longmire *et al.* had reported the same conclusion whereby GH therapy doubled the risk of second neoplasm in childhood cancer survivors [40]. Generally, most studies report that replacing circulating GH in humans does not promote cancer. However, while there were no additional cases relative to the general population, there was no data comparing GH-treated with GH-deficient untreated children for ethical reasons. Given the finding of no malignancies in the aforementioned GH/IGF-1 deficiency referred to above, one would predict that such a comparison would show an increase in cancer incidence on GH replacement to normal levels. This would be concordant with the many animal studies verifying the resistance of GH/IGF-1-deficient animals to cancer.

Animal models

The prospect that GH is an etiologic factor in tumorigenesis was evident from the early clinical observation that hypophysectomy inhibited metastasis and progression of specific malignancies [41], and that high doses of GH induced neoplasms in rats [42]. Supporting these early observations, it was noted that transgenic mice overexpressing human GH exhibited higher incidences of tumors in mammary glands [43,44] and livers (Table 1) [45]. These mice have constitutively activated hepatic STAT3, Src, ERK and Akt [46]. An intermediatory role of IGF-1 in many GH actions is concordant with the observation that overexpression of IGF-1 in the mammary epithelium leads to development of mammary cancers [47,48]. Similarly, expression of constitutively active IGF-1R leads to early development of mammary and salivary gland adenocarcinomas [48]. In GH-transgenic mice crossed with SOCS-2-knockout mice, loss of the GH signaling antagonist SOCS-2 was found to be associated with increased local IGF-1 production and multiple hyperplastic and lymphoid polyps [49].

Conversely, GHR-knockout mice display a lower and delayed incidence of neoplastic disease with substantially fewer fatal neoplastic lesions, particularly lymphomas and pulmonary adenoma/carcinomas compared with wild-type littermates [50]. Thus, 83% of C57Bl6 littermate controls died naturally from neoplastic diseases, whereas only 42% of the GHR-deleted mice died from neoplasms in this study. In animal models of carcinogenesis, such as mammary tumors driven by the Simian virus 40 large T antigen, tumors in GHR-deleted mice are also markedly reduced in size (50 vs 776 mm^3) and number (3.2 ± 1.2 vs 9.8 + 1.4) compared with those observed in the wild-type mice [51]. Likewise, lit/lit mice that are characterized by a nonfunctional GHRH receptor with GH and IGF-1 levels less than 10% of wild-type counterparts, exhibit marked retardation of human MCF-7 breast cancer xenograft growth (average: 35 large tumors in wild-type vs five in lit/lit by day 39 after implantation [52]). GH-deficient dwarf rats (dw/dw with 20% normal serum IGF-1) are resistant to mammary tumors induced by the carcinogen nitrosomethylurea (tumor incidence 100% in wild-type vs 4.8% in dw/dw rats) with an average tumor load of 7.0 per wild-type rat vs 1.0 per dw/dw rat. Hormone replacement of dw/dw rats with estrogen, progesterone, GH or IGF-1 revealed a similar tumor incidence and tumor burden to wild-type rats only with bGH replacement, and a lesser increase with IGF-1 replacement (62% incidence with an average of 1.6 tumors per rat), [53]. This study was confirmed by Shen *et al.* with the additional finding that halting GH replacement led to tumor regression [54]. Likewise, development of prostate carcinomas in the Probasin/TAg rat is markedly decreased on a dw/dw background such that by 52 weeks of age, the majority of dw/dw rats did not develop carcinomas, while all control Probasin/TAg rats did. Indeed, by 10 weeks of age, the dorsal and ventral prostate showed 100% tumor incidence in normal rats, while the GH-deficient dw/dw rats did not have measurable tumors [55].

It is clinically relevant that mice transgenic for the GH antagonist G120R GH (with 46% normal serum IGF-1) are partially resistant to 7,12-dimethylbenz(a)anthracene (DMBA)-induced mammary tumors (31.6% free of tumors vs 68% tumor free for the antagonist mice at 39 weeks after treatment) [56]. Accordingly, treatment of mice harboring MCF-7 xenografts with large doses of pegvisomant (an improved clinical version of the G120R GH antagonist) resulted in 70–80% suppression of circulating IGF-1 and a 30% decrease in tumor volume together with a twofold reduction in proliferation and a twofold increase in apoptosis. However, no effect on IGF-1-independent MDA-MB235 or MDA-MB231

xenografts was evident [57]. Regression of all 15 human meningioma xenografts in nude mice was induced by daily pegvisomant treatment over 8 weeks at 45 mg/kg. Interestingly, this was accompanied by only a 20% decrease in serum IGF-1 [58], suggesting a direct action of GH on this cancer. A similar study with colorectal cancer-205 xenografts by Dagnaes-Hansen *et al.* showed a marked decrease in tumor weight (~40%) and increased apoptosis with second daily administration of 60 mg/kg pegvisomant, accompanied by a decrease in serum IGF-1 to 36% of the control value [59].

These differences in tumor progression might relate to the extent of IGF-1 availability, as IGF-1 has been shown to act *in vitro* as a tumor promoter by increasing proliferation and decreasing apoptosis, and by promoting angiogenesis and metastasis [4]. Indeed, local expression of IGF-1 in mouse mammary tissue resulted in spontaneous mammary tumors in 30% of mice [60]. Alternatively, these differences might also relate to GH availability or to a combination of both GH and IGF-1 availability. Some conclusions can be drawn from mouse models with lower levels of circulating IGF-1 but which have normal/elevated tissue expression as a result of selective knockout of hepatic IGF-1 expression (liver IGF-1-deleted or LID mice). These mice have approximately 50% of normal circulating IGF-1, which results in a 40% significant decline in azoxymethane-induced colon adenocarcinoma number, largely as a result of increased apoptosis [61]. An earlier study with orthotopically transplanted colon-38 adenocarcinomas found the circulating IGF-1 in their LID mice to be approximately 25% of normal, and this was associated with a substantial decrease in the number of mice with palpable colon tumors from 57 to 31%, together with a significant increase in tumor latency from 23 to 27 days [62]. Hepatic metastases were also significantly decreased from 44 to 31%, and these improvements were reversed with IGF-1 administration. Generation of mammary tumors by chemical or genetic means is also decreased in LID mice [63]. Both the DMBA carcinogen model and the C3(1)/Simian virus 40 large T-antigen expressing mouse model show decreased incidence and onset in LID mice. The decrease for DMBA-treated mice is from 56 to 26% incidence, and latency from 60 to 74 days, while with the large T-antigen model approximately 60% of mice developed one tumor compared with approximately 40% with two tumors in control mice. At 4 weeks, the tumor volume in the large T-antigen model was approximately 50% of the control mice volume. These modest differences contrast with the striking blockade to tumor development seen in the GHR-deleted mice and the GH-deficient rats and mice discussed previously. This could be a result of insufficiently low circulating IGF-1 in the LID mice, or of paracrine IGF-1 generation in response to activation of the ubiquitous GHR. The elevated circulating GH consequent to lowered circulating IGF-1 in the LID mice would not appear to be making a major contribution to cancer promotion, since the LID mice do have a significantly lower tumor burden.

These studies clearly indicate the involvement of endocrine GH and IGF-1 in tumor growth promotion, and indicate that effective therapeutic options for cancer treatment need to drastically lower serum IGF-1.

Table 1. Animal models implicating growth hormone/IGF-1 in cancer incidence and progression.

Cancer status	Animal model	Ref.
Increased mammary tumor	hGH-transgenic mice	[43,103]
Increased hepatic tumor	hGH-transgenic mice	[45]
Increased mammary tumor	Mammary epithelial overexpression of IGF-1	[47,60]
Increased mammary and salivary adenocarcinoma	Constitutively active IGF-1 receptor	[48]
Decreased lymphoma and pulmonary adenoma/carcinoma	GH-receptor null	[50]
Decreased mammary tumors	SV40 large T antigen in GHR null	[51]
Decreased number of mammary tumors	GH120 receptor antagonist-transgenic mice with DMBA	[56]
Decreased growth of MCF-7 xenografts	*lit/lit* GH-deficient mice	[52]
Decreased growth of mammary tumors	*dw/dw* GH-deficient rat treated with NMU	[53,54]
Decreased prostate carcinomas	Probasin T-antigen rat crossed with *dw/dw*	[55]
Decreased colon adenocarcinoma	LID mice treated with azoxymethane	[61]
Decreased mammary tumor incidence	LID mice treated with DMBA	[63]
Decreased mammary tumor incidence	SV40 large T antigen in LID mice	[63]
Decreased growth of colon 38 adenocarcinoma, some reversal with IGF-1 treatment	LID mice	[62]
Decrease in MCF-7 xenograft growth	Pegvisomant-treated nude mice	[57]
Regression of meningioma xenografts	Pegvisomant-treated nude mice	[58]
Regression of Colo 205 xenografts	Pegvisomant-treated nude mice	[59]

DMBA: 7,12-dimethylbenz[α]anthracene; GH: Growth hormone; hGH: Human growth hormone; LID: Liver IGF-1 deficient; MCF: Michigan cancer foundation; NMU: *N*-methyl-*N*-nitrosourea; SV40: Simian virus 40.

GHR expression & cancer

The GHR is expressed in almost all cells, and its expression is subject to control by nine alternate first exons in humans [64]. The GHR transcript has been found to be overexpressed in a limited range of cancers, notably prostate carcinoma, glioblastoma, neuroectodermal tumors, adult T-cell lymphoma, kidney clear cell carcinoma and parathyroid adenoma (see Table 2) [201].

Table 2. Summary of oncomine data for overexpression of growth hormone 1, growth hormone 2 and growth hormone receptor transcript expression (top 10% or better) compared with normal tissue.

Transcript	Cancer type	Oncomine reference
GH1	Prostate carcinoma	Liu orostate
	Bladder urothelial carcinoma	Dyrskjot bladder 3
	Colon, mucinous adenocarcinoma	Kurashina colon
	Ovarian clear-cell carcinoma	Hendrix ovarian
GH2	Prostate carcinoma	LaTulippe prostate
	Chronic adult T-cell leukemia/lymphoma	Choi leukemia
	Bladder urothelial carcinoma	Dyrskjot bladder 3
	Colon mucinous adenocarcinoma	Kurashina colon
	Ovarian mucinous adenocarcinoma	Hendrix ovarian
	Ovarian endometrioid carcinoma	Hendrix ovarian
GHR	Prostate carcinoma	Liu prostate 2, Yu prostate, Varambally
	Prostatic intraepithelial neoplasia	Tomlins prostate
	Glioblastoma	Liang brain, Lee brain
	Primitive neuroectodermal tumor	Pomeroy brain
	Acute adult T-cell leukemia/lymphoma	Choi leukemia
	Clear-cell sarcoma of the kidney	Cutcliffe renal
	Parathyroid gland adenoma	Morrison parathyroid

GH: Growth hormone; GHR: Growth hormone receptor.
Data from [201].

In addition, immunohistochemical and quantitative PCR studies have reported GHR overexpression in a high proportion of invasive breast ductal carcinoma [65], adrenal cortical neoplasms [66] and in colorectal cancer [67]. Moreover, elevated serum GH-binding protein (derived from the GHR by cleavage, and a measure of GHR expression [68]) is associated with a threefold increase in breast cancer incidence [69]. Immunohistochemical assessment has also revealed GHR overexpression in melanoma [70] and prostate carcinoma [71]. This expression has been found to be not only cytoplasmic but also within the nucleus (see later). To date, there are no reports of constitutively active GHR mutations.

Autocrine GH & cancer

15 years ago, expression of GH was reported in the mammary tissue of dogs in response to progesterone administration, resulting in acromegalic symptoms [72]. The hormone is synthesized in the hyperplastic ductular epithelium of the mammary gland, since GH mRNA was present in dog and cat epithelia, and was shown to be elevated by progesterone [73]. As recently reported by Illera's group, expression of GH protein in canine mammary tissue is markedly (20-fold) elevated in malignant tumors, and less so in benign tumors and dysplasias [74]. This expression correlates with a 12-fold increase in IGF-1 protein expression and a fourfold increase in estradiol content of the malignant tumors, with a correspondingly lower but still elevated expression of IGF-1 and estradiol in benign tumors [74]. Increased mammary GH and IGF-1 correlated with increased serum GH and IGF-1, with serum levels of GH greater than 6 ng/ml and IGF-1 greater than 43 ng/ml resulting in death of the majority of dogs within 6 months from neoplasia [13]. Is this striking evidence for autocrine/paracrine actions of GH in cancer promotion evident in humans?

The study of Mol *et al.* reported the presence of GH transcripts in human mammary tissue but with no evident relation to presence of carcinogenesis, and apparently decreased transcript in most carcinomas [73]. Raccurt *et al.* later reported increased GH protein in three intraductal carcinoma samples relative to normal tissue, but not in invasive ductal carcinomas [75]. They also provided ISH and qPCR evidence for GH transcript expression in these three carcinomas. Recently, Ratkaj *et al.* used IHC to study human GH expression in a larger series (n = 40) of ductal invasive breast carcinomas and fibroadenomas, and concluded that GH was expressed in all fibroadenomas and their stroma, but in only 55% of ductal carcinomas and 20% of their stromal tissue [76]. There was no correlation between GH expression and tumor size or tumor grade. A search of the Oncomine database reveals underexpression of GH1 and no listing for GH2 transcripts in invasive ductal breast carcinoma against normal tissue, in contrast to the prolactin transcript, which is highly expressed [201]. In a survey of GH transcript expression across breast cancer lines, van Garderen and Schalken found only three of ten lines expressed GH1 transcript by PCR [77], (including MCF-7 cells, confirmed by Gil-Puig [78]), although all express GHR transcripts. Thus, it appears that humans are unlike dogs in overexpression of paracrine/autocrine GH in mammary cancer, but rather rely on prolactin.

What about other cancers?

Many human prostate cancers overexpress GH1 or GH2 and GHR transcripts as evidenced in the Oncomine database (Table 2) [201]. Furthermore, an immunohistochemical study of 20 prostate cancers and 17 controls reported a fourfold increase in human GH expression in prostatic carcinoma Gleason scores 6–8. Co-expression of GH and GHR isoforms has also been reported at protein and mRNA levels in prostate cancer cell lines (e.g., ALVA-41, PC-3, DU 145) [71,79], with van Garderen and Schalken reporting six of seven prostate cancer lines expressing GH1 transcripts, and all expressing GHR transcripts [77]. Association of autocrine GH expression with prostate cancer contrasts with clinical studies show that acromegaly is associated with prostate hypertrophy but not malignancy [80], and the observation that GH replacement in GHD patients increases prostate size to normal without any increase in neoplasia [81]. As previously noted, absence of GH or GHR signaling results in resistance to T-antigen induced prostate cancer in mice and rats [55,82]. Loss of GH/IGF1 activity is also associated with impaired development of the prostatic ductal branching architecture that results from IGF-1 deficiency [83]. A reasonable hypothesis to explain these findings is that autocrine GH acts in a different manner from endocrine GH to promote

cancer formation, whereas endocrine GH promotes hypertrophy in an IGF-1-dependent manner. This situation may apply to other cancers overexpressing GH1 and GH2 evident in the Oncomine database, such as chronic adult T-cell leukemia, ovarian mucinous carcinoma, endometrioid and clear-cell adenocarcinomas, and bladder urothelial cancers (Table 2) [201]. The GHR itself is also reported as overexpressed in a range of neoplasias (see earlier). Moreover, since human GH can activate the human prolactin receptor [84], the presence of overexpressed prolactin receptor in prostate cancer, T-cell leukemias and ovarian adenocarcinomas [201] raises the possibility that autocrine GH may also drive oncogenesis in these cancers.

The oncogenic actions of forced autocrine expression of human GH in immortalized human breast lines has been extensively studied by Lobie's group. Thus, Zhu *et al.* have reported that overexpression of autocrine GH in mammary epithelial cell lines (particularly MCF-7 cells) results in increased cell proliferation, transformation and invasion, with an epithelial to mesenchymal transition [85]. This is associated with an altered transcript expression profile, with a number of oncogenic genes being upregulated by autocrine GH overexpression [86]. Autocrine GH led to increased expression of the oncogenic homeobox protein Hox-A1 and telomerase protein together with downregulation of junctional plakoglobin and increased DNA methyltransferase-3 activity resulting in methylation of the plakoglobin promoter [87]. Human GH overexpression also resulted in increased activity of matrix metalloproteases-2 and -9, redistribution of E-cadherin to the cytoplasm and increased secretion of trefoil factor 3 (*TFF3*), proposed to mediate the oncogenic actions of autocrine GH by Lobie's group by paracrine actions on adjacent cells (Figure 2) [87]. Autocrine production of human GH was associated with increased angiogensis in xenografts, in accord with its ability to recruit endothelial cell precursors and to induce VEGF [88]. Of interest, autocrine human GH-driven proliferation of MCF-7 cells, transcriptional activation and cell spreading was reported to be completely blocked by the addition of exogenous human GHR-specific antagonist B2036/pegvisomant [89]. These studies indicate that overexpression of human GH in transformed cells is oncogenic. Is there, then, a difference between autocrine and endocrine GH signaling? van den Eijnden and Strous examined this question in ts20 cells, finding that GHR signaling in cells with autocrine GH does not manifest before the Golgi, and is associated with a very low level of chronic STAT5 and GHR tyrosine phosphorylation, but robust induction of a STAT5-responsive luciferase reporter [90]. Sustained GHR signaling would be associated with induction of negative-feedback regulators such as SOCS proteins, hence the pulsatile nature of pituitary GH secretion. It would appear that sustained autocrine GH stimulation does something different, for example, results in the gain of a phenotype characteristic of oncogenic transformation, yet sustained endocrine GH stimulation (as in acromegaly) results in only a modest increase in cancer susceptibility. One is driven to the conclusion that intracellular signaling events are important in the transformation process, particularly since Strous' group found that autocrine GH-expressing cells are insensitive to external (endocrine) GH [90]. Conversely, Lobie's group have reported that exogenous B2036/pegvisomant blocks autocrine growth, implying that autocrine GH is secreted and acts externally (or that the antagonist is internalized at high concentrations). It may be that both a hormone-induced signal from the plasma membrane and an intracellular signal are necessary for full autocrine action by GH.

Nuclear GHR & cancer

A likely possibility for altered intracellular signaling relates to the presence of the GHR in the cell nucleus, since this increases cell sensitivity to STAT5 [91]. Tissue immunohistochemistry reveals that the nuclear GHR is present in many proliferating cells, including a variety of cancers, such as breast cancer [92], colorectal carcinoma [93], hepatocellular carcinoma [94], melanoma [70] and uterine cervical neoplasms [95]. The translocation of a transmembrane receptor into the nucleus is known to occur for the EGFR, the FGF receptor and IFN-γ receptor [96], and is often associated with cell transformation. Full-length GHR is translocated to the nucleus in a GH- and importin-β-dependent manner in cell models, and *in vivo* in response to regeneration after partial hepatectomy in the rat, which is a GH-dependent process [91]. There is a high correlation between the nuclear GHR and cell proliferation during the liver regeneration process and targeting the GHR to the nucleus by fusion with a nuclear localization signal markedly increased the cell proliferative response to autocrine GH via STAT5 activation in pro-B cells, resulting in constitutively activated STAT5. Moreover, pro-B BaF3 cell lines stably expressing nuclear-targeted GHR become transformed, and form solid tumors in immunocompromised mice. This is associated with upregulation of transcripts for a number of genes involved in oncogenesis such as survivin, dysadherin and *MybBP*. Accordingly, a high proportion of nuclear GHR cells are evident in sections of highly proliferative lymphomas [91]. Further examination of the mechanism involved led to the identification of an important RNA splicing protein and transcriptional co-activator, CoAA, which binds to the extracellular domain of the receptor in response to GHs, potentially facilitating nuclear translocation by means of its nuclear localization motif [97]. Transfection of pro-B cells with CoAA markedly enhanced the proliferative response to GHs, but not to IL-3, the physiological cytokine for these pro-B cells. CoAA is an oncogene related to Ewing's sarcoma protein and translocated in liposarcoma (TLS) oncoproteins, which is amplified in lymphoma, non-small cell carcinoma and squamous cell carcinoma [98], and can drive osteosarcoma proliferation *in vitro* [99]. It is also a potent co-activator of the estrogen receptor, which is highly relevant to breast cancer [100].

GH & prolactin receptor activation in cancer

As mentioned previously, human GH also activates the human prolactin receptor [84], although lower species have GHs and prolactins specific for their cognate receptors. PRL can upregulate local IGF-1 expression in breast cancer cells, resulting in downstream activation of Erk1/2 and Akt [101], and PRL and IGF-1 augment neoplastic progression synergistically [102]. Following the initial observation that human GH-transgenic mice develop mammary cancer (human GH activates both GH and prolactin receptors in mice) [103], Wennbo *et al.* created rat prolactin-transgenic and bovine GH-transgenic

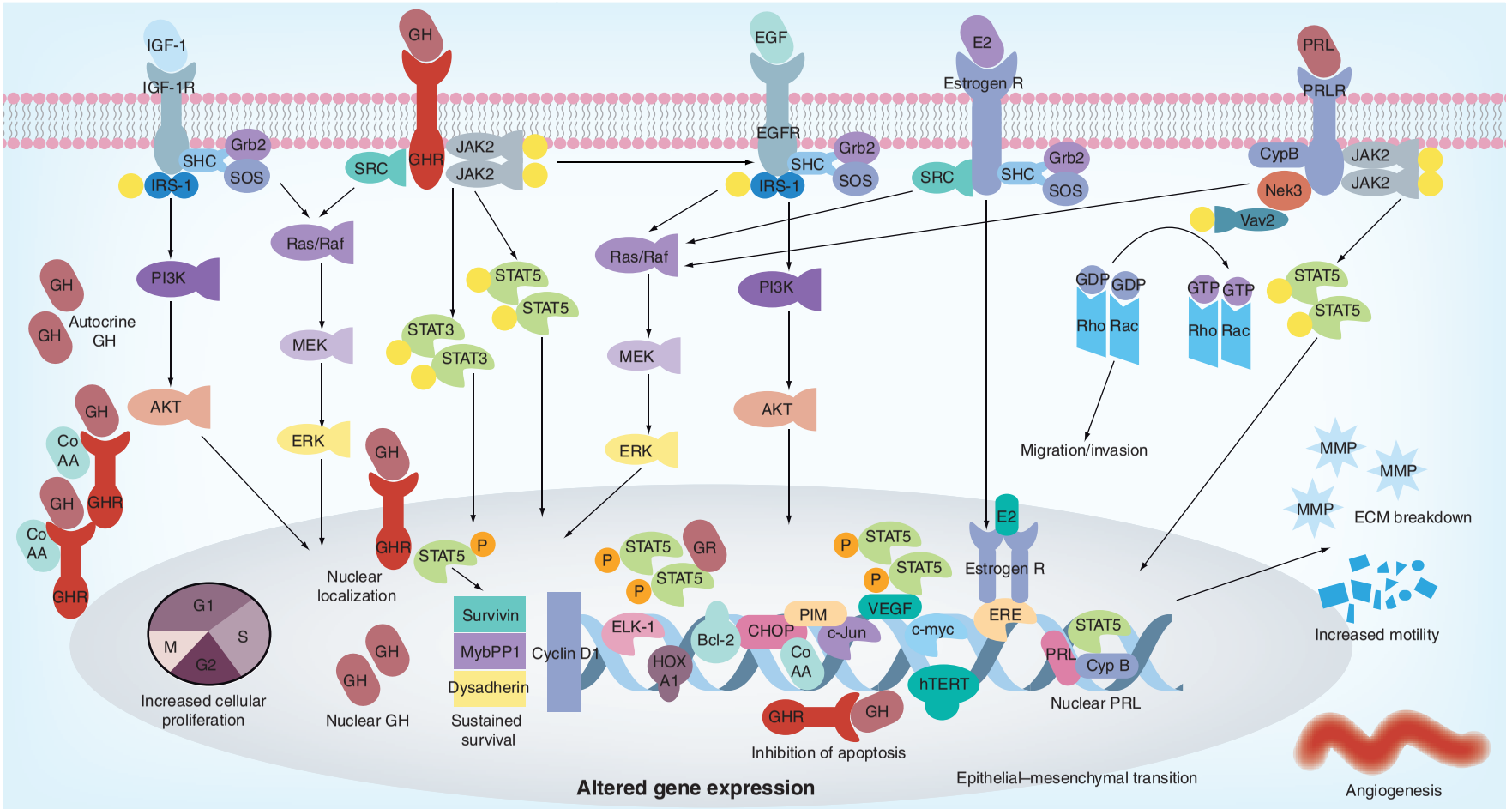

Figure 2. Oncogenic signaling by growth hormone and prolactin. GH and PRL signaling via Jak2 mediate many of the downstream responses through phosphorylation of STAT transcription factors, MAP kinases and other kinase cascades. STAT5 and STAT3 are major contributors to the downstream signaling and upregulate key proliferative genes. In PRLR-mediated signaling the phosphorylation of Vav2 (a guanosine nucleotide exchange factor that stimulates the Rho/Rac protein family) by Nek3 allows it to enhance the activity of Rac responsible for enhanced motility and invasion. The somatotrophic effects of GH are mediated by IGF-1 and its receptor (IGF-1R) serves as a potent proliferative signaling system that stimulates cell growth and promotes cell survival. The proliferative actions of IGF-1 are mediated by the association of receptor tyrosine kinase with SHC, Grb2 and SOS that activate the Ras and MAPK cascade (Raf, Mek and Erk1/2). This cascade culminates in activation of Elk-1 and other transcription factors. The anti-apoptotic effects are mediated by the phosphorylation of IRS-1 via the PI3K pathway resulting in the activation of Akt and mTOR. A cell exhibiting upregulation of these key signaling molecules or lack of a negative feedback has increased mitogenic potential with inhibition of apoptotic pathways. GHR nuclear localization, a function of highly proliferative cells, can promote in tumorigensis via the Jak2/STAT5 pathway together with CoAA, dependent on autocrine GH. This results in dysregulation of expression of survivin, dysadherin and Mybbp1a – genes associated with tumorigenesis. PRL can also be translocated into the nucleus by binding to CypB, which enhances the STAT5 DNA-binding activity and prolactin-induced STAT5-mediated gene expression. Autocrine GH increases cell proliferation (via HoxA1, TFF3, Jak/STAT, MAPK, Cyclin D1, c-myc, hTERT), survival (via TFF3, Bcl2, CHOP, Jak/STAT) and migration/invasion/EMT (via TFF3, MMP, γ-catenin) and angiogenesis (TFF3, VEGF) by differential regulation of bracketed genes. estrogen receptor, androgen receptor and EGFR upregulated by GH signaling (Figure 1) also contributes to tumor promotion by genomic and plasma membrane actions.
ECM: Extracellular matrix; GH: Growth hormone; GHR: Growth hormone receptor; PRL: Prolactin.

mice, which target their prolactin and GHRs, respectively [104]. Only in the prolactin transgenics were mammary tumors evident, supporting the oncogenic role of autocrine/paracrine prolactin in mammary tumorigenesis. This may be a consequence of the differences in level of receptor expression for GH and prolactin in the mammary gland since both receptors have similar signaling pathways. The role of prolactin in breast cancer has been extensively reviewed by Clevenger *et al.* [105]. Clinical and animal model studies also support a role for autocrine prolactin in prostatic cancer progression [106,107] and elevated prolactin receptor expression is evident in colorectal carcinoma and metastases [108]. These findings can be accommodated in a model of abnormal signaling by these two closely related class-1 cytokine receptors involving excessive activation, particularly of STAT5, but also of STAT3 (Figures 1 & 2) [109–111].

The role of STAT5 activation in cancer

Constitutively activated STAT5 can act as an oncogene, and is a common feature of hematopoietic proliferative diseases. This is a consequence of activating mutations in the JAK kinase or relevant cytokine receptor such as JAK V617F [13,112,113], TEL-JAK2 [114], Bcr-abl [115] and MPL W515L [116]. Activation of STAT5 has been shown to be critical for transformation by several of these oncogenic mutations [117–119]. There is now accumulating evidence that activated STAT5 plays a vital role in promoting a broad range of cancers, including prostate cancer [120], melanoma [121,122], hepatocellular carcinoma [123] and breast cancer [124]. Activation of STAT5 has also been found to increase tumor growth and aggressiveness of hepatocellular carcinoma and squamous epithelial cell carcinoma by induction of epithelial–mesenchymal transition [123,125]. Induction of senescence is a common feature of oncogenes [126] and expression of constitutively active STAT5 has also been shown to induce senescence [127,128].

Several studies investigating human melanoma patient samples and melanoma cell lines have shown that phosphorylated STAT5 is a common feature in melanoma, particularly in metastasis [82,121,122]. Knockdown of STAT5 by RNAi in melanoma cells reduced Bcl-2 and cyclinD2 transcription, reduced cell viability and induced apoptosis, and expression of a dominant negative (C-terminal truncated) STAT5 inhibited expression of Bcl-2, leading to G1 arrest and enhanced cell death [121,122]. In a fish model of melanoma, constitutive activation of STAT5 has shown to correlate with the aggressiveness of the melanoma [129], suggesting that activation of STAT5 plays an important role in metastasis. In a 3D skin reconstruction model of metastatic melanoma, differentiation and invasion is inhibited by roscovitine [130], which is an inhibitor of cyclin-dependent kinases [131] and STAT5 activity [132].

Similarly, activated STAT5 has been detected in the majority of prostate cancer specimens, particularly in high histological grade cancers, but not in normal prostate epithelium [99,133]. It has recently been shown that activated STAT5 promotes growth and metastatic behavior of human prostate cancer cells *in vitro* and *in vivo* [120,134–136] and expression of a dominant-negative STAT5 induces cell death in both androgen-independent and androgen-sensitive prostate cancer cell lines [133]. Interestingly, STAT5 is able to synergise with androgen receptor by upregulating androgen receptor expression, which results in upregulation of STAT5 expression. The liganded androgen receptor and STAT5 interact in prostate cancer cells and enhance each other's nuclear uptake [137]. Because both the GHR and the prolactin receptor activate STAT5 as a key signaling pathway, it is likely that both autocrine/paracrine and endocrine GH and prolactin action would enhance active (oncogenic) STAT5 generation.

Many studies have shown STAT5 to be a major player in breast cancer [124], for example, expression of dominant-negative STAT5A in T47D breast cancer cells induces apoptosis [138], however, STAT5A and STAT5B show distinct effects in human mammary carcinoma cell lines [110]. Transgenic mice expressing a constitutively active variant of STAT5 (a C-terminal 44 amino acid deleted STAT5 fused to the JAK2 kinase domain via residues 677–847 of STAT6) specifically in mammary epithelium via the β-lactoglobulin regulatory sequences are predisposed to mammary tumor formation [139]. However, it is interesting to note that overexpression of the C-terminal deleted dominant-negative form of STAT5 from the same regulatory sequences also predisposes mice to mammary tumors; although the tumors from activated STAT5 expression showed a more differentiated phenotype suggesting different mechanisms are at play [140].

To date there has been no identification of a constitutively active mutation of GHR, however, with current whole genome sequencing regimes of large numbers of tumor samples it is likely that such mutations may be identified, similar to those identified for other class-1 cytokine receptors such as the thrombopoietin receptor W515L/K [141] and S505N [142] activating mutations, and the constitutively active prolactin receptor found in benign tumors [143].

Expert commentary

It is clear that GH/IGF-1 is necessary for the progression of a wide range of cancers in rodents and dogs. However, the situation is not so clear with humans, since only one study has reported on cancer incidence in GHR/GH-deficient patients. This needs to be rectified with further clinical data.

The relationship between autocrine GH expression and cancer incidence/progression needs to be firmly established with comprehensive studies of clinical samples.

The basis for the transforming actions of autocrine GH needs to be fully explored using cells with modest levels of GH expression corresponding to those evident in particular cancers. Prostate carcinoma would be a good model for these studies, because both autocrine GH and highly expressed GHR are present in prostate cancers.

There is no significant risk above that of the general population resulting from therapeutic replacement with GH. However, use of GH for prolonged periods at supraphysiologic levels could contribute to increased cancer risk, particularly colon and thyroid cancer, as it does in acromegaly.

Five-year view

Given the animal and human data supporting critical involvement of the GH–IGF-1 axis in cancer incidence and progression, the development of GH antagonists for use alone or in conjunction

with IGF-1R blockers, is of key importance. While pegvisomant is partially effective in suppressing cancer in animal models, it is disadvantaged by high cost and likely impairment of its action by elevated plasma GH resulting from lowered IGF-1 feedback. Therefore, other means of suppressing GH secretion or action would be most useful. Nevertheless, clinical trials of pegvisomant in cancer in conjunction with other adjuvant therapies appear warranted. The ability of GH and IGF-1 to confer resistance to radiotherapy [144,145] and chemotherapy [146] is a further reason for use of GH antagonists.

Given the potential role of GH in promoting stem cell activation [136,147], we can expect to see studies relating GH action to cancer stem cells and GH in the future.

Finally, while no activating clinical mutations in the GHR have been identified to date, this is a reasonable probability based on other activating mutations in cytokine receptors. Screening for activating mutations in GH/IGF-1-dependent cancers such as prostate cancer and lymphoma would appear warranted.

Financial & competing interests disclosure

Michael J Waters is supported by grants from the National Health and Medical Research Council (Australia). The authors have no other relevant affiliations or financial involvement with any organization or entity with a financial interest in or financial conflict with the subject matter or materials discussed in the manuscript apart from those disclosed.

No writing assistance was utilized in the production of this manuscript.

Key issues

- Epidemiological studies implicate increased growth hormone (GH)–IGF-1 axis activity in promotion of certain cancers (e.g., prostate, colon and breast cancer).
- Deficiency of endocrine GH or deletion of the GH receptor confers resistance to a wide range of cancers in rodents and humans.
- The GH antagonist pegvisomant has efficacy in slowing tumor development in animal models, including human xenografts.
- GH receptors are overexpressed in a range of cancers.
- Autocrine/paracrine GH may contribute substantially to cancer promotion in humans, as it does in dogs.
- The transforming activity of autocrine GH appears to involve sensitization to STAT5 and potentially STAT3 action.
- Both GH and prolactin can contribute to cancer progression since they both activate STAT5 and STAT3, and autocrine GH can activate the prolactin receptor in humans.
- GH and IGF-1 will synergise to promote cancer cell proliferation, survival and metastasis.

References

Papers of special note have been highlighted as:
• of interest

1 Nilsson A, Carlsson B, Isgaard J, Isaksson OG, Rymo L. Regulation by GH of insulin-like growth factor-I mRNA expression in rat epiphyseal growth plate as studied with *in situ* hybridization. *J. Endocrinol.* 125(1), 67–74 (1990).

2 Yakar S, Liu JL, Stannard B *et al.* Normal growth and development in the absence of hepatic insulin-like growth factor I. *Proc. Natl Acad. Sci. USA* 96(13), 7324–7329 (1999).

3 Jenkins PJ, Mukherjee A, Shalet SM. Does growth hormone cause cancer? *Clin. Endocrinol. (Oxf.)* 64(2), 115–121 (2006).

4 Samani AA, Yakar S, LeRoith D, Brodt P. The role of the IGF system in cancer growth and metastasis: overview and recent insights. *Endocr. Rev.* 28(1), 20–47 (2007).

• **An authoritative and comprehensive review describing the cancer promoting actions of IGF-1.**

5 Hanahan D, Weinberg RA. The hallmarks of cancer. *Cell* 100(1), 57–70 (2000).

6 Harrela M, Koistinen H, Kaprio J *et al.* Genetic and environmental components of interindividual variation in circulating levels of IGF-I, IGF-II, IGFBP-1, and IGFBP-3. *J. Clin. Invest.* 98(11), 2612–2615 (1996).

7 Pollak M. The question of a link between insulin-like growth factor physiology and neoplasia. *Growth Horm. IGF Res.* 10(Suppl. B), S21–S24 (2000).

8 Laban C, Bustin SA, Jenkins PJ. The GH–IGF-I axis and breast cancer. *Trends Endocrinol. Metab.* 14(1), 28–34 (2003).

9 Yamauchi T, Ueki K, Tobe K *et al.* Tyrosine phosphorylation of the EGF receptor by the kinase Jak2 is induced by growth hormone. *Nature* 390(6655), 91–96 (1997).

10 Frank SJ. Mechanistic aspects of crosstalk between GH and PRL and ErbB receptor family signaling. *J. Mammary Gland Biol. Neoplasia.* 13(1), 119–129 (2008).

11 Brooks AJ, Wooh JW, Tunny KA, Waters MJ. Growth hormone receptor; mechanism of action. *Int. J. Biochem. Cell Biol.* 40(10), 1984–1989 (2008).

12 Gunnell D, Okasha M, Smith GD, Oliver SE, Sandhu J, Holly JM. Height, leg length, and cancer risk: a systematic review. *Epidemiol. Rev.* 23(2), 313–342 (2001).

13 Queiroga FL, Perez-Alenza D, Silvan G, Pena L, Lopes CS, Illera JC. Serum and intratumoural GH and IGF-I concentrations: Prognostic factors in the outcome of canine mammary cancer. *Res. Vet. Sci.* 89(3), 396-403 (2010).

14 Lundqvist E, Kaprio J, Verkasalo PK *et al.* Co-twin control and cohort analyses of body mass index and height in relation to breast, prostate, ovarian, corpus uteri, colon and rectal cancer among Swedish and Finnish twins. *Int. J. Cancer* 121(4), 810–818 (2007).

15 Key TJ, Appleby PN, Reeves GK, Roddam AW. Insulin-like growth factor 1 (IGF1), IGF binding protein 3 (IGFBP3), and breast cancer risk: pooled individual data analysis of 17 prospective studies. *Lancet Oncol.* 11(6), 530–542 (2010).

16 Peyrat JP, Bonneterre J, Hecquet B *et al.* Plasma insulin-like growth factor-1 (IGF-1) concentrations in human breast cancer. *Eur. J. Cancer* 29A(4), 492–497 (1993).

17 Dupont J, Le Roith D. Insulin-like growth factor 1 and oestradiol promote cell proliferation of MCF-7 breast cancer cells: new insights into their synergistic effects. *Mol. Pathol.* 54(3), 149–154 (2001).

18 Byrne C, Colditz GA, Willett WC, Speizer FE, Pollak M, Hankinson SE. Plasma insulin-like growth factor (IGF) I, IGF-binding protein 3, and mammographic density. *Cancer Res.* 60(14), 3744–3748 (2000).

19 Kleinberg DL, Wood TL, Furth PA, Lee AV. Growth hormone and insulin-like growth factor-I in the transition from normal mammary development to preneoplastic mammary lesions. *Endocr. Rev.* 30(1), 51–74 (2009).

20 Rudd MF, Webb EL, Matakidou A *et al.* Variants in the GH–IGF axis confer susceptibility to lung cancer. *Genome Res.* 16(6), 693–701 (2006).

21 Le Marchand L, Donlon T, Seifried A, Kaaks R, Rinaldi S, Wilkens LR. Association of a common polymorphism in the human *GH1* gene with colorectal neoplasia. *J. Natl Cancer Inst.* 94(6), 454–460 (2002).

22 Menashe I, Maeder D, Garcia-Closas M *et al.* Pathway analysis of breast cancer genome-wide association study highlights three pathways and one canonical signaling cascade. *Cancer Res.* 70(11), 4453–4459 (2010).

23 Canzian F, McKay JD, Cleveland RJ *et al.* Genetic variation in the growth hormone synthesis pathway in relation to circulating insulin-like growth factor-I, insulin-like growth factor binding protein-3, and breast cancer risk: results from the European prospective investigation into cancer and nutrition study. *Cancer Epidemiol. Biomarkers Prev.* 14(10), 2316–2325 (2005).

24 Diorio C, Brisson J, Berube S, Pollak M. Genetic polymorphisms involved in insulin-like growth factor (IGF) pathway in relation to mammographic breast density and IGF levels. *Cancer Epidemiol. Biomarkers Prev.* 17(4), 880–888 (2008).

25 Lai JH, Vesprini D, Zhang W, Yaffe MJ, Pollak M, Narod SA. A polymorphic locus in the promoter region of the *IGFBP3* gene is related to mammographic breast density. *Cancer Epidemiol. Biomarkers Prev.* 13(4), 573–582 (2004).

26 Verheus M, Maskarinec G, Woolcott CG *et al. IGF1*, *IGFBP1*, and *IGFBP3* genes and mammographic density: the Multiethnic Cohort. *Int. J. Cancer* 127(5), 1115–1123 (2010).

27 Morimoto LM, Newcomb PA, White E, Bigler J, Potter JD. Insulin-like growth factor polymorphisms and colorectal cancer risk. *Cancer Epidemiol. Biomarkers Prev.* 14(5), 1204–1211 (2005).

28 Friedrichsen DM, Hawley S, Shu J *et al. IGF-I* and *IGFBP-3* polymorphisms and risk of prostate cancer. *Prostate* 65(1), 44–51 (2005).

29 Park K, Kim JH, Jeon HG, Byun SS, Lee E. Influence of *IGFBP3* gene polymorphisms on IGFBP3 serum levels and the risk of prostate cancer in low-risk Korean men. *Urology* 75(6), 1516, e1–e7 (2010).

30 Rowlands MA, Gunnell D, Harris R, Vatten LJ, Holly JM, Martin RM. Circulating insulin-like growth factor peptides and prostate cancer risk: a systematic review and meta-analysis. *Int. J. Cancer* 124(10), 2416–2429 (2009).

31 Rinaldi S, Cleveland R, Norat T *et al.* Serum levels of IGF-I, IGFBP-3 and colorectal cancer risk: results from the EPIC cohort, plus a meta-analysis of prospective studies. *Int. J. Cancer* 126(7), 1702–1715 (2010).

32 Wolpin BM, Meyerhardt JA, Chan AT *et al.* Insulin, the insulin-like growth factor axis, and mortality in patients with nonmetastatic colorectal cancer. *J. Clin. Oncol.* 27(2), 176–185 (2009).

33 Stattin P, Bylund A, Rinaldi S *et al.* Plasma insulin-like growth factor-I, insulin-like growth factor-binding proteins, and prostate cancer risk: a prospective study. *J. Natl Cancer Inst.* 92(23), 1910–1917 (2000).

34 Renehan AG, Brennan BM. Acromegaly, growth hormone and cancer risk. *Best Pract. Res. Clin. Endocrinol. Metab.* 22(4), 639–657 (2008).

• **The most recent summary of the numerous studies relating acromegaly to cancer risk.**

35 Loeper S, Ezzat S. Acromegaly: re-thinking the cancer risk. *Rev. Endocr. Metab. Disord.* 9(1), 41–58 (2008).

36 Colao A, Pivonello R, Auriemma RS *et al.* The association of fasting insulin concentrations and colonic neoplasms in acromegaly: a colonoscopy-based study in 210 patients. *J. Clin. Endocrinol. Metab.* 92(10), 3854–3860 (2007).

37 Shevah O, Laron Z. Patients with congenital deficiency of IGF-I seem protected from the development of malignancies: a preliminary report. *Growth Horm. IGF Res.* 17(1), 54–57 (2007).

• **The first study to quantify incidence of malignancies in growth hormone (GH) receptor/IGF-1 deficiency in man.**

38 Chernausek SD. Growth and development: how safe is growth hormone therapy for children? *Nat. Rev. Endocrinol.* 6(5), 251–253 (2010).

39 Bell J, Parker KL, Swinford RD, Hoffman AR, Maneatis T, Lippe B. Long-term safety of recombinant human growth hormone in children. *J. Clin. Endocrinol. Metab.* 95(1), 167–177 (2010).

40 Ergun-Longmire B, Mertens AC, Mitby P *et al.* Growth hormone treatment and risk of second neoplasms in the childhood cancer survivor. *J. Clin. Endocrinol. Metab.* 91(9), 3494–3498 (2006).

41 Luft R, Olivecrona H. Hypophysectomy in the treatment of malignant tumors. *Cancer* 10(4), 789–794 (1957).

42 Moon HD, Simpson ME, Li CH, Evans HM. Neoplasms in rats treated with pituitary growth hormone; pulmonary and lymphatic tissues. *Cancer Res.* 10(5), 297–308 (1950).

43 Tornell J, Carlsson B, Pohjanen P, Wennbo H, Rymo L, Isaksson O. High frequency of mammary adenocarcinomas in metallothionein promoter-human growth hormone transgenic mice created from two different strains of mice. *J. Steroid Biochem. Mol. Biol.* 43(1–3), 237–242 (1992).

44 Bates P, Fisher R, Ward A, Richardson L, Hill DJ, Graham CF. Mammary cancer in transgenic mice expressing insulin-like growth factor II (IGF-II). *Br. J. Cancer* 72(5), 1189–1193 (1995).

45 Snibson KJ, Bhathal PS, Adams TE. Overexpressed growth hormone (GH) synergistically promotes carcinogen-initiated liver tumour growth by promoting cellular proliferation in emerging hepatocellular neoplasms in female and male GH-transgenic mice. *Liver* 21(2), 149–158 (2001).

46 Miquet JG, Gonzalez L, Matos MN *et al.* Transgenic mice overexpressing GH exhibit hepatic upregulation of GH-signaling mediators involved in cell proliferation. *J. Endocrinol.* 198(2), 317–330 (2008).

47 Hadsell DL, Murphy KL, Bonnette SG, Reece N, Laucirica R, Rosen JM. Cooperative interaction between mutant p53 and des(1–3)IGF-I accelerates mammary tumorigenesis. *Oncogene* 19(7), 889–898 (2000).

48 Carboni JM, Lee AV, Hadsell DL *et al.* Tumor development by transgenic expression of a constitutively active insulin-like growth factor I receptor. *Cancer Res.* 65(9), 3781–3787 (2005).

49 Michaylira CZ, Simmons JG, Ramocki NM *et al.* Suppressor of cytokine signaling-2 limits intestinal growth and enterotrophic actions of IGF-I *in vivo*. *Am. J. Physiol. Gastrointest. Liver Physiol.* 291(3), G472–G481 (2006).

50 Ikeno Y, Hubbard GB, Lee S *et al.* Reduced incidence and delayed occurrence of fatal neoplastic diseases in growth hormone

receptor/binding protein knockout mice. *J. Gerontol. A Biol. Sci. Med. Sci.* 64(5), 522–529 (2009).

- **Describes causes of death in GH receptor null mice, showing a markedly decreased death rate from cancers.**

51 Zhang X, Mehta RG, Lantvit DD *et al.* Inhibition of estrogen-independent mammary carcinogenesis by disruption of growth hormone signaling. *Carcinogenesis* 28(1), 143–150 (2007).

52 Yang XF, Beamer WG, Huynh H, Pollak M. Reduced growth of human breast cancer xenografts in hosts homozygous for the lit mutation. *Cancer Res.* 56(7), 1509–1511 (1996).

53 Thordarson G, Semaan S, Low C *et al.* Mammary tumorigenesis in growth hormone deficient spontaneous dwarf rats; effects of hormonal treatments. *Breast Cancer Res. Treat.* 87(3), 277–290 (2004).

54 Shen Q, Lantvit DD, Lin Q *et al.* Advanced rat mammary cancers are growth hormone dependent. *Endocrinology* 148(10), 4536–4544 (2007).

55 Wang Z, Prins GS, Coschigano KT *et al.* Disruption of growth hormone signaling retards early stages of prostate carcinogenesis in the C3(1)/T antigen mouse. *Endocrinology* 146(12), 5188–5196 (2005).

56 Pollak M, Blouin MJ, Zhang JC, Kopchick JJ. Reduced mammary gland carcinogenesis in transgenic mice expressing a growth hormone antagonist. *Br. J. Cancer* 85(3), 428–430 (2001).

57 Divisova J, Kuiatse I, Lazard Z *et al.* The growth hormone receptor antagonist pegvisomant blocks both mammary gland development and MCF-7 breast cancer xenograft growth. *Breast Cancer Res. Treat.* 98(3), 315–327 (2006).

- **Provides clear evidence that the GH antagonist pegvisomant is able to regress human breast cancer line growth *in vivo*.**

58 McCutcheon IE, Flyvbjerg A, Hill H *et al.* Antitumor activity of the growth hormone receptor antagonist pegvisomant against human meningiomas in nude mice. *J. Neurosurg.* 94(3), 487–492 (2001).

59 Dagnaes-Hansen F, Duan H, Rasmussen LM, Friend KE, Flyvbjerg A. Growth hormone receptor antagonist administration inhibits growth of human colorectal carcinoma in nude mice. *Anticancer Res.* 24(6), 3735–3742 (2004).

60 de Ostrovich KK, Lambertz I, Colby JK *et al.* Paracrine overexpression of insulin-like growth factor-1 enhances mammary tumorigenesis *in vivo*. *Am. J. Pathol.* 173(3), 824–834 (2008).

61 Olivo-Marston SE, Hursting SD, Lavigne J *et al.* Genetic reduction of circulating insulin-like growth factor-1 inhibits azoxymethane-induced colon tumorigenesis in mice. *Mol. Carcinog.* 48(12), 1071–1076 (2009).

62 Wu Y, Yakar S, Zhao L, Hennighausen L, LeRoith D. Circulating insulin-like growth factor-I levels regulate colon cancer growth and metastasis. *Cancer Res.* 62(4), 1030–1035 (2002).

63 Wu Y, Cui K, Miyoshi K *et al.* Reduced circulating insulin-like growth factor I levels delay the onset of chemically and genetically induced mammary tumors. *Cancer Res.* 63(15), 4384–4388 (2003).

64 Waters MJ. The growth hormone receptor. In: *The Handbook of Physiology.* Kostyo JL, Goodman HM (Eds). Oxford University Press, NY, USA, 397–444 (1999).

65 Gebre-Medhin M, Kindblom LG, Wennbo H, Tornell J, Meis-Kindblom JM. Growth hormone receptor is expressed in human breast cancer. *Am. J. Pathol.* 158(4), 1217–1222 (2001).

66 Lin CJ, Mendonca BB, Lucon AM, Guazzelli IC, Nicolau W, Villares SM. Growth hormone receptor messenger ribonucleic acid in normal and pathologic human adrenocortical tissues – an analysis by quantitative polymerase chain reaction technique. *J. Clin. Endocrinol. Metab.* 82(8), 2671–2676 (1997).

67 Wu X, Liu F, Yao X, Li W, Chen C. Growth hormone receptor expression is up-regulated during tumorigenesis of human colorectal cancer. *J. Surg. Res.* 143(2), 294–299 (2007).

68 Harrison SM, Barnard R, Ho KY, Rajkovic I, Waters MJ. Control of growth hormone (GH) binding protein release from human hepatoma cells expressing full-length GH receptor. *Endocrinology* 136(2), 651–659 (1995).

69 Pazaitou-Panayiotou K, Kelesidis T, Kelesidis I *et al.* Growth hormone-binding protein is directly and IGFBP-3 is inversely associated with risk of female breast cancer. *Eur. J. Endocrinol.* 156(2), 187–194 (2007).

70 Lincoln DT, Sinowatz F, Kolle S, Takahashi H, Parsons P, Waters M. Up-regulation of growth hormone receptor immunoreactivity in human melanoma. *Anticancer Res.* 19(3A), 1919–1931 (1999).

71 Weiss-Messer E, Merom O, Adi A *et al.* Growth hormone (GH) receptors in prostate cancer: gene expression in human tissues and cell lines and characterization, GH signaling and androgen receptor regulation in LNCaP cells. *Mol. Cell Endocrinol.* 220(1–2), 109–123 (2004).

72 Mol JA, van Garderen E, Selman PJ, Wolfswinkel J, Rijinberk A, Rutteman GR. Growth hormone mRNA in mammary gland tumors of dogs and cats. *J. Clin. Invest.* 95(5), 2028–2034 (1995).

73 Mol JA, Henzen-Logmans SC, Hageman P, Misdorp W, Blankenstein MA, Rijnberk A. Expression of the gene encoding growth hormone in the human mammary gland. *J. Clin. Endocrinol. Metab.* 80(10), 3094–3096 (1995).

74 Queiroga FL, Perez-Alenza MD, Silvan G, Pena L, Lopes CS, Illera JC. Crosstalk between GH/IGF-I axis and steroid hormones (progesterone, 17β-estradiol) in canine mammary tumours. *J. Steroid Biochem. Mol. Biol.* 110(1–2), 76–82 (2008).

75 Raccurt M, Lobie PE, Moudilou E *et al.* High stromal and epithelial human GH gene expression is associated with proliferative disorders of the mammary gland. *J. Endocrinol.* 175(2), 307–318 (2002).

76 Ratkaj I, Stajduhar E, Vucinic S *et al.* Integrated gene networks in breast cancer development. *Funct. Integr. Genomics* 10(1), 11–19 (2010).

77 van Garderen E, Schalken JA. Morphogenic and tumorigenic potentials of the mammary growth hormone/growth hormone receptor system. *Mol. Cell Endocrinol.* 197(1–2), 153–165 (2002).

78 Gil-Puig C, Blanco M, Garcia-Caballero T, Segura C, Perez-Fernandez R. Pit-1/GHF-1 and GH expression in the MCF-7 human breast adenocarcinoma cell line. *J. Endocrinol.* 173(1), 161–167 (2002).

79 Chopin LK, Veveris-Lowe TL, Philipps AF, Herington AC. Co-expression of GH and GHR isoforms in prostate cancer cell lines. *Growth Horm. IGF Res.* 12(2), 126–136 (2002).

80 Colao A, Marzullo P, Spiezia S *et al.* Effect of two years of growth hormone and insulin-like growth factor-I suppression on prostate diseases in acromegalic patients. *J. Clin. Endocrinol. Metab.* 85(10), 3754–3761 (2000).

81 Colao A, Di Somma C, Spiezia S, Filippella M, Pivonello R, Lombardi G. Effect of growth hormone (GH) and/or testosterone replacement on the prostate in GH-deficient adult patients. *J. Clin. Endocrinol. Metab.* 88(1), 88–94 (2003).

82 Wang W, Edington HD, Rao UN *et al.* Effects of high-dose IFNα2b on regional lymph node metastases of human melanoma: modulation of STAT5, FOXP3, and IL-17. *Clin. Cancer Res.* 14(24), 8314–8320 (2008).

83 Ruan W, Powell-Braxton L, Kopchick JJ, Kleinberg DL. Evidence that insulin-like growth factor I and growth hormone are required for prostate gland development. *Endocrinology* 140(5), 1984–1989 (1999).

84 Cunningham BC, Bass S, Fuh G, Wells JA. Zinc mediation of the binding of human growth hormone to the human prolactin receptor. *Science* 250(4988), 1709–1712 (1990).

85 Zhu T, Starling-Emerald B, Zhang X *et al.* Oncogenic transformation of human mammary epithelial cells by autocrine human growth hormone. *Cancer Res.* 65(1), 317–324 (2005).

86 Xu XQ, Emerald BS, Goh EL *et al.* Gene expression profiling to identify oncogenic determinants of autocrine human growth hormone in human mammary carcinoma. *J. Biol. Chem.* 280(25), 23987–24003 (2005).

87 Perry JK, Mohankumar KM, Emerald BS, Mertani HC, Lobie PE. The contribution of growth hormone to mammary neoplasia. *J. Mammary Gland Biol. Neoplasia.* 13(1), 131–145 (2008).

• **Comprehensive review of the autocrine/paracrine actions of GH in cancer.**

88 Brunet-Dunand SE, Vouyovitch C, Araneda S *et al.* Autocrine human growth hormone promotes tumor angiogenesis in mammary carcinoma. *Endocrinology* 150(3), 1341–1352 (2009).

89 Kaulsay KK, Zhu T, Bennett W, Lee KO, Lobie PE. The effects of autocrine human growth hormone (hGH) on human mammary carcinoma cell behavior are mediated via the hGH receptor. *Endocrinology* 142(2), 767–777 (2001).

90 van den Eijnden MJ, Strous GJ. Autocrine growth hormone: effects on growth hormone receptor trafficking and signaling. *Mol. Endocrinol.* 21(11), 2832–2846 (2007).

91 Conway-Campbell BL, Wooh JW, Brooks AJ *et al.* Nuclear targeting of the growth hormone receptor results in dysregulation of cell proliferation and tumorigenesis. *Proc. Natl Acad. Sci. USA* 104(33), 13331–13336 (2007).

• **Provides evidence for a role of nuclear localized GH receptor in cancer promotion via synergy with STAT5.**

92 Mertani HC, Garcia-Caballero T, Lambert A *et al.* Cellular expression of growth hormone and prolactin receptors in human breast disorders. *Int. J. Cancer* 79(2), 202–211 (1998).

93 Lincoln DT, Kaiser HE, Raju GP, Waters MJ. Growth hormone and colorectal carcinoma: localization of receptors. *In Vivo* 14(1), 41–49 (2000).

94 Garcia-Caballero T, Mertani HM, Lambert A *et al.* Increased expression of growth hormone and prolactin receptors in hepatocellular carcinomas. *Endocrine* 12(3), 265–271 (2000).

95 Dehari R, Nakamura Y, Okamoto N, Nakayama H. Increased nuclear expression of growth hormone receptor in uterine cervical neoplasms of women under 40 years old. *Tohoku J. Exp. Med.* 216(2), 165–172 (2008).

96 Lo HW, Hung MC. Nuclear EGFR signalling network in cancers: linking EGFR pathway to cell cycle progression, nitric oxide pathway and patient survival. *Br. J. Cancer* 94(2), 184–188 (2006).

97 Conway-Campbell BL, Brooks AJ, Robinson PJ, Perani M, Waters MJ. The extracellular domain of the growth hormone receptor interacts with coactivator activator to promote cell proliferation. *Mol. Endocrinol.* 22(9), 2190–2202 (2008).

98 Sui Y, Yang Z, Xiong S *et al.* Gene amplification and associated loss of 5′ regulatory sequences of CoAA in human cancers. *Oncogene* 26(6), 822–835 (2007).

99 Li X, Hoeppner LH, Jensen ED, Gopalakrishnan R, Westendorf JJ. Co-activator activator (CoAA) prevents the transcriptional activity of Runt domain transcription factors. *J. Cell. Biochem.* 108(2), 378–387 (2009).

100 Auboeuf D, Dowhan DH, Li X *et al.* CoAA, a nuclear receptor coactivator protein at the interface of transcriptional coactivation and RNA splicing. *Mol. Cell Biol.* 24(1), 442–453 (2004).

101 Carver KC, Schuler LA. Prolactin does not require insulin-like growth factor intermediates but synergizes with insulin-like growth factor I in human breast cancer cells. *Mol. Cancer Res.* 6(4), 634–643 (2008).

102 Carver KC, Arendt LM, Schuler LA. Complex prolactin crosstalk in breast cancer: new therapeutic implications. *Mol. Cell Endocrinol.* 307(1–2), 1–7 (2009).

103 Tornell J, Rymo L, Isaksson OG. Induction of mammary adenocarcinomas in metallothionein promoter-human growth hormone transgenic mice. *Int. J. Cancer* 49(1), 114–117 (1991).

104 Wennbo H, Gebre-Medhin M, Gritli-Linde A, Ohlsson C, Isaksson OG, Tornell J. Activation of the prolactin receptor but not the growth hormone receptor is important for induction of mammary tumors in transgenic mice. *J. Clin. Invest.* 100(11), 2744–2751 (1997).

105 Clevenger CV. Role of prolactin/prolactin receptor signaling in human breast cancer. *Breast Dis.* 18, 75–86 (2003).

106 Dagvadorj A, Collins S, Jomain JB *et al.* Autocrine prolactin promotes prostate cancer cell growth via Janus kinase-2-signal transducer and activator of transcription-5a/b signaling pathway. *Endocrinology* 148(7), 3089–3101 (2007).

107 Rouet V, Bogorad RL, Kayser C *et al.* Local prolactin is a target to prevent expansion of basal/stem cells in prostate tumors. *Proc. Natl Acad. Sci. USA* 107(34), 15199–15204 (2010).

108 Harbaum L, Pollheimer MJ, Bauernhofer T *et al.* Clinicopathological significance of prolactin receptor expression in colorectal carcinoma and corresponding metastases. *Mod. Pathol.* 23(7), 961–971 (2010).

109 Mohankumar KM, Perry JK, Kannan N *et al.* Transcriptional activation of signal transducer and activator of transcription (STAT) 3 and STAT5B partially mediate homeobox A1-stimulated oncogenic transformation of the immortalized human mammary epithelial cell. *Endocrinology* 149(5), 2219–2229 (2008).

110 Tang JZ, Zuo ZH, Kong XJ *et al.* Signal transducer and activator of transcription (STAT)-5A and STAT5B differentially regulate human mammary carcinoma cell behavior. *Endocrinology* 151(1), 43–55 (2010).

111 Tang JZ, Kong XJ, Banerjee A *et al.* STAT3α is oncogenic for endometrial carcinoma cells and mediates the oncogenic effects of autocrine human growth hormone. *Endocrinology* 151(9), 4133–4145 (2010).

112 Levine RL, Gilliland DG. JAK-2 mutations and their relevance to myeloproliferative disease. *Curr. Opin Hematol.* 14(1), 43–47 (2007).

113 Morgan KJ, Gilliland DG. A role for JAK2 mutations in myeloproliferative diseases. *Annu. Rev. Med.* 59, 213–222 (2008).

114 Lacronique V, Boureux A, Valle VD *et al.* A TEL-JAK2 fusion protein with constitutive kinase activity in human leukemia. *Science* 278(5341), 1309–1312 (1997).

115 Carlesso N, Frank DA, Griffin JD. Tyrosyl phosphorylation and DNA binding activity of signal transducers and activators of

transcription (STAT) proteins in hematopoietic cell lines transformed by Bcr/Abl. *J. Exp. Med.* 183(3), 811–820 (1996).

116 Pikman Y, Lee BH, Mercher T *et al.* MPLW515L is a novel somatic activating mutation in myelofibrosis with myeloid metaplasia. *PLoS Med.* 3(7), e270 (2006).

117 Funakoshi-Tago M, Tago K, Abe M, Sonoda Y, Kasahara T. STAT5 activation is critical for the transformation mediated by myeloproliferative disorder-associated JAK2 V617F mutant. *J. Biol. Chem.* 285(8), 5296–5307 (2010).

118 Hoelbl A, Schuster C, Kovacic B *et al.* STAT5 is indispensable for the maintenance of Bcr/Abl-positive leukaemia. *EMBO Mol. Med.* 2(3), 98–110 (2010).

119 Schwaller J, Parganas E, Wang D *et al.* STAT5 is essential for the myelo- and lymphoproliferative disease induced by TEL/JAK2. *Mol. Cell* 6(3), 693–704 (2000).

120 Gu L, Vogiatzi P, Puhr M *et al.* STAT5 promotes metastatic behavior of human prostate cancer cells *in vitro* and *in vivo*. *Endocr. Relat. Cancer* 17(2), 481–493 (2010).

121 Mirmohammadsadegh A, Hassan M, Bardenheuer W *et al.* STAT5 phosphorylation in malignant melanoma is important for survival and is mediated through Srs and Jak1 kinases. *J. Invest. Dermatol.* 126(10), 2272–2280 (2006).

122 Hassel JC, Winnemoller D, Schartl M, Wellbrock C. STAT5 contributes to antiapoptosis in melanoma. *Melanoma Res.* 18(6), 378–385 (2008).

123 Lee TK, Man K, Poon RT *et al.* Signal transducers and activators of transcription 5b activation enhances hepatocellular carcinoma aggressiveness through induction of epithelial-mesenchymal transition. *Cancer Res.* 66(20), 9948–9956 (2006).

124 Wagner KU, Rui H. Jak2/STAT5 signaling in mammogenesis, breast cancer initiation and progression. *J. Mammary Gland Biol. Neoplasia.* 13(1), 93–103 (2008).

• **A substantial review describing the dual role of JAK/STAT5 signaling in breast cancer initiation and metastasis.**

125 Koppikar P, Lui VW, Man D *et al.* Constitutive activation of signal transducer and activator of transcription 5 contributes to tumor growth, epithelial–mesenchymal transition, and resistance to epidermal growth factor receptor targeting. *Clin. Cancer Res.* 14(23), 7682–7690 (2008).

126 Prieur A, Peeper DS. Cellular senescence *in vivo*: a barrier to tumorigenesis. *Curr. Opin Cell Biol.* 20(2), 150–155 (2008).

127 Mallette FA, Gaumont-Leclerc MF, Huot G, Ferbeyre G. Myc down-regulation as a mechanism to activate the Rb pathway in STAT5a-induced senescence. *J. Biol. Chem.* 282(48), 34938–34944 (2007).

128 Mallette FA, Moiseeva O, Calabrese V, Mao B, Gaumont-Leclerc MF, Ferbeyre G. Transcriptome analysis and tumor suppressor requirements of STAT5-induced senescence. *Ann. NY Acad. Sci.* 1197, 142–151 (2010).

129 Schartl M, Wilde B, Laisney JA, Taniguchi Y, Takeda S, Meierjohann S. A mutated EGFR is sufficient to induce malignant melanoma with genetic background-dependent histopathologies. *J. Invest. Dermatol.* 130(1), 249–258 (2010).

130 Mohapatra S, Coppola D, Riker AI, Pledger WJ. Roscovitine inhibits differentiation and invasion in a three-dimensional skin reconstruction model of metastatic melanoma. *Mol. Cancer Res.* 5(2), 145–151 (2007).

131 Senderowicz AM. Small-molecule cyclin-dependent kinase modulators. *Oncogene* 22(42), 6609–6620 (2003).

132 Mohapatra S, Chu B, Wei S *et al.* Roscovitine inhibits STAT5 activity and induces apoptosis in the human leukemia virus type 1-transformed cell line MT-2. *Cancer Res.* 63(23), 8523–8530 (2003).

133 Ahonen TJ, Xie J, LeBaron MJ *et al.* Inhibition of transcription factor STAT5 induces cell death of human prostate cancer cells. *J. Biol. Chem.* 278(29), 27287–27292 (2003).

134 Dagvadorj A, Kirken RA, Leiby B, Karras J, Nevalainen MT. Transcription factor signal transducer and activator of transcription 5 promotes growth of human prostate cancer cells *in vivo*. *Clin. Cancer Res.* 14(5), 1317–1324 (2008).

135 Kazansky AV, Spencer DM, Greenberg NM. Activation of signal transducer and activator of transcription 5 is required for progression of autochthonous prostate cancer: evidence from the transgenic adenocarcinoma of the mouse prostate system. *Cancer Res.* 63(24), 8757–8762 (2003).

136 Ginestier C, Wicha MS. Mammary stem cell number as a determinate of breast cancer risk. *Breast Cancer Res.* 9(4), 109 (2007).

137 Tan SH, Dagvadorj A, Shen F *et al.* Transcription factor STAT5 synergizes with androgen receptor in prostate cancer cells. *Cancer Res.* 68(1), 236–248 (2008).

138 Yamashita H, Iwase H, Toyama T, Fujii Y. Naturally occurring dominant-negative STAT5 suppresses transcriptional activity of estrogen receptors and induces apoptosis in T47D breast cancer cells. *Oncogene* 22(11), 1638–1652 (2003).

139 Iavnilovitch E, Groner B, Barash I. Overexpression and forced activation of stat5 in mammary gland of transgenic mice promotes cellular proliferation, enhances differentiation, and delays postlactational apoptosis. *Mol. Cancer Res.* 1(1), 32–47 (2002).

140 Iavnilovitch E, Cardiff RD, Groner B, Barash I. Deregulation of STAT5 expression and activation causes mammary tumors in transgenic mice. *Int. J. Cancer* 112(4), 607–619 (2004).

141 Pardanani AD, Levine RL, Lasho T *et al.* MPL515 mutations in myeloproliferative and other myeloid disorders: a study of 1182 patients. *Blood* 108(10), 3472–3476 (2006).

142 Ding J, Komatsu H, Wakita A *et al.* Familial essential thrombocythemia associated with a dominant-positive activating mutation of the *c-MPL* gene, which encodes for the receptor for thrombopoietin. *Blood* 103(11), 4198–4200 (2004).

143 Bernichtein S, Touraine P, Goffin V. New concepts in prolactin biology. *J. Endocrinol.* 206(1), 1–11 (2010).

144 Lempereur L, Brambilla D, Scoto GM *et al.* Growth hormone protects human lymphocytes from irradiation-induced cell death. *Br. J. Pharmacol.* 138(8), 1411–1416 (2003).

145 Wu X, Wan M, Li G *et al.* Growth hormone receptor overexpression predicts response of rectal cancers to pre-operative radiotherapy. *Eur. J. Cancer* 42(7), 888–894 (2006).

146 Zatelli MC, Minoia M, Mole D *et al.* Growth hormone excess promotes breast cancer chemoresistance. *J. Clin. Endocrinol. Metab.* 94(10), 3931–3938 (2009).

147 Blackmore DG, Golmohammadi MG, Large B, Waters MJ, Rietze RL. Exercise increases neural stem cell number in a growth hormone-dependent manner, augmenting the regenerative response in aged mice. *Stem Cells* 27(8), 2044–2052 (2009).

Website

201 Oncomine database www.oncomine.org